THE ALKALOIDS
Chemistry and Biology

VOLUME **65**

Edited by

Geoffrey A. Cordell
Evanston, Illinois

ELSEVIER

Amsterdam • Boston • Heidelberg • London • New York • Oxford
Paris • San Diego • San Francisco • Singapore • Sydney • Tokyo
Academic Press is an imprint of Elsevier

ACADEMIC
PRESS

Academic Press is an imprint of Elsevier
84 Theobald's Road, London WC1X 8RR, UK
Radarweg 29, PO Box 211, 1000 AE Amsterdam, The Netherlands
Linacre House, Jordan Hill, Oxford OX2 8DP, UK
30 Corporate Drive, Suite 400, Burlington, MA 01803, USA
525 B Street, Suite 1900, San Diego, CA 92101-4495, USA

First edition 2008

ISBN: 978-0-12-374296-4
ISSN: 1099-4831

Printed and bound in USA

08 09 10 11 12 10 9 8 7 6 5 4 3 2 1

CONTRIBUTORS

Hans-Joachim Knölker, Department Chemie, Technische Universität Dresden, Dresden, Germany

Kethiri R. Reddy, Department Chemie, Technische Universität Dresden, Dresden, Germany

PREFACE

This is the latest volume in the series ''*The Alkaloids: Chemistry and Biology*'' and covers a group of alkaloids comprising the carbazole nucleus. Single-topic volumes in this series have been rare, and the last one discussed antitumor alkaloids and was published as Volume 25 in 1985. This is the first volume dedicated to a single alkaloid structure type since Volume 8, which dealt with the monoterpene indole alkaloids over 40 years ago.

This background places in context how significant this remarkably extensive and exceptionally well-organized single volume review of the ''*Chemistry and Biology of Carbazole Alkaloids*'' by Knölker and Reddy actually is. It brings together for the first time all of the alkaloids that have been isolated from plant, microbial, and marine sources, which possess, in any aspect of their structure, a carbazole nucleus. The alkaloids are reviewed from the detailed aspects of their structure elucidation, and for the first time an approach is offered with respect to an overall view of their biogenetic pathways, which differ substantially based on the further structural elements of which the carbazole is a core feature. These discussions are followed by a detailed exposition of how the significance of these alkaloids has been enhanced through the determination of several important, clinically relevant, biological properties. Finally, the authors offer a comprehensive presentation of the many synthetic approaches to the various carbazole alkaloids, from the simple alkaloids to the more complex alkaloids, including the bis-alkaloids.

Geoffrey A. Cordell
Evanston, Illinois, USA

CHAPTER 1

Introduction

The initial discovery of carbazole in the anthracene fraction of coal tar followed by the first isolation of the antimicrobial murrayanine (3-formyl-1-methoxycarbazole) from the plant *Murraya koenigii* Spreng., started the enormous development of carbazole chemistry. Since then, there has been a strong interest in this area by chemists and biologists due to the intriguing structural features and promising biological activities associated with many carbazole alkaloids. The progress in the chemistry of carbazole alkaloids is emphasized by the publication of several reviews and book chapters covering the field (1–10).

In this series, three earlier reviews on carbazole alkaloids were published by Kapil (1), Husson (2), and Chakraborty (3) in the Volumes 13, 26, and 44, respectively. The present chapter introduces a new classification of carbazole alkaloids and summarizes the recent synthetic efforts. The nomenclature of carbazole alkaloids used in this review is that of *Chemical Abstracts*. As shown in Scheme 1.1, the conventional tricyclic ring system of carbazole **1** is denoted by A, B, and C, and the numbering starts from ring A. The term carbazole generally refers to a 9*H*-carbazole.

Several hypotheses have been proposed for the biogenesis of carbazole alkaloids (see Chapter 3 of this review). However, there is no deep experimental knowledge of the biosynthesis of this class of alkaloids. A comparison of the structural features of carbazole alkaloids isolated from higher plants suggests that 3-methylcarbazole (**2**) may represent the key intermediate in their biosynthesis (Scheme 1.1).

In the present review, we summarize the occurrence, biogenesis, biological activity, and the chemistry of carbazole alkaloids, which have been classified based on their natural sources, ring system, and substitution pattern. While a comprehensive overview is given on all carbazole alkaloids isolated from natural sources, only their total syntheses published since 1990 are discussed.

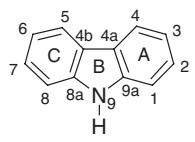

1

Carbazole Numbering

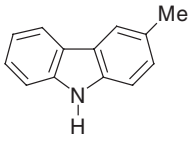

2 3-Methylcarbazole

Scheme 1.1

CHAPTER 2

Occurrence, Isolation, and Structure Elucidation

A large number of carbazole alkaloids has been isolated from higher plants of the genera *Murraya*, *Glycosmis*, and *Clausena*, all belonging to the family Rutaceae (subtribe Clauseninae, tribe Clauseneae, subfamily Aurantioideae). The occurrence of carbazole alkaloids in these three genera of the Rutaceae is of chemotaxonomic importance and justifies their classification as an independent subtribe. Carbazoles have also been reported from other genera, such as *Micromelum* of the family Rutaceae (subtribe Micromelinae), *Ekebergia* of the Meliaceae, and *Cimicifuga* of the Ranunculaceae. The genus *Murraya*, especially the species *Murraya euchrestifolia* Hayata, represents the richest source of carbazole alkaloids among all terrestrial plants. Various monomeric and also bis-carbazole alkaloids, formed by the combination of two of the monomeric units, have been reported from the genus *Murraya*. It is noteworthy that, while *Murraya koenigii* grown in Indian soil did not afford any bis-carbazole alkaloids, the same species grown in a green house in Japan from seeds collected in Taiwan generated bis-carbazole alkaloids. Depending on the seasonal and geographical variation, the genus *Murraya* is known to provide different alkaloids. Moreover, carbazole alkaloids have been isolated from several different *Streptomyces* species. The indolocarbazole alkaloids have been obtained from microorganisms, slime molds, and marine sources. Further natural sources for carbazole alkaloids are for example the blue-green alga *Hyella caespitosa*, species of the genera *Aspergillus*, *Actinomadura*, *Didemnum*, and *Iotrochota*, and the human pathogenic yeast *Malassezia furfur*.

The natural sources of carbazole alkaloids are listed in Table 2.1. Carbazole and various alkylcarbazoles have also been obtained from other sources, such as coal tar, petroleum oil, soil humus, the polluted atmosphere of industrial areas, as well as cigarette smoke.

I. CARBAZOLE ALKALOIDS FROM HIGHER PLANTS

The isolation of carbazole (**1**), 3-methylcarbazole (**2**), and several oxidized derivatives of 3-methylcarbazole from taxonomically related higher plants of the genera *Glycosmis*, *Clausena*, and *Murraya* (family Rutaceae) indicates that the aromatic methyl group of the biogenetic key intermediate 3-methylcarbazole can be eliminated oxidatively (5,6). Most of the carbazole alkaloids isolated from the

Table 2.1 Biological sources of carbazole alkaloids

A. Higher plants	*Murraya euchrestifolia* Hayata
	M. koenigii Spreng.
	M. siamensis Craib.
	Clausena anisata Hook.
	C. heptaphylla Wight & Arn.
	C. excavata Burm f.
	C. indica Oliver
	C. lansium (Lour.) Skeels
	C. harmandiana Pierre ex. Guillaumin [syn. *C. wampi* (Blanco) Oliv.]
	G. arborea (Roxb.) DC.
	G. parviflora (Sims) Little
	G. mauritiana Tanaka
	G. montana Pierre
	Glycosmis pentaphylla (Retz.) DC. (syn. *G. arborea* (Roxb.) DC.
	Micromelum ceylanicum Wight
	M. hirsutum Oliver
	Ekebergia senegalensis Fuss.
	Cimicifuga simplex Wormsk. ex DC.
B. Other sources	*Streptoverticillium ehimense*
(i) Microbial sources (schizomycophyta)	*S. mobaraense*
	Streptomyces chromofuscus DC 118
	S. exfoliates 2419-SVT2
	Streptomyces sp.
	S. staurosporeus Anaya
	Actinomadura madurae
	A. melliaura
	Arcyria denudata
	Aspergillus flavus
	A. tubingensis
	Nocardia aerocoligenes
	Nocardiopsis dassonvillei
	Nocardiopsis sp.
(ii) Marine sources (cyanophyta)	*Hyella caespitosa* Bron et Flah
	Tedania ignis
	Nostoc sphaericum
	Tolypothrix tjipanasensis
	New Zealand Ascidian
	Australian Ascidian *Didemnum* sp.
	Marine Sponge *Iotrochota* sp.
	Marine Sponge *Dictyodendrilla verongiformis*
(iii) Diverse sources	Bovine urine
	Malassezia furfur (human pathogenic yeast)

Rutaceae family (11) have a one-carbon-substituent at position 3 of the carbazole nucleus and an oxygen substituent at position 1 or 2. The structure of these alkaloids can vary from simple substituted carbazoles to molecules containing complex terpene moieties.

A. Tricyclic Carbazole Alkaloids

1 Carbazole

Carbazole (**1**) was isolated first from the anthracene fraction of coal tar in 1872 by Graebe and Glaser (12). In 1987, almost a century later, Bhattacharyya *et al.* reported for the first time the isolation of carbazole (**1**) from a plant source, *Glycomis pentaphylla* (13) (Scheme 2.1). Structural assignment of carbazole (**1**) was based on UV, IR, and mass spectral data, as well as direct comparison with an authentic sample.

2 3-Methylcarbazole and Non-Oxygenated Congeners

Chakraborty (14), Joshi (15), and Connolly *et al.* (16) reported independently the isolation of 3-methylcarbazole (**2**) from the roots of different *Clausena* species, such as *Clausena heptaphylla*, *Clausena indica*, and *Clausena anisata*. In 1987, Bhattacharyya *et al.* isolated 3-methylcarbazole (**2**), along with carbazole (**1**), from the root bark of *Glycosmis pentaphylla* (13). A decade later, 3-methylcarbazole (**2**) was obtained by Chakrabarty *et al.* from the chloroform extract of the roots of *M. koenigii* (17). In 1998, Wu *et al.* isolated 3-methylcarbazole (**2**) during a study of the antiplatelet aggregation activity of the acetone extract of the root bark of *M. euchrestifolia* (18). In the IR spectrum (ν_{max} 3450, 1600, 1493, 1390, 885, 808 cm^{-1}), the band at 808 cm^{-1}, which is characteristic of 3-methylcarbazole, confirms the position of the methyl group (19). The UV spectrum (λ_{max} 230, 236, 243, 260, 296, 330 nm) was superimposible with that of 3-methylcarbazole and confirmed the structural assignment (20,21).

In 1988, Furukawa *et al.* reported the isolation of 3-formylcarbazole (**3**) from the root bark of *M. euchrestifolia* (22). Three years later, McChesney and El-Feraly isolated 3-formylcarbazole (**3**), along with methyl carbazole-3-carboxylate (**4**), from the roots of *Clausena lansium* (23). The roots of this ornamental tree are used in traditional medicine in Taiwan to treat bronchitis and malaria (23). In 1992, Bhattacharyya *et al.* described the isolation and structural elucidation of 3-formylcarbazole (**3**) from *G. pentaphylla* (24).

3-Formylcarbazole has UV spectral characteristics as reported previously in the literature (25–27). The IR spectrum showed the band of an NH group (3460 cm^{-1}) and of a conjugated carbonyl function (1685 cm^{-1}). The ^{1}H-NMR and ^{13}C-NMR

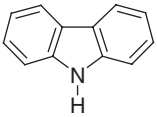

1 Carbazole

Scheme 2.1

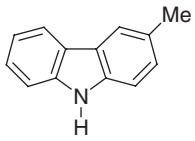

2 3-Methylcarbazole

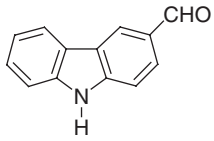

3 3-Formylcarbazole

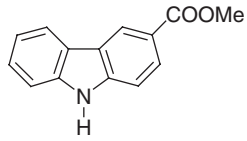

4 Methyl carbazole-3-carboxylate

Scheme 2.2

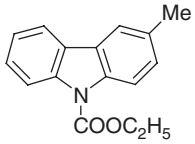

5 9-Carbethoxy-3-methylcarbazole

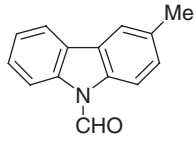

6 9-Formyl-3-methylcarbazole

Scheme 2.3

spectrum confirmed the presence of an aldehyde group at position 3. In the aromatic region, the ^{1}H-NMR spectrum of methyl carbazole-3-carboxylate (**4**) is very similar to that of 3-formylcarbazole (**3**). The methyl ester was indicated by a singlet at δ 3.91 for the methoxy group and, in the ^{13}C-NMR spectrum, by a signal at δ 168.0 for the ester carbonyl group. In addition to the spectroscopic proof, chemical support was derived from transformation into the corresponding acid and remethylation with diazomethane to afford methyl carbazole-3-carboxylate (**4**) (Scheme 2.2).

In 1997, Chakrabarty *et al.* reported the isolation of 9-carbethoxy-3-methylcarbazole (**5**) and 9-formyl-3-methylcarbazole (**6**) from the roots of *M. koenigii* (17). These metabolites are the first 9-formyl and 9-carbethoxy carbazole derivatives obtained from plant sources. 9-Formyl-3-methylcarbazole (**6**) showed weak cytotoxicity against both mouse melanoma B16 and adriamycin-resistant P388 mouse leukemia cell lines. The structural assignment of these two alkaloids was based on the IR- and ^{1}H-NMR spectra which were lacking any signal of an NH group. Additional structural support for 9-carbethoxy-3-methylcarbazole (**5**) was provided by the similarity of the UV absorption spectrum with that of a synthetic sample, obtained by reaction of 3-methylcarbazole with ethyl chloroformate in the presence of base. Further structural support for 9-formyl-3-methylcarbazole (**6**) was derived from a comparison of the UV spectrum and the IR carbonyl absorption (1696 cm^{-1}) with those of an authentic sample of 9-formyl-3-methylcarbazole (1700 cm^{-1}), prepared by the treatment of 3-methylcarbazole (**2**) with 98% formic acid (17) (Scheme 2.3).

3 1-Oxygenated Tricyclic Carbazole Alkaloids

The higher plants of the genus *Murraya* (family Rutaceae), which are trees growing in Southern Asia, are the major source of 1-oxygenated carbazole alkaloids. Extracts of the leaves and bark of this tree have been used in traditional medicine for analgesia and local anesthesia, and for the treatment of eczema, rheumatism, and dropsy. Murrayafoline A (**7**) was isolated from the ethanolic extract of the root bark of *M. euchrestifolia* collected in Taiwan (28,29). Recently, Cuong *et al.* isolated the same alkaloid from *Glycosmis stenocarpa* Guillaumin collected in Northern Vietnam (30).

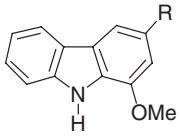

7 Murrayafoline A
R = Me
8 Koenoline
R = CH_2OH
9 Murrayanine
R = CHO
10 Mukoeic acid
R = COOH
11 Mukonine
R = COOMe

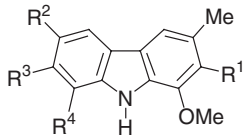

7 Murrayafoline A
R^1,R^2,R^3,R^4 = H
12 Murrayastine
R^1,R^2 = H; R^3,R^4 = OMe
13 Clausenapin
R^1 = prenyl; R^2,R^3,R^4 = H
14 Clausenine
R^1,R^3,R^4 = H; R^2 = OMe

Scheme 2.4

The UV spectrum [λ_{max} 225, 243, 251 (sh), 292, 330, and 334 (sh) nm] of murrayafoline-A (**7**) was similar to that of other 1-oxygenated carbazoles. The ^{1}H-NMR spectrum of (**7**), with a three-proton signal at δ 6.9–7.3 and a signal at δ 7.87 for H-5, indicated an unsubstituted C-ring. The signals for a methoxy substituent at δ 3.76 and an aromatic methyl group at δ 2.40, along with the signals for H-4 and H-2 at δ 7.33 and 6.55, respectively, suggested a C-1 methoxy and a C-3 methyl group. This regiochemistry was confirmed by NOE experiments. Thus, murrayafoline-A (**7**) was assigned as 1-methoxy-3-methylcarbazole, previously described as an intermediate in the synthesis of murrayanine (**9**) (Scheme 2.4) (31).

The cytotoxic carbazole alkaloid koenoline (**8**) was isolated from the root bark of *M. koenigii* (32). Koenoline exhibited the characteristic UV spectrum (λ_{max} 241, 251, 289, and 323 nm) of a 1-methoxycarbazole derivative. In addition, the IR spectrum indicated an NH (3445 cm^{-1}) and an OH group (3235 cm^{-1}), as well as an aromatic system (1585 and 1500 cm^{-1}). The ^{1}H-NMR spectrum showed the signals of an aromatic methoxy (δ 4.01), a benzylic methylene group (δ 4.5), H-2 and H-4 as two broad singlets at δ 6.95 and 7.66, and an unsubstituted C-ring. Based on these spectroscopic data, koenoline was structurally assigned as **8**. Further confirmation was derived from the ^{13}C-NMR data and a partial synthesis by sodium borohydride reduction of murrayanine (**9**) (31).

Chakraborty *et al*. reported the isolation of murrayanine (**9**) independently from two different genera of the family Rutaceae, *M. koenigii* (33) and *C. heptaphylla* (34). More recently, Cuong *et al*. isolated murrayanine (**9**) from *G. stenocarpa* Guillaumin from Northern Vietnam (30). Murrayanine (**9**) showed antimicrobial properties against human pathogenic fungi (35). The UV spectrum of murrayanine (**9**) (λ_{max} 238, 244, 273, 288, and 327 nm) was strikingly similar to that of 3-formylcarbazole (**3**). The IR spectrum showed the presence of an NH group (3450 cm^{-1}), an aromatic aldehyde (2800, 1681 cm^{-1}), and an aromatic ring (1631, 1613, 1585 cm^{-1}). In addition, peaks at 850 and 725 cm^{-1} suggested tetra- and di-substituted aromatic rings. The ^{1}H-NMR spectrum showed an aldehyde proton (δ 9.98), an aromatic

methoxy group (δ 3.96), and six aromatic protons (δ 8.09, 7.39). The spectroscopic data confirmed structure **9** (3-formyl-1-methoxycarbazole) for murrayanine. This structural assignment was further supported by chemical transformation into known carbazole derivatives.

Mukoeic acid (**10**) was obtained from the stem bark of *M. koenigii*. It represents the first carbazole carboxylic acid isolated from a plant source (36,37). The characteristic UV spectrum (λ_{max} 235, 270, and 320 nm) of a 1-methoxycarbazole derivative, as well as the presence of bands for an NH (3431 cm^{-1}), a COOH group (1690 cm^{-1}), and a substituted aromatic ring (1635, 1613, 1609, 763, and 735 cm^{-1}) in the IR spectrum, supported the assigned structure. The ^{1}H-NMR spectrum of methyl mukoate, obtained by methylation of mukoeic acid with diazomethane, showed the presence of a carbomethoxy and a methoxy group at δ 4.02 and 4.07, and a deshielded aromatic proton at δ 8.53 (assigned to the proton at C-4 of the carbazole framework). In addition to the spectroscopic data, further structural support was derived from decarboxylation of mukoeic acid to 1-methoxycarbazole. This chemical transformation suggested the presence of a carboxylic group at C-3 and a methoxy group at C-1.

The corresponding methyl ester of mukoeic acid, mukonine (**11**), was also isolated from *M. koenigii* (4). The UV spectrum (λ_{max} 236, 274, and 320 nm) was very similar to that of mukoeic acid. The IR spectrum showed bands for an NH (3350 cm^{-1}) and a COOMe group (1700 cm^{-1}), and for an aromatic system (1600, 1510 cm^{-1}). The data indicated that mukonine was a methyl 1-methoxycarbazole-3-carboxylate, which was confirmed by hydrolysis of mukonine to mukoeic acid. The co-occurrence of murrayafoline-A (**7**), koenoline (**8**), murrayanine (**9**), mukoeic acid (**10**), and mukonine (**11**) in plants of the genus *Murraya* suggests that they are biosynthesized by *in vivo* oxidation of murrayafoline-A (**7**) (Scheme 2.4).

In 1986, Furukawa *et al.* isolated murrayastine (**12**) from the stem bark of *M. euchrestifolia* collected in Taiwan (38). The UV spectrum (λ_{max} 224, 247, 255, 298, 322, and 336 nm) and the IR spectrum (ν_{max} 1630 and 1585 cm^{-1}) indicated a carbazole framework. The ^{1}H-NMR spectrum showed an aromatic methyl signal (δ 2.47), three aromatic methoxy groups (δ 3.95, 3.96, and 4.00), and *meta*-coupled H-4 (δ 7.32) and H-2 (δ 6.65) signals. The enhancement of the signals at H-2 and H-4 on irradiation at the aromatic methyl group suggested C-3 as the position for the methyl group. The *ortho*-coupled H-5 signal (δ 7.56, d, J=8.0 Hz) demonstrated that positions C-5 and C-6 were unsubstituted. The spectral data suggested structure **12** for murrayastine, which was confirmed by synthesis (38).

Clausenapin (**13**) was isolated from the leaves of *C. heptaphylla* (39). Prior to its isolation, it was known as a Huang–Minlon reduction product of indizoline (4). The UV spectrum of clausenapin (λ_{max} 224, 240, 250, 290, 320, and 335 nm) was similar to that of 1-methoxycarbazole, which was also supported by the IR data. The ^{1}H-NMR spectrum showed signals for a prenyl side chain (δ 1.75, 1.85, 3.62, and 5.3), an aromatic methyl (δ 2.28), an unsubstituted C ring (δ 7.1–7.4 and 7.9), and a H-4 singlet (δ 7.5). Isolation of 3-methylcarbazole from zinc dust distillation, the similarity of the UV spectrum with 1-methoxycarbazole, and the singlet for the proton at C-4 suggested that the prenyl chain was at position 2. From these spectral studies, structure **13** was assigned to clausenapin. This structure was further supported by the previously reported Huang–Minlon reduction product of indizoline (**16**) (see Scheme 2.5) (4).

In 1995, Chowdhury *et al*. isolated clausenine (**14**) from the alcoholic extract of the stem bark of *C. anisata* (40). The UV (λ_{max} 226, 242, 299, 298, 340, and 354 nm) and the IR spectrum showed the presence of an NH group (3400 cm^{-1}) and a substituted aromatic system with a carbazole framework (1580, 1218, 940, 840, 820 cm^{-1}). The ^{1}H-NMR spectrum exhibited an aromatic methyl signal (δ 2.42), two aromatic methoxy groups (δ 3.80 and 3.92), and *meta*-coupled H-4 (δ 7.54) and H-2 (δ 6.74) signals. The *ortho*-coupled H-8 (δ 7.32, d, J=8.0 Hz), along with the *ortho*- and *meta*-coupled H-7 signal (δ 6.92, dd, J=8.0, 2.0 Hz), and the *meta*-coupled H-5 (δ 7.44, d, J=2.0 Hz) demonstrated that the positions C-2, C-4, C-5, C-7, and C-8 were unsubstituted. Based on all these spectral data, structure **14** was assigned to clausenine (Scheme 2.4).

6-Methoxymurrayanine (3) (3-formyl-1,6-dimethoxycarbazole) (**15**) was isolated from the roots of *C. lansium* (23). The roots of *C. lansium* were used to treat bronchitis and malaria. The UV (λ_{max} 227, 239, 251, 294, 335, and 349 nm) and IR spectra showed the presence of a 3-formylcarbazole framework. The ^{1}H-NMR data were similar to murrayanine (**9**), with an additional methoxy group for one of the aromatic hydrogens at the C-ring of the carbazole. Since the signal for H-5 (δ 7.90) is not *ortho*-coupled, an additional methoxy could be located at C-6. This structural conclusion was also supported by the ^{13}C-NMR spectrum.

Indizoline (**16**) was isolated from the roots of *C. indica* (15). The UV spectrum (λ_{max} 237, 247, 275, 294, and 330 nm) is similar to 3-formylcarbazole (with the exception of a hyperchromic shift of the maximum at λ 275 nm), which was also supported by the IR data. The ^{1}H-NMR spectrum showed signals at δ 1.70 (3*H*, J=1.0 Hz, methyl), 1.85 (3*H*, J=1.0 Hz, methyl), 3.9 (2*H*, benzylic methylene), and 5.25 (1*H*, vinylic proton) indicative of the presence of a prenyl side chain attached to the aromatic ring. Moreover, the presence of an aromatic methoxy group (δ 3.29), an aldehyde (δ 10.3), an unsubstituted C-ring (δ 7.4, 3*H*, m and δ 8.02, 1*H*, dd, J=2, 7 Hz), and a deshielded H-4 singlet (δ 8.4), due to the proximity of the aldehyde function at C-3, were observed. On Huang–Minlon reduction, indizoline gave a compound having a UV spectrum similar to that of 1-methoxycarbazole. The singlet nature of the C-4 proton and the substitution at the positions 1 and 3, strongly suggested that the prenyl side chain was located at C-2. On this basis, indizoline was formulated as **16**. This assignment was confirmed by an independent synthesis of its reduction product **13** (see Scheme 2.4) (4), which later was isolated from *C. heptaphylla* and named clausenapin (**13**) (see Scheme 2.4) (39).

Although ekeberginine (**17**) is an alkaloid closely related structurally to indizoline (**16**), it was isolated from two different sources, the stem bark of *Ekebergia senegalensis* (Meliaceae) (41) and the combined extracts of the stem bark and roots of *C. anisata* (16). The ^{1}H-NMR spectrum **17** was similar to that of indizoline, except for the absence of the deshielded C-4 proton and the presence of a C-2 proton at δ 7.43 as a singlet. The position of the prenyl group was unambiguously assigned at C-4 of the carbazole ring by using 2D long-range δ_C/δ_H correlation combined with the 1D proton-coupled ^{13}C-NMR spectrum. Thus, C-4b has ^{3}J correlations with H-6 and H-8, while C-4a has ^{3}J correlations with H-5 and the C-1 methylene protons of the prenyl group. Therefore, structure **17** was assigned to ekeberginine. This structural assignment also supports the structure of readily formed *N*-methylekeberginine.

Clausenal (**18**) was isolated from the ethanolic extract of the leaves of *C. heptaphylla*. Clausenal showed promising activity against Gram-positive and

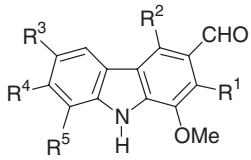

9 Murrayanine
R^1,R^2,R^3,R^4,R^5 = H

15 6-Methoxymurrayanine
(3-Formyl-1,6-dimethoxycarbazole)
R^1,R^2,R^4,R^5 = H; R^3 = OMe

16 Indizoline
R^1 = prenyl; R^2,R^3,R^4,R^5 = H

17 Ekeberginine
R^1,R^3,R^4,R^5 = H; R^2 = prenyl

18 Clausenal
R^1,R^2,R^3,R^4 = H; R^5 = OMe

19 Clausine Q
R^1,R^2,R^3,R^5 = H; R^4 = OH

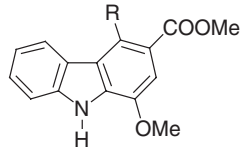

11 Mukonine
R = H

20 Clausamine D
R = prenyl

21 Clausamine E
R = (E)HC=CHC(OH)Me_2

22 Clausamine G
R = (E)HC=CHC(OOH)Me_2

Scheme 2.5

Gram-negative bacteria, and fungi (42). The UV spectrum (λ_{max} 231, 257, 261, and 327 nm) is characteristic of a 3-formylcarbazole. The IR data suggested the presence of an NH (3400 cm^{-1}), an aldehyde (1660 cm^{-1}), and an aromatic ring (1610, 1576 cm^{-1}). The ^{1}H-NMR spectrum showed signals for NH (δ 8.80, br s), CHO (δ 10.28, s), H-4 (δ 8.60, d, J=2.8 Hz), H-5 (δ 7.78, dd, J=8.0, 1.5 Hz), H-2 (δ 7.44, d, J=1.8 Hz), H-6 (7.25, m), H-7 (δ 6.98, dd, J=8.0, 1.8 Hz), as well as two singlets for two aromatic methoxy groups (δ 4.07, 4.02). In addition, a mass spectral fragment at m/z 227 represented a formylcarbazole residue, while the peaks at m/z 240 (M^+–15) and 212 (227−15) suggested the presence of two aromatic methoxy groups. In consideration of the ^{1}H-NMR and ^{13}C-NMR data, the two methoxy groups were placed at C-1 and C-8, and the formyl group at C-3. Based on these spectral data, the structure of clausenal was assigned as 1,8-dimethoxy-3-formylcarbazole (**18**). This structure was confirmed by synthesis using a Japp–Klingemann reaction and Fischer indolization.

Clausine Q (**19**) was isolated from the acetone extract of the root bark of *Clausena excavata* (43). The UV spectrum (λ_{max} 242, 286, 297, 325, and 338 nm) was characteristic of a 3-formylcarbazole. The ^{1}H-NMR spectrum showed the presence of CHO (δ 10.01, s), H-4 (δ 8.19, d, J=1.2 Hz), H-5 (δ 7.99, d, J=8.0 Hz), H-2 (δ 7.38, d, J=1.2 Hz), H-6 (δ 6.84, dd, J=8.5, 2.2 Hz), H-8 (δ 7.07, d, J=2.2 Hz), and an aromatic methoxy group (δ 4.06). Two *meta*-coupled protons (H-2 and H-4), a *meta*-coupled proton at C-8, and an *ortho*- and *meta*-coupled proton at C-6 suggested clausine Q to be a 1,7-disubstituted-3-formylcarbazole. The positional assignments for OH at C-7 and OMe at C-1 were confirmed by NOE experiments. Thus, the structure of clausine Q suggested was established as **19** (Scheme 2.5).

In 2000, Itoigawa *et al*. (44) isolated clausamine D (**20**), clausamine E (**21**), and clausamine G (**22**) from the acetone extract of branches of *C. anisata*. Clausamine G is

the first example of a naturally occurring, peroxygenated carbazole alkaloid. All of these carbazole alkaloids showed antitumor-promoting activity against TPA (12-*O*-tetradecanoylphorbol-13-acetate)-induced EBV-EA (Epstein–Barr virus early antigen) activation (44).

The UV spectrum (λ_{max} 222, 240, 248, 256, 269, 310, 321, and 335 nm) of clausamine D (**20**) was characteristic of a 1-oxygenated 3-carbomethoxy carbazole. The IR spectrum showed the presence of NH (3467 cm^{-1}) and COOMe (1709 cm^{-1}). The presence of a carbomethoxy functionality at the carbazole nucleus was additionally confirmed by the characteristic mass fragmentation at m/z 292 (M^+-OMe) and 264 ($M^+-COOMe$). The ^{1}H-NMR spectrum showed the presence of a prenyl side chain attached to the aromatic ring, and a set of four C–H protons at δ 8.14 (d, J=8.1 Hz), 7.27 (t, J=8.1 Hz), 7.44 (t, J=8.1 Hz), and 7.49 (d, J=8.1 Hz) for H-5, H-6, H-7, and H-8, respectively. Moreover, the ^{1}H-NMR spectrum exhibited a singlet at δ 7.46 for H-2 and two signals for aromatic methoxy groups at δ 4.03 and 3.93. These data, combined with biogenetic considerations, suggested the presence of a 1-oxygenated 3-substituted carbazole skeleton with no substituents on the C-ring. NOE results, combined with ^{1}H and ^{13}C-NMR data, unequivocally confirmed structure **20** for clausamine D. This structure was also supported by the synthesis of **20** *via* *O*-methylation of clausine F (**32**) (see Scheme 2.7).

The UV spectrum (λ_{max} 224, 239, 273, 322, and 337 nm) of clausamine E (**21**) was similar to that of clausamine D (**20**). The ^{1}H-NMR spectrum also showed a signal pattern similar to that of clausamine D, except for the absence of signals of a prenyl group. Doublets at δ 7.37 and 6.00 with a large coupling constant of J=16.1 Hz indicated the presence of an (*E*)-disubstituted double bond. Moreover, a 6-proton-singlet at δ 1.55 due to two methyl groups was observed. These data, and two significant mass fragment ion peaks at m/z 321 (M^+-H_2O) and 280 ($M^+-C(OH)Me_2$), suggested the presence of the side chain [(*E*)-CH═CHC(OH)Me_2]. Based on these data, structure **21** was assigned to clausamine E.

The UV spectrum (λ_{max} 223, 236, 270, 313, 321, and 333 nm) of clausamine G (**22**) and the doublets in the ^{1}H-NMR spectrum at δ 7.47 and 5.92 with a large coupling constant of J=16.5 Hz indicated the presence of an (*E*)-disubstituted double bond. A 6-proton-singlet at δ 1.60 resulted from two equivalent methyl groups. These data confirmed the similarity of clausamine G (**22**) and clausamine E (**21**). The observation of a broad singlet at δ 9.56, exchangeable with D_2O, together with a significant mass fragment ion peak at m/z 281 ($M^+-C(OOH)Me_2+H$) suggested the presence of a side chain [(*E*)-CH═CHC(OOH)Me_2]. Based on the spectral data, structure **22** was assigned to clausamine G. This structure was additionally supported by transformation of clausamine G into clausamine E on reaction with triphenylphosphine (Scheme 2.5).

1-Hydroxy-3-methylcarbazole (**23**) was isolated from the stem bark of *M. koenigii* (45). The UV spectrum (λ_{max} 225, 242, 290, and 331 nm) was similar to that of 3-methylcarbazole (**2**) (see Scheme 2.2). The IR spectrum showed the presence of an NH group (3400 cm^{-1}), an OH substituent (3283 cm^{-1}), and an aromatic ring (1615, 1580 cm^{-1}). The aromatic region of the ^{1}H-NMR spectrum showed an unsubstituted C-ring along with a proton at C-4 (doublet at δ 7.5, J=2.0 Hz) exhibiting a *meta*-coupling with the proton at C-2. Based on this evidence, the alkaloid was assigned as 1-hydroxy-3-methylcarbazole (**23**). Further structural support was

derived from a zinc dust distillation of 1-hydroxy-3-methylcarbazole (**23**), which led to 3-methylcarbazole (**2**) (see Scheme 2.2).

O-Demethylmurrayanine (**24**) was isolated from the combined extracts of the stem bark and roots of *C. anisata* (16). Preliminary color tests of the isolated fraction showed a phenolic hydroxy group. The UV spectrum (λ_{max} 226, 244, 255, 278, 291, 336, and 346 nm) gave evidence for a 3-formylcarbazole. The presence of a hydroxy group and a conjugated aldehyde group was additionally confirmed by the strong absorptions at 3460 and 1670 cm^{-1} in the IR spectrum. The ^{1}H-NMR spectrum showed the presence of deshielded *meta*-coupled (J=1.4 Hz) protons at δ 8.15 and 7.33 (H-4 and H-2), along with the proton of an aldehyde group (δ 9.89) and an *ortho*-disubstituted aromatic ring pattern for the unsubstituted C ring. The structural assignment was additionally supported by the ^{13}C-NMR spectrum and led to structure **24** for *O*-demethylmurrayanine.

In 1996, Wu *et al*. reported the isolation of clausine E (**25**) from the stem bark of *C. excavata* (46). One year later, Ito *et al.* reported the isolation of the same alkaloid from the same source and named it clauszoline-I (**25**) (47). This alkaloid showed inhibition of rabbit platelet aggregation and caused vasocontraction. The UV, IR, and ^{1}H-NMR spectra were similar to those of mukoeic acid (**10**) with respect to the position of substituents. The presence of a carbomethoxy group at C-3 was indicated by an IR band at 1703 cm^{-1}. Moreover, two significant mass fragments at m/z 210 (M^+−OMe) and 182 (M^+−COOMe) confirmed the presence of a carbomethoxy group. On the basis of these spectral data, structure **25** was assigned to clausine E (clauszoline-I) (Scheme 2.6).

Chowdhury *et al*. isolated 6,7-dimethoxy-1-hydroxy-3-methylcarbazole (**26**) from the leaves of *M. koenigii* (48). This alkaloid has shown high activity against both Gram-positive and Gram-negative bacteria and fungi. The UV spectrum (λ_{max} 235, 285, 305, and 330 nm) was characteristic of a carbazole nucleus. Besides a color test, the presence of a phenolic hydroxy group was confirmed by a strong absorption at 3305 cm^{-1} in the IR spectrum. The ^{1}H-NMR signal for the hydroxy proton was similar to that of 1-hydroxycarbazole. In carbazole alkaloids the protons at C-4 and C-5 appear at higher field. Therefore, the signals at δ 7.64 and 7.45 were assigned to

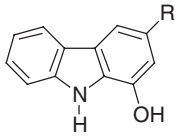

23 1-Hydroxy-3-methylcarbazole
R = Me

24 *O*-Demethylmurrayanine
R = CHO

25 Clausine E (Clauszoline-I)
R = COOMe

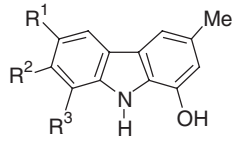

23 1-Hydroxy-3-methylcarbazole
R^1,R^2,R^3 = H

26 6,7-Dimethoxy-1-hydroxy-3-methylcarbazole
R^1,R^2 = OMe; R^3 = H

27 Murrayafoline B
R^1=H; R^2 = OMe, R^3 = prenyl

28 Clausenol
R^1 = OMe; R^2,R^3 = H

Scheme 2.6

H-4 and H-5. However, the proton at δ 7.45 is comparatively more shielded, suggesting the presence of a methoxy group at the *ortho* position. The singlet nature of this proton also suggests two methoxy groups at adjacent positions. The proton at δ 7.45 was thus assigned to H-5 and the *meta*-coupled doublet at δ 7.64 to H-4. Consequently, the methyl group could be attached to C-3. The singlet at δ 6.85 was assigned to H-8, and a *meta*-coupled doublet at δ 6.80 was assigned to H-2. All of the spectral evidence confirmed this alkaloid as 6,7-dimethoxy-1-hydroxy-3-methylcarbazole (**26**). Further structural support came from its ^{13}C-NMR spectrum, as well as its preparation as an advanced synthetic intermediate in the total synthesis of koeniginequinone B (**114**) (49) (see Section I.A.7, Scheme 2.21).

Murrayafoline-B (**27**) was obtained as a colorless syrup from the root bark of *M. euchrestifolia* (29). The UV spectrum (λ_{max} 230, 247, 255, 302, and 324 nm), and a bathochromic shift in alkali solution, indicated a phenolic carbazole. Additional support was derived from its IR data (ν_{max} 3600, 3475, 1620, 1595 cm^{-1}). The ^{1}H-NMR spectrum showed the presence of an aromatic methyl group (δ 2.42), an aromatic methoxy group (δ 3.90), and a prenyl side chain (δ 1.72, 1.88, 3.90, and 5.31). Moreover, it exhibited two broad singlets arising from H-2 (δ 6.56) and H-4 (δ 7.32), and two signals with *ortho*-coupling for H-5 (δ 7.72, J=9.0 Hz) and H-6 (δ 6.82, J=9.0 Hz). These spectral data led to structure **27** for murrayafoline-B, which was additionally confirmed by its photooxidation to murrayaquinone B (**108**) (29) (see Scheme 2.21).

Clausenol (**28**) was isolated from the alcoholic extract of the stem bark of *C. anisata* (40). The UV (λ_{max} 228, 253, 303, and 356 nm) and the IR spectrum [ν_{max} 3395 (NH, OH), 1620, 1580 (aromatic ring system), 975, 850, and 820 cm^{-1} (substituted aromatic ring)] suggested the presence of a carbazole ring. The ^{1}H-NMR spectrum was very similar to that of clausenine (**14**), except for the signal of a hydroxy group at δ 10.56 (exchangeable with deuterium oxide), which was present instead of a methoxy signal. This assignment was additionally supported by a color test, as well as the transformation of **28** into clausenine (**14**) by methylation with diazomethane (see Scheme 2.4). The spectral data and the chemical transformation confirmed structure **28** for clausenol. Additional structural support was derived from total synthesis using a Japp–Klingemann reaction and Fischer indolization (40) (Scheme 2.6).

In 1992, Wu *et al*. isolated two new 4-prenylcarbazole alkaloids, clausine D (**29**) and clausine F (**32**), from the stem bark of *C. excavata*, collected in Taiwan. These alkaloids showed inhibition of platelet aggregation (50). Four years later, clausine I (**30**) was isolated from the same natural source, along with clausine E (**25**). This alkaloid showed inhibition of rabbit platelet aggregation and caused vasocontraction (46). Clausine I (**30**) and clausine E (**25**) have the same molecular formula. However, clausine I (**30**) is regioisomeric to lansine (**69**) (see Scheme 2.14). In the same year, clausine J (**31a**) and clausine G (**33**) were isolated from the same natural source (51) (Scheme 2.7).

The UV spectrum (λ_{max} 225, 242, 253, 276, 289, and 351 nm) of clausine D (**29**) was similar to that of *O*-demethylmurrayanine (**24**), which also represents a 3-formyl-1-hydroxycarbazole framework. The presence of a hydroxy group and a conjugated aldehyde group was further supported by strong absorptions at 3380 and 1655 cm^{-1} in the IR spectrum. The ^{1}H-NMR spectrum was very similar to that of *O*-demethylmurrayanine, except for the presence of a prenyl group (δ 1.65,

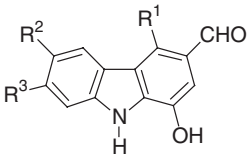

24 *O*-Demethylmurrayanine
$R^1,R^2,R^3 = H$

29 Clausine D
R^1=prenyl; $R^2,R^3 = H$

30 Clausine I
$R^1,R^3 = H$; $R^2 = OMe$

31a Clausine J
$R^1 = H$; $R^2 = OMe$; $R^3 = OH$

31b Clausine Z
$R^1,R^3 = H$; $R^2 = OH$

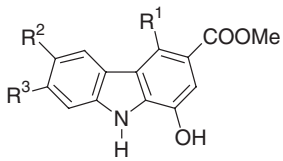

25 Clausine E (Clauszoline-I)
$R^1,R^2,R^3 = H$

32 Clausine F
R^1 = prenyl; $R^2,R^3 = H$

33 Clausine G
$R^1,R^3 = H$; $R^2 = OMe$

34 Clausine R
$R^1,R^2 = H$; $R^3 = OH$

35 Clausamine F
$R^1 = (E)HC{=}CHC(OH)Me_2$; $R^2,R^3 = H$

Scheme 2.7

1.88, 4.33, and 5.26) and the absence of a strongly deshielded proton at C-4. The presence of a prenyl group was further confirmed by the observation of a mass fragmentation ion at m/z 223 ($M^+-CH{=}CMe_2-H$) and by the ^{13}C-NMR signals at δ 27.2 (t), 123.9 (d), 132.7 (s), 18.3 (q), and 26.6 (q). The location of the prenyl side chain at C-4 was further explained by the downfield shift of the benzylic protons of the prenyl group at δ 4.33. These spectral data suggested structure **29** for clausine D, which was unambiguously confirmed by its NOESY and HMBC spectra (50).

The UV spectrum (λ_{max} 223, 242, 255, 278, 296, 341, and 353 nm) of clausine I (**30**) resembled that of *O*-demethylmurrayanine (**24**), which suggests a 1-hydroxy-3-formylcarbazole framework. The presence of a hydroxy group and a conjugated aldehyde group was further confirmed in the IR spectrum by strong absorptions at 3400 and 1640 cm^{-1}, respectively. The ^{1}H-NMR spectrum was similar to that of *O*-demethylmurrayanine, except for the presence of a methoxy group at δ 3.98 and the coupling pattern of the C-ring, which shows an *ortho*-coupled proton at C-8 (δ 7.56, d, J=9.0 Hz), an *ortho*- and *meta*-coupled proton at C-7 (δ 7.10, dd, J=9.0, 2.5 Hz), and a *meta*-coupled proton at C-5 (δ 7.78, d, J=2.5 Hz). The spectral data indicated that clausine I has a structure similar to *O*-demethylmurrayanine, but with a methoxy group at the 6-position. Based on this evidence, structure **30** was assigned to clausine I. This assignment was additionally supported by NOESY and HMBC experiments (46).

The UV spectrum (λ_{max} 235, 255, 289, 305, and 347 nm) of clausine J (**31a**) was similar to that of *O*-demethylmurrayanine (**24**) and thus indicated a 1-hydroxy-3-formylcarbazole skeleton. The presence of a hydroxy group and a conjugated aldehyde group was confirmed by strong absorptions at 3430 and 1650 cm^{-1} in the IR spectrum. The ^{1}H-NMR signal for the hydroxy proton of **31a** was similar to that of 1-hydroxycarbazole at δ 9.31. The signal for the 3-formyl proton at δ 9.94, along with signals for two *meta*-coupled protons, H-2 and H-4 (J=1.0 Hz) at δ 7.30 and 8.10

supported the 1-hydroxy-3-formylcarbazole partial structure. This assignment was strongly supported by NOE's of the signal for the formyl proton with the two protons H-2 and H-4. Based on this NOE experiment, the additional two singlets at δ 7.09 and 7.74 were assigned to H-8 and H-5, respectively. The signals for an additional hydroxy group at δ 7.80 and for a methoxy group at δ 3.98, along with the existence of an NOE between the methoxy group and H-5, indicated that the methoxy group is attached to C-6, while the second hydroxy group is at C-7. On the basis of these spectral data, structure **31a** was assigned to clausine J representing 1,7-dihydroxy-3-formyl-6-methoxycarbazole (51).

In 2005, Potterat *et al*. reported the isolation of clausine Z (**31b**) from the ethanolic extract of the stem and leaves of *C. excavata*. This alkaloid exhibits inhibitory activity against cyclin-dependent kinase 5 (CDK5) and has protective effects on cerebellar granule neurons *in vitro* (52). The UV spectrum (λ_{max} 223, 243, 256, 279, 299, 340, and 357 nm) was similar to that of clausine I (**30**), which indicates a 1-hydroxy-3-formylcarbazole framework. The presence of a hydroxy group and a conjugated aldehyde group was confirmed by strong absorptions at 3407 and 1649 cm^{-1} in the IR spectrum. The ^{1}H-NMR data were very similar to those of clausine I (**30**) however, instead of a methoxy signal an additional hydroxy signal was present at δ 9.07, which was exchangeable with deuterium oxide. The spectral data suggest that clausine Z has a 6-*O*-demethylclausine I structure and thus, structure **31b** was assigned to clausine Z. Additional support for this structural assignment derived from ROESY, HSQC, and HMBC experiments.

The UV spectrum (λ_{max} 244, 269, and 323 nm) of clausine F (**32**) resembled that of mukoeic acid (**10**) (see Scheme 2.4) indicating a 1-oxygenated-3-carboxycarbazole framework. The ^{1}H-NMR spectrum was very similar to that of clausine D (**29**), except for the presence of a carbomethoxy signal at δ 3.83 instead of an aldehyde proton at δ 10.34 as in clausine D. The presence of a carbomethoxy group was also supported in the IR spectrum by a band at 1670 cm^{-1} for an aromatic ester. The presence of a carbomethoxy group was further supported by the mass fragmentation ion at m/z 250 ($M^{+}-COOMe$). The ^{13}C-NMR spectrum exhibited signals for a carbonyl carbon and for a methoxy group at δ 168.85 and 51.53, respectively. Based on these spectral data and additionally supported by NOESY and HMBC experiments, structure **32** was assigned to clausine F (50).

The UV spectrum (λ_{max} 224, 272, 282, 316, and 353 nm) of clausine G (**33**) showed a strong similarity to that of clausine I (**30**). The aromatic region in the ^{1}H-NMR spectrum was also very similar to clausine I with respect to the chemical shifts and splitting pattern. The presence of a carbomethoxy group at C-3 was indicated by the signal of a methoxy group at δ 3.89 in the ^{1}H-NMR spectrum, a carbonyl signal at δ 168.0 in the ^{13}C-NMR spectrum, and a band at 1670 cm^{-1} in the IR spectrum. Based on these spectral data, clausine G was assigned as 3-carbomethoxy-1-hydroxy-6-methoxycarbazole (**33**). This structural assignment was additionally confirmed by NOE experiments and $^{1}H-^{13}C$ long-range correlations in the HMBC spectrum (51).

Clausine R (**34**) was isolated from the acetone extract of the root bark of *C. excavata* (43). The UV spectrum (λ_{max} 241, 282, and 320 nm) resembled that of mukoeic acid (**10**) (see Scheme 2.4), which indicated a 1-oxygenated 3-carboxycarbazole framework. The ^{1}H-NMR spectrum is similar to that of clausine Q (**19**) (see Scheme 2.5), except for the presence of a carbomethoxy signal at δ 3.86 instead of the aldehyde proton at δ 10.01 as in clausine Q. The presence of a carbomethoxy group

was also supported in the IR spectrum by a band at 1695 cm^{-1} for an aromatic ester, and by the mass fragmentation ion at m/z 198 (M^+−COOMe). The signal of the methoxy group at δ 3.86 showed no NOE with the signals of any other protons. The presence of an NOE between the signals for the hydroxy group at δ 8.89 and H-2 at δ 7.48 and NOEs between the signals for the second hydroxy group at δ 8.41 with H-6 at δ 6.79 and H-8 at δ 7.03 suggested one hydroxy group to be located at C-1 and the other at C-7. Based on these spectral data, structure **19** was assigned to clausine R.

Clausamine F (**35**) was isolated along with other clausamine derivatives (**20**–**22**) (see Scheme 2.5) from the acetone extract of branches of *C. anisata*. All these alkaloids showed antitumor-promoting activity against TPA-induced EBV-EA (Epstein-Barr virus early antigen) activation in Raji cells (44). The UV spectrum (λ_{max} 223, 242, 272, 324, and 341 nm) and the IR spectrum (ν_{max} 1508, 1558, 1699, 3300, and 3456 cm^{-1}) of clausamine F (**35**) were similar to that of clausamine E (**21**). These absorptions are characteristic of a 1-oxygenated 3-carbomethoxy carbazole framework. The ^{1}H-NMR spectrum also showed a signal pattern similar to that of clausamine E. However, instead of the singlet for the C-1 methoxy group, an additional broad D_2O exchangeable signal was apparent, which was assigned to the hydroxy group. The spectral data confirmed structure **35** for clausamine F (Scheme 2.7).

In 1996 Wu *et al.* isolated the optically active carbazole–pyranocoumarin dimer, carbazomarin-A (**36**) from the methanolic extract of the stem bark of *C. excavata*. This was the first carbon–carbon linked carbazole–pyranocoumarin dimer found in nature. Although its optical rotation value is known ([α] −27.03, *c* 0.0259, $CHCl_3$), its absolute configuration has not been assigned (53).

The UV spectrum (λ_{max} 215, 240, 253, 267, 326, 338, and 356 nm) and the IR spectrum (ν_{max} 1595, 1610, 1670, and 3400 cm^{-1}) of carbazomarin-A (**36**) clearly indicated a 1-oxygenated 3-carboxycarbazole alkaloid. The aromatic region in the ^{1}H-NMR spectrum shows four, mutually coupled protons at δ 7.26 (1*H*, m), 7.43 (2*H*, m), and 8.03 (1*H*, d, *J*=8.0 Hz), assigned to a non-substituted C-ring. The strongly deshielded singlet at δ 8.21 was assigned to C-4 of the substituted A-ring. The ^{1}H−^{13}C long-range correlation between the carbonyl carbon (δ 173.3) and H-4 (δ 8.21) suggested that the carbomethoxy substituent is attached at C-3. The other signals in the olefinic and aromatic region were found to be very similar to those of nordentatin, a 8′-dimethylallyl-5′-hydroxy-dimethylpyranocoumarin nucleus (54). In contrast to nordentatin, one double bond of the pyran ring was reduced to a single bond, which presented a –CH_2CH– group as double doublet (dd) at δ 2.11, 2.25, and 5.17. The carbon–carbon linkage between C-2 and C-4″ of the carbazole and the dihydropyranocoumarin framework was established based on NOESY and ^{1}H−^{13}C long-range correlations in the HMBC spectrum. The mass fragmentation ions at m/z 312 (M^+−[$C_{14}H_{11}NO_3$] carbazole nucleus) and at 241 (M^+−[$C_{19}H_{22}O_4$] dihydropyranocoumarin−H) provided additional support for the carbazole–pyranocoumarin dimer. From these spectral data, structure **36** was assigned to carbazomarin-A (53) (Scheme 2.8).

4 2-Oxygenated Tricyclic Carbazole Alkaloids

Among the large number of carbazole alkaloids that have been isolated from *M. koenigii* are also many 2-oxygenated derivatives. In 1985, Bhattacharyya *et al.* isolated 2-methoxy-3-methylcarbazole (**37**) from the petroleum ether extract of the seeds of *M. koenigii* (55). The UV spectrum (λ_{max} 235, 255, 300, and 328 nm) and the IR

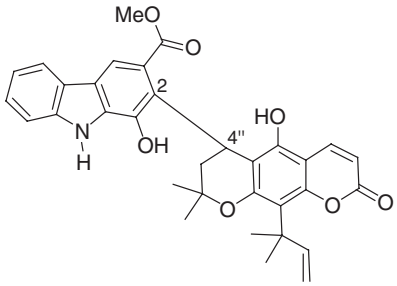

36 Carbazomarin-A

Scheme 2.8

spectrum (ν_{max} 750, 820, 1208, 1600, and 1640 cm^{-1}) suggested a carbazole skeleton. In the ^{1}H-NMR spectrum, a complex multiplet of four, mutually coupled protons at δ 7.20−7.40 indicated a non-substituted C-ring. In addition, the signals for an aromatic methoxy group (δ 3.77), an aromatic methyl group (δ 2.35), and H-4 (δ 7.50) and H-1 (δ 6.95) confirmed 2-methoxy-3-methylcarbazole (**37**) as the structure. Further support was obtained by transformation of **37** into known derivatives (14,56).

In 1990, Lange *et al.* isolated *O*-methylmukonal (**38**) from the roots of *Murraya siamensis* (57). Two years later, Bhattacharyya *et al.* reported the isolation of the same alkaloid from the roots of a different natural source, *G. pentaphylla*, and named it glycosinine (**38**) (24). More recently, Kongkathip *et al.* reported the isolation of *O*-methylmukonal (**38**) from the rhizomes and the roots of another natural source, *C. excavata* (58). Moreover, they reported for the first time that **38** showed anti-HIV-1 activity.

The UV and IR spectral data of *O*-methylmukonal (**38**) indicated the presence of a 3-formylcarbazole skeleton. The ^{1}H-NMR spectrum showed signals at δ 8.88, 10.49, and 3.99 for the NH, CHO, and aromatic methoxy groups, respectively. In addition, four aromatic protons at δ 7.40 (d, J=8.0 Hz), 7.38 (t, J=8.0 Hz), 7.25 (t, J=8.0 Hz), and 8.00 (d, J=8.0 Hz) for H-8, H-7, H-6, and H-5, respectively, confirmed that the C-ring was unsubstituted. The deshielded singlet at δ 8.56 was assigned to H-4 and the singlet at δ 6.88 was assigned to H-1. On the basis of this spectroscopic evidence, structure **38** was proposed for *O*-methylmukonal (glycosinine) (57). This assignment was additionally supported by the ^{13}C-NMR data and by oxidation of 2-methoxy-3-methylcarbazole (**37**) with DDQ to *O*-methylmukonal (**38**) (24).

In 1993, Wu *et al.* reported the isolation of clausine L (*O*-methylmukonidine) (**39**) from the leaves of *C. excavata* (59). One year later, Bhattacharyya *et al.* isolated the same alkaloid from the stem bark of a different natural source, *M. koenigii*, and named it methyl 2-methoxycarbazole-3-carboxylate (**39**) (45). The UV spectrum (λ_{max} 235, 242, 269, 281, 319, and 333 nm) showed the presence of a 2-oxygenated-3-carbonylcarbazole nucleus. The IR spectrum indicated an NH group (3350 cm^{-1}), a COOMe group (1700 cm^{-1}), and an aromatic system (1635, 1605 cm^{-1}). In the ^{1}H-NMR spectrum, four mutually coupled aromatic protons at δ 8.07, 7.48, 7.34, and 7.19 showed that the C-ring was lacking substituents. The presence of a deshielded singlet at δ 8.52, which was assigned to a proton at C-4 *ortho* to the carbomethoxy group, in addition to a further sharp singlet at δ 7.14 for H-1, established the position

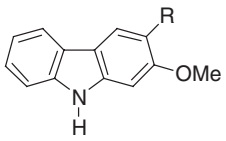

37 2-Methoxy-3-methylcarbazole
R = Me

38 *O*-Methylmukonal (Glycosinine)
R = CHO

39 Clausine L (*O*-Methylmukonidine, Methyl 2-methoxycarbazole-3-carboxylate)
R = COOMe

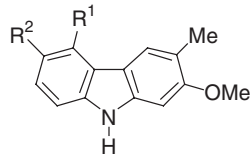

37 2-Methoxy-3-methylcarbazole
R^1,R^2 = H

40 Glycozolidine
R^1 = H; R^2 = OMe

41 Glycozolidol
R^1 = H; R^2 = OH

42 Glybomine A
R^1 = OMe; R^2 = H

Scheme 2.9

of the aromatic methoxy group at C-2. On the basis of these spectroscopic data, structure **39** was assigned to clausine L. Moreover, this assignment was supported by the ^{13}C-NMR spectrum and NOE experiments (Scheme 2.9).

In 1966, Chakraborty *et al.* reported the isolation of glycozolidine (**40**) from the root bark of *G. pentaphylla* (60,61). In 1999, glycozolidine (**40**) was also isolated by Chakravarty *et al.* from the roots of a different *Glycosmis* species, *Glycosmis arborea* (62). The IR spectrum of **40** exhibited bands at ν_{max} 3450 (NH), 1625 (aromatic system), 1208 (aromatic methyl ether), 813 cm^{-1} (substituted aromatic ring). The IR data, in agreement with the UV spectrum (λ_{max} 233, 237, 260, and 309 nm), indicated the presence of a carbazole ring system. The ^{1}H-NMR spectrum showed signals of an aromatic methyl group (δ 2.35), two aromatic methoxy groups (δ 3.77 and 3.90) and two, non-*ortho*-coupled protons, H-4 and H-5, at δ 7.17 and 7.45, respectively. In addition, two aromatic protons at δ 6.97 and 7.02, along with a shielded aromatic proton at δ 6.52, were shown. The ^{1}H-NMR signals and their coupling pattern suggested that glycozolidine has substituents at C-2, C-3, and C-6. The spectroscopic assignment was additionally supported by the following chemical transformations of glycozolidine: first, zinc dust distillation to 3-methylcarbazole; second, heating with solid potassium hydroxide at 270–300°C to afford 2,6-dihydroxy-3-methylcarbazole; and third, chemoselective demethylation with hydrogen bromide (48%) to 6-hydroxy-2-methoxy-3-methylcarbazole. Raney-nickel reduction of 6-hydroxy-2-methoxy-3-methylcarbazole *via* the corresponding tosylate afforded 2-methoxy-3-methylcarbazole. Based on these degradation studies and the spectral data, structure **40** was assigned to glycozolidine (61,62). This structural assignment was confirmed by total synthesis of the natural product (63,64).

Two decades later, Bhattacharyya *et al.* reported the isolation of glycozolidol (**41**) from the roots of *G. pentaphylla* (65). This alkaloid attracted interest due to its antibacterial activity against Gram-positive and Gram-negative bacteria. The UV spectrum (λ_{max} 232, 260, and 305 nm) showed the presence of a carbazole nucleus. The IR spectrum exhibited bands at 3500 (OH), 3440 (NH), 1625, 1600 (aromatic system), 1380 (C-methyl), 1208 (aromatic ether), and 850 cm^{-1} (substituted aromatic system). In the ^{1}H-NMR spectrum, singlets for an aromatic methyl group (δ 2.38), an

aromatic methoxy group (δ 3.7), and H-1 and H-4 at δ 6.92 and 7.45 were visible and indicated substituents at C-2 and C-3. The signal for H-5 appeared as a *meta*-coupled doublet at δ 7.2 (J=2.0 Hz), H-7 as an *ortho*- and *meta*-coupled doublet of doublets at δ 6.75 (J=8.0, 2.0 Hz), and H-8 as an *ortho*-coupled doublet at δ 7.08 (J=8.0 Hz). Thus, a 6-substitution of the carbazole was suggested. In addition to these peaks, two broad singlets at δ 10.8 and 8.0, both exchangeable with D_2O, confirmed the presence of hydroxy and NH protons. The resonance of the hydroxy proton of glycozolidol was similar to that of 6-hydroxy-3-methylcarbazole (66,67), a fact which supports a 6-hydroxycarbazole. On the basis of these spectroscopic data, structure **41** was assigned to glycozolidol. Additional support for this assignment was derived from the methylation of glycozolidol (**41**) with diazomethane to glycozolidine (**40**) (60–62).

In 2004, Itoigawa and Furukawa *et al.* reported the isolation of glybomine A (**42**) from the stem of *G. arborea* collected at Mymensing in Dhaka, Bangladesh (68). Glybomine A was the first example of a 2,5-dioxygenated carbazole alkaloid from a natural source and showed antitumor-promoting activity against (12-*O*-tetradecanoylphorbol-13-acetate) TPA-induced EBV-EA activation. The UV spectrum (λ_{max} 239, 294, 330, and 316 nm) and the IR absorption at ν_{max} 3475 cm^{-1} for a NH, confirmed the carbazole framework. The ^{1}H-NMR spectrum exhibited signals for an aromatic methyl group (δ 2.29), two aromatic methoxy groups (δ 3.87, 4.03), and an NH group (δ 10.09). Moreover, in the aromatic region, two singlets at δ 6.99 and 7.94 and three signals for contiguous protons at δ 6.65, 7.02, and 7.18 were observed. The spectroscopic data, supported by NOE experiments, suggested the two methoxy groups to be at positions 2 and 5, and the methyl group at position 3 on the carbazole system. Therefore, structure **42** was assigned to glybomine A (Scheme 2.9).

Furukawa *et al.* isolated isomurrayafoline B (**43**) (69) and murrayaline A (**44**) (38,70) from the root bark of *M. euchrestifolia* collected in Taiwan. The UV spectrum [λ_{max} 213, 237, 264, 310, and 330 (sh) nm] of isomurrayafoline B (**43**) was characteristic of a carbazole nucleus. The ^{1}H-NMR spectrum showed the presence of an aromatic methyl group (δ 2.38), an aromatic methoxy group (δ 3.90), a prenyl side chain (δ 1.74, 1.88, 3.60, and 5.30), and two broad singlets at δ 4.74 and 7.70, exchangeable with D_2O, for OH and NH. In the aromatic region, two broad singlets arising from H-1 (δ 6.82) and H-4 (δ 7.67), and *ortho*-coupled proton signals (J=8.0 Hz) for H-5 (δ 7.70) and H-6 (δ 6.82) suggested C-2, C-3, C-7, and C-8 as the positions of the substituents. In NOE experiments, irradiation at the signal for the methyl group resulted in an enhancement of the signal for H-4, irradiation at the methoxy group led to an enhancement of H-6, and irradiation at the signal for the benzylic methylene protons of the prenyl moiety led to no signal enhancement. Thus, structure **43** was assigned to isomurrayafoline B (69).

The UV spectrum [λ_{max} 226, 260 (sh), 304, and 383 nm] and the IR spectrum (ν_{max} 1580, 1590, 1600, 1630, 1650, and 3370 cm^{-1}) of murrayaline A (**44**) indicated a carbazole derivative with a formyl group (1650 cm^{-1}). The ^{1}H-NMR spectrum confirmed this assignment from the signals for one aromatic methyl (δ 2.35) and two aromatic methoxy groups (δ 3.90, 3.98), as well as the signals of four aromatic protons at δ 6.91 (s), 7.95 (s), 6.77 (d, J=9.0 Hz), and 8.02 (d, J=9.0 Hz). In NOE experiments, irradiation at the signal for the aromatic methyl group led to an enhancement of the signal for H-4 and irradiation at the signals for the methoxy groups resulted in an enhancement of the signals for H-1 and H-6. These NOEs indicated the positions 2 and 7 for the two methoxy groups and position 3 for the

methyl group. Therefore, murrayaline A was formulated as 2,7-dimethoxy-8-formyl-3-methylcarbazole (**44**). This structural assignment was confirmed by synthesis (38).

Reisch *et al.* isolated murrayanol (**45**) from the fruits of *M. koenigii* (71). The UV spectrum [λ_{max} 208, 236, 262, 296 (sh), 316 (sh), and 328 (sh) nm] and the IR spectrum (ν_{max} 1470, 1540, 1610, 1650, 2960, 3440, and 3560 cm^{-1}) suggested a phenolic carbazole derivative. The ^{1}H-NMR spectrum showed characteristic signals of a geranyl side chain, signals for the OH and NH protons at δ 4.76 and 7.73 (exchangeable with D_2O), a methyl group at C-3 (δ 2.38), and a methoxy group at C-7 (δ 3.91). The presence of a geranyl group was additionally confirmed by the mass fragmentation ion at m/z 240 ($M^+ - CH{=}CMeCH_2CH_2CH{=}CMe_2$). On cyclization, murrayanol provided 9-methoxymahanimbicine (for mahanimbicine (**147**), see Scheme 2.28). This transformation demonstrated the similarity of their substitution pattern. Based on the spectroscopic and chemical evidence, structure **45** was assigned to murrayanol (Scheme 2.10).

Clausine P (**46**) was isolated from the acetone extract of the root bark of *C. excavata* (43). The UV spectrum [λ_{max} 212, 236, 251 (sh), 261 (sh), 290 (sh), 317, and 330 nm] and the IR spectrum (ν_{max} 1635 and 3400 cm^{-1}) were characteristic of a carbazole derivative. The ^{1}H-NMR spectrum exhibited a signal for a methyl group (δ 2.29) at C-3 and two methoxy groups (δ 3.89, 3.96) at C-2 and C-8. In the aromatic region, three, mutually *ortho*-coupled (J=7.8 Hz) protons at δ 6.85, 7.03, and 7.54 were assigned to H-7, H-6, and H-5, respectively. Two singlets at δ 7.06 and 7.76 were assigned to H-1 and H-4. These assignments for the ^{1}H-NMR signals were additionally supported by NOEs between 3-Me (δ 2.29) and H-4 (δ 7.76), 2-OMe (δ 3.89) and H-1 (δ 7.06), and 8-OMe (δ 3.96) and H-7 (δ 6.85). The spectroscopic data confirmed that **46** is the structure of clausine P.

Bhattacharyya and Chowdhury reported the isolation of glycozolidal (**47**) from the roots of *G. pentaphylla* (72). The UV and the IR data of glycozolidal were characteristic of a 3-formylcarbazole. The ^{1}H-NMR spectrum showed signals for a formyl group (δ 9.9), two aromatic methoxy groups (δ 3.7 and 3.9), a proton at C-4 (δ 8.4, deshielded due to the formyl group at C-3), and a *meta*-coupled (J=2.0 Hz)

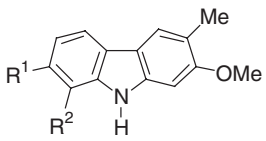

43 Isomurrayafoline B
R^1 = OMe; R^2 = prenyl

44 Murrayaline A
R^1 = OMe; R^2 = CHO

45 Murrayanol
R^1 = OH; R^2 = geranyl

46 Clausine P
R^1 = H; R^2 = OMe

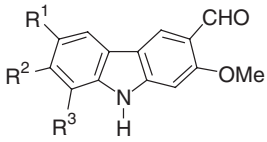

38 *O*-Methylmukonal (Glycosinine)
R^1,R^2,R^3 = H

47 Glycozolidal
R^1 = OMe, R^2, R^3 = H

48 7-Methoxy-*O*-methylmukonal
(3-Formyl-2,7-dimethoxycarbazole)
R^1,R^3 = H; R^2 = OMe

49 Atanisatin
R^1,R^2 = H; R^3 = prenyl

Scheme 2.10

proton at C-5 (δ 7.6), indicating a substitution at C-6. The proton at C-4 showed neither an *ortho*- nor a *meta*-coupling, which indicated the presence of a substituent at C-2. Following all these spectral observations, structure **47** was formulated for glycozolidal. This assignment was confirmed by synthesis of glycozolidal (**47**) from glycozolidine (**40**) (see Scheme 2.9) using DDQ oxidation (72).

Lange *et al.* isolated 7-methoxy-*O*-methylmukonal (3) (3-formyl-2,7-dimethoxy-carbazole) (**48**) from the roots of *M. siamensis* (57). More recently, Kongkathip *et al.* described the isolation of the same natural product from the rhizomes and roots of *C. excavata* (58). This group also reported for the first time the anti-HIV-1 activity of 7-methoxy-*O*-methylmukonal (**48**). The UV and IR data indicated a 3-formylcarbazole derivative. The ^{1}H-NMR spectral data were similar to those of *O*-methylmukonal (**38**) (see Scheme 2.9), except for the presence of an additional methoxy group at δ 3.90. The signals for H-5 at δ 7.87 with an *ortho*-coupling (J=8.3 Hz), and for H-6 at δ 6.88 with an *ortho*- and a *meta*-coupling (J=8.3, 2.2 Hz), suggested C-7 as the position of this methoxy group. Based on the spectroscopic evidence and additional support by the ^{13}C-NMR data, structure **48** was assigned to 7-methoxy-*O*-methylmukonal. Okorie reported the isolation of atanisatin (**49**) from the stem of *C. anisata* (73) (Scheme 2.10).

In 1996, Wu *et al.* isolated clausine H (**50**) and clausine K (**51**) from the stem bark of *C. excavata* (46). These alkaloids showed an inhibition of rabbit platelet aggregation and caused vasocontraction. Later, Ito *et al.* isolated clausine H and clausine K from the same natural source and named them clauszoline C (**50**) (74) and clauszoline-J (**51**) (47). More recently, Kongkathip *et al.* isolated clauszoline-J (**51**) from the rhizomes and roots of the same natural source, *C. excavata*, and described its anti-HIV-1 activity (58).

The UV and IR data of clausine H (clauszoline-C) (**50**) indicated the presence of a carbazole nucleus. The ^{1}H-NMR spectrum showed signals of three methoxy groups at δ 3.82, 3.86, and 3.89. In the aromatic region, a deshielded singlet for H-4 at δ 8.40 indicated the presence of a carbomethoxy group at C-3 and a methoxy group at C-2. The H-5 at δ 7.94 with an *ortho*-coupling (J=7.7 Hz), H-6 at δ 6.82 with an *ortho*- and a *meta*-coupling (J=7.7, 2.4 Hz) and H-8 at δ 7.02 with a *meta*-coupling (J=2.4 Hz) indicated the presence of a methoxy group at C-7. The singlet at δ 7.10 for H-1 led to the proposed structure with a second methoxy group at C-2. Moreover, a characteristic IR band at ν_{max} 1710 cm^{-1}, two significant mass fragments at m/z 254 (M^+-OMe) and 223 (M^+-COOMe$-$H), and the ^{13}C-NMR signals at δ 167.41 and 51.62 suggested the presence of a carbomethoxy substituent at the carbazole framework. Based on the spectroscopic data and additional support from NOE experiments, structure **50** was assigned to clausine H (clauszoline-C) (Scheme 2.11).

The UV, IR, and ^{1}H-NMR spectra of clausine K (clauszoline-J) (**51**) were almost identical to those of clausine H (clauszoline-C) (**50**). The most significant difference between their spectra was the presence of IR bands at ν_{max} 3315 (br) and 1666 cm^{-1} and the absence of one methoxy group resonance in the ^{1}H-NMR spectrum, which indicated the presence of a carboxy group instead of a carbomethoxy group at C-3 of the carbazole framework. This conclusion was supported by two characteristic mass fragments at m/z 254 (M^+-OH) and 226 (M^+-COOH). The spectroscopic evidence combined with NOE experiments led to structure **51** for clausine K (clauszoline-J). This assignment was confirmed by methylation of **51** with diazomethane to afford clausine H (**50**) (46) (Scheme 2.11).

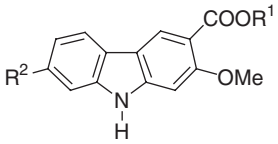

39 Clausine L (*O*-Methylmukonidine, Methyl 2-methoxycarbazole-3-carboxylate)
R^1 = Me; R^2 = H

50 Clausine H (Clauszoline-C)
R^1 = Me; R^2 = OMe

51 Clausine K (Clauszoline-J)
R^1 = H; R^2 = OMe

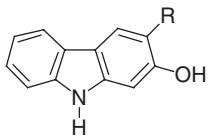

52 2-Hydroxy-3-methylcarbazole
R = Me

53 Mukonal
R = CHO

54 Mukonidine
R = COOMe

Scheme 2.11

In the mid-1980s, Bhattacharyya and Chakraborty isolated 2-hydroxy-3-methylcarbazole (**52**) (75) and mukonal (**53**) (76) from the roots and stem bark of *M. koenigii*. The UV and IR spectra of 2-hydroxy-3-methylcarbazole (**52**) confirmed the presence of an aromatic carbazole system. The ^{1}H-NMR spectrum showed an aromatic methyl group at δ 2.33 and two proton signals at δ 8.1 and 8.2 for OH and NH, respectively, both of which were exchangeable with D_2O. In the aromatic region of the ^{1}H-NMR spectrum, a complex 4-proton-multiplet at δ 7.1−8.0 indicated a non-substituted C-ring of the carbazole nucleus. The shielded singlet at δ 7.0 and the deshielded singlet at δ 7.68, assigned to H-1 and H-4, respectively, indicated the presence of a methyl group at C-3 and a hydroxy group at C-2. On zinc dust distillation, 2-hydroxy-3-methylcarbazole afforded 3-methylcarbazole, indicating the presence of a methyl group at C-3. Based on the spectroscopic data and chemical transformations, structure **52** was assigned as 2-hydroxy-3-methylcarbazole (75). Further confirmation for this structural assignment was derived from direct comparison with an authentic sample of synthetic material (56).

The UV spectrum (λ_{max} 234, 247, 278, 297, 316, and 342 nm) and the IR spectrum [ν_{max} 1590, 1610 (aromatic system), 1640 (chelated aldehyde), and 3380 (OH, NH) cm^{-1}] of mukonal (**53**) are characteristic of a 3-formylcarbazole derivative. This conclusion was supported by the ^{1}H-NMR spectrum which showed a singlet for an aldehyde proton at δ 10.16 and two signals at δ 11.0 and 11.76 for NH and OH, both exchangeable with D_2O. In the aromatic region, a complex, four-proton-multiplet at δ 7.3−8.0 suggested that ring C of the carbazole nucleus is unsubstituted. The deshielded singlet at δ 8.4 was assigned to H-4, which is *ortho* to the aldehyde group. The position of the hydroxy group was assigned at C-2, because of its chelation to the formyl group, and based on the fact that H-4 exhibited no *meta*-coupling. The shielded singlet of H-1 at δ 7.0 supported this assignment. On decarbonylation with Pd/C, mukonal provided 2-hydroxycarbazole, confirming the position of the hydroxy group at C-2. Based on the spectroscopic and chemical support, structure **53** was assigned to mukonal (76). A direct comparison with an authentic sample of synthetic material confirmed this assignment (77).

In 1978, Chakraborty *et al.* reported the isolation of mukonidine (**54**) from the stem bark of *M. koenigii* (78). In their investigation of the root bark of *C. excavata* in

1993, Wu *et al.* isolated mukonidine (**54**) along with its *O*-methyl derivative, clausine L (**39**) (see Scheme 2.9) (59). However, the spectroscopic and physical data of Chakraborty's *O*-methylmukonidine were not identical with those of clausine L (59,78). Based on the agreement of the data of synthetic mukonidine with those of Wu's mukonidine (59), it was concluded that Chakraborty's mukonidine (78) may have a different structure (79–81). The UV, IR, and ^{1}H-NMR spectra of mukonidine (**54**) were very similar to those of clausine L (**39**) (see Scheme 2.9), except for the presence of a signal for an aromatic hydroxy group at δ 11.07 instead of an aromatic methoxy group. Based on the spectroscopic evidence Wu *et al.* assigned structure **54** to mukonidine (59). Four years later, this structural assignment was strongly supported by comparison with the spectroscopic data of synthetic mukonidine (80,81) (Scheme 2.11).

In 1993, Furukawa *et al.* isolated mukoenine-A (**55**) from the root and stem bark of *M. koenigii* (82). One year later, Reisch *et al.* reported the isolation of the same natural product from the same natural source and named it girinimbilol (83). The UV spectrum [λ_{max} 217, 238, 260 (sh), 288, 300, 321 (sh), 333, and 356 nm] of mukoenine-A (**55**) exhibited the typical absorption of a 2-oxygenated carbazole derivative. The ^{1}H-NMR spectrum showed the signal for an aromatic methyl group at δ 2.40, a broad singlet at δ 7.84 for the NH group, and a further singlet at δ 5.18 for the OH group. The presence of a prenyl group was indicated by the signals at δ 1.79 and 1.91 (each singlets for three protons), 3.62 (2*H*, d, *J*=7.1 Hz), and 5.37 (1*H*, t, *J*=7.1 Hz). Further support for the prenyl group was derived from the characteristic mass fragmentation ion at *m*/*z* 209 ($M^+-CH=CMe_2-H$). In the aromatic region of the ^{1}H-NMR spectrum, a four-proton signal including a low-field H-5 at δ 7.93 (1*H*, d, *J*=7.7 Hz), suggested an unsubstituted carbazole C-ring. The high-field singlet at δ 7.68 was assigned to H-4. NOE experiments were used to identify the positions of the methyl, hydroxy, and prenyl groups at C-3, C-2, and C-1, respectively. Based on this spectroscopic evidence, structure **55** was assigned to mukoenine-A (Scheme 2.12).

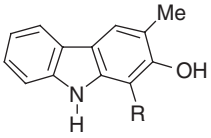

52 2-Hydroxy-3-methylcarbazole
R = H

55 Mukoenine-A (Girinimbilol)
R = prenyl

56 Mahanimbinol (Mahanimbilol)
R = geranyl

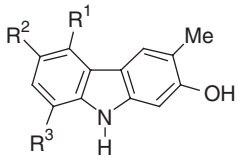

57 Carbalexin A
R^1 = OMe; R^2,R^3 = H

58 Carbalexin B
R^1,R^2 = H; R^3 = OMe

59 Carbalexin C
R^1,R^3 = H; R^2 = OMe

60 Glybomine B
R^1 = prenyl; R^2 = OMe; R^3 = H

61 Glybomine C
R^1 = prenyl; R^2 = OH; R^3 = H

Scheme 2.12

In 1980, Rama Rao *et al.* isolated mahanimbinol (**56**) from the stem wood of *M. koenigii* (84). Fourteen years later, Reisch *et al.* reported the isolation of the same natural product from the same natural source and named it mahanimbilol (83). In 2001, Boyd *et al.* also reported the isolation of mahanimbilol from the organic extract of *M. siamensis* (85).

The UV, IR, and ^{1}H-NMR spectra of mahanimbinol (**56**) are very similar to those of mukoenine-A (**55**), with the exception of differences in the signals resulting from the side chain at C-1. The ^{1}H-NMR spectrum showed three signals for methyl groups at δ 1.58, 1.65, and 1.86, a 4-proton-multiplet at δ 2.03−2.14, a doublet for the benzylic methylene group at δ 3.56, and two multiplets for vinyl protons at δ 5.04 and 5.34. These data indicate that **56** has a geranyl group at C-1 instead of the prenyl group of **55**. Further support for this conclusion was derived from the mass fragmentation ion at m/z 210 (M^+−CH═CMeCH$_2$CH$_2$CH═CMe$_2$). The structural similarity of mahanimbinol (**56**) and mukoenine-A (**55**) was additionally confirmed by the ^{13}C-NMR chemical shifts. Based on the spectroscopic data, mahanimbinol was structurally assigned as **56** (Scheme 2.12).

In 2001, Greger *et al.* isolated the stress-induced carbazole phytoalexins carbalexin A (**57**), B (**58**), and C (**59**) from the leaves of *Glycosmis parviflora*. These carbazole alkaloids showed strong antifungal activity in bioautographic tests on TLC plates with *Cladosporium herbarum* (86).

The UV spectrum (λ_{max} 239, 293, 317, and 330 nm) of carbalexin A (**57**) showed the typical absorptions of a 2-hydroxy-3-methylcarbazole framework. The ^{1}H-NMR spectrum exhibited signals of an aromatic methyl group at δ 2.41, an aromatic methoxy group at δ 4.07, and an NH group at δ 7.89. Moreover, the aromatic region showed a shielded singlet at δ 6.82 for H-1, a deshielded singlet at δ 8.02 for H-4, and three contiguous, mutually *ortho*-coupled (J=8.0 Hz) protons at δ 6.65, 7.25, and 6.98 for H-6, H-7, and H-8, respectively. Based on these spectroscopic data, the following positions were assigned to the substituents: C-2 for the hydroxy group, C-3 for the methyl group, and C-5 for the methoxy group. Therefore, structure **57** was assigned to carbalexin A (Scheme 2.12).

The UV and the IR spectrum of carbalexin B (**58**) were very similar to those of carbalexin A, indicating the presence of a 2-hydroxy-3-methylcarbazole skeleton also for carbalexin B. The ^{1}H-NMR spectrum showed the presence of singlets for an aromatic methyl group at δ 2.40 and an aromatic methoxy group at δ 4.00, and a broad singlet for an NH group at δ 8.04. In the aromatic region, the two singlets for H-1 at δ 6.87 and H-4 at δ 7.76 suggested a similar substitution pattern at the A-ring of the carbazole framework of **58** as found for carbalexin A (**57**). The three, mutually *ortho*-coupled (J=8.0 Hz) protons at δ 6.83, 7.11, and 7.55 were assigned to H-7, H-6, and H-5, respectively, and indicated that the position of the methoxy group was at C-8. Based on this spectroscopic support, structure **58** was assigned to carbalexin B (Scheme 2.12).

The UV spectrum [λ_{max} 231, 263 (sh), and 310 nm] of carbalexin C (**59**) indicated a 2-hydroxy-3-methylcarbazole. The ^{1}H-NMR spectrum showed signals for an aromatic methyl group (δ 2.40), an aromatic methoxy group (δ 3.91), a shielded singlet for H-1 (δ 6.52), and two, non-*ortho*-coupled proton signals for H-4 and H-5 (δ 7.74 and 7.44). The *ortho*-coupling (J=8.6 Hz) of the aromatic protons H-7 at δ 6.96 and H-8 at δ 7.25, and the *meta*-coupling (J=2.5 Hz) between H-5 at δ 7.44 and H-7 at δ 6.96, indicated that the methoxy group is located at C-6. Based on these spectral data, structure **59** was assigned to carbalexin C (Scheme 2.12).

In 2004, Furukawa and co-workers reported the isolation of glybomine B (**60**) and glybomine C (**61**), along with glybomine A (**42**) (see Scheme 2.9), from the stem of *G. arborea* (68). This group of carbazole alkaloids showed antitumor-promoting activity against (12-*O*-tetradecanoylphorbol-13-acetate) TPA-induced EBV-EA activation.

The UV spectrum [λ_{max} 217, 263 (sh), 307, 336 (sh), and 339 nm] of glybomine B (**60**) indicated a 2,6-dioxygenated-3-methylcarbazole derivative. The ^{1}H-NMR spectrum exhibited signals for an aromatic methyl group (δ 2.39), an aromatic methoxy group (δ 3.87), a prenyl side chain (δ 1.70, 1.93, 3.92, 5.32), and two broad singlets, which were exchangeable with D_2O, for the OH and the NH group (δ 4.85 and 7.68). In the aromatic region, H-1 and H-4 appeared as singlets at δ 6.77 and 7.82, indicating the presence of substituents at C-2 and C-3. The two doublets for H-7 and H-8 at δ 6.99 and 7.13 with an *ortho*-coupling (J=8.4 Hz) demonstrated that two further substituents were present at C-5 and C-6. The individual positions of the hydroxy group at C-2, the methyl group at C-3, the prenyl group at C-5, and the methoxy group at C-6 were confirmed by NOE experiments. These spectroscopic data, supported by the results of HMBC correlations, led to the assignment of structure **60** for glybomine B. The UV and the IR spectrum of glybomine C (**61**) were similar to those of glybomine B (**60**). In the ^{1}H-NMR spectrum of glybomine C (**61**), the chemical shifts of the signals and their coupling pattern were to a large extent in agreement with that of glybomine B (**60**), except for the signal of the methoxy group of glybomine B (δ 3.87) which was not present. Based on the spectroscopic data and supported by the results of NOE experiments and HMBC correlations, structure **61** was assigned for glybomine C (Scheme 2.12).

In 1991, Furukawa *et al.* described the isolation and structural elucidation of euchrestine-C (**62**) (87) and of racemic euchrestine-E (**63**) (70) from the stem bark of *M. euchrestifolia*. The UV spectrum (λ_{max} 212, 237, 266, 306, 320, and 329 nm) of euchrestine-C (**62**) showed the typical absorptions for a 2,7-dioxygenated carbazole skeleton. Further support for this assignment of the framework derived from its IR spectrum (ν_{max} 3380, 3470, and 3600 cm^{-1}). The ^{1}H-NMR spectrum exhibited the signals characteristic of a geranyl side chain and of an aromatic methyl group (δ 2.38). The geranyl group was additionally confirmed by the presence of the characteristic mass fragmentation ion at m/z 226 ($M^+-CH=CMeCH_2$ $CH_2CH=CMe_2$). In the aromatic region, H-1 and H-4 appeared as singlets at δ 6.81 and 7.65, respectively, suggesting substitution at C-2 and C-3. The two doublets for H-6 and H-5 at δ 6.70 and 7.63 with an *ortho*-coupling (J=8.4 Hz) indicated further substituents at C-7 and C-8. Based on this spectroscopic evidence, structure **62** was assigned to euchrestine-C (Scheme 2.13).

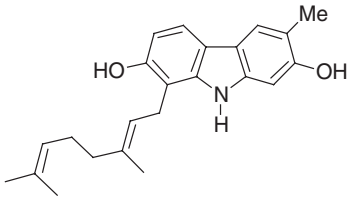

62 Euchrestine-C

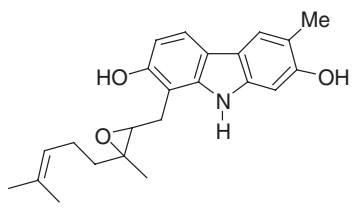

63 Euchrestine-E

Scheme 2.13

The UV and IR spectra of euchrestine-E (**63**) were similar to those of euchrestine-C (**62**). The pattern of signals in the ^{1}H-NMR spectrum resembled that of euchrestine-C, except for the signals of some protons of the side chain. The characteristic ^{1}H-NMR data and the mass fragment ion at m/z 226 (resulting from the cleavage of a benzylic bond in the molecular ion) indicated the presence of a geranyl side chain with an oxirane ring. Based on the spectroscopic data and additional support by two-dimensional ^{1}H−^{1}H correlation spectroscopy (^{1}H−^{1}H COSY), structure **63** was assigned to euchrestine-E (Scheme 2.13).

In 1991, Furukawa *et al.* reported the isolation of murrayaline-B (**64**) (70), euchrestine-A (**65**), euchrestine-B (**66**), and euchrestine-D (**67**) (87) from the stem bark of *M. euchrestifolia*. Ten years later, Nakatani *et al.* reported the isolation of euchrestine-B (**66**) from the leaves of a different natural source, *M. koenigii*. Euchrestine-B showed radical scavenging activity against 1,1-diphenyl-2-picrylhydrazyl (DPPH) (88).

The UV spectrum [λ_{max} 223, 259 (sh), 303, and 380 nm] and the IR spectrum (ν_{max} 1600, 1635, 1660, 3380, and 3400 cm^{-1}) of murrayaline-B (**64**) were similar to those of murrayaline-A (**44**) (see Scheme 2.10). The ^{1}H-NMR spectrum showed the presence of an aromatic methyl group (δ 2.34) and an aromatic methoxy group (δ 4.02). In the aromatic region, H-1 and H-4 appeared as singlets at δ 7.20 and 7.73 indicating a substitution at C-2 and C-3. The two doublets for H-6 and H-5, respectively, at δ 6.89 and 8.16 with an *ortho*-coupling (J=8.7 Hz), indicated the presence of two further substituents at C-7 and C-8. The sharp singlet at δ 10.58, characteristic of an aldehyde group, suggested that murrayaline-B represents a formylcarbazole. Two deuterium-exchangeable broad singlets at δ 8.42 and 10.79 indicated the presence of an OH and NH group. These spectroscopic data supported by NOE experiments led to structure **64** for murrayaline-B. The transformation of murrayaline-B (**64**) into murrayaline-A (**44**) by *O*-methylation with methyl iodide confirmed this structural assignment (70).

The UV spectrum (λ_{max} 213, 236, 265, 295, 313, 318, and 329 nm) of euchrestine-A (**65**) was very similar to that of euchrestine-C (**62**) (see Scheme 2.13). The fact that the structures were closely related was additionally supported by the IR data (ν_{max} 3400, 3470, and 3600 cm^{-1}). Also, the coupling pattern in the ^{1}H-NMR spectrum of euchrestine-A was similar to that of euchrestine-C, except for the presence of a prenyl side chain (δ 1.78, 1.89, 3.59, and 5.36) at C-8 instead of the geranyl group. The presence of a prenyl group was confirmed by a mass fragmentation ion at m/z 225 (M^+−CH═CMe_2−H). Based on the spectroscopic data, structure **65** was assigned to euchrestine-A (87).

The UV spectrum (λ_{max} 212, 238, 264, 310, 318, and 331 nm) and the IR spectrum (ν_{max} 3380, 3470, and 3600 cm^{-1}) of euchrestine-B (**66**) were very similar to those of euchrestine-C (**62**) (see Scheme 2.13). The ^{1}H-NMR spectrum of euchrestine-B showed strong agreement with that of euchrestine-C, including the presence of a geranyl side chain at C-8. However, the 3-proton-singlet at δ 3.90 indicated the presence of a methoxy group instead of the hydroxy group at C-7. This regiochemical assignment was supported by NOE experiments. The spectroscopic data led to structure **66** for euchrestine-B (87).

The UV spectrum [λ_{max} 212, 238, 265, 312, and 321 (sh) nm] and the IR spectrum (ν_{max} 3600, 3470, and 3380 cm^{-1}) of euchrestine-D (**67**) showed the characteristic absorptions of a 2,6-dioxygenated carbazole framework. The ^{1}H-NMR spectrum

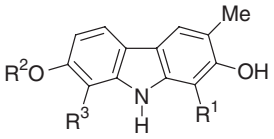

64 Murrayaline-B
R^1 = H; R^2=Me; R^3 = CHO

65 Euchrestine-A
R^1,R^2 = H; R^3 = prenyl

66 Euchrestine-B
R^1 = H; R^2 = Me; R^3 = geranyl

67 Euchrestine-D
R^1 = geranyl; R^2,R^3 = H

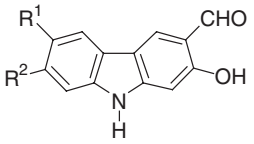

53 Mukonal
R^1,R^2 = H

68 7-Methoxymukonal
(3-Formyl-2-hydroxy-7-methoxycarbazole)
R^1 = H; R^2 = OMe

69 Lansine
R^1 = OMe; R^2 = H

70 Clausanitin
R^1 = H; R^2 = prenyl

Scheme 2.14

exhibited signals of an aromatic methyl group (δ 2.38) and a geranyl side chain. The presence of a geranyl side chain was additionally supported by a mass fragmentation ion at m/z 226 ($M^+ - CH{=}CMeCH_2CH_2CH{=}CMe_2$). In the aromatic region of the ^{1}H-NMR spectrum, H-4 appeared as a singlet at δ 7.56 indicating the presence of substituents at C-1, C-2, and C-3. The *ortho*-coupling (J=8.4 Hz) of H-5 at δ 7.74 and the *ortho*- and *meta*-coupling (J=8.4, 2.4 Hz) of H-6 at δ 6.68 suggested a substitution at C-7. This conclusion was in agreement with the presence of a *meta*-coupled (J=2.4 Hz) H-8 at δ 6.82. Treatment of euchrestine-D with diazomethane gave the corresponding dimethyl ether. NOE experiments with this dimethyl ether unequivocally confirmed structure **67** for euchrestine-D (Scheme 2.14) (87).

In 1988, Pummangura *et al.* reported the isolation of 7-methoxymukonal (3) (3-formyl-2-hydroxy-7-methoxycarbazole) (**68**) from the root bark of *Clausena harmandiana* (89). The UV spectrum [λ_{max} 224, 240, 290 (sh), 300, and 338 nm] and the IR spectrum (ν_{max} 1640 and 3280 cm^{-1}) of 7-methoxymukonal indicated the presence of a 3-formylcarbazole with a chelated hydroxy group. The ^{1}H-NMR spectrum showed a close similarity with that of 7-methoxy-*O*-methylmukonal (**48**) (see Scheme 2.10), except for the signal of one methoxy group which was replaced by the signal of a hydroxy group (δ 11.40) and was chelated to the formyl group (δ 10.11) at C-3. Based on the spectroscopic data and additional support by the ^{13}C-NMR spectrum, structure **68** was assigned to 7-methoxymukonal (3) (3-formyl-2-hydroxy-7-methoxycarbazole) (89).

In 1980, Kapil *et al.* reported the isolation of lansine (**69**) from the ethanolic extract of the leaves of *C. lansium* (90). The UV spectrum (λ_{max} 233, 248, 309, 340 and 368 nm) was characteristic of a 3-formylcarbazole. The IR spectrum (ν_{max} 1620, 1645, and 3300 cm^{-1}) confirmed the presence of an NH group and a chelated carbonyl function. The ^{1}H-NMR spectrum demonstrated a strong agreement with that of glycozolidal (**47**) (see Scheme 2.10), except for the signal of one methoxy group which was replaced by the signal of a hydroxy group and was chelated to the formyl group (δ 9.91) at C-3. The spectroscopic data led to structure **69** for lansine. This

structural assignment was additionally supported by *O*-methylation of lansine with methyl iodide to *O*-methyllansine, which was identical in all spectral data with 2,6-dimethoxy-3-formylcarbazole (27) (glycozolidal) (72).

In 1975, Okorie reported the isolation of clausanitin (**70**) from the roots of *C. anisata* (73). The UV spectrum [λ_{max} 239, 249 (sh), 278, 288 (sh), 297, and 340 nm] and the IR spectrum (ν_{max} 1610, 1635, 3300, and 3400 cm^{-1}) of clausanitin were characteristic of a 3-formylcarbazole derivative. The ^{1}H-NMR spectrum showed the presence of sharp singlets for a formyl proton (δ 9.87) and a deuterium-exchangeable hydroxy proton (δ 11.75) along with the signals of a prenyl side chain (δ 1.72, 1.85, 3.62, 5.33). In the aromatic region, two singlets, assigned to H-1 (δ 7.34) and H-4 (δ 8.00), appeared at shielded and deshielded positions, and indicated the presence of a formyl group at C-3 and of a hydroxy group at C-2. Moreover, the *ortho*-coupling (J=7.0 Hz) of the signal for H-5 at δ 7.90, the *ortho*- and *meta*-coupling (J=7.0, 2.0 Hz) of the signal for H-6 at δ 7.31, and the presence of an additional aromatic signal for H-8 at δ 7.37 suggested that the prenyl side chain was located at C-7. Based on these spectroscopic data, structure **70** was assigned to clausanitin (Scheme 2.14).

In 1996, Wu *et al.* reported the isolation of clausine A (**71**) from the methanol extract of the stem bark of *C. excavata* (51). The UV spectrum (λ_{max} 202, 218, 241, 268 (sh), 275, 288, and 352 nm) and the IR spectrum [ν_{max} 1625 (aromatic system), 1650 (chelated aldehyde), and 3400 (OH or NH) cm^{-1}] of clausine A were very similar to those of mukonal (**53**) (see Scheme 2.11), which indicated a 3-formyl-2-hydroxy-carbazole framework. This assignment was supported by the ^{1}H-NMR spectrum which showed a singlet for an aldehyde proton at δ 9.99 and two D_2O-exchangeable proton signals at δ 10.85 and 11.42 for the NH and OH group, respectively. The presence of a 3-formyl and a 2-hydroxy group was also evident by the upfield shift of H-1 (δ 6.94) and the downfield shift of H-4 (δ 8.44). In addition to these two singlets, the aromatic region exhibited the signals of three mutually *ortho*-coupled (J=8.0 Hz) protons at δ 6.99, 7.17, and 7.68, assigned to H-7, H-6, and H-5 at the C-ring of the carbazole nucleus. Thus, the position of the methoxy group (3-proton-singlet at δ 3.99) was concluded to be at C-8. On the basis of the spectroscopic evidence, structure **71** was assigned to clausine A (Scheme 2.15).

Three years later, Wu *et al.* reported the isolation of clausine O (**72**) from the acetone extract of the root bark of *C. excavata* (43). The UV spectrum [λ_{max} 223, 240, 252 (sh), 291 (sh), 301, 321 (sh), and 340 nm] and the IR spectrum (ν_{max} 1620, 3330 and 3375 cm^{-1}) of clausine O indicated a 3-formylcarbazole framework with a chelated hydroxy group. The ^{1}H-NMR spectrum showed strong agreement with that of 7-methoxymukonal (**68**) (see Scheme 2.14), except for the methoxy group at the C-ring of the carbazole nucleus which was replaced by a further hydroxy group (δ 8.46). The hydroxy group on the carbazole-A-ring was chelated to the formyl group (δ 9.95) at C-3. The spectroscopic data led to structure **72** for clausine O.

In 1997, Ito *et al.* isolated clauszoline-M (**73**) from the roots, the stem bark, and the leaves of *C. excavata* (47). The characteristic absorptions in the UV and the IR spectrum indicated a 3-formyl-2-hydroxy-carbazole framework. The IR band at (ν_{max} 1651 cm^{-1}) and the ^{1}H-NMR signals at δ 9.99 (CHO) and 11.44 (OH, D_2O-exchangeable) suggested the presence of strongly hydrogen-bonded formyl and hydroxy groups, thus supporting the 3-formyl-2-hydroxycarbazole moiety. In addition to these peaks, the ^{1}H-NMR spectrum showed in the aromatic region

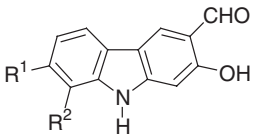

71 Clausine A
R^1 = H; R^2 = OMe

72 Clausine O
R^1 = OH; R^2 = H

73 Clauszoline-M
R^1 = H; R^2 = OH

74 Murrayaline-C
R^1 = OMe; R^2 = CHO

75 Murrayaline-D
R^1 = OMe; R^2 = geranyl

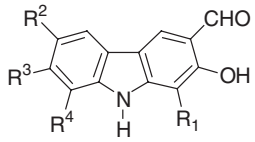

76 Heptaphylline
R^1 = prenyl; R^2,R^3,R^4 = H

77 Heptazoline
R^1 = prenyl; R^2,R^3 = H; R^4 = OH

78 6-Methoxyheptaphylline
R^1 = prenyl; R^2 = OMe; R^3,R^4 = H

79 7-Methoxyheptaphylline
R^1 = prenyl; R^2,R^4 = H; R^3 = OMe

80 Clausine B
R^1,R^3 = H; R^2,R^4 = OMe

81 Clausine S
R^1 = $CH_2CH(OH)C(Me)=CH_2$;
R^2,R^3,R^4 = H

Scheme 2.15

three, mutually *ortho*-coupled (J=7.7 Hz) proton signals at δ 6.90, 7.05 and 7.58, which were assigned to H-7, H-6, and H-5, respectively. The two singlets at δ 6.94 and 8.40 resulted from H-1 and a deshielded H-4, respectively. Based on these spectroscopic data and additional support from the ^{13}C-NMR spectrum, structure **73** was assigned to clauszoline-M.

In 1991, Furukawa *et al.* isolated murrayaline-C (**74**) and murrayaline-D (**75**) from the stem bark of *M. euchrestifolia* collected in Taiwan (70). The UV spectrum [λ_{max} 223, 259 (sh), 303, and 380 nm] and the IR spectrum (ν_{max} 1610, 1640, 1660, 3400, and 3420 cm^{-1}) of murrayaline-C (**74**) indicated the presence of a 3-formyl-2-hydroxycarbazole framework. The ^{1}H-NMR spectrum of murrayaline-C (**74**) showed a similar signal and coupling pattern as that of murrayaline-B (**64**) (see Scheme 2.14), except for the signal of the aromatic methyl group, which was missing and replaced by two additional low-field singlets at δ 9.95 and 11.41. The signal at δ 9.95 was typical of an aldehyde proton attached at C-3. The other singlet at δ 11.41 was assigned to a strongly hydrogen-bonded hydroxy proton located *ortho* to the aldehyde group. These assignments were additionally supported by NOE experiments. On the basis of the spectroscopic evidence, structure **74** was assigned to murrayaline-C (70).

The UV spectrum [λ_{max} 243, 255 (sh), 287, 330, 357, 364, and 368 nm] and the IR spectrum [ν_{max} 1582, 1620 (aromatic system), 1680 (chelated aldehyde), and 3400 (OH or NH) cm^{-1}] of murrayaline-D (**75**) were characteristic of a 3-formyl-2-hydroxycarbazole. This assignment was supported by the ^{1}H-NMR spectrum, which showed a singlet for an aldehyde proton at δ 9.98 and a D_2O-exchangeable proton signal at δ 8.54 for an NH group. In addition to these two peaks, the ^{1}H-NMR spectrum exhibited signals for an aromatic methoxy group at δ 3.95 and for the

geranyl side chain. The presence of a geranyl side chain was additionally supported by the mass fragmentation ion at m/z 254 ($M^+ - CH=CMeCH_2CH_2CH=CMe_2$). In the aromatic region, two, mutually *ortho*-coupled (J=8.8 Hz) proton signals for H-5 at δ 7.88 and H-6 at δ 6.95 confirmed the substitution pattern of the C-ring. The two singlets for H-1 at δ 7.40 and H-4 at δ 8.08 (deshielded by the formyl group at C-3) supported the regiochemical assignments for the substituents on the A-ring. Based on these spectral data, structure **75** was assigned to murrayaline-D (70).

Various heptaphylline derivatives, differing in their substitution pattern of the C-ring, were isolated from different *Clausena* species. In 1967, Joshi *et al*. reported the isolation of heptaphylline (**76**) from the roots of *C. heptaphylla* (26). The UV spectrum (λ_{max} 234, 278, 298, and 346 nm) and the IR spectrum [ν_{max} 1618 (aromatic system), 1640 (chelated aldehyde), and 3300 (OH or NH) cm^{-1}] of heptaphylline were characteristic of a 3-formyl-2-hydroxycarbazole. The ^{1}H-NMR spectrum showed signals for a prenyl side chain (δ 1.66, 1.83, 3.60, and 5.35), a formyl substituent (δ 9.9), an NH group (δ 10.3), and a chelated hydroxy group (δ 11.7). In the aromatic region, a multiplet of four protons at δ 7.1−8.3 indicated an unsubstituted C-ring and the singlet at δ 8.25 for H-4 was strongly deshielded due to the presence of an *ortho*-formyl group. Based on these spectroscopic data, structure **76** was assigned to heptaphylline (26,91). This assignment was additionally supported by synthesis of heptaphylline starting from 3-formyl-2-hydroxy-carbazole and prenyl bromide (91) (Scheme 2.15).

In 1970, Chakraborty *et al*. described the isolation of heptazoline (**77**) from the stem bark of *C. heptaphylla* (92). The UV spectrum (λ_{max} 240, 275, and 298 nm) and the IR spectrum (ν_{max} 1500, 1580, 1623, 3150, and 3450 cm^{-1}) of heptazoline indicated the presence of a 3-formyl-2-hydroxycarbazole framework. The ^{1}H-NMR spectrum showed signals for a prenyl side chain (δ 1.65, 1.81, 3.63, and 5.30), a formyl group (δ 9.91), a D_2O-exchangeable NH group (δ 11.25), and two phenolic hydroxy groups (δ 9.82 and 11.5). In the aromatic region, H-4 of the carbazole nucleus was strongly deshielded and appeared as a singlet at δ 8.28 indicating the close proximity of the formyl group at C-3 and the absence of a proton at C-2. The proton at C-5 appeared as doublet of doublets with an *ortho*- and a *meta*-coupling (J=8.0, 2.0 Hz) indicating the presence of protons at C-6 and C-7 and the presence of a substituent at C-8, which thus was assigned as the position of the second hydroxy group. Based on this spectroscopic analysis, structure **77** was assigned to heptazoline.

In 1972, Joshi *et al*. isolated 6-methoxyheptaphylline (**78**) from the roots of *C. indica* (93). The UV spectrum (λ_{max} 235, 283, 311, and 341 nm) of 6-methoxyheptaphylline closely resembled that of heptaphylline (**76**), and thus indicated a 3-formyl-2-hydroxycarbazole framework containing a chelated hydroxy group. This assignment was supported by the IR spectrum. The ^{1}H-NMR spectrum confirmed the similarity with heptaphylline (**76**), but also showed the presence of an additional methoxy group at δ 3.29. The position of the methoxy group was unequivocally assigned at C-6. This regiochemical assignment was deduced from the signals for the aromatic protons of the carbazole C-ring, which appeared as a doublet with a *meta*-coupling (J=2.0 Hz) at δ 7.45 (H-5), a doublet with an *ortho*-coupling (J=7.5 Hz) at δ 7.3 (H-8), and a doublet of doublets with an *ortho*- and a *meta*-coupling (J=7.5, 2.0 Hz) at δ 7.0 (H-7). Based on these spectroscopic data, structure **78** was assigned to 6-methoxyheptaphylline.

In 1988, Pummangura *et al.* reported the isolation of 7-methoxyheptaphylline (**79**) from the root bark of *C. harmandiana* (89). The UV spectrum [λ_{max} 224, 240, 290 (sh), 300, and 338 nm] and the IR spectrum (ν_{max} 1640 and 3280 cm^{-1}) of 7-methoxyheptaphylline were very similar to those of 7-methoxymukonal (**68**) (see Scheme 2.14), indicating the presence of a 3-formyl-2-hydroxycarbazole with a chelated hydroxy group. The ^{1}H-NMR spectrum confirmed the similarity with 7-methoxymukonal (**68**), but showed signals for an additional prenyl side chain (δ 1.63, 1.79, 3.53, and 5.29). The presence of a prenyl group was supported by the mass fragmentation ion at m/z 253 ($M^+-CH=CMe_2-H$). The absence of an upfield aromatic singlet of H-1 as for 7-methoxymukonal (**68**), indicated that the prenyl group was located at C-1. These spectroscopic data were strongly supported by the ^{13}C-NMR spectrum and thus, led to the assignment of structure **79** for 7-methoxyheptaphylline (89,94).

In 1996, Wu *et al.* isolated clausine B (**80**) from the stem bark of *C. excavata* (46). Clausine B showed inhibition of rabbit platelet aggregation and caused vasocontraction. Three years later, the same group described the isolation and structural elucidation of an optically active ($[\alpha]_D$ +159.09, c 0.0022, MeOH) carbazole alkaloid, clausine S (**81**) from the root bark of *C. excavata*. The absolute stereochemistry of clausine S is still unknown (43).

The UV spectrum (λ_{max} 235, 269, 278, 304, and 357 nm) and the IR spectrum [ν_{max} 1600, 1610 (aromatic system), 1640 (chelated aldehyde), and 3400 (OH, NH) cm^{-1}] of clausine B (**80**) were similar to those of mukonal (**53**) (see Scheme 2.11) and thus indicated a 3-formyl-2-hydroxycarbazole framework. This assignment was confirmed by the ^{1}H-NMR spectrum, which showed a singlet of an aldehyde proton at δ 9.95 and two D_2O-exchangeable proton signals at δ 10.60 and 11.36 for the NH and OH groups, respectively. Moreover, the ^{1}H-NMR spectrum exhibited two, three-proton singlets at δ 3.87 and 3.96 for two methoxy groups. In the aromatic region, the singlet for H-1 was shielded at δ 6.89 and the singlet for H-4 was deshielded at δ 8.38. These signals and their chemical shifts confirmed the presence of a formyl group at C-3 and of a hydroxy group at C-2. The two doublets at δ 6.62 for H-7 and at δ 7.24 for H-5 with a *meta*-coupling (J=2.0 Hz) suggested that the two methoxy groups were located at C-6 and C-8. These spectroscopic assignments were additionally supported by NOE and HMBC experiments and led to structure **80** for clausine B (46).

The UV and IR spectra of clausine S (**81**) were similar to those of clausine B (**80**) indicating a 3-formyl-2-hydroxy-carbazole. Further support for this assignment derived from the ^{1}H-NMR spectrum, which showed a singlet of an aldehyde proton at δ 9.98, a signal for the hydroxy group at δ 11.81, and a deshielded singlet at δ 8.35 for H-4. Moreover, four signals of mutually *ortho*-coupled (J=8.0 Hz) protons at δ 7.21, 7.37, 7.53, and 8.07 indicated that the C-ring was unsubstituted. The presence of one set of CH_2CH-ABX signals at δ 3.05 (dd, J=14.0, 8.6 Hz), 3.28 (dd, J=14.0, 4.0 Hz) and 4.49 (m), singlets at δ 4.74 and 4.92 for a terminal olefinic methylene group, a signal at δ 1.86 for an olefinic methyl group, and a D_2O-exchangeable doublet (J=4.0 Hz) at δ 4.30 for the aliphatic hydroxy group suggested a $-CH_2CH(OH)C(Me)=CH_2$ side chain at C-1. The presence of this side chain was additionally confirmed by the mass fragmentation ion at m/z 224 [$M^+-CH_2CH(OH)C(Me)=CH_2$], which results from cleavage at the benzylic position. On the basis of these spectroscopic data, structure **81** was assigned to clausine S (Scheme 2.15) (43).

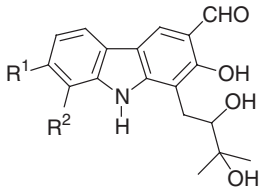

82 Clauszoline-D
$R^1 = H$; $R^2 = OH$

83 Clausine U
$R^1 = OH$; $R^2 = H$

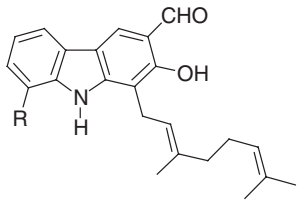

84 Clauszoline-F
R = OH

85 Clausenatine A (Mukoenine-B)
R = H

Scheme 2.16

In 1996, Ito *et al.* reported the isolation of clauszoline-D (**82**) and clauszoline-F (**84**) from the stem bark of *C. excavata* (74). Clauszoline-D (**82**) was obtained from nature in racemic form. Three years later, Wu *et al.* described the isolation of clausine U (**83**) and clausenatine A (**85**) from the acetone extract of the root bark of the same natural source (43). Clausine U (**83**) was isolated in optically active form ($[\alpha]_D$−72.85, *c* 0.0151, MeOH). However, the absolute stereochemistry of clausine U is still unknown (43). Prior to the isolation of clausenatine A (**85**), Furukawa *et al.* reported in 1993 the isolation of the same natural product from the root and stem bark of *M. koenigii* and named it mukoenine-B (82) (Scheme 2.16).

The UV spectrum [λ_{max} 217, 242, 276, 292, 301 (sh), and 356 nm] of clauszoline-D (**82**) is characteristic of a 2,8-dioxygenated 3-formylcarbazole. Moreover, the IR spectrum [ν_{max} 1600 (aromatic system), 1631 (chelated aldehyde), and 3330 (OH or NH) cm^{-1}] of clauszoline-D confirmed a 3-formyl-2-hydroxycarbazole. The ^{1}H-NMR spectrum showed signals for a formyl group at δ 9.97, an NH group at δ 10.43, and two hydroxy groups at δ 11.77 and 8.95. A deshielded singlet at δ 8.30 for H-4 suggested that the formyl substituent was located at C-3. Three, mutually *ortho*-coupled (*J*=7.7 Hz) signals at δ 7.57, 7.05, and 6.88 for H-5, H-6, and H-7, respectively, indicated the presence of a substituent at C-8. The substituent at C-1 was shown to be a dihydroxylated prenyl chain, indicated by two signals for methyl groups at δ 1.30 and 1.31, attached to an oxygen-substituted tertiary carbon, and an ABX signal with geminal and vicinal couplings at δ 3.46 (1*H*, dd, *J*=14.3, 1.8 Hz) and 2.89 (1*H*, dd, *J*=9.5, 14.3 Hz), and two signals for OH groups at δ 4.28 and 3.72. Two characteristic mass fragmentation ions at *m/z* 270 [M^+−C(OH)Me_2] and 240 [M^+−CH(OH)C(OH)Me_2] additionally supported the presence of this side chain. The spectroscopic assignments were confirmed by NOE experiments and led to structure **82** for clauszoline-D (74) (Scheme 2.16).

The UV spectrum [λ_{max} 221, 240 (sh), 245, 254, 288, 303 (sh), 324 (sh), and 339 nm] and the IR spectrum (ν_{max} 1620, and 3400 cm^{-1}) of clausine U (**83**) were very similar to those of clauszoline-D (**82**) and indicated a 3-formyl-2-hydroxycarbazole framework. The ^{1}H-NMR spectrum confirmed the similarity of clausine U to clauszoline-D, but showed the signal for an additional hydroxy group at C-7. This regiochemistry was deduced from the signals for the aromatic protons, which appeared as a doublet with an *ortho*-coupling (*J*=8.3 Hz) at δ 7.85 (H-5), a doublet of doublets with an *ortho*- and a *meta*-coupling (*J*=8.3, 2.0 Hz) at δ 6.76 (H-6), and a

doublet with a *meta*-coupling (J=2.0 Hz) at δ 6.96 (H-8). These spectroscopic data, additionally supported by the ^{13}C-NMR spectrum, as well as HMQC, HMBC, and NOESY spectra, led to structure **83** for clausine U (43).

The UV spectrum [λ_{max} 216, 242, 276, 291, 300 (sh), and 354 nm] of clauszoline-F (**84**) is characteristic of a 2,8-dioxygenated 3-formylcarbazole chromophore. Moreover, the IR spectrum [ν_{max} 1585 (aromatic system), 1630 (chelated aldehyde), and 3300 (OH or NH) cm^{-1}] of clauszoline-F indicated a 3-formyl-2-hydroxycarbazole. The ^{1}H-NMR spectrum differs from that of clauszoline-D (**82**) only in the presence of signals for a geranyl side chain instead of those for a dihydroxyisopentyl side chain. This geranyl side chain was further supported by the mass fragmentation ion at m/z 240 ($M^+-CH=CMeCH_2CH_2CH=CMe_2$). The position of the geranyl side chain at C-1 was unequivocally confirmed by NOE experiments. Because of the structural similarity to clauszoline-D, and based on the spectroscopic data, structure **84** was assigned to clauszoline-F (74).

The UV spectrum [λ_{max} 222, 238, 284 (sh), 294, 331, and 342 (sh) nm] supported by the IR spectrum of clausenatine A (mukoenine-B) (**85**) indicated the presence of a 3-formylcarbazole with a chelated hydroxy group. The ^{1}H-NMR spectrum was very similar to that of clauszoline-F (**84**), except for the lack of a signal for a second hydroxy group on the C-ring of the carbazole nucleus. This was confirmed by the signals of four protons at δ 8.04 (d, J=7.8 Hz), 7.18 (t, J=7.8 Hz), 7.33 (t, J=7.8 Hz), 7.44 (d, J=7.8 Hz) for H-5, H-6, H-7, and H-8, respectively, indicating an unsubstituted C-ring. The spectroscopic data led to the assignment of structure **85** for clausenatine A (mukoenine-B) (43,82) (Scheme 2.16).

5 C-Ring Oxygenated Tricyclic Carbazole Alkaloids

Since 1966, several carbazole alkaloids which are oxygenated at the C-ring were isolated from different natural sources. Glycozoline (**86**) was the first member of this class of alkaloids and was obtained from the stem bark of *G. pentaphylla* (95,96). In 1991, glycozoline (**86**) was also isolated by McChesney and El-Feraly from the roots of *C. lansium* (23). In Taiwan, the roots of this ornamental tree are used in traditional medicine for the treatment of bronchitis and malaria (23). In 1999, Chakravarty *et al.* isolated glycozoline (**86**) from the roots of *G. arborea* (62).

The UV spectrum (λ_{max} 227, 252, 264, and 304 nm) and the IR spectrum [ν_{max} 1208 (aromatic ether), 1380 (C-methyl), 1595, 1600 (aromatic system), and 3500 (NH) cm^{-1}] of glycozoline were characteristic of a 6-methoxycarbazole framework. The ^{1}H-NMR spectrum showed the presence of signals for an NH group (δ 7.80), two aromatic protons (δ 7.50), a multiplet of four aromatic protons (δ 6.80–7.18), an aromatic methoxy group (δ 3.90), and an aromatic methyl group (δ 2.50). The spectroscopic data confirmed that glycozoline is 6-methoxy-3-methylcarbazole (**86**) (96,62). Chemical support for this structural assignment was derived through transformation into known carbazole derivatives (96) and total synthesis (97).

In 2001, Chakravarty *et al.* described the isolation and structural elucidation of glycoborine (**87**) from the roots of *G. arborea* (98). The UV spectrum (λ_{max} 244, 287, 324, and 337 nm) of glycoborine was characteristic of a carbazole chromophore. The ^{1}H-NMR spectrum showed the presence of signals for an NH proton (δ 7.87), an aromatic methoxy group (δ 4.06), and an aromatic methyl group (δ 2.52). A strongly deshielded signal at δ 8.11 for H-4 suggested that the methyl group is located at C-3 and the methoxy group at C-5. Two, mutually *ortho*-coupled (J=7.9 Hz) protons at

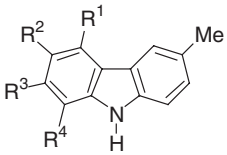

86 Glycozoline
R^1,R^3,R^4 = H; R^2 = OMe

87 Glycoborine
R^1 = OMe; R^2,R^3,R^4 = H

88 Glycozolicine
R^1,R^2,R^3 = H; R^4 = OMe

89 Siamenol
R^1,R^4 = H; R^2 = prenyl; R^3 = OH

90 Clausenalene
R^1,R^4 = H; R^2,R^3 = -OCH_2O-

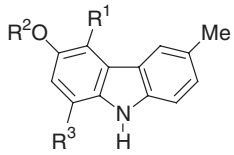

91 Glycozolinine (Glycozolinol)
R^1,R^2,R^3 = H

92 Glycomaurrol
R^1 = prenyl; R^2,R^3 = H

93 Eustifoline-C
R^1 = geranyl; R^2,R^3 = H

94 1-Formyl-3-methoxy-6-methylcarbazole
(8-Formyl-6-methoxy-3-methylcarbazole)
R^1 = H; R^2 = Me; R^3 = CHO

Scheme 2.17

δ 7.25 and 7.19 for H-1 and H-2, respectively, supported this assignment for the regiochemistry of the A-ring. Three signals of contiguous protons at δ 6.65 (d, J=7.9 Hz), 6.98 (dd, J=7.9, 0.6 Hz), and 7.30 (dd, J=7.9, 7.9 Hz) for H-6, H-8, and H-7, respectively, indicated that the location of the methoxy substituent must be C-5. The spectroscopic data, supported by ^{13}C-NMR, COSY, NOESY, HSQC, and HMBC spectra, led to 5-methoxy-3-methylcarbazole as the structure of glycoborine (**87**). This assignment was additionally confirmed by synthesis (98).

In 1992, Bhattacharyya *et al.* reported the isolation of glycozolicine (**88**) from the roots of *G. pentaphylla*, and originally assigned the structure as 5-methoxy-3-methylcarbazole (24). On their isolation of glycoborine (**87**) in 2001, Chakravarty *et al.* reassigned glycozolicine (**88**) as 8-methoxy-3-methylcarbazole (98) (Scheme 2.17).

The UV spectrum (λ_{max} 227, 244, 288, 325, and 330 nm) and the IR spectrum [ν_{max} 1380 (C-methyl), 1590, 1610 (aromatic system), and 3450 (NH) cm^{-1}] of glycozolicine indicated a 3-methylcarbazole. The ^{1}H-NMR spectrum exhibited signals for an NH proton at δ 8.16, an aromatic methoxy group at δ 4.00, and an aromatic methyl group at δ 2.52. In the aromatic region, a deshielded broad singlet at δ 7.84 for H-4 suggested that C-3 is the position of the methyl substituent. This regiochemical assignment was supported by the presence of signals for two, mutually *ortho*-coupled (J=8.2 Hz) protons at δ 7.34 (H-1) and δ 7.23 (H-2). Signals for three contiguous protons at δ 6.88 (d, J=7.6 Hz), 7.13 (dd, J=7.6, 7.6 Hz), and 7.64 (d, J=7.6 Hz) for H-7, H-6, and H-5, respectively, indicated that the methoxy substituent must at C-8. Based on these spectroscopic data, and supported by the ^{13}C-NMR, COSY, NOESY, HSQC, and HMBC spectra, glycozolicine was assigned as 8-methoxy-3-methylcarbazole (**88**). This structural assignment was confirmed by synthesis *via* Fischer indolization of 2-methoxyphenylhydrazine and 4-methylcyclohexanone (98).

In 2000, Boyd *et al.* described the isolation of siamenol (**89**) from the organic extract of *M. siamensis* (85). Siamenol exhibited HIV-inhibitory activity. The UV

spectrum [λ_{max} 216, 238, 261, 308, and 328 (sh) nm] and the IR spectrum indicated the presence of a 3-methylcarbazole. The ^{1}H-NMR spectrum showed signals for a prenyl side chain (δ 1.75, 3.42, and 5.43) and an aromatic methyl group (δ 2.42). The presence of a prenyl group was further supported by the mass fragmentation ion at m/z 210 ($M^+-CH=CMe_2$). In the aromatic region, the signals for H-4 at δ 7.63 with a *meta*-coupling (d, J=1.0 Hz), H-1 at δ 7.17 with an *ortho*-coupling (d, J=8.5 Hz), and H-2 with an *ortho*- and a *meta*-coupling (dd, J=8.5, 1.0 Hz) at δ 7.01 suggested a substitution at C-3. The two singlets at δ 6.81 for H-8 and at δ 7.62 for H-5 indicated that two additional substituents are present at C-6 and C-7. Based on these spectroscopic data and additional support from the ^{13}C-NMR, COSY, NOESY, HMQC, and HMBC spectra, structure **89** was assigned to siamenol.

In 1993, Bhattacharyya *et al.* reported the isolation of clausenalene (**90**) from the stem bark of *C. heptaphylla* (99). This was the first report of a methylenedioxycarbazole alkaloid from a plant source. The UV spectrum (λ_{max} 236, 312, 336, and 353 nm) and the IR spectrum [ν_{max} 1520, 1620 (aromatic system), and 3391 (NH) cm^{-1}] of clausenalene indicated, by their characteristic absorptions, the presence of a carbazole nucleus. The ^{1}H-NMR spectrum showed signals for an NH proton at δ 7.90, an aromatic methyl group at δ 2.30, and an aromatic methylenedioxy group at δ 6.00. In the aromatic region, a deshielded singlet at δ 7.74 for H-4 and two, mutually *ortho*-coupled (J=7.0 Hz) protons at δ 7.10 for H-1 and δ 7.30 and for H-2, suggested that C-3 is the position of the methyl substituent. Moreover, a deshielded singlet at δ 7.45 for H-5 and a shielded singlet at δ 6.80 for H-8 indicated that the methylenedioxy function is bound to C-6 and C-7. The spectroscopic data together with the ^{13}C-NMR spectrum led to the conclusion that clausenalene (**90**) was 3-methyl-6,7-methylenedioxycarbazole. This structural assignment was confirmed by a total synthesis using a Japp–Klingemann reaction and Fischer indolization starting from 2-hydroxymethylene-5-methylcyclohexanone and 3,4-methylenedioxyphenyldiazonium chloride.

In 1983, Mukherjee *et al.* described the isolation and structural elucidation of glycozolinine (**91**) from the seeds of *G. pentaphylla* (66). One year later, Bhattacharyya *et al.* reported the isolation of the same carbazole alkaloid from the roots of the same source and renamed it glycozolinol (**91**) (67). The UV spectrum (λ_{max} 224, 254, 269, and 298 nm) and the IR spectrum [ν_{max} 1390 (C-methyl), 1570, 1630 (aromatic system), and 3440 (NH) cm^{-1}] of glycozolinine (glycozolinol) (**91**) were very similar to those of glycozoline (**86**), indicating the presence of a 6-oxygenated-3-methylcarbazole framework. The ^{1}H-NMR spectrum emphasized the close similarity of glycozolinine (glycozolinol) (**91**) to glycozoline (**86**), with the exception of the signal for a hydroxy group at δ 11.04, instead of a signal for a methoxy group. These spectroscopic data led to structure **91** for glycozolinine (glycozolinol). Additional chemical support for this structural assignment was derived from transformation into known carbazole derivatives, including conversion into glycozoline by treatment with diazomethane (66), and total synthesis (67).

In 1989, Reisch *et al.* described the isolation and structural elucidation of glycomaurrol (**92**) from the dichloromethane extract of the stem bark of *Glycosmis mauritiana* (100). Glycomaurrol (**92**) was considered as a biogenetic precursor of glycomaurin (eustifoline-A) (**172**) (see Chapter 2.5, Scheme 2.36). The UV spectrum [λ_{max} 230, 243 (sh), 255 (sh), 268 (sh), 289 (sh), 298, and 327 nm] indicated the presence of a 6-oxygenated-3-methylcarbazole framework. The ^{1}H-NMR spectrum

showed two, deuterium-exchangeable, broad singlets at δ 4.87 and 7.82 for the protons of the OH and NH groups, respectively. The IR spectrum confirmed the presence of these functional groups from the bands at ν_{max} 3390 for OH and 3200 cm^{-1} for NH. Moreover, the ^{1}H-NMR spectrum exhibited signals for an aromatic methyl group (δ 2.52) and a prenyl side chain (δ 1.76, 1.95, 3.99, and 5.40). The presence of a prenyl group was additionally supported by the mass fragmentation ion at m/z 209 ($M^+-CH=CMe_2-H$). In the aromatic region, a deshielded broad singlet at δ 7.93 for H-4, and a multiplet at δ 7.19–7.31 for H-1 and H-2, suggested the presence of a methyl substituent at C-3. For the C-ring, two, mutually *ortho*-coupled (J=8.5 Hz) protons at δ 6.95 and 7.13 confirmed the positions of the prenyl side chain at C-5 and of the hydroxy group at C-6 of the carbazole framework. Based on these spectroscopic data and the ^{13}C-NMR spectrum, structure **92** was assigned to glycomaurrol. Further chemical support for this structural assignment was derived from transformation into known carbazole derivatives.

In 1990, Ito and Furukawa described the isolation and structural elucidation of eustifoline-C (**93**) from the root bark of *M. euchrestifolia* collected in Taiwan in December (101). Eustifoline-C (**93**) was considered a biogenetic precursor of eustifoline-B (**173**) (see Chapter 2.5, Scheme 2.36). The UV spectrum (λ_{max} 231, 258, 268, 290, 300, 325, and 357 nm) and the IR spectrum of eustifoline-C were very similar to those of glycomaurrol (**92**). The ^{1}H-NMR spectrum emphasized the close similarity of eustifoline-C (**93**) to glycomaurrol (**92**), with the exception of the signals for a geranyl side chain at C-5 instead of the signals for the prenyl group. The presence of a geranyl side chain was additionally supported by the mass fragmentation ion at m/z 210 ($M^+-CH=CMeCH_2CH_2CH=CMe_2$) resulting from cleavage at the benzylic position. The position of the geranyl side chain as a substituent at C-5 of the carbazole framework was supported by NOE experiments with *O*-methyleustifoline-C, which was prepared by treatment of eustifoline-C with diazomethane. Based on the spectroscopic evidence, structure **93** was assigned to eustifoline-C.

In 2001, Chowdhury *et al.* isolated 1-formyl-3-methoxy-6-methylcarbazole (8-formyl-6-methoxy-3-methylcarbazole) (**94**) from the leaves of *M. koenigii* (48). This carbazole alkaloid exhibited inhibitory activity against both Gram-positive and Gram-negative bacteria, and against fungi. The UV spectrum (λ_{max} 227, 262, 303, and 398 nm) was characteristic of a 1-formylcarbazole (=8-formylcarbazole) nucleus. This assignment was supported by the IR spectrum [ν_{max} 1208 (aromatic ether), 1580, 1605 (aromatic system), 1665 (C=O), 2760 (aldehyde C–H) and 3405 (NH) cm^{-1}]. The ^{1}H-NMR spectrum showed the presence of signals for an aldehyde proton at δ 10.50, an NH proton at δ 9.61, an aromatic methyl group at δ 2.32, and an aromatic methoxy group at δ 4.03. In the aromatic region, the protons at the C-ring, H-5 (δ 8.05, d, J=2.5 Hz) and H-7 (δ 7.45, d, J=2.5 Hz) exhibited no *ortho*-coupling, and thus indicated a substitution at C-6. The *meta*-coupling of H-4 (δ 7.82, d, J=2.5 Hz) indicated that the position of the methyl group was C-3. Based on the UV spectrum, the formyl group was assigned to position 8. The ^{1}H-NMR spectrum indicated the presence of a formyl and a methoxy group on the same ring of the carbazole skeleton. The spectroscopic evidence led to 1-formyl-3-methoxy-6-methylcarbazole (8-formyl-6-methoxy-3-methylcarbazole) (**94**). This structural assignment was additionally confirmed by transformation of 1-formyl-3-methoxy-6-methylcarbazole

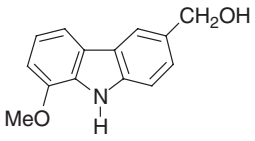

95 Mukoline

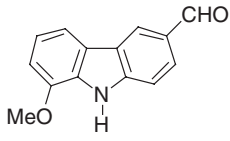

96 Mukolidine

Scheme 2.18

into a known natural product, glycozoline (**86**), on decarbonylation with Pd–C, and by total synthesis (46) (Scheme 2.17).

In 1982, Chakraborty *et al.* described the isolation and structural elucidation of mukoline (**95**) and mukolidine (**96**) from the roots of *M. koenigii* (102) (Scheme 2.18). The UV spectrum (λ_{max} 221, 242, 252, 258, 280, 290, and 320 nm) and the IR spectrum (ν_{max} 1610, 3240, and 3440 cm^{-1}) of mukoline (**95**) indicated the presence of an 8-(1-)methoxycarbazole chromophore. The ^{1}H-NMR spectrum showed signals for an NH proton at δ 8.22, a hydroxy group at δ 4.45, deshielded benzylic methylene protons at δ 4.75, and an aromatic methoxy group at δ 3.90. The aromatic region exhibited a doublet with *meta*-coupling (J=2.0 Hz) for H-4, and signals for five further protons in the range of δ 7.00−7.90. Based on these spectroscopic data, structure **95** was assigned for mukoline. This structural assignment was chemically supported by transformation into the corresponding *O*-acetyl and *N*-methyl derivatives, total synthesis, and conversion into mukolidine (**96**) by oxidation with active MnO_2 (102).

The UV spectrum (λ_{max} 238, 248, 275, 290, and 330 nm) and the IR spectrum (ν_{max} 1660, and 3185 cm^{-1}) of mukolidine (**96**) indicated a 3-formylcarbazole framework. The ^{1}H-NMR spectrum exhibited signals for an aldehyde proton at δ 10.80, an NH proton at δ 8.60, and an aromatic methoxy group at δ 4.05. The aromatic region showed signals for H-4 at δ 8.15, H-5 at δ 8.08, and four other aromatic protons between δ 7.30−7.60. Based on these spectroscopic data, structure **96** was assigned to mukolidine. This structural assignment was supported by transformation into mukoline (**95**) on borohydride reduction, and by synthesis starting from 2-(hydroxymethylene)cyclohexanone and toluenediazonium chloride using Japp–Klingemann conditions (102) (Scheme 2.18).

In 1991, McChesney and El-Feraly described the isolation and structural elucidation of 3-formyl-6-methoxycarbazole (**97**) from the roots of *C. lansium* (23). The roots of this ornamental tree are used in traditional medicine in Taiwan to treat bronchitis and malaria (23). In 2005, Franzblau *et al.* isolated the same natural product from the stem bark of *Micromelum hirsutum* (103). They reported that 3-formyl-6-methoxycarbazole (**97**) shows *in vitro* anti-TB activity against the H_{37}Rv strain of *Mycobacterium tuberculosis*.

The UV spectrum (λ_{max} 229, 245, 281, 297, and 334 nm) and the IR spectrum (ν_{max} 1675, and 3310 cm^{-1}) indicated a 3-formylcarbazole framework for this alkaloid. The ^{1}H-NMR spectrum exhibited signals for an aldehyde proton at δ 10.06, an NH proton at δ 10.72, and an aromatic methoxy group at δ 3.90. In the aromatic region, H-5 (δ 7.80) and H-7 (δ 7.10) showed a mutual *meta*-coupling (J=2.4 Hz), and H-8 (δ 7.40) appeared as a doublet with an *ortho*-coupling (J=8.8 Hz). Thus, these signals suggested C-6 as the position of the methoxy substituent. The deshielded signal for

H-4 (δ 8.66, br s) with no *ortho*-coupling, and the mutually *ortho*-coupled (J=8.2 Hz) signals for H-1 (δ 7.58) and H-2 (δ 7.92), indicated that the formyl substituent was located at C-3. The spectroscopic data confirmed the structure as 3-formyl-6-methoxycarbazole (**97**). This assignment was additionally supported by the ^{13}C-NMR spectrum.

In 1997, Ito *et al*. described the isolation and structural elucidation of clauszoline-K (**98**) from the stem bark of *C. excavata* (47). The UV spectrum of clauszoline-K indicated a 3-formylcarbazole. The IR spectrum with a band at ν_{max} 1680 cm^{-1}, and the ^{1}H-NMR spectrum with a singlet at δ 10.08, confirmed the presence of a formyl group. Moreover, the ^{1}H-NMR spectrum showed a singlet for an aromatic methoxy group at δ 3.92 and two sets of three-spin systems in the aromatic region. The first set showed signals for H-1 at δ 7.47 (d, J=8.4 Hz), H-2 at δ 7.91 (dd, J=8.4, 1.5 Hz), and H-4 at δ 8.51 (d, J=1.5 Hz). The most deshielded signal at δ 8.51 was assigned to H-4 due to the *ortho*-formyl group. Another set of signals for aromatic protons at δ 6.94 (dd, J=8.4, 2.2 Hz), 6.96 (d, J=2.2 Hz), and 8.00 (d, J=8.4 Hz) was assigned to H-6, H-8, and H-5, respectively. Additional NOE experiments supported the assignment of the proton signals. The spectroscopic data confirmed that structure **98** represents clauszoline-K.

In 1992, Furukawa *et al.* reported the isolation of 3-formyl-7-hydroxycarbazole (**99**) from the root bark of *M. euchrestifolia* (104). The UV spectrum [λ_{max} 233, 245 (sh), 273, 288, and 326 nm] and the IR spectrum (ν_{max} 1673 and 3336 cm^{-1}) of 3-formyl-7-hydroxycarbazole were very similar to those of clauszoline-K (**98**), indicating a 3-formylcarbazole framework. The ^{1}H-NMR spectrum confirmed the structural similarity to clauszoline-K, and showed the presence of a hydroxy group instead of the methoxy group. All of the spectroscopic data supported the structure of 3-formyl-7-hydroxycarbazole (**99**) (Scheme 2.19).

In 2005, Franzblau *et al.* isolated micromeline (**100**) from the stem bark of *M. hirsutum* (103). This alkaloid exhibited *in vitro* anti-TB activity against the H_{37}Rv strain of *Mycobacterium tuberculosis* and against the Erdman strain of *M. tuberculosis*

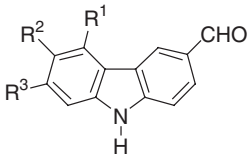

97 3-Formyl-6-methoxycarbazole
R^1,R^3 = H; R^2 = OMe

98 Clauszoline-K
R^1,R^2 = H; R^3 = OMe

99 3-Formyl-7-hydroxycarbazole
R^1,R^2 = H; R^3 = OH

100 Micromeline
R^1 = prenyl; R^2 = OH; R^3 = H

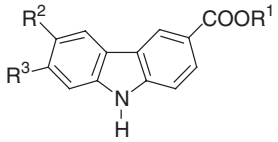

101 Clausine C (Clauszoline-L)
R^1 = Me; R^2 = H; R^3 = OMe

102 Clausine M
R^1 = Me; R^2 = H; R^3 = OH

103 Clausine N
R^1,R^2 = H; R^3 = OMe

104 Methyl 6-methoxycarbazole-3-carboxylate
R^1 = Me; R^2 = OMe; R^3 = H

Scheme 2.19

in a J774 mouse macrophage model. The UV spectrum (λ_{max} 316 and 329 nm) and the IR spectrum [ν_{max} 1670 (conjugated carbonyl), 3317 (OH), and 3394 (NH) cm^{-1}] of micromeline indicated the presence of a 3-formylcarbazole. This assignment was supported by the ^{1}H-NMR spectrum which showed signals for an aldehyde proton at δ 10.05, an NH proton at δ 10.67, an OH proton at δ 7.99, and a prenyl side chain at δ 1.69, 1.99, 4.02, and 5.32. A deshielded doublet of doublets with *meta*- and *para*-coupling (J=1.6, 0.5 Hz) at δ 8.65 for H-4, and two, mutually *ortho*-coupled (J=8.5 Hz) signals for H-1 at δ 7.60 and for H-2 at δ 7.91, confirmed that C-3 is the position of the formyl substituent. For the C-ring of the carbazole framework, two, mutually *ortho*-coupled (J=8.5 Hz) protons at δ 7.11 and 7.29 suggested the positions of the prenyl side chain and the hydroxy group at C-5 and C-6, respectively. Based on these spectroscopic data and additional support by the ^{13}C-NMR, COSY, NOESY, HMQC, and HMBC spectra, structure **100** was assigned to micromeline.

In 1996, Wu *et al*. described the isolation and structural elucidation of clausine C (**101**) from the stem bark of *C. excavata* (51). One year later, Ito *et al*. isolated the same natural product from the same source and named it clauszoline-L (**101**) (47). The UV spectrum [λ_{max} 218, 238 (sh), 248, 281, and 320 (sh) nm] was characteristic of a 3-carbomethoxycarbazole. This assignment was supported by the IR spectrum [ν_{max} 1610 (aromatic system), 1709 (carbomethoxy), and 3469 (NH) cm^{-1}]. The ^{1}H-NMR spectrum resembled that of clauszoline-K (**98**), except for the appearance of an additional methoxy signal instead of the signal for the formyl group at C-3. The additional methoxy signal at δ 3.97 in the ^{1}H-NMR spectrum, an IR band at 1709 cm^{-1}, and two significant mass fragments at m/z 224 (M^+-OMe) and 196 ($M^+-COOMe$) indicated the presence of a carbomethoxy group at C-3. Based on these spectroscopic data, which were supported by NOE experiments (47), structure **101** was assigned to clausine C (clauszoline-L).

In 1999, Wu *et al*. described the isolation and structural elucidation of clausine M (**102**) and clausine N (**103**) from the acetone extract of the root bark of *C. excavata* (43). The UV spectrum [λ_{max} 219, 239 (sh), 249, 283, and 318 (sh) nm] and the IR spectrum [ν_{max} 1610 (aromatic system), 1690 (carbomethoxy), 3330 (OH), and 3375 (NH) cm^{-1}] of clausine M (**102**) were similar to those of clausine C (**101**), indicating a 3-carbomethoxycarbazole framework. The ^{1}H-NMR spectrum confirmed the structural similarity to clausine C (**101**), but showed a signal for a hydroxy group at δ 8.51 instead of the methoxy signal. The presence of a hydroxy group was supported by the IR band at 3330 cm^{-1}. The spectroscopic data led to structure **102** for clausine M. This structural assignment was additionally supported by NOE experiments (43).

Clausine N (**103**) represents an isomer of clausine M (**102**) and shows similar UV and IR spectra. The ^{1}H-NMR spectrum confirmed the structural similarity to clausine M (**102**), but exhibited signals for a methoxy group at C-7 (δ 3.88) and for a carboxyl group at C-3 instead of the signals for the carboxymethyl and hydroxy groups. The presence of a methoxy substituent was confirmed by two characteristic mass fragments at m/z 226 (M^+-Me) and 198 (M^+-COMe). Based on these spectroscopic data, structure **103** was assigned to clausine N (43).

In 1991, McChesney and El-Feraly reported the isolation of methyl 6-methoxy-carbazole-3-carboxylate (**104**) from the roots of *C. lansium* (23). In Taiwan the roots of this ornamental tree are used in folk medicine for the treatment of bronchitis and malaria (23). The UV spectrum [λ_{max} 227, 241 (sh), 266 (sh), and 285 nm] and the IR

spectrum (ν_{max} 1705 and 3300 cm^{-1}) of methyl 6-methoxycarbazole-3-carboxylate (**104**) closely resembled those of clausine C (**101**), indicating the structural similarity. The ^{1}H-NMR spectrum showed signals for an NH proton at δ 10.36 and two aromatic methoxy groups at δ 3.96 and 4.03. In the aromatic region, H-5 at δ 7.70 and H-7 at δ 7.18 exhibited a mutual *meta*-coupling (J=1.8 Hz), and H-8 at δ 7.42 appeared as a doublet with an *ortho*-coupling (J=7.8 Hz). These signals indicated that the location of the methoxy substituent was at C-6 on the C-ring. The deshielded signal for H-4 (δ 8.93, br s) was also lacking an *ortho*-coupling, and the two protons H-1 (δ 7.48) and H-2 (δ 8.27) showed a mutual *ortho*-coupling (J=7.8 Hz). Thus, for the A-ring it was concluded that the methyl ester was located at C-3. The presence of a methyl ester group was supported by the IR band at 1705 cm^{-1}. The spectroscopic data confirmed the structure of methyl 6-methoxycarbazole-3-carboxylate (**104**) (Scheme 2.19).

6 9-Oxygenated Tricyclic Carbazole Alkaloids

In 1988, Furukawa *et al.* reported the isolation of *N*-methoxy-3-formylcarbazole (3-formyl-9-methoxycarbazole) (**105**) from the root bark of *M. euchrestifolia* (22). This was the first example of a 9-oxygenated tricyclic carbazole alkaloid isolated from a natural source. The UV spectrum (λ_{max} 236, 272, 288, and 320 nm) and the IR spectrum (ν_{max} 1600, 1620, and 1680 cm^{-1}) of *N*-methoxy-3-formylcarbazole (**105**) indicated the presence of a 3-formylcarbazole framework. This assignment was confirmed by the ^{1}H-NMR spectrum which showed the signal for an aldehyde proton at δ 10.12. Moreover, the ^{1}H-NMR spectrum resembled closely that of 3-formylcarbazole, and exhibited an additional signal for a methoxy group at δ 4.27. The presence of a methoxy substituent was supported by the mass fragment at m/z 194 (M^+−OMe). The absence of an NH proton in the ^{1}H-NMR spectrum, and the presence of seven aromatic CH signals in the ^{13}C-NMR and DEPT spectrum, led to the assignment of the methoxy group at the *N*-atom. These spectral data confirmed the structure of *N*-methoxy-3-formylcarbazole (**105**) (Scheme 2.20).

Four years later, Furukawa *et al.* described the isolation and structural elucidation of *N*-methoxy-3-hydroxymethylcarbazole (3-hydroxymethyl-9-methoxycarbazole) (**106**) from the root bark of *M. euchrestifolia* (104). The UV spectrum (λ_{max} 237, 263, 283, and 334 nm) of *N*-methoxy-3-hydroxymethylcarbazole (**106**) was similar to that of *N*-methoxy-3-formylcarbazole (**105**), but exhibited some bathochromic shifts of the bands. The ^{1}H-NMR spectrum confirmed the structural similarity to *N*-methoxy-3-formylcarbazole, but showed the signal for a hydroxymethyl group at δ 4.86 instead of the signal for a formyl group. The presence of a hydroxymethyl group was supported by an IR band at 3450 cm^{-1} and a characteristic mass fragment at m/z 167. The ^{13}C-NMR spectrum of *N*-methoxy-3-hydroxymethylcarbazole supported the

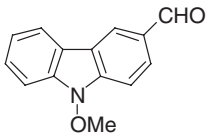

105 3-Formyl-9-methoxycarbazole
(N-methoxy-3-formylcarbazole)

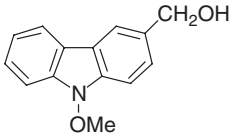

106 3-Hydroxymethyl-9-methoxycarbazole
(N-methoxy-3-hydroxymethylcarbazole)

Scheme 2.20

structural similarity to *N*-methoxy-3-formylcarbazole. The spectroscopic data confirmed the structure of *N*-methoxy-3-hydroxymethylcarbazole (**106**). This assignment was additionally supported by NOE experiments and chemical transformation into known carbazole derivatives.

7 Tricyclic Carbazole-1,4-quinone Alkaloids

The carbazole-1,4-quinones represent an important family of carbazole alkaloids (105,106). Except for clausenaquinone A (**112**), all carbazole-1,4-quinones isolated from natural sources have a 3-methylcarbazole-1,4-quinone skeleton. The plants of the genus *Murraya* (Rutaceae) are the major natural source of carbazole-1,4-quinone alkaloids. In 1983, Furukawa *et al.* reported the first isolation of a carbazole-1,4-quinone, murrayaquinone A (**107**), from the root bark of *M. euchrestifolia* collected in Taiwan (28,29). In subsequent years, the same group reported the isolation of various carbazole-1,4-quinones from the root or stem bark of the same plant: murrayaquinone B (**108**) (28,29), murrayaquinone C (**109**) (28,29), murrayaquinone D (**110**) (29), and murrayaquinone E (**111**) (70) (Scheme 2.21).

The UV spectrum [λ_{max} 225, 258, 293 (sh), and 398 nm] and the IR spectrum (ν_{max} 1595, 1650, and 3200 cm^{-1}) of murrayaquinone A (**107**) indicated the presence of a carbazole-1,4-quinone nucleus. This was supported by the ^{13}C-NMR spectrum with two signals for carbonyl carbons at δ 183.40 and 180.40. The ^{1}H-NMR spectrum showed signals for a vinylic methyl group as a doublet (J=1.5 Hz) at δ 2.19 and an olefinic proton as a quartet (J=1.5 Hz) at δ 6.51, both exhibiting a long-range coupling. In the aromatic region, a signal for a deshielded proton which appeared as a doublet of triplets (J=1.0, 5.0 Hz) at δ 8.23 could be assigned to H-5 due to the deshielding effect of the C-4 carbonyl moiety. A three-proton multiplet at δ 7.30–7.60 was assigned to H-6, H-7, and H-8. The spectroscopic data and a total synthesis confirmed structure **107** for murrayaquinone A (28,29).

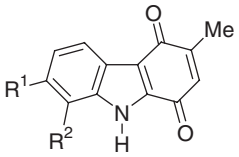

107 Murrayaquinone A
R^1,R^2 = H

108 Murrayaquinone B
R^1 = OMe; R^2 = prenyl

109 Murrayaquinone C
R^1 = OMe; R^2 = geranyl

110 Murrayaquinone D
R^1 = OH; R^2 = geranyl

111 Murrayaquinone E
R^1 = OH; R^2 = prenyl

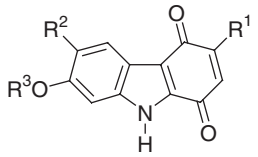

112 Clausenaquinone A
R^1 = OMe; R^2 = Me; R^3 = H

113 Koeniginequinone A
R^1,R^3 = Me; R^2 = H

114 Koeniginequinone B
R^1,R^3 = Me; R^2 = OMe

Scheme 2.21

The UV spectrum [λ_{max} 231, 264, 310 (sh), and 404 nm] and the IR spectrum (ν_{max} 1610, 1640, 1655, and 3280 cm^{-1}) of murrayaquinone B (**108**) were very similar to those of murrayaquinone A (**107**), indicating a carbazole-1,4-quinone framework. This assignment was supported by the ^{13}C-NMR spectrum which exhibited two signals for carbonyl carbons at δ 183.70 and 179.80. The ^{1}H-NMR spectrum showed signals for a vinylic methyl group as a doublet at δ 2.13 and an olefinic proton as a quartet at δ 6.42, both with an allylic coupling (J=1.5 Hz), an aromatic methoxy group at δ 3.91, and a prenyl side chain (δ 1.74, 1.85, 3.57, and 5.23). The presence of a prenyl side chain was supported by the mass fragmentation ion at m/z 254 ($M^+-CH=CMe_2$). In the aromatic region, two, mutually *ortho*-coupled (J=9.0 Hz) protons at δ 7.02 and 7.98 could be assigned to H-6 and H-5. Moreover, the observation of an NOE of 15.9% between the signals for H-6 at δ 6.02 and the methoxy group at δ 3.91 confirmed the position of the methoxy group at C-7 and of the prenyl group at C-8. On the basis of these spectroscopic data, structure **108** was assigned to murrayaquinone B (28,29).

The UV spectrum [λ_{max} 233, 267, and 410 nm] and the IR spectrum (ν_{max} 1610, 1645, 1655, and 3440 cm^{-1}) of murrayaquinone C (**109**) were very similar to those of murrayaquinone B (**108**), indicating a carbazole-1,4-quinone framework. This assignment was supported by two signals for carbonyl carbons in the ^{13}C-NMR spectrum at δ 183.60 and 179.70. The ^{1}H-NMR spectrum confirmed the structural similarity to murrayaquinone B (**108**), and also exhibited signals for a geranyl side chain instead of the signals for a prenyl side chain. The mass fragmentation ion at m/z 308 ($M^+-CH=CMeCH_2CH_2CH=CMe_2$), resulting from cleavage at the benzylic position, supported the presence of a geranyl side chain. The spectroscopic data, confirmed by NOE experiments and total synthesis, led to structure **109** for murrayaquinone C (28,29).

The UV spectrum [λ_{max} 234, 266, and 415 nm] and the IR spectrum (ν_{max} 1610, 1645, 1660, and 3440 cm^{-1}) of murrayaquinone D (**110**) were very similar to those of murrayaquinone C (**109**), thus indicating the presence of a carbazole-1,4-quinone framework. The ^{1}H-NMR spectrum confirmed the structural similarity to murrayaquinone C (**109**), but showed the signal for a hydroxy group (δ 5.52) instead of the signal for a methoxy group. Based on the spectroscopic data, structure **110** was assigned to murrayaquinone D (29).

The UV spectrum [λ_{max} 232, 262, and 406 nm] and the IR spectrum (ν_{max} 1620, 1650, 3400, and 3430 cm^{-1}) of murrayaquinone E (**111**) resembled those of murrayaquinone B (**108**) and indicated the presence of a carbazole-1,4-quinone framework. In the IR spectrum, the bands at ν_{max} 1620 and 1650 cm^{-1} are characteristic of a carbazole-1,4-quinone. The ^{1}H-NMR spectrum confirmed the similarity to murrayaquinone B (**108**), but exhibited the signal of a hydroxy group instead of the signal for a methoxy group. The presence of a hydroxy group was supported by the mass fragmentation ion at m/z 278 (M^+-OH). These spectroscopic data led to structure **111** for murrayaquinone E (70).

In 1994, Wu *et al*. described the isolation and structural elucidation of clausenaquinone A (**112**) from the stem bark of *C. excavata* (107). This carbazole-1,4-quinone alkaloid exhibited potent inhibitory activity of rabbit platelet aggregation induced by arachidonic acid, as well as cytotoxicity in the HCT-8, RPMI-7951, and TE-671 tumor cells. The UV spectrum (λ_{max} 228, 265, 295, and 419 nm) and the IR spectrum (ν_{max} 1600, 1625, 1660, 3260, and 3370 cm^{-1}) of clausenaquinone A

indicated a carbazole-1,4-quinone. The ^{1}H-NMR spectrum showed signals for an aromatic methyl group at δ 2.33, an aromatic methoxy group at δ 3.88, and a vinyl proton at δ 5.78 assigned to H-2. A deshielded broad singlet at δ 8.17 for H-5 suggested the presence of a carbonyl group at C-4 and a methyl group at C-6. A shielded broad singlet at δ 7.04 could be assigned to H-8. A broad singlet at δ 7.82, corresponding to a D_2O-exchangeable proton, confirmed the presence of a hydroxy group at C-7. Based on the spectroscopic data, structure **112** was assigned to clausenaquinone A. This structural assignment was additionally supported by HMBC spectra and by total synthesis (107).

In 1998, Saha and Chowdhury described the isolation of koeniginequinone A (**113**) and koeniginequinone B (**114**) from the stem bark of *M. koenigii* (49), which represented the first report of carbazole-1,4-quinone alkaloids from this plant. The UV spectrum [λ_{max} 227, 260, and 286 (sh), 387 nm] and the IR spectrum (ν_{max} 1639, 1652, and 3280 cm^{-1}) of koeniginequinone A (**113**) indicated a carbazole-1, 4-quinone framework. In the IR spectrum, the bands at ν_{max} 1639 and 1652 cm^{-1} are typical of a carbazole-1,4-quinone. The ^{1}H-NMR spectrum showed signals for a vinylic methyl group (doublet at δ 2.09), an olefinic proton (quartet at δ 6.39, both with an allylic coupling of J=1.3 Hz), and an aromatic methoxy group at δ 3.81. In the aromatic region, two, mutually *ortho*-coupled (J=8.0 Hz) protons at δ 8.03 and 6.93 were assigned to H-5 and H-6, respectively, due to the deshielding effect of the C-4 carbonyl moiety and the shielding effect of the methoxy group at C-7. A shielded doublet at δ 7.04 with a *meta*-coupling (J=1.8 Hz) was assigned to H-8, confirming the position of the methoxy group at C-7. These spectroscopic data led to the structure of 7-methoxy-3-methylcarbazole-1,4-quinone (**113**) for koeniginequinone A. This assignment was confirmed by synthesis using a Japp–Klingemann reaction and Fischer indolization (49).

The UV spectrum [λ_{max} 225, 263, 293 (sh), and 464 nm] and the IR spectrum (ν_{max} 1641, 1650, and 3284 cm^{-1}) of koeniginequinone B (**114**) indicated a carbazole-1, 4-quinone. The presence of this framework was supported by the characteristic carbazole-1,4-quinone bands in the IR spectrum at ν_{max} 1641 and 1650 cm^{-1}. The ^{1}H-NMR spectrum showed signals for a vinylic methyl group (doublet at δ 2.12), an olefinic proton (quartet at δ 6.42, both with an allylic coupling of J=1.2 Hz), and two aromatic methoxy groups at δ 3.94 and 3.97. In the aromatic region, the singlet at δ 7.56 for H-5 was deshielded by the C-4 carbonyl moiety, and the shielded singlet at δ 6.84 was assigned to H-8. Moreover, these signals confirmed the positions of the two methoxy groups at C-6 and C-7. Based on the spectroscopic data, koeniginequinone B was assigned as 6,7-dimethoxy-3-methylcarbazole-1,4-quinone (**114**). A total synthesis by a Japp–Klingemann reaction and Fischer indolization supported this structural assignment (49) (Scheme 2.21).

B. Pyranocarbazole Alkaloids

1 Pyrano[3,2-*a*]carbazole Alkaloids

In 1964, Chakraborty *et al.* isolated girinimbine (**115**) from the stem bark of *M. koenigii* (108). Girinimbine represented the first pyrano[3,2-*a*]carbazole alkaloid isolated from natural sources. Later, Joshi *et al.* isolated the same alkaloid from the roots of a different source, *C. heptaphylla* (91). Based on chemical degradation studies,

Chakraborty *et al.* proposed originally that the pyran ring and the aromatic methyl group of girinimbine are attached to different aromatic rings of the carbazole framework (108). Five years later, Dutta and Quasim reassigned the structure of girinimbine based on NMR studies and proposed that the pyran ring and the methyl group of girinimbine are connected to the same aromatic ring (109). This structural assignment was in agreement with biogenetic considerations and supported by Joshi *et al.* (91,110). The UV spectrum (λ_{max} 223, 238, 288, 330, 342, and 358 nm) of girinimbine (**115**) indicated a carbazole. The IR spectrum (ν_{max} 1580, 1620, and 3290 cm^{-1}) showed the presence of an NH function and an aromatic system. The ^{1}H-NMR spectrum exhibited signals for an NH at δ 7.75, two aromatic protons at δ 7.50, three aromatic protons at δ 7.08, and an aromatic methyl group at δ 2.23. A six-proton singlet at δ 1.42 and symmetrical doublets at δ 5.45 and 6.25 suggested a 2,2-dimethyl-Δ^3-pyran ring fused to the carbazole nucleus. The presence of a 2,2-dimethyl-Δ^3-pyran ring was supported by the mass fragmentation ion at m/z 248 (M^+-Me). Based on these spectroscopic data, structure **115** was assigned to girinimbine.

In 1968, Narasimhan *et al.* reported the isolation of koenimbin (**116**) from the fruits of *M. koenigii* (111). One year later, Kapil *et al.* isolated the same carbazole alkaloid from the leaves of the same source (112). The UV spectrum (λ_{max} 230, 240, 300, 340, and 360 nm) and the IR spectrum (ν_{max} 1580, 1650, and 3400 cm^{-1}) of koenimbin (**116**) indicated a carbazole framework. The ^{1}H-NMR spectrum showed signals for an NH, an aromatic methoxy group, and an aromatic methyl group. In the aromatic region, two deshielded singlets at δ 7.61 and 7.40 were assigned to H-4 and H-5, respectively. The proton at C-5 was slightly shielded compared to the corresponding proton of mahanimbine (**139**) (see Scheme 2.27). Therefore, the position of the methoxy group was assigned to C-6. Moreover, the ^{1}H-NMR spectrum confirmed the presence of a fused 2,2-dimethyl-Δ^3-pyran ring. The spectroscopic data were supported by chemical transformation into known carbazole derivatives and led to 6-methoxygirinimbine (**116**) as the structure for koenimbin (111).

In 1969, Kapil *et al.* described the isolation and structural elucidation of koenigicine (**118**) (6,7-dimethoxygirinimbine) from the leaves of *M. koenigii* (112). Only one year later, Joshi and Narasimhan isolated from the same natural source an identical carbazole alkaloid and named it koenimbidine (110) and koenidine (113). During their investigation Narasimhan *et al.* isolated, along with koenidine (**118**), koenine (**117**) and koenigine (**119**), which differ in the oxygen substitution pattern at the positions 6 and 7 (113). In 1982, Bowen and Perera reported the isolation of koenigine (**119**) from the leaves of *Micromelum zeylanicum*, a species restricted to Sri Lanka. The name of the plant in Sinhalese is Walkarapincha (wild *M. koenigii*) (114). The ^{1}H-NMR spectra confirm that all these alkaloids have a pyrano[3,2-*a*]carbazole framework (Scheme 2.22).

Koenine (**117**) gave a positive ferric chloride test, which indicated the presence of a phenolic group. The ^{1}H-NMR spectrum showed signals for an aromatic methyl group and a 2,2-dimethyl-Δ^3-pyran ring. In the aromatic region, H-7 (δ 6.74) exhibited an *ortho*-coupling (J=8.0 Hz) with H-8 (δ 7.18), and a *meta*-coupling (J=2.0 Hz) with H-5 (δ 7.20). The signal for H-4 appeared at (δ 7.55) as a deshielded singlet. The ^{1}H-NMR spectroscopic data unambiguously confirmed the positions of the 2,2-dimethyl-Δ^3-pyran ring at C-1 and C-2, the methyl group at C-3, and the hydroxy group at C-6. Therefore, koenine was assigned as 6-hydroxygirinimbine

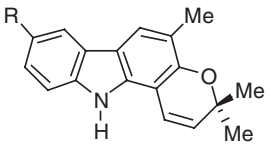

115 Girinimbine
R = H

116 Koenimbin
R = OMe

117 Koenine
R = OH

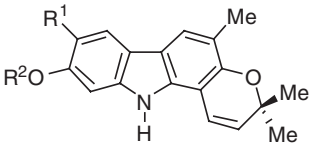

118 Koenigicine (Koenimbidine, Koenidine)
R^1 = OMe; R^2 = Me

119 Koenigine
R^1 = OMe; R^2 = H

120 Murrayamine-A
(7-Hydroxygirinimbine, Mukoenine-C)
R^1,R^2 = H

120a *O*-Methylmurrayamine A
R^1 = H; R^2 = Me

Scheme 2.22

(**117**). This structural assignment was confirmed by the conversion of koenine into koenimbin *via* methylation (113).

The UV spectra of koenigicine (**118**) and koenigine (**119**) were strikingly similar to the UV spectrum of koenimbin (**116**), indicating a similar carbazole chromophore. The ^{1}H-NMR spectrum of koenigicine (**118**) showed signals for an aromatic methyl group, two aromatic methoxy groups and a 2,2-dimethyl-Δ^3-pyran ring. The signal for H-4 represented a deshielded singlet at δ 7.58, suggesting the presence of a methyl substituent at C-3 and a 2,2-dimethyl-Δ^3-pyran ring fused at C-1 and C-2. The 2,2-dimethyl-Δ^3-pyran ring was confirmed by the mass fragmentation ion at m/z 308 (M^+-Me). In addition, H-5 appeared as a deshielded singlet at δ 7.48 and H-8 as a shielded singlet at δ 6.93, which confirmed the positions of the two methoxy groups at C-6 and C-7. Based on these spectroscopic data, koenigicine was assigned as 6,7-dimethoxygirinimbine (**118**) (112,113).

The ^{1}H-NMR spectrum of koenigine (**119**) was similar to that of koenigicine (**118**). However, koenigine has one hydroxy group and one methoxy group instead of two methoxy groups, as in koenigicine. The presence of a hydroxy group was supported by a positive ferric chloride test. Based on the chemical shift of H-8 (δ 6.81) in koenigine the position of the hydroxy group was assigned to C-7. The spectroscopic data led to structure **119** for koenigine. This structural assignment was supported by conversion of koenigine into koenigicine *via* methylation (113).

In 1991, Wu reported the isolation of murrayamine-A (**120**) from the leaves of *M. euchrestifolia* (115). Two years later, Furukawa *et al*. isolated the same alkaloid from the roots of *M. koenigii* and named it mukoenine-C (82). The UV spectrum [λ_{max} 221, 240, 287 (sh), 294, 342, 349, and 360 nm] of murrayamine-A indicated a carbazole framework. The ^{1}H-NMR spectrum showed singlets for an NH group at δ 7.76 and a phenolic hydroxy group at δ 4.91. This was supported by IR bands at 3419 and 3044 cm^{-1}. In the aromatic region, H-4 appeared as a deshielded singlet at δ 7.53, suggesting that the methyl substituent at C-3 and the 2,2-dimethyl-Δ^3-pyran ring were fused at C-1 and C-2. The presence of a 2,2-dimethyl-Δ^3-pyran ring was

confirmed by the mass fragmentation ion at m/z 264 (M^+-Me). The signals for H-5 with an *ortho*-coupling (J=8.2 Hz) at δ 7.72, and H-6 with an *ortho*- and a *meta*-coupling (J=8.2, 2.2 Hz) at δ 6.68, suggested C-7 as the position for the hydroxy group. This assignment was in agreement with the *meta*-coupling (J=2.2 Hz) of H-8 at δ 6.81. The position of the hydroxy group at C-7 was supported by the marked diamagnetic shifts observed for the signals of H-6 (Δ −0.21) and H-8 (Δ −0.3) of *O*-acetylmurrayamine A. Therefore, murrayamine-A was assigned as 7-hydroxygirinimbine (**120**) (82,115).

In 2003, Nakatani *et al.* reported the isolation of *O*-methylmurrayamine A (**120a**) from the leaves of *M. koenigii*. *O*-Methylmurrayamine A (**120a**) showed radical scavenging activity against the 1,1-diphenyl-2-picrylhydrazyl (DPPH) radical (116). Prior to its isolation from nature, this alkaloid was known as a synthetic derivative of murrayamine-A (**120**), obtained by methylation with diazomethane (115). The UV spectrum [λ_{max} 221, 240, 283 (sh), 294, 341 (sh), and 357 (sh) nm] of *O*-methylmurrayamine A (**120a**) was very similar to that of murrayamine-A (**120**), indicating the presence of a pyranocarbazole framework. This was supported by the IR spectrum. The ^{1}H-NMR spectrum of *O*-methylmurrayamine A differs from that of murrayamine-A only by the signal of an aromatic methoxy group at δ 3.90 instead of a hydroxy group. In the ^{13}C-NMR spectrum, the signal for the methoxy group appeared at δ 55.7. Based on the spectroscopic data, structure **120a** was assigned to *O*-methylmurrayamine A (116) (Scheme 2.22).

In 1997, Mester and Reisch described the isolation and structural elucidation of mupamine (**121**) from the root bark of *C. anisata* (117). The UV spectrum of mupamine (**121**) resembled that of girinimbine (**115**) (see Scheme 2.22), indicating the presence of a similar chromophore. The ^{1}H-NMR spectrum showed signals for an NH group at δ 8.03 and an aromatic methoxy group at δ 3.99. This assignment was supported by IR bands at 3370 and 2840 cm^{-1}. In the aromatic region, H-4 appeared as a deshielded singlet at δ 7.63, suggesting the presence of a methyl substituent at C-3 and a 2,2-dimethyl-Δ^3-pyran ring fused at C-1 and C-2. The 2,2-dimethyl-Δ^3-pyran ring was confirmed by the mass fragmentation ion at m/z 278 (M^+-Me). Moreover, the aromatic region showed three, mutually *ortho*-coupled (J=7.8 Hz) signals for H-5, H-6, and H-7 at δ 7.53, 7.09, and 6.80, respectively, suggesting C-8 as the position of the methoxy group. The spectroscopic data led to 8-methoxygirinimbine (**121**) as the structure for mupamine (117).

In 1983, Ganguly *et al.* reported the isolation of mukonicine (**122**) from the leaves of *M. koenigii* (118). The UV spectrum of mukonicine (**122**) resembled that of koenimbin (**116**) (see Scheme 2.22), indicating a similar chromophore. This assignment was supported by the IR spectrum [ν_{max} 1385 (C-Me), 1648 (C-OMe), and 3440 (NH) cm^{-1}]. The ^{1}H-NMR spectrum showed signals for an NH proton at δ 7.81, an aromatic methyl group at δ 2.30, two aromatic methoxy groups at δ 3.90, and a 2,2-dimethyl-Δ^3-pyran ring. In the aromatic region, the signal for H-4 appeared as a deshielded singlet at δ 7.56, suggesting the regiochemistry with a methyl group at C-3 and a 2,2-dimethyl-Δ^3-pyran ring fused at C-1 and C-2. The presence of a 2,2-dimethyl-Δ^3-pyran ring was supported by the mass fragmentation ion at m/z 308 (M^+-Me). The signal for H-5 appeared at higher field (δ 7.40), indicating that one of the two methoxy groups was located at C-6, similar to koenimbin (**116**) (see Scheme 2.22). The position of the second methoxy group was assigned to C-8 because the signal for H-7 appeared at much higher field (δ 6.88) than H-5. Therefore, mukonicine was assigned as 6,8-dimethoxygirinimbine (**122**) (118).

In 2003, Hao *et al.* isolated from the aerial parts of *M. koenigii* the optically active carbazole alkaloid **123**, with a rare arylpropanyl substitution, and named it murrayanine (119). However, since 1965 murrayanine is known as 3-formyl-1-methoxycarbazole (**9**) isolated by Chakraborty *et al.* from the stem bark of *M. koenigii* (33,34) (see Scheme 2.4). Therefore, in order to avoid confusion in the future, we suggest to rename this ''new murrayanine'' as murrayanine B (**123**) and this name is used for **123** throughout this article. Murrayanine B (**123**) showed a specific rotation of $[\alpha]_D^{25} + 8.0$ (*c* 0.74, MeOH), but its absolute configuration is not known. The UV spectrum (λ_{max} 225, 238, 300, and 342 nm) of murrayanine B (**123**) indicated a carbazole framework. The ^{1}H-NMR spectrum exhibited signals for an NH and a phenolic hydroxy group as two broad singlets at δ 9.73 and 4.75. The IR spectrum supported this assignment with bands at 3440 and 3410 cm^{-1}. Moreover, the ^{1}H-NMR spectrum showed the presence of a koenigine (**119**) moiety (see Scheme 2.22) and an 11-carbon residue. The structure of the latter was indicated by signals for a –OCH_2–CHR^1–CHR^2–O– group. This assignment was supported by the mass fragmentation ion at *m*/*z* 210 (M−307) as well as COSY and HMBC spectra.

The ^{1}H-NMR spectrum showed the presence of an isolated, two-spin system at δ 6.81 with a *meta*-coupling (*J*=1.9 Hz), indicating a symmetrically substituted aromatic residue. The presence of two methoxy groups on this aromatic ring at C-6″ and C-8″ was revealed by NMR analysis, while the hydroxy group at C-7″ was determined with the help of mass and NMR spectroscopic data. The NMR spectra of murrayanine B and koenigine differed at C-8. The signal for C-8 in the ^{13}C-NMR spectrum of murrayanine B indicated substitution, whereas a CH signal was observed for the C-8 of koenigine. This assignment was confirmed by ^{1}H–^{13}C long-range correlations between H-2″ at δ 3.88 and the carbons at δ 148.3 (C-7), 110.9 (C-8), and 131.8 (C-8a), as well as between the methylene protons at δ 4.02 (H-1″) and the carbon at δ 110.9 (C-8). The connection of C-7 and C-3″ *via* an oxygen was determined by the ^{1}H–^{13}C long-range correlations between H-3″ at δ 5.46 and C-7 at δ 148.3. The relative configuration of C-2″ and C-3″ was determined as *trans* based on the coupling constant (*J*=7.8 Hz) and ROESY correlations between H-1″ and H-3″. The spectroscopic data led to structure **123** for murrayanine B (119) (Scheme 2.23).

Chakraborty *et al.* reported the isolation of murrayacine (**124**), a formyl analog of girinimbine from two different natural sources *M. koenigii* (120,121) and *C. heptaphylla* (122). The UV spectrum (λ_{max} 226, 282, and 301 nm) and the IR spectrum (ν_{max} 1675 and 3250 cm^{-1}) of murrayacine (**124**) indicated

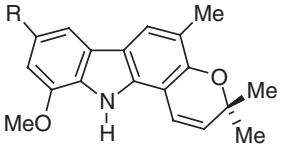

121 Mupamine
R = H

122 Mukonicine
R = OMe

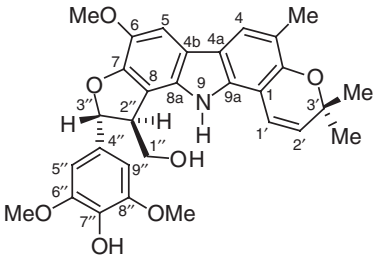

123 Murrayanine-B

Scheme 2.23

a 3-formylcarbazole. The presence of a formyl group was confirmed by the formation of a 2,4-dinitrophenylhydrazone. The ^{1}H-NMR spectrum showed signals for an aldehyde proton (δ 10.68), an NH (δ 12.0), and a 2,2-dimethyl-Δ^3-pyran ring. The deshielded singlet at δ 8.40 for H-4 suggested the position of the formyl substituent at C-3 and the 2,2-dimethyl-Δ^3-pyran ring fused to C-1 and C-2. The presence of a 2,2-dimethyl-Δ^3-pyran ring was confirmed by the mass fragmentation ion at m/z 262 (M^+-Me). A multiplet of four aromatic protons at δ 7.35–8.15 indicated an unsubstituted C-ring. Based on the spectroscopic data, structure **124** was assigned to murrayacine. This assignment was supported by the transformation of **124** into known carbazole derivatives (110,121).

In 1990, Lange *et al.* isolated 7-methoxymurrayacine (**125**) from the roots of *M. siamensis* (57). The UV and IR spectra of 7-methoxymurrayacine (**125**) were very similar to those of murrayacine (**124**) indicating a 3-formylcarbazole. The ^{1}H-NMR spectrum of 7-methoxymurrayacine also resembled that of murrayacine. However, the C-ring substitution pattern was similar to that of murrayamine-A (**120**) (see Scheme 2.22), indicating the presence of a substituent at C-7. This regiochemical assignment was supported by the ^{1}H-NMR spectrum which showed an *ortho*-coupled (J=8.4 Hz) H-5 at δ 7.84, an *ortho*- and *meta*-coupled (J=8.4, 2.2 Hz) H-6 at δ 6.86, and a *meta*-coupled (J=2.2 Hz) H-8 at δ 6.90. These spectroscopic data led to structure **125** for 7-methoxymurrayacine.

In 1996, Ito *et al.* reported the isolation of clauszoline-G (**126**) from the stem bark of *C. excavata* collected in Singapore (74). The UV spectrum [λ_{max} 204, 234, 245 (sh), 278, 300, and 361 nm] and the IR spectrum (ν_{max} 1578, 1631, 1658, and 3263 cm^{-1}) of clauszoline-G (**126**) indicated a 3-formylcarbazole framework. The ^{1}H-NMR spectrum showed signals for an NH at δ 10.58, a phenolic hydroxy group at δ 8.90, and a formyl group at δ 10.48. In the aromatic region, H-4 appeared as a deshielded singlet at δ 8.33, suggesting the position of the formyl substituent at C-3 and the 2,2-dimethyl-Δ^3-pyran ring fused to C-1 and C-2. The presence of a 2,2-dimethyl-Δ^3-pyran ring was confirmed by the mass fragmentation ion at m/z 278 (M^+-Me). In the aromatic region, the ^{1}H-NMR spectrum showed signals for three, mutually *ortho*-coupled (J=7.7 Hz) protons at δ 7.61, 7.04, and 6.88 (H-5, H-6, and H-7), suggesting the presence of a substituent at C-8. Based on these spectral data, clauszoline-G was assigned as 8-hydroxymurrayacin (**126**).

In 1974, Chakraborty *et al.* isolated heptazolidine (**127**) from *C. heptaphylla* (123). The UV spectrum (λ_{max} 230, 238, 278, 282, and 335 nm) and the IR spectrum (ν_{max} 965, 1190, 1510, 1650, and 3400 cm^{-1}) of heptazolidine indicated a pyranocarbazole framework. The ^{1}H-NMR spectrum showed signals for an NH (δ 8.1), an aromatic methoxy group (δ 3.98), and an aromatic methyl group (δ 2.3). The shielded singlet at δ 7.50 was assigned to H-5 and indicated the position of the methoxy group to be at C-6. Moreover, the aromatic region exhibited a *meta*-coupled (J=2.0 Hz) signal at δ 7.67 for H-4, and two, mutually *ortho*-coupled (J=8.5 Hz) signals at δ 7.18 and 6.94. The coupling pattern of the ^{1}H-NMR spectrum suggested the position of the methyl group at C-3 and the presence of a 2,2-dimethyl-Δ^3-pyran ring fused to C-7 and C-8 of the carbazole framework. This assignment was supported by the mass fragmentation ion at m/z 278 (M^+-Me). The spectroscopic data were additionally confirmed by transformation into known carbazole derivatives as well as total synthesis, and led to structure **127** for heptazolidine (123,124).

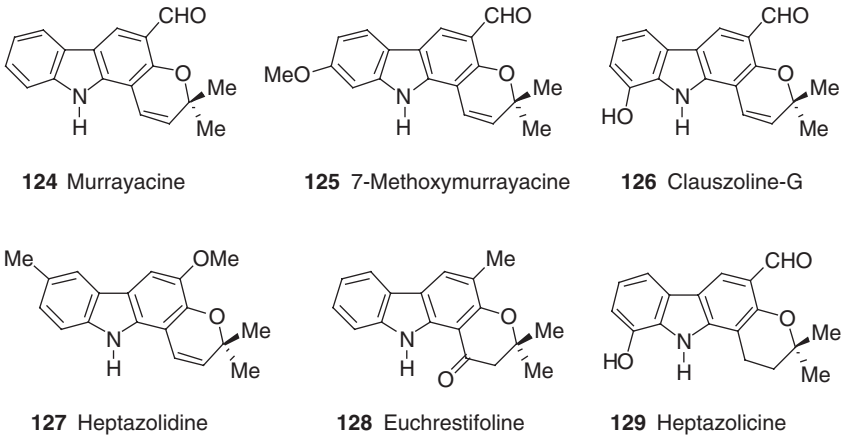

124 Murrayacine **125** 7-Methoxymurrayacine **126** Clauszoline-G

127 Heptazolidine **128** Euchrestifoline **129** Heptazolicine

Scheme 2.24

In 1996, Wu *et al*. reported the isolation of euchrestifoline (**128**) from the leaves of *M. euchrestifolia* collected in May (125). Depending on the season, a constitutional variation is observed for the carbazole alkaloids obtained from the leaves of this species. Previously, **128** was prepared by Chakraborty and Islam as an intermediate for the synthesis of girinimbine (**115**) (126) (see Scheme 2.22). The UV spectrum (λ_{max} 231, 255, 284, 291, 330, and 386 nm) of euchrestifoline was typical of a carbazole. The ^{1}H-NMR spectrum showed singlets for an aromatic methyl group at δ 2.39 and H-4 at δ 8.02. The deshielding of H-4 suggested the position of the methyl group at C-3. Moreover, the four mutually coupled signals at δ 7.23, 7.39, 7.48, and 7.95 for H-6, H-7, H-8, and H-5, indicated an unsubstituted C-ring. A broad signal at low field (δ 10.14) along with IR bands at 3440 (NH) and 1650 (C=O) cm^{-1} suggested the presence of a keto-carbazole with an intramolecular hydrogen bonding. The remaining signals, including two methyl groups adjacent to the oxygen functionality as singlet at δ 1.54 and a singlet for a methylene group at δ 2.83, confirmed the dimethylpyranone ring fused to C-1 and C-2 of the carbazole framework. Based on these spectral data, structure **128** was assigned to euchrestifoline (125).

In 1984, Chowdhury *et al.* isolated heptazolicine (**129**) from the roots of *C. heptaphylla* (127). The UV spectrum (λ_{max} 242, 275, and 300 nm) of heptazolicine (**129**) indicated a 3-formylcarbazole. This assignment was supported by the IR spectrum [ν_{max} 1700 (CHO), 3000 (NH), and 3260 (OH, hydrogen-bonded) cm^{-1}]. The ^{1}H-NMR spectrum showed signals for an NH at δ 10.4, a phenolic hydroxy group at δ 11.2, and a formyl group at δ 9.8. Two symmetrical triplets (J=7 Hz) at δ 3.03 and δ 1.98, along with a sharp singlet for six protons at δ 1.45, indicated the 2,2-dimethyldihydropyran ring. The presence of a 2,2-dimethyldihydropyran ring was supported by the mass fragmentation ion at m/z 280 (M^+−Me). In the aromatic region, H-4 appeared as a deshielded singlet at δ 8.3, suggesting the position of the formyl substituent at C-3 and the 2,2-dimethyldihydropyran fused to C-1 and C-2. The *ortho*- and *meta*-coupling (J=8.0, 2.0 Hz) of H-5 at δ 7.5 showed that C-6 and C-7 were unsubstituted. This conclusion was in agreement with the two-proton multiplet at δ 6.7–7.2 for H-6 and H-7. The signals for the aromatic protons and the downfield shift of the hydroxy proton (δ 11.2) confirmed the position of the hydroxy group at

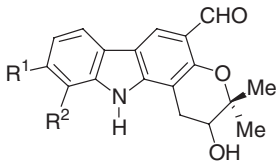

130 Clauszoline-E
R^1 = H; R^2 = OH

131 Clausine T
R^1 = OH; R^2 = H

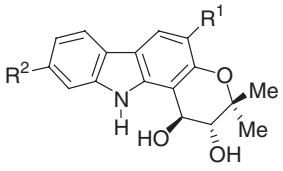

132 Clausine W
R^1 = CHO; R^2 = OH

133 Dihydroxygirinimbine
R^1 = Me; R^2 = H

Scheme 2.25

C-8. The spectroscopic data, supported by transformation into known carbazole derivatives, led to structure **129** for heptazolicine (Scheme 2.24).

In 1996, Ito *et al*. isolated clauszoline-E (**130**) from the stem bark of *C. excavata* in racemic form (74). The UV spectrum (λ_{max} 242, 273, and 292 nm) of clauszoline-E (**130**) indicated a 3-formylcarbazole framework. This assignment was supported by the IR spectrum [ν_{max} 1650 (CHO), 3479 (NH), and 3287 (OH) cm^{-1}]. The ^{1}H-NMR spectrum showed signals for an NH at δ 11.30, a phenolic hydroxy group at δ 9.85, and a formyl group at δ 10.35. The presence of a 2,2-dimethyl-3-hydroxydihydropyran ring was indicated by two three-proton singlets at δ 1.38 and 1.30 for the geminal dimethyl group attached to the α-oxygen carbon atom, a multiplet at δ 3.83 coupled (1*H*, *J*=5.5 Hz) with a hydroxy proton at δ 5.32, and a doublet of doublets due to the benzylic methylene group at δ 3.17 (1*H*, *J*=17.1, 5.1 Hz) and 2.83 (1*H*, *J*=17.1, 7.0 Hz). In the aromatic region, H-4 appeared as a deshielded singlet at δ 8.24, suggesting the position of the formyl substituent at C-3 and the 2,2-dimethyl-3-hydroxydihydropyran fused to C-1 and C-2. Three, mutually *ortho*-coupled (*J*=7.7 Hz) signals for H-5, H-6, and H-7 at δ 7.52, 6.97, and 6.80, respectively, suggested the position of the hydroxy group at C-8. Based on the spectroscopic data, which were additionally supported by ^{13}C-NMR, NOE, and HMBC spectra, structure **130** was assigned to clauszoline-E.

In 1997, Wu *et al*. described the isolation of clausine T (**131**) and clausine W (**132**) from the root bark of *C. excavata* (128) (Scheme 2.25). Both alkaloids were obtained from Nature in optically active form: $[\alpha]_D$ –82.1 (*c* 0.0341, MeOH) for **131** and $[\alpha]_D$ –3.41 (*c* 1.002, MeOH) for **132**. However, their absolute configuration is still unknown.

The UV spectrum [λ_{max} 242, 249, 274, 285 (sh), 302, and 345 nm] and the IR spectrum (ν_{max} 1590, 1610, and 3400 cm^{-1}) of clausine T (**131**) indicated a 3-formylcarbazole. The ^{1}H-NMR spectrum of clausine T was similar to that of clauszoline-E (**130**), but differed in the position of the hydroxy group. The aromatic region showed a deshielded singlet for H-4 at δ 8.13, a doublet with an *ortho* coupling (*J*=8.4 Hz) for H-5 at δ 7.88, a doublet of doublets with an *ortho*- and a *meta*-coupling (*J*=8.4, 2.1 Hz) for H-6 at δ 6.76, and a doublet with a *meta*-coupling (*J*=2.1 Hz) for H-8 at δ 6.91. Thus, the position of the hydroxy group was assigned at C-7. These spectroscopic data, additionally supported by the ^{13}C-NMR spectrum and NOE experiments, led to structure **131** for clausine T (128).

The UV and IR spectra of clausine W (**132**) resembled those of clausine T (**131**), indicating a 3-formyl-7-hydroxypyranocarbazole skeleton. The ^{1}H-NMR spectrum confirmed the similarity to clausine T, except for the substitution pattern of the

dihydropyran ring. The heteroaliphatic region exhibited signals of four, mutually-coupled protons at δ 3.81 (dd, J=7.5, 5.2 Hz), 4.58 (d, J=7.0 Hz), 4.86 (d, J=5.2 Hz), and 4.92 (dd, J=7.5, 7.0 Hz). Of these four signals, the two doublets at δ 4.58 and 4.86 were exchangeable with D_2O and the two other signals showed a vicinal diaxial coupling (J=7.5 Hz) indicating a –CH(OH)CH(OH)– moiety with a *trans*-diol configuration. The two singlets at δ 1.31 and 1.55 were assigned to the geminal dimethyl group of the pyran ring. Based on these spectroscopic data and additional support by ^{13}C-NMR, NOESY, HSQC, and HMBC spectra, structure **132** was assigned to clausine W (128).

In 1985, Furukawa *et al.* reported the isolation of dihydroxygirinimbine (**133**) from the root bark of *M. euchrestifolia* collected in Taiwan (129). Although this alkaloid was obtained in optically active form ($[\alpha]_D$ –4, MeOH), the absolute configuration remains unknown. The UV spectrum (λ_{max} 238, 254, 259, 303, and 332 nm) of dihydroxygirinimbine was typical of a 3-methylcarbazole, which was supported by the IR spectrum. The ^{1}H-NMR spectrum indicated an aromatic methyl group at δ 2.28, along with a *trans*-2′,2′-dimethyl-3′,4′-dihydroxydihydropyran ring similar to clausine W (**132**). In the aromatic region, H-4 appeared at δ 7.72, suggesting C-3 as the position of the methyl substituent. Moreover, four, mutually-coupled protons at δ 7.06, 7.24, 7.50, and 7.96 indicated an unsubstituted C-ring of the carbazole. Based on these spectroscopic data, structure **133** was assigned to dihydroxygirinimbine (Scheme 2.25).

In 1996, Wu *et al.* described the isolation of murrayamine-I (**134**) and murrayamine-K (**135**) from the acetone extract of the leaves of *M. euchrestifolia* collected in November (130). The UV spectrum [λ_{max} 222, 240, 281 (sh), 295, 324, 349, and 360 nm] of murrayamine-I (**134**) indicated a 2,7-dioxygenated carbazole framework. This assignment was supported by the IR spectrum. Except for the substitution pattern of the pyran ring, the ^{1}H-NMR spectrum resembled that of murrayamine-A (**120**) (see Scheme 2.22), suggesting a similar structure. In the olefinic region, two doublets at δ 5.64 and 6.75, with a mutual coupling of J=9.8 Hz, confirmed the annulated pyran ring with two geminal substituents. A singlet at δ 1.50 indicated a quaternary methyl group. Two diasterotopic protons belonging to the same methylene group, which appeared as doublets (J=11.5 Hz) at δ 4.17 and 4.26, and a singlet at δ 2.02 for an acetate, showed that the other geminal substituent was an acetoxymethylene group. The mass fragmentation ion at m/z 264 ($M^+ - CH_2OCOCH_3$) supported this assignment. These spectroscopic data led to structure **134** for murrayamine-I (130).

The UV spectrum [λ_{max} 237, 279 (sh), 288, 327, 344, and 359 nm] of murrayamine-K (**135**) indicated a 3-methylcarbazole, which was supported by the IR spectrum. The ^{1}H-NMR spectrum resembled that of murrayamine-I (**134**). The only difference was that murrayamine-K has an unsubstituted carbazole C-ring, as concluded from the four, mutually-coupled protons at δ 7.18, 7.31, 7.37, and 7.91. Based on these spectroscopic data and additional support by the ^{13}C-NMR data as well as NOE experiments, structure **135** was assigned to murrayamine-K (130).

In 1986, Furukawa *et al.* reported the isolation of pyrayafoline A (**136**) from the stem bark of *M. euchrestifolia* (38,87). The UV spectrum [λ_{max} 239, 286 (sh), 295, and 334 nm] and the IR spectrum (ν_{max} 1590, 1605, and 1625 cm^{-1}) of pyrayafoline A (**136**) suggested a carbazole framework. The ^{1}H-NMR spectrum showed signals for an aromatic methyl group, an aromatic methoxy group, and a 2,2-dimethyl-Δ^3-pyran

ring. In the aromatic region, H-5 and H-6 appeared as *ortho*-coupled (J=8.0 Hz) doublets at δ 7.63 and 6.67, indicating the position of the pyran ring at C-7 and C-8. Moreover, H-1 appeared as a shielded singlet at δ 6.83 and H-4 as a deshielded singlet at δ 7.62, indicating the position of the methoxy group at C-2 and of the methyl group at C-3. Based on the spectroscopic data and additional support by synthesis, structure **136** was assigned to pyrayafoline A (38).

Five years later, the same group isolated from the same natural source further pyranocarbazole alkaloids, pyrayafoline C (**137**) and pyrayafoline D (**138**), which were obtained in racemic form (87). In 1992, Reisch *et al.* described the isolation of pyrayafoline D from the fruits of a different natural source, *M. koenigii*, and named it isomahanine (**138**). The absolute configuration of isomahanine is not known (71). In 2003, Nakatani *et al.* reported the isolation of isomahanine (**138**) from the leaves of *M. koenigii* in optically active form: $[\alpha]_D^{25}$ − 38.2 (*c* 0.22, $CHCl_3$). However, the absolute configuration at the stereogenic center has not been assigned. Pyrayafoline D (isomahanine) (**138**) exhibited radical scavenging activity against the 1,1-diphenyl-2-picrylhydrazyl (DPPH) radical (116) and significant cytotoxicity against HL-60 cells (131).

The UV spectrum [λ_{max} 238, 286 (sh), 296, and 323 nm] of pyrayafoline C (**137**) resembled that of pyrayafoline A (**136**) suggesting a similar chromophore. This conclusion was supported by the IR spectrum. The ^{1}H-NMR spectrum was also very similar to that of pyrayafoline A (**136**), except for the presence of a hydroxy group instead of the methoxy group. The spectroscopic data led to structure **137** for pyrayafoline C. This assignment was additionally supported by methylation of pyrayafoline C with diazomethane to give pyrayafoline A (**136**) (Scheme 2.26) (38).

The UV spectrum [λ_{max} 238, 288 (sh), 296, and 331 nm] and the IR spectrum (ν_{max} 3380, 3480, and 3600 cm^{-1}) of pyrayafoline D (**138**) resembled those of pyrayafoline C (**137**), indicating a similar carbazole framework. The ^{1}H-NMR spectrum of pyrayafoline D (**138**) differs from that of pyrayafoline C (**137**) only by the presence of signals at δ 1.75 (2*H*, m), 2.15 (2*H*, m), 5.10 (1*H*, t), 1.57 (3*H*, s), and 1.65 (3*H*, s), assignable to the side chain $-CH_2CH_2CH{=}CMe_2$, instead of the signal for one of the methyl groups at the pyran ring of pyrayafoline C (**137**) The presence of this side chain was supported by the mass fragmentation ion at m/z 264 ($M^+ - CH_2CH_2CH{=}CMe_2$). Based on the spectroscopic data, structure **138** was

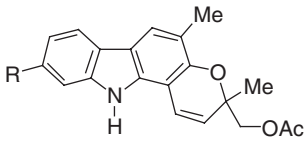

134 Murrayamine-I
R = OH

135 Murrayamine-K
R = H

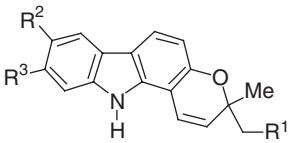

136 Pyrayafoline A
R^1 = H; R^2 = Me; R^3 = OMe

137 Pyrayafoline C
R^1 = H; R^2 = Me; R^3 = OH

138 Pyrayafoline D (Isomahanine)
R^1 = prenyl; R^2 = Me; R^3 = OH

Scheme 2.26

assigned to pyrayafoline D. Additional structural support was derived from NOE experiments with the methyl ether of pyrayafoline D, obtained by methylation using diazomethane (87) (Scheme 2.26).

In 1966, Chakraborty *et al*. described the isolation of (+)-mahanimbine (**139a**) from *M. koenigii* (132). Two years later, Narasimhan *et al.* corrected the structural assignment of Chakraborty. Although alkaloid **139a** was obtained in optically active form ($[\alpha]_D$ +52), the absolute configuration is still unknown (111,133). Later, the racemic alkaloid, (±)-mahanimbine (**139b**), was isolated independently from two different *Murraya* species, *M. euchrestifolia* (29) and *M. siamensis* (85).

The UV spectrum (λ_{max} 277, 288, 328, 343, and 357 nm) and the IR spectrum (ν_{max} 1600, 1650, and 3330 cm^{-1}) of (+)-mahanimbine (**139a**) resembled that of girinimbine (**115**) (see Scheme 2.22), indicating a 3-methylpyranocarbazole. The ^{1}H-NMR spectrum differs from that of girinimbine (**115**) only by the presence of signals at δ 1.67–1.87 (2*H*, m), 1.93–2.21 (2*H*, m), 5.13 (1*H*, m), 1.57 (3*H*, s), and 1.63 (3*H*, s), assignable to the $-CH_2CH_2CH{=}CMe_2$ side chain, instead of one signal of a methyl group at the pyran ring. The presence of this side chain was supported by the mass fragmentation ion at m/z 258 ($M^+ - CH_2CH_2CH{=}CMe_2$). Based on these spectroscopic data, structure **139a** was assigned to (+)-mahanimbine (111,133). Additional support for this assignment was derived from total synthesis and transformation into known carbazole derivatives (133) (Scheme 2.27).

In 1991, Wu reported the isolation of murrayamine-C (**141**) and murrayamine-B (**142**) from the leaves of *M. euchrestiolia* collected in Taiwan. Both alkaloids were obtained from Nature in racemic form (115) (Scheme 2.28). One year later, the same group reported the isolation of a structurally different carbazole from the fruits of the same natural source and gave an identical name, murrayamine-C* (**140**). This alkaloid was also obtained in racemic form (134) (Scheme 2.27). In 1979, Chakraborty *et al*. assigned the same structure to mahanimboline, which was isolated from the root bark of *M. koenigii* (135). A close comparison of the spectroscopic data of mahanimboline with those of murrayamine-C* (**140**) showed that they were different alkaloids. Therefore, mahanimboline must have another structure, which is yet to be assigned (134).

The UV spectrum (λ_{max} 222, 238, 278, 288, 327, 342, and 358 nm) of murrayamine-C* (**140**) resembled that of girinimbine (**115**) (see Scheme 2.22), indicating the presence of a similar 3-methylpyranocarbazole. The ^{1}H-NMR spectrum differs from that of girinimbine (**115**) only in the presence of signals at δ 1.70 as a singlet for an allylmethyl (3*H*), δ 4.83 and 4.93 as singlets for the vinyl protons (2*H*),

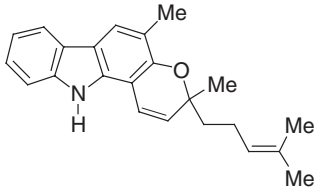

139a (+)-Mahanimbine
139b (±)-Mahanimbine

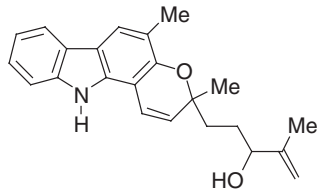

140 Murrayamine-C*
(Mahanimboline)

Scheme 2.27

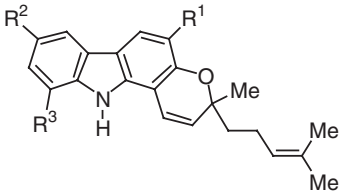

141 Murrayamine-C
R^1 = H; R^2 = Me; R^3 = OMe
142 Murrayamine-B
R^1 = Me; R^2 = H; R^3 = OMe
143 Murrayacinine
R^1 = CHO; R^2,R^3 = H
144 Murrayamine-N
R^1 = H; R^2 = CHO; R^3 = OMe

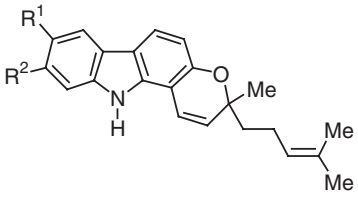

145 Murrayamine-J
R^1 = CHO; R^2 = H
146 (–)-Isomahanimbine
R^1 = Me; R^2 = H
147 (+)-Mahanimbicine
R^1 = Me; R^2 = H

Scheme 2.28

δ 4.07 as a multiplet for a carbinol proton (1*H*), and δ 1.79 as a multiplet for the vicinal methylene protons (4*H*) of the side chain $-CH_2CH_2CH(OH)C(Me)=CH_2$. These signals replace the signal of one of the methyl groups on the pyran ring in the ^{1}H-NMR spectrum of girinimbine (**115**). The presence of this side chain was confirmed by proton decoupling experiments and the mass fragmentation ion at m/z 248 ($M^+ - CH_2CH_2CH(OH)C(Me)=CH_2$). Based on these spectral data, structure **140** was assigned to murrayamine-C*. This structure was further supported by the difference NOE experiment (134) (Scheme 2.27).

The UV spectrum (λ_{max} 241, 274, 285, 340, and 353) of murrayamine-C (**141**) indicates the presence of a 1,7-dioxygenated carbazole chromophore. This was confirmed by the IR spectrum. The ^{1}H-NMR spectrum showed a similar C-ring substitution pattern with that of pyrayafoline D (**138**) (see Scheme 2.26). However, the A-ring substitution pattern was completely different. Thus, the ^{1}H-NMR spectrum showed the presence of an aromatic methyl at δ 2.49, an aromatic methoxy at δ 3.97, and two aromatic singlets at δ 7.33 for a deshielded C-4 proton and at δ 6.65 for a shielded C-2 proton. Based on these spectral data, and the similarity with the C-ring substitution pattern of pyrayafoline D, the structure **141** was assigned to murrayamine-C. This structure was further supported with the ^{13}C-NMR data, as well as NOE experiments (115).

The UV (λ_{max} 272, 283, 330, 341, and 357 nm) and IR (ν_{max} 1580, 1645, and 3433 cm^{-1}) spectra of murrayamine-B (**142**) resembled those of (+)-mahanimbine (**139a**) (see Scheme 2.27) indicating the presence of a similar 3-methylpyranocarbazole framework. The ^{1}H-NMR spectrum differs from that of (+)-mahanimbine (**139a**) only in the C-ring substitution pattern of the carbazole nucleus. Thus, the ^{1}H-NMR spectrum showed the presence of an aromatic methoxy group at δ 4.0 and, in the aromatic region, three, mutually *ortho*-coupled (J=7.8 Hz) C-5, C-6, and C-7 protons at δ 7.52, 7.10, and 6.81, respectively, suggesting the presence of a methoxy group at C-8. Based on these spectral data, and the structural similarity with that of (+)-mahanimbine, the structure **142** was assigned to murrayamine-B. This structure was further supported by NOE experiments (115).

In 1974, Chakraborty *et al.* reported the isolation of murrayacinine (**143**), a formyl analog of (±)-mahanimbine (**139b**) from the stem bark of *M. koenigii*. The absolute configuration of this isolate is also not known (77). The UV (λ_{max} 234, 280, 301, and 312 nm) and IR (ν_{max} 1590, 1610, 1670, and 3360 cm^{-1}) spectra of murrayacinine (**143**) showed the presence of a 3-formylcarbazole framework. On borohydride reduction, murrayacinine gave the corresponding alcohol, the UV spectrum of which resembled that of (±)-mahanimbine (**139b**) (see Scheme 2.27) and confirmed it to be a formyl analog of (±)-mahanimbine (**139b**). This structure was also supported by the mass fragmentation ions at *m/z* 262 ($M^+-CH_2CH_2CH=CMe_2$) and 234 ($M^+-CH_2CH_2CH=CMe_2-CO$). Based on these spectral data and comparison with the known UV data of (±)-mahanimbine (**139b**) and 3-formylcarbazole, structure **143** was assigned to murrayacinine. Further support for this structure comes from its synthesis (77).

In 1996, Wu *et al.* reported the isolation of murrayamine-N (**144**) and murrayamine-J (**145**) from the leaves of *M. euchrestifolia* collected in November. The absolute configurations of these alkaloids are not assigned (130). The UV [λ_{max} 248, 271 (sh), 289, 300, and 313 nm] and IR (ν_{max} 1590, 1668, 1750, and 3333 cm^{-1}) spectra of murrayamine-N (**144**) were similar to those of murrayamine-C (**141**) indicating the presence of a similar pyranocarbazole chromophore. The ^{1}H-NMR spectrum differs from that of murrayamine-C (**141**) only in the presence of a C-3 formyl group at δ 10.03 instead of the aromatic methyl group. The presence of a formyl group at C-3 was unequivocally confirmed by the downfield shift of the C-4 (δ 8.07) and C-2 (δ 7.41) protons by about 0.75 ppm as compared to the C-4 (δ 7.33) and C-2 (δ 6.65) protons of murrayamine-C. Based on these spectral data, structure **144** was assigned to murrayamine-N. This structure was further supported by the NOE experiments (130).

The UV (λ_{max} 243, 267, 290, 311, and 346 (sh) nm) and IR (ν_{max} 1575, 1646, 1667, 2856, and 3331 cm^{-1}) spectra of murrayamine-J (**145**) resembled those of murrayamine-N (**144**), indicating the presence of a similar 3-formylpyranocarbazole chromophore. The ^{1}H-NMR spectrum differs from that of murrayamine-N (**144**) only in the A-ring substitution pattern of the carbazole nucleus. In the aromatic region, H-4 (δ 8.46) and H-2 (δ 7.89) were mutually *meta*-coupled (J=1.7 Hz), indicating the presence of a formyl group at C-3. This assignment was supported by the signal for H-1, which appeared as a doublet at δ 7.44 with an *ortho*-coupling (J=8.4 Hz). Based on these spectroscopic data and the similarity to murrayamine-N, structure **145** was assigned to murrayamine-J (130).

In 1970, Joshi *et al.* reported the isolation of (−)-isomahanimbine (**146**), a methyl analog of murrayamine-J (**145**) from the leaves of *M. koenigii*. Although, murrayamine-J (**145**) was isolated from Nature in optically active form ($[\alpha]_D$ −6, *c* 2.1, $CHCl_3$), the absolute configuration is still not known (110). In the same year, Kapil *et al.* isolated the opposite enantiomer ($[\alpha]_D^{30}$ + 18.6, *c* 0.86, $CHCl_3$) from the same source and named it (+)-mahanimbicine (**147**). The absolute configuration of this alkaloid is also unknown (136).

The UV (λ_{max} 238, 281, 290, 335, and 354 nm) and IR (ν_{max} 1580, 1600, 1638, 3410, and 3440 cm^{-1}) spectra of (−)-isomahanimbine (**146**) were similar to those of murrayamine-C (**141**) (see Scheme 2.28) indicating the presence of a similar pyranocarbazole framework. The ^{1}H-NMR spectrum indicated a similar C-ring substitution pattern with that of murrayamine-C (**141**) (see Scheme 2.28). However,

the A-ring substitution pattern was completely different. Thus, in the aromatic region, H-1 (δ 7.15) and H-2 (δ 7.05) were mutually *ortho*-coupled (J=8.0 Hz), and H-4 appeared as a broad singlet at δ 7.68, indicating the presence of a methyl group at C-3. The position of the methyl group was supported by the *meta*-coupling (J=1.0 Hz) of H-2. Based on these spectroscopic data, structure **146** was assigned to (−)-isomahanimbine. Additional support for this structure was derived from the transformation into known carbazole derivatives (110).

In 1970, Narasimhan *et al.* described the isolation of (−)-mahanine (**148**) in optically active form ($[\alpha]_D$ −24.4) from the leaves of *M. koenigii* (113,133). Three decades later, Nakatani *et al.* isolated from the same natural source the opposite enantiomer, (+)-mahanine (**149**) (88). In 1999, Ramsewak *et al.* reported the isolation of mahanine from the leaves of the same natural source. However, its absolute configuration was not mentioned (137). In 1991, Wu reported the isolation of (+)-mahanine (**149**) from a different *Murraya* species, *M. euchrestifolia* (115). This alkaloid showed a specific rotation of $[\alpha]_D$ +34 (*c* 2.0, $CHCl_3$), and its CD spectrum displayed a positive Cotton effect in the region of 265–276 nm due to the styrene chromophore, indicating a negative chirality of the pyranocarbazole ring system. Therefore, the absolute configuration of (+)-mahanine (**149**) was *S* at C-3′. Consequently, (−)-mahanine (**148**) has an *R* configuration (115). In 2002, (+)-mahanine (**149**) was also isolated by Nakahara *et al.* from the twigs of *Micromelum minutum* (138). This alkaloid showed a wide variety of biological activities, including cytotoxicity against the tumor cell line HL60 (131,138), antimutagenicity against heterocyclic amines such as 3-amino-1,4-dimethyl-5*H*-pyrido[4,3-*b*]indole (Trp-P-1), and antimicrobial activity against *Bacillus cereus* and *Staphylococcus aureus* (138).

The UV spectrum [λ_{max} 221, 240, 285 (sh), 294, 342, and 357 nm] of (+)-mahanine (**149**) resembled that of murrayamine-A (**120**) (see Scheme 2.22), indicating the presence of a similar pyranocarbazole framework. This assignment was supported by the IR spectrum. The ^{1}H-NMR spectrum differs from that of murrayamine-A only by the signals at δ 1.73 (2*H*, t), 2.14 (2*H*, m), 5.10 (1*H*, t), 1.57 (3*H*, s), and 1.65 (3*H*, s) resulting from the side chain $-CH_2CH_2CH{=}CMe_2$, which replaces one of the methyl groups on the pyran ring of murrayamine-A (**120**). The presence of this side chain was supported by the mass fragmentation ion at m/z 264 ($M^+ - CH_2CH_2CH{=}CMe_2$). Based on these spectral data, structure **149** was assigned to (+)-mahanine (115) (Scheme 2.29).

In 2003, Nakatani *et al.* reported the isolation of *O*-methylmahanine (**149a**) from the leaves of *M. koenigii* (116). Although this alkaloid was isolated in optically active form ($[\alpha]_D^{25}$ + 3.0, *c* 0.10, $CHCl_3$), the absolute configuration is unknown. *O*-Methylmahanine (**149a**) showed radical scavenging activity against 1,1-diphenyl-2-picrylhydrazyl (DPPH) radical (116). Prior to its isolation, the same compound was known synthetically in racemic form as DL-*O*-methylmahanine (139).

The UV spectrum [λ_{max} 221, 241, 285 (sh), 296, 343, and 358 (sh) nm] of *O*-methylmahanine (**149a**) resembled that of (+)-mahanine (**149**), indicating a similar pyranocarbazole framework. This conclusion was supported by the IR spectrum. The ^{1}H-NMR spectrum differs from that of (+)-mahanine (**149**) only in the presence of an aromatic methoxy group at δ 3.88 instead of the hydroxy group. This assignment was confirmed by the ^{13}C-NMR signal at δ 55.7. Based on these spectral data, structure **149a** was assigned to *O*-methylmahanine (116) (Scheme 2.29).

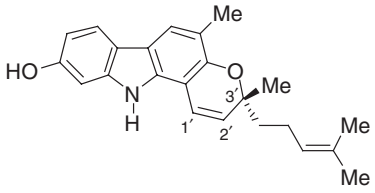

148 (–)-Mahanine

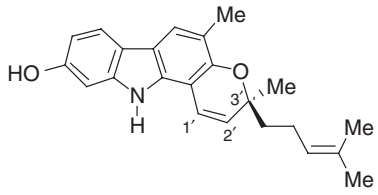

149 (+)-Mahanine

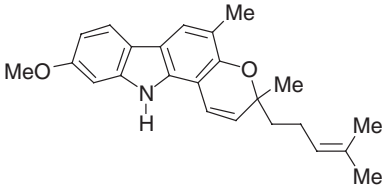

149a *O*-Methylmahanine

Scheme 2.29

2 Cyclic Monoterpenoid Pyrano[3,2-*a*]carbazole Alkaloids

In 1969, Dutta *et al.* reported the isolation of a pentacyclic pyrano[3,2-*a*]carbazole alkaloid (currayanin) from *M. koenigii* and assigned its structure as **150** (140,141). This alkaloid was obtained from Nature in racemic form (141). The name currayanin derives from the vernacular name of this plant: currypatta or curry-leaf tree. One year later, Chakraborty *et al.* described the isolation of the same alkaloid from the stem bark of the same source in optically active form ($[\alpha]_D^{30} + 20$, $CHCl_3$) and named it murrayazolidine (142). In 1969, Kapil *et al.* isolated from the leaves of *M. koenigii* a pentacyclic pyrano[3,2-*a*]carbazole alkaloid cyclomahanimbine (**151**) in racemic form (143). In 1974, Bandaranayake *et al.* achieved the synthesis of cyclomahanimbine (**151**) by heating (±)-mahanimbine (**139**) (see Scheme 2.27) in benzene under reflux in the presence of an ion-exchange resin (Dowex-50W-X8, H^+) (144). Independently, Bandaranayake and Narasimhan *et al.* examined the structure of optically active murrayazolidine and racemic currayanin and reassigned the structure as **151** (141,144). In 1983, Furukawa *et al.* reported the relative stereochemistry of cyclomahanimbine based on the X-ray structure of (±)-murrafoline (**178**) (see Scheme 2.38) which is a C–C dimer of girinimbine (**115**) (see Scheme 2.22) and cyclomahanimbine (145,146). Two years later, the same authors reported the isolation of racemic cyclomahanimbine from the root bark of *M. euchrestifolia* (29). In 1974, Chakraborty *et al.* revised the structure of optically active murrayazolidine to racemic cyclomahanimbine (**151**) (147) (Scheme 2.30). In 1992, Reisch *et al.* also reported the isolation of murrayazolidine (**151**), which was identical with cyclomahanimbine and curryanin, from the fruits of *M. koenigii* and confirmed the relative stereochemistry by X-ray analysis (71).

The UV spectrum (λ_{max} 246, 251, 257, 307, and 341 nm) of cyclomahanimbine (**151**) indicates the presence of a carbazole framework with an ether oxygen at C-2. This assignment was supported by the IR spectrum [ν_{max} 1602, 1615 (aromatic system), and 3425 (NH) cm^{-1}]. On hydrogenation, cyclomahanimbine yielded the corresponding dihydro derivative, which did not show any shift of the absorption

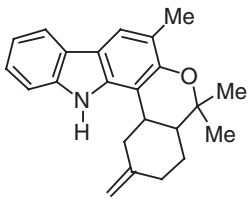

150

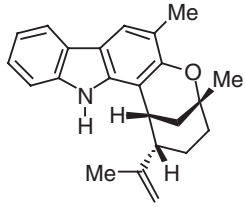

151 Cyclomahanimbine
(Murrayazolidine,Curryanin)

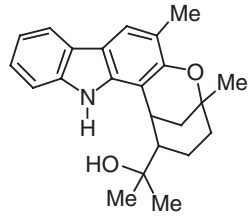

152 Murrayazolinine

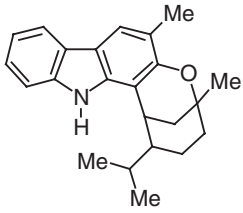

153 Exozoline

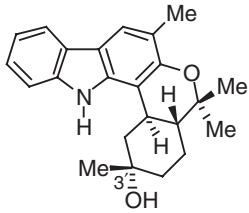

154 Murrayamine-O

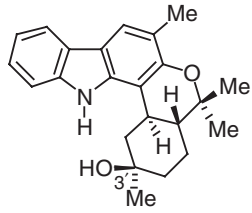

155 Murrayamine-P

Scheme 2.30

maxima, indicating that the double bond in the alkaloid is not conjugated with the carbazole system. The ^{1}H-NMR spectrum resembled that of (+)-mahanimbine (**139a**) (see Scheme 2.27). However, cyclomahanimbine showed two additional vinylic protons at δ 4.72, a vinylic methyl group at δ 2.33, and a benzylic methine proton at δ 3.11. These spectral data, and the characteristic mass fragmentation at m/z 248 (M^+-83), indicated the presence of a 2,2-substituted pyran system. Based on these spectroscopic data, structure **151** was assigned to cyclomahanimbine (143). This structural assignment was supported by two independent syntheses, starting from murrayazoline (**163a**) (see Scheme 2.32) and (+)-mahanimbine (**139a**) (see Scheme 2.27) (141,143,144,148), and by transformation into known carbazole derivatives (143), as well as X-ray analysis (71).

In 1973, Chakraborty *et al*. reported the isolation of murrayazolinine (**152**) from the stem bark of *M. koenigii*. The absolute configuration of murrayazolinine is not known (148). The UV (λ_{max} 240, 253, 258, and 304 nm) and IR [ν_{max} 1610, 1630 (aromatic system), and 3400 (NH) cm^{-1}] spectra of murrayazolinine (**152**) resembled those of cyclomahanimbine (**151**), indicating a similar carbazole framework. The ^{1}H-NMR spectrum differs from that of cyclomahanimbine only by the presence of a hydroxy isopropyl group instead of the vinylic methyl group. This conclusion was supported by the IR band at 3250 (OH) cm^{-1}, as well as by the isolation of acetone during the chromic acid oxidation of murrayazolinine. The presence of a $-CH_2CH_2CHC(OH)(Me)_2$ group annulated at the dihydropyran ring was confirmed by the mass fragmentation ion at m/z 248 ($M^+-CH_2CH_2CHC(OH)(Me)_2$). Based on these spectral data, structure **152** was assigned to murrayazolinine. Direct support for this structure derived from dehydration of murrayazolinine (**152**) with phosphorous oxychloride to murrayazoline (**163a**) (see Scheme 2.32).

In 1978, Ganguly and Sarkar reported the isolation of exozoline (**153**) from the leaves of *M. exotica* (149). The UV (λ_{max} 242, 256, and 306 nm) and IR [ν_{max} 1615, 1625 (aromatic system), and 3440 (NH) cm^{-1}] spectra of exozoline (**153**) resembled those of cyclomahanimbine (**151**), indicating a similar carbazole framework. The ^{1}H-NMR spectrum of exozoline is similar to that of cyclomahanimbine, but showed a six-proton doublet at δ 0.62 instead of the signals for the isopropenyl group. Based on the spectral data, the structure of exozoline (**153**) was confirmed as dihydrocyclomahanimbine. This assignment was supported by the superimposable IR spectrum of dihydrocyclomahanimbine obtained by hydrogenation of cyclomahanimbine (**151**).

In 1995, Wu *et al.* reported the isolation of two C-3′ epimeric, cannabinol-skeletal carbazole alkaloids, murrayamine-O (**154**) and murrayamine-P (**155**) from the root bark of *M. euchrestifolia* (150). Although these two diasteromeric alkaloids were obtained in optically active form ($[\alpha]_D$ –137.6, *c* 0.07, $CHCl_3$) and ($[\alpha]_D$ +92, *c* 0.015, $CHCl_3$), respectively, their absolute configuration is not known. However, the relative configuration was assigned based on 2D-NMR studies (150). In the same year, Wu *et al.* also reported the isolation of murrayamine-D (**156**) from the leaves of the same plant collected in winter (February). This alkaloid contains the same bicyclic terpenoid skeleton as murrayazolidine (**151**), but has a hydroxy group at C-7 of the carbazole nucleus. Therefore, murrayamine-D (**156**) is a 7-hydroxymurrayazolidine. The absolute configuration of murrayamine-D is not known (151). One year later in spring (May), the same group isolated from the leaves of *M. euchrestifolia* murrayamine-H (**157**), murrayamine-F (**158**), and murrayamine-G (**159**). The absolute configuration of these alkaloids is still not known (125). The plant shows strong seasonal variations of carbazole alkaloids. Therefore, the pharmacological activity of the extracts from this traditional Chinese medicinal plant is dependent on the collection time, which may be explained by the variation of the biologically active carbazole alkaloids (125) (Scheme 2.31).

The UV spectrum [λ_{max} 240, 254, 258 (sh), 304, 319 (sh), and 332 nm] of murrayamine-O (**154**) indicates a 2-oxygenated carbazole. This assignment was confirmed by the IR spectrum [ν_{max} 1614 (aromatic system), 3200 (OH), and 3450 (NH) cm^{-1}]. The presence of a hydroxy group was supported by the mass fragmentation ion at *m*/*z* 248 $(M^+-18)\cdot$ The ^{1}H-NMR spectrum showed the presence

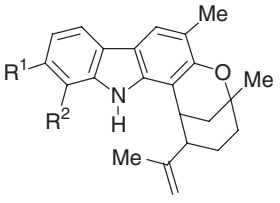

156 Murrayamine-D
(7-Hydroxymurrayazolidine)
R^1 = OH; R^2 = H

157 Murrayamine-H
R^1 = H; R^2 = OMe

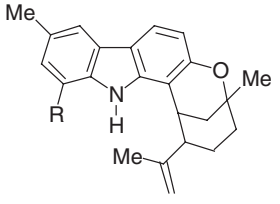

158 Murrayamine-F
R = OMe

159 Murrayamine-G
R = H

Scheme 2.31

of a broad singlet for an NH proton at δ 8.61. In the aromatic region, a downfield singlet at δ 7.59 for H-4, and four, mutually-coupled protons at δ 7.07, 7.20, 7.33, and 7.84 for H-6, H-7, H-8, and H-5, respectively, indicated a 1,3-disubstituted-2-oxygenated carbazole framework. The aromatic methyl group, supported by a characteristic signal at δ 2.22, was located at C-3. Nine of the eleven double bond equivalents corresponded to the carbazole nucleus. The lack of olefinic protons indicated that the additional two double bond equivalents were due to two rings. Based on ^{13}C-NMR, DEPT, and QUAT (unprotonated ^{13}C-nuclear only) spectra of murrayamine-O (**154**), the remaining skeleton consisted of ten carbon atoms: three methyl groups, three methylene groups, two methine carbons, and two quaternary carbons, suggesting a 3′-hydroxy-3′,7′,7′-trimethyloxadecalin ring fused to C-1 and C-2 of ring A of the carbazole. This assignment was confirmed by HMBC and COSY spectra. The relative configurations were confirmed by the splitting patterns, coupling constants, and NOESY experiments. Based on the spectroscopic data, structure **154** was assigned to murrayamine-O (150) (Scheme 2.30).

The UV [λ_{max} 240, 254, 257 (sh), 304, 319 (sh), and 331 nm] and IR (ν_{max} 1609, 3377, and 3522 cm^{-1}) spectra of **155** resembled those of murrayamine-O (**154**), indicating a similar carbazole framework. The ^{1}H-NMR and ^{13}C-NMR spectra of murrayamine-P were also similar to those of murrayamine-O (**154**), except for the NOESY correlations. This assignment was confirmed by an HMBC spectrum, which emphasized that murrayamine-P differed from murrayamine-O only by the relative configuration at C-3′. Therefore, structure **155** was assigned to murrayamine-P (150) (Scheme 2.30).

The UV (λ_{max} 239, 266, 315, and 324 nm) and IR [ν_{max} 1620 (aromatic system), and 3429 (NH) cm^{-1}] spectra of murrayamine-D (**156**) resembled those of murrayazolidine (**151**) (see Scheme 2.30) indicating a similar carbazole framework. The ^{1}H-NMR spectrum confirmed the same A-ring substitution pattern as that of murrayazolidine (**151**). However, the C-ring substitution pattern was completely different. Thus, in the aromatic region, H-5 (δ 7.69) and H-6 (δ 6.65) were mutually *ortho*-coupled (J=8.4 Hz), and H-8 (δ 6.78) was only *meta*-coupled (J=2.2 Hz), indicating C-7 as the position of the hydroxy group. The location of the hydroxy group was confirmed by the *meta*-coupling (J=2.2 Hz) of H-5 with H-8. The presence of a hydroxy group was supported by a broad IR band between 3200 and 3600 cm^{-1}. Based on the spectral data, the structure of murrayamine-D (**156**) was assigned as 7-hydroxymurrayazolidine. This assignment was confirmed by NOE experiments (151) (Scheme 2.31).

The UV (λ_{max} 243, 255, 301, and 329 nm) and IR [ν_{max} 1580, 1628 (aromatic system), and 3435 (NH) cm^{-1}] spectra of murrayamine-H (**157**) resembled those of murrayamine-D (**156**) indicating a similar carbazole framework. The ^{1}H-NMR spectrum showed a close similarity to murrayamine-D, except for the carbazole C-ring substitution pattern which confirmed the presence of an aromatic methoxy group at δ 3.99, instead of the aromatic hydroxy group. Thus, in the aromatic region, H-5, H-6, and H-7 were mutually *ortho*-coupled (J=7.8 Hz) at δ 7.50, 7.06, and 6.78, respectively, indicating that the position of the methoxy group is at C-8. The downfield shift of H-5 at δ 7.50, along with the *meta*-coupling (J=1.2 Hz) to H-7, confirmed the position of the methoxy group. Based on these spectral data, structure **157** was assigned to murrayamine-H. This structural assignment was supported by NOE experiments (125).

The UV spectrum [λ_{max} 244, 256 (sh), 303, and 328 (sh) nm] of murrayamine-F (**158**) is very similar to that of murrayamine-H (**157**) indicating a similar carbazole framework. This assignment was supported by the IR spectrum. The ^{1}H-NMR spectrum showed similar substituents, including an aromatic methyl group at δ 2.49, an aromatic methoxy group at δ 3.97, and a bicyclic ring with isopropenyl and methyl substituents. However, the aromatic methyl and methoxy substituents were in different positions as compared to murrayamine-H (**157**). Besides these substituents, the aromatic region showed two, *ortho*-coupled (J=8.4 Hz) doublets at δ 7.69 and 6.70, assigned to H-5 and H-6, respectively. Furthermore, two, *meta*-coupled protons appeared as broad singlets at δ 6.62 and 7.32, assigned to H-2 and H-4, respectively. The chemical shift and the coupling pattern of the signals for the aromatic protons confirmed structure **158** for murrayamine-F. This assignment was supported by an NOE difference spectrum (125).

The UV (λ_{max} 241, 262, and 307 nm) and IR [ν_{max} 1617 (aromatic system), and 3465 (NH) cm^{-1}] spectra of murrayamine-G (**159**) resembled those of murrayamine-F (**158**), indicating a similar carbazole framework. The ^{1}H-NMR spectrum was also similar to that of murrayamine-F, but the signal for the methoxy group was absent. In the aromatic region, H-4 (δ 7.71) showed a *meta*-coupling (J=1.0 Hz) with H-2 (δ 7.10), which had an additional *ortho*-coupling (J=8.3 Hz) with H-1 (δ 7.22), indicating the position of the aromatic methyl group at C-3, as in murrayamine-F. Based on these spectroscopic data, structure **159** was assigned to murrayamine-G. This assignment was supported by NOE experiments (125) (Scheme 2.31).

In 1969, Kapil *et al*. reported the isolation of bicyclomahanimbine (**160**) from the leaves of *M. koenigii*. Although, bicyclomahanimbine was isolated in optically active form $[\alpha]_D^{23}$ − 1.23 ($CHCl_3$), the absolute configuration is not known (143). One year later, the same authors isolated from the same natural source bicyclomahanimbicine (**161**), an isomer of bicyclomahanimbine (**160**). The absolute configuration of this alkaloid is also not known (136). Four years after their isolation, Bandaranayake *et al*. revised the original structure of these alkaloids (144). In 1995, Wu *et al*. reported the isolation of bicyclomahanimbine (**160**) from the leaves of a different *Murraya* species, *M. euchrestifolia* (151) (Scheme 2.32).

The UV spectrum (λ_{max} 242, 255, 260, and 305 nm) of bicyclomahanimbine (**160**) shows the typical absorption of a 2-hydroxy-3-methylcarbazole skeleton. This assignment was supported by the IR spectrum [ν_{max} 1605, 1625 (aromatic system), and 3455 (NH) cm^{-1}]. The aromatic region of the ^{1}H-NMR spectrum resembled that of (±)-mahanimbine (**139b**) (see Scheme 2.27) and cyclomahanimbine (**151**) (see Scheme 2.30), indicating a similar aromatic substitution pattern on the carbazole framework. However, the monoterpene moiety fused at C-1 and C-2 was different. In consideration of the molecular formula, and the absence of two double bonds present in (±)-mahanimbine (**139b**), bicyclomahanimbine (**160**) was proposed as a hexacyclic base with a cyclobutane system. The presence of a cyclobutane ring was supported by the downfield shift (Δ −0.72) of the methyl group at δ 0.71 in bicyclomahanimbine when compared to the methyl group of (±)-mahanimbine at δ 1.43 (29). Based on these spectroscopic data and the structural similarity to cannabicyclol, which was determined by X-ray analysis, structure **160** was assigned to bicyclomahanimbine (143,144).

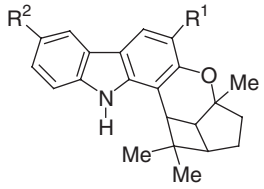

160 Bicyclomahanimbine
R^1 = Me; R^2 = H

161 Bicyclomahanimbicine
R^1 = H; R^2 = Me

162 Murrayamine-M
R^1 = H; R^2 = CHO

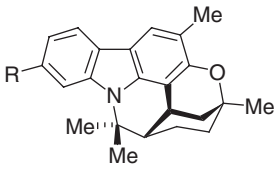

163a Murrayazoline
(Mahanimbidine,Curryangin)
R = H

163b (+)-Murrayazoline
R = H

164 Murrayamine-E
(7-Hydroxymurrayazoline)
R = OH

Scheme 2.32

The UV (λ_{max} 243, 257, 263, and 305 nm) and IR [ν_{max} 1610 (aromatic system), and 3445 (NH) cm^{-1}] spectra of bicyclomahanimbicine (**161**) resembled those of bicyclomahanimbine (**160**) indicating a similar carbazole framework. The ^{1}H-NMR spectrum showed similar substituents, including an aromatic methyl group at δ 2.51 and a dihydropyran ring. However, the position of the aromatic methyl group was different. The aromatic region showed the presence of two *ortho*-coupled (J=8.0 Hz) doublets at δ 7.76 and 6.74, assigned to H-5 and H-6, respectively. Furthermore, a *meta*-coupled proton appeared as a broad singlet at δ 7.76 and was assigned to H-4, and a two-proton multiplet at δ 7.21 to H-1 and H-2. The chemical shifts and the coupling patterns of the signals in the aromatic region, as well as the similarity to bicyclomahanimbine, led to structure **161** for bicyclomahanimbicine (136,144).

In 1996, Wu *et al*. reported the isolation of murrayamine-M (**162**), a formyl analog of bicyclomahanimbicine (**161**) from the leaves of *M. euchrestifolia* collected in November in Taiwan. The UV spectrum [λ_{max} 243, 254 (sh), 292, and 325 nm] of murrayamine-M (**162**) indicated a 3-formylcarbazole. This assignment was supported by the IR spectrum [ν_{max} 1605 (aromatic system), 1675 (CHO), and 3300 (NH) cm^{-1}]. The ^{1}H-NMR spectrum resembled that of bicyclomahanimbicine (**161**), but exhibited a formyl group (δ 10.08) at C-3 instead of the aromatic methyl group. The deshielded *meta*-coupled (J=1.7 Hz) H-4 at δ 8.48 confirmed the position of the formyl group at C-3. Based on the spectral data, structure **162** was assigned to murrayamine-M (Scheme 2.32). The absolute configuration of **162** is not known (130).

In 1969, Dutta *et al*. isolated curryangin (**163a**) from the stem bark of *M. koenigii* in racemic form (152). In the same year, Kapil *et al*. described the isolation of the same alkaloid, also as a racemate, from the leaves of *M. koenigii* and named it mahanimbidine (**163a**) (143). In 1972, Chakraborty *et al*. reported the third isolation of this structure from *M. koenigii* and named it murrayazoline (**163a**). From the X-ray structure determination it was clear that this isolation again provided the natural product in racemic form (153). In 1985, Furukawa *et al*. isolated this alkaloid in optically active form ($[\alpha]_D$ +2.25, $CHCl_3$) from the root bark of *M. euchrestifolia* and named it (+)-murrayazoline (**163b**). However, the absolute configuration has not been determined (29).

The UV spectrum (λ_{max} 239, 266, and 308 nm) of murrayazoline (**163a**) indicated a 2-oxygenated carbazole. The ^{1}H-NMR spectrum showed the presence of three methyl singlets at δ 1.26, 1.43, and 1.90, which are typical of methyl groups attached to carbon bearing an electronegative atom, and a fourth singlet at δ 2.33 for an aromatic methyl group. Along with these four methyl groups, a benzylic methine proton appeared as a broad multiplet at δ 3.33. The lack of an NH proton, and of olefinic protons, indicated the hexacyclic structure of this alkaloid with a carbazole *N*-atom common to two rings. Based on the spectral data and an X-ray analysis, structure **163a** was assigned to murrayazoline (153). This assignment was additionally supported by the synthesis of murrayazoline (**163a**) starting from (±)-mahanimbine (**139b**) (see Scheme 2.27) (141,143,152).

In 1995, Wu *et al.* reported the isolation of murrayamine-E (**164**) from the leaves of *M. euchrestifolia* collected in February in Taiwan. Murrayamine-E (**164**) was obtained in optically active form $[\alpha]_D$ –39.68 (*c* 0.133, $CHCl_3$). However, the absolute configuration was not determined. The relative stereochemistry was confirmed by a NOESY spectrum and an X-ray analysis (151). The UV spectrum [λ_{max} 245, 273, 316, and 335 (sh) nm] of murrayamine-E (**164**) indicated a 1-substituted-3-methyl-2,7-dioxygenated carbazole. This assignment was supported by the IR spectrum [ν_{max} 1608, 1623 (aromatic system), and 3358 (OH) cm^{-1}]. The ^{1}H-NMR spectrum differed from that of murrayazoline (**163a**) only in the substitution pattern of the carbazole C-ring by the presence of an additional aromatic hydroxy group at δ 4.70. From the aromatic splitting pattern of the carbazole C-ring, the hydroxy group was located at C-7. The aromatic region showed signals for two *ortho*-coupled (*J*=9.0 Hz) protons at δ 7.75 and 6.78, assigned to H-5 and H-6, respectively. Moreover, H-6 showed an additional *meta*-coupling (*J*=2.4 Hz) with H-8, which appeared at δ 6.99. Based on the spectral data, the structure of murrayamine-E (**164**) was assigned as 7-hydroxymurrayazoline (Scheme 2.32). Additional support for this assignment was derived from a NOESY spectrum and an X-ray crystal structure analysis (151) (Scheme 2.31).

In 1982, Chakraborty *et al.* reported the isolation of isomurrayazoline (**165**), a regioisomer of murrayazoline (**163a**) (see Scheme 2.32), from the stem bark of *M. koenigii*. This alkaloid was obtained from Nature in optically active form ($[\alpha]_D$ −7.33, $CHCl_3$). However, its absolute configuration is not known. The UV (λ_{max} 240, 253, 258, 303, and 330 nm) and IR [ν_{max} 1605 (aromatic system) cm^{-1}] spectra of isomurrayazoline (**165**) resembled those of murrayazoline (**163a**) (see Scheme 2.32), indicating a similar pyranocarbazole framework. The ^{1}H-NMR spectrum confirmed the similarity with signals for an aromatic methyl group at δ 2.35 and a hexacyclic carbazole ring. However, the methyl group was located at a different position on the carbazole framework. The aromatic region showed signals for five aromatic protons as a one-proton multiplet at δ 7.95, an unresolved two-proton doublet at δ 7.55, and a two-proton multiplet at δ 7.13–7.33. The aromatic substitution pattern was very similar to that of (−)-isomahanimbine (**146**) (see Scheme 2.28). Based on the spectroscopic data, structure **165** was assigned to isomurrayazoline. Additional proof for this assignment was obtained by the transformation of isomurrayazoline (**165**) to isomurrayazolinine by acid-catalyzed hydration (154) (Scheme 2.33).

In 1989, the same authors reported the isolation of murrayazolinol (**166**) from the same natural source as a minor carbazole alkaloid (155). In 1995, this alkaloid was also obtained by Ahmad as a minor carbazole alkaloid from the benzene extract of

the root bark of *Murraya exotica* (156). The absolute configuration of murrayazolinol (**166**) has not been determined (155,156).

The UV spectrum (λ_{max} 245, 265, and 305 nm) of murrayazolinol (**166**) is similar to that of murrayazoline (**163a**) (see Scheme 2.32), indicating a similar pyranocarbazole framework. The IR spectrum [ν_{max} 1350, 1380 (C-methyl), 1620, 1650 (aromatic system), 3360 (OH) cm^{-1}] confirmed the pyranocarbazole structure with an additional OH group. The ^{1}H-NMR spectrum of murrayazolinol exhibited signals for an aromatic methyl group at δ 2.34, and confirmed an aromatic substitution pattern similar to murrayazoline (**163a**). The difference was in the substitution of the monoterpenoid moiety. The ^{1}H-NMR spectrum of the monoterpenoid moiety of murrayazoline showed a signal for the carbinyl hydrogen of a secondary alcohol, which appeared as a doublet of doublets (J=7.2 Hz) at δ 3.80. The presence of a secondary hydroxy group was confirmed by the mass fragmentation ion at m/z 314 ($M^+-CH_3-H_2O$). Based on the spectroscopic data, structure **166** was assigned to murrayazolinol (155) (Scheme 2.33).

3 Pyrano[2,3-*a*]carbazole Alkaloids

In 1996, Ito *et al.* reported the isolation of clauszoline-A (**167**) and clauszoline-B (**168**) from the acetone extract of the stem bark of *C. excavata* collected in Singapore (74). These alkaloids represented the first, naturally occurring 2,8-dioxygenated-3-formylcarbazole alkaloids with a dimethylpyran ring fused to C-7 and C-8 of the carbazole nucleus. The extracts of the leaves and bark of this tree have been used in traditional medicine for the treatment of snakebites and abdominal pain (74). One year later, the same group isolated another pyrano[2,3-*a*]carbazole alkaloid, clauszoline-H (**169**), from the roots of the same natural source in Japan (47) (Scheme 2.34).

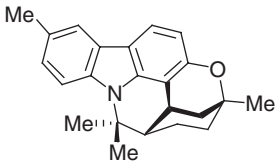

165 Isomurrayazoline

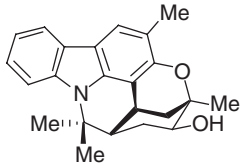

166 Murrayazolinol

Scheme 2.33

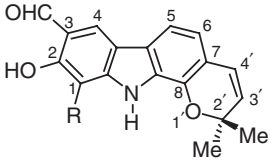

167 Clauszoline-A
R = prenyl

168 Clauszoline-B
R = H

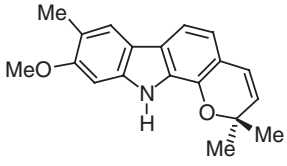

169 Clauszoline-H

Scheme 2.34

The UV spectrum (λ_{max} 240, 265, 306, and 375 nm) of clauszoline-A (**167**) indicated a carbazole framework. This assignment was supported by the IR spectrum [ν_{max} 1630 (aromatic system), 3440 (br) (OH), and 3450 (NH) cm^{-1}]. The ^{1}H-NMR spectrum showed signals for an NH at δ 8.31 (broad singlet), a strongly hydrogen-bonded hydroxy group at δ 11.64, a formyl group at δ 9.89, and a prenyl side chain (δ 1.79, 1.94, 3.65, and 5.36). The prenyl side chain was confirmed by the mass fragmentation ion at m/z 306 ($M^+-CH=CMe_2$). In the aromatic region, the deshielded singlet at δ 7.98 was assigned to H-4 based on the deshielding caused by the C-3 carbonyl group. The singlet for H-4 suggested the position of the hydroxy group at C-2 and of the prenyl side chain at C-1. Moreover, two, mutually *ortho*-coupled (J=7.7 Hz) proton signals at δ 7.44 and 6.90 were assigned to H-5 and H-6, indicating substitution at C-7 and C-8. The six-proton singlet at δ 1.53, together with symmetrical doublets at δ 5.63 and 6.48, suggested the presence of a 2,2-dimethyl-Δ^3-pyran ring. The fusion of the pyran ring at C-7 and C-8 of the carbazole nucleus was confirmed by an NOE enhancement between H-6 (δ 6.90) and H-4′ (δ 6.48). The 2,2-dimethyl-Δ^3-pyran ring was confirmed by the mass fragmentation ion at m/z 346 (M^+-Me), which could represent the carbazolo-pyrrylium ion. On the basis of these spectral data, structure **167** was assigned to clauszoline-A (74).

The UV [λ_{max} 242, 252 (sh), 264, 291 (sh), 304, and 376 nm] and IR [ν_{max} 1630 (aromatic system), 3300 (br) (OH), and 3450 (NH) cm^{-1}] spectra of clauszoline-B (**168**) resembled those of clauszoline-A (**167**), indicating a pyranocarbazole framework. The ^{1}H-NMR spectrum also showed a signal pattern similar to that of clauszoline-A, except for the presence of a high-field, one-proton singlet at δ 6.83, instead of signals for the prenyl side chain. Based on the spectroscopic data, structure **168**, representing a deprenylated clauszoline-A, was assigned to clauszoline-B. This assignment was supported by NOE experiments (74).

The UV spectrum [λ_{max} 230, 258, 288, 310, and 363 nm] of clauszoline-H (**169**) was very similar to that of clauszoline-B (**168**), indicating a pyranocarbazole. This assignment was supported by the IR spectrum. The ^{1}H-NMR spectrum of clauszoline-H (**169**) differs from that of clauszoline-B (**168**) only in the substituents at the A-ring of the carbazole nucleus. The ^{1}H-NMR spectrum showed signals for an aromatic methyl group at δ 2.34 and an aromatic methoxy group at δ 3.90, instead of a formyl group and a strongly hydrogen-bonded hydroxy group, as in clauszoline-B. Based on these spectral data, and additional support by NOE experiments, structure **169** was assigned to clauszoline-H (47).

4 Pyrano[2,3-*b*]carbazole Alkaloids

In 1991, Furukawa *et al*. reported the isolation of pyrayafoline B (**170**) from the stem bark of *M. euchrestifolia* collected in May in Taiwan (87). In the same year, the same group isolated a further pyrano[2,3-*b*]carbazole alkaloid, pyrayafoline E (**171**), from the stem bark of *M. euchrestifolia*. Pyrayafoline E was isolated from Nature in racemic form (70). These alkaloids are the first members of the naturally occurring 2,7-dioxygenated-3-methylcarbazole alkaloids having a dimethyl pyran ring fused to C-6 and C-7 of the carbazole nucleus (70,87) (Scheme 2.35).

The UV spectrum [λ_{max} 228, 252, 285, 296 (sh), 329, and 353 nm] of pyrayafoline B (**170**) indicated a carbazole framework. This assignment was supported by the IR spectrum. The ^{1}H-NMR spectrum showed a singlet for an NH proton at δ 7.70, a

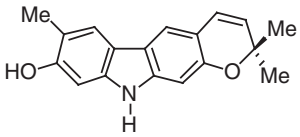

170 Pyrayafoline B

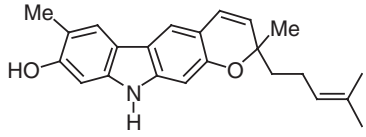

171 Pyrayafoline E

Scheme 2.35

broad singlet for a hydroxy group at δ 4.94, and a singlet for an aromatic methyl group at δ 2.37. A six-proton singlet at δ 1.46, assigned to the geminal dimethyl group at the pyran ring, and the symmetrical doublets at δ 5.58 and 6.48 indicated a 2,2-dimethyl-Δ^3-pyran ring. The presence of a 2,2-dimethyl-Δ^3-pyran ring was supported by the mass fragmentation ion at m/z 264 (M^+-Me), which could be represented by the carbazolopyrylium ion. Furthermore, the aromatic region showed the presence of four, one-proton singlets at δ 6.74, 7.62, 7.49, and 6.71. The two low-field singlets at δ 7.62 and 7.49 were assigned to H-4 and H-5, both deshielded by the carbazole nucleus. *O*-Methylation of pyrayafoline B with diazomethane gave the corresponding monomethyl ether, suggesting the presence of a phenolic group in pyrayafoline B. The spectral data of pyrayafoline B, supported by NOE experiments with the corresponding monomethyl ether, led to structure **170** for pyrayafoline B. This assignment was unequivocally confirmed by a spectroscopic comparison with the synthetic monomethyl ether of pyrayafoline B, obtained by a palladium(II)-mediated synthesis starting from 7-acetylaminochromene and 4-bromo-2-methoxy-toluene (87).

The UV [λ_{max} 233 (sh), 252, 284, 330 (sh), and 354 nm] and IR [ν_{max} 1625 (aromatic system), 3380 (br) (OH), and 3470 (NH) cm^{-1}] spectra of pyrayafoline E (**171**) resembled those of pyrayafoline B (**170**), indicating a similar pyranocarbazole framework. The ^{1}H-NMR spectrum differed from that of pyrayafoline B (**170**) only by the presence of signals at δ 1.70 (2*H*, m), 2.13 (2*H*, m), 5.10 (1*H*, t), 1.57 (3*H*, s), and 1.65 (3*H*, s), assigned to the $-CH_2CH_2CH=CMe_2$ side chain, instead of the signal for one of the methyl groups at the pyran ring of pyrayafoline B (**170**). The presence of this side chain was confirmed by the mass fragmentation ion at m/z 264 ($M^+-CH_2CH_2CH=CMe_2$). Based on the spectral data, structure **171** was assigned to pyrayafoline E (70) (Scheme 2.35).

5 Pyrano[2,3-*c*]carbazole Alkaloids

In 1989, Reisch *et al.* reported the isolation of glycomaurin (**172**) from the stem bark of *G. mauritiana*. This alkaloid represents the first example of a naturally occurring, 6-oxygenated-3-methylcarbazole having a dimethylpyran ring fused to the carbazole nucleus at C-5 and C-6 (100). In the following year, Ito and Furukawa isolated the same alkaloid from the root bark of *M. euchrestifolia* and named it eustifoline-A (101). Along with eustifoline-A (**172**), they also reported the isolation of the corresponding prenyl analog, eustifoline-B (**173**). The absolute configuration of this alkaloid is not known (101) (Scheme 2.36).

The UV spectrum (λ_{max} 232, 262, 273, 286, 314, 324, and 378 nm) of eustifoline-A (glycomaurin) (**172**) indicated a carbazole framework. This assignment was

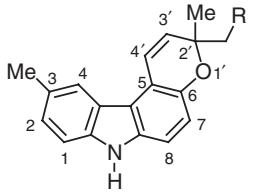

172 Eustifoline-A (Glycomaurin)
R = H

173 Eustifoline-B
R = prenyl

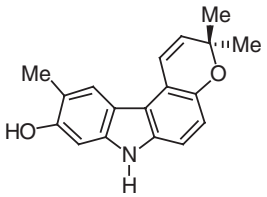

174 Glycoborinine

Scheme 2.36

supported by the IR spectrum. The ^{1}H-NMR spectrum showed a singlet for an NH proton at δ 10.06 and an aromatic methyl group at δ 2.48. In addition, a six-proton singlet at δ 1.45, assignable to the geminal dimethyl group of the pyran ring, and the symmetrical doublets at δ 5.90 and 7.36 indicated a 2,2-dimethyl-Δ^3-pyran ring. The presence of a 2,2-dimethyl-Δ^3-pyran ring was supported by the mass fragmentation ion at m/z 248 (M^+-Me). In the aromatic region, a deshielded, *meta*-coupled (J=0.7 Hz) doublet at δ 7.99 for H-4, and the mutually *ortho*-coupled (J=8.4 Hz) H-1 and H-2 at δ 7.36 and 7.19, respectively, suggested the position of the methyl group at C-3. Furthermore, H-2 at δ 7.19 showed a *meta*-coupling (J=0.7 Hz) with H-4, confirming the position of methyl substituent at C-3. For the carbazole C-ring, two, mutually *ortho*-coupled (J=8.4 Hz) protons at δ 6.84 and 7.25 indicated the fusion of the dimethylpyran ring at C-5 and C-6. The annulation of the pyran ring at C-5 and C-6 of the carbazole nucleus was confirmed by NOE experiments. Based on the spectroscopic data, structure **172** was assigned to eustifoline-A (101). This assignment was supported by the synthesis of **172** from glycozolinine (**91**), as well as glycomaurrol (**92**) (100) (see Scheme 2.17).

The UV spectrum (λ_{max} 230, 268, 304, 324, and 362 nm) of eustifoline-B (**173**) is very similar to that of eustifoline-A (glycomaurin) (**172**) indicating a similar pyranocarbazole. This assignment was supported by the IR spectrum. The ^{1}H-NMR spectrum signal pattern of eustifoline-B (**173**) was also similar to that of eustifoline-A, except for the presence of signals at δ 1.78 (2*H*, m), 2.17 (2*H*, m), 5.11 (1*H*, t), 1.58 (3*H*, s), and 1.65 (3*H*, s), assignable to the side chain $-CH_2CH_2CH=CMe_2$. The presence of this side chain was supported by the mass fragmentation ion at m/z 248 ($M^+-CH_2CH_2CH=CMe_2$). Based on these spectral data, structure **173** was assigned to eustifoline-B (101).

In 1999, Chakravarty *et al*. reported the isolation of glycoborinine (**174**) from the roots of *G. arborea* (62). The UV spectrum (λ_{max} 262, 269, 293, and 335 nm) of glycoborinine (**174**) resembled that of eustifoline-A (glycomaurin) (**172**), indicating a similar carbazole framework. The ^{1}H-NMR spectrum differed from that of eustifoline-A (**172**) only in the A-ring substitution pattern. In the aromatic region, H-4 (δ 7.79) and H-1 (δ 6.82) appeared as broad singlets, indicating the position of a methyl group at C-3 and a hydroxy group at C-2. Based on these spectral data, structure **174** was assigned to glycoborine. This assignment was supported by the ^{13}C-NMR, COSY, NOESY, HSQC, and HMBC spectra (62) (Scheme 2.36).

6 Pyranocarbazole-1,4-quinone Alkaloids

In 1985, Furukawa *et al.* reported the isolation of pyrayaquinone-A (**175**) and pyrayaquinone-B (**176**) from the root bark of *M. euchrestifolia* (157). Three years later, the same authors reported a further pyranocarbazole-1,4-quinone alkaloid, pyrayaquinone-C (**177**) from the root bark of the same natural source. The absolute configuration of this isolate is not known (22) (Scheme 2.37).

The UV [λ_{max} 220 (sh), 252, 308 (sh), and 460 nm] and IR (ν_{max} 1610, 1630, 1640, and 1660 cm^{-1}) spectra of pyrayaquinone-A (**175**) indicated the presence of a carbazole-1,4-quinone nucleus. The ^{1}H-NMR spectrum showed signals for a vinylic methyl group as a doublet (J=1.5 Hz) at δ 2.16, and an olefinic proton as a quartet (J=1.5 Hz) at δ 6.46, both having a long-range coupling. In addition, a six-proton singlet at δ 1.48, assigned to the geminal dimethyl group on the pyran ring, and the symmetrical doublets at δ 5.72 and 6.48 indicated a 2,2-dimethyl-Δ^3-pyran ring. The presence of a 2,2-dimethyl-Δ^3-pyran ring was supported by the mass fragmentation ion at m/z 278 (M^+-Me). In the aromatic region, H-5 appeared downfield (δ 7.79) as a singlet due to the deshielding effect of the C-4 carbonyl moiety. The upfield singlet at δ 6.83 was assigned to H-8. The chemical shifts and the splitting pattern of the signals in the aromatic region indicated the fusion of the pyran ring at C-6 and C-7 of the carbazole nucleus. The spectral data, combined with biogenetic considerations, suggested structure **175** for pyrayaquinone-A (157). Additional support for this assignment was derived from synthesis (157).

The UV [λ_{max} 229 (sh), 248, 295 (sh), and 410 nm] and IR (ν_{max} 1605, 1635, 1640, and 1650 cm^{-1}) spectra of pyrayaquinone-B (**176**) resembled those of pyrayaquinone-A (**175**) indicating a 3-methylcarbazole-1,4-quinone. The ^{1}H-NMR spectrum indicated similar substituents as for pyrayaquinone-A, including an aromatic methyl group at δ 2.14 and a 2,2-dimethyl-Δ^3-pyran ring, which was annulated at a different position. The aromatic region showed the presence of two *ortho*-coupled (J=9.0 Hz) doublet protons at δ 7.94 and 6.86, assigned to H-5 and H-6, respectively. The chemical shifts and the splitting pattern of the signals in the aromatic region, suggested structure **176** for pyrayaquinone-B (157). This assignment was supported by synthesis (157).

The UV spectrum [λ_{max} 248, 275 (sh), 294, and 392 nm] of pyrayaquinone-C (**177**) resembled that of pyrayaquinone-B (**176**) indicating a 3-methylcarbazole-1,4-quinone. This assignment was supported by the IR spectrum. The ^{1}H-NMR

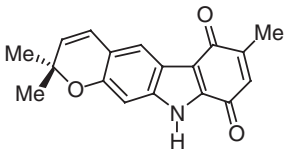

175 Pyrayaquinone-A

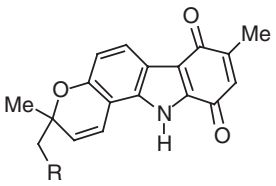

176 Pyrayaquinone-B
R = H

177 Pyrayaquinone-C
R = prenyl

Scheme 2.37

spectrum of pyrayaquinone-C (**177**) was also similar to that of pyrayaquinone-B, except for the presence of signals at δ 1.76 (2*H*, m), 2.12 (2*H*, m), 5.09 (1*H*, t), 1.56 (3*H*, s), and 1.65 (3*H*, s), assignable to the side chain $-CH_2CH_2CH{=}CMe_2$. The presence of this side chain attached to the pyran ring was confirmed by the mass fragmentation ion at m/z 278 ($M^+ - CH_2CH_2CH{=}CMe_2$). Based on the spectral data, structure **177** was assigned to pyrayaquinone-C (22) (Scheme 2.37).

C. Bis-Carbazole Alkaloids

The bis-carbazole alkaloids contain previously known monomeric carbazoles as structural subunits. All bis-carbazole alkaloids were isolated only from plants of the genus *Murraya*, until 1996, when clausenamine-A (**203**) (see Scheme 2.48) was isolated from the stem bark of *C. excavata*. The plant *M. euchrestifolia* is one of the richest sources of carbazole alkaloids. The bis-carbazoles often co-occur with monomeric carbazoles in the root bark, stem bark, and leaves of this plant (3,5–7,158,159). The aspect of atropisomerism for axially chiral, bis-carbazoles was considered only recently. Thus, in many cases it is not clear whether the isolated natural products are racemic or enantiomerically pure. Moreover, little attention has been paid to the relationship between their stereochemistry and biological activity.

In 1983, Furukawa *et al.* isolated the first bis-carbazole alkaloid, murrafoline-A [(±)-murrafoline] (**178**) from the root bark of *M. euchrestifolia*. Murrafoline-A consists of a dihydrogirinimbine unit (*cf.* girinimbine (**115**) Scheme 2.22) attached at C-12 to the C-8 of cyclomahanimbine (**151**) (see Scheme 2.30). Both monomeric carbazole alkaloids co-occur with murrafoline-A (**178**). This alkaloid was isolated from nature in racemic form. The complete structure and relative stereochemistry of murrafoline-A were confirmed by an X-ray analysis (145,146) (Scheme 2.38).

The UV spectrum [λ_{max} 243, 260 (sh), 307, and 332 (sh) nm] of murrafoline-A (**178**) indicated a carbazole framework. This assignment was supported by the IR spectrum. The ^{1}H-NMR spectrum showed signals for two aromatic methyl groups at δ 2.28 and 2.37, a vinylic methyl group at δ 1.54, three tertiary methyl groups at a carbon linked to an oxygen, a triplet and a multiplet at δ 4.58 and 3.24 due to benzylic protons, and overlapping unresolved signals for thirteen protons in the aromatic region between δ 6.70 and 7.90 (two of which disappeared on treatment with deuterated water). The mass fragmentation showed a peak at m/z 297 along with the molecular ion peak at m/z 594, confirming the presence of a bis-carbazole

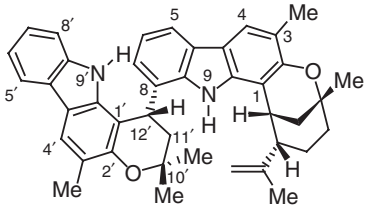

178 Murrafoline-A [(±)-Murrafoline]

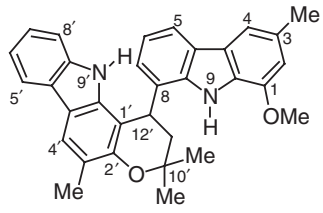

179 Murrafoline-B

Scheme 2.38

framework. Based on these spectral data and an X-ray analysis, the structure for murrafoline-A [(±)-murrafoline] was assigned as **178** (145).

From the same natural source, Furukawa *et al.* isolated in 1985 and 1993 further bis-carbazole alkaloids: murrafoline-B (**179**), -C (**180a**), -D (**181**) (146,160), -G (**182**), and -H (**183**) (146). In 2006, the same authors reported a further derivative of murrafoline, murrafoline-I (**180b**), from *M. koenigii* (131). Murrafoline-I (**180b**) induced apoptosis in HL-60 cells by activation of the caspase-9/caspase-3 pathway, through mitochondrial dysfunction (131). The common structural feature of all these murrafoline congeners is a dihydrogirinimbine attached at C-12 to a second carbazole moiety. All of these murrafolines were obtained from Nature as racemates (146,160) (Schemes 2.38–2.40).

The UV spectrum [λ_{max} 240, 292, 304, and 330 nm] of murrafoline-B (**179**) indicated the presence of a bis-carbazole framework. This assignment was supported by the IR spectrum, as well as the mass fragmentation which showed a peak at m/z 237 along with the molecular ion peak at m/z 474. The ^{1}H-NMR spectrum showed signals for one aromatic methoxy group at δ 3.87, two aromatic methyl groups at δ 2.48 and 2.49, and a dimethyldihydropyran ring (δ 2.30, 2.38, 4.69, 1.46, and 1.56). From decoupling experiments, it was concluded that the carbazole had one unsubstituted C-ring, and another C-ring with a substitution at C-8. NOE experiments supported the positions of the substituents. The spectral data and the mass fragmentations at m/z 263 and 211 indicated that the monomeric units of this alkaloid are murrayafoline-A and girinimbine. All of the spectral data led to structure **179** for murrafoline-B, which consists of a dihydrogirinimbine (*cf.* girinimbine (**115**) Scheme 2.22) attached at C-12 to C-8 of murrayafoline-A (**7**) (see Scheme 2.4) (146,160). This assignment was supported by ^{13}C-NMR and COSY spectra (146) and finally by synthesis (reaction of murrayafoline-A and girinimbine with Nafion 117 in refluxing aqueous methanol) (160) (Scheme 2.38).

The UV (λ_{max} 242, 251, 291, 328, and 342 nm) and IR (ν_{max} 1610, and 3460 cm^{-1}) spectra of murrafoline-C (**180a**) indicated a bis-carbazole framework. This assignment was supported by the mass fragmentation ion at m/z 256. The ^{1}H-NMR spectrum showed signals for two aromatic methyl groups at δ 2.24 and 2.47. The observation of ABX type signals at δ 2.27, 2.31, and 4.63 and AB-type signals at δ 5.56

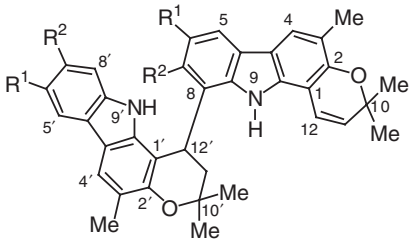

180a Murrafoline-C
R^1,R^2 = H

180b Murrafoline-I
R^1 = OMe; R^2 = OH

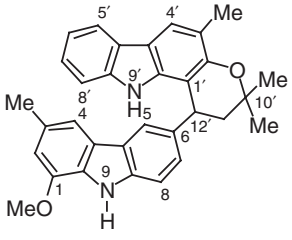

181 Murrafoline-D

Scheme 2.39

and 6.07, and tertiary methyl groups at δ 1.38, 1.41, 1.42, and 1.54, suggested the presence of a 4-substituted 2,2-dimethyldihydropyran ring and a 2,2-dimethylpyran ring. The similarity of the ^{1}H-NMR spectra of murrafoline-C and murrafoline-B suggested that both alkaloids had the same linkage between C-12 and C-8 of the two carbazole units. Thus, the murrafoline-C structure **180a** consists of a dihydrogirinimbine unit that is attached at C-12 to the C-8 of girinimbine (**115**) (160). This assignment was supported by NOESY and HMBC spectra (146) (Scheme 2.39).

The UV spectrum [λ_{max} 240, 256 (sh), 296, 332, and 345 nm] of murrafoline-D (**181**) indicated a bis-carbazole framework. This assignment was supported by the IR spectrum. The mass fragmentation showed a peak at m/z 237, along with the molecular ion peak at m/z 474. The ^{1}H-NMR spectrum showed similar substituents as for murrafoline-B (**179**) (see Scheme 2.38), including two aromatic methyl groups at δ 2.38 and 2.45, an aromatic methoxy group at δ 3.97, and a 4-substituted 2,2-dimethyldihydropyran ring, indicating the presence of a dihydrogirinimbine and a murrayafoline-A (**7**) unit (see Scheme 2.4). However, the two monomeric carbazole units have different attachment points. The characteristic aromatic C-ring signals for murrayafoline-A confirmed the linkage of C-6 of murrayafoline-A to C-12 of dihydrogirinimbine, which was supported by HMBC and NOE experiments. Based on these spectral data, structure **181** was assigned to murrafoline-D (146). This assignment was confirmed by the ^{13}C-NMR data (146), and finally by synthesis through the reaction of murrayafoline-A and girinimbine with Nafion 117 in refluxing aqueous methanol (146,160) (Scheme 2.39).

The UV spectrum [λ_{max} 243, 254 (sh), 293, 332, and 343 (sh) nm] of murrafoline-G (**182**) resembled that of murrafoline-D (**181**) (see Scheme 2.39), indicating a bis-carbazole framework with similar monomeric units. The ^{1}H-NMR spectrum showed signals for substituents similar to those of murrafoline-D (**181**) (see Scheme 2.39), including aromatic methyl groups at δ 2.39 and 1.73, an aromatic methoxy group at δ 3.96, and a 4-substituted 2,2-dimethyldihydropyran ring, indicating a dihydrogirinimbine unit and a murrayafoline-A (**7**) unit, with different attachments of the two monomeric carbazole units. The signal for the methyl group at C-3 of the murrayafoline-A unit of murrafoline-G exhibited an abnormal high-field shift (δ 1.73) as compared to the corresponding methyl group (δ 2.45) of murrafoline-D (**181**). The lack of a deshielded H-4 and signals of four, mutually *ortho*-coupled (J=8.6 Hz) protons at δ 8.35, 7.21, 7.43, and 7.69 for H-5 to H-8 confirmed the linkage of C-4 of murrayafoline-A to C-12 of dihydrogirinimbine. Based on the spectroscopic

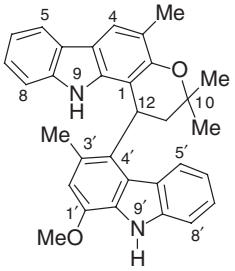

182 Murrafoline-G

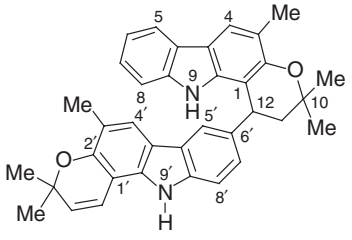

183 Murrafoline-H

Scheme 2.40

data, structure **182** was assigned to murrafoline-G. The assignment was supported by ^{13}C-NMR data, NOE experiments (146), and finally by synthesis through the reaction of murrayafoline-A and girinimbine with Nafion 117 in refluxing aqueous methanol (146) (Scheme 2.40).

The UV spectrum [λ_{max} 239, 256 (sh), 292, 331, and 345 nm] of murrafoline-H (**183**) resembled that of murrafoline-C (**180a**) (see Scheme 2.39) and indicated a dimeric carbazole with similar monomeric units. The ^{1}H-NMR spectrum showed a similarity to murrafoline-C (**180a**) (see Scheme 2.39), with signals for two aromatic methyl groups at δ 2.38 and 2.26, and a 4-substituted 2,2-dimethyldihydropyran ring. This indicated the presence of a dihydrogirinimbine unit and a girinimbine (**115**) unit (see Scheme 2.22), but with a different attachment of the monomeric carbazole units. Furthermore, the aromatic region of the girinimbine unit showed the presence of H-4 as a singlet at δ 7.64, along with two *ortho*-coupled (J=8.1 Hz) protons at δ 7.09 and 7.30, and a *meta*-coupled (J=1.8 Hz) doublet at δ 7.93. This low-field *meta*-coupled doublet was assigned to C-5, and indicated the linkage of C-6 of girinimbine with C-12 of dihydrogirinimbine. The linkage at C-6 was supported by the presence of an additional *meta*-coupling (J=1.8 Hz) for H-7 (δ 7.09). Based on the spectral data, structure **183** was assigned to murrafoline-H. This assignment was confirmed by ^{13}C-NMR data, NOE experiments, and synthesis (146) (Scheme 2.40).

In 1988, Furukawa *et al.* isolated murrafoline-E (**184**) and murrafoline-F (**185**) from the root bark of *M. euchrestifolia*. Murrafoline-E was the third example of an *N*-benzyl-linked bis-carbazole alkaloid from a *Murraya* plant, while murrafoline-F was the first *N*-methoxy-bis-carbazole alkaloid (22).

The UV spectrum [λ_{max} 238, 255 (sh), 263 (sh), 328, 340, and 352 (sh) nm] of murrafoline-E (**184**) indicated a carbazole. This assignment was supported by the IR spectrum. The mass fragmentation with two base peaks at m/z 262 and 211 suggested a bis-carbazole with girinimbine (**115**) and murrayafoline-A (**7**) units. The ^{1}H-NMR spectrum showed signals for an aromatic methyl group at δ 2.51, an aromatic methoxy group at δ 3.94, a 2,2-dimethyl-Δ^3-pyran ring [δ 1.41 (6*H*, s), 5.79 and 6.92 (each 1*H*, d, J=10.0 Hz)], and a benzylic methylene attached to a nitrogen atom at δ 6.01. Moreover, the ^{1}H–^{1}H COSY spectrum showed two, four-spin systems in the aromatic region indicating the lack of substituents on the C-ring of both carbazole skeletons. Based on these spectral data and NOE experiments, structure **184** was assigned to murrafoline-E (22) (Scheme 2.41).

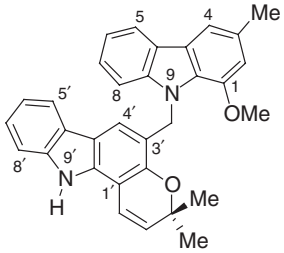

184 Murrafoline-E

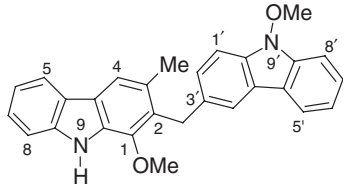

185 Murrafoline-F

Scheme 2.41

The UV spectrum [λ_{max} 239, 252 (sh), 261 (sh), 285 (sh), 296, 326, and 340 nm] of murrafoline-F (**185**) indicated a carbazole. The ^{1}H-NMR spectrum showed signals for an aromatic methyl at δ 2.38 and two aromatic methoxy groups at δ 3.93 and 4.14. The ^{1}H–^{1}H COSY spectrum showed two, four-spin and one, three-spin system, suggesting unsubstituted C-rings for both carbazole units and a 3-substituted A-ring in one of the carbazoles. The signals at δ_H 4.43 (2*H*) and δ_C 32.2 in the ^{1}H- and ^{13}C-NMR spectra, and a mass fragment at m/z 223 (M^+-196–H), indicated the methylene linkage between two carbazole moieties of this bis-carbazole. The strong mass fragment at m/z 390 (M^+−OMe), and the presence of 12 sp^2 carbons as doublets in the ^{13}C-NMR spectrum, indicated that one methoxy group was located on the nitrogen of the carbazole. Based on the spectral data and NOE experiments, structure **185** was assigned to murrafoline-F (22) (Scheme 2.41).

In 1990, Furukawa *et al.* reported the isolation of murrastifoline-A (**186**), -B (**187**), -C (**188**), and -D (**189**) from the root bark of *M. euchrestifolia* (161). Later, the same authors isolated further murrastifoline derivatives, murrastifoline-E (**190**) (101) and murrastifoline-F (**191**) (82) from the same natural source. Their common substructure is a 1-methoxy-3-methylcarbazole [murrayafoline A (**7**)], which is attached at the *N*-atom to a second carbazole moiety. For murrastifoline A (**186**), murrastifoline-B (**187**), and murrastifoline-F (**191**) no optical rotations were mentioned. Murrastifoline-D (**189**) was isolated as a racemate and murrastifoline-E (**190**) in optically active form: $[\alpha]_D$ −5.7 (*c* 0.035, $CHCl_3$). However, the absolute configuration of murrastifoline-E (**190**) is still not known. In 2001, Bringmann *et al.* described the enantiomeric resolution and the chiroptical properties of murrastifoline-F (**191**) (162) (Schemes 2.42–2.44).

The murrastifolines exhibited characteristic carbazole UV spectra. Their ^{1}H-NMR spectra showed signals for aromatic methoxy (δ 3.57–4.11) and methyl groups (δ 2.52–2.56). In the aromatic region, signals of a four-spin system and two singlets for H-4 (δ 7.56–7.63) and H-2 (δ 6.85–7.00) were observed. The ^{1}H-NMR spectra, NOE studies, and mass fragments at m/z 210 or 211 confirmed murrayafoline A (**7**) as the common structural unit for all murrastifolines (Schemes 2.42–2.44).

The ^{1}H-NMR spectrum of murrastifoline-A (**186**) showed, besides the signals for murrayafoline A, a broad singlet for an NH (δ 10.45), and singlets for an aromatic methyl (δ 2.48) and a methoxy (δ 4.03) group. In the aromatic region, the two singlets at δ 7.54 and 6.88 were assigned to H-4 and H-2, respectively. Furthermore, the

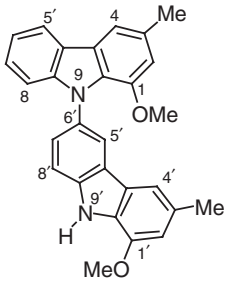

186 Murrastifoline-A

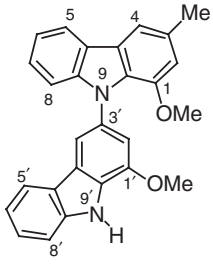

187 Murrastifoline-B

Scheme 2.42

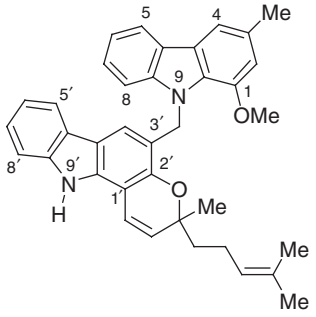

188 Murrastifoline-C

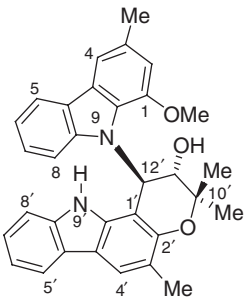

189 Murrastifoline-D

Scheme 2.43

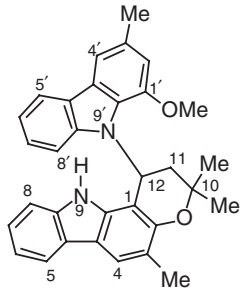

190 Murrastifoline-E

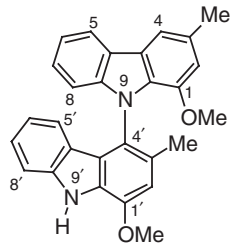

191 Murrastifoline-F

Scheme 2.44

aromatic region showed an *ortho*-coupling (J=7.9 Hz) for H-7 (δ 7.40) and H-8 (δ 7.67), and a deshielded *meta*-coupled (J=2.0 Hz) H-5 (δ 8.10), indicating the linkage of C-6 of one murrayafoline A unit to the *N*-atom of a second. This linkage was confirmed by the additional *meta*-coupling of H-7 (δ 7.40) with H-5. The spectral data and NOE experiments led to structure **186** for murrastifoline-A (161) (Scheme 2.42).

The ^{1}H-NMR spectrum of murrastifoline-B (**187**) showed signals for an NH proton (broad singlet at δ 10.59) and an aromatic methoxy group (δ 4.03). The aromatic region exhibited a four-spin system, suggesting an unsubstituted C-ring and two *meta*-coupled (J=1.5 Hz) singlets at δ 7.04 and 7.81 for H-2 and H-4, respectively, indicating a linkage between C-3 of one murrayafoline A unit with the *N*-atom of a second. Based on the spectral data and NOE experiments, structure **187** was assigned to murrastifoline-B (161) (Scheme 2.42).

The mass fragmentation of murrastifoline-C (**188**) at m/z 330 and 211 indicated the presence of mahanimbine (**139**) (see Scheme 2.27) along with the murrayafoline A unit. In addition to the ^{1}H-NMR spectral data of murrayafoline A, murrastifoline-C showed a four-spin system suggesting an unsubstituted C-ring. The symmetrical doublets at δ 5.77 and 6.96, and a three-proton singlet at δ 1.38, were assigned to olefinic protons and a tertiary methyl group at the pyran ring. The signals at δ 1.70 (2*H*, m), 2.08 (2*H*, m), 5.14 (1*H*, t), 1.59 (3*H*, s), and 1.67 (3*H*, s) were assigned to the $-CH_2CH_2CH{=}CMe_2$ side chain of the pyran ring. This side chain was

confirmed by the mass fragmentation ion at m/z 457 ($M^+-CH_2CH_2CH=CMe_2$). The ^1H–^1H COSY and NOESY spectra showed a correlation between the broad singlet at δ 7.36 for H-4 and the two-proton singlet at δ 6.03, assigned to the benzylic methylene protons linked to the *N*-atom of murrayafoline A. Based on the spectral data, structure **188** was assigned to murrastifoline-C (161) (Scheme 2.43).

The mass spectrum of murrastifoline-D (**189**), with fragments at m/z 280 and 211, confirmed the murrayafoline A unit. The second carbazole unit was deduced from the ^1H-NMR spectrum, which showed signals for geminal dimethyl groups at δ 1.55 and 1.42, and a doublet of doublets (J=5.9, 9.2 Hz) at δ 4.38, coupled with a hydroxy proton at δ 4.48 (J=5.9 Hz). The doublet (J=9.2 Hz) at δ 7.21 was assigned to H-12′ of the benzylic carbon attached to the nitrogen of murrayafoline A. The spectral data indicated a 2,2-dimethyl-3-hydroxy-4-substituted dihydropyran ring. The *trans* relationship between substituents at C-11′ and C-12′ was confirmed by the coupling constant (J=9.2 Hz) of the methine protons and the absence of an NOE between them. The aromatic region showed a singlet at δ 7.87 for H-4, and a four-spin system indicating an unsubstituted carbazole C-ring. Based on the spectral data and NOE experiments, structure **189** was assigned to murrastifoline-D (161) (Scheme 2.43).

The UV spectrum (λ_{max} 239, 255, 291, 331, and 348 nm) of murrastifoline-E (**190**) resembled that of murrastifoline-D (**189**) (see Scheme 2.43) indicating a bis-carbazole with similar monomeric carbazole units. The ^1H-NMR spectrum confirmed the structural similarity to murrastifoline-D (**189**), but was lacking the signal for the hydroxy function of the 4-substituted 2,2-dimethyl dihydropyran ring, which was indicated by signals for the geminal dimethyl groups at δ 1.50 and 1.48, a doublet of doublets (J=7.3, 11.0 Hz) at δ 7.42, and a two-proton multiplet at δ 2.23. The doublet of doublets at δ 7.42 was assigned to H-12 of the benzylic carbon attached to the nitrogen of the murrayafoline A unit. The spectral data confirmed that murrastifoline-E (**190**) is a deoxygenated murrastifoline-D. This assignment was supported by ^{13}C-NMR data and NOE experiments (101) (Scheme 2.44).

The ^1H-NMR spectrum of murrastifoline-F (**191**) showed singlet signals for two aromatic methyl groups (δ 2.05, 2.55), two methoxy groups (δ 3.33, 4.10), three aromatic protons (δ 6.67, 6.88, and 7.67), and an NH group (δ 8.27). The ^1H–^1H COSY spectrum showed two, four-spin systems suggesting an unsubstituted C-ring in both carbazole units. The spectral data and the NOE experiments confirmed that the basic structural subunit of murrastifoline-F (**191**) is murrayafoline A (**7**), which co-occurs with **191** in the plant. The linkage of the two murrayafoline A molecules is between the *N*-atom of one unit and C-4 of the second unit. Therefore, structure **191** was assigned to murrastifoline-F (82) (Scheme 2.44).

In 1990, Furukawa *et al.* described the isolation and structural elucidation of chrestifoline-A (**192**), -B (**193**), and -C (**194**) from the root bark of *M. euchrestifolia*. The chrestifolines contain 1-methoxy-3-methylcarbazole [murrayafoline A (**7**)] as the common structural subunit, which is linked to the second carbazole *via* the methyl group at C-3. Chrestifoline-C (**194**) was isolated from nature in optically active form: $[\alpha]_D$ −5.6 (c 0.054, $CHCl_3$). However, the absolute configuration is not known (161) (Schemes 2.45 and 2.46).

All of the chrestifoline alkaloids have a UV spectrum characteristic of a carbazole chromophore. The ^1H-NMR spectra of all these alkaloids showed signals for an NH proton at δ 10.16 or 10.31, an aromatic methoxy group at δ 3.84 or 3.85, and a 2H singlet at δ 4.78–5.80 assigned to the benzylic methylene protons connected to

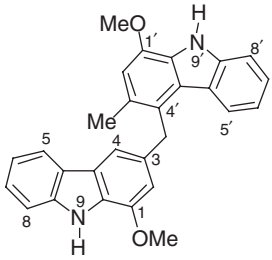

192 Chrestifoline-A

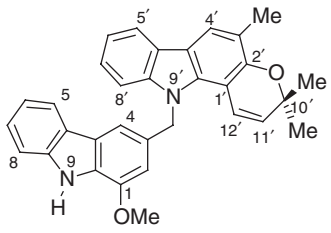

193 Chrestifoline-B

Scheme 2.45

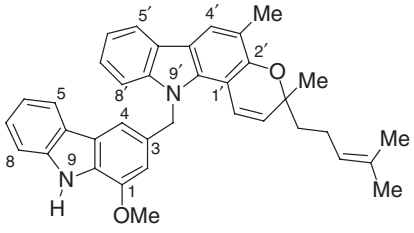

194 Chrestifoline-C

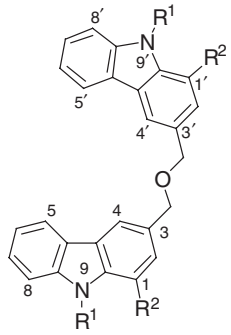

195 Oxydimurrayafoline
R^1 = H; R^2 = OMe

196 3,3′-[Oxybis(methylene)]bis-(9-methoxy-9*H*-carbazole)
R^1 = OMe; R^2 = H

Scheme 2.46

the *N*-atom of the second carbazole nucleus. In the aromatic region, signals of a four-spin system and two singlets for H-2 at δ 7.00 or 6.90 and H-4 at δ 7.39 or 7.38 were observed. This aromatic splitting pattern, supported by NOE studies and the mass fragment at m/z 210, indicated the presence of a 1-methoxy-3-(substituted methylene)carbazole nucleus as a common structural unit of the chrestifolines.

The ^{1}H-NMR spectrum of chrestifoline-A (**192**) showed additional signals of a four-spin system indicating an unsubstituted C-ring, a methoxy group at δ 4.02, an aromatic methyl group at δ 2.47, a singlet for an aromatic proton at δ 6.94, and an NH singlet at δ 10.28. The spectral data, supported by NOE studies, confirmed structure **192** for chrestifoline-A. This assignment was supported by the mass spectrum displaying m/z 420 as the base peak and a fragment at m/z 210 (161) (Scheme 2.45).

The mass fragmentation of chrestifoline-B (**193**) at m/z 263 and 248, and a molecular ion at m/z 472 and a base peak at m/z 210, indicated the presence of girinimbine (**115**) (see Scheme 2.22) as the second, monomeric carbazole unit. The ^{1}H-NMR spectrum of this bis-carbazole alkaloid showed signals of a four-spin

system indicating an unsubstituted C-ring, an aromatic methyl group at δ 2.27, a deshielded H-4 at δ 7.81, and signals for a 2,2-dimethyl-Δ^3-pyran ring at δ 1.36 (6*H*, s), and δ 5.53 and 6.91 (each 1*H*, d, *J*=9.9 Hz). Based on the spectral data and NOE experiments, structure **193** was assigned to chrestifoline-B (161) (Scheme 2.45).

The mass fragments of chrestifoline-C (**194**) at *m*/*z* 331 and 210 (base peak) indicated mahanimbine (**139**) (see Scheme 2.27) as the second carbazole unit. The ^{1}H-NMR spectra of chrestifoline-C showed signals for a deshielded H-4 at δ 7.81 and a four-spin system indicating an unsubstituted C-ring. The symmetrical doublets at δ 5.53 and 6.95 and the three-proton singlet at δ 1.34 were assigned to the olefinic protons and the tertiary methyl group of the pyran ring. The signals at δ 1.68 (2*H*, m), 2.04 (2*H*, m), 5.00 (1*H*, t), 1.45 (3*H*, s), and 1.54 (3*H*, s) confirmed the side chain –$CH_2CH_2CH{=}CMe_2$, attached to the quaternary carbon of the pyran ring. The presence of this side chain was supported by the mass fragmentation ion at *m*/*z* 457 ($M^+ - CH_2CH_2CH{=}CMe_2$). Based on the spectroscopic data and NOE experiments, structure **194** was assigned to chrestifoline-C (161) (Scheme 2.46).

In 1987, Furukawa *et al*. reported the isolation of oxydimurrayafoline (**195**) from the root bark of *M. euchrestifolia*. This alkaloid represented the first example of a dimeric carbazole alkaloid with an ether linkage (69). The UV spectrum (λ_{max} 242, 253, 294, 324, and 337 nm) and the base peak at *m*/*z* 211 in the mass spectrum of oxydimurrayafoline (**195**) indicated a symmetrical dimeric carbazole with two murrayafoline A units. The ^{1}H-NMR spectrum resembled that of murrayafoline A (**7**), except for the presence of a singlet at δ 4.76 instead of the singlet for the aromatic methyl group in murrayafoline A at δ 2.42. The singlet at δ 4.76 suggested a benzylic oxymethylene moiety. The spectral data, supported by NOE experiments, led to structure **195** for oxydimurrayafoline (Scheme 2.46).

In 2005, Rahman and Gray isolated 3,3′-[oxybis(methylene)]bis(9-methoxy-9*H*-carbazole) (**196**) from the stem bark of *M. koenigii* (163). This alkaloid showed potent activity against Gram-negative bacteria and fungi. Alkaloid **196** represented the first example of an ether linked, symmetrical dimeric carbazole with *N*-methoxycarbazole units (163). The UV spectrum (λ_{max} 237, 264, 293, and 329 nm) of 3,3′-[oxybis(methylene)]bis(9-methoxy-9*H*-carbazole) (**196**) resembled that of 3-hydroxymethyl-*N*-methoxycarbazole (**106**) (see Scheme 2.20) indicating the presence of a similar monomeric carbazole unit. The ^{1}H-NMR spectrum was also very similar and indicated the presence of two symmetrical 3-hydroxymethyl-*N*-methoxycarbazole (**106**) units linked *via* a methylene ether. The methylene protons at δ 4.78 showed HMBC correlations to C-1, C-3, and C-4, as well as direct (^1J) and long-range (^3J) correlations to the methylene carbons at δ 72.7. The latter correlation confirmed the bismethylene ether linkage of the dimer, similar to that of oxydimurrayafoline (**195**). Based on the spectroscopic data and the structural similarity to 3-hydroxymethyl-*N*-methoxycarbazole (**106**), structure **196** was assigned to 3,3′-[oxybis(methylene)]bis (9-methoxy-9*H*-carbazole) (Scheme 2.46).

In 1983, Furukawa *et al*. isolated bismurrayafoline-A (**197**) and -B (**200**) from *M. euchrestifolia* (164). The absolute configuration of bismurrayafoline-B is not known (164) (Scheme 2.47).

The UV spectrum [λ_{max} 228, 244, 253 (sh), 284 (sh), 293, and 340 nm] of bismurrayafoline-A (**197**) indicated a dimer of murrayafoline A (**7**) (see Scheme 2.4). This assignment was supported by the IR spectrum and the mass fragmentation which showed a peak at *m*/*z* 210 along with the molecular ion peak at *m*/*z* 420. The

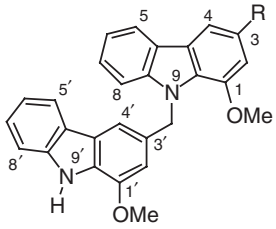

197 Bismurrayafoline-A
R = Me

198 Bismurrayafolinol
R = CH_2OH

199 Chrestifoline-D
R = CHO

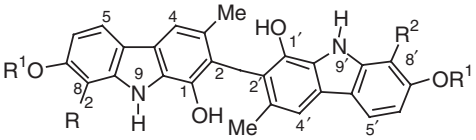

200 Bismurrayafoline-B
R^1 = Me; R^2 = prenyl

201 Bismurrayafoline-C
R^1 = H; R^2 = geranyl

202 Bismurrayafoline-D
R^1 = Me; R^2 = geranyl

Scheme 2.47

^{1}H-NMR spectrum of bismurrayafoline-A (**197**) showed singlets for an aromatic methyl group (δ 2.46), two methoxy (δ 3.71, 3.82) groups, and four aromatic protons δ 6.62 (2*H*), 7.32 (1*H*), and 7.36 (1*H*). Moreover, two, four-spin systems indicated that the C-rings of both carbazole units were unsubstituted. The two-proton singlet at δ 5.83 and the base peak at *m*/*z* 210 confirmed the benzylic methylene group bound to the *N*-atom. Based on the spectral data, structure **197** was assigned to bismurrayafoline-A. Additional support for this assignment was derived from the transformation to murrayafoline A by hydrogenation (164) (Scheme 2.47).

In 1987, Furukawa *et al*. described the isolation of bismurrayafolinol (**198**) from the root bark of *M. euchrestifolia* (69). The UV spectrum (λ_{max} 225, 244, 252, 281, 292, and 340 nm) of bismurrayafolinol (**198**) resembled that of bismurrayafoline-A (**197**) indicating a similar dimeric carbazole framework. This assignment was supported by the IR spectrum and the mass fragmentation which showed a peak at *m*/*z* 210. Moreover, the ^{1}H-NMR spectrum was also similar to that of bismurrayafoline-A (**197**), except for the presence of the signal for an aromatic hydroxymethylene group at δ 4.86 instead of an aromatic methyl group at δ 2.46. The spectroscopic data led to structure **198** for bismurrayafolinol. This structure was unequivocally confirmed by synthesis of the acetate of natural murrayafolinol starting from murrayanine (**9**) (see Scheme 2.4) (69) (Scheme 2.47).

Two years after the isolation of the chrestifolines **192–194** (see Schemes 2.45 and 2.46), the same authors obtained chrestifoline-D (**199**) from the same natural source. Similar to the previous chrestifolines, this alkaloid had a 1-methoxy-3-methylene-carbazole unit.

The UV spectrum (λ_{max} 223, 241, 250, 275, 291, and 335 nm) of chrestifoline-D (**199**) resembled that of bismurrayafoline-A (**197**), indicating a similar dimeric carbazole framework. The ^{1}H-NMR spectrum was also similar to that of bismurrayafoline-A (**197**), except for the presence of a low-field singlet at δ 10.07 for a formyl group instead of the signal for an aromatic methyl group. This assignment was supported by the IR band at ν_{max} 1680 cm^{-1}. The spectral data, supported by NOE experiments, led to structure **199** for chrestifoline-D. Additional

support for this assignment derived from the synthesis of bismurrayafoline-A (**197**) by DDQ-oxidation (104) (Scheme 2.47).

The UV spectrum [λ_{max} 225 (sh), 240, 265 (sh), 285 (sh), 312, and 333 (sh) nm] of bismurrayafoline-B (**200**), and its bathochromic shift in alkali, indicated a phenolic carbazole. This conclusion was supported by the IR spectrum (ν_{max} 3550, 3450, and 1615 cm^{-1}). The 19 carbon signals of the ^{13}C-NMR spectrum, the molecular ion peak at m/z 588, and the peak at m/z 294 confirmed a symmetrical dimeric carbazole with two equivalent monomer units. The ^{1}H-NMR spectrum of bismurrayafoline-B (**200**) was similar to that of murrayafoline B (**27**) (see Scheme 2.6), except for some differences in the chemical shifts and the lack of a signal for H-2 at δ 6.56 (for murrayafoline B). The spectroscopic data and NOE experiments confirmed a 2,2′-linkage of the two murrayafoline B units and led to structure **200** for bismurrayafoline-B (164) (Scheme 2.47).

In 1991, Furukawa *et al.* described the isolation of bismurrayafoline-C (**201**) and -D (**202**) from the stem bark of *M. euchrestifolia*. Bismurrayafoline-D represents the dimethyl ether of bismurrayafoline-C. The absolute configuration of both alkaloids is not known (70). The UV spectrum [λ_{max} 226, 235, 260 (sh), 285, 311, and 335 (sh) nm] of bismurrayafoline-C (**201**) resembled that of bismurrayafoline-B (**200**), indicating a similar carbazole framework. The ^{1}H-NMR spectrum of bismurrayafoline-C was also very similar to that of bismurrayafoline-B (**200**), except for the presence of signals for an aromatic hydroxy group and a geranyl moiety instead of the aromatic methoxy group and the prenyl moiety. The spectral data supported by NOE experiments led to structure **201** for bismurrayafoline-C. This assignment was supported by additional NOE studies with the corresponding tetra-*O*-methyl ether obtained by the treatment of bismurrayafoline-C (**201**) with diazomethane (70) (Scheme 2.47).

The UV and IR spectra of bismurrayafoline-D (**202**) resembled those of bismurrayafoline-C (**201**), indicating a similar bis-carbazole framework. The ^{1}H-NMR spectrum was also similar to that of bismurrayafoline-C, except for an additional singlet at δ 3.89 for a methoxy group. The geranyl side chain was supported by the mass fragmentation ion at m/z 239 (M^{2+}−CH═CMeCH$_2$CH$_2$CH═CMe$_2$), and a doubly charged molecular ion at m/z 362 (M^{2+}). The spectroscopic data, supported by NOE experiments with bismurrayafoline-D and the corresponding di-*O*-methyl ether, led to structure **202** for bismurrayafoline-D (70) (Scheme 2.47).

In 1996, Wu *et al.* reported the isolation of clausenamine-A (**203**) from the methanol extract of the stem bark of *C. excavata*, which is used in traditional medicine in China for the treatment of poisonous snakebites (53). Four years later, Zhang and Lin reported the *in vitro* cytotoxic activity of clausenamine-A (**203**) and its synthetic analogs against a variety of human cancer cell lines (165). The UV spectrum (λ_{max} 218, 235, 257, 307, and 343 nm) of clausenamine-A (**203**) and the ^{1}H-NMR singlets at δ 2.44 and 8.95, typical of an aromatic methyl group and a carbazole NH, indicated a 3-methylcarbazole framework. The 15 carbon signals in the ^{13}C-NMR spectrum, the molecular ion peak at m/z 512, and the peak at m/z 256 confirmed it as a symmetrical dimeric carbazole. Moreover, The ^{1}H-NMR spectrum showed a low-field singlet at δ 7.81 for H-4 and *meta*-coupled (J=2.0 Hz) doublets at δ 6.45 and 7.13 for H-7 and H-5, supported by an NOE of the signal at δ 7.81 (H-4) with the signal at δ 7.13 (H-5). Additional NOEs of the methoxy group at δ 3.77 with H-7, and of the other methoxy group at δ 3.82 with H-5 and H-7, indicated the positions of the

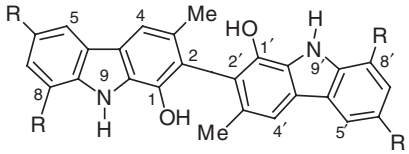

203 Clausenamine-A
R = OMe

204 Bis(*O*-demethylmurrayafoline A)
R = H

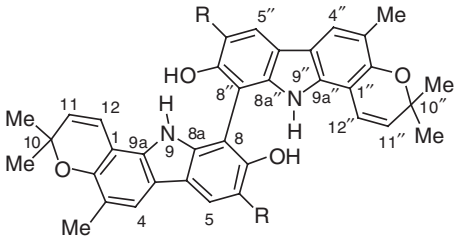

205 8,8″-Biskoenigine
R = OMe

206 Bis-7-hydroxygirinimbine-A
R = H

Scheme 2.48

methoxy groups at C-8 and C-6. The hydroxy-substituted C-1 at δ 152.2 showed in an HMBC experiment a correlation with the NH at δ 8.95 confirming a C-2–C-2′ carbon–carbon linkage of the dimeric carbazole. Based on these spectroscopic data, structure **203** was assigned to clausenamine-A (53) (Scheme 2.48).

In 1995, Bringmann *et al.* reported the antiplasmodial activity of the non-natural bis(*O*-demethylmurrayafoline A) (**204**) against *Plasmodium falciparum in vitro*. Along with the antimalarial activity, an enantiomeric resolution and the chiroptical properties of this alkaloid were described (166). The ^{1}H-NMR spectrum of bis(*O*-demethylmurrayafoline A) (**204**) resembled that of clausenamine-A (**203**), except for the lack of two aromatic methoxy group signals and the presence of two, four-spin systems, indicating a similar dimeric carbazole with unsubstituted C-rings in both carbazole units. Based on the spectroscopic data, structure **204** was assigned to bis(*O*-demethylmurrayafoline A) (166–168).

In 2002, Hao *et al.* isolated 8,8″-biskoenigine (**205**) from *M. koenigii* (119,169). Although, this alkaloid was optically active and exhibited a specific rotation of $[\alpha]_D^{25} + 139.6$ (*c* 1.0, $CHCl_3$) (119), the absolute configuration is unknown. 8,8″-biskoenigine (**205**) showed antiosteoporotic activity in the cathepsin B (CAT-B) model (119). The UV spectrum [λ_{max} 225, 301, and 343 nm] of 8,8″-biskoenigine (**205**) indicated a dimeric carbazole framework. This assignment was supported by the IR spectrum and the mass spectrum which showed a peak at m/z 308 and the molecular ion peak at m/z 616. Nineteen carbon signals in the ^{13}C-NMR spectrum suggested a symmetrical dimeric carbazole. The ^{1}H-NMR spectrum of 8,8″-biskoenigine was very similar to that of koenigine (**119**) (see Scheme 2.22), except for the absence of the C-8 methine proton indicating a linkage between C-8 and C-8″. This linkage was supported by the upfield shifts of C-7 (C-7″) and C-8a (C-8a″). The spectroscopic data led to structure **205** for 8,8″-biskoenigine (119,169). This structural assignment was additionally confirmed by the ^{13}C-NMR spectrum (119,169) and by synthesis *via* an oxidative coupling of koenigine with $FeCl_3$ in the solid state (119) (Scheme 2.48).

In 1991, Wang *et al.* reported the isolation of bis-7-hydroxygirinimbine-A (**206**) and -B (**207**) from the leaves of *M. euchrestifolia*. The absolute configuration of these alkaloids is not known (170). The UV spectrum (λ_{max} 226, 295, and 343 nm) of bis-7-hydroxygirinimbine-A (**206**) is very similar to that of 8,8″-biskoenigine (**205**),

indicating a similar dimeric carbazole framework. The ^{1}H-NMR spectrum of bis-7-hydroxygirinimbine-A (**206**) also resembled that of 8,8″-biskoenigine (**205**), except for the absence of the singlet (δ 4.05) for the two aromatic methoxy groups at C-6 and C-6′, and the presence of a doublet for H-6 (H-6′) at δ 6.98 with an *ortho*-coupling (J=8.55 Hz) to H-5 (H-5′) at δ 7.89. The molecular ion peak at m/z 556, along with the peak at m/z 263, confirmed the dimeric nature of this carbazole alkaloid. Based on the spectroscopic data, structure **206** was assigned to bis-7-hydroxygirinimbine-A. Additional support for this assignment was derived from an HMBC spectrum and NOE experiments with the di-*O*-methyl ether of bis-7-hydroxygirinimbine-A, prepared by the treatment of bis-7-hydroxygirinimbine-A (**206**) with diazomethane (170) (Scheme 2.48).

The UV spectrum (λ_{max} 224, 296, and 345 nm) of bis-7-hydroxygirinimbine-B (**207**) resembled that of bis-7-hydroxygirinimbine-A (**206**) suggesting a similar dimeric carbazole. The ^{1}H- and ^{13}C-NMR spectra indicated the presence of two 7-hydroxygirinimbine units. NOE experiments with the di-*O*-methyl ether of bis-7-hydroxygirinimbine-B confirmed that the two 7-hydroxygirinimbine units, in contrast to bis-7-hydroxygirinimbine-A (**206**), had a linkage from C-6 of the first to C-8′ of the second unit. On the basis of the spectroscopic data, structure **207** was assigned to bis-7-hydroxygirinimbine-B (170) (Scheme 2.49).

In 1993, Furukawa *et al.* isolated bismahanine (**208**) from the acetone extract of the stem bark of *M. koenigii* (82). Ten years later, Nakatani *et al.* obtained the same alkaloid in optically active form ($[\alpha]_D^{25}$ + 4.0, *c* 0.65, $CHCl_3$) from the dichloromethane extract of the leaves of the same natural source (116). However, the absolute configuration was not determined. Bismahanine (**208**) showed radical scavenging activity against the 1,1-diphenyl-2-picrylhydrazyl (DPPH) radical (116). The UV spectrum (λ_{max} 223, 245, 297, 331, 341, and 359 nm) of bismahanine (**208**) resembled that of (+)-mahanine (**149**) (see Scheme 2.29) indicating a similar pyranocarbazole unit. The ^{1}H-NMR spectrum was also similar to that of bis-7-hydroxygirinimbine-B (**207**), except for the signals at δ 1.71 (2*H*, m), 1.77 (2*H*, m), 2.15 (4*H*, m), 5.08 (1*H*, t), 5.12 (1*H*, t), 1.54 (3*H*, s), 1. 56 (3*H*, s), 1.60 (3*H*, s), and 1.63 (3*H*, s). These signals were assigned to the two side chain –$CH_2CH_2CH{=}CMe_2$ units, replacing a methyl group on the pyran ring of bis-7-hydroxygirinimbine-B (**207**). The side chain was confirmed

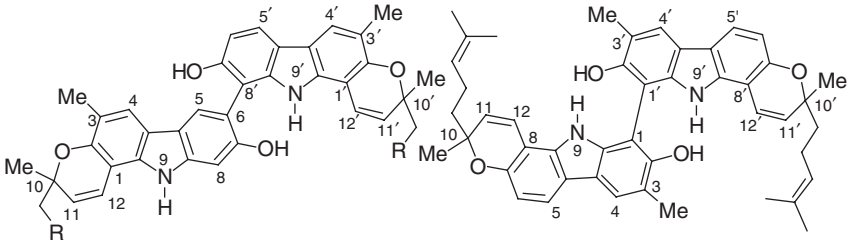

207 Bis-7-hydroxygirinimbine-B
R = H

208 Bismahanine
R = prenyl

209 Bisisomahanine

Scheme 2.49

by the mass fragmentation ion at m/z 609 ($M^+-CH_2CH_2CH=CMe_2$), 347 ($M^{2+}+1$), and 263 ($M^{2+}-CH_2CH_2CH=CMe_2$). Based on the spectral data, structure **208** was assigned to bismahanine (82) (Scheme 2.49).

In 2004, Cuong *et al*. reported the isolation of bisisomahanine (**209**) from the roots of *G. stenocarpa* (30). Bisisomahanine was obtained in optically active form ($[\alpha]_D^{20}$ − 13.1, *c* 0.25, $CHCl_3$). However, the absolute configuration is not known. This alkaloid represented the first dimeric prenylated pyranocarbazole alkaloid with a 1,1′-linkage (30).

The UV spectrum (λ_{max} 224, 245, 298, and 335 nm) of bisisomahanine (**209**) resembled that of isomahanine (pyrayafoline D) (**138**) (see Scheme 2.26) indicating a similar monomeric pyranocarbazole unit. This assignment was supported by the IR spectrum (ν_{max} 1621, 3362, and 3470 cm^{-1}). The presence of 23 signals in the ^{13}C-NMR spectrum, and the molecular ion peak at m/z 692, confirmed a symmetrical dimeric carbazole alkaloid. The 1D- and 2D-NMR spectra of bisisomahanine (**209**) were also similar to those of isomahanine (pyrayafoline D), with the exception of an additional, non-hydrogen substituted, aromatic carbon signal at δ 99.1, and the absence of the aromatic methine signal for H-1 (C-1) in the ^{1}H- and ^{13}C-NMR spectra. The spectroscopic data and the NOESY experiments suggested the C-1/C-1′-linkage of the two isomahanine (pyrayafoline D) monomers. Additional support by HMBC, HMQC, and ^{1}H–^{1}H COSY spectra confirmed structure **209** for bisisomahanine (30) (Scheme 2.49).

In 1991, Ito and Furukawa reported the isolation of murranimbine (**210**) from the root bark of *M. euchrestifolia* collected in Taiwan. This alkaloid was isolated in racemic form (171). The UV spectrum (λ_{max} 240, 260, 306, and 336 nm) of murranimbine (**210**) indicated a carbazole framework. This assignment was supported by the IR spectrum. The mass spectrum, which showed a peak at m/z 263 and the molecular ion peak at m/z 526, suggested a dimeric carbazole. The ^{1}H-NMR spectrum showed signals for two aromatic methyl groups at δ 2.30 and 2.32, four geminal methyl groups at δ 0.60, 1.54, 1.44, and 1.60, and a D_2O-exchangeable NH signal at δ 10.55. The ^{1}H–^{1}H COSY spectrum exhibited two sets of signals for four aromatic protons, including the characteristic H-5 and H-5′ of the carbazole units, and two deshielded signals at δ 7.65 and 8.00 with a long-range coupling to the aromatic methyl groups. The latter signals also showed NOEs with the aromatic methyl groups. The spectral data confirmed that the aromatic C-ring and H-4 of the carbazole nucleus were unsubstituted. A ^{1}H–^{1}H COSY spectrum showed the relationships of the signals at δ 6.12 (H-12′, *J*=2.9 Hz), 2.74 (H-11′, *J*=2.9, 5.1 Hz), 4.07 (H-12), 2.21 (H-11, *J*=5.1, 12.8 Hz), and 2.08 (H-11), and suggested that murranimbine contained two girinimbine (**115**) (see Scheme 2.22) units. Analysis of the HMBC spectrum of murranimbine confirmed the connectivity of the two units, and thus the structure of murranimbine **210**. The relative stereochemistry was assigned based on NOE experiments (171) (Scheme 2.50).

In 2003, Nakatani *et al*. reported the isolation of bispyrayafoline (**211**) and 1,6′-[9,9′,10,10′-tetrahydro-2,7′-dihydroxy-3,7′,10,10′-tetramethyl-10,10′-bis(4-methyl-3-pentenyl)]bipyrano[3,2-*a*]carbazole (**212**), both in optically active form: $[\alpha]_D^{25}$ + 55.0 (*c* 0.12, $CHCl_3$) and $[\alpha]_D^{25}$ + 22.2 (*c* 0.09, $CHCl_3$), from the leaves of *M. koenigii* (116). The absolute configurations of **211** and **212** remain unknown. Both alkaloids showed radical scavenging activity against the 1,1-diphenyl-2-picrylhydrazyl (DPPH) radical (116). In 2006, Furukawa *et al*. reported the isolation of the alkaloid **212** from the same source

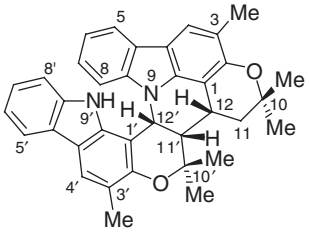

210 Murranimbine

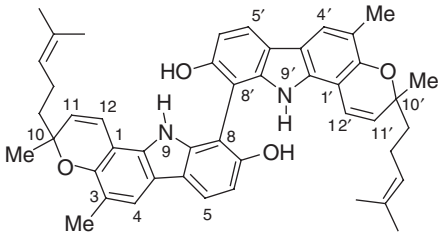

211 Bispyrayafoline

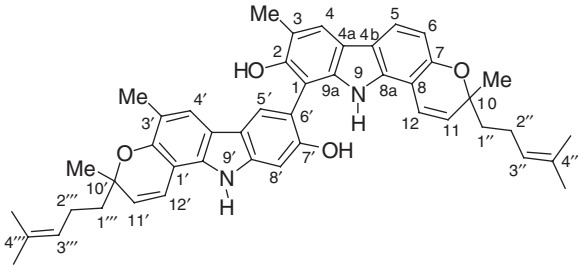

212 Mahabinine-A

Scheme 2.50

and named it mahabinine-A (131). Mahabinine-A (**212**) induced apoptosis in HL-60 cells by activation of the caspase-9/caspase-3 pathway, through mitochondrial dysfunction (131).

The UV spectrum (λ_{max} 224, 243, 298, and 327 nm) of bispyrayafoline (**211**) was similar to that of (+)-mahanine (**149**) (see Scheme 2.29) and indicated the monomeric pyranocarbazole unit. The presence of 23 signals in the ^{13}C-NMR spectrum and a molecular ion peak at m/z 692 confirmed a symmetrical dimeric carbazole. The ^{1}H- and ^{13}C-NMR spectra resembled those of (+)-mahanine (**149**), with the exception of an additional non-hydrogen substituted aromatic carbon signal at δ 99.0 and the lack of the aromatic methine signal for H-1 (C-1) in the ^{1}H- and ^{13}C-NMR spectra. The spectroscopic data confirmed the C-8/C-8′ linkage between the (+)-mahanine monomers and led to structure **211** for bispyrayafoline (116) (Scheme 2.50).

The UV spectrum (λ_{max} 224, 243, 298, and 327 nm) of mahabinine-A (**212**) resembled that of bismahanine (**208**) (see Scheme 2.49) indicating a similar dimeric carbazole framework. The ^{1}H- and ^{13}C-NMR spectra were also similar to those of bismahanine, except for the signal of one additional aromatic methyl group indicating the presence of an isomahanine (**138**) unit (see Scheme 2.26). The ^{1}H-NMR spectrum showed two, *ortho*-coupled (J=8.3 Hz) aromatic protons at δ 6.71 and 7.70. The HMBC spectrum with cross-peaks between the aromatic proton at δ 6.71 and C-8 at δ 104.8, as well as C-4b at δ 117.9, suggested that the aromatic proton was located at C-6. The HMBC correlation of the other *ortho*-coupled aromatic proton at δ 7.70 and the aromatic carbon atoms at δ 136.0 (C-8a) and at δ 150.9 (C-7) indicated that the aromatic proton at δ 7.70 was located at C-5. Moreover, HMBC

correlations between the aromatic methyl group (δ 2.47) and δ 121.4 (C-4), 117.5 (C-3), and 150.0 (C-2) indicated that the aromatic methyl group was located at C-3. The assignments of the aromatic proton at δ 6.71 to C-6 and of the aromatic methyl group at δ 2.47 to C-3 were confirmed by NOESY experiments. The spectroscopic data confirmed the presence of isomahanine (**138**) (see Scheme 2.26) linked at C-1 to the second carbazole unit. The HMBC spectrum of mahabinine-A (**212**) indicated the linkage to the mahanine (**149**) (see Scheme 2.29) unit: thus, H-5′ (δ 7.88) showed a correlation to C-1 (δ 104.1) of the isomahanine unit, confirming the C-6′/C-1-linkage between mahanine and isomahanine. The linkage was supported by NOESY correlations between H-5′ of the mahanine unit to both OH and NH of the isomahanine unit. Based on these spectroscopic data, structure **212** was assigned to mahabinine-A (**212**) (116) (Scheme 2.50).

In 1993, Furukawa *et al.* reported the isolation of bis-2-hydroxy-3-methylcarbazole (**213**), bismurrayaquinone-A (**215**), and bikoeniquinone-A (**216**) from the acetone extract of the root bark of *M. koenigii* (82). Bismurrayaquinone-A and bikoeniquinone-A were the first examples of dimeric carbazolequinone alkaloids isolated from Nature. The absolute configurations of these alkaloids are not known (82). However, two years later, Bringmann *et al.* described the enantiomeric resolution and the chiroptical properties of bismurrayaquinone-A (**215**) (167) (Schemes 2.51 and 2.52).

The UV spectrum [λ_{max} 237, 260 (sh), 304, and 336 nm] of bis-2-hydroxy-3-methylcarbazole (**213**) resembled that of 2-hydroxy-3-methylcarbazole (**52**) (see

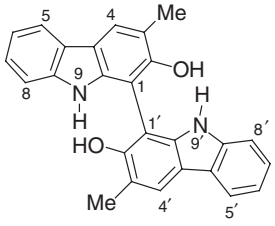

213 Bis-2-hydroxy-3-methylcarbazole
1,1′-Bis(2-hydroxy-3-methylcarbazole)

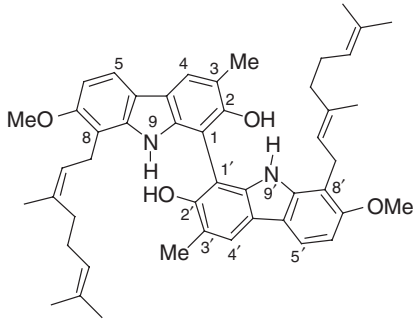

214 Bismurrayafoline E

Scheme 2.51

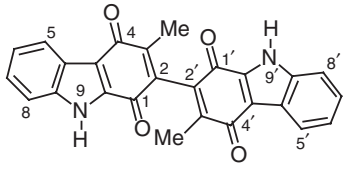

215 Bismurrayaquinone-A

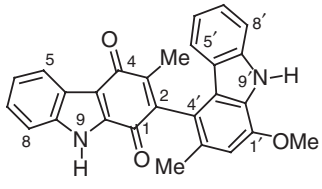

216 Bikoeniquinone-A

Scheme 2.52

Scheme 2.11) indicating a similar carbazole unit. The EI-MS spectrum showed a molecular ion peak at m/z 392, and a peak at m/z 196, suggesting a symmetrical dimeric carbazole with two, 2-hydroxy-3-methylcarbazole units. The ^{1}H-NMR spectrum was also similar to that of 2-hydroxy-3-methylcarbazole (**52**), except for the lack of the signal for H-1 (H-1′), indicating a C-1/C-1′-linkage between the two 2-hydroxy-3-methylcarbazole units. Based on the spectroscopic data and additional support by NOE experiments, structure **213** was assigned to bis-2-hydroxy-3-methylcarbazole (82).

In 1999, Rashid *et al*. isolated bismurrayafoline E (**214**) from the leaves of *M. koenigii* (172). The FAB mass spectrum of bismurrayafoline E (**214**) showed a molecular ion peak at m/z 725 (M^++H), identical to that of bismurrayafoline-D (**202**) (see Scheme 2.47), indicating a similar dimeric carbazole framework. The ^{1}H-NMR spectrum was almost superimposable on that of bismurrayafoline-D (**202**). However, the HSQC and HMBC spectra confirmed the position of the methyl groups at C-3 (C-3′) and the hydroxy groups at C-2 (C-2′) in bismurrayafoline E, as compared to C-3 (C-3′) and C-1 (C-1′) in bismurrayafoline-D. Thus, a C-1/C-1′-linkage was suggested for bismurrayafoline E. Based on the spectroscopic data, structure **214** was assigned to bismurrayafoline E (172) (Scheme 2.51).

The UV spectrum (λ_{max} 225, 252, 291, and 392 nm) of bismurrayaquinone-A (**215**) resembled that of murrayaquinone A (**107**) (see Scheme 2.21) indicating a similar carbazole unit. The IR spectrum showed a strong band at ν_{max} 1650 cm^{-1}. The ^{1}H-NMR spectrum was also similar to that of murrayaquinone A, except for the lack of a signal for H-2 (H-2′). The spectroscopic data confirmed structure **215** for bismurrayaquinone-A (82) (Scheme 2.52).

The ^{1}H-NMR and the ^{1}H–^{1}H COSY spectrum of bikoeniquinone-A (**216**) showed the presence of two sets of four mutually coupling aromatic proton signals, a one-proton singlet at δ 6.94, two methyl groups attached to sp^2-carbon atoms, a methoxy group at δ 4.01, and two D_2O-exchangeable protons at δ 11.70 and 10.36, assigned to NH groups. The spectroscopic data suggested the presence of two different monomeric carbazole units in bikoeniquinone-A, which were assigned as murrayaquinone A (**107**) (see Scheme 2.21) and murrayafoline A (**7**) (see Scheme 2.4). The presence of these monomeric units was supported by a strong IR absorption at ν_{max} 1645 cm^{-1}, typical UV bands at λ_{max} 227, 240, 257, 289, and 331 nm, and a mass fragmentation at m/z 211. These spectroscopic data, and the NOEs between the two methyl singlets at δ 1.81 and 2.26, indicated a C-2/C-4′–linkage between murrayaquinone A (**107**) and murrayafoline A (**7**). In conclusion, structure **216** was assigned to bikoeniquinone-A (82) (Scheme 2.52).

D. Carbazolelactone Alkaloids

In 1998, Ito *et al*. isolated clausamine-A (**217**), -B (**218**), and -C (**219**), each in their racemic form from the branches of *C. anisata* (173). The clausamines have a 1-oxygenated carbazole framework with an annulated six-membered lactone in the 3,4-position. They represented the first examples of naturally occurring carbazole alkaloids with a lactone moiety (173). Later in the same year, Wu *et al*. reported four further carbazolelactone alkaloids, clausevatine-D (**220**), -E (**221**), -F (**222**), and -G (**223**), from the root bark of *C. excavata* (Rutaceae) (174). This plant is a wild shrub

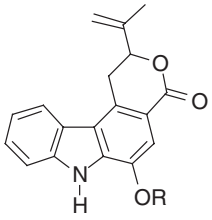

217 Clausamine-A
R = H
218 Clausamine-B
R = Me

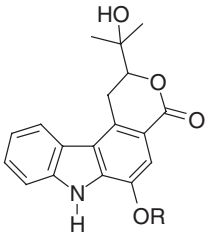

219 Clausamine-C
R = Me
220 Clausevatine-D
R = H

Scheme 2.53

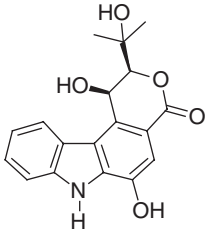

221 Clausevatine-E

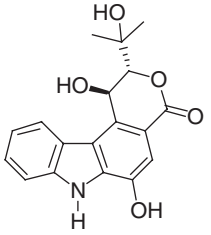

222 Clausevatine-F

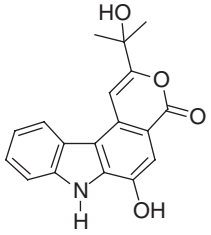

223 Clausevatine-G

Scheme 2.54

that is used in traditional medicine for the treatment of snakebites and abdominal pain. In nature, except clausevatine-G (**223**), clausevatine-D (**220**) $[\alpha]_D$ 5.7 (*c* 0.932, MeOH), -E (**221**) $[\alpha]_D$ –92.4 (*c* 0.0552, MeOH), and -F (**222**) $[\alpha]_D$ –199.0 (*c* 0.0203, MeOH) were isolated in their optically active form. Although these isolates were available in nature in their enantiopure form, except for the relative stereochemistry of clausevatine-D and -E, their absolute stereochemistry is not known (174) (Schemes 2.53 and 2.54).

The UV spectrum [λ_{max} 248, 269, 278 (sh), 310 (sh), and 322 nm] of clausamine-A (**217**) was similar to that of clausine F (**32**) (see Scheme 2.7), indicating the presence of a 1-oxygenated-3-carboxy-4-substituted carbazole framework. The ^{1}H- and ^{13}C-NMR spectra of clausamine-A suggested the presence of an NH group at δ_H 10.94 and a lactone carbonyl group at δ_C 166.03. This assignment was supported by the IR data at ν_{max} 3462 and 1697 cm^{-1}. In addition, the IR spectrum also showed the presence of a hydroxy group at ν_{max} 3329 (br) cm^{-1} and the ^{1}H-NMR spectrum showed in the aromatic region, the presence of a set of four-spin protons, along with a lone singlet at δ 7.55 for H-2. Furthermore, the ^{1}H- and ^{13}C-NMR spectra showed the signals assignable to a vinyl methyl group at δ_H 1.98 and δ_C 18.57, a vinyl methylene at δ_H 5.26, 5.07, and δ_C 113.58, a methine at δ_H 5.12 and δ_C 81.18 on a carbon bearing an oxygen atom, a methylene carbon at δ_H 3.71, 3.52, and δ_C 29.80, and a quaternary vinyl carbon at δ_C 144.82. Based on these spectral data, and HMBC

and NOE experiments, the structure **217** was assigned to clausamine-A. This structure was further supported with the significant mass fragmentation ions at m/z 223 ($M^+-OCMeC{=}CH_2$) and 195 ($M^+-OCMeC{=}CH_2-CO$) (173) (Scheme 2.53).

The UV spectrum [λ_{max} 248, 269, 278 (sh), 310 (sh), and 321 nm] of clausamine-B (**218**) was similar to that of clausamine-A (**217**), indicating a similar carbazole framework. The ^{1}H-NMR spectrum also showed a similar signal pattern to that of clausamine-A, except for an additional aromatic methoxy group at δ 4.07. This assignment was supported by the ^{13}C-NMR signal at δ 55.94. In NOE experiments, irradiation of the methoxy group at δ 4.07 resulted in a 20% area increase of the signal at δ 7.66 (H-2). Based on these spectral data, structure **218** was assigned to clausamine-B. This structure was further supported with the HMBC spectrum, as well as the significant mass fragmentation pattern at m/z 237 ($M^+-OCMeC{=}CH_2$) and 209 ($M^+-OCMeC{=}CH_2-CO$) (173) (Scheme 2.53).

The UV spectrum [λ_{max} 249, 270, 278 (sh), 312 (sh), and 322 nm] of clausamine-C (**219**) was similar to that of clausamine-B (**218**) indicating the presence of a similar carbazole framework. This was also discernible for its IR spectrum with the presence of bands at ν_{max} 3464, 3400 (br), and 1703 cm^{-1} for the NH, OH, and lactone carbonyl groups, respectively. The ^{1}H-NMR spectrum also showed a similar signal pattern to that of clausamine-B, except for the difference on the substitution pattern of the lactone nucleus. Further, the ^{1}H-NMR spectrum showed ABC-type signals at δ 3.67 (1*H*, dd, *J*=3.3, 16.1 Hz), 3.47 (1*H*, dd, *J*=12.8, 16.1 Hz), and 4.47 (1*H*, dd, *J*=3.7, 12.8 Hz), and two aliphatic methyl singlets at δ 1.50 and 1.47 attached to a carbon atom bearing an oxygen function. The spectral data indicate a 1-hydroxy-1-methyl-ethyl substitution at the lactone nucleus. This assignment was additionally supported by the mass fragment ion at m/z 267 (M^+-CMe_2OH+H) in the EI-MS. Based on these spectral data, structure **219** was assigned to clausamine-C. This structure was confirmed by HMBC experiments (173) (Scheme 2.53).

The UV spectrum [λ_{max} 241, 251, 272, 278 (sh), and 325 nm] of clausevatine-D (**220**) was similar to that of clausamine-A (**217**), indicating a similar 1-oxygenated-3-carbonyloxycarbazole framework. The ^{1}H-NMR spectrum resembled that of clausamine-C (**219**), except for the presence of a downfield, D_2O-exchangeable aromatic hydroxy group at C-1 (δ 9.14), instead of the aromatic methoxy group of clausamine-C. Based on these spectral data, structure **220** was assigned to clausevatine-D. This assignment was additionally supported by HMQC, HMBC, and NOESY spectra (174) (Scheme 2.53).

The UV spectrum [λ_{max} 240, 251, 271, 282, 315 (sh), and 325 nm] of clausevatine-E (**221**) resembled that of clausevatine-D (**220**), indicating a similar 1-oxygenated-3-carbonyloxycarbazole. The ^{1}H-NMR spectrum was also similar to that of clausevatine-D with an aliphatic hydroxy group at δ 5.45 replacing one of the benzylic protons. Based on the chemical shifts, coupling constants, and NOE analysis of the benzylic and homobenzylic protons, the relative stereochemistry of the benzylic hydroxy and 1-hydroxy-1-methyl-ethyl group was assigned to be *cis*. Based on the spectroscopic data, structure **221** was assigned to clausevatine-E (174) (Scheme 2.54).

The UV, IR, and ^{1}H-NMR spectra of clausevatine-F (**222**) were very similar to those of clausevatine-E (**221**) indicating that the two alkaloids are diastereoisomers. The differences between these two alkaloids were only in the chemical shifts and coupling constants of the benzylic and homobenzylic protons, and indicated a *trans*

stereochemistry of both substituents. Based on these spectral data, structure **222** was assigned to clausevatine-F. This structural assignment was supported by ^{13}C-NMR and NOE spectra (174) (Scheme 2.54).

The UV spectrum [λ_{max} 223, 264 (sh), 274, 287, and 338 nm] of clausevatine-G (**223**) was similar to that of clausevatine-D (**220**), indicating a similar 1-oxygenated-3-carbonyloxycarbazole. The ^{1}H-NMR spectrum also resembled that of clausevatine-D, except for the lack of benzylic protons and the presence of an olefinic singlet at δ 7.65, indicating a double bond at the lactone ring conjugated to the carbazole. Based on these spectral data, and additional support from the ^{13}C-NMR and NOE spectra, structure **223** was assigned to clausevatine-G (174) (Scheme 2.54).

E. Furocarbazole Alkaloids

In 1990, Ito and Furukawa reported the isolation of furostifoline (**224**) and the isomeric eustifoline-D (**227**) from the root bark of *M. euchrestifolia*. These were the first furocarbazole alkaloids obtained from a natural source (101). Seven years later, Wu *et al.* reported the isolation of further furocarbazole alkaloids, furoclausine-A (**225**) and furoclausine-B (**226**) from the root bark of a different plant source, *C. excavata* (128). Furoclausine-B (**226**) was isolated from nature in optically active form $[\alpha]_D$ –32.73 (*c* 0.022, MeOH), however, the absolute stereochemistry is not known (128,175,176) (Scheme 2.55).

The UV spectrum (λ_{max} 238, 274, and 334 nm) of furostifoline (**224**) indicates the presence of a 2-oxygenated carbazole framework. The ^{1}H-NMR spectrum showed the presence of a NH at δ 8.28 and an aromatic methyl group at δ 2.67. The aromatic region showed signals for a low-field H-4 at δ 7.79, a four-spin system indicating the presence of an unsubstituted C-ring, and two doublets with a vicinal-coupling (*J*=2.0 Hz) at δ 7.73 and 7.00 for H-2′ and H-3′ on the furan ring, respectively. The spectral data, supported by NOE results, led to structure **224** for furostifoline (101) (Scheme 2.55).

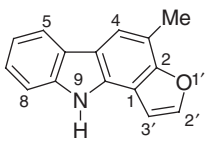

224 Furostifoline

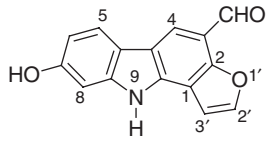

225 Furoclausine-A

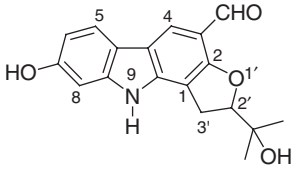

226 Furoclausine-B

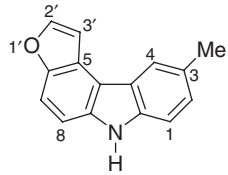

227 Eustifoline-D

Scheme 2.55

The UV spectrum of [λ_{max} 239, 288 (sh), 301, and 345 nm] of furoclausine-A (**225**) resembled that of clausine T (**131**) (see Scheme 2.25) indicating a similar 2,7-dioxygenated-3-formylcarbazole. The ^{1}H-NMR spectrum of furoclausine-A was also very similar to that of clausine T (**131**), except for the absence of all aliphatic signals and the presence of two extra aromatic doublets at δ 7.27 and 7.99 with a characteristic small vicinal coupling (J=2.3 Hz) suggesting the presence of a furan ring instead of the dihydropyran ring of clausine T. This assignment was confirmed by NOE and HMBC experiments. Based on the spectroscopic data, structure **225** was assigned to furoclausine-A. This assignment was supported by ^{13}C-NMR and HMQC spectra (128) (Scheme 2.55).

The UV spectrum of [λ_{max} 231 (sh), 286 (sh), 301, and 339 nm] of furoclausine-B (**226**) resembled that of furoclausine-A (**225**) indicating a similar carbazole nucleus. The ^{1}H-NMR spectrum was also very similar to that of furoclausine-A, except for the absence of two aromatic protons of the furan ring and the presence of two diastereotopic protons for a methylene group at δ 3.40 (d, J=8.3 Hz) and 3.41 (d, J=8.0 Hz) coupled with a tertiary proton at δ 4.92 (1*H*, dd, J=8.3, 8.0 Hz), two methyl singlets at δ 1.21, and a singlet for a hydroxy group at δ 3.60, indicating the presence of a (2-hydroxyisopropyl)dihydrofuran ring. Based on these spectral data, and the structural similarity with furoclausine-A, the structure **226** was assigned for furoclausine-B (128) (Scheme 2.55).

The UV spectrum (λ_{max} 224, 268, 298, 310, and 340 nm) of eustifoline-D (**227**) indicated the presence of a carbazole framework. The ^{1}H-NMR spectrum showed signals for an NH at δ 8.10 and an aromatic methyl group at δ 2.58. The aromatic region exhibited signals for a low-field H-4 at δ 7.97, mutually *ortho*-coupled H-1 and H-2 at δ 7.40 and 7.26, and H-7 and H-8 at δ 7.58 and 7.35, indicating the presence of substitutions at C-3, C-5, and C-6 of the carbazole moiety. Two, vicinally-coupled (J=2.0 Hz) 1*H* signals at δ 7.81 (doublet) and 7.32 (double doublet) were assigned to H-2′ and H-3′ on the furan ring system, respectively. The C-3′ proton showed an additional coupling (J=0.7 Hz) with H-7 at δ 7.58 (1*H*, doublet of doublets, J=8.7, 0.7 Hz). Based on these data, and an NOE of H-3′ on the furan ring (δ 7.32) and H-4 (δ 7.97), structure **227** was assigned to eustifoline-D (101) (Scheme 2.55).

F. Pyrido[4,3-*b*]carbazole Alkaloids

In 1959, Goodwin *et al*. reported the isolation of the fully aromatized pyrido[4,3-*b*]carbazole alkaloids ellipticine (**228**) and 9-methoxyellipticine (**229**) from the leaves of *Ochrosia elliptica* Labill. and *Ochrosia sandwicensis* A.DC. of the Apocynaceae family (177). In the following years, different groups reported the isolation of the same alkaloids from several different plants in the Apocynaceae family namely, *Aspidosperma subincanum* Mart. (178), *Ochrosia maculata* Jacq. (*Ochrosia borbonica* J.F. Gmel.) (179), *Bleekeria vitiensis* (Markgr.) A.C. Sm. (180), *Ochrosia moorei* F. Muell. ex Benth. (181), *Ochrosia acuminata* Trimen (182), as well as the Loganiaceae family, *Strychnos dinklagei* Gilg. (183). Two years later, from the stem bark of *S. dinklagei* Gilg., the same authors reported further ellipticine congeners, 9-hydroxyellipticine (**230**), 13-oxoellipticine (**231**), and 12-hydroxyellipticine (**232**) (184) (Scheme 2.56).

Since the isolation of ellipticine and its congeners from natural sources, and the initial discovery of their anticancer activity in various experimental and human

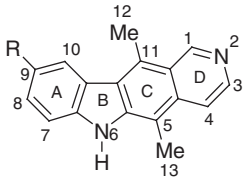

228 Ellipticine
R = H

229 9-Methoxyellipticine
R = OMe

230 9-Hydroxyellipticine
R = OH

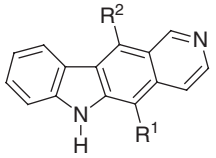

231 13-Oxoellipticine
R^1 = CHO; R^2 = Me

232 12-Hydroxyellipticine
R^1 = Me; R^2 = CH_2OH

Scheme 2.56

tumor systems, a widespread interest in the chemistry and biology of these alkaloids has emerged (185–196). This development resulted in the commercialization of ellipticine derivatives for clinical use in the treatment of myleoblastic leukemia, advanced breast cancer, and other solid tumors (197–201).

The UV spectrum (λ_{max} 224, 237, 245, 275, 285, 293, 331, 346, 380, and 400 nm) of ellipticine (**228**) indicated a pyrido[4,3-*b*]carbazole framework. The ^{1}H-NMR spectrum showed signals for two aromatic methyl groups at δ 2.50 and 2.97 and a D_2O-exchangeable NH at δ 11.10. The aromatic region showed a deshielded *ortho*-coupled (J=8.5 Hz) doublet at δ 8.10, a three-proton multiplet at δ 6.98–7.25, indicating an unsubstituted A-ring of the pyrido[4,3-*b*]carbazole nucleus, two, mutually *ortho*-coupled (J=6.0 Hz) protons at δ 7.65 and 8.15, and a deshielded singlet at δ 9.42. These data indicated the pyrido[4,3-*b*]carbazole framework. The assignment of the ^{13}C-NMR data was achieved through INEPT experiments (202). Based on these spectral data, structure **228** was assigned to ellipticine (183). This assignment was unambiguously confirmed by total synthesis (178), as well as transformation into further ellipticine derivatives (177).

The UV spectrum (λ_{max} 246, 277, 294, 337, 353, and 403 nm) of 9-methoxyellipticine (**229**) resembled that of ellipticine (**228**) indicating a similar pyrido[4,3-*b*]carbazole framework (177). The ^{1}H-NMR spectrum was also very similar to that of ellipticine, except for the presence of an additional aromatic methoxy group at δ 3.97 and the difference in the A-ring substitution pattern of the pyrido[4,3-*b*]carbazole nucleus. The aromatic region showed signals for the mutually *ortho*-coupled (J=8.7 Hz) H-8 and H-7 at δ 7.17 and 7.42, respectively, a deshielded H-10 at δ 7.91 as a doublet with a *meta*-coupling (J=2.4 Hz) to H-8 at δ 7.17, indicating the position of the aromatic methoxy group at C-9. Based on the spectral data, structure **229** was assigned to 9-methoxyellipticine (182). This assignment was unambiguously confirmed by synthesis (203) and transformation into 9-methoxyellipticine derivatives (177).

The UV spectrum (λ_{max} 245, 277, 294, 338, 352, and 400 nm) of 9-hydroxyellipticine (**230**) resembled that of 9-methoxyellipticine (**229**) indicating the presence of a similar pyrido[4,3-*b*]carbazole framework. The ^{1}H-NMR spectrum was also very similar to that of 9-methoxyellipticine (**229**), except for the presence of a hydroxy

group at δ 9.06 instead of the aromatic methoxy group at δ 3.97. The presence of the hydroxy group was confirmed by the characteristic mass fragmentation at m/z 245 (M^+-OH). Based on these spectral data, structure **230** was assigned to 9-hydroxyellipticine (184). This structure was unambiguously confirmed by synthesis (204).

The UV spectrum [λ_{max} 239 (sh), 261, 291, 335, 358, and 404 nm] of 13-oxoellipticine (**231**) resembled that of ellipticine (**228**), indicating a similar pyrido[4,3-*b*]carbazole framework. The ^{1}H-NMR spectrum was also very similar to that of ellipticine (**228**), except for the presence of an aldehyde group at δ 11.05 instead of the aromatic methyl group at C-5 (δ 2.71) of ellipticine. The aldehyde functionality was confirmed by characteristic IR bands at ν_{max} 1655 (C═O) and 2820 (aldehyde CH) cm^{-1}, and a mass fragmentation at m/z 231 (M^+-CHO). Based on these spectral data, structure **231** was assigned to 13-oxoellipticine. This assignment was supported by transformation into 13-oxoellipticine derivatives (205).

The UV spectrum [λ_{max} 278 (sh), 289, 295, and 315 (sh) nm] of 12-hydroxyellipticine (**232**) resembled that of ellipticine (**228**) indicating a similar pyrido[4,3-*b*]carbazole framework. The ^{1}H-NMR spectrum was also similar to that of ellipticine (**228**), except for the presence of a hydroxymethylene group instead of one of the aromatic methyl groups, which was supported by a two-proton singlet at δ 5.48, assigned to the methylene group, and a signal for a D_2O-exchangeable aliphatic hydroxy group at δ 5.44. The hydroxymethylene function at C-11 was confirmed by transformation of 12-hydroxyellipticine to the corresponding *O*-acetyl derivative (184). Based on these spectroscopic data, structure **232** was assigned to 12-hydroxyellipticine (184) (Scheme 2.56).

In 1957, Schmutz *et al.* reported the isolation of (+)-guatambuine (*u*-alkaloid C) (**233**), a tetrahydro-derivative of olivacine, from *Aspidosperma ulei* Markgr. (206,207). In the following year, Carvalho-Ferreira *et al.* reported the same alkaloid from a different *Aspidosperma* species, *Aspidosperma longipetiolatum* Kuhlm. In Brazil, this plant is known as guatambu amarelo (208,209). In 1961, Ondetti and Deulofeu reported the isolation of (+)-guatambuine (**233**) from the root bark of *Aspidosperma australe* Müll. Arg., along with (−)-guatambuine (**233**), and from the stem bark, (±)-guatambuine (**233**) and olivacine (**238a**) (210,211). It is interesting to note that two optical isomers and the racemic form of guatambuine have been obtained from the same natural source. Although, (+)-guatambuine (**233**) $[\alpha]_D^{25} + 112.0$ (*c* 0.990, pyridine) (207), $[\alpha]_D^{25} + 106$ (pyridine) (208), $[\alpha]_D^{29} + 112.0 \pm 3.0$ (*c* 0.485, pyridine), and (−)-guatambuine (**233**) $[\alpha]_D^{26} - 106.0 \pm 2.0$ (pyridine) were isolated in optically active form, the absolute stereochemistry is not known (210,211). In 1959, Woodward *et al.* reported the isolation of *N*-methyltetrahydroellipticine (**234**) from *A. subincanum* Mart. (178). In 1967, Burnell and Casa reported the isolation of (±)-guatambuine (**233**) from the bark of a different *Aspidosperma* species, *Aspidosperma vargasii* A.DC., together with *N*-methyltetrahydroellipticine (**234**) and 9-methoxyolivacine (**238b**) (212).

The UV spectrum (λ_{max} 240, 250, 262, 299, and 330 nm) of (±)-guatambuine (**233**) indicated a carbazole framework (210,211). The ^{1}H-NMR spectrum showed signals for an aromatic methyl group at δ 2.41 and an *N*-methyl group at δ 2.54 as singlets, along with a doublet (J=6.3 Hz) for an aliphatic methyl group at δ 1.52. The ^{1}H-NMR spectrum also showed two ddd-signals (J=5.7, 6.0, and 11.7 Hz) at δ 2.79 and 3.19 for the protons at two C-3, a two-proton multiplet at δ 2.94 for H-4, and a one-proton

quartet (J=6.3 Hz) at δ 3.89 for H-1. The aromatic region showed signals for a downfield H-11 as a singlet at δ 7.70, a four-spin system, indicating an unsubstituted tetrahydropyrido[4,3-*b*]carbazole A-ring. Based on these spectral data, and additional support by ^{13}C-NMR, HMBC, and HMQC spectra, structure **233** was assigned to (±)-guatambuine (213). This assignment was unambiguously confirmed by synthesis from olivacine (**238a**) (see Scheme 2.58) (210,211).

The UV spectrum (λ_{max} 239, 260, 290, 319, and 330 nm) of *N*-methyltetrahydroellipticine (**234**) resembled that of (±)-guatambuine (**233**) indicating a similar tetrahydropyrido[4,3-*b*]carbazole framework. The ^{1}H-NMR spectrum was also very similar to that of (±)-guatambuine (**233**), except for the presence of a singlet at δ 2.68 for an aromatic methyl group instead of the doublet at δ 1.52 for the aliphatic methyl group of (±)-guatambuine, and two equivalent C-1 protons as singlet at δ 3.70, along with a four-proton multiplet at δ 2.92 for H-3 and H-4. These spectral data led to structure **234** for *N*-methyltetrahydroellipticine (212).

In 1995, Moreti *et al.* reported the isolation of janetine (**235**), 3,4-dihydroolivacine (**237**), olivacine (**238a**), and 3-hydroxytetrahydroolivacine (**239**) from the stem bark of *Peschiera buchtienii* (H. Winkl.) Markgr. (syn. *Tabernaemontana buchtienii* H. Winkl.) (214). This tree is common in the Chapare region of Bolivia, and is locally used for the treatment of leishmaniasis (214). Although, janetine (**235**) was isolated from Nature in its optically active form $[\alpha]_D$ +8 (*c* 0.95, EtOH), the absolute stereochemistry is not known (214). In 1958, Schmutz and Hunziker reported the isolation of 3,4-dihydroellipticine (*u*-alkaloid D) (**236**) from *A. ulei* (207). Three years later, the same authors reported the isolation of the same alkaloid, 3,4-dihydroellipticine (**236**) along with 3,4-dihydroolivacine (**237**) as an inseparable mixture (215). In 1961, Büchi *et al.* reported the isolation of 3,4-dihydroellipticine (**236**), together with *N*-methyl-tetrahydroellipticine (**234**) and ellipticine (**228**) (see Scheme 2.56) from a different *Aspidosperma* species, *A. subincanum* (216). In 1982, Michel *et al.* reported the isolation of 3,4-dihydroellipticine (**236**) from the stem bark of *S. dinklagei* (Loganiaceae) (184). In 1958, Schmutz and Hunziker reported the isolation of olivacine (**238a**), an isomeric structure of ellipticine (**228**) (see Scheme 2.56) from *Aspidosperma olivaceum* Müll. Arg. (217). In the following years, olivacine (**238a**) was also isolated from other species of the genera *Aspidosperma*, namely, *A. longepetiolatum* (209), *A. australe* (218), and of the genus *Tabernaemontana*, *Tabernaemontana psychotrifolia* H.B. & K. (219) (Schemes 2.57 and 2.58).

The UV spectrum (λ_{max} 240, 250, 262, 298, and 328 nm) of janetine (**235**) resembled that of (±)-guatambuine (**233**), indicating a similar tetrahydropyrido[4,3-*b*]carbazole framework. The ^{1}H-NMR spectrum was similar to that of (±)-guatambuine, except for the lack of the *N*-methyl group at δ 2.54. The assignment was supported by the mass fragment at m/z 250 (M^+). Based on these spectral data and additional support by ^{13}C-NMR, COSY, HMBC, and HMQC spectra, structure **235** was assigned to janetine (214).

The UV spectrum (λ_{max} 235, 270 (sh), 279, 301, 312, and 378 nm) of **236** indicated a dihydropyrido[4,3-*b*]carbazole framework. This assignment was supported by the IR spectrum (ν_{max} 843, 1028, 1167, 1410, 1595, and 1615 cm^{-1}). The structure for 3,4-dihydroellipticine was confirmed by synthesis from ellipticine and comparison of the IR and UV spectra, melting points and R_f values. Additional support for this assignment derived from the transformation into derivatives of 3,4-dihydroellipticine (216).

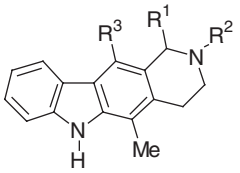

233 Guatambuine
R^1,R^2 = Me; R^3 = H

234 *N*-Methyltetrahydroellipticine
R^1 = H; R^2,R^3 = Me

235 Janetine
R^1 = Me; R^2,R^3 = H

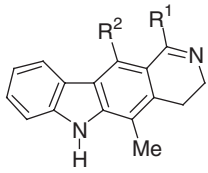

236 3,4-Dihydroellipticine
R^1 = H; R^2 = Me

237 3,4-Dihydroolivacine
R^1 = Me; R^2 = H

Scheme 2.57

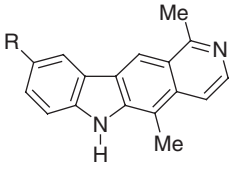

238a Olivacine
R = H

238b 9-Methoxyolivacine
R = OMe

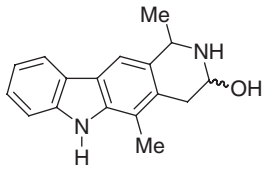

239 3-Hydroxytetrahydroolivacine

Scheme 2.58

The UV spectrum (λ_{max} 235, 274, 282, 298, 310, and 370 nm) of 3,4-dihydroolivacine (**237**) indicated a dihydropyrido[4,3-*b*]carbazole framework. The ^{1}H-NMR spectrum showed signals for an NH proton at δ 8.25, two aromatic methyl groups at δ 2.40 and 2.55, and two triplets (J=7.0 Hz) at δ 2.80 and 3.70 for the C-4 and C-3 protons. The aromatic region showed signals for H-11 as a downfield singlet at δ 8.10, a four-spin system indicating an unsubstituted A-ring of the dihydropyrido [4,3-*b*]carbazole. Based on these spectroscopic data, structure **237** was assigned to 3,4-dihydroolivacine (214).

The UV spectrum (λ_{max} 218, 235, 265, 289, and 324 nm) of olivacine (**238a**) indicated a pyrido[4,3-*b*]carbazole framework (220). The ^{1}H-NMR spectrum showed signals for two aromatic methyl groups at δ 2.90 and 3.20. The aromatic region showed signals for H-11 as a deshielded singlet at δ 8.70, a four-spin system indicating an unsubstituted pyrido[4,3-*b*]carbazole A-ring, and two mutually *ortho*-coupled (J=6.3 Hz) protons at δ 7.80 and 8.17, indicating a methyl-substituted pyrido[4,3-*b*]carbazole framework. Based on these spectral data, structure **238a** was assigned for olivacine (214). This assignment was unambiguously confirmed by synthesis (220), as well as transformation into known derivatives (210,211).

The UV spectrum (λ_{max} 222, 239, 269, 290, and 323 nm) of 9-methoxyolivacine (**238b**) resembled that of olivacine (**238a**), indicating a similar pyrido[4,3-*b*]carbazole framework. The ^{1}H-NMR spectrum was also similar to that of olivacine, except for

the presence of an additional aromatic methoxy group and the difference in the A ring substitution pattern of the pyrido[4,3-*b*]carbazole nucleus. The aromatic region showed, instead of the four-spin proton system, a three-spin proton system in which H-10 at δ 7.50 was only *meta*-coupled to H-8 at δ 7.00. The *ortho*-coupling of H-8 to H-7 at δ 7.31 confirmed the position of the aromatic methoxy group at C-9. Based on these spectroscopic data, structure **238b** was assigned to 9-methoxyolivacine. The assignment was additionally supported by transformation into derivatives and comparison of their spectral data (212).

The UV spectrum (λ_{max} 242, 251, 261, 297, and 329 nm) of 3-hydroxytetrahydroolivacine (**239**) resembled that of janetine (**235**) (see Scheme 2.57), indicating a similar tetrahydropyrido[4,3-*b*]carbazole framework. The ^{1}H-NMR spectrum was also similar to that of janetine, except for the presence of an additional aliphatic hydroxy group. The spectral data indicated a hydroxylated janetine. This assignment was by the mass fragment at m/z 266 (M^+), which is 16 more than for janetine. The position of the hydroxy group was assigned to C-3 based on the presence of a triplet (1*H*, *J*=2.0 Hz) at δ 4.90, which suggested a hemiaminal group. Based on these spectral data, structure **239** was assigned to 3-hydroxytetrahydroolivacine (214).

In 1981, Potier *et al.* reported the isolation of *N*-oxyellipticine (**240**) from *O. moorei* (181). In the following year, Michel *et al.* reported the isolation of another *N*-oxyellipticine derivative, *N*-oxy-13-oxoellipticine (**241**), from the stem bark of *S. dinklagei* (184). Five years later, the same authors isolated from the bark of the same natural source, a novel, natural, bis-ellipticine alkaloid, strellidimine (**242**), in racemic form (221). Strellidimine represented the first example of a natural bis-ellipticine alkaloid, containing a 9-hydroxyellipticine (**230**) unit (see Scheme 2.56) linked to a 3,4-dihydroellipticine (**236**) unit (see Scheme 2.57) (221) (Scheme 2.59).

The UV spectrum (λ_{max} 240, 268, 278, 288, 295, and 330 nm) of *N*-oxyellipticine (**240**) resembled that of ellipticine (**228**) (see Scheme 2.56), indicating a similar pyrido[4,3-*b*]carbazole framework (222). Comparison of the mass spectrum of *N*-oxyellipticine at m/z 262 (M^+), with that of ellipticine (**228**) showed only the presence of an additional oxygen as an *N*-oxy function. This conclusion was supported by comparison with the spectral data of synthetic *N*-oxyellipticine, obtained by oxidation of ellipticine (**228**) with H_2O_2 in dichloromethane, and by reduction of *N*-oxyellipticine with zinc to ellipticine. Based on these comparisons,

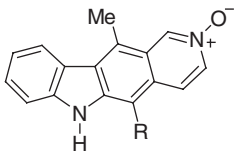

240 *N*-Oxyellipticine
R = Me

241 *N*-Oxy-13-oxoellipticine
R = CHO

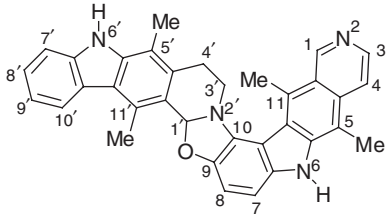

242 Strellidimine

Scheme 2.59

structure **240** was assigned to *N*-oxyellipticine (222). This assignment was unequivocally confirmed by an X-ray crystal structure analysis (223) (Scheme 2.59).

The UV spectrum [λ_{max} 233 (sh), 287 (sh), 296, 323 (sh), and 354 nm] of *N*-oxy-13-oxoellipticine (**241**) indicated a pyrido[4,3-*b*]carbazole framework. The ^{1}H-NMR spectrum was very similar to that of 13-oxoellipticine (**231**) (see Scheme 2.56), except for the upfield shift of H-1 and H-3 at δ 9.28 and 8.48, when compared to the corresponding signals for 13-oxoellipticine for H-1 at δ 10.0 and for H-3 at δ 9.15. The *N*-oxy function was supported by the mass fragment at m/z 276 (M^+). Based on these spectral data, structure **241** was assigned to *N*-oxy-13-oxoellipticine. This assignment was unequivocally confirmed by transformation of *N*-oxy-13-oxoellipticine to 13-oxoellipticine (**231**) (see Scheme 2.56) (184).

The UV spectrum [λ_{max} 244, 253, 265, 279, 298, 327 (sh), 340, and 410 nm] of strellidimine (**242**) indicated a highly conjugated, polyaromatic system with at least one pyridine ring. The chemical ionization mass spectrum (CI-MS) (NH_3) showed a molecular ion at m/z 509 (M^++H), along with two fragment ions at m/z 263 and 247, typical of hydroxyellipticine and dihydroellipticine units. The ^{1}H-NMR spectrum of strellidimine showed most of the characteristic signals of these two monomeric units, although there were differences in the aromatic region, when compared to the spectra of 9-hydroxyellipticine (**230**) (see Scheme 2.56) and 3,4-dihydroellipticine (**236**) (see Scheme 2.57). The two signals typical for H-10 of 9-hydroxyellipticine and for H-1 of 3,4-dihydroellipticine were absent, whereas the two signals of H-7 and H-8 of the hydroxyellipticine moiety appeared as a simple AB system at δ 7.34 and 7.29, respectively. A singlet typical of an isolated proton at C-2 of a 2,3-dihydrooxazole ring appeared at δ 6.55. Based on these spectral data, structure **242** was assigned to strellidimine. This assignment was confirmed by synthesis *via* oxidative coupling of 9-hydroxyellipticine (**230**) and 3,4-dihydroellipticine (**236**) in phosphate buffer with horseradish peroxidase-H_2O_2 (221) (Scheme 2.59).

G. Miscellaneous Carbazole Alkaloids

In 1993, Kusano *et al.* isolated 2-hydroxy-7-methyl-9*H*-carbazole (**243**) from the aerial parts of *Cimicifuga simplex* Wormsk. ex DC. (224). Six years later, Wu *et al.* reported the isolation of clausine V (**244**) from the root bark of *C. excavata* (43) (Scheme 2.60). The UV spectrum (λ_{max} 236, 261, and 305 nm) of 2-hydroxy-7-methyl-9*H*-carbazole (**243**) indicated a 2-hydroxycarbazole. This assignment was supported by the IR spectrum [ν_{max} 1611 (aromatic system), 2700–3000 (OH), and 3400 (NH) cm^{-1}]. The presence of a hydroxy function was confirmed by transformation into the corresponding *O*-acetate and comparison with 2-hydroxy-7-methyl-9*H*-carbazole.

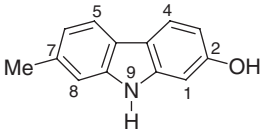

243 2-Hydroxy-7-methyl-9*H*-carbazole

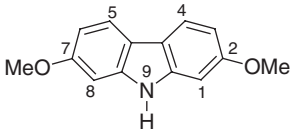

244 Clausine V

Scheme 2.60

The ^{1}H-NMR spectrum showed signals for an aromatic methoxy group at δ 2.45 and two sets of three-spin systems in the aromatic region. The first set appeared at δ 6.79 (d, J=2.1 Hz), 6.68 (dd, J=8.3, 2.1 Hz), and 7.80 (d, J=8.3 Hz), and was assigned to H-1, H-3, and a deshielded H-4, respectively. The signals of the second set appeared at δ 6.89 (dd, J=8.8, 1.7 Hz), 7.13 (br s), and 7.77 (d, J=8.8 Hz), and were assigned to H-6, H-8, and a deshielded H-5, respectively. Based on these spectral data and additional support by ^{13}C-NMR, COSY, NOESY, HMBC, and HMQC spectra, structure **243** was assigned to 2-hydroxy-7-methyl-9*H*-carbazole (224).

The UV spectrum (λ_{max} 208, 236, 261, 311, and 319 nm) of clausine V (**244**) indicated a 2,7-dioxygenated carbazole framework. This assignment was supported by the IR spectrum [ν_{max} 1615 (aromatic system), and 3380 (NH) cm^{-1}]. The ^{1}H-NMR spectrum showed a signal for an NH proton at δ 10.13 and a singlet for two aromatic methoxy groups at δ 3.84. In the aromatic region, a set of mutually *ortho*-coupled (J=8.4 Hz) protons at δ 7.84 and 6.76 for H-4, H-5, H-3, and H-6, appeared together with a set of *meta*-coupled (J=2.3 Hz) protons at δ 6.98 for H-1 and H-8, indicating the presence of methoxy groups at C-2 and C-7. These spectral data confirmed a symmetrical carbazole and led to structure **244** for clausine V (43).

II. CARBAZOLE ALKALOIDS FROM OTHER SOURCES

While 1- and 2-oxygenated tricyclic carbazole alkaloids were isolated primarily from higher plants, various tricyclic carbazole alkaloids, which are 3-oxygenated or 3,4-dioxygenated, were obtained from alternative natural sources, such as microbial, marine, and mammalian sources.

A. Tricyclic Carbazole Alkaloids

1 3-Oxygenated Tricyclic Carbazole Alkaloids

Since the late 1960s, several carbazole alkaloids oxygenated in the 3-position were isolated from diverse natural sources, the majority of which were isolated from different plant sources. However, in 1979, Moore *et al.* reported the isolation of two unusual, non-basic, 3-oxygenated carbazole alkaloids, hyellazole (**245**) and chloro-hyellazole (**246**), from the blue-green marine algae *Hyella caespitosa* (225). These alkaloids have structures entirely different from those of the carbazole alkaloids isolated from terrestrial plants.

The UV spectrum [λ_{max} 226, 232, 238 (sh), 250 (sh), 260 (sh), 292 (sh), 304, 338, and 352 nm] of hyellazole (**245**) indicated a carbazole framework. This assignment was supported by the IR band at ν_{max} 3490 (NH) cm^{-1}. The ^{1}H-NMR spectrum of hyellazole (**245**) showed signals for an aromatic methyl group at δ 2.14, an aromatic methoxy group at δ 3.99, and an NH group at δ 9.52. In the aromatic region at δ 7.35–7.60 appeared a complex multiplet for 6*H*, indicating the presence of a phenyl group along with H-8 of the carbazole nucleus at δ 7.50. Additionally, the aromatic region showed the presence of a deshielded H-4 at δ 7.70 as a singlet, indicating substitution at C-1, C-2, and C-3, along with three, mutually *ortho*-coupled protons at δ 8.08, 7.28, and 7.11 for deshielded H-5, H-7, and H-6, respectively. Based on these

spectral data and additional support from the ^{13}C-NMR spectrum, structure **245** was assigned to hyellazole (225).

The UV [λ_{max} 220, 235, 242, 255 (sh), 272 (sh), 300 (sh), 310, 348, and 360 nm] spectrum of chlorohyellazole (**246**) resembled that of hyellazole (**245**). The ^{1}H-NMR spectrum was also similar to that of hyellazole (**245**), except for the absence of H-6, as shown by two, mutually *meta*-coupled protons at δ 8.13 and 7.27, assigned to a deshielded H-5 and H-7, respectively, indicating the position of the chlorine atom to be at C-6. These spectral data led to structure **246** for chlorohyellazole. This assignment was unequivocally confirmed by an X-ray crystal structure analysis (225).

In 1989, Kato *et al.* reported the isolation of carazostatin (**247**) from *Streptomyces chromofuscus*. Carazostatin represents a novel radical scavenger more active than butylated hydroxytoluene (BHT) (226). Moreover, it exhibits strong inhibitory activity against the free radical-induced, lipid peroxidation in liposomal membranes, and shows stronger antioxidant activity than α-tocopherol (227).

The UV spectrum (λ_{max} 218, 235, 254, 266, 303, and 342 nm) of carazostatin (**247**) indicated a 3-hydroxycarbazole framework. This assignment was supported by the IR spectrum [ν_{max} 1590 (aromatic system), 3360 (OH), and 3460 (NH) cm^{-1}]. The presence of OH and NH functions were confirmed by transformation of carazostatin into *N,O*-dimethylcarazostatin, and comparison of the data. The ^{1}H-NMR spectrum of carazostatin (**247**) showed an aromatic methyl (δ 2.38) and two broad singlet protons for NH (δ 7.77) and OH (δ 4.72) groups. The presence of an *n*-heptyl group was indicated by ^{1}H-NMR signals at δ 2.87 (2*H*, t, *J*=7.9 Hz), 1.65 (2*H*, m), 1.30–1.46 (8*H*, m), and 0.91 (3*H*, t, *J*=7.0 Hz). The aromatic region showed signals for a low-field H-4 at δ 7.31, and a four-spin system indicating an unsubstituted C-ring of the carbazole. The NOE studies with *N,O*-dimethylcarazostatin confirmed the position of the hydroxy, aromatic methyl, and *n*-heptyl groups at C-3, C-2, and C-1, respectively. On the basis of these spectral data, and additional support from the ^{13}C-NMR, COSY, and HMBC spectra, structure **247** was assigned to carazostatin (226) (Scheme 2.61).

In 1990, Seto *et al.* described the isolation of antiostatin A_1 (**248**), A_2 (**249**), A_3 (**250**), A_4 (**251**), B_2 (**252**), B_3 (**253**), B_4 (**254**), and B_5 (**255**) from *Streptomyces cyaneus* 2007-SV$_1$. The antiostatins represent the first carbazole derivatives with an acetamido group or a substituted urea chain, and exhibited strong inhibitory activity against free radical-induced lipid peroxidation (228) (Scheme 2.62).

The UV spectrum (λ_{max} 220, 238, 301, 338, and 350 nm) of antiostatin A_1 (**248**) indicated the presence of a carbazole framework. This was also discernible from its IR spectrum. The ^{1}H-NMR spectrum of antiostatin A_1 (**248**) showed an *N*-acetyl group (δ 2.47, 3*H*, s and 9.68, 1*H*, br s), an aromatic methyl group (δ 2.40), a phenolic

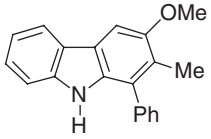

245 Hyellazole

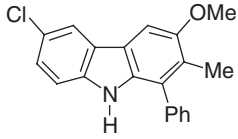

246 Chlorohyellazole

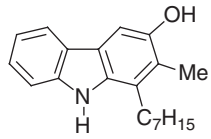

247 Carazostatin

Scheme 2.61

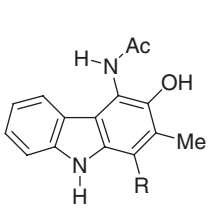

248 Antiostatin A_1
R = $(CH_2)_4Me$

249 Antiostatin A_2
R = $(CH_2)_2CHMeCH_2Me$

250 Antiostatin A_3
R = $(CH_2)_4CHMe_2$

251 Antiostatin A_4
R = $(CH_2)_6Me$

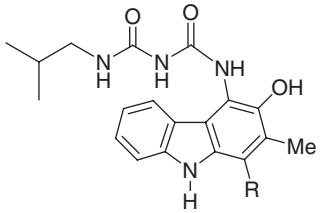

252 Antiostatin B_2
R = $(CH_2)_5Me$

253 Antiostatin B_3
R = $(CH_2)_4CHMe_2$

254 Antiostatin B_4
R = $(CH_2)_6Me$

255 Antiostatin B_5
R = $(CH_2)_5CHMe_2$

Scheme 2.62

hydroxy group (δ 8.05), and an NH group (δ 10.16). The presence of an *n*-pentyl group was indicated by ^{1}H-NMR signals at δ 2.97 (2*H*, t), 1.65 (2*H*, m), 1.45 (2*H*, m), 1.37 (2*H*, m), and 0.89 (3*H*, t). The aromatic region showed signals for a four-spin system indicating an unsubstituted C-ring of the carbazole nucleus. From the HMBC spectra, and comparison of the ^{13}C-NMR spectra with those of carazostatin (**247**) (see Scheme 2.61), the *n*-pentyl, aromatic methyl, aromatic hydroxy, and *N*-acetyl groups were located at C-1, C-2, C-3, and C-4 of the carbazole nucleus. Based on the spectral data, structure **248** was assigned to antiostatin A_1 (228). Comparison of the ^{1}H-NMR and mass spectral data of antiostatin A_1 (**248**) with those of the antiostatins A_2, A_3, and A_4 confirmed the structures for **249**, **250**, and **251**.

The UV spectrum (λ_{max} 218, 238, 301, 338, and 352 nm) of antiostatin B_4 (**254**) resembled that of antiostatin A_1 (**248**), indicating a similar carbazole framework. This was also supported from its IR spectrum. The ^{1}H-NMR spectrum of antiostatin B_4 (**252**) was also very similar to that of antiostatin A_1 (**248**), except for the presence of an isobutylurea group instead of the acetyl group. Moreover, C-1 was substituted by an *n*-heptyl side chain, as supported by peaks at δ 2.98 (2*H*, t), 1.66 (2*H*, m), 1.47 (2*H*, m), 1.36 (2*H*, m), 1.30 (2*H*, m), 1.28 (2*H*, m), and 0.89 (3*H*, t). Based on these spectroscopic data, and additional support from the ^{13}C-NMR and HMBC spectra, structure **254** was assigned to antiostatin B_4 (228). Comparison of the ^{1}H-NMR and mass spectral data of antiostatin B_4 (**254**) with those of the antiostatins B_2, B_3, and B_5 confirmed the structures for **252**, **253**, and **255** (228) (Scheme 2.62).

In 1997, Seto *et al.* reported the isolation of the novel neuronal protecting substances, carbazomadurin A (**256**) and carbazomadurin B (**257**) from *Actinomadura madurae* 2808-SV1. Carbazomadurin B (**257**) was isolated from Nature in optically active form $[\alpha]_D^{24} + 4.0$ (*c* 0.05, MeOH). However, the absolute configuration was not determined (229) (Scheme 2.63).

The UV spectrum [λ_{max} 237, 249 (sh), 289 (sh), 299, 347, and 357 nm] of carbazomadurin B (**257**) indicated a carbazole framework. The ^{1}H-NMR spectrum showed an aromatic methyl at δ 2.26, a hydroxymethyl at δ 5.01, and an NH group at

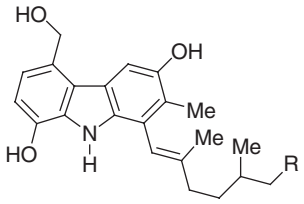

256 Carbazomadurin A
R = H

257 Carbazomadurin B
R = Me

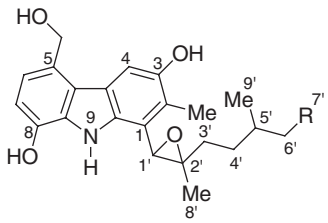

258 Epocarbazolin A
R = H

259 Epocarbazolin B
R = Me

Scheme 2.63

δ 8.89. The DQF-COSY and HMBC spectra revealed the presence of alkyl, aromatic methyl, and hydroxy groups at C-1, C-2, and C-3 of the A-ring of the carbazole, which was also supported by the presence of a deshielded H-4 at δ 7.59. Based on the 2D-NMR DQF-COSY and HMBC spectra, the structure of the alkyl side chain was confirmed as 2,5-dimethylhept-1-ene. The stereochemistry of the double bond in the 2,5-dimethylhept-1-ene side chain was assigned as *E* based on NOE spectra. Moreover, the HMBC spectrum indicated the presence of a hydroxymethyl group at C-5, and a second hydroxy group at C-8, which was supported by two aromatic protons at δ 6.92 and 6.72 for H-6 and H-7, respectively. Based on these spectroscopic data, structure **257** was assigned to carbazomadurin B (229).

The UV spectrum [λ_{max} 237, 250 (sh), 289 (sh), 299, 345, and 357 nm] of carbazomadurin A (**256**) resembled that of carbazomadurin B (**257**), indicating a similar carbazole framework. The ^{1}H-NMR spectrum was also similar to that of carbazomadurin B (**257**), except for the signals of the alkyl side chain. Detailed analysis of the DQF-COSY and HMBC spectra confirmed a 2,5-dimethylhex-1-ene side chain at C-1 with the same configuration of the double bond. Based on the spectral data, structure **256** was assigned to carbazomadurin A (229).

In 1993, Oki *et al.* isolated the novel carbazole antibiotics epocarbazolin A (**258**) and B (**259**) from the culture broth of *Streptomyces anulatus* T688-8 (230). They represent the first carbazole alkaloids with an epoxide moiety in a side chain, and are the epoxides corresponding to carbazomadurin A (**256**) and B (**257**). Epocarbazolin A (**258**) $[\alpha]_D^{26}$ + 75.0 (*c* 0.5, MeOH) and B (**259**) $[\alpha]_D^{26}$ + 78.0 (*c* 0.5, MeOH) were obtained from Nature in optically active form. However, their absolute configuration is not known. These alkaloids showed potent 5-lipoxygenase inhibitory activity and weak antibacterial activity (230) (Scheme 2.63).

The UV spectrum [λ_{max} 233, 250 (sh), 289 (sh), 300, 344, and 358 nm] of epocarbazolin B (**259**) resembled that of carbazomadurin B (**257**) indicating the presence of a similar carbazole framework. The ^{1}H-NMR spectrum was also similar to that of carbazomadurin B (**257**), except for the presence of an epoxide instead of the double bond in the side chain. This epoxide was confirmed by the chemical shifts of C-1′ and C-2′ (δ 64.7 and 63.9), and the C–H coupling constant of C-1′ and H-1′ (*J*=175 Hz). Additional support for this assignment was derived from COSY experiments. The structure was unequivocally supported by COSY and NOESY

studies of *N*,*O*-tetramethylepocarbazolin B, prepared by the permethylation of epocarbazolin B with MeI in the presence of NaH in DMF (230).

The UV spectrum [λ_{max} 234, 250 (sh), 289 (sh), 299, 345, and 359 nm] of epocarbazolin A (**258**) resembled that of epocarbazolin B (**259**), indicating a similar carbazole framework. The ^{1}H-NMR spectrum was also similar to that of epocarbazolin B (**259**), but lacked the signal for one methylene group in the alkyl side chain, indicating a 3-methylbutyl group instead of the 3-methylpentyl group. This assignment was supported by the FAB-mass spectrum with a molecular ion at m/z 369 (M^+). Based on the spectral data, and additional support from the ^{13}C-NMR spectrum, structure **258** was assigned to epocarbazolin A (230).

2 3,4-Dioxygenated Tricyclic Carbazole Alkaloids

A broad range of structurally diverse 3,4-dioxygenated carbazole alkaloids, such as the carbazomycins A–F (**260-265**) and the neocarazostatins A–C (**266-268**) were isolated from different *Streptomyces* species.

In 1980, Nakamura *et al.* reported the isolation of carbazomycin A (**260**) and B (**261**) from *Streptomyces ehimense* H 1051-MY 10 (231). These structurally unique alkaloids (232,233), biogenetically derived from tryptophan (234), were the first antibiotics with a carbazole framework. Six years later, Marumo *et al.* reported the isolation of carbazomycin E (carbazomycinal) (**264**) and F (6-methoxycarbazomycinal) (**265**) from a different *Streptoverticillium* species of the strain KCC U-0166 (235). Subsequently, these alkaloids were isolated by Nakamura *et al.* from *S. ehimense* H 1051-MY 10, along with further members of the carbazomycin family, carbazomycin C (**262**) and D (**263**) (236). Carbazomycin A and B inhibit the growth of phytopathogenic fungi and have antibacterial and antiyeast activities (231). Carbazomycin B (**261**) and C were shown to inhibit 5-lipoxygenase (237).

The UV spectrum (λ_{max} 223, 242, 293, 327, and 340 nm) of carbazomycin A (**260**) indicates the presence of a carbazole framework (231). The ^{1}H-NMR spectrum showed a signal for an NH proton at δ 7.89, two aromatic methyl groups at δ 2.40, and two aromatic methoxy groups at δ 3.92 and 4.13. The aromatic region showed overlapping of three proton signals at δ 7.13−7.42 and a deshielded *ortho*- and *meta*-coupled (J=7.0, 2.0 Hz) dd-signal for H-5 at δ 8.25 suggesting the lack of substituents on ring C of the carbazole nucleus. Based on the ^{13}C-NMR decoupling technique and their chemical shift positions, two aromatic methyl and two aromatic methoxy groups were assigned to the C-1, C-2, C-3, and C-4 positions of the carbazole nucleus, respectively. Moreover, this assignment was supported by the presence of two aromatic methyl carbons at higher field (δ_C 12.6 and 13.6) than the usual values (δ_C 15∼25) and two methoxy carbons at lower field (δ_C 60.5 and 61.1) than the usual values (δ_C 53∼57). Additionally, the position of the aromatic methoxy group at C-3 was supported by the mass fragment at m/z 212 (M^+-CH_3–CO) in the EI-MS. Based on these spectroscopic data, structure **260** was assigned to carbazomycin A (232) (Scheme 2.64).

The UV spectrum (λ_{max} 224, 245, 289, 330, and 340 nm) of carbazomycin B (**261**) resembled that of carbazomycin A (**260**), indicating a similar carbazole framework (231). The ^{1}H-NMR spectrum was similar to that of carbazomycin A, except for the presence of a phenolic hydroxy group at δ 6.21 instead of the C-4 methoxy group at δ 4.13. The presence of a hydroxy group at C-4 was confirmed by the transformation of carbazomycin B into 4-deoxycarbazomycin B (reduction of *O*-tosylcarbazomycin B

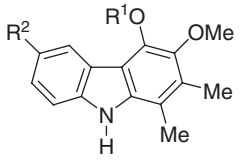

260 Carbazomycin A
R^1 = Me; R^2 = H
261 Carbazomycin B
R^1,R^2 = H
262 Carbazomycin C
R^1 = H; R^2 = OMe
263 Carbazomycin D
R^1 = Me; R^2 = OMe

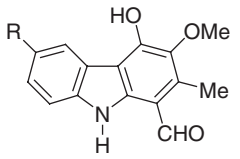

264 Carbazomycin E
R = H
265 Carbazomycin F
R = OMe

Scheme 2.64

over Raney nickel) and transformation into carbazomycin A by *O*-methylation with diazomethane (231,232). Based on the spectral data, structure **261** was assigned to carbazomycin B. This assignment was unequivocally confirmed by an X-ray crystallographic analysis (233).

The UV spectrum [λ_{max} 227, 245, 287 (sh), 341, and 354 nm] of carbazomycin C (**262**) resembled that of carbazomycin B (**261**) indicating a similar carbazole framework. The ^{1}H-NMR spectrum was also similar to that of carbazomycin B, except for the difference in the C-ring aromatic substitution pattern and the presence of an additional aromatic methoxy group at δ 3.84. In the aromatic region, the deshielded H-5 showed a *meta*-coupling (J=2.4 Hz) at δ 7.7 indicating a methoxy group at C-6. This assignment was supported by the mutually *ortho*-coupled (J=8.8 Hz) aromatic protons at δ 6.91 and 7.31, assigned to H-7 and H-8. Moreover, H-7 at δ 6.91 showed a *meta*-coupling (J=2.4 Hz) with H-5 (δ 7.7). The ^{13}C-NMR spectrum also supported these assignments. Due to the shifts induced by the presence of the methoxy groups, the signals for C-5, C-6, C-7, and C-8 appeared at δ 106.2, 154.0, 113.9, and 111.5, respectively. Based on these spectral data, structure **262** was assigned to carbazomycin C. Additional structural support derived from transformation into carbazomycin D (**263**) by *O*-methylation of **262** with dimethyl sulfate and potassium carbonate in boiling acetone (236). The assignment was unequivocally confirmed by X-ray crystallographic analysis (238).

The UV spectrum [λ_{max} 229, 247, 291 (sh), 340, and 356 nm] of carbazomycin D (**263**) resembled that of carbazomycin C (**262**) indicating a similar carbazole framework. The ^{1}H-NMR spectrum was also similar to that of carbazomycin C, except for the presence of an additional aromatic methoxy group at δ 4.06 instead of the aromatic hydroxy group (δ 8.06). These data suggested an *O*-methyl ether of carbazomycin C for carbazomycin D. Based on the spectral data, structure **263** was assigned to carbazomycin D. This structure was unambiguously confirmed by *O*-methylation of carbazomycin C (**262**) using dimethyl sulfate and potassium carbonate in boiling acetone (236).

The UV spectrum (λ_{max} 227, 263, 295, 320, and 372 nm) of carbazomycin E (**264**) indicated a carbazole framework. The ^{1}H-NMR spectrum showed the signal of an

aldehyde group (δ_H 10.41, δ_C 189.4). The aldehyde group was confirmed by characteristic IR bands at ν_{max} 1660 (C═O) and 2860 (aldehyde CH) cm^{-1}. Moreover, the ^{1}H-NMR spectrum showed signals for an aromatic methyl, a methoxy, and a hydroxy group at δ 2.77, 3.81, and 9.57, respectively. The aromatic region showed the signals of a four-spin system, indicating an unsubstituted C-ring of the carbazole. This assignment was confirmed by four aromatic CH-signals in the ^{13}C-NMR spectrum. Based on NOE experiments, the positions of the aromatic methyl and aldehyde groups were assigned to C-2 and C-1, respectively. The position of the aromatic methoxy group at C-3 was supported by the mass fragmentation ion at m/z 212 (M^+-CH_3–CO) in the EI-MS. Based on these spectral data, structure **264** was assigned to carbazomycin E (235).

The UV spectrum (λ_{max} 227, 268, 295, 310, and 382 nm) of carbazomycin F (**265**) resembled that of carbazomycin E (**264**) indicating the presence of a similar carbazole framework. The ^{1}H-NMR spectrum was also similar to that of carbazomycin E, except for an additional aromatic methoxy group at δ 3.93, and the difference in the aromatic substitution pattern. The aromatic region showed an *ortho*- and *meta*-coupled (J=8.5, 2.7 Hz) doublet of doublets at δ 7.05, a doublet with an *ortho*-coupling (J=8.5 Hz) at δ 7.38, and another broad doublet proton with a *meta*-coupling (J=2.7) at δ 7.72. The most deshielded proton at δ 7.72 was assigned to H-5. The chemical shifts and the splitting pattern in the aromatic region suggested C-6 as the position for the second aromatic methoxy group. This assignment was confirmed by a long-range selective proton decoupling (LSPD) experiment. Based on these spectral data, structure **265** was assigned to carbazomycin F. This structure was unambiguously confirmed by *O*-methylation of carbazomycin E (**264**) (235).

In 1991, Kato *et al*. reported the isolation of the neocarazostatins A (**266**), B (**268**), and C (**267**) from the culture of *Streptomyces* species strain GP 38 (239). Although, the neocarazostatins A (**266**) $[\alpha]_D^{25}$ − 36.0 (*c* 0.1, MeOH), B (**268**) $[\alpha]_D^{25}$ − 24.0 (*c* 0.1, MeOH), and C (**267**) $[\alpha]_D^{25}$ − 92.0 (*c* 0.1, MeOH) were optically active, their absolute configuration was not determined. The neocarazostatins exhibited strong inhibitory activity against the free radical-induced lipid peroxidation (239) (Scheme 2.65).

The UV spectrum (λ_{max} 230, 250, 271, 292, 331, and 345 nm) of neocarazostatin A (**266**) resembled that of carbazomycin B (**261**) (see Scheme 2.64), indicating a similar carbazole framework. In the ^{13}C-NMR spectrum, 12 signals due to the carbazole nucleus in neocarazostatin A were almost identical to those of the analogous carbons

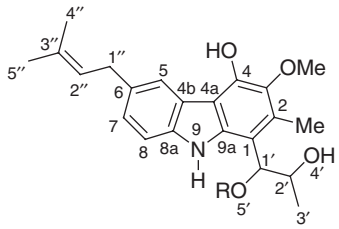

266 Neocarazostatin A
R = H

267 Neocarazostatin C
R = Me

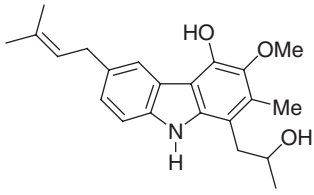

268 Neocarazostatin B

Scheme 2.65

in the spectrum of carbazomycin B, except for the signals assigned to C-1 and C-6, indicating a 1,6-disubstituted carbazomycin B-type chromophore for neocarazostatin A. Moreover, the ^{1}H-, ^{13}C-NMR, and ^{1}H–^{1}H COSY spectra of neocarazostatin A indicated the existence of the partial structures –CHOHCHOHMe and –CH_2CH=CMe_2. Furthermore, the HMBC spectrum showed long-range couplings of H-1′ (CH) to C-1, C-2, and C-9a, and of H-1″ (CH_2) to C-5, C-6, and C-7, indicating the attachment of partial structure –CHOHCHOHMe to C-1 and of CH_2CH=CMe_2 to C-6. Based on these spectral data, structure **266** was assigned to neocarazostatin A (239).

The UV spectrum (λ_{max} 231, 250, 271, 292, 331, and 345 nm) of neocarazostatin C (**267**) resembled that of neocarazostatin A (**266**), indicating a similar carbazole framework. The ^{1}H-NMR and ^{13}C-NMR spectra of neocarazostatin C were also similar to those of neocarazostatin A, except for the presence of one methoxy group (δ_H 3.25, δ_C 56.9). The HMBC spectrum showed the long-range coupling of the *O*-methyl protons to C-1′. Based on the spectral data, structure **267** was assigned to neocarazostatin C (239).

The UV spectrum (λ_{max} 228, 249, 270, 292, 331, and 344 nm) of neocarazostatin B (**268**) resembled that of neocarazostatin A (**266**), indicating a similar carbazole. Comparison of the mass fragmentation (*m*/*z* 353, M^+) in the EI-MS spectrum of neocarazostatin B (**268**) with that of neocarazostatin A (**266**) confirmed a deoxy-derivative of neocarazostatin A. The ^{1}H-NMR and ^{13}C-NMR spectra of neocarazostatin B also resembled those of neocarazostatin A, except for the signals of H-1′ (δ_H 2.93 and 3.03, instead of 4.92) and C-1′ (δ_C 38.6, instead of 76.5). Based on the spectroscopic data, structure **268** was assigned to neocarazostatin B (239).

3 Tricyclic Carbazole-1,4-quinol Alkaloids

In 1988, Nakamura *et al*. reported the isolation of carbazomycins G (**269**) and H (**270**) from the culture broth of *Streptoverticillium ehimense*. These alkaloids have a structurally unique carbazole-1,4-quinol framework and were obtained from Nature in racemic form. Carbazomycin G showed moderate antifungal activity against *Trichophyton* species (238).

The UV spectrum [λ_{max} 214, 253, 272 (sh), 278, and 340 nm] of carbazomycin G (**269**) indicated a carbazole. The ^{1}H-NMR spectrum showed signals for an NH at δ 12.27, an aromatic methoxy group at δ 3.71, and two methyl groups. However, the signals for the methyl groups appeared at higher field than aromatic methyl signals, such as those of carbazomycin B (**251**) (δ 2.35 and 2.39) (see Scheme 2.64). The signal at δ 2.01 was assigned to an olefinic methyl group, and the other signal at δ 1.60 to a tertiary methyl group at an oxy-substituted carbon. This assignment was confirmed by the ^{13}C-NMR methyl signals at δ 10.1 and 27.9, assigned to the vinylic methyl group and the tertiary methyl group, respectively. Moreover, the ^{13}C-NMR spectrum showed signals for a quaternary carbon at δ 67.3 and a carbonyl carbon at δ 177.5. The ^{1}H-NMR spectrum showed a three-proton multiplet at δ 7.21–7.50 and a deshielded signal for H-5 at δ 8.05, indicating an unsubstituted C-ring. The spectral data, and biogenetic considerations, of the carabazomycins led to structure **269** for carbazomycin G. The assignment was confirmed by an X-ray crystallographic analysis (238).

The UV spectrum (λ_{max} 214, 253, 261 (sh), 292, and 340 nm) of carbazomycin H (**270**) resembled that of carbazomycin G (**269**), indicating a similar carbazole framework. The ^{1}H-NMR spectrum was also similar to that of carbazomycin G,

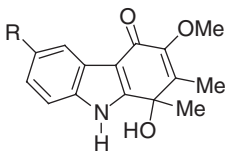

269 Carbazomycin G
R = H

270 Carbazomycin H
R = OMe

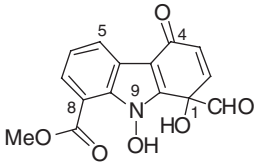

271 Coproverdine

Scheme 2.66

except for an additional aromatic methoxy group at δ 3.84, and the difference in the C-ring aromatic substitution pattern. The aromatic region showed an *ortho*- and *meta*-coupled (J=8.8, 2.4 Hz) dd at δ 6.85, a doublet with an *ortho*-coupling (J=8.8 Hz) at δ 7.39, and another deshielded broad doublet with a *meta*-coupling (J=2.4) at δ 7.66, assigned to H-5. The chemicals shifts in the aromatic region, and the coupling constants, confirmed the position of the aromatic methoxy group at C-6. Based on the spectroscopic data, structure **270** was assigned to carbazomycin H. This assignment was supported by the ^{13}C-NMR spectrum (238) (Scheme 2.66).

In 2002, Munro *et al.* reported the isolation of coproverdine (**271**) from a New Zealand Ascidian. The name of this isolate was derived from the descriptor attached to the voucher specimen (green sheep-shit-like in appearance), hence coproverdine (*copro* Greek dung, *ovis* Latin sheep, *verde* Latin green). This alkaloid was isolated from Nature in optically active form $[\alpha]_D^{20}$ − 8.0 (*c* 0.36, EtOH). However, the absolute configuration was not assigned. Coproverdine showed cytotoxic activity against a variety of murine and human tumor cell lines (240).

The UV spectrum (λ_{max} 208, 270, 302, and 382 nm) of coproverdine (**271**) indicated a carbazole framework. The NMR spectrum showed the presence of an aldehyde group (δ_H 10.13, δ_C 192.7), and a methyl ester (δ_H 4.06, δ_C 53.4 and 168.2), along with a carbonyl carbon at δ 186.6. The aldehyde group was confirmed by the characteristic IR band at ν_{max} 1665 (C═O). The ^{1}H-NMR spectrum showed the presence of three, mutually *ortho*-coupled (J=8.0 Hz) protons at δ 7.84, 7.39, and 7.28, indicating the presence of a 1,2,3-trisubstituted aromatic ring, and a *cis*-double bond (J=10.2 Hz) at δ 6.25 and 7.01. The HMBC spectrum confirmed the methyl ester functionality at C-8, the oxo group at C-4, and the formyl group at C-1 of the carbazole nucleus. The UV data and carbon chemical shift calculations suggested C-1 and N-9 as the positions for the remaining two hydroxy groups. This assignment was confirmed by the characteristic IR bands at ν_{max} 3500 cm^{-1} (broad) and 3690 cm^{-1} (sharp), for both hydrogen-bonded and free hydroxy groups. Based on the spectroscopic data, and additional support from COSY, HSQC, and HMBC spectra, structure **271** was assigned to coproverdine (240) (Scheme 2.66).

4 Tricyclic Carbazole-3,4-quinone Alkaloids

In the past decade, Seto *et al.* reported the isolation of a series of unprecedented carbazole-3,4-quinone alkaloids from various *Streptomyces* species. In 1993, the first example of a carbazole-3,4-quinone alkaloid, carquinostatin A (**278**) was isolated

from *Streptomyces exfoliatus* 2419-SVT2. This alkaloid was shown to be a potent neuronal cell protecting substance that also exhibited free radical scavenging activity. Carquinostatin A was isolated from Nature in enantiopure form, and the absolute stereochemistry at C-2′ was determined by the Mosher method to be *R*. Although this alkaloid was available in enantiopure form, the optical rotation could not be measured due to strong absorption in the visible range (241). One year later, another 6-prenyl-carbazole-3,4-quinone alkaloid, carquinostatin B (**279**), was isolated from the same source. Carquinostatin B presented as a hydroxycarquinostatin A, was a potent neuronal cell protecting substance, and was isolated from Nature in optically active form. However, the optical rotation could not be determined due to strong visible region absorption. By analogy with carquinostatin A, the absolute configuration at C-2′ was assigned as *R*. Based on NOE studies with the dimethylketal of carquinostatin B, the absolute configuration at C-1′ was assigned as *S* (242,243). In 1998, Grammel *et al.* reported the isolation of the carquinostatins A (**278**) and B (CS-79B) (**279**) from a *Streptomyces tendae* bald mutant, created by acriflavine treatment. These carbazole alkaloids showed antibacterial activity (244). In 1995, lavanduquinocin (**280**), a structurally intriguing carbazole-3,4-quinone alkaloid, with a monoterpenoidal β-cyclolavandulyl side chain in the 6-position, was isolated from *Streptomyces viridochromogenes* 2942-SVS3. Lavanduquinocin exhibited strong neuronal cell protecting activity. Using Mosher's method, the absolute configuration at C-2′ was determined as *R* (245). In the same year, a series of carbazole-3,4-quinones, named carbazoquinocin A (**272**), B (**273**), C (**274**), D (**275**), E (**276**), and F (**277**), were isolated from *Streptomyces violaceus* 2448-SVT2. The carbazoquinocins exhibited strong inhibitory activity against lipid peroxidation. Among the various carbazoquinocins, carbazoquinocin A (**272**) and D (**275**) have a secondary stereogenic center at the 1-alkyl side chain. Although they were optically active, their absolute configuration was not assigned (246) (Schemes 2.67 and 2.68).

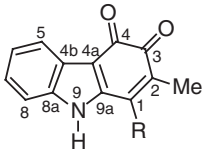

272 Carbazoquinocin A
R = $(CH_2)_2CHMeCH_2Me$

273 Carbazoquinocin B
R = $(CH_2)_4CHMe_2$

274 Carbazoquinocin C
R = $(CH_2)_6Me$

275 Carbazoquinocin D
R = $(CH_2)_4CHMeCH_2Me$

276 Carbazoquinocin E
R = $(CH_2)_5CHMe_2$

277 Carbazoquinocin F
R = $(CH_2)_6CHMe_2$

Scheme 2.67

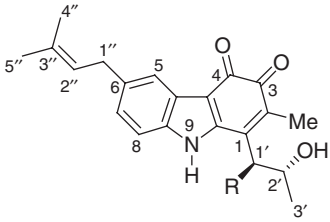

278 Carquinostatin A
R = H

279 Carquinostatin B
R = OH

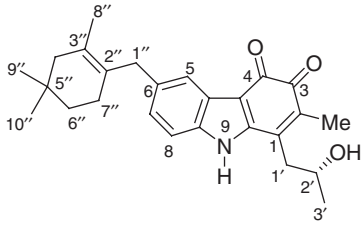

280 Lavanduquinocin

Scheme 2.68

The UV (λ_{max} 228, 264, and 398 nm) and IR (ν_{max} 1625, 1640 (sh), and 3440 cm^{-1}) spectral data of carbazoquinocin C (**274**) indicated a carbazole-3,4-quinone. This assignment was confirmed in the ^{13}C-NMR spectrum by two carbonyl carbon signals at δ 183.5 and 172.7, and by typical carbazole-3,4-quinone bands in the IR spectrum at ν_{max} 1625 and 1640 cm^{-1}. The ^{1}H-NMR spectrum of carbazoquinocin C (**274**) showed an aromatic methyl group at δ 1.90 and an *n*-heptyl group at δ 2.67 (2*H*, t, *J*=7.5 Hz), 1.55 (2*H*, m), 1.45 (2*H*, m), 1.31 (2*H*, m), 1.27 (2*H*, m), 1.25 (2*H*, m), and 0.85 (3*H*, t, *J*=8.0 Hz). The aromatic region showed signals for a low-field H-5 at δ 7.85, a three-proton multiplet at δ 7.23 (2*H*) and 7.50 (1*H*) assigned to H-6, H-7 and H-8, respectively, indicating an unsubstituted C-ring. In the ^{1}H-^{13}C long-range HMBC spectrum, the terminal methylene protons (C-1′) of the *n*-heptyl group showed coupling to C-1 (δ_C 142.2), C-2 (δ_C 133.1), and C-9a (δ_C 145.7). Moreover, the aromatic methyl group coupled to C-1 (δ_C 142.2), C-2 (δ_C 133.1), and C-3 (δ_C 183.5), indicated the position of the *n*-heptyl group at C-1, and the aromatic methyl group at C-2. Based on the spectroscopic data, structure **274** was assigned to carbazoquinocin C (246) (Scheme 2.67).

The UV (λ_{max} 228, 264, and 398 nm) and IR [ν_{max} 1625, 1640 (sh), and 3440 cm^{-1}] spectral data of carbazoquinocin D (**275**) were identical to those of carbazoquinocin C (**274**), indicating the presence of a similar carbazole-3,4-quinone framework. Chemically, the presence of a carbazole-3,4-quinone function was established by formation of an *o*-phenylenediamine adduct. The ^{1}H- and ^{13}C-NMR spectra of carbazoquinocin D were also very similar to those of carbazoquinocin C, except for the presence of a 5-methylheptyl residue in place of the *n*-heptyl group. Thus, the ^{1}H-NMR spectrum of carbazoquinocin D showed a doublet (3*H*, *J*=7.0 Hz), and a triplet (3*H*, *J*=6.5 Hz) for the aliphatic methyl groups, and the chemical shifts of the corresponding aliphatic methyl carbons in the ^{13}C-NMR spectrum were shifted to higher fields (δ 19.1 and 11.2, respectively) due to a γ-effect. Based on these spectral data, and the structural similarity to carbazoquinocin C, the structure **275** was assigned to carbazoquinocin D (246) (Scheme 2.67).

A close comparison of the HRFAB-MS and ^{1}H-NMR spectral data of the carbazoquinocins A (**272**), B (**273**), E (**276**), and F (**277**) with those of the carbazoquinocins C (**274**) and D (**275**) indicated the presence of a 3-methylpentyl, 5-methylhexyl, 6-methylheptyl, and 7-methyloctyl residue, respectively, in place of the

carbazoquinocin C (**274**) C-1 *n*-heptyl and carbazoquinocin D (**275**) 5-methylheptyl group. Based on these spectral data, and the structural similarities to the carbazoquinocins C (**274**) and D (**275**), the structures **272**, **273**, **276**, and **277** were assigned to carbazoquinocins A, B, E, and F, respectively (246) (Scheme 2.67).

The UV (λ_{max} 230, 267, and 425 nm) and IR [ν_{max} 1615, 1640 (sh), 1660 (sh), 3220, and 3450 cm^{-1}] spectral data of carquinostatin A (**278**) were similar to those of carbazoquinocin C (**274**) (see Scheme 2.67), indicating the presence of a similar carbazole-2-methyl-3,4-quinone framework. This was substantiated by the ^{13}C-NMR showing two carbonyl carbon signals at δ 183.5 and 172.6, as well as typical carbazole-3,4-quinone bands in the IR spectrum at ν_{max} 1615 and 1640 cm^{-1}. Chemically, the presence of a carbazole-3,4-quinone function was established by the formation of an *o*-phenylenediamine adduct. A close comparison of the ^{1}H- and ^{13}C-NMR spectra of carquinostatin A (**278**) with those of neocarazostatin B (**268**) (see Scheme 2.65) indicated that carquinostatin A is structurally related to neocarazostatin B with a masked carbazole-3,4-hydroquinone (*ortho*-hydroquinone) unit. This was further supported by the ^{1}H–^{13}C long-range HMBC spectrum, as well as NOE experiments. Based on this spectroscopic analysis, the structure **278** was assigned for carquinostatin A (241) (Scheme 2.68).

The UV (λ_{max} 230, 267, and 425 nm) and IR [ν_{max} 1615, 1640 (sh), 1660 (sh), 3220, and 3450 cm^{-1}] spectra of carquinostatin B (**279**) were similar to those of carquinostatin A (**278**), indicating the presence of a similar carbazole-3,4-quinone framework. The comparison of the mass fragmentation ion m/z 354 (M^{+}+1) in the HRFAB-MS spectrum of carquinostatin B (**279**) with carquinostatin A (**278**) showed it to be a hydroxy derivative of carquinostatin A. The ^{1}H- and ^{13}C-NMR spectra of carquinostatin B were also very similar to those of carquinostatin A, except for the signals due to H-1′ (δ_H 4.70 in place of 2.75) and C-1′ (δ_C 73.9 in place of 37.7). Based on these spectral data, and the structural similarity to carquinostatin A, structure **279** was assigned to carquinostatin B. This structure was further supported by DQF-COSY and HMBC spectra (243) (Scheme 2.68).

The UV (λ_{max} 232, 269, and 429 nm) and IR [ν_{max} 1615, 1640 (sh), 1660 (sh), 3220, and 3450 cm^{-1}] spectra of lavanduquinocin (**280**) were similar to those of carquinostatin A (**278**), indicating the presence of a similar carbazole-3,4-quinone framework. The ^{1}H- and ^{13}C-NMR spectra of lavanduquinocin (**280**) were also very similar to those of carquinostatin A, except for the presence of a cyclolavandulyl moiety in place of a prenyl side chain at C-6 of the carbazole nucleus. Thus, the DQF-COSY spectrum showed the coupling between the C-6″ methylene protons at δ 1.24 with the C-7″ methylene protons at δ 1.84, which also showed long-range coupling with the C-4″ (δ 1.78) and C-1″ (δ 3.41) methylene protons. Further, the HMBC spectrum showed coupling between the C-5″ methyl protons at δ 0.84 to C-4″ (δ_C 45.6), C-5″ (δ_C 28.9), and C-6″ (δ_C 35.4). In addition, the C-3″ allylic methyl proton at δ 1.73 showed coupling to C-2″ (δ_C 127.3), C-3″ (δ_C 125.6), and C-4″ (δ_C 45.6). Furthermore, the C-1″ protons at δ 3.41 showed coupling to C-2″ (δ_C 127.3), C-3″ (δ_C 125.6), and C-7″ (δ_C 26.8), establishing the connectivity between C-1″ (δ_C 38.4) and C-2″ (δ_C 127.3). These results indicated the presence of a cyclolavandulyl moiety at C-6 of the carbazole nucleus. These spectral data, together with the similarities to the data of carquinostatin A, established the structure **280** for lavanduquinocin (245) (Scheme 2.68).

B. Benzocarbazole Alkaloids

In the past decade, a few examples of benzoannulated carbazole ring systems were found in nature as marine products. In 1993, Chan *et al.* reported a novel marine benzocarbazole alkaloid, purpurone (**281**) from the marine sponge *Iotrochota* sp. in its racemic form. Purpurone, as indicated by its name, is purple in color. This represents the first example of a benzocarbazole alkaloid with a biphenylene quinone methide functionality. The isolate showed ATP-citrate lyase (ACL) inhibitory activity (247).

The UV spectrum (λ_{max} 216, 296, and 500 nm) of purpurone (**281**) showed a bathochromic shift on addition of base, indicating the presence of phenolic groups. The IR spectrum showed a strong hydroxy band at ν_{max} 3100–3600 cm^{-1} and a carbonyl band at 1680 cm^{-1} which was assigned to a highly conjugated carbonyl group. This was substantiated by the ^{13}C-NMR carbonyl carbon signal at δ 185.4. The HRFAB mass spectrum, in combination with the NMR spectral data, established a molecular formula of $C_{40}H_{27}NO_{11}$. The ^{1}H- and ^{13}C-NMR spectra showed only 22 carbon signals and 9 proton signals, indicating purpurone to be a highly symmetrical molecule in which the nitrogen atom, one oxygen atom, and four carbon atoms lie in a plane of symmetry. Permethylation of purpurone with diazomethane gave an unstable nonamethyl derivative with five methyl signals in a ratio of 2:2:2:2:1 indicating the presence of nine phenolic groups, one of which lies in the plane of symmetry, and four phenolic groups in each symmetrical unit, along with one carbonyl function. The presence of a tyramine unit in the plane of symmetry is evident from the NMR spectra.

The HMBC correlations from the C-1″ proton signal at δ 2.95 to the 6a and 7a carbon signals at δ 156.1 indicated that the tyramine nitrogen was attached to the symmetrical units, each $C_{16}H_9O_5$, through this aromatic carbon atom. The downfield shift for this carbon shows conjugation to a carbonyl carbon. Further, the ^{1}H-NMR spectral data and the HMBC correlations indicated the presence of two, symmetrically located, 4-substituted, 1,2-dihydroxyphenyl rings at C-6 and C-8 of the benzocarbazole nucleus. Additional support came from NOE experiments. The remaining signals in the ^{1}H-NMR spectrum were at δ 7.45 (s, 2*H*) and 7.80 (s, 2*H*). The HETCOR spectrum indicated the δ_C values for these carbons as 115.1 and 114.1, respectively. The HMBC spectrum showed that both of these proton signals were correlated with the ^{13}C-NMR signals at δ 149.0 and 150.1, which were assigned to the phenolic carbons C-3, C-11 and C-2, C-12, respectively. These proton signals were therefore on two, symmetrically located, 1,2-disubstituted 4,5-dihydroxyphenyl rings. The HMBC spectrum showed a strong correlation between the ^{1}H-NMR signal at δ 7.45 and the ^{13}C-NMR signal at δ 185.4, the carbonyl groups must be adjacent to the 1,2-disubstituted 4,5-dihydroxyphenyl rings. This experiment led to the assignment of δ_H 7.45 for the C-4 and C-10 protons, and δ_C 185.4 for the C-5 and C-9 carbonyl carbons. Based on this spectroscopic analysis, the structure **281** was assigned for purpurone (247) (Scheme 2.69).

Four years later, Kang and Fenical reported the isolation of ningalin D (**282**) from a marine ascidian of the genus *Didemnum* collected in Western Australia, near Ningaloo Reef. On the basis of the restricted rotation and also because of the apparent helicity, **282** could be chiral. However, from the marine source, it was available only in racemic form (248).

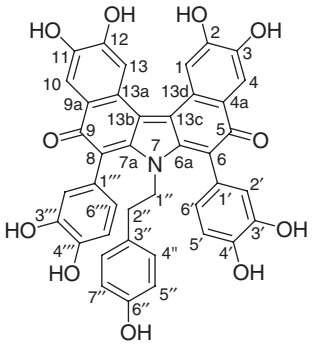

281 Purpurone

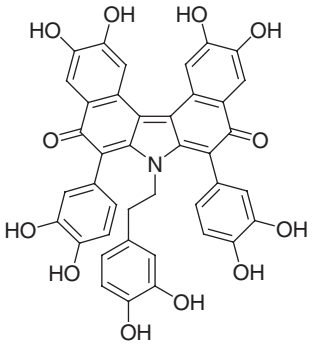

282 Ningalin D

Scheme 2.69

The UV (λ_{max} 206, 294, and 508 nm) and IR (ν_{max} 1665, 3000–3700 cm^{-1}) spectra of ningalin D (**282**) were very similar to those of purpurone (**281**), indicating the presence of a similar benzocarbazole framework with a biphenylene quinone methide functionality. Comparison of the HRFAB mass spectrum of ningalin D with that of purpurone showed it to be a hydroxy-derivative of purpurone. The ^{1}H- and ^{13}C-NMR spectra of ningalin D were also very similar to those of purpurone, except for the presence of an additional hydroxy group at C-5″ of the phenethyl aromatic ring, showing the presence of a dopamine unit in place of a tyramine unit in the plane of the symmetry of ningalin D. Thus, the ^{1}H-NMR spectrum showed two, mutually coupled (J=6.5 Hz) triplet methylene protons at δ 2.13 and 2.95 for C-2″ and C-1″, respectively. Further, in the aromatic region, two, mutually *ortho*-coupled (J=7.5 Hz) C-8″ and C-7″ protons at δ 5.95 and 6.30, respectively, and one *meta*-coupled (J=1.5 Hz) C-4″ proton at δ 6.12, indicated the presence of a dopamine moiety. Based on these spectral data, and the structural similarity to those of purpurone, the structure **282** was assigned for ningalin D. This structure was further supported by the HMBC and NOESY spectra (248) (Scheme 2.69).

C. Pyrrolo[2,3-*c*]carbazole Alkaloids

Since the late eighties, pyrrolocarbazole alkaloids began to emerge as a new class of condensed heteroarylcarbazoles. Until the early nineties, these compounds were known from their synthetic origin due to their broad spectrum of bioactivities, such as anticancer, antidiabetic, neurotropic, and protein kinase C (PKC) inhibitory properties (249). In 1993, Sato *et al.* isolated the novel pyrrolo[2,3-*c*]carbazole alkaloids, **289**, **290**, and **291** from a dark green marine sponge, *Dictyodendrilla* sp. These compounds showed inhibitory activities against bovine lens aldose reductase. Although, **290** and **291** have a stereogenic center, they were obtained in optically inactive form (no Cotton effect) (250). A decade later, Fusetani *et al.* reported the isolation of further pyrrolo[2,3-*c*]carbazole alkaloids, the dictyodendrins A (**283**), B (**284**), C (**286**), D (**287**), and E (**288**), along with the previously known carbazole alkaloid **290** from the same Japanese marine invertebrate, the marine sponge *Dictyodendrilla verongiformis*. Dictyodendrins A–E were the first telomerase-inhibitory marine natural products.

Despite the presence of a stereogenic center, the CD spectrum of dictyodendrin A (**283**) exhibited no Cotton effect, indicating its racemic nature. This was proven by chiral reverse phase HPLC (251).

Dictyodendrin A (**283**) showed UV maxima at λ_{max} 208, 227, 328, and 480 nm. The IR spectrum indicated the presence of a strong hydroxy band at ν_{max} 3408 cm^{-1}, and an ester carbonyl band at 1724 cm^{-1}. The ^{1}H-NMR spectrum showed the presence of a signal for an NH proton at δ 9.96, 13 methine signals between δ 5.9 and 7.5, along with two methylenes at δ 2.19, 3.73, and an ester methoxy group at δ 3.52. The presence of an ester function was supported by the ^{13}C-NMR signal at δ 174.1 for the ester carbonyl carbon. Interpretation of the COSY spectral data, together with HMBC correlations, led to the establishment of four, 4-substituted phenols in which ring H was connected to the C-4 carbon of the pyrrolo[2,3-*c*]carbazole nucleus, and ring E was connected to the C-1 carbon of the pyrrolo[2,3-*c*]carbazole nucleus. However, ring G was linked to a methylene carbon C-2‴ (δ_H 2.19, δ_C 36.2). Furthermore, HMBC cross peaks were observed between H-3″ (H-8″) and C-1″, between H-1″ and C-8″, and between H-1″ and C-2, connecting ring F to the C-1″ methine (δ_H 5.28, δ_C 48.9), which was linked to a methoxycarbonyl functionality and C-2″ of ring F. The three, contiguous, aromatic protons at δ 5.94, 6.56, and 7.17 for C-10, C-9, and C-8, respectively, indicated the further substitution on C-7 of the A ring of the pyrrolo[2,3-*c*]carbazole nucleus. The HMBC cross peaks (H-10/C-10b, C-6a; H-9/C-10a, C-7; H-8/C-6a; N-6/C-10b, C-10a, C-6a, C-5a) indicated the fusion of ring A with a pyrrole, leading to a 2,3,7-trisubstituted indole. Based on this spectral analysis, the structure **283** was assigned to dictyodendrin A. This structure was further supported by the transformation of dictyodendrin A to the 7-*O*-sodium sulfate salt of **289** (see Scheme 2.72) (251) (Scheme 2.70).

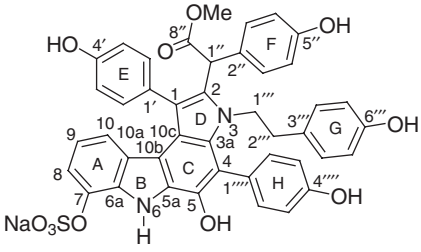

283 Dictyodendrin A

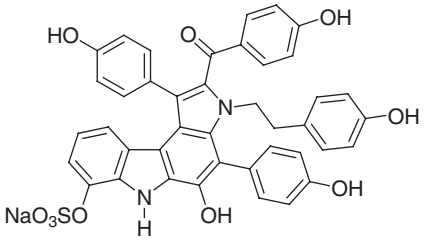

284 Dictyodendrin B

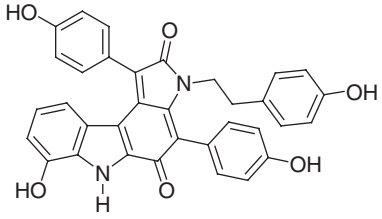

285

Scheme 2.70

Dictyodendrin B (**284**) showed UV maxima at λ_{max} 228, 305, and 397 nm. The IR spectrum indicated the presence of a strong hydroxy band at ν_{max} 3381 cm^{-1} and a conjugated ketone band at 1608 cm^{-1}. Comparison of the HRFAB mass spectrum of dictyodendrin B with that of dictyodendrin A showed it to be an oxidative decarboxylation product of dictyodendrin A. This was supported by the presence of a conjugated ketone carbon signal at δ 191.8 in its ^{13}C-NMR spectrum, as well as the absence of an ester methoxy group and the C-1″ methine signals in its NMR spectra. Furthermore, similar to dictyodendrin A, the NMR spectra showed the presence of four, 4-substituted phenols, an isolated ethylene unit, and a 2,3,7-trisubstituted indole, indicating the presence of the similar common core. Based on these spectral data, and the structural similarity to dictyodendrin A, the structure **284** was assigned to dictyodendrin B. This structure was unequivocally established by transformation of dictyodendrin B into pyrrolidinone **285** by treament with acid, the same pyrrolidinone was also obtained by acid treatment of the 7-*O*-sodium sulfate salt of **289** (see Scheme 2.72) (251) (Scheme 2.70).

The UV (λ_{max} 238, 277, 302, and 415 nm) and IR (ν_{max} 1602, 3362 cm^{-1}) spectra of dictyodendrin C (**286**) were similar to those of dictyodendrins A (**283**) and B (**284**), indicating the presence of a similar carbazole framework. The ^{1}H-NMR spectrum showed the absence of C-1″ and ring F, which was substantiated by the ^{13}C-NMR data. The C-9 unit attached at C-2 in dictyodendrin A was replaced by an oxygen atom, which was in agreement with HR-FABMS and NMR data, indicating dictyodendrin C to be the 10-sulfate of pyrrolidinone. Based on this spectral analysis, the structure **286** was assigned to dictyodendrin C. This structure was unequivocally established by the transformation of dictyodendrin C to pyrrolidinone **285** (see Scheme 2.70) by acid hydrolysis (251) (Scheme 2.71).

The UV (λ_{max} 243, 276, 305, and 416 nm) and IR (ν_{max} 1602, 3454 cm^{-1}) spectra of dictyodendrin D (**287**) were very similar to those of dictyodendrin C (**286**), indicating the presence of a similar carbazole framework. The FABMS data, showed that the molecular ion peak is 80 units larger than that of dictyodendrin C. Furthermore, sequential loss of SO_3 and $NaSO_3$ suggested the presence of two sulfate groups. The NMR spectra of dictyodendrin D were also very similar to those of dictyodendrin C, except that in the ^{1}H-NMR spectrum, a downfield shift

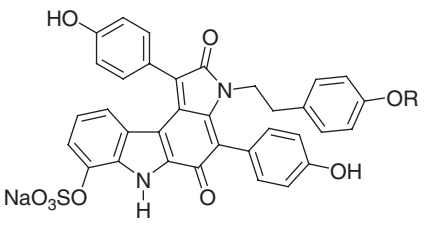

286 Dictyodendrin C
R = H

287 Dictyodendrin D
R = SO_3H

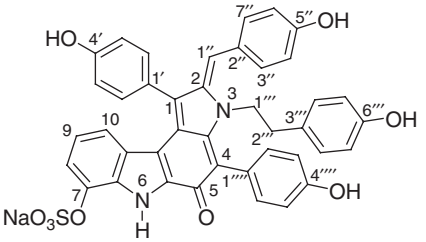

288 Dictyodendrin E

Scheme 2.71

of 0.5 ppm was observed for H-5‴ and H-7‴, assigning dictyodendrin D as the 7‴-*O*-sulfate of dictyodendrin C. Based on these spectral data and the structural similarity to dictyodendrin C, the structure **287** was assigned to dictyodendrin D. This structure was unequivocally established by the transformation of dictyodendrin D into pyrrolidinone **285** (see Scheme 2.70) by acid hydrolysis (251) (Scheme 2.71).

Dictyodendrin E (**288**) showed UV maxima at λ_{max} 230, 280, and 464 nm. Similar to dictyodendrin C (**286**), the ^{1}H-NMR spectrum of dictyodendrin E showed the presence of four, 4-substituted phenols, an isolated ethylene unit, and a 2,3,7-trisubstituted indole, indicating the presence of a similar common core. Furthermore, in place of a keto group at C-2, the isolate showed the presence of a vinyl proton connected to a 4-substituted phenol. This was established with the HMBC spectrum in which a vinyl proton at δ 5.99 (H-1′) showed long-range coupling to C-1 and C-3″ (C-7″). Further, from the ROESY spectrum, the geometry of this double bond ($\Delta^{2,1''}$) was established to be *Z*. Based on these spectral data, and the structural similarity to dictyodendrin C, the structure **288** was assigned to dictyodendrin E. This structure was unequivocally established by the transformation of dictyodendrin E into pyrrolidinone **285** (see Scheme 2.70) through acid treatment (251) (Scheme 2.71).

The UV spectrum (λ_{max} 231, 281, and 482 nm) of pyrrolo[2,3-*c*]carbazole alkaloid **289** was very similar to that of dictyodendrin E (**288**), indicating the presence of a similar carbazole framework. The NMR spectra of **289** were also very similar to those of dictyodendrin E (**288**), except for the presence of an *O*-sulfate group at C-7 and a methoxycarbonyl group instead of the C-1″ vinyl proton. The presence of a methoxycarbonyl group was supported by the presence of an IR band at ν_{max} 1691 cm^{-1}, as well as long-range coupling between the methoxy protons (δ 3.17) and the carbonyl carbon (δ 171.3) in the HMBC spectrum. Further, the presence of a 7-*O*-sulfate group was supported from its HRFAB-MS. Based on these spectral data and the structural similarity to those of dictyodendrin E, the structure **289** was assigned for this isolate (250) (Scheme 2.72).

The UV spectrum (λ_{max} 229, 288, 324, 391, and 475 nm) of the pyrrolo[2,3-*c*]carbazole alkaloid **290** showed the presence of a pyrrolo[2,3-*c*]carbazole framework with a spirolactone structure. The ^{1}H-NMR spectrum indicated the presence of two

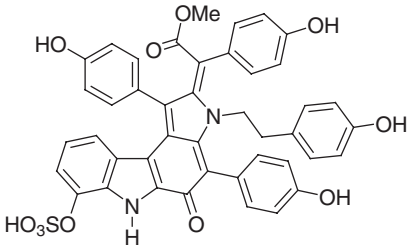

289

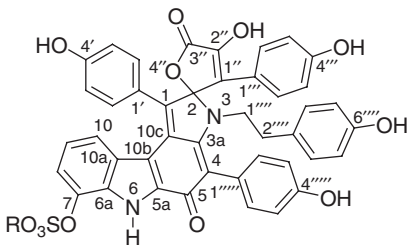

290 R = Na

291 R = H

Scheme 2.72

methylene protons at δ 2.37 and 2.97, assignable to an isolated ethylene group and unresolved broad signals for 22 protons as multiplets. In the aromatic region, the three contiguous aromatic protons at δ 5.74, 6.61, and 7.15 for C-10, C-9, and C-8, respectively, indicated further substitution at C-7 of the A ring of a pyrrolo[2,3-*c*]carbazole nucleus. The ^{13}C-NMR spectrum indicated the presence of two methylene carbon atoms at δ 36.8 and 47.5, and a carbonyl carbon atom at δ 181.6, along with many unassignable aromatic carbon atoms. The isolate was hydrolyzed chemically with trifluoroacetic acid, and enzymatically with sulfatase to the corresponding hydroxy derivative, indicating the presence of a sulfate group. The ^{1}H-NMR spectrum of this hydroxy derivative showed an upfield shift for the C-10 (δ 5.43) and C-8 protons (δ 6.54) compared with **290**, while the other protons did not shift as much. This established the position of the sulfate group at C-7. Transformation of this hydroxy derivative to the corresponding acetate, and the X-ray crystallographic analysis of this acetate, led unequivocally to the structure **290** for the pyrrolo[2,3-*c*]carbazole alkaloid (250) (Scheme 2.72).

The UV spectrum (λ_{max} 229, 289, 324, 391, and 475 nm) of the pyrrolo[2,3-*c*]carbazole alkaloid **291** was identical to that of **290**, indicating the presence of a similar pyrrolo[2,3-*c*]carbazole spirolactone framework. Comparison of the spectral data of this isolate with those of the pyrrolo[2,3-*c*]carbazole alkaloid **290** indicated it to be an acid form of **290**. This was further established by the chemical conversion of **291** to the corresponding 7-hydroxy derivative. Based on these spectral data, and the close structural similarity to **290**, the structure **291** was assigned to this compound (250) (Scheme 2.72).

D. Indolo[2,3-*a*]carbazole Alkaloids

The indolocarbazole family is comprised of five different isomeric ring systems based on the fusion and orientation of the indole ring and the C-ring of the carbazole nucleus (8). Among these, the most interesting structural class are the indolo[2,3-*a*]carbazoles, since many natural products bear this basic framework, and show a wide range of potent biological activities (252–260). The other structural classes of indolocarbazoles and their derivatives have been studied in much less detail due to the fact that they are not present in natural products, and there is a lack of knowledge of their biological activities. However, several aza analogs of indolo[3,2-*a*]carbazoles were shown to be powerful benzodiazepine receptor ligands (261,262). Moreover, in the mid-1990s derivatives of the indolo[3,2-*b*]carbazole attracted interest due to their affinity to the 2,3,7,8-tetrachlorodibenzo-*p*-dioxin (TCDD) receptor [also referred to as the aryl hydrocarbons (Ah) receptor protein] (263–266) which plays an important physiological role.

Previously in the literature, for simplicity, under indolo[2,3-*a*]carbazole natural products, only the indolo[2,3-*a*]carbazoles with and without the pyrrolo[3,4-*c*]ring were considered. The recent past has witnessed an explosive growth of these natural products. Due to this, and the difference in the aglycon framework, in this article we have classified the indolo[2,3-*a*]carbazoles with a pyrrolo[3,4-*c*]ring as indolo[2,3-*a*]pyrrolo[3,4-*c*]carbazole alkaloids, and the indolo[2,3-*a*]carbazoles without a pyrrolo[3,4-*c*]ring as simple indolo[2,3-*a*]carbazole alkaloids.

1 Indolo[2,3-*a*]pyrrolo[3,4-*c*]carbazole Alkaloids

The majority of indolocarbazole alkaloids, isolated so far from nature, are derivatives of the indolo[2,3-*a*]pyrrolo[3,4-*c*]carbazole ring system **292**. They have been isolated from soil organisms, slime molds, and marine sources (3,7,8,252–255), and have shown a broad range of potent biological activities, such as antifungal, antimicrobial, antitumor, and antihypertensive activity (3,7,256–260,267–270). Their activity as potent inhibitors of protein kinase C (PKC) has received special attention, and was the focus of several investigations (8,257,258,271–280). The history of these natural products dates back about 30 years (Scheme 2.73).

In 1977, Ōmura *et al*. isolated the first indolo[2,3-*a*]pyrrolo[3,4-*c*]carbazole alkaloid from *Streptomyces staurosporeus* Awaya (281), and subsequently from several other actinomycetes (267,268). Initially, this alkaloid was called AM-2282, but later it was named staurosporine (**295**) (282,283). From Nature, this isolate was obtained in its optically active form $[\alpha]_D^{25} + 35.0$ (*c* 1.0, MeOH) (281). The absolute configuration of this isolate was initially assigned from circular dichroism (CD) measurements (284). However, this assignment was revised based on anomalous dispersion measurements performed on crystalline 4′-*N*-methylstaurosporine methiodide, which was prepared from staurosporine (**295**). Based on this X-ray crystallographic analysis, the absolute stereochemistry of staurosporine (**295**) was revised to be 2′*S*, 3′*R*, 4′*R*, and 6′*R* (285). Staurosporine has very interesting biological activities (280), including antimicrobial (281,286,287), antihypertensive (286,287), cytotoxic (271), inhibition of PKC (271,288), and platelet aggregation inhibition (268).

Since 1997, the number of isolated and structurally elucidated indolo[2,3-*a*]pyrrolo[3,4-*c*]carbazole alkaloids has grown considerably (8,255,258). Almost 10 years later, Kase *et al*. reported the isolation of K-252c (**293**) from the culture broth of *Nocardiopsis* sp. K-290. The structure of K-252c represents the aglycon of staurosporine (**295**), therefore, **293** is named staurosporinone (273,274). In 1994, Horton *et al*. reported the isolation of the staurosporine aglycon (K-252c) from a different source, the marine ascidian *Eudistoma* sp., collected off the coast of West Africa (275). Staurosporine aglycone (K-252c) showed strong inhibition of PKC isoenzymes (273,275), and also potent *in vitro* cytotoxicity against the human lung cancer A549 and P388 murine leukemia cell lines (275). In 1996, Cai *et al*. reported the isolation of a 6-alkylated derivative of staurosporine aglycon, 6-isopropoxymethyl-K-252c (**294**) from *S. longisporoflavus* strain R-19 (289).

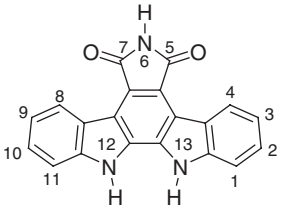

292 Indolo[2,3-*a*]pyrrolo [3,4-*c*]carbazole

Scheme 2.73

The UV spectrum [λ_{max} 230, 238 (sh), 246 (sh), 257 (sh), 287, 320 (sh), 331, 341, and 358 nm] of staurosporinone (K-252c) (**293**) showed the presence of an indolo[2,3-*a*]pyrrolo[3,4-*c*]carbazole framework. The IR spectrum indicated the presence of an NH band at ν_{max} 3440 cm^{-1} and an amide band at 1648 cm^{-1}. The presence of NH groups at δ 11.38 and 11.56, and a secondary amide at δ 8.49, were also established from its ^{1}H-NMR spectrum. Further, the NMR spectra of this isolate were very similar to those of K-252a (**330**) (see Scheme 2.85), except for the absence of the sugar moiety. This was also in agreement with the HR-MS. Hydrolysis of K-252a (**330**) gave staurosporinone (K-252c) (**293**), establishing it to be the aglycon of K-252a. Based on these spectral data, and the structural similarity to K-252a, the structure **293** was established for K-252c (274) (Scheme 2.74).

The ^{1}H-NMR spectrum of 6-isopropoxymethyl-K-252c (**294**) was very similar to that of staurosporinone (K-252c) (**293**), except for the presence of isopropoxy signals at δ 1.17 as a doublet and a multiplet at δ 3.80 along with a singlet at δ 5.14, assignable to methylene protons attached to a nitrogen atom. The ^{13}C-NMR spectrum also showed the presence of isopropoxymethyl signals, together with those attributed to staurosporinone. The location of the additional isopropoxymethyl group at the lactam nitrogen was supported by the shifts of the 4c, 5, 7, and 7a carbon signals by more than 2 ppm in comparison to staurosporinone. Based on these spectral data, and the structural similarity to staurosporinone, the structure **294** was assigned to 6-isopropoxymethyl-K-252c (289).

The UV spectrum [λ_{max} 243, 267 (sh), 292, 322 (sh), 335, 356, and 372 nm] of (+)-staurosporine (AM-2282) (**295**) was very similar to that of staurosporinone (**293**), indicating the presence of a similar indolo[2,3-*a*]pyrrolo[3,4-*c*]carbazole framework. The IR spectrum indicated the presence of an NH band at ν_{max} 3500 cm^{-1} and an amide band at 1675 cm^{-1}. The structure and relative stereochemistry of this isolate were established by X-ray crystallographic analysis of the methanol solvate (282,283). The structure **295**, indicating the presence of an indolocarbazole subunit, wherein two

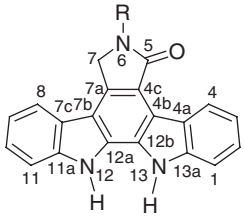

293 Staurosporinone (K-252c)
Staurosporine Aglycone
R = H

294 6-Isopropoxymethyl-K-252c
R = CH_2OCHMe_2

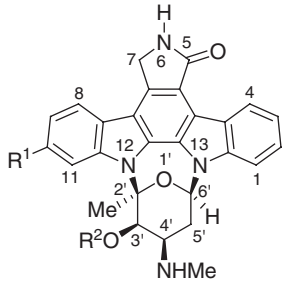

295 (+)-Staurosporine (AM-2282)
R^1 = H; R^2 = Me

296 TAN-999
R^1 = OMe; R^2 = Me

297 *O*-Demethylstaurosporine
(3'-*O*-Demethylstaurosporine)
R^1,R^2 = H

Scheme 2.74

indole nitrogens are bridged by glycosyl linkages, was unambiguously confirmed by its ^{1}H-, ^{13}C-NMR, COSY, NOESY, selective INEPT, HMBC, and HMQC spectra (290). Furthermore, in addition to the relative stereochemistry, the absolute stereochemistry of staurosporine was assigned to be 2′*S*, 3′*R*, 4′*R*, and 6′*R* based on X-ray crystallographic analysis of 4′-*N*-methylstaurosporine methiodide (285). Based on these data, the structure **295** was assigned to (+)-staurosporine (AM-2282).

In 1989, Tanida *et al.* reported the isolation of a 10-methoxy derivative of staurosporine, TAN-999 (**296**) from the culture broths of *Nocardiopsis dassonvillei* C-71425 in its optically active form $[\alpha]_D$ +42.0 (*c* 0.50, DMF). This isolate functions as a macrophage activator, useful for the treatment of mycosis, bacterial infection, and cancer (291,292).

The UV spectrum [λ_{max} 245, 296, 341, 352 (sh), and 368 nm] of TAN-999 (**296**) was very similar to that of (+)-staurosporine (**295**), indicating the presence of a similar indolo[2,3-*a*]carbazole framework with a lactam function. This was also discernible from its IR spectrum with the presence of an NH band at ν_{max} 3430 cm^{-1} and an amide band at 1680 cm^{-1}. The ^{1}H-NMR spectrum of TAN-999 was also very similar to that of (+)-staurosporine, except for the presence of an additional methoxy group at δ 3.95, resulting in the presence of a 1,2,4-trisubstituted aromatic ring instead of a 1,2-disubstituted aromatic ring. The location of this additional methoxy group was assigned to C-10, based on ^{1}H–^{1}H COSY, ^{1}H–^{13}C COSY, refocused INEPT, and COLOC experiments. In the COLOC spectrum (*J*=4.2 Hz), a C-10 quaternary carbon (δ 157.49) was correlated with the methoxy protons (δ 3.95) and the C-8 aromatic proton (δ 7.75). The NOE experiment showed a cross-peak between the methoxy protons (δ 3.95) and two aromatic protons (H-9 and H-11). Furthermore, an NOE was observed between the aromatic (H-11) and methyl protons (H′-6, δ 2.33). These data establish the presence of this additional methoxy group (δ 3.95) at C-10. Based on these spectral data, and the structural similarity to (+)-staurosporine, the structure **296** was assigned to TAN-999 (293) (Scheme 2.74).

In 1995, Hoehn *et al.* reported the isolation of *O*-demethylstaurosporine (3′-*O*-demethylstaurosporine) (**297**) from a blocked mutant of *S. longisporoflavus* R 19 (294). In nature, this was isolated in its optically active form $[\alpha]_D^{20} + 82.0 \pm 1.1$ (*c* 1%, DMSO), and was less potent than (+)-staurosporine (**295**), but showed more selective inhibition of PKC subtypes α, β-2, and γ (294).

The UV (λ_{max} 244, 293, 335, 355, and 372 nm) and IR (ν_{max} 1660 and 3420 cm^{-1}) spectra of *O*-demethylstaurosporine (3′-*O*-demethylstaurosporine) (**297**) were very similar to those of (+)-staurosporine (**295**), indicating the presence of a similar indolo[2,3-*a*]carbazole framework with a lactam function. The ^{1}H- and ^{13}C-NMR spectra of *O*-demethylstaurosporine (3′-*O*-demethylstaurosporine) (**297**) were also very similar to those of (+)-staurosporine, except for the absence of a methoxy group at δ_H 3.32 and δ_C 57.2. In addition, the carbon signal for C-3′ was significantly shifted from δ 82.7 to 68.9. Based on these data, and the structural similarity to (+)-staurosporine, the structure **297** was assigned to *O*-demethylstaurosporine (3′-*O*-demethylstaurosporine). This structure was unambiguously established by a bioconversion experiment with a blocked mutant of *S. longisporoflavus* M 13 transforming *O*-demethylstaurosporine (3′-*O*-demethylstaurosporine) quantitatively into (+)-staurosporine (294) (Scheme 2.74).

In 1992, Kinnel and Scheuer reported the isolation of 11-hydroxystaurosporine (**298**) and 3,11-dihydroxystaurosporine (**299a**) from the Pohnpei brown tunicate,

Eudistoma sp. (295). These were the first examples of naturally occurring, enantiopure indolo[2,3-*a*]carbazole alkaloids from a marine organism. Based on the specific rotation, $[\alpha]_D$ +10.3 (*c* 0.30, MeOH), of 11-hydroxystaurosporine (**298**) and the CD spectrum of 3,11-dihydroxystaurosporine (**299a**), the absolute configurations of these isolates were presumed to be similar to that of (+)-staurosporine (**295**) (see Scheme 2.74). These isolates were active against human nasopharyngeal cancer cells, and 3,11-dihydroxystaurosporine (**299a**) was more potent than (+)-staurosporine (**295**) in PKC inhibition (295). In 1999, 3,11-dihydroxystaurosporine (**299a**) was also isolated by Boyd *et al*. from a different natural source, the prosobranch mollusk *Coriocella nigra* collected in the Philippines (296).

The UV [λ_{max} 246, 256, 292, 300, 334 (sh), 356, and 374 nm] and IR (ν_{max} 1660 and 3400 cm^{-1}) spectra of 11-hydroxystaurosporine (**298**) were very similar to those of (+)-staurosporine (**295**) (see Scheme 2.74), indicating the presence of a similar indolo[2,3-*a*]carbazole framework with a lactam function. The ^{1}H- and ^{13}C-NMR spectra of 11-hydroxystaurosporine (**298**) were also very similar to those of (+)-staurosporine, except for the absence of the C-11 proton. But there was an exchangeable proton, indicating the presence of a phenolic group, at δ 10.6. The presence of a phenolic hydroxy group was supported from its HRFAB-MS. In addition, this isolate formed a diacetate, indicating the presence of the secondary amine and the phenol. Based on these data, and the structural similarity to (+)-staurosporine, the structure **298** was assigned to 11-hydroxystaurosporine. This structure was further supported by the HMBC and NOE spectra (295) (Scheme 2.75).

The ^{1}H-NMR spectrum of 3,11-dihydroxystaurosporine (**299a**) was very similar to that of 11-hydroxystaurosporine (**298**), except for the absence of one proton in the aromatic region. Decoupling experiments showed that the second aromatic ring is 1,2,4-trisubstituted, and the C-4 proton is shifted to δ 8.69 with *meta*-coupling (*J*=2.7 Hz). This shielding effect of the C-4 proton, together with HRFAB-MS, indicated the presence of an additional oxygen atom *ortho* to the C-4 carbon. Based

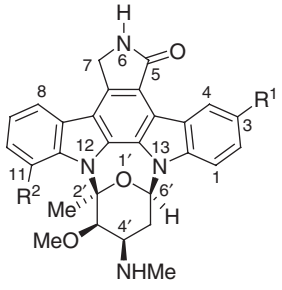

298 11-Hydroxystaurosporine
R^1 = H; R^2 = OH

299a 3,11-Dihydroxystaurosporine
R^1,R^2 = OH

299b 3-Hydroxystaurosporine
R^1 = OH, R^2 = H

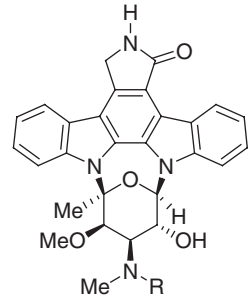

300 4′-*N*-Methyl-5′-hydroxystaurosporine
R = Me

301 5′-Hydroxystaurosporine
R = H

Scheme 2.75

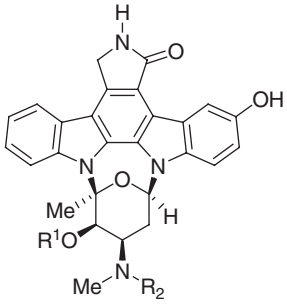

302 3-Hydroxy-4′-*N*-methylstaurosporine
R^1,R^2 = Me

303 3-Hydroxy-3′-*O*-demethylstaurosporine
R^1,R^2 = H

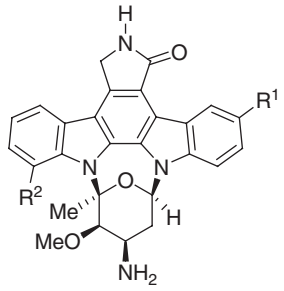

304 3-Hydroxy-4′-*N*-demethylstaurosporine
R^1 = OH; R^2 = H

305 11-Hydroxy-4′-*N*-demethylstaurosporine
R^1 = H; R^2 = OH

306 4′-*N*-Demethylstaurosporine
R^1,R^2 = H

Scheme 2.76

on these spectral data, and the structural similarity to 11-hydroxystaurosporine (**298**), the structure **299a** was assigned to 3,11-dihydroxystaurosporine (295).

In 1999, Schupp *et al.* reported the isolation of 3-hydroxystaurosporine (**299b**) (Scheme 2.75), 3-hydroxy-3′-*O*-demethylstaurosporine (**303**), 11-hydroxy-4′-*N*-demethylstaurosporine (**305**), and 4′-*N*-demethylstaurosporine (**306**) (see Scheme 2.76), along with the previously known staurosporinone (**293**), (+)-staurosporine (**295**), and *O*-demethylstaurosporine (3′-*O*-demethylstaurosporine) (**297**) (see Scheme 2.74) from the marine ascidian *Eudistoma toealensis* and its predatory flatworm *Pseudoceros* sp. (Pseudocerotidae). Except for 3-hydroxy-3′-*O*-demethylstaurosporine (**303**) and 11-hydroxy-4′-*N*-demethylstaurosporine (**305**), the remaining staurosporine derivatives were isolated in their protonated form (297). In the same year, prior to Schupp's report Boyd *et al.* already reported the isolation of 11-hydroxy-4′-*N*-demethylstaurosporine (**305**), along with the previously known 3,11-dihydroxystaurosporine (**299a**) (see Scheme 2.75), from a different natural source, the prosobranch mollusk *Coriocella nigra* collected in the Philippines (296).

The ^{1}H-NMR spectrum of 3-hydroxystaurosporine (**299b**) was very similar to that of (+)-staurosporine (**295**) (see Scheme 2.74), except for the absence of one proton in the aromatic region. Decoupling experiments showed that the second aromatic ring is 1,2,4-trisubstituted, and the C-4 proton is shifted to δ 8.71 with *meta*-coupling (J=1.8 Hz). This shielding effect of the C-4 proton indicated the presence of an additional oxygen atom *ortho* to the C-4 carbon. Based on these spectral data, and the structural similarity to (+)-staurosporine (**295**), the structure **299b** was assigned to 3-hydroxystaurosporine. This structure was further supported by the COSY, HMBC, and HMQC spectra (297) (Scheme 2.75).

In 2000, Baz *et al.* reported the isolation of 4′-*N*-methyl-5′-hydroxystaurosporine (**300**) and 5′-hydroxystaurosporine (**301**), along with (+)-staurosporine (**295**) (see Scheme 2.74), from the culture broth of a marine *Micromonospora* sp. strain L-31-CLCO-002. In nature, these isolates were available in their enantiopure form with a

specific rotation of $[\alpha]_D$ +30.0 (*c* 0.11, $CHCl_3$) for 4′-*N*-methyl-5-hydroxystaurosporine and $[\alpha]_D$ +53.0 (*c* 0.10, $CHCl_3$) for 5′-hydroxystaurosporine. The relative configurations of these staurosporine analogs were determined by NMR analysis (298).

The UV (λ_{max} 242, 291, 320, 334, 354, and 370 nm) and IR (ν_{max} 1670 and 3400 cm^{-1}) spectra of 4′-*N*-methyl-5′-hydroxystaurosporine (**300**) were very similar to those of (+)-staurosporine (**295**) (see Scheme 2.74), indicating the presence of a similar indolo[2,3-*a*]carbazole framework with a lactam function. The NMR spectra of 4′-*N*-methyl-5′-hydroxystaurosporine (**300**) were also very similar to those of (+)-staurosporine (**295**) (see Scheme 2.74), except for the difference in the substitution pattern of the sugar moiety. Thus, the ^{1}H-NMR spectrum showed two shielded *N*-methyl singlets at δ 2.37 and a doublet (*J*=9.9 Hz) for the C-5′ proton at δ 4.43 and the C-3′ singlet at δ 3.95, and a shielded doublet (*J*=9.9 Hz) for the C-4′ proton at δ 3.02, indicating the presence of additional methyl and hydroxy groups at the C-4′ *N*-methyl and the C-5′ carbon, respectively. Based on these spectral data, and the structural similarity to (+)-staurosporine (**295**), the structure **300** was assigned to 4′-*N*-methyl-5′-hydroxystaurosporine. This structure was further supported by the ^{13}C-NMR and NOESY spectra (298) (Scheme 2.75).

The UV (λ_{max} 242, 291, 320, 334, 354, and 370 nm) and IR (ν_{max} 1670 and 3400 cm^{-1}) spectra of 5′-hydroxystaurosporine (**301**) were identical to those of 4′-*N*-methyl-5′-hydroxystaurosporine (**300**), indicating the presence of a similar carbazole framework. The ^{1}H-NMR spectrum of 5′-hydroxystaurosporine (**301**) also closely resembled that of 4′-*N*-methyl-5′-hydroxystaurosporine, except for the presence of a three-proton singlet at δ 2.17 in place of a six-proton singlet at δ 2.37, indicating the addition of one C-4′-*N*-methyl group. This was also in agreement with the FAB-MS data. Based on these spectral data, and the close structural similarity to 4′-*N*-methyl-5′-hydroxystaurosporine (**300**), the structure **301** was assigned to 5′-hydroxystaurosporine. This structure was unambiguously established by the transformation of 5′-hydroxystaurosporine (**301**) to 4′-*N*-methyl-5′-hydroxystaurosporine (**300**) by *N*-methylation with methyl iodide in acetone with potassium carbonate (298) (Scheme 2.75).

In 2002, Schupp *et al.* reported the isolation of 3-hydroxy-4′-*N*-methylstaurosporine (**302**), 3-hydroxy-4′-*N*-demethylstaurosporine (**304**) (see Scheme 2.76) and 3′-*O*-demethyl-4′-*N*-demethylstaurosporine (**307**) (see Scheme 2.77), along with the

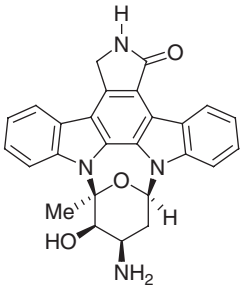

307 3′-*O*-Demethyl-4′-*N*-demethylstaurosporine

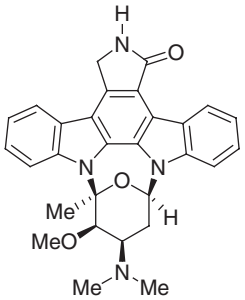

308 *N*-Methylstaurosporine

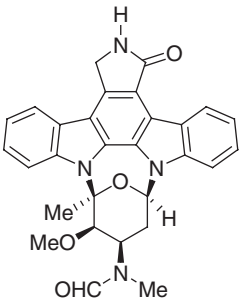

309 *N*-Formylstaurosporine

Scheme 2.77

previously known 11-hydroxystaurosporine (**298**) (see Scheme 2.75) and *N*-methylstaurosporine (**308**) (see Scheme 2.77), from the marine ascidian *E. toealensis* and its predatory flatworm *Pseudoceros* sp. (Pseudocerotidae). The CD measurements of all these staurosporine derivatives confirmed that they have a similar 2′*S*, 3′*R*, 4′*R*, and 6′*R* absolute configuration as (+)-staurosporine (**295**) (see Scheme 2.74) (299). Prior to Schupp's isolation, *N*-methylstaurosporine (**308**) was already known by Cai *et al.* at Ciba-Geigy from *S. longisporoflavus* (300).

The UV spectrum (λ_{max} 287, 297, 308, 324, 342, 366, and 385 nm) of 3-hydroxy-4′-*N*-methylstaurosporine (**302**) was similar to that of (+)-staurosporine (**295**) (see Scheme 2.74), indicating the presence of a similar indolocarbazole framework with a lactam function. The ESI-MS spectrum showed a molecular ion at m/z 497 (M^++H), together with the daughter ion at m/z 354, characteristic of the oxygenated indolocarbazole moiety in 3-hydroxy-4′-*N*-methylstaurosporine (**302**). The ^{1}H-NMR spectrum was similar to that of (+)-staurosporine (**295**), except for a broad methyl signal at δ 2.94 corresponding to two *N*-methyl groups. Based on the HMQC and HMBC experiments, the two other methyl groups at δ 2.35 and 2.59 were assignable to the C-3′ methoxy and C-2′ methyl groups, respectively. Furthermore, the aromatic region showed a characteristic, three-proton coupling pattern, in which there was an upfield shift for the *meta*-coupled (J=2.5 Hz) C-4 proton (δ 8.77). The absence of the C-3 proton, and the corresponding upfield shifts of the C-4 (δ 8.77) and C-2 (δ 7.07) protons, indicated the presence of an additional hydroxy group at C-3. Based on these spectral data, and the structural similarity to (+)-staurosporine, the structure **302** was assigned to 3-hydroxy-4′-*N*-methylstaurosporine. This structure was further supported by the ^{13}C-NMR and COSY spectra (299) (Scheme 2.76).

The UV (λ_{max} 237, 251, 270, 297, 342, 366, and 384 nm) spectrum of 3-hydroxy-3′-*O*-demethylstaurosporine (**303**) was very similar to that of *O*-demethylstaurosporine (3′-*O*-demethylstaurosporine) (**297**) (see Scheme 2.74), indicating the presence of a similar indolo[2,3-*a*]carbazole framework with a lactam function. The ^{1}H- and ^{13}C-NMR spectra of 3-hydroxy-3′-demethylstaurosporine (**303**) were also very similar to those of *O*-demethylstaurosporine (3′-*O*-demethylstaurosporine) (**297**), except for the absence of one proton in the aromatic region. The ^{1}H–^{1}H COSY spectrum showed a characteristic three-proton aromatic coupling pattern in which the C-4 proton was shifted to δ 8.74 with *meta*-coupling (J=2.4 Hz), indicating the presence of an additional oxygen atom *ortho* to the C-4 carbon. This 1,2,4-trisubstituted aromatic pattern was also supported by the absence of the C-3 proton and the upfield shifts of the C-4 and C-2 protons compared to *O*-demethylstaurosporine (3′-*O*-demethylstaurosporine). Based on these spectral data, and the structural similarity to *O*-demethylstaurosporine (3′-*O*-demethylstaurosporine) (**297**), the structure **303** was assigned to 3-hydroxy-3′-*O*-demethylstaurosporine. This structure was further supported by the COSY, HMBC, and HMQC spectra (297) (Scheme 2.76).

The UV spectrum (λ_{max} 287, 297, 342, 366, and 384 nm) of 3-hydroxy-4′-*N*-demethylstaurosporine (**304**) was very similar to that of 3-hydroxy-4′-*N*-methylstaurosporine (**302**), indicating the presence of a similar indolocarbazole framework with a lactam function. The ESI-MS spectrum showed a molecular ion at m/z 469 (M^++H), together with a daughter ion at m/z 354, indicating the presence of an oxygenated indolocarbazole moiety, together with the absence of two methyl groups in the sugar

moiety. The ^{1}H-NMR spectrum was also similar to that of 3-hydroxy-4′-*N*-methylstaurosporine (**302**), except for the absence of a broad methyl signal at δ 2.94 corresponding to two *N*-methyl groups. Furthermore, the C-4′ proton showed a downfield shift (δ 4.12) when compared to the C-4′ proton (δ 3.92) of 3-hydroxy-4′-*N*-methylstaurosporine (**302**), establishing the absence of methyl groups at C-4′-nitrogen. Based on these spectral data, and the structural similarity to 3-hydroxy-4′-*N*-methylstaurosporine, the structure **304** was assigned to 3-hydroxy-4′-*N*-demethylstaurosporine. This structure was further supported by the COSY spectrum (299) (Scheme 2.76).

The UV spectrum (λ_{max} 290, 354, and 371 nm) of 11-hydroxy-4′-*N*-demethylstaurosporine (**305**) was similar to that of 11-hydroxystaurosporine (**298**) (see Scheme 2.75), indicating the presence of a similar indolocarbazole framework (296). The ESI-MS spectrum of 11-hydroxy-4′-*N*-demethylstaurosporine was identical to that of 3-hydroxy-4′-*N*-demethylstaurosporine (**304**) with a molecular ion at m/z 469 (M^{+}+H) and a daughter ion at m/z 354, establishing that these two are regioisomeric, oxygenated, indolocarbazole alkaloids (299). The ^{1}H-NMR spectrum of 11-hydroxy-4′-*N*-demethylstaurosporine was also very similar to that of 11-hydroxystaurosporine (**298**) (see Scheme 2.75), except for the presence of the NH_2 protons at δ 8.45 as a broad singlet in place of the *N*-methyl protons at δ 2.55. The absence of a CH_2 group was supported from its HRFAB-MS. Based on these spectral data, and the structural similarity to 11-hydroxystaurosporine, the structure **305** was assigned to 11-hydroxy-4′-*N*-demethylstaurosporine. This structure was further supported by the HMBC and NOE spectra (296) (Scheme 2.76).

The ^{1}H- and ^{13}C-NMR spectra of 4′-*N*-demethylstaurosporine (**306**) were very similar to those of (+)-staurosporine (**295**) (see Scheme 2.74), except for the absence of the C-4′-*N*-methyl at δ_H 2.83 and δ_C 31.3, indicating the presence of an NH_2 group at C-4′. Based on these spectral data, and the close structural similarity to (+)-staurosporine, the structure **306** was assigned to 4′-*N*-demethylstaurosporine (297) (Scheme 2.76).

The UV spectrum (λ_{max} 291, 322, 334, 355, and 372 nm) of 3′-*O*-demethyl-4′-*N*-demethylstaurosporine (**307**) was very similar to that of (+)-staurosporine (**295**) (see Scheme 2.74), indicating the presence of a similar indolo[2,3-*a*]pyrrolo[3,4-*c*]carbazole framework. The NMR spectra of 3′-*O*-demethyl-4′-*N*-demethylstaurosporine were also very similar to those of (+)-staurosporine (**295**), except for the difference in the substitution pattern of the sugar moiety. Thus, the ^{1}H-NMR spectrum showed only one methyl signal at δ 2.41. From the HMBC experiments this methyl group was correlated with C-2′, indicating the location of this methyl at C-2′, and there were no methyl signals representing the 3′-OMe and 4′-NMe, as in (+)-staurosporine. Further, the presence of a (+)-staurosporine indolocarbazole moiety was supported by the mass fragmentation ion at m/z 338 in the EI-MS. Based on these spectral data, and the close structural similarity to (+)-staurosporine, the structure **307** was assigned to 3′-*O*-demethyl-4′-*N*-demethylstaurosporine (299) (Scheme 2.77).

The IR (ν_{max} 1685 and 3450 cm^{-1}) spectrum of *N*-methylstaurosporine (**308**) was similar to that of 4′-*N*-methyl-5′-hydroxystaurosporine (**300**) (see Scheme 2.75), indicating the presence of a similar indolo[2,3-*a*]carbazole framework with a lactam function (300). The ^{1}H-NMR spectrum of *N*-methylstaurosporine (**308**) was very similar to that of (+)-staurosporine (**295**), except for a broad methyl signal at δ 2.94 corresponding to two *N*-methyl groups. Based on these spectral data, and the

close structural similarity to (+)-staurosporine, the structure **308** was assigned to *N*-methylstaurosporine. This structure was further supported by the ^{13}C-NMR, HMBC, and HMQC spectra (299) (Scheme 2.77).

In 1995, Cai *et al.* reported the isolation of several metabolites related to staurosporine, *N*-formylstaurosporine (**309**) (see Scheme 2.77), *N*-acetoxymethoxystaurosporine (**310**), 4′-*N*-demethyl-*N*-formyl-*N*-hydroxystaurosporine (**311**), and 4′-demethylamino-4′-nitrostaurosporine (**312**) (see Scheme 2.78) from *S. longisporoflavus* R19 strain (301). Prior to this report, *N*-formylstaurosporine (**309**) had been described in the patent literature (302).

Comparison of the HREI-MS of *N*-formylstaurosporine (**309**) with (+)-staurosporine (**295**) (see Scheme 2.74) indicated the presence of an additional carbonyl group. The EI-MS spectrum mass fragmentation ion at m/z 466 (M^+–CO) indicated the presence of a formyl group. Additionally, the presence of an aldehyde functionality was confirmed by the characteristic IR bands at ν_{max} 1670 (C═O), 2840 (aldehyde CH) cm^{-1}. The ^{1}H- and ^{13}C-NMR spectra of *N*-formylstaurosporine (**308**) were also very similar to those of (+)-staurosporine (**295**), except for the presence of an additional aldehyde group (δ_H 8.18 and δ_C 162.8). The position of this formyl group was established at the 4′-*N* atom by recording a high temperature ^{1}H-NMR spectrum. The 4′-*N*-methyl group at 30°C split into two separate signals due to the *syn* and *anti* conformations of the formyl group. However, at 150°C only one signal was observed due to the rapid conformational interchange of the formyl group. Based on these spectral analyses and the close structural similarity to (+)-staurosporine, the structure **309** was assigned to *N*-formylstaurosporine (301) (Scheme 2.77).

Comparison of the HREI-MS of *N*-acetoxymethoxystaurosporine (**310**) with (+)-staurosporine (**295**) (see Scheme 2.74) indicated the presence of an additional $C_3H_4O_3$ residue. The ^{1}H- and ^{13}C-NMR spectra of *N*-acetoxymethoxystaurosporine (**309**) were also very similar to those of (+)-staurosporine (**295**), except for the presence of a singlet methyl group at δ 1.76 and the doublets at δ 4.55 and 4.46 of a methylene group. From the two ^{13}C-NMR signals at δ 20.3 and 169.0, the methyl group (δ_H 1.76) was indicated to be part of an acetate function. The position of the CH_2O at the 4′-*N* atom was established by basic hydrolysis of *N*-acetoxymethoxystaurosporine (**310**) to *N*-hydroxystaurosporine. Based on these spectral analyses, chemical correlation to *N*-hydroxystaurosporine, and the close structural similarity to (+)-staurosporine, the structure **310** was assigned to *N*-acetoxymethoxystaurosporine (301) (Scheme 2.78).

The ^{1}H-NMR spectrum of 4′-*N*-demethyl-*N*-formyl-*N*-hydroxystaurosporine (**311**) was very similar to that of (+)-staurosporine (**295**), except for the absence of the *N*-methyl group in the sugar moiety and the presence of two, rather broad, signals at δ 8.1 and 9.4 assignable to *N*-formyl and *N*-hydroxy groups, respectively. The presence of a formyl group was confirmed by the observation of a ^{13}C-NMR signal at δ 160.0. Furthermore, the characteristic IR bands at ν_{max} 1665 (C═O), 2860 (aldehyde CH), and 3400 (OH) cm^{-1} indicated the presence of *N*-formyl and *N*-hydroxy groups. Based on these spectral data, and the close structural similarity to (+)-staurosporine, the structure **311** was assigned to 4′-*N*-demethyl-*N*-formyl-*N*-hydroxystaurosporine (301) (Scheme 2.78).

The ^{1}H-NMR spectrum of 4′-demethylamino-4′-nitrostaurosporine (**312**) was very similar to that of (+)-staurosporine (**295**) (see Scheme 2.74), except for the absence of the *N*-methyl group and the strong, downfield shift of the C-4′ proton from δ 3.33 to

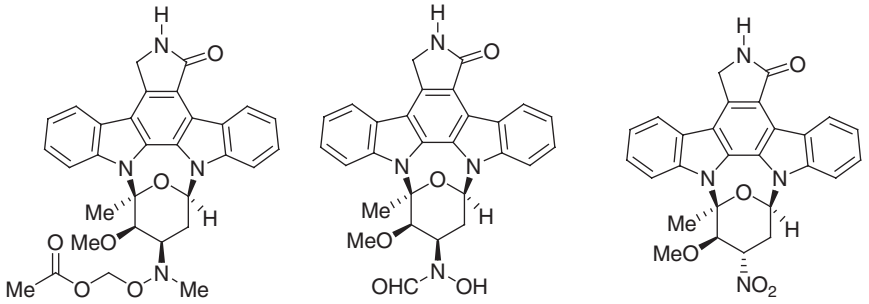

310 *N*-Acetoxymethoxy-staurosporine

311 4′-*N*-Demethyl-*N*-formyl-*N*-hydroxystaurosporine

312 4′-Demethylamino-4′-nitrostaurosporine

Scheme 2.78

4.53 in the sugar moiety. Comparison of the HREI-MS of **312** with (+)-staurosporine (**295**) (see Scheme 2.74) indicated the presence of two additional oxygen atoms. These data, together with the ^{1}H-NMR data, indicated the presence of a nitro group in position C-4′. Further, the presence of a nitro group was supported by a characteristic, very strong absorption band in the IR spectrum at ν_{max} 1590 cm^{-1}, as well as the expected ^{13}C-NMR shifts for the C-3′, C-4′, and C-5′ signals. Based on these spectral data, and the close structural similarity to (+)-staurosporine, the structure **312** was assigned to 4′-demethylamino-4′-nitrostaurosporine. This structure was further supported by NOE experiments (301) (Scheme 2.78).

In 1989, Tanida *et al*. reported the isolation of the oxime analog of staurosporine, TAN-1030A (**313**) from culture broth of *Streptomyces* sp. C-71799, along with previously known (+)-staurosporine (**295**) (see Scheme 2.74) (291). In 1995, Cai *et al*. also reported TAN-1030A (**313**) from a different *Streptomyces* sp., *S. longisporoflavus* R19 strain (301). TAN-1030A (**313**) was shown to activate macrophage function in mice (291).

The UV [λ_{max} 244 (sh), 263 (sh), 275 (sh), 289, 319 (sh), 333, 352, and 369 nm] and IR (ν_{max} 1680 and 3430 cm^{-1}) spectra of TAN-1030A (**313**) were very similar to those of (+)-staurosporine (**295**) (see Scheme 2.74), indicating the presence of a similar indolo[2,3-*a*]pyrrolo[3,4-*c*]carbazole framework. The ^{1}H-NMR spectrum of TAN-1030A (**313**) was also very similar to that of (+)-staurosporine (**295**), except for the presence of a D_2O-exchangeable proton at δ 10.45 in place of the *N*-methyl group at δ 1.44 in the sugar moiety. Further, in the ^{13}C-NMR spectrum, a quaternary carbon at δ 145.1 appeared in place of the staurosporine C-4′ methine signal (δ 50.0). These NMR data indicated the presence of an oxime function at the C-4′ position. Hydrogenation of (−)-TAN-1030A with Pt-black afforded the corresponding C-4′ amino derivative, which, on acetylation with Ac_2O-pyridine, gave the corresponding *N*-acetyl derivative. These chemical reactions confirmed the presence of an oxime function. Furthermore, the oxime proton at δ 10.45 showed NOE enhancement with the C-3′ methoxy (δ 3.43) and the C-2′ methyl (δ 2.47), indicating the *syn* stereochemistry of the oxime function at C-4′ relative to the methoxy group. Based on these spectral data and the structural similarities to (+)-staurosporine the structure **313**, was assigned to TAN-1030A. This structure was further supported by the COSY, NOESY, and COLOC spectra (291,293) (Scheme 2.79).

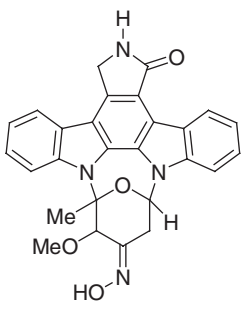

313 TAN-1030A

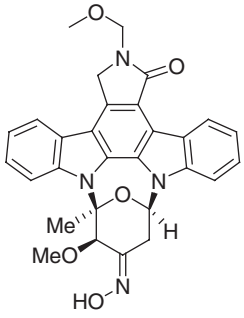

314 6-Methoxymethyl-TAN-1030A

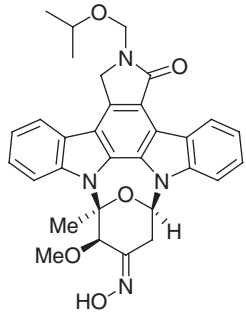

315 6-Isopropoxymethyl-TAN-1030A

Scheme 2.79

In 1996, Cai *et al*. reported the isolation of several metabolites related to TAN-1030A, 6-methoxymethyl-TAN-1030A (**314**), 6-isopropoxymethyl-TAN-1030A (**315**), 4′-deoxime-4′-oxo-TAN-1030A (**316**), and 4′-deoxime-4′-oxo-3′-epi-TAN-1030A (**317**) from *S. longisporoflavus* strain R-19 (289). The ^{1}H-NMR spectrum of 6-methoxymethyl-TAN-1030A (**314**) was very similar to that of TAN-1030A (**313**), except for the absence of a lactam proton at nitrogen 6, suggesting a substitution at this center. Further, the ^{1}H-NMR spectrum showed a singlet for methylene protons at δ 5.12 and a methoxy group at δ 3.29, indicating the presence of a methoxymethyl (CH_2OMe) group at the lactam nitrogen. The presence of this additional methoxymethyl group was also supported by the comparison of the HREI-MS with that of TAN-1030A (**313**). Based on these spectral data, and the structural similarities to TAN-1030A (**313**), the structure **314** was assigned to 6-methoxymethyl-TAN-1030A. This structure was further supported by the ^{13}C-NMR spectrum (289) (Scheme 2.79).

The ^{1}H-NMR spectrum of 6-isopropoxymethyl-TAN-1030A (**315**) was very similar to that of 6-methoxymethyl-TAN-1030A (**314**), except for the difference in the substitution pattern on the lactam nitrogen 6. Comparison of the HREI-MS with that of 6-methoxymethyl-TAN-1030A indicated the presence of an isopropyl group instead of a methyl group. The presence of this additional isopropoxy group was also established from the ^{1}H-NMR spectrum by the presence of a six-proton doublet at δ 1.17 assignable to two methyl groups, and a one-proton multiplet at δ 3.80, assignable to an isopropoxy methine proton. Based on these spectral data, and the structural similarities to 6-methoxymethyl-TAN-1030A (**314**), the structure **315** was assigned to 6-isopropoxymethyl-TAN-1030A. This structure was further supported by the ^{13}C-NMR spectrum (289) (Scheme 2.79).

The ^{1}H-NMR spectrum of 4′-deoxime-4′-oxo-TAN-1030A (**316**) was very similar to that of TAN-1030A (**313**) (see Scheme 2.79), except for the downfield shift of the C-3′ and C-5′ signals. Comparison of the HRFAB-MS of **316** with TAN-1030A (**313**) (see Scheme 2.79), indicated the lack of nitrogen and hydrogen atoms. These data, together with the ^{1}H-NMR data, indicated the presence of a ketone function at position C-4′. Furthermore, the presence of a keto group was supported by a typical ketone band in the IR spectrum at ν_{max} 1730 cm^{-1}, as well as a carbonyl carbon signal at δ 200.6 in the ^{13}C-NMR spectrum. Based on these spectral data, and the structural

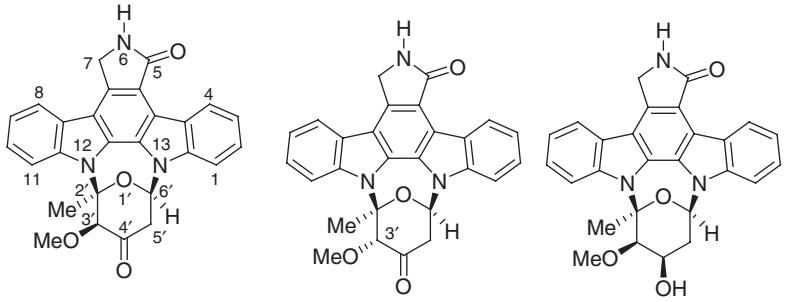

316 4′-Deoxime-4′-oxo-TAN-1030A **317** 4′-Deoxime-4′-oxo-3′-epi-TAN-1030A **318** RK-286C

Scheme 2.80

similarities to TAN-1030A (**313**), the structure **316** was assigned to 4′-deoxime-4′-oxo-TAN-1030A (289) (Scheme 2.80).

The ^{1}H-NMR spectrum of 4′-deoxime-4′-oxo-3′-epi-TAN-1030A (**317**) was quite similar to that of 4′-deoxime-4′-oxo-TAN-1030A (**316**), except for the differences in the position of the 2′-methyl group, and the C-3′ and C-5′ signals. Furthermore, the ^{13}C-NMR spectrum showed shifts of about 4 ppm for the 2′-methyl group, and the C-3′ and C-5′ signals. The NOE difference experiments indicated that these two indolocarbazoles are C-3′ epimeric compounds. 4′-Deoxime-4′-oxo-3′-epi-TAN-1030A (**317**) showed no pronounced NOE (3%) as compared to the 13% NOE for 4′-deoxime-4′-oxo-TAN-1030A (**316**), on the proton at C-3′ by irradiation at the equatorial 2-methyl group, indicating a *cis*-relationship between the C-2′ methyl and the C-3′ methoxy groups of **317**. Structural support came from the observed long-range effects in the ^{13}C-NMR spectrum. Based on these spectral data, and the structural similarities to 4′-deoxime-4′-oxo-TAN-1030A (**316**), the structure **317** was assigned to 4′-deoxime-4′-oxo-3′-epi-TAN-1030A (289) (Scheme 2.80).

In 1990, Isono *et al.* reported the isolation of RK-286C (**318**) from the culture filtrate and the mycelium extract of *Streptomyces* sp. RK-286 (303). In nature, this isolate was obtained in its optically active form $[\alpha]_D^{20} + 45.3$ (*c* 0.22, EtOAc). Based on similar CD curves, the absolute configuration of this isolate was assigned to be similar to that of (+)-staurosporine (**295**) (see Scheme 2.74) (284). RK-286C has shown PKC inhibitory activity and platelet aggregation *in vitro*, as well as weak antifungal activity (303).

The UV spectrum [λ_{max} 245, 266 (sh), 292, 322 (sh), 335, 356, and 372 nm] of RK-286C (**318**) was identical to that of (+)-staurosporine (**295**) (see Scheme 2.74), indicating the presence of a similar indolo[2,3-*a*]pyrrolo[3,4-*c*]carbazole framework. This was also discernible from its IR spectrum. The ^{1}H- and ^{13}C-NMR spectra of RK-286C were also very similar to those of (+)-staurosporine (**295**), except for the presence of a D_2O-exchangeable proton at δ 4.17, in place of the corresponding C-4′ methylamino protons at δ 1.44 and 3.33. Besides these spectral differences, the C-4′ proton and carbon also showed a downfield shift, further supporting the presence of a hydroxy group. Based on these spectral data, and the structural similarity to (+)-staurosporine, the structure **318** was assigned to RK-286C. This structure was further supported by the COSY spectrum (284) (Scheme 2.80).

Two years later, the same authors also reported the 3′-epimer of RK-286C, RK-1409B (**319**), from the culture broth of *Streptomyces platensis* subsp. *malvinus* RK-1409. In nature, this isolate was obtained in its optically active form $[\alpha]_D^{22}$ + 147.0 (*c* 0.2, DMSO). RK-1409B showed inhibition of PKC and weak antifungal activity (304).

The UV spectrum [λ_{max} 245, 267 (sh), 293, 320 (sh), 336, 357, and 374 nm] of RK-1409B (**319**) was identical to that of RK-286C (**318**) (see Scheme 2.80), indicating the presence of a similar indolo[2,3-*a*]pyrrolo[3,4-*c*]carbazole framework. This was also discernible from its IR spectrum. The ^{1}H- and ^{13}C-NMR spectra of RK-1409B (**319**) were also very similar to those of RK-286C (**318**), except for some differences in the chemical shifts for the sugar moiety, indicating that RK-1409B is a stereoisomer of RK-286C. The relative stereochemistry of the hydroxy group at C-4′ was determined to be axial by the small coupling constants of 4′-H ($J_{3',4'}$=4.3 Hz, $J_{4',5'a}$=5.5 Hz, and $J_{4',5'b}$=4.3 Hz), and the axial orientation of the methoxy group at C-3′ was supported by an NOE between 11-H and 3′-H, indicating that RK-1409B and RK-286C were epimers at the C-3′ position. The CD spectra of RK-1409B and RK-286C exhibited quite similar curves, showing that the absolute stereochemistry at C-2′ and C-6′ were the same in RK-286C. Based on these spectral data, and the structural similarity to RK-286C, the structure **319** was assigned to RK-1409B. This structure was further supported by the COSY and HMBC spectra (304) (Scheme 2.81).

In 1994, McAlpine *et al*. reported the isolation of MLR-52 (**320**), along with (+)-staurosporine (**295**) (see Scheme 2.74), from the fermentation broth and mycelia of *Streptomyces* sp. AB 1869R-359. In nature, this isolate was obtained in its optically active form $[\alpha]_D$ +68.0 (*c* 0.093, MeOH). This isolate has shown inhibition of PKC and potent *in vitro* immunosuppressive activity (305).

The UV spectrum (λ_{max} 234, 286, 317, 332, 351, and 368 nm) of MLR-52 (**320**) was similar to that of RK-286C (**318**) (see Scheme 2.80), indicating the presence of a similar indolo[2,3-*a*]pyrrolo[3,4-*c*]carbazole framework. This was also discernible from its IR spectrum. The ^{1}H- and ^{13}C-NMR spectra of MLR-52 (**320**) were similar to those of RK-286C (**318**) (see Scheme 2.80), except for the different substitution pattern of the sugar moiety. Thus, the ^{1}H-NMR spectrum showed a one-proton doublet at δ 4.16 for the C-5′ proton, in place of a two-proton multiplet at δ 2.41 and 2.61, indicating a hydroxy group at this carbon. Furthermore, the presence of an additional oxygen atom was supported from the HRFAB-MS. An axial–axial

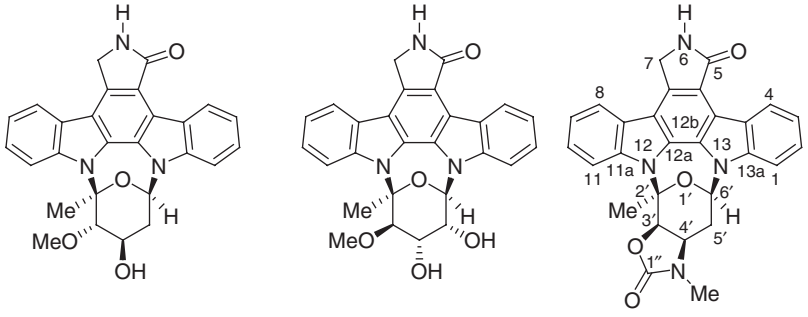

319 RK-1409B **320** MLR-52 **321** ZHD-0501

Scheme 2.81

coupling constant (J=10.3 Hz) between the proton signals for H-3′ and H-4′ at δ 4.14 and 3.57, respectively, indicated that the 3′-methoxy and the 4′-hydroxy groups are equatorial to each other. Further, the proton at C-5′ showed a small coupling constant (J=2.6 Hz) with the C-4′ hydrogen indicating an axial hydroxy group at C-5′. Based on these spectral data, and the structural similarity to RK-286C, the structure **320** was assigned to MLR-52. This structure was further supported by the COSY and HMBC spectra (305) (Scheme 2.81).

In 2005, Han *et al.* reported the isolation of a novel, naturally occurring, staurosporine analog, ZHD-0501 (**321**) from the fermentation broth of a marine-derived *Actinomadura* sp. 007. This was the first example of a staurosporine analog carrying a heterocycle fused to the pyran ring, and it has shown *in vitro* anticancer activity against mammalian cancer cells. In nature, this isolate was obtained in its optically active form $[\alpha]_D^{20} + 83.2$ (*c* 0.10, MeOH) (306).

The UV spectrum [λ_{max} 243 (sh), 275 (sh), 290, 318, 332, 351, and 369 nm] of ZHD-0501 (**321**) was very similar to that of (+)-staurosporine (**295**) (see Scheme 2.74), indicating the presence of a similar indolo[2,3-*a*]pyrrolo[3,4-*c*]carbazole framework. This was also discernible from its IR spectrum. The ^{1}H- and ^{13}C-NMR spectra of ZHD-0501 (**321**) were also very similar to those of (+)-staurosporine (**295**), except for the difference in the sugar moiety, establishing the presence of a similar aglycon. Analysis of the PFG COSY and PFG HMQC spectra indicated the structural units related to the proton spin system in the sugar moiety. The HMBC correlations of 2′-Me/C-2′, 2′-Me/C-3′, and H-6′/C-2′ showed the presence of a methyl pyranose ring system. Further, the HMBC correlations of H-3′/C-1″, H-4′/C-1″, *N*-Me/C-1″, and *N*-Me/C-4′ confirmed the *N*-methyl oxazolone ring fused to C-3′ and C-4′ in the sugar moiety. Additionally, the presence of an oxazolone was also established by its IR spectrum, with the oxazolone carbonyl band at ν_{max} 1680 cm^{-1}. Based on the aglycon chemical shifts, and the HMBC correlations between H-6′ and the carbons C-12b and C-13a, the carbons C-2′ and C-6′ in the sugar ring could be connected to *N*-12 and *N*-13 in the aglycon. The stereochemistry of ZHD-0501 was established on the basis of the coupling constants of the protons on the pyran ring and the results of difference NOE experiments. Based on these spectral analyses, and the structural similarities to (+)-staurosporine, the structure **321** was assigned to ZHD-0501 (306) (Scheme 2.81).

In 1990, researchers at Bristol-Myers Squibb reported the isolation of Bmy-41950 (**322**) from *S. staurosporeus* strain R10069 (ATCC 55006). This isolate showed *in vitro* activity against human colon cancer cells (HCT-116) (307). Two years later, Isono *et al.* reported the isolation of the same natural product from a different *Streptomyces* sp., *S. platensis* subsp. *malvinus* RK-1409 and named it RK-1409 (7-oxostaurosporine) (**322**) (308,309). In nature, this isolate was obtained in its optically active form $[\alpha]_D^{20} + 38.3$ (*c* 0.06, $CHCl_3$) (309). The PKC inhibitor RK-1409 (7-oxostaurosporine) inhibited the morphological change of a human erythroleukemia cell line, K-562, induced by phorbol 12,13-dibutyrate (PDBu), and also showed a weak antimicrobial activity against *Chlorella vulgaris* and *Pyricularia oryzae* (308).

The UV spectrum [λ_{max} 238, 260, 287, 305 (sh), 317, 340, and 410 nm] of Bmy-41950 (RK-1409, 7-oxostaurosporine) (**322**) indicated the presence of an indolo[2,3-*a*]pyrrolo[3,4-*c*]carbazole-5,7(6*H*)-dione framework. This was also discernible from its IR spectrum. The ^{1}H-NMR spectrum of Bmy-41950 (RK-1409, 7-oxostaurosporine) (**322**) was very similar to that of (+)-staurosporine (**295**) (see Scheme 2.74), except for

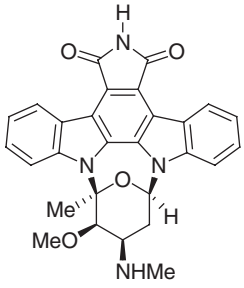

322 Bmy-41950
(RK-1409, 7-Oxostaurosporine)

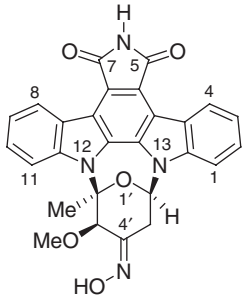

323 7-Oxo-TAN-1030A

Scheme 2.82

the difference in the aglycon moiety. Thus, the ^{1}H-NMR spectrum indicated the absence of the C-7 methylene protons at δ 4.97 and 5.03. Further, a strong downfield shift of the C-8 proton from δ 7.87 to 9.35 indicated the presence of an oxo group at C-7. The presence of this additional oxygen atom in place of two hydrogen atoms was also supported by the HREI-MS. Furthermore, oxidation of (+)-staurosporine (**295**) with *tert*-butyl hydroperoxide and Mn(III)acetylacetonate gave 7-oxostaurosporine, whose spectral data were identical with those of RK-1409 (7-oxostaurosporine) and having the same absolute stereochemistry as that of (+)-staurosporine, and establishing unambiguously the structure and absolute stereochemistry of natural Bmy-41950 (RK-1409, 7-oxostaurosporine) as **322**. Based on these spectroscopic data, the structural similarity to (+)-staurosporine (**295**), and the chemical evidence, the structure **322** was assigned to Bmy-41950 (RK-1409, 7-oxostaurosporine) (309) (Scheme 2.82).

In 1996, Cai *et al*. reported the isolation of the 7-oxygenated TAN-1030A derivatives, 7-oxo-TAN-1030A (**323**), and 7-hydroxy-TAN-1030A (**324**), along with the 7-hydroxy derivative of (+)-staurosporine, UCN-01 (**325a**) from *S. longisporoflavus* strain R-19 (289). Prior to Cai's report, in 1987, Takahashi *et al*. isolated UCN-01 (**325a**) from a different strain of the genus *Streptomyces*, N-71. UCN-01 was shown to inhibit PKC, protein kinase A (PKA), had antitumor activity against murine lymphotic leukemia P388 *in vivo*, and cytotoxic effects on the growth of HeLa S3 cells (310,311). In nature, UCN-01 was isolated in its optically active form $[\alpha]_D^{22} + 132.0$ (*c* 0.3, MeOH) (311). Based on the CD spectral results, UCN-01 was assigned to be a β-7-hydroxy isomer (289). Two years later, the same authors also reported the isolation of UCN-01 (**325a**), together with its C-7-epimer, UCN-02 (**325b**), from a different strain of the genus *Streptomyces*, N-126. In nature, UCN-02 was also isolated in its optically active form $[\alpha]_D^{22} - 38.6$ (*c* 0.35, MeOH) (279,312). Based on the known β-configuration at C-7 for UCN-01 (289), UCN-02 was assigned to be the 7α-hydroxy isomer. In acid or alkaline media, UCN-01 and UCN-02 are in equilibrium. UCN-02 was shown to inhibit PKC and protein kinase A (PKA) and showed cytotoxic effects on the growth of HeLa S3 cells (279).

Comparison of the HREI-MS of 7-oxo-TAN-1030A (**323**) with TAN-1030A (**313**) (see Scheme 2.79) indicated the presence of one additional oxygen in place of two hydrogens. The ^{1}H-NMR spectrum of 7-oxo-TAN-1030A (**323**) was very similar to

that of TAN-1030A (**313**), except for the absence of the C-7 methylene protons at δ 4.95, and a strong downfield shift of the C-8 proton signal from δ 7.96 to 9.08, indicating the presence of an oxo group at C-7. Based on these spectral data, and structural similarity to TAN-1030A (**313**), the structure **323** was assigned to 7-oxo-TAN-1030A (289) (Scheme 2.82).

Comparison of the HRFAB-MS of 7-hydroxy-TAN-1030A (**324**) with TAN-1030A (**313**) (see Scheme 2.79), indicated the presence of one additional oxygen atom. The ^{1}H-NMR spectrum of 7-hydroxy-TAN-1030A (**324**) was also very similar to that of TAN-1030A (**313**), except for the presence of two, one-proton doublets (J=11.0 Hz) at δ 6.41 and 6.53, indicating the presence of a proton and a hydroxy group at C-7, respectively, in place of the two-proton singlet (δ 4.95) for the protons at C-7 in TAN-1030A (**313**). The presence of a hydroxy group at C-7 was further supported by the downfield shift of the C-8 proton signal from δ 7.96 to 8.42. Based on these spectral data, and the structural similarity to TAN-1030A (**313**), the structure **324** was assigned for 7-hydroxy-TAN-1030A (289) (Scheme 2.83).

The UV spectrum [λ_{max} 240, 264 (sh), 274 (sh), 300, 326 (sh), 338 (sh), 358, and 374 nm] of UCN-01 (**325a**) resembles closely that of (+)-staurosporine (**295**) (see Scheme 2.74), indicating the presence of a similar indolo[2,3-*a*]pyrrolo[3,4-*c*]carbazole framework. This was also discernible from its IR spectrum. The ^{1}H-NMR spectrum of UCN-01 (**325a**) was very similar to that of (+)-staurosporine (**295**), except for the presence of signals at δ 6.39 (1*H*, dd, J=9.8, 1.1 Hz) and 6.44 (1*H*, d, J=9.8 Hz). On D_2O addition, the signal at δ 6.39 changed to a singlet and the signal at δ 6.44 collapsed, indicating the 7-methine proton and the 7-hydroxy proton, respectively. Furthermore, in a proton decoupling experiment, the signal at δ 6.39 was changed to a doublet (J=9.8 Hz) on irradiation of the 6-imino proton at δ 8.72 (1*H*, d, J=1.1 Hz). In the ^{13}C-NMR spectrum, the C-7 carbon appeared as a doublet at δ 78.4 in place of a triplet at δ 45.3 in (+)-staurosporine (311). The NOE studies indicated a similar absolute stereochemistry as (+)-staurosporine, except for the configuration of the 7-hydroxy group (279). CD spectral analysis indicated a β-configuration at the 7-hydroxy group (289). Based on these spectroscopic analyses, and the structural similarity to (+)-staurosporine, the structure **325a** was assigned to UCN-01 (279,289,311) (Scheme 2.83).

The UV, IR, and EI-MS spectral data of UCN-02 (**325b**) were identical to those of UCN-01 (**325a**), except for the optical rotation and the R_f value on TLC. The ^{1}H- and

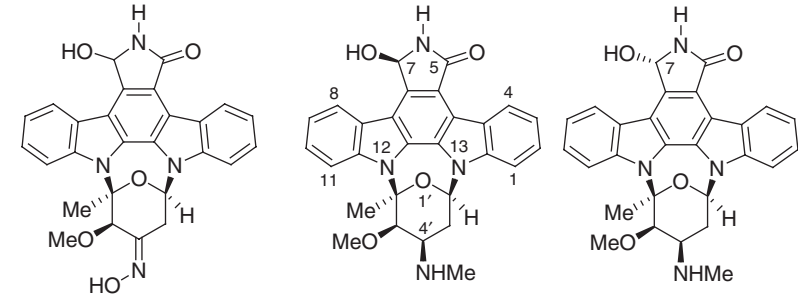

324 7-Hydroxy-TAN-1030A **325a** UCN-01 **325b** UCN-02

Scheme 2.83

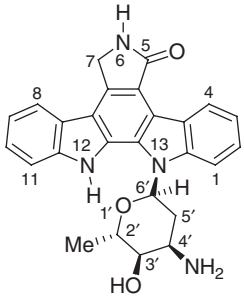

326 Holyrine A

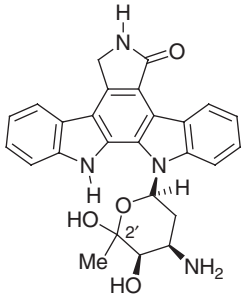

327 Holyrine B

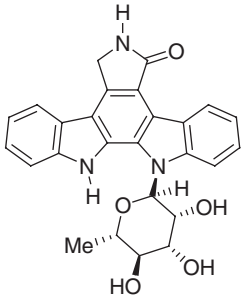

328 K-252d

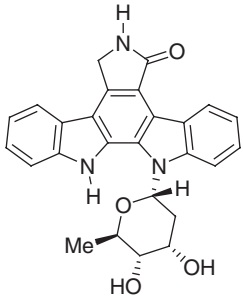

329 RK-286D

Scheme 2.84

^{13}C-NMR spectra were also very similar to those of UCN-01 (**325a**), except for the chemical shift difference of H-7, indicating that UCN-02 (**325b**) is a diastereomer of UCN-01 (**325a**) at the C-7 position, with an α-configuration of the 7-hydroxy group. Based on these data, and the close structural similarity to UCN-01 (**325a**), the structure **325b** was assigned to UCN-02 (279) (Scheme 2.83).

In 1999, Andersen *et al.* reported the isolation of holyrine A (**326**) and holyrine B (**327**), along with the previously known K-252d (**328**) (Scheme 2.84), (+)-staurosporine (**295**), and *O*-demethylstaurosporine (**297**) (see Scheme 2.74) from the cultures of an *Actinomycete* st. N96C-47, isolated from the North Atlantic Ocean near Holyrood. Holyrine A (**326**) and holyrine B (**327**) have only a single attachment of their sugar moiety to the aromatic aglycon, similar to K-252d (**328**) (Scheme 2.84) and rebeccamycin (**337**) (see Scheme 2.86) (313).

Prior to Andersen's report, Kase *et al.* had already reported the isolation of K-252d (**328**), along with K-252b (**331**) (see Scheme 2.85) and K-252c (**293**) (see Scheme 2.74), from the culture broth of *Nocardiopsis* sp. K-290 (273). All these isolates were shown to be potent inhibitors of PKC (273). In nature, K-252d (**328**) $[\alpha]_D^{20} + 35.0$ (*c* 0.4, MeOH) and K-252b (**331**) $[\alpha]_D^{20} + 97.0$ (*c* 0.6, DMF) were isolated in their optically active forms (273,274). In the same year, the same authors also reported the isolation of K-252a (**330**) (see Scheme 2.85) from a different *Nocardiopsis* sp., K-252a (272). Prior to the isolation of K-252a (**330**), Sezaki *et al.* reported the same natural product as SF-2370 (**330**) from a different natural source, *Actinomadura* sp. SF-2370 in its optically active form $[\alpha]_D^{25} - 57.0$ (*c* 0.1, MeOH) (314). The antibiotic K-252a

(SF-2370) (**330**) showed extremely potent inhibitory activity on PKC (272), as well as weak antibacterial and antifungal activities (314). In 1992, Isono *et al*. isolated a novel indolocarbazole antibiotic, RK-286D (**329**), along with the previously known (+)-staurosporine (**295**) (see Scheme 2.74) and RK-286C (**318**) (see Scheme 2.80), from the mycelial cake of *Streptomyces* sp. RK-286. In nature, RK-286D was isolated in optically active form $[\alpha]_D^{20} - 60.0$ (*c* 0.13, MeOH), showing the structural relation to RK-286C (**318**) (315) (see Scheme 2.80).

The ^{1}H-NMR spectrum of holyrine A (**326**) was very similar to that of 3′-*O*-demethyl-4′-*N*-demethylstaurosporine (**307**) (see Scheme 2.77), except for the presence of a mutually coupled (*J*=7.2 Hz) one-proton quartet at δ 4.61 and a three-proton doublet at δ 1.60 in place of the C-2′ methyl singlet proton at δ 2.41 of 3′-*O*-demethyl-4′-*N*-demethylstaurosporine (**307**), indicating the presence of a proton and a methyl group at C-2′ of the glycon. Further, a detailed analysis of the COSY, HMQC, and HMBC revealed that the aglycon in **326** was different from the aglycon in **307** by the presence of a proton at *N*-12 (δ 11.75). Strong anisotropic neighboring group deshielding of the C-4 proton at δ 9.47 by the C-5 lactam carbonyl differentiated the two, four-spin aromatic systems in the aglycon. These data, in conjunction with the HMBC correlation between the *N*-12 proton (δ 11.75) and C-11 (δ 111.6), showed that the glycon was attached to the aglycon at *N*-13. Furthermore, NOE experiments and coupling constant analysis established the same relative stereochemistry as for the glycon substituents in 3′-*O*-demethyl-4′-*N*-demethylstaurosporine (**307**). Based on these spectral data, and the close structural similarity to 3′-*O*-demethyl-4′-*N*-demethylstaurosporine, the structure **326** was assigned to holyrine A (313) (Scheme 2.84).

Comparison of the HRFAB-MS of holyrine B (**327**) with holyrine A (**326**) indicated the presence of one additional oxygen atom. The ^{1}H-NMR spectrum of holyrine B (**327**) was very similar to that of holyrine A (**326**), except for the presence of a methyl singlet at δ 1.59 in place of the methyl doublet at δ 1.60 and the absence of the resonance assigned to the C-2′ proton at δ 4.61. These ^{1}H-NMR changes, together with the additional oxygen atom in the molecular formula of **327**, indicated the presence of a hydroxy functionality at C-2′. The HMBC correlations observed between the C-2′ methyl (δ 1.59) and the C-2′ and C-3′ carbons at δ 99.0 and 67.6, respectively, confirmed the presence of a hemiketal functionality at C-2′. The close similarity of the chemical shifts and multiplicities of the C-3′, C-4′, C-5′, and C-6′ resonances in the ^{1}H-NMR spectra of the holyrines A and B indicated the identical relative stereochemistries at C-3′ to C-6′. However, the relative configuration at C-2′ was not assigned. Based on these spectral data and the close structural similarity to holyrine A, the structure **327** was assigned to holyrine B (313) (Scheme 2.84).

The UV spectrum [λ_{max} 242 (sh), 248 (sh), 260 (sh), 280 (sh), 322, 335, 347, and 364 nm] of K-252d (**328**) was similar to that of staurosporinone (K-252c) (**293**) (see Scheme 2.74), indicating the presence of a similar indolo[2,3-*a*]pyrrolo[3,4-*c*]carbazole framework. Comparison of the ^{1}H-NMR spectrum of K-252d (**328**) with that of staurosporinone (K-252c) (**293**) suggested it to be an *N*-glycoside of K-252c. The HREI-MS spectrum of this isolate revealed the composition of the sugar moiety as $C_6H_{11}O_4$. Hydrolysis of K-252d (**328**) gave a water soluble substance which was identical with rhamnose. The optical rotation and CD spectral data of the 4-nitrobenzoate of methyl-α-rhamnopyranoside obtained from K-252d (**328**) were

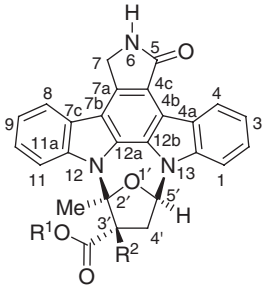

330 K-252a (SF-2370)
R^1 = Me; R^2 = OH

331 K-252b
R^1 = H; R^2 = OH

332 3′-Methylamino-3′-deoxy-K-252a
R^1 = Me; R^2 = NHMe

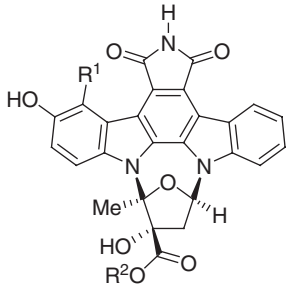

333 (+)-Indocarbazostatin
R^1 = H; R^2 = Et

334 (–)-Indocarbazostatin B
R^1 = NH_2; R^2 = Et

335 (+)-Indocarbazostatin C
R^1 = H; R^2 = Me

336 (–)-Indocarbazostatin D
R^1 = NH_2; R^2 = Me

Scheme 2.85

identical with those of an authentic sample synthesized from l-rhamnose. Further, ^{1}H- and ^{13}C-NMR long-range ^{1}H–^{1}H and ^{1}H–^{13}C-couplings constants showed that the glycon was attached at *N*-13 to the α-L-rhamnopyranosyl, indicating K-252d as 13-*N*-(α-L-rhamnopyranosyl)-252c. Based on these spectral data, and the structural similarity to K-252c and methyl-α-rhamnopyranoside, the structure **328** was established for K-252d (274) (Scheme 2.84).

The UV spectrum [λ_{max} 233, 278 (sh), 290, 320 (sh), 335, 347, and 364 nm] of RK-286D (**329**) was similar to that of K-286C (**318**) (see Scheme 2.80), indicating the presence of a similar indolo[2,3-*a*]pyrrolo[3,4-*c*]carbazole framework. The ^{1}H-NMR spectrum of RK-286D (**329**) was also similar to that of K-286C (**318**), except for the difference in the sugar moiety, establishing the presence of a similar aglycon. Analysis of the decoupling experiments and NOE difference spectrum revealed that the sugar moiety of RK-286D is digitoxose, attached to *N*-13 of the aglycon. The digitoxosepyranosyl moiety is in the $^1C_4$ conformation with the relative stereochemistry as shown in the structure **329**. However, the absolute stereochemistry remains to be determined. Based on these spectral data, and the structural similarity to K-286C (**318**), the structure **329** was assigned to RK-286D (315) (Scheme 2.84).

The UV spectrum [λ_{max} 248, 264 (sh), 280 (sh), 320 (sh), 333, 350, and 367 nm] of K 252a (SF-2370) (**330**) was very similar to that of (+)-staurosporine (**295**) (see Scheme 2.74), showing the presence of a similar indolo[2,3-*a*]pyrrolo[3,4-*c*]carbazole framework. The IR spectrum indicated the presence of an NH and OH band at ν_{max} 3420 cm^{-1}, an ester band at 1730 cm^{-1}, and an amide band at 1663 cm^{-1}. The ^{1}H-NMR spectrum of K 252a (**330**) was similar to that of (+)-staurosporine (**295**), except for the difference in the sugar moiety, establishing the presence of a similar aglycon. The presence of a similar aglycon as in (+)-staurosporine (**295**) was also supported by the NOE spectrum. Further, the long-range coupling pattern of the sugar moiety determined from the COLOC spectrum between the 4′-methylene protons to the

C-3′, C-2′, and the carbonyl carbons, the methyl protons to the C-3′ and C-2′ carbons, and the C-5′ proton to the C-2′ carbon, indicated the location of the methoxycarbonyl group at the C-3′ position and the methyl group at the C-2′ position. Furthermore, proton homo decoupling experiments showed the presence of methine and methylene protons at the C-5′ and C-4′ positions. These spectral data indicated the presence of a 2-deoxyfuranoside. Additionally, the observation of a long-range coupling between H-5′ and C-12b, and the NOE (9.1%) between the C-2′ methyl and C-11 protons, indicated that C-5′ is bonded to *N*-13 and C-2′ to *N*-12. Based on these spectroscopic analyses, and the structural similarity to (+)-staurosporine, the structure **330** was assigned to K-252a (SF-2370). This structure and the configuration at C-3′ was unambiguously established from its X-ray analysis (274) (Scheme 2.85).

The UV spectrum [λ_{max} 246, 268 (sh), 280 (sh), 323, 337, 353, and 371 nm] of K-252b (**331**) was very similar to that of K 252a (**330**), indicating the presence of a similar indolo[2,3-*a*]pyrrolo[3,4-*c*]carbazole framework. The ^{1}H- and ^{13}C-NMR spectra of K-252b (**331**) were also very similar to those of K-252a (SF-2370) (**330**), except for the absence of the methoxycarbonyl methyl signal at δ_H 3.94 and δ_C 52.6. The compound obtained by hydrolysis of K-252a was identical with **331**, which on methylation with diazomethane gave K-252a, indicating K-252b as the 3′-carboxylic acid of K-252a. Based on these spectral data, and the structural similarity to K-252a (**330**), the structure **331** was assigned to K-252b (274) (Scheme 2.85).

In 1996, Cai *et al.* from Ciba-Geigy reported the isolation of 3′-methylamino-3′-deoxy-K-252a (**332**), along with the previously known K-252c (**293**) (see Scheme 2.74) and K-252a (**330**), from *S. longisporoflavus* (276). The IR spectrum of 3′-methylamino-3′-deoxy-K-252a (**332**) was very similar to that of K-252a (**330**), showing the presence of similar functional groups. The ^{1}H-NMR spectrum of 3′-methylamino-3′-deoxy-K-252a (**332**) was also very similar to that of K-252a (**330**), except for the difference in the sugar moiety, indicating the presence of a similar aglycon. In addition to the peaks of K-252a, the ^{1}H-NMR spectrum also showed the presence of a three-proton doublet at δ 1.92, and a one-proton quartet at δ 2.44 assignable to an NHMe in place of the C-3′-hydroxy group of K-252a. Further, comparison of the ^{13}C-NMR data of **330** and **332** showed that the alkaloids are identical, except for the upfield shift of the C-3′ carbon from δ 84.9 to 78.0, and the quartet methyl carbon at δ 32.2, assignable to the NHMe group. Based on these spectral data, and the structural similarity to K-252a, the structure **332** was assigned to 3′-methylamino-3′-deoxy-K-252a (300) (Scheme 2.85).

In 2002, Ubukata *et al.* reported the isolation of (+)-indocarbazostatin (**333**) and (−)-indocarbazostatin B (**334**) from a culture broth of *Streptomyces* sp. TA-0403 (316,317). Two years later, the same authors reported the isolation of two further indocarbazostatin derivatives, (+)-indocarbazostatin C (**335**) and (−)-indocarbazostatin D (**336**), along with the previously known (+)-indocarbazostatin (**333**) and (−)-indocarbazostatin B (**334**) from a different mutant strain, *Streptomyces* sp. MUV-6-83 (318). These isolates function as novel inhibitors of nerve growth factor (NGF)-induced neuronal differentiation in PC12 cells in the nanomolar range (316,318). In nature, (+)-indocarbazostatin (**333**) $[\alpha]_D^{26} + 51.3$ (*c* 0.05, MeOH) and (−)-indocarbazostatin B (**334**) $[\alpha]_D^{26} - 48.7$ (*c* 0.05, MeOH) (317), (+)-indocarbazostatin C (**335**) $[\alpha]_D^{26} + 50.0$ (*c* 0.05, MeOH), and (−)-indocarbazostatin D (**336**) $[\alpha]_D^{26} - 44.0$ (*c* 0.05, MeOH) (318), were isolated in their optically active form, and their relative and absolute configurations were assigned as shown in their respective structures based on MM2, MOPAC, and CONFLEX calculations, and CD analyses (317,318).

The UV spectrum (λ_{max} 236, 283, 290, and 326 nm) of (+)-indocarbazostatin (**333**) indicated the presence of a hetero-substituted indolo[2,3-*a*]pyrrolo[3,4-*c*]carbazole-5,7(6*H*)-dione framework. This was also discernible from its IR spectrum. The ^{1}H- and ^{13}C-NMR, ^{1}H–^{1}H-COSY, PFG HMQC, and PFG HMBC spectral data revealed the presence of a hydroxy group at C-9 of the indolo[2,3-*a*]pyrrolo[3,4-*c*]carbazole-5,7(6*H*)-dione framework and the 2-deoxyfuranoside sugar moiety. The observed long-range coupling between H-5′ and C-12b, and the NOE between the C-2′ methyl and C-11 protons, indicated that C-5′ and C-2′ of the 2-deoxyfuranoside are bonded to *N*-13 and *N*-12 of the aglycon, respectively. Further, the ^{1}H-NMR spectrum showed the presence of a hydroxy signal, along with ethyl ester signals with unusually low δ values due to the anisotropic affect of the aglycon chromophore. Based on these spectral data, the structure **333** was assigned to (+)-indocarbazostatin (317) (Scheme 2.85).

The UV spectrum (λ_{max} 236, 270, 292, and 327 nm) of (−)-indocarbazostatin B (**334**) was very similar to that of (+)-indocarbazostatin (**333**) indicating the presence of a similar indolo[2,3-*a*]pyrrolo[3,4-*c*]carbazole-5,7(6*H*)-dione framework. This was also discernible from its IR spectrum. The ^{1}H-NMR spectrum of (−)-indocarbazostatin B (**334**) was very similar to that of (+)-indocarbazostatin (**333**), except for the difference in the aglycon moiety. Thus, the ^{1}H-NMR spectrum showed the absence of a *meta*-coupled (J=2.7 Hz) C-8 aromatic proton at δ 8.97. This was further supported by the ^{13}C-NMR spectrum with the presence of a C-8 singlet carbon at δ 134.0 in place of the doublet carbon at δ 111.5 in (+)-indocarbazostatin (**333**). Further, a 10 ppm high field shift of the 7c carbon indicated the presence of an amino group at C-8. The presence of this additional NH_2 group in place of one hydrogen atom was supported from the FAB-MS. Based on the differential NOE, COSY, PFG HMQC, PFG HMBC, ^{13}C-NMR chemical shift calculations and biosynthetic considerations, the relative and absolute configurations of (−)-indocarbazostatin B (**334**) were similar to those of (+)-indocarbazostatin (**333**). However, an opposite optical rotation and the totally different CD spectrum from that of (+)-indocarbazostatin (**333**) could be explained by the CONFLEX calculations of the molecule. The results showed a negative atropisomeric chirality (left handed twist) in the 7b∼7c axis, because of repulsion from steric hindrance between the C-8 amino group and the C-7 carbonyl group. Based on these spectroscopic analyses, and the structural similarity to (+)-indocarbazostatin (**333**), the structure **334** was assigned to (−)-indocarbazostatin B (317) (Scheme 2.85).

The UV and IR spectra of (+)-indocarbazostatin C (**335**) were very similar to those of (+)-indocarbazostatin (**333**), indicating the presence of a similar indolo[2,3-*a*]pyrrolo[3,4-*c*]carbazole-5,7(6*H*)-dione framework. The ^{1}H- and ^{13}C-NMR spectra were also very similar to those of (+)-indocarbazostatin (**333**), except for the methyl ester function at δ 3.05 in place of an ethyl ester. Further, ^{1}H- and ^{13}C-NMR analyses including NOE experiments established that (+)-indocarbazostatin C (**335**) is the C-3′ methyl ester analog of (+)-indocarbazostatin (**333**). Analysis of the NMR and CD spectral data of the (+)-indocarbazostatin C (**335**) revealed the same absolute configuration as for (+)-indocarbazostatin (**333**). Based on these spectral data, and the structural similarity to (+)-indocarbazostatin (**333**), the structure **335** was assigned to (+)-indocarbazostatin C (318) (Scheme 2.85).

The UV and IR spectra of (−)-indocarbazostatin D (**336**) were very similar to those of (−)-indocarbazostatin B (**334**), indicating the presence of a similar

indolo[2,3-*a*]carbazole framework. The ^{1}H- and ^{13}C-NMR spectra were also very similar to those of (−)-indocarbazostatin B (**334**), except for the presence of a C-3′ methyl ester function at δ 3.13 in place of an ethyl ester. The presence of a methyl ester function at C-3′ was established from the differential NOE experiments and the C–H long-range coupling pattern of (−)-indocarbazostatin D (**336**). The comparable UV and CD spectra of (−)-indocarbazostatin B (**334**) and (−)-indocarbazostatin D (**336**) showed the presence of similar absolute configurations in these alkaloids. Further, similar to (−)-indocarbazostatin B (**334**), the unusual CD spectrum was explained by the negative atropisomeric chirality in the 7b∼7c axis. Based on these spectral data, and the structural similarity to (−)-indocarbazostatin B (**334**), the structure **336** was assigned to (−)-indocarbazostatin D (318) (Scheme 2.85).

Independently, in 1985, researchers at Bristol-Myers reported the isolation of rebeccamycin (**337**) (269,319,320) and 1-dechlororebeccamycin (**338**) (321) from the fermentation of *Saccharothrix aerocolonigenes* (formerly *Nocardia aerocoligenes*), strain C38383-RK-2 (ATCC 39243). Recently, the genus name for strain ATCC 39243 was changed from *Saccharothrix* to *Lechevalieria* (322). In nature, rebeccamycin (**337**) $[\alpha]_D^{20}$ + 143.0 (*c* 1.02, THF) and 1-dechlororebeccamycin (**338**) $[\alpha]_D^{20}$ + 128.1 (*c* 1.01, THF) were isolated in their optically active forms (323). Rebeccamycin has shown a broad spectrum of *in vivo* activity in tumor-bearing murine models such as P-388 leukemia, L1210 leukemia, and B16 melanoma. It inhibits the growth of human lung adenocarcinoma cells *in vitro* and produces single-strand breaks in the DNA of these cells (269,324). 1-Dechlororebeccamycin (**338**) inhibits Gram-positive and Gram-negative bacteria, as well as mammalian neoplasms, such as the murine leukemia P-388 (321) (Scheme 2.86).

The UV spectrum [λ_{max} 238, 256 (sh), 293 (sh), 314, 362 (sh), and 390 (sh) nm] of rebeccamycin (**337**) indicated the presence of an indolo[2,3-*a*]pyrrolo[3,4-*c*]carbazole-5,7(6*H*)-dione framework. This was also discernible from its IR spectrum. The ^{1}H-NMR spectrum indicated the presence of an amide NH at δ 11.37 and an indole NH at δ 10.30, in addition to signals for aromatic protons and a sugar moiety. Unlike (+)-staurosporine (**295**) (see Scheme 2.74), where the lactam function deshielded only the *ortho* C-4 proton, the C-4 and C-8 aromatic protons in rebeccamycin are both deshielded due to the anisotropic deshielding effect of the phthalimide function.

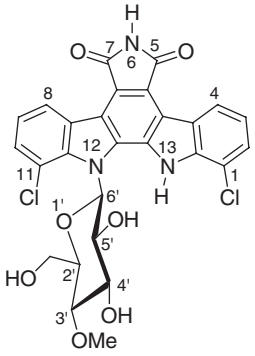

337 Rebeccamycin

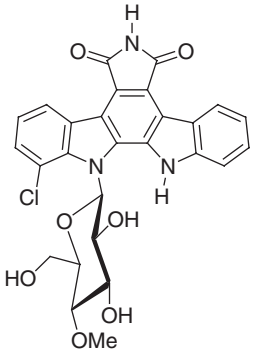

338 1-Dechlororebeccamycin

Scheme 2.86

In consideration of the ^{1}H-NMR signals of the glycosidic and aglycon signals, a 4-*O*-methylglycosidic linkage with the aglycon was indicated. From the chemical shifts of the C-6′ proton of rebeccamycin and its tetraacetate (obtained from rebeccamycin and acetic anhydride/pyridine) the sugar residue was either a *C*- or *N*-glycoside attached to the aglycon. Finally, the structure was deduced from X-ray crystallographic analysis (319) and its absolute configuration from the total synthesis (325). Based on these spectral data and X-ray analysis, the structure **337** was assigned to rebeccamycin (Scheme 2.86).

Comparison of the HREI-MS of 1-dechlororebeccamycin (**338**) with that of rebeccamycin (**337**), indicated the presence of one hydrogen atom in place of a chlorine atom. The ^{1}H-NMR spectrum of 1-dechlororebeccamycin (**338**) was similar to that of rebeccamycin (**337**), except for the difference in the aromatic pattern of the aglycon. Thus, in place of a one-proton doublet at δ 7.69 for the C-2 proton, a two-proton multiplet at δ 7.63 was apparent, assignable to the C-1 and C-2 protons. Further, the ^{13}C-NMR spectrum indicated the presence of only one singlet carbon signal at δ 116.4 assignable to C-11 in place of the two singlet carbon signals at δ 116.0 and 116.5 in rebeccamycin, assignable to the C-1 and C-11 carbon atoms, respectively, establishing the absence of the chlorine atom at C-1. Based on these spectral data, and the structural similarity to rebeccamycin, the structure **338** was assigned to 1-dechlororebeccamycin (323) (Scheme 2.86).

In 1986, researchers at Bristol-Myers and Schering Plough reported the isolation of AT2433-A1 (**339**), AT2433-A2 (**340**), AT2433-B1 (**341**), and AT2433-B2 (**342**) from the cultured broth of *Actinomadura melliaura* ATCC 39691 [previously known as *A. melliaura* sp. nov. (SCC 1655)] (326–328). Structurally, these isolates were closely related to rebeccamycin (**337**) (see Scheme 2.86) and were active against Gram-positive bacteria, such as *Micrococcus luteus* (ATCC 9341), *Bacillus subtilis* (ATCC 6633), *Staphylococcus aureus* (A 9537), *Streptococcus faecalis* (A 20688), and *Streptococcus faecium* (ATCC 9790). Further, AT2433-B2 (**342**) has shown activity against the Gram-negative bacterium *Escherichia coli* SS 1431. In addition, AT2433-A1 (**339**), and AT2433-B1 (**340**) showed antitumor activity against the transplantable murine P-388 leukemia (326,327).

The UV spectrum [λ_{max} 235, 283, 316, and 395 nm] of AT2433-A1 (**339**) was similar to that of rebeccamycin (**337**) (see Scheme 2.86), indicating the presence of a similar indolo[2,3-*a*]pyrrolo[3,4-*c*]carbazole-5,7(6*H*)-dione framework. This was also discernible from its IR spectrum. The ^{1}H-NMR spectrum of AT2433-A1 (**339**) showed the absence of a phthalimide NH signal at δ 11.37 of rebeccamycin (**337**) (see Scheme 2.86), and the presence of a methyl singlet at δ 3.25, indicating a methyl substitution on this nitrogen. Also, the aromatic region showed an additional aromatic proton at δ 7.88, suggesting that one of the chlorine atoms of rebeccamycin was absent. This was confirmed from its CI-MS and IR spectrum, by the presence of strongly split absorption bands at ν_{max} 759 and 768 cm^{-1} due to the asymmetric substitution by a chlorine atom in the aromatic ring. Further, the crucial information regarding the carbohydrate units, and their mutual relationship, was obtained from the EI-MS spectrum of the more volatile tetraacetate derivative of AT2433-A1 (**339**). Similar to rebeccamycin, the *N*-glycosidic linkage of the 4-*O*-methylglucopyranoside was readily apparent for AT2433-A1 (**339**) by inspection of the ^{1}H- and ^{13}C-NMR data. In the ^{13}C-NMR, the signals for the C-2′ methylene were shifted downfield to 66.0 ppm, indicating the position of further substitution. In addition, the triplet for the hydroxy

proton of the C-6′ methylene hydroxy was absent in AT2433-A1, showing the linkage of the amino sugar at this position. The structure, methyl 2,4-dideoxy-4-*N*-methylaminopentapyranoside, of the amino sugar was elucidated by additional MS, NMR, and CD studies of the methanolytic degradation product of AT2433-A1. The high temperature ^{1}H-NMR spectrum of 3,4-di-*p*-bromobenzoate, obtained from the degradation product of AT2433-A1, showed the α-configuration at C-6″ and an equatorial substitution of the pyranose ring at C-3″ and C-4″. Further, the CD spectrum was negative, indicating the chirality of the 3,4-di-*p*-bromobenzoate as α-d-*threo*. In addition, the CD spectra of AT2433-A1 (**339**) and rebeccamycin were superimposable, indicating an identical chirality for the two alkaloids thereby establishing both the relative and absolute structure of AT2433-A1 as **339**. Based on these spectroscopic analyses, and the close structural similarity to rebeccamycin, the structure **339** was assigned to AT2433-A1 (328) (Scheme 2.87).

The UV spectrum [λ_{max} 234, 286, 314, and 394 nm] of AT2433-A2 (**340**) was similar to that of AT2433-A1 (**339**) indicating the presence of a similar indolo[2,3-*a*]pyrrolo[3,4-*c*]carbazole-5,7(6*H*)-dione framework. The ^{1}H-NMR spectrum of AT2433-A2 (**340**) was also similar to that of AT2433-A1 (**339**), except for the absence of a methyl group at δ 2.22, indicating AT2433-A2 as the 3″-*N*-demethyl derivative of AT2433-A1. The absence of a CH_2 group was also supported by its field desorption (FD)-MS. Further, the CD spectrum was identical to that of AT2433-A1, indicating the similar relative and absolute structure of AT2433-A2. Based on these spectral data, and the close structural similarity to AT2433-A1, the structure **340** was assigned to AT2433-A2 (328) (Scheme 2.87).

The UV spectrum [λ_{max} 234, 284, 316, and 400 nm] of AT2433-B1 (**341**) was very similar to that of AT2433-A1 (**339**), indicating the presence of a similar indolo[2,3-*a*]pyrrolo[3,4-*c*]carbazole-5,7(6*H*)-dione framework. The ^{1}H-NMR spectrum of AT2433-B1 (**341**) was also very similar to that of AT2433-A1 (**339**), except for the

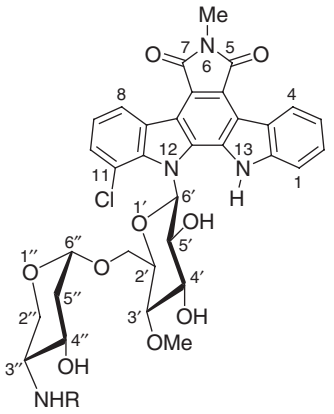

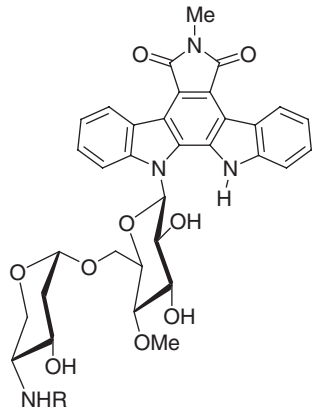

339 AT2433-A1
R = Me

340 AT2433-A2
R = H

341 AT2433-B1
R = Me

342 AT2433-B2
R = H

Scheme 2.87

presence of a proton at δ 8.14, indicating the absence of a chlorine atom at C-11. The presence of this additional hydrogen atom in place of a chlorine atom was also supported from its FD-MS. Further, the CD spectrum was identical to that of AT2433-A1, indicating a similar relative and absolute structure of AT2433-B1. Based on these spectral data, and the close structural similarity to AT2433-A1, the structure **341** was assigned for AT2433-B1 (328) (Scheme 2.87).

The UV spectrum [λ_{max} 233, 282, 315, and 400 nm] of AT2433-B2 (**342**) was very similar to that of AT2433-B1 (**341**), indicating the presence of a similar indolo[2,3-*a*]pyrrolo[3,4-*c*]carbazole-5,7(6*H*)-dione framework. The ^{1}H-NMR spectrum of AT2433-B2 (**342**) was also very similar to that of AT2433-B1 (**341**), except for the absence of a methyl group at δ 2.19, indicating AT2433-B2 as the 3″-*N*-demethyl derivative of AT2433-B1. The absence of a CH_2 group was also supported from its FD-MS. Further, the CD spectrum was identical to that of AT2433-B1, indicating a similar relative and absolute structure of AT2433-B2. Based on these spectral data, and the close structural similarity to AT2433-B1, the structure **342** was assigned to AT2433-B2 (328) (Scheme 2.87).

In 1991, Bonjouklian *et al*. reported the isolation of 15 different tjipanazoles from an extract of the blue-green alga *Tolypothrix tjipanasensis* (strain DB-1-1). Among these 15 different tjipanazoles only tjipanazole J (**343**) has the indolo[2,3-*a*]pyrrolo[3,4-*c*]carbazole framework analogous to 7-hydroxy-TAN-1030A (**324**), UCN-01 (**325a**), and UCN-02 (**325b**) (see Scheme 2.83), while the others have a simple indolo[2,3-*a*]carbazole framework (329).

The UV spectrum [λ_{max} 238, 259, 303, 339, 338, and 369 nm] of tjipanazole J (**343**) was similar to that of UCN-01 (**325a**) (see Scheme 2.83), indicating the presence of a similar indolo[2,3-*a*]pyrrolo[3,4-*c*]carbazole framework. Comparison of the ^{1}H-NMR spectrum of tjipanazole J (**343**) with UCN-01 (**325a**), showed the absence of a sugar moiety, along with the disubstituted aglycon. Thus, in the aromatic region, deshielded, two-proton doublets with *meta*-coupling (J=2.4 Hz) at δ 8.34 and 9.17 together with two sets of mutually *ortho*-coupled (J=8.3 Hz) protons at δ 7.44, 7.47, 7.76, and 7.79, indicating the presence of two chlorine atoms *ortho* to the deshielded protons were observed. The locations (C-3 and C-9) of these chlorine atoms were established by an additional *meta*-coupling (J=2.4 Hz) for the protons at δ 7.44 and 7.47. The presence of two chlorine atoms was evident from the FD-MS. Based on these spectral data and the structural similarity to UCN-01 (**325a**), the structure **343** was assigned to tjipanazole J. This structure was further supported by the ^{13}C-NMR spectrum (329) (Scheme 2.88).

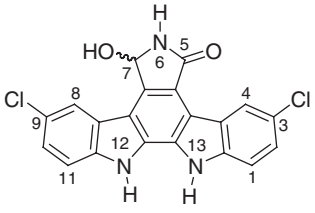

343 Tjipanazole J

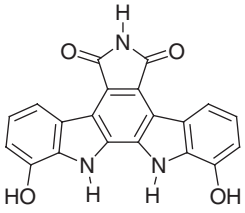

344 BE-13793C

Scheme 2.88

In 1991, Kojiri *et al*. reported the isolation of BE-13793C (**344**), an alkaloid isomeric with the arcyriaflavins C (**347**) and D (**348**) (see Scheme 2.89), from the culture broth of *Streptoverticillium mobaraense* strain BA 13793 collected in Seto, Aichi Perfecture, Japan. BE-13793C (**344**) showed strong inhibitory activity against topoisomerases I and II and inhibited the growth of doxorubicin-resistant or vincristine-resistant P-388 murine leukemia cell lines, as well as their parent P-388 cell line (330).

Comparison of the ^{1}H- and ^{13}C-NMR spectra with those of rebeccamycin (**337**) (see Scheme 2.86), and LSPD experiments on BE-13793C (**344**), indicated the absence of a sugar moiety and the presence of hydroxy groups in place of chlorine atoms in the aglycon. The presence of hydroxy functions was further established by the transformation of this isolate into the corresponding diacetyl derivative, whose ^{1}H-NMR spectrum showed the presence of a six-proton singlet at δ 2.52 in place of a two-proton hydroxy signal at δ 10.20. The UV spectrum [λ_{max} 236, 255 (sh), 283, 311, and 395 (sh) nm] of this diacetyl derivative was very similar to that of rebeccamycin (**337**), indicating the presence of a similar indolo[2,3-*a*]pyrrolo[3,4-*c*]carbazole-5,7(6*H*)-dione framework. Further, the integration of the ^{1}H-NMR spectrum and the number of carbon atoms in the ^{13}C-NMR spectrum were half those observed in the HRFAB-MS, indicating the symmetrical nature of BE-13793C. Based on these spectral data and the structural similarity to rebeccamycin (**337**), the structure **344** was assigned to BE-13793C (330) (Scheme 2.88).

In 1980, Steglich *et al*. reported the isolation of arcyriaflavins B (**346**) and C (**347**) from the fruiting bodies of the slime mold *Arcyria denudata* (Myxomycetes) (254,331,332). Two years later, the same authors reported the isolation of the same natural products from a different slime mold, *Metatrichia vesparium* (Myxomycetes) (333). In the following years, arcyriaflavin A (**345**) was isolated from a different *Arcyria* species, *Arcyria nutans* (252,254), and arcyriaflavin D (**348**) was isolated from a different slime mold, *Dictydiaethalium plumbeum* (254). Except for arcyriaflavin D, which has a 2,9-dihydroxylation pattern, the other arcyriaflavin derivatives were classified according to the number of hydroxy groups present in the 2- and 10-positions. The arcyriaflavins exhibit moderate antibiotic and antifungal activities (254). In 1994, McConnell *et al*. reported the isolation of arcyriaflavin A (**345**) from a different natural source, the marine ascidian *Eudistoma* sp., collected off the coast of West Africa (275). Recently, Ishibasi *et al*. isolated arcyriaflavin C (**347**) from a different species of *Arcyria*, *Arcyria ferruginea*. Further, arcyriaflavin C (**347**) was isolated, along with arcyriaflavin B (**346**), from the fruiting bodies of the slime mold, *Tubifera casparyi*. Arcyriaflavin C exhibited nanomolar range cell-cycle inhibition effects at the G1 and G2/M stages (334).

The UV spectrum [λ_{max} 235, 257, 272, 281, 300 (sh), 314, and 402 nm] of arcyriaflavin A (**345**) was similar to that of Bmy-41950 (RK-1409, 7-oxostaurosporine) (**322**), indicating the presence of an indolo[2,3-*a*]pyrrolo[3,4-*c*]carbazole-5,7(6*H*)-dione framework (252). The ^{1}H-NMR spectrum of arcyriaflavin A (**345**) was similar to that of Bmy-41950 (RK-1409, 7-oxostaurosporine) (**322**), except for the absence of a sugar moiety, and the presence of two NH protons at δ 10.01 and 11.72. This was also supported from its HRFAB-MS. Based on these data, and the structural similarity to Bmy-41950 (RK-1409, 7-oxostaurosporine) (**322**), the structure **345** was assigned to arcyriaflavin A (275). This structure was unequivocally established from spectrometric comparison with synthetic arcyriaflavin A (335,336) (Scheme 2.89).

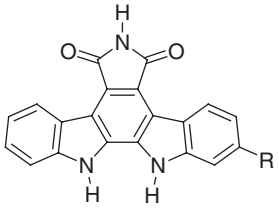

345 Arcyriaflavin A
R = H

346 Arcyriaflavin B
R = OH

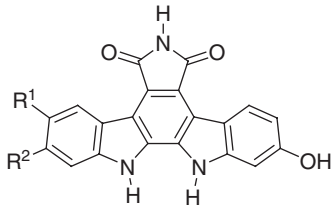

347 Arcyriaflavin C
R^1 = H; R^2 = OH

348 Arcyriaflavin D
R^1 = OH; R^2 = H

Scheme 2.89

The UV spectrum (λ_{max} 229, 271, 280, 323, and 414 nm) of arcyriaflavin B (**346**) was similar to that of arcyriaflavin A (**345**), indicating the presence of a similar indolo[2,3-*a*]carbazole framework. The ^{1}H-NMR spectrum of arcyriaflavin B (**346**) was also similar to that of arcyriaflavin A (**345**), except for the differences in the splitting pattern of one of the aromatic rings. Thus, the ^{1}H-NMR spectrum showed the presence of two, deshielded, aromatic protons at δ 8.96 and 9.15 as doublets and a broad doublet assignable to the C-4 and C-8 protons, respectively, in place of a two-proton signal at δ 8.99. Further, in place of three, one-proton signals at δ 7.80, 7.55, and 7.35 in arcyriaflavin A (**345**), arcyriaflavin B (**346**) showed the presence of a three-proton multiplet at δ 7.24–7.80 assignable to the C-9, C-10, and C-11 protons, and mutually *meta*-coupled (J=2.1 Hz) signals at δ 7.16 and 6.27 assignable to the C-1 and C-3 protons, respectively. In addition, the C-3 proton at δ 6.27 showed a further *ortho*-coupling (J=8.6 Hz) with a deshielded C-4 proton at δ 8.96, indicating the location of the hydroxy group at C-2 position. Furthermore, the position of the hydroxy group at the C-2 carbon was supported by the presence of a singlet carbon signal at δ 157.5 in the ^{13}C-NMR spectrum. Based on these spectral data, and the structural similarity to arcyriaflavin A (**345**), the structure **346** was assigned to arcyriaflavin B (331) (Scheme 2.89).

The UV spectrum [λ_{max} 229, 255 (sh), 270, 280, 318 (sh), 330.5 (sh), and 422 nm] of arcyriaflavin C (**347**) was similar to that of arcyriaflavin A (**345**), indicating the presence of a similar indolo[2,3-*a*]carbazole framework. The ^{1}H-NMR spectrum showed the presence of a broad two-proton singlet at δ 11.92, assignable to two NH protons, and a further broad one-proton singlet at δ 9.56, which was assignable to the phthalimide NH proton. Additionally, the aromatic region showed the presence of three sets of two-proton signals, in which one set appeared in a deshielded region as an *ortho*-coupled (J=8.4 Hz) doublet at δ 8.93, a second set appeared as a doublet with *meta*-coupling (J=2.2 Hz) at δ 7.13, and a third set appeared in a shielded environment at δ 6.89 as a double doublet with *ortho*- and *meta*-coupling (J=8.4, 2.2 Hz), indicating the location of two hydroxy groups at the C-2 and C-10 positions. Based on these spectral data, the structure **347** was assigned for arcyriaflavin C. This structure was unequivocally established by spectrometric comparison with synthetic arcyriaflavin C obtained by the acid-mediated cyclization of arcyriarubin C (**351**) (see Scheme 2.90) (331) (Scheme 2.89).

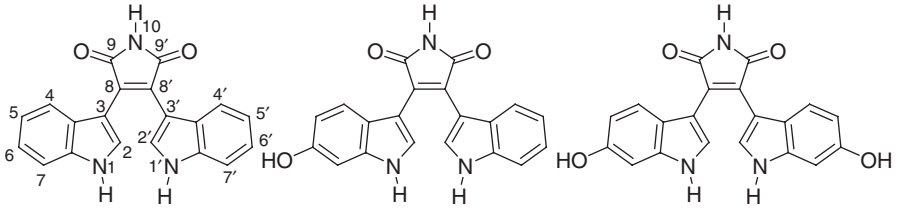

349 Arcyriarubin A **350** Arcyriarubin B **351** Arcyriarubin C

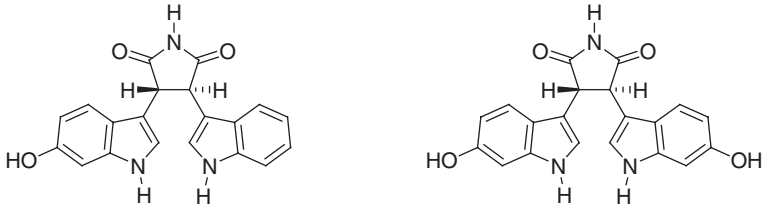

352 Dihydroarcyriarubin B **353** Dihydroarcyriarubin C

Scheme 2.90

The UV spectrum (λ_{max} 229, 327, and 418 nm) of arcyriaflavin D (**348**) was similar to that of arcyriaflavin C (**347**), indicating the presence of a similar indolo[2,3-*a*]carbazole framework. The ^{1}H-NMR spectrum of arcyriaflavin D (**348**) was similar to that of arcyriaflavin C (**347**), except for the differences in the splitting pattern of one of the aromatic rings. Thus, the aromatic region of the ^{1}H-NMR spectrum indicated the presence of a deshielded, *meta*-coupled (J=2.2 Hz) proton at δ 8.37, together with two, mutually *ortho*-coupled (J=8.5 Hz) protons at δ 7.00 and 7.55. Further, a high-field proton signal (δ 7.00) showed a *meta*-coupling (J=2.2 Hz) with the low-field proton signal (δ 8.37), establishing the location of a second hydroxy group at C-9. Based on these spectral data, and the structural similarity to arcyriaflavin C (**347**), the structure **348** was assigned to arcyriaflavin D (337) (Scheme 2.89).

2 2,3-Bis(indol-3-yl)maleimide Alkaloids

In the early 1980s, Steglich *et al.* reported the isolation of a series of biogenetically closely related bisindolylmaleimides, arcyriarubins B (**350**) and C (**351**) (254,331,332), dihydroarcyriarubin B (**352**) (252,254), (Scheme 2.90), arcyroxepin A (**354**) (254,331,332), and arcyriaverdin C (**355**) (254,255) (see Scheme 2.91), along with the indolo[2,3-*a*]pyrrolo[3,4-*c*]carbazole alkaloids, arcyriaflavins B (**346**) and C (**347**) (331) (see Scheme 2.89), from the red sporangia of the slime mold *A. denudata*. Arcyriarubin A (**349**) was present in this organism in only small amounts (252,254). Similar to the arcyriaflavins, the arcyriarubins also exhibit moderate antibiotic and antifungal activities (254).

In 2003, Ishibasi *et al.* reported the isolation of a further, biogenetically closely related, bisindolylmaleimide, dihydroarcyriarubin C (**353**), along with the previously known, arcyriarubin C (**351**) (Scheme 2.90) and arcyriaflavin C (**347**) (see Scheme 2.89), from the fruit bodies of a different *Arcyria* species, *A. ferrugine*. The CD spectral data of dihydroarcyriarubin C (**353**) indicated it to be racemic. However, the

^{1}H-NMR spectral data showed the *trans*-relative stereochemistry for the protons of the dihydromaleimide ring (334).

The UV spectrum [λ_{max} 248 (sh), 276, 284 (sh), 371, and 465 nm] of arcyriarubin A (**349**) indicated the presence of a bisindolylmaleimide framework (252). This was also discernible from its IR spectrum with the presence of carbonyl bands at ν_{max} 1710 and 1750 cm^{-1} for the maleimide function. The ^{1}H-NMR spectrum of arcyriarubin A (**349**) showed only half of the full set of signals, indicating a symmetrical structure for this alkaloid. The splitting and position of the aromatic signals, and the two indolic NH protons at δ 11.59 in the ^{1}H-NMR spectrum, indicated that the maleimide is substituted by two indol-3-yl groups. Based on these spectral data, the structure **349** was assigned to arcyriarubin A (338). This structure was unequivocally established by spectrometric comparison with synthetic arcyriarubin A, obtained by the reaction of indolylmagnesium bromide with 2,3-dibromo-*N*-methylmaleimide as the crucial step (252,338) (Scheme 2.90).

The UV spectrum [λ_{max} 281, 392 (sh), and 465 nm] of arcyriarubin B (**350**) was similar to that of arcyriarubin A (**349**), indicating the presence of a similar bisindolylmaleimide framework. This was also discernible from its IR spectrum. The ^{1}H-NMR spectrum of arcyriarubin B (**350**) was also similar to that of arcyriarubin A (**349**), except for the differences in the splitting pattern of one of the aromatic rings of the indole nucleus. Thus, the ^{1}H-NMR spectrum showed the presence of two mutually *ortho*-coupled (J=8.7 Hz) protons at δ 6.72 and 6.24 assignable to the C-4 and C-5 protons, respectively. The C-5 proton signal at δ 6.24 showed a *meta*-coupling (J=2.1 Hz) with the C-7 proton signal at δ 6.85, indicating the location of the OH function at C-6. The location of this hydroxy group at C-6 was further supported by the shift of the C-7 carbon signal at δ 97.7 in the ^{13}C-NMR spectrum. Further, in the ^{1}H-NMR spectrum, two indolic NH protons appeared at different chemical shift values (δ 10.78 and 10.52) indicating the unsymmetrical nature of the alkaloid, in which the maleimide unit is substituted by two, different indol-3-yl groups. Based on these spectral data, and the structural similarity to arcyriarubin A (**349**), the structure **350** was assigned to arcyriarubin B (252,331). This structure was unequivocally established by spectrometric comparison with synthetic arcyriarubin B (338) (Scheme 2.90).

The UV spectrum (λ_{max} 283 and 474 nm) of arcyriarubin C (**351**) was similar to that of arcyriarubin B (**350**), indicating the presence of a similar bisindolylmaleimide framework. This was also discernible from its IR spectrum. The ^{1}H-NMR spectrum of arcyriarubin C (**351**) showed only half of the full set of signals, indicating the symmetrical structure of this alkaloid. The position and splitting pattern in the aromatic region of the ^{1}H-NMR spectrum, and the two indolic NH protons at δ 10.42, indicated that the maleimide unit is substituted by two (6-hydroxy)indol-3-yl groups. Further, the position of the C-7 and C-7′ signals at δ 97.7 in the ^{13}C-NMR spectrum, indicated the location of the hydroxy groups at C-6 and C-6′ of the indole nucleus. Based on these spectral data, and the structural similarity to arcyriarubin B (**350**), the structure **351** was assigned to arcyriarubin C (331).

The IR spectrum of dihydroarcyriarubin B (**352**) showed the presence of carbonyl bands at ν_{max} 1710 and 1770 cm^{-1}, indicating the presence of a dihydromaleimide function. The ^{1}H-NMR spectrum showed the presence of an AB quartet at δ 4.48 and 4.53 assignable to the methylene protons of the dihydromaleimide ring.

The structure, and the *trans*-relative stereochemistry, of dihydroarcyriarubin B (**352**) was confirmed by comparison of the product obtained from arcyriarubin B (**350**) by palladium-catalyzed hydrogen transfer from cyclohexene in boiling xylene. Under these conditions, only the thermodynamically more stable *trans*-diastereomer was formed. Based on these data, and the spectroscopic comparison with the hydrogenation product of arcyriarubin B (**350**), the structure **352** was assigned to dihydroarcyriarubin B (252) (Scheme 2.90).

The ^{1}H- and ^{13}C-NMR spectra of dihydroarcyriarubin C (**353**) were very similar to those of arcyriarubin C (**351**), except for the presence of one sp^{3} methine proton at δ 4.44, which was assignable to the C-8 proton. The HMBC spectrum showed a cross peak from H-8 to C-8 (δ_C 48.2), and this HMBC correlation may be assigned to H-8 to C-8′ (or H-8′ to C-8), indicating the symmetrical structure of this alkaloid. This structure was further supported by its ^{1}H–^{1}H COSY and HMQC spectra (334). Comparison of the ^{1}H-NMR spectral data of synthetic *cis*- and *trans*-dihydroarcyriarubin A (339) indicated the *trans*-relative stereochemistry for the natural dihydroarcyriarubin C (**353**). Based on these spectral data, and comparison with arcyriarubin C (**351**), as well as with synthetic *trans*-dihydroarcyriarubin A, the structure **353** was assigned to dihydroarcyriarubin C (334,339) (Scheme 2.90).

The UV spectrum [λ_{max} 226 (sh), 273, 283 (sh), 362, and 471 nm] of arcyroxepin A (**354**) indicated the presence of a bisindolylmaleimide framework. This was also discernible from its IR spectrum with the presence of carbonyl bands at ν_{max} 1710 and 1760 cm^{-1} for the maleimide function. The ^{1}H-NMR spectrum of arcyroxepin A (**354**) showed three, mutually *ortho*-coupled (J=8.0 Hz) protons at δ 7.18, 7.32, and 7.38 in the aromatic region, along with a fourth proton whose shape and position depended very strongly on the measuring conditions. The indole NH protons appeared as singlet at δ 9.82, and no signal was observed for the C-2 and C-2′ protons, indicating the presence of a third oxygen between these two carbons. Based on these spectral data, the structure **354** was assigned to arcyroxepin A (331) (Scheme 2.91).

The UV spectrum [λ_{max} 256 (sh), 336, 433, and 634 nm] of arcyriaverdin C (**355**) indicated the presence of a bisindolylmaleimide framework with an extended conjugation (252). The structure of arcyriaverdin C (**355**) was confirmed by chemical correlation of arcyriaverdin C (**355**) with arcyriarubin C (**351**) (see Scheme 2.90) by oxidation of the latter with lead tetraacetate in chloroform. Based on these data, and spectroscopic comparison with the oxidation product of arcyriarubin C (**351**), the structure **355** was assigned to arcyriaverdin C (252) (Scheme 2.91).

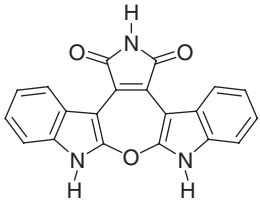

354 Arcyroxepin A

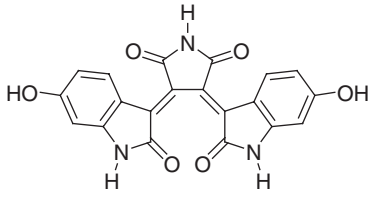

355 Arcyriaverdin C

Scheme 2.91

3 Simple Indolo[2,3-*a*]carbazole Alkaloids

In 1990, Moore *et al.* reported the isolation of 5-cyano-6-methoxy-11-methylindolo[2,3-*a*]carbazole (**357**), along with a minor component, 6-cyano-5-methoxyindolo[2,3-*a*]carbazole (**358**), from the blue-green alga *Nostoc sphaericum* EX-5-1 (340). These were the first, naturally occurring, indolo[2,3-*a*]carbazole alkaloids with a simple indolo[2,3-*a*]carbazole (**356**) framework (Scheme 2.92). These alkaloids are moderately active against herpes simplex virus type 2 and are weakly cytotoxic against murine and human cancer cell lines (340).

The UV spectrum (λ_{max} 234, 252, 290, 338, 354, and 372 nm) of 5-cyano-6-methoxy-11-methylindolo[2,3-*a*]carbazole (**357**) indicated the presence of an indolo[2,3-*a*]carbazole framework. The IR spectrum indicated the presence of a sharp band at ν_{max} 2200 cm^{-1} for a nitrile group. The ^1H- and ^{13}C-NMR spectral data indicated the presence of an aromatic methoxy group (δ_H 4.21 and δ_C 62.0) and an *N*-methyl group (δ_H 4.34 and δ_C 31.8). Further, a ^1H–^1H COSY experiment suggested the presence of an indolic NH and two, independent, *ortho*-disubstituted benzenoid rings. The HMQC and HMBC spectral data, including NOE experiments, established the presence of an indolo[2,3-*a*]carbazole system. The relative positions of the methoxy and *N*-methyl groups were established at C-6 and *N*-11, respectively, by the detection of a NOE between the signals for the OMe protons and H-4 and the correlation of H-4 and the protons of the *N*-methyl group with C-11a in the HMBC experiment. The position of the cyano group at C-6 was established by one-dimensional ^{13}C–^{13}C decoupling experiments. The downfield chemical shift for the C-5 carbon showed the presence of the cyano group at this position, and the location of the methoxy group at the adjacent carbon, C-6. Based on these spectral data, the structure **357** was assigned to 5-cyano-6-methoxy-11-methylindolo[2,3-*a*]carbazole (340) (Scheme 2.93).

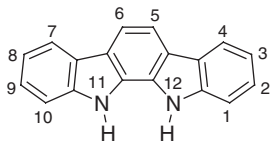

356 Indolo[2,3-*a*]carbazole

Scheme 2.92

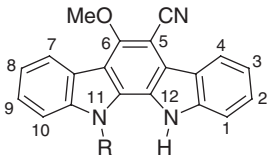

357 5-Cyano-6-methoxy-11-methylindolo[2,3-*a*]carbazole
R = Me

358 5-Cyano-6-methoxyindolo[2,3-*a*]carbazole
R = H

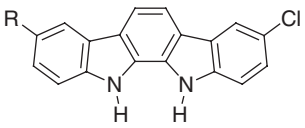

359 Tjipanazole D
R = Cl

360 Tjipanazole I
R = H

Scheme 2.93

The ^{1}H- and ^{13}C-NMR spectra of 5-cyano-6-methoxyindolo[2,3-*a*]carbazole (**358**) were very similar to those of 5-cyano-6-methoxy-11-methylindolo[2,3-*a*]carbazole (**357**), except for the absence of the signals for the *N*-methyl group at δ_H 4.34 and δ_C 31.8, and the presence of an additional NH proton signal at δ_H 11.41. Based on these spectral data, and the structural similarity to 5-cyano-6-methoxy-11-methylindolo[2,3-*a*]carbazole (**357**), the structure **358** was assigned to 5-cyano-6-methoxy-11-methylindolo[2,3-*a*]carbazole (340) (Scheme 2.93).

In 1991, Bonjouklian *et al.* reported, from a bioactivity-directed isolation of the blue-green alga *T. tjipanasensis* (strain DB-1-1), an extraordinary array of indolo[2,3-*a*]carbazoles, the tjipanazoles (**343** and **359-372**). Of these, only tjipanazole J (**343**) (see Scheme 2.88) has the characteristic pyrrolo[3,4-*c*]ring. Whereas tjipanazoles D (**359**) and I (**360**) are simple chlorinated indolo[2,3-*a*]carbazoles, tjipanazoles G1 (**363**) and G2 (**366**) are non-chlorinated indolo[2,3-*a*]carbazole *N*-glycosides, whereas tjipanazoles A1 (**361**), A2 (**364**), B (**369**), C1 (**362**), C2 (**367**), C3 (**365**), C4 (**368**), E (**370**), F1 (**371**), and F2 (**372**) are chlorinated indolo[2,3-*a*]carbazole *N*-glycosides (329) (Schemes 2.93–2.97).

The UV spectrum (λ_{max} 259, 291, 331, and 366 nm) of tjipanazole D (**359**) indicated the presence of an indolo[2,3-*a*]carbazole framework. The ^{1}H-NMR spectrum

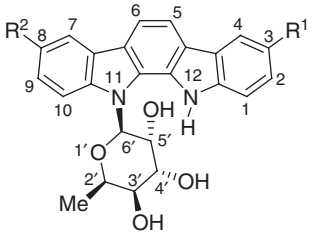

361 Tjipanazole A1
R^1,R^2 = Cl

362 Tjipanazole C1
R^1 = Cl; R^2 = H

363 Tjipanazole G1
R^1,R^2 = H

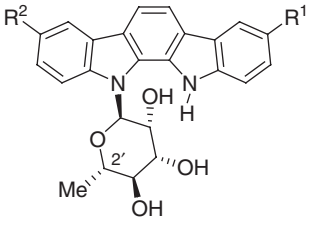

364 Tjipanazole A2
R^1,R^2 = Cl

365 Tjipanazole C3
R^1 = Cl; R^2 = H

366 Tjipanazole G2
R^1,R^2 = H

Scheme 2.94

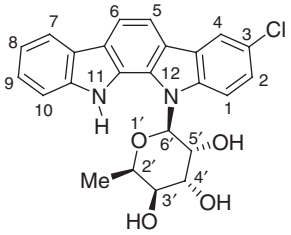

367 Tjipanazole C2

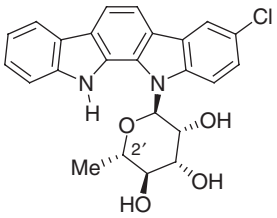

368 Tjipanazole C4

Scheme 2.95

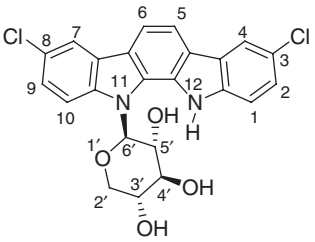

369 Tjipanazole B

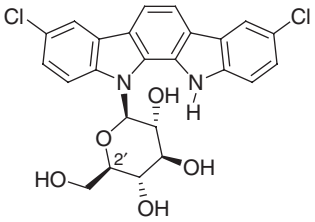

370 Tjipanazole E

Scheme 2.96

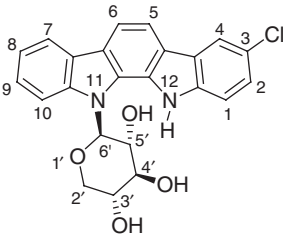

371 Tjipanazole F1

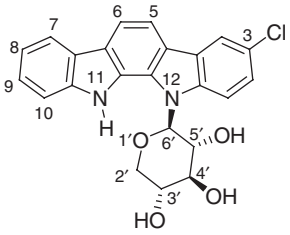

372 Tjipanazole F2

Scheme 2.97

showed the presence of a deshielded, two-proton singlet at δ 8.20, assignable to the C-4 and C-7 protons, indicating the presence of chlorine atoms at the C-3 and C-8 carbons. The positions of the chlorine atoms were additionally supported by the three, two-proton doublet signals at δ 7.35, 7.60, and 8.00, assignable to the C-2, and C-9, C-1, and C-10, and C-5 and C-6 protons, respectively. This was also supported by the HRFAB-MS. Based on these spectral data, the structure **359** was assigned for tjipanazole D. This structure was unequivocally established by spectrometric comparison of synthetic tjipanazole D, obtained by the coupling of two equivalents of 4-chlorophenylhydrazine with 1,2-cyclohexanedione under Fischer–Borsche conditions (329) (Scheme 2.93).

The UV spectrum (λ_{max} 259, 289, 329, and 361 nm) of tjipanazole I (**360**) was very similar to that of tjipanazole D (**359**), indicating the presence of a similar indolo[2,3-*a*]carbazole framework. The ^{1}H-NMR spectrum of tjipanazole I (**360**) was also very similar to that of tjipanazole D (**359**), except for the difference in the splitting pattern of one of the aromatic rings. Thus, the ^{1}H-NMR spectrum indicated the presence of four, mutually coupled signals at δ 7.20, 7.36, 7.59, and 8.15, assignable to the C-8, C-9, C-10, and C-7 protons, respectively, and establishing the absence of substitution on this aromatic ring. Comparison of the HRFAB-MS of tjipanazole I with that of tjipanazole D, indicated the absence of one chlorine atom. Based on these spectral data, and the structural similarity to tjipanazole D (**359**), the structure **360** was assigned to tjipanazole I (329) (Scheme 2.93).

The UV spectrum (λ_{max} 261, 294, 333, 354, and 371 nm) of tjipanazole A1 (**361**) was very similar to that of tjipanazole D (**359**) (see Scheme 2.93), indicating the presence of a similar indolo[2,3-*a*]carbazole framework. Comparison of the ^{1}H-NMR spectral

data of tjipanazole A1 (**361**) with those of tjipanazole D (**359**) (see Scheme 2.93) indicated the presence of similar aromatic peaks to those of tjipanazole D, except for an absent indole nitrogen proton and a new hexopyranose ring where the anomeric carbon was attached to the indole nitrogen. Proton decoupling and NOE experiments indicated that the sugar moiety was a β-6-deoxygulosyl unit which was attached to one of the nitrogens of a 3,8-dichloroindole[2,3-*a*]carbazole (tjipanazole D). The β-configuration at the 6-deoxygulosyl unit was also supported from its CD spectrum. Based on these spectral data, and the structural similarity to tjipanazole D (**359**), the structure **361** was assigned to tjipanazole A1. This structure was unequivocally established by spectrometric comparison of tjipanazole D and 6-deoxy-D-gulose obtained by acidic solvolysis of tjipanazole A1 (329) (Scheme 2.94).

The ^{1}H-NMR spectrum of tjipanazole C1 (**362**) was very similar to that of tjipanazole A1 (**361**), except for the difference in the splitting pattern of one of the aromatic rings. Thus, the ^{1}H-NMR spectrum indicated the presence of four, mutually coupled protons at δ 7.24, 7.42, 7.69, and 8.16 assignable to the C-8, C-9, C-10, and C-7 protons, respectively, indicating no substitution on this aromatic ring. Proton decoupling and NOE experiments indicated that the β-6-deoxygulosyl sugar unit was attached to *N*-11 of a 3-chloroindole[2,3-*a*]carbazole. Based on these spectral data and the structural similarity to tjipanazole A1 (**361**), the structure **362** was assigned to tjipanazole C1.

Comparison of the ^{1}H-NMR spectrum of tjipanazole G1 (**363**) with that of tjipanazole C1 (**362**) indicated the absence of a chlorine atom at C-3 of the aglycon. This was also clear from the ^{1}H-NMR spectrum by the presence of an additional, mutually *ortho*-coupled (J=8.4 Hz), triplet proton signal at δ 7.22, assignable to the C-3 proton. Based on these spectral data and the close structural similarity to tjipanazole C1 (**362**), the structure **363** was assigned to tjipanazole G1 (329) (Scheme 2.94).

The UV spectrum (λ_{max} 261, 294, 333, 354, and 371 nm) of tjipanazole A2 (**364**) was identical to that of tjipanazole A1 (**361**), indicating the presence of a similar indolo[2,3-*a*]carbazole framework. The ^{1}H-NMR spectrum of tjipanazole A2 (**364**) also showed the presence of a similar structure, except for the difference in the configuration of the 2′-methyl group of the sugar moiety, indicating that tjipanazole A2 is a stereoisomer of tjipanazole A1. Comparison of the proton and carbon chemical shifts with the values for K-252d (**328**) (see Scheme 2.84) indicated that the sugar unit is a β-rhamnosyl. This was supported by comparison with the L-rhamnose that was obtained by acid hydrolysis of tjipanazole A2. Based on these spectral data and the structural similarity to tjipanazole A1 (**361**), the structure **364** was assigned to tjipanazole A2 (329) (Scheme 2.94).

Comparison of the ^{1}H-NMR spectrum of tjipanazole C3 (**365**) with that of tjipanazole C1 (**362**) indicated that these two alkaloids are C-2′-epimers. Proton decoupling and NOE experiments indicated that the sugar moiety was a β-rhamnosyl unit which was attached to *N*-11 of 3-chloroindolo[2,3-*a*]carbazole. Based on these spectral data and the structural similarity to tjipanazole C1 (**362**), the structure **365** was assigned to tjipanazole C3 (329) (Scheme 2.94).

Comparison of the ^{1}H-NMR spectrum of tjipanazole G2 (**366**) with that of tjipanazole G1 (**363**) showed the presence of a similar structure, except for the difference in the configuration of the 2′-methyl group of the sugar moiety, showing

that these two alkaloids are C-2′-epimers, with a β-rhamnosyl sugar unit. Thus, in the ^{1}H-NMR spectrum, the C-2′-methyl showed a downfield shift (δ 1.76, d, J=7.2 Hz), indicating the presence of an α-C-2′ methyl group, and the C-2′ hydrogen showed an upfield shift (δ 4.58, q, J=7.2 Hz), indicating a β-C-2′ hydrogen. Based on these spectral data and the structural similarity to tjipanazole G1 (**363**), the structure **366** was assigned to tjipanazole G1 (329) (Scheme 2.94).

The ^{1}H-NMR spectrum of tjipanazole C2 (**367**) was very similar to that of tjipanazole C1 (**362**), except for the attachment of a β-6-deoxygulosyl sugar unit at *N*-12 of a 3-chloroindolo[2,3-*a*]carbazole. The nature of this sugar unit, and its regiochemistry with respect to the chloro substituent, was established with proton decoupling and NOE experiments. Based on these spectral data and the structural similarity to tjipanazole C1 (**362**), the structure **367** was assigned to tjipanazole C2 (329) (Scheme 2.95).

Comparison of the ^{1}H-NMR spectrum of tjipanazole C4 (**368**) with that of tjipanazole C2 (**367**) indicated that these two alkaloids are C-2′-epimers. Proton decoupling and NOE experiments indicated that the sugar moiety was a β-rhamnosyl unit which was attached to *N*-12 of a 3-chloroindolo[2,3-*a*]carbazole. Based on these spectral data and the structural similarity to tjipanazole C2 (**367**), the structure **368** was assigned to tjipanazole C4 (329) (Scheme 2.95).

The UV spectrum (λ_{max} 259, 292, 330, 349, and 366 nm) of tjipanazole B (**369**) was similar to that of tjipanazole A1 (**361**) (see Scheme 2.94), indicating the presence of a similar 3,8-dichloroindolo[2,3-*a*]carbazole framework. Comparison of the ^{1}H- and ^{13}C-NMR spectral data of tjipanazole B (**369**) with those of tjipanazole A1 (**361**) (see Scheme 2.94) indicated the presence of similar aromatic peaks to those of tjipanazole A1, but differed in the nature of the sugar moiety. Proton decoupling experiments suggested that the sugar moiety was a β-xylosyl unit, which was attached to one of the nitrogens of a 3,8-dichloroindole[2,3-*a*]carbazole (tjipanazole D). The β-configuration of the xylosyl unit was also supported by comparison of the optical rotation of the α- and β-methyl-D-xyloside triacetates obtained from xylose. Based on these spectral data and the structural similarity to tjipanazole A1, the structure **369** was assigned to tjipanazole B. This structure was unequivocally established by spectrometric comparison of tjipanazole D and D-xylose obtained by acidic solvolysis of tjipanazole B (329) (Scheme 2.96).

The UV spectrum (λ_{max} 259, 23, 332, 350, and 368 nm) of tjipanazole E (**370**) was very similar to that of tjipanazole B (**369**), indicating the presence of a similar 3,8-dichloroindolo[2,3-*a*]carbazole framework. Comparison of the ^{1}H- and ^{13}C-NMR spectral data of tjipanazole E (**370**) with those of tjipanazole B (**369**) indicated the presence of a similar structure to tjipanazole B, except for the nature of the sugar moiety which was shown to be a β-glucosyl unit, and was attached to one of the nitrogens of a 3,8-dichloroindole[2,3-*a*]carbazole (tjipanazole D). The structure **370** was confirmed by spectrometric comparison of tjipanazole D and D-glucose obtained by acidic hydrolysis of tjipanazole E. The absolute stereochemistry of the sugar was unequivocally established by the synthesis of tjipanazole E by *N*-glycosidation of tjipanazole D using the procedure described by Robins *et al.* (341). Based on these data and the structural similarity to tjipanazole B (**369**), the structure **370** was assigned to tjipanazole E (329) (Scheme 2.96).

The ^{1}H-NMR spectrum of tjipanazole F1 (**371**) was very similar to that of tjipanazole C1 (**362**) (see Scheme 2.94), except for the nature of the sugar unit

attached at *N*-11 of a 3-chloroindolo[2,3-*a*]carbazole. The nature of this sugar unit, which was assigned to be a β-xylosyl unit, and its regiochemistry with respect to the chloro substituents, was established with proton decoupling and NOE experiments. Based on these spectral data and the structural similarity to tjipanazole C1 (**362**), the structure **371** was assigned for tjipanazole F1 (329) (Scheme 2.97).

Comparison of the ^{1}H-NMR spectrum of tjipanazole F2 (**372**) with that of tjipanazole F1 (**371**) indicated that these two are regioisomeric 3-chloroindolo[2,3-*a*]carbazole derivatives. Proton decoupling and NOE experiments, indicated that the β-xylosyl sugar moiety was attached to *N*-12 of a 3-chloroindolo[2,3-*a*]carbazole. Based on these spectral data and the structural similarity to tjipanazole F1 (**371**), the structure **372** was assigned to tjipanazole F2 (329) (Scheme 2.97).

E. Imidazo[4,5-*a*]pyrrolo[3,4-*c*]carbazole Alkaloids

In 1998, Berlinck *et al.* reported on the bioassay-guided fractionation of the crude methanol extract of the Brazilian ascidian *Didemnum granulatum* to afford two novel imidazo[4,5-*a*]pyrrolo[3,4-*c*]carbazole alkaloids, granulatimide (**374**) and isogranulatimide (**375**) (342), along with previously known (343) didemnimide A (**373**). From a biogenetic perspective, it appears that the co-occurring didemnimide A (**373**) represents the precursor for the two pentacyclic alkaloids granulatimide (**374**) and isogranulatimide (**375**). These two alkaloids are the first examples of a new class of G2-specific cell-cycle check point inhibitors, and they were identified through a rational screening program (342). Three years later, from the same natural source, the same authors reported 6-bromogranulatimide (**376**), and the previously known (342) granulatimide (**374**) (344).

The UV spectrum of didemnimide A (**373**) with λ_{max} 430 nm indicates the presence of an indole ring with additional conjugation at the C-3 position through the maleimide ring. This was also discernible from its IR spectrum with the presence of asymmetric and symmetric stretching of the imide carbonyl groups at ν_{max} 1702 and 1755 cm^{-1}, respectively. The mass fragmentation pattern observed in the HREIMS at m/z 207 (M^+-71) for the imide unit, m/z 140 [(M^+-71)-−67] for the imidazole unit, and m/z 91 [(M^+-71)-115] for the indole unit, showed the presence of a novel indole–maleimide–imidazole carbon skeleton. The ^{1}H-NMR spectrum of didemnimide A (**373**) indicated the presence of a 3-substituted indole with four mutually *ortho*-coupled (J=7.8 Hz) protons at δ 7.64, 7.18, 7.27, and 7.55, assignable to the C-4, C-5, C-6, and C-7 protons, respectively, along with a singlet proton signal at δ 8.48 for C-2, and a broad singlet NH proton at δ 12.90. The remaining singlets at δ 8.18 and 8.12 were assignable to the imidazole ring protons. The connectivities of the indole and imidazole rings were established by HMBC experiments. Based on these spectral data, the structure **373** was assigned to didemnimide A. This structure was unequivocally established from its X-ray crystallographic analysis (343) (Scheme 2.98).

The UV spectrum (λ_{max} 210, 231, 280, and 470 nm) of granulatimide (**374**), indicated the presence of a polycyclic aromatic framework. The IR spectrum indicated the presence of NH and amide carbonyl groups at ν_{max} 3246 and 1698 cm^{-1}, respectively. Comparison of the HRFABMS of didemnimide A (**373**) with that of granulatimide (**374**) indicated a difference of two hydrogen atoms. The ^{1}H-NMR

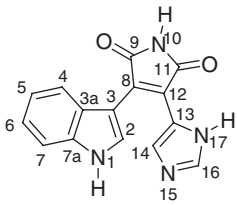

373 Didemnimide A

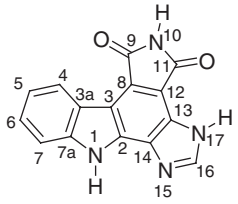

374 Granulatimide

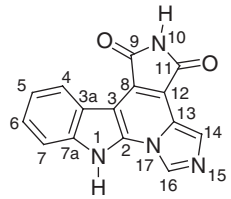

375 Isogranulatimide

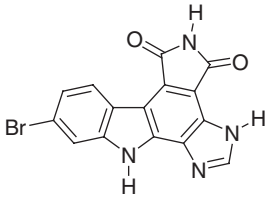

376 6-Bromogranulatimide

Scheme 2.98

data showed that the two alkaloids were closely related, except for the absence of an aromatic proton signal corresponding to C-14 (one of the imidazole ring protons) at δ 7.71 and the indole C-2 proton at δ 8.05 (a singlet in didemnimide A), indicating a bond between the C-2 carbon of the indole fragment and the C-14 carbon of the imidazole fragment. This was also shown by the ^{13}C-NMR singlet carbon signals at δ 135.4 and 133.4, instead of doublet carbon signals at δ 130.7 and 119.6 for the C-2 and C-14 carbons in didemnimide A, respectively. A planar, polycyclic, aromatic structure for granulatimide could be explained by the large chemical shifts observed for the C-4 proton (δ 8.89) relative to the chemical shift observed for the C-4 proton in didemnimide A (δ 7.07) and was attributed to a neighboring group effect of the C-9 maleimide carbonyl in granulatimide. Based on these spectral data, the structure **374** was assigned to granulatimide. In addition to COSY and NOE spectra, this structure was unequivocally established by spectrometric comparison of synthetic granulatimide obtained by the photocyclization of didemnimide A (342) (Scheme 2.98).

The UV spectrum (λ_{max} 210, 231, 280, and 470 nm) of isogranulatimide (**375**) was identical to that of granulatimide (**374**), indicating a similar polycyclic aromatic framework. This was also discernible from its IR spectrum by the presence of an NH and an imide carbonyl band at ν_{max} 3294 and 1678 cm^{-1}, respectively. Comparison of the NMR spectral data of isogranulatimide (**375**) with those of granulatimide (**374**) showed the presence of two imidazole protons at δ 8.10 and 9.12 in place of one imidazole proton (δ 8.50) in granulatimide (**374**). These signals did not show any HMBC/HMQC correlations or NOEs. The NH proton (*N*-17) at δ 13.57, corresponding to granulatimide (**374**) was absent, indicating a bond between this nitrogen of the imidazole fragment and the C-2 carbon of the indole fragment. Based on these spectral data and the structural similarity to granulatimide (**374**), the structure **375** was assigned to isogranulatimide. In addition to the COSY spectrum, this structure was unequivocally established by spectrometric comparison with synthetic isogranulatimide obtained as a minor product by the photolytic cyclization of didemnimide A (342) (Scheme 2.98).

The UV spectrum (λ_{max} 236, 282, 308, and 386 nm) of 6-bromogranulatimide (**376**) was similar to that of granulatimide (**374**), indicating the presence of a similar pentacyclic imidazo[4,5-*a*]pyrrolo[3,4-*c*]carbazole framework. The ^{1}H- and ^{13}C-NMR spectral data of 6-bromogranulatimide (**376**) were also very similar to those of granulatimide (**374**), except for the presence of a bromine atom in place of the C-6 proton. This was also discernible from its HREIMS. Based on these spectral data and the structural similarity to granulatimide (**374**), the structure **376** was assigned to 6-bromogranulatimide. This structure was further supported by the HMQC and HMBC spectra (344) (Scheme 2.98).

F. Quinolino[4,3-*b*]carbazole-1,4-quinone Alkaloids

In 1999, Rickards *et al*. reported the isolation of calothrixins A (**377**) and B (**378**) from photoautrophic cultures of *Calothrix* cyanobacteria (345). These two, novel, pentacyclic carbazole alkaloids contain a quinolino[4,3-*b*]carbazole-1,4-quinone framework. Calothrixins A and B inhibit the growth of a chloroquin-resistant strain of the malaria parasite *P. falciparum* and human HeLa cancer cells (345).

The UV spectrum (λ_{max} 292, 362, and 413 nm) of calothrixin A (**377**) was unaffected by acid, but shifted reversibly to longer wavelengths on the addition of aqueous sodium hydroxide, indicating the presence of an ionizable acid group on the pentacyclic quinolino[4,3-*b*]carbazole-1,4-quinone chromophore. The ^{1}H-NMR spectrum showed the presence of an isolated proton singlet at δ 8.88, and two-spin systems, each containing four adjacent aromatic protons, indicating the presence of two, *ortho*-disubstituted benzenoid rings, each with only one carbon substituent. The second substituent on each ring was nitrogen, as indicated by the deshielding (δ 138.4 and 143.1) of the *N*-substituted ring carbons. The ^{1}H and ^{13}C shifts of these spin systems closely resembled those of the indole rings of 5-cyano-6-methoxyindolo[2,3-*a*]carbazole (**358**) (see Scheme 2.93) indicating a similar indole system. The ^{1}H and ^{13}C resonances of another spin system were shifted downfield, indicating a different environment. The isolated singlet proton at δ 8.88 showed three-bond correlation between *N*-5 and C-4a, in addition to correlations to the carbonyl carbon at δ 178.4, and to the resonances at δ 130.0 and 122.1, indicating a quinoline structure. These data indicated a fused pentacyclic ring system with indole and quinoline systems as the terminal rings. The presence of an *N*-oxide group was supported with the weak, variable intensity ion at *m*/*z* 314, carrying an extra oxygen atom relative to *m*/*z* 298 in its EIMS spectrum, which could be explained by the variable loss of an oxygen atom in the EIMS, due to thermal decomposition in the ion source before ionization. The EI-MS spectrum fragmentation ions at *m*/*z* 297 (M^{+}–OH), 286 (M^{+}–CO), 258 [(M^{+}-28)–CO] also indicated the presence of an *N*-oxide and two carbonyl carbons in the molecule. Based on these spectral data, the structure **377** was assigned to calothrixin A. This structure was unequivocally supported by the absence of any NOEs between the indole and quinoline systems, and the absence of long-range ^{1}H and ^{13}C correlations, as well as by X-ray crystallographic analysis (345) (Scheme 2.99).

The UV spectrum (λ_{max} 283, 352, and 405 nm) of calothrixin B (**378**) was similar to that of calothrixin A (**377**) indicating the presence of a similar pentacyclic quinolino[4,3-*b*]carbazole-1,4-quinone chromophore. Close comparison of the HREIMS of calothrixin B (**378**) with that of calothrixin A (**377**) indicated that

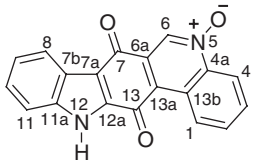

377 Calothrixin A

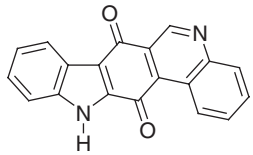

378 Calothrixin B

Scheme 2.99

calothrixin B (**378**) was the *N*-5-deoxy analog of calothrixin A. The ^{1}H- and ^{13}C-NMR spectral data of calothrixin B showed significant differences in their chemical shifts only near N-5. Thus, the C-4, C-4a, and C-6 resonances of calothrixin B were 8–15 ppm downfield of those in calothrixin A, and the H-4 and H-6 resonances of calothrixin B were respectively 0.44 upfield and 0.73 ppm downfield of those in calothrixin A, paralleling the shifts observed for the corresponding nuclei in quinoline and quinoline *N*-oxide. Based on these spectral data and the structural similarity to calothrixin A (**377**), the structure **378** was assigned for calothrixin B (345) (Scheme 2.99).

G. Sesquiterpenoid Carbazole Alkaloids

In 1989, Gloer *et al.* reported the isolation of tubingensin A (**379**) from the hexane extract of the sclerotia of the fungus *Aspergillus tubingensis*. Tubingensin A has a unique 9*H*-octahydronaphtho[3,4-*b*]carbazole pentacyclic framework. Moreover, tubingensin A is active against the widespread crop pest *Heliothis zea* and displays *in vitro* antiviral activity against herpes simplex virus type 1 (346). In the same year, the same authors isolated the cytotoxic hexacyclic carbazole alkaloid, tubingensin B (**380**) from the same source. Tubingensin B exhibited similar biological activity as found for tubingensin A, but was more cytotoxic to HeLa cells (IC_{50} 4 μg/mL for **380** vs. 23 μg/mL for **379**) (347). One year later, the same group reported the isolation of aflavazole **381**, a new anti-insectan carbazole metabolite from a different *Aspergillus* sp., *Aspergillus flavus* sclerotia. Aflavazole showed strong antifeedant activity against the fungivorous beetle *Carpophilus hemipterus* (348). In nature, tubingensin A (**379**) $[\alpha]_D^{20}$ + 13.6 (*c* 1.0, $CHCl_3$) (322,324), tubingensin B (**380**) $[\alpha]_D$ –6.7 (*c* 0.80, $CHCl_3$) (322), and aflavazole (**381**) $[\alpha]_D$ +2.8 (*c* 0.35, MeOH) (348) were isolated in their optically active form.

In 2001, Sings *et al.* isolated two indole diterpene alkaloids, dihydrotubingensins A (**382**) and B (**383**) (349), together with the previously known tubingensins A (**379**) (346) and B (**380**) (347). Dihydrotubingensins A and B were the first dihydrocarbazole-containing alkaloids isolated from a living system. Dihydrotubingensin B (**380**) was obtained in its optically active $[\alpha]_D^{20}$ − 50.0 (*c* 0.1, MeOH) form (349).

The UV spectrum (λ_{max} 218, 239, 262, 302, 326, and 340 nm) of tubingensin A (**379**) shows the presence of a carbazole framework. The ^{1}H-NMR spectrum of tubingensin A (**379**) indicated the presence of a 2,3-disubstituted carbazole substructure. The selective INEPT spectrum showed correlations of H-5 with C-3, C-4, C-7, and C-9, the correlations of H-10 with C-2, C-4, C-12, and C-20, and the correlations of H-27 with

C-3, C-10, C-11, and C-13. Among these, C-10 represents a four-bond correlation, and the absence of measurable coupling between H-10 and H-27 is in agreement with the observed correlation and their *para*-orientation. The partial structure assigned with these selective INEPT correlations supports the long-range correlation of the three protons at C-29 with C-14, C-15, C-16, and C-20, and the correlation of the three protons at C-28 with C-15, C-16, and C-17. The protons at C-13 were significantly downfield shifted, suggesting the attachment of C-13 to a sp^2 center. The presence of a 4-methyl-3-pentenyl group was clearly shown by the ^{1}H-NMR decoupling experiments and ^{13}C-NMR data. The connectivity of these partial structures was established by selective INEPT experiments, in which the downfield C-13 protons of the C-13–C-14 ethylene unit were long-range coupled to two aromatic C-11 and C-12 quaternary carbons, the C-27 aromatic methine, and the C-15 aliphatic quaternary carbon. The upfield C-14 protons of the C-13–C-14 ethylene unit correlated with both the C-15 and C-20 aliphatic quaternary carbons and the C-12 aromatic quaternary carbon. Finally, the C-10 downfield aromatic proton correlated with the C-20 aliphatic quaternary carbon which has the 4-methyl-3-pentenyl substituent. The relative stereochemistry of tubingensin A, as shown in structure **379**, was based on biogenetic considerations, NOESY correlation, and Dreiding models. Based on these spectroscopic analyses, structure **379** was assigned to tubingensin A (346) (Scheme 2.100).

The UV spectrum (λ_{max} 218, 237, 260, 299, 325, and 338 nm) of tubingensin B (**380**) was very similar to that of tubingensin A (**379**), indicating the presence of a similar carbazole framework. Comparison of the ^{1}H-NMR spectrum of tubingensin B (**380**) with that of tubingensin A (**379**) indicated that these two alkaloids are structural isomers with a similar 2,3-disubstituted carbazole substructure. This was also supported with homonuclear decoupling and ^{1}H–^{1}H COSY experiments. In addition, the selective INEPT and COSY data indicated the presence of a second isolated ethylene moiety, and an isopropyl group attached to a third quaternary carbon. In the selective INEPT experiments, the isopropyl C-24 methine proton and the C-13 methylene protons both correlated with C-12 and C-23. The C–H proton of the hydroxylated methine (H-19) correlated with C-11, and the aromatic proton singlets (H-10 and H-27) correlated with C-20 and C-23, respectively. The relative stereochemistry of tubingensin B, as shown in structure **380**, was based on NOESY correlation and Dreiding models. Based on these spectroscopic analyses, structure **380** was assigned to tubingensin B (347) (Scheme 2.100).

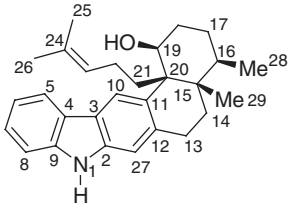

379 Tubingensin A

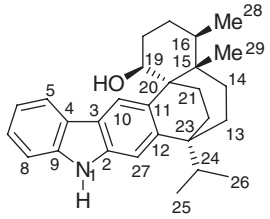

380 Tubingensin B

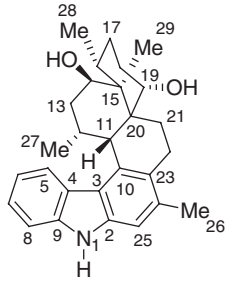

381 Aflavazole

Scheme 2.100

The UV spectrum (λ_{max} 219, 243, 263, 297, 327, and 341 nm) of aflavazole (**381**) indicated the presence of a carbazole framework. The ^{13}C-NMR spectrum of aflavazole (**381**) showed the presence of 12 aromatic carbons similar to those of tubingensins A (**379**) and B (**380**), without any other multiple bonds, indicating the presence of three additional rings and a similar carbazole moiety. The ^{1}H-NMR decoupling and COSY experiments and selective INEPT data, indicated the presence of a 2,3,4-trisubstituted carbazole substructure, and the presence of an isolated ethylene unit and an aromatic methyl group showing a benzylic coupling to a broad singlet at δ 7.12 assignable to the C-25 proton. The selective INEPT correlations of H-11 with C-3, C-10, and C-23, indicated the direct attachment of C-11 to C-10 of the carbazole nucleus. The three protons of C-26 showed correlations to aromatic C-23, C-24, and C-25, thereby locating the aromatic methyl group *meta* to C-11, and confirming its position *ortho* to C-25. Irradiation of the isolated ethylene protons of C-22 at δ 2.89 showed the polarization transfer to C-10, C-23, and C-24, thus establishing the linkage of C-22 to C-23. Similarly, the H-21 ethylene protons showed the polarization transfer to C-19 and C-20, indicating the linkage of C-20 to C-21. The relative stereochemistry of aflavazole, as shown in structure **381**, was based on NOESY correlations. Based on these spectroscopic analyses, the structure **381** was assigned to aflavazole (348) (Scheme 2.100).

Comparison of the ^{1}H-NMR spectrum of dihydrotubingensin A (**382**) with that of tubingensin A (**379**) indicated the absence of the C-10 and C-27 aromatic singlets at δ 7.92 and 7.11, respectively, and the presence of two additional methylene signals at δ 3.26–3.41. This was also established from the HRESIMS spectrum. Based on these spectral data, and the close structural similarity to tubingensin A (**379**), the structure **382** was assigned to dihydrotubingensin A. This structure was unequivocally established by transformation of dihydrotubingensin A (**382**) into tubingensin A (**379**) (see Scheme 2.100) by mild air oxidation (349) (Scheme 2.101).

The UV spectrum (λ_{max} 227 and 281 nm) of dihydrotubingensin B (**383**) indicated the presence of a substituted indole framework, rather than a carbazole framework. Close comparison of the ^{1}H-NMR spectrum of dihydrotubingensin B (**383**) with that of tubingensin B (**380**) indicated the absence of two aromatic signals corresponding to H-10 and H-27 at δ 8.05 and 7.32, respectively, with the presence of two additional downfield-shifted methylene signals at δ 3.34 and 3.53 for the C-10 protons, and at δ 3.66 for the C-27 protons. This was also deduced from the HRESIMS and ^{13}C-NMR spectral data. The presence of a dihydrocarbazole unit was also established through long-range ^{1}H–^{13}C-NMR correlations obtained from the HMBC experiment. Based

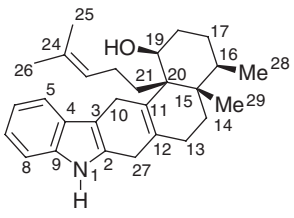

382 Dihydrotubingensin A

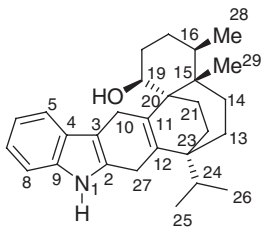

383 Dihydrotubingensin B

Scheme 2.101

on these spectral data and the close structural similarity to tubingensin B (**380**), structure **383** was assigned to dihydrotubingensin B. This structure was unequivocally established by transformation of dihydrotubingensin B (**383**) into tubingensin B (**380**) (see Scheme 2.100) by mild air oxidation (349) (Scheme 2.101).

H. Miscellaneous Carbazole Alkaloids

In 1991, Dillman and Cardellina reported the isolation of 1-methylcarbazole (**384**) from extracts of the sponge *Tedania ignis* collected in the shallow waters of Bermuda (350). This was the first report on the isolation of 1-methylcarbazole from a marine invertebrate (350). Prior to this isolation, 1-methylcarbazole was detected, along with other methylcarbazole derivatives as major components of cigarette smoke condensate (351). This isolate showed insecticidal and antimicrobial activity (352), but was shown to be non-mutagenic (353).

In 1983, Luk *et al.* reported the isolation of 3-chlorocarbazole (**385**) from female bovine urine using a benzodiazepine receptor binding assay. This was the first example of a carbazole alkaloid isolated from mammalian tissues (354). The UV spectrum [λ_{max} 215, 223, 229, 236, 246, 260, 291 (sh), 297, 319 (sh), 330, and 343 nm] of 3-chlorocarbazole (**385**) showed the presence of a carbazole framework, which was supported by its IR spectrum. The ^{1}H-NMR spectrum showed the presence of two sets of multiplets at δ 7.18–7.50 and 7.90–8.15 assignable to five and three protons, respectively, indicating the absence of one proton of 9*H*-carbazole. These spectral data, coupled with a characteristic mass fragmentation at m/z 166 (M^+-Cl), indicated the presence of a chlorine at C-3 of the carbazole nucleus. Based on these spectral data, structure **385** was assigned to 3-chlorocarbazole (354). This structure was unequivocally established by comparison with a synthetic sample (355) (Scheme 2.102).

In 1999, Brown *et al.* reported the isolation of two regioisomeric dibromocarbazole alkaloids, 3,6-dibromocarbazole (**386**) and 2,7-dibromocarbazole (**388**), along with 3,6-diiodocarbazole (**387**) from one colony of the epilithic encrusting cyanobacterium *Kyrtuthrix maculans* on Hong Kong shores. Although all these

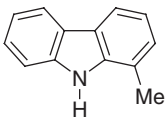

384 1-Methylcarbazole

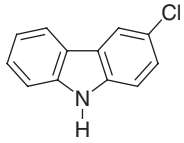

385 3-Chlorocarbazole

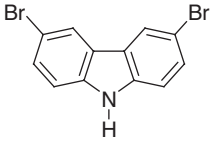

386 3,6-Dibromocarbazole

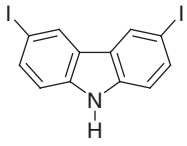

387 3,6-Diiodocarbazole

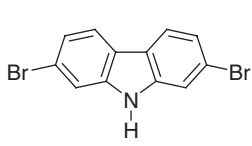

388 2,7-Dibromocarbazole

Scheme 2.102

alkaloids were known previously through organic synthesis, this was the first report of their occurrence as natural products (356). Recently, Zhu and Hites isolated a further polybrominated carbazole, 1,3,6,8-tetrabromocarbazole, from the sediment cores of Lake Michigan. This was the first report of the isolation of a tetrabromocarbazole from the environment (357).

The ^{1}H- and ^{13}C-NMR spectra of 3,6-dibromocarbazole (**386**) showed only half of the full set of signals, indicating the symmetrical structure for this alkaloid. The presence of two bromine atoms was clearly established by the HREIMS. The position and splitting pattern in the aromatic region of the ^{1}H-NMR spectrum, along with one broad singlet at δ 8.11 assignable to the NH proton indicated the location of the two bromine atoms at C-3 and C-6 on the carbazole nucleus. In addition, the ^{13}C-NMR chemical shifts also supported the position of these bromine atoms. Based on these spetral data, the structure **386** was assigned to 3,6-dibromocarbazole. This structure was unequivocally established by comparison with a commercially available sample of 3,6-dibromocarbazole (356) (Scheme 2.102).

The ^{1}H-NMR spectrum of 3,6-diiodocarbazole (**387**) showed the same set of protons as 3,6-dibromocarbazole (**386**), except for their downfield shift. These spectral data, together with the HREIMS, indicated the presence of two iodine atoms in place of two bromine atoms. In addition, the ^{13}C-NMR chemical shifts also supported the presence of iodine atoms. Based on these spectral analyses, and the close structural similarity to 3,6-dibromocarbazole, the structure **387** was assigned to 3,6-diiodocarbazole (356).

The HREIMS of 2,7-dibromocarbazole (**388**) was identical to that of 3,6-dibromocarbazole (**386**). Differences were identified in the chemical shifts and splitting pattern of the ^{1}H-NMR spectrum. Thus, a deshielded, two-proton doublet at δ 7.87 with *ortho*-coupling (J=8.3 Hz), assignable to the C-4 and C-5 protons, indicated the location of two bromine atoms at the C-2 and C-7 positions of the carbazole nucleus. This was also evident from the shielded *ortho*- and *meta*-coupled (J=8.3, 1.5 Hz) two-proton double doublet at δ 7.36, assignable to the C-3 and C-6 protons. Further, a mutually *meta*-coupled (J=1.5 Hz) two-proton doublet at δ 7.57, assignable to the C-1 and C-9 protons, supported the location of the two bromine atoms *ortho* to these carbons. Based on these spectral analyses and the HREIMS identical to that of 3,6-dibromocarbazole (**386**), the regioisomeric dibromocarbazole structure **388** was assigned to 2,7-dibromocarbazole (Scheme 2.102) (356).

Recently, Steglich *et al*. isolated pityriazole (**389**), along with malasseziazoles A (**390**), B (**391**), and C (**392**), from cultures of the human pathogenic yeast *Malassezia furfur*. Malasseziazoles A–C (**390**–**392**) were the first natural products with an indolo[3,2-*b*]carbazole framework (358). The UV spectrum [λ_{max} 221, 279, and 336 (sh) nm] of pityriazole (**389**) showed the presence of a carbazole framework. This was supported by the IR spectrum. The ^{1}H-NMR spectrum of pityriazole (**389**) showed the presence of a broad OH peak at δ 17.10 assignable to an aromatic hydroxy group, and a singlet at δ 10.16 assignable to a NH. In the aromatic region, a deshielded C-4 proton appeared as a singlet at δ 8.40, indicating substitution at C-1, C-2, and C-3 of the carbazole nucleus. Four, mutually coupled protons at δ 7.89, 7.02, 7.13, and 7.30 assignable to the C-5, C-6, C-7, and C-8 protons, respectively, established the absence of substitution on the C-ring of the carbazole nucleus. In addition to these peaks, the ^{1}H-NMR also showed the protons corresponding to a 1*H*-indol-3-yl group, which was also supported by ^{1}H–^{1}H COSY experiments. Along with these spectral data,

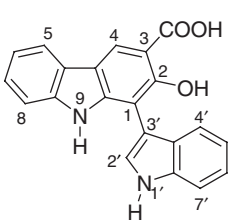

389 Pityriazole

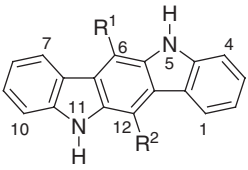

390 Malasseziazole A
R^1 = COCOOH; R^2 = H

391 Malasseziazole B
R^1 = COCOOH; R^2 = CHO

392 Malasseziazole C
R^1 = COOH; R^2 = CHO

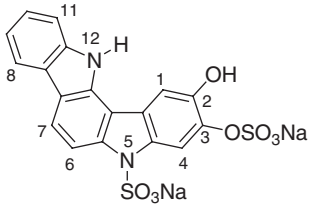

393 Ancorinazole

Scheme 2.103

HMBC and HMQC correlations indicated the presence of a 1*H*-indol-3-yl group at C-1, a hydroxy group at C-2, and a carboxylic group at C-3 of the carbazole nucleus. Based on these spectral data, the structure **389** was assigned to pityriazole (358) (Scheme 2.103).

The UV spectrum (λ_{max} 211, 225, 255, 305, 375, and 447 nm) of malasseziazole A (**390**) showed the presence of an indolo[3,2-*b*]carbazole framework. The ^{1}H-NMR spectrum of malasseziazole A (**390**) showed signals for two, 2,3-disubstituted, 1*H*-indole moieties interconnected by a $C_4H_2O_3$ unit containing a –C(═O)COOH group. This was supported by ^{1}H–^{1}H COSY experiments. Further structural support came from the HMBC and HMQC correlations. Based on these spectral analyses, the structure **390** was assigned to malasseziazole A (358) (Scheme 2.103).

The UV spectrum [λ_{max} 209, 230 (sh), 242 (sh), 275 (sh), 306, 409, and 482 nm] of malasseziazole B (**391**) was similar to that of malasseziazole A (**390**), indicating the presence of a similar indolo[3,2-*b*]carbazole framework. The ^{1}H-NMR spectrum of malasseziazole B (**391**) was also very similar to that of malasseziazole A (**390**), except for the absence of the C-12 singlet proton at δ 8.40, along with the presence of an aldehyde proton at δ 11.55. This aldehyde proton showed correlations with the C-11a, C-12, and C-12a carbons in the HMBC experiment. Based on these spectral analyses and the structural similarity to malasseziazole A (**390**), the structure **391** was assigned to malasseziazole B (358) (Scheme 2.103).

The UV spectrum [λ_{max} 214, 226 (sh), 247, 268, 308, 391, and 462 nm] of malasseziazole C (**392**) was similar to that of malasseziazole B (**391**), indicating the presence of a similar indolo[3,2-*b*]carbazole framework. The ^{1}H-NMR spectrum of malasseziazole C (**392**) was also very similar to that of malasseziazole B (**391**), except for the presence of a carboxylic group in place of an α-ketocarboxylic group. This was evident from its ^{13}C-NMR spectrum, by the absence of an α-ketocarboxylic carbonyl carbon at δ 198.6, as well as a downfield shift (δ 126.5) of the carboxylic group attached to the C-6 carbon. The structure was also supported by the HMBC and HMQC correlations. Based on these spectral analyses and the structural similarity to malasseziazole B (**391**), the structure **392** was assigned to malasseziazole C (358) (Scheme 2.103).

In 2002, Boyd *et al*. reported the isolation of ancorinazole (**393**) from the aqueous extract of the sponge *Ancorina* sp., collected in New Zealand. This was the first natural product with an indolo[3,2-*a*]carbazole framework (359). The UV spectrum [λ_{max} 243, 280, 296 (sh), 308, 341, and 357 nm] of ancorinazole (**393**) indicated the presence of a polycyclic aromatic framework. The HRFAB-MS of the pseudomolecular ion of ancorinazole (**393**) at m/z 469 (M^+–Na), indicated the molecular formula $C_{18}H_{10}O_8N_2S_2Na_2$. The FAB-MS peaks at m/z 427 (M^+–H–Na–SO_2) and 413 (M^++H–Na–SO_3), indicated the loss of SO_2 and SO_3 from (M^+–H) and (M^++H), respectively. In addition to these mass spectral data, IR spectral bands at ν_{max} 1053, 1232, and 1262 cm^{-1} supported the presence of sulfate and sulfamate groups. Additional support for the sulfate functionality was obtained chemically with the formation of a white precipitate ($BaSO_4$) by acid hydrolysis in the presence of $BaCl_2$. The ^{1}H-NMR spectrum showed three singlets at δ 7.92, 8.09, and 8.67 in which the signal at δ 8.67 was an exchangeable proton assignable to a hydroxy group. These data indicated substitutions at the C-2 and C-3 positions of the indolo[3,2-*a*]carbazole framework. The aromatic region showed four, mutually-coupled protons at δ 8.07, 7.16, 7.32, and 7.58 assignable to the C-8, C-9, C-10, and C-11 protons, respectively, indicating an *ortho*-disubstituted aromatic ring. Two *ortho*-coupled (J=9.0 Hz) protons, which were assignable to C-6 and C-7 of the indolocarbazole framework, appeared at δ 8.00 and 8.02. A series of 1D-TOCSY-experiments, as well as HMBC correlations, supported this assignment. Additionally, the [3,2-*a*]fusion geometry of the indolocarbazole, the position of the sulfate group at C-3 and a sulfonate at *N*-5, were supported by NOE experiments. Based on these spectral analyses, the structure **393** was assigned to ancorinazole. Further evidence for this structure comes from its transformation into the corresponding hydrolysis product 2,3-dihydroxy-indolo[3,2-*a*]carbazole by treatment with mild acid (359) (Scheme 2.103).

CHAPTER 3

Biogenesis of Carbazole Alkaloids

A closer examination of all the carbazole alkaloids isolated and studied so far presents several interesting biogenetic features of these molecules. The most important one is the origin of the indole nucleus and of the ring A. With some rare exceptions, the alkaloids having an extra methyl group (or its equivalent) at the 3-position are isolated from higher plants, whereas the others are obtained from several different sources. Based on their natural occurrence, the carbazole alkaloids isolated to date were classified under these two main categories, and their biosyntheses is discussed consequently. Some of the biosynthetic pathways discussed below are lacking clear experimental support, and are based on rational, delineated proposals.

I. CARBAZOLE ALKALOIDS FROM HIGHER PLANTS

The occurrence of 3-methylcarbazole (**2**) and its oxidative congeners 3-formylcarbazole (**3**) and methyl carbazole-3-carboxylate (**4**), from the taxonomically related genera *Murraya*, *Clausena*, and *Glycosmis* of the family Rutaceae, sub-family Aurantoidae, of higher plants, provides clear evidence for the *in vivo* oxidation of the methyl group in 3-methylcarbazole. This was supported by the photochemical oxidation of the 3-methyl group of carbazole alkaloids (360). Further support derives from the co-occurrence of a diverse range of 1- and 2-oxygenated 3-methylcarbazoles and their oxidative variants from the genus *Murraya*, and the closely allied genera *Clausena* and *Glycosmis* of the family Rutaceae (see Scheme 3.4) (8,361). Whatever may be the progenitor of the carbazole nucleus in nature, it is clear from these findings that 3-methylcarbazole (**2**) is the key precursor for the carbazoles isolated from higher plants.

The route of formation of the carbazole nucleus is still far from understood, and has been variously considered to arise from 3-prenylquinolone *via* a pathway involving shikimic acid (**394**) and mevalonic acid (MVA) (**400**) (Scheme 3.1) (1,112,362–366), anthranilic acid (**397**) and prephenic acid (**404**) *via* a pathway involving shikimic acid (**394**) (Scheme 3.2) (367), and also tryptophan (**408**) involving the mevalonate (**400**) pathway (Scheme 3.3) (133). All of these pathways lack experimental proof. However, based on the occurrence of the diverse carbazole alkaloids derived from anthranilic acid (**397**) in the family Rutaceae, the pathway

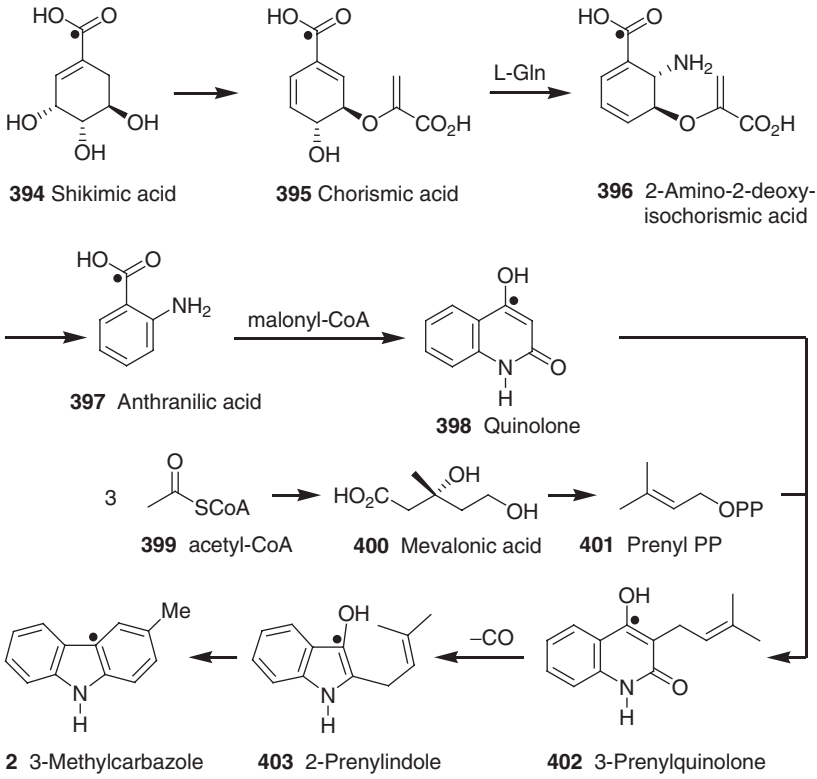

Scheme 3.1

described in Scheme 3.1 is regarded as more rational, and is the most widely accepted among these biogenetic pathways to carbazole alkaloids in higher plants.

In the biogenetic pathway depicted in Scheme 3.1 (362–366), the formation of 3-methylcarbazole (**2**) it is considered to arise from 3-prenylquinolone (**402**) through 2-prenylindole (**403**). Although 2-prenylindole alkaloids are rare in nature, there is another major source in the Rutaceae in the form of the dimeric indoles of *Flindersia fournieri*, such as isoborreverine, which could arise from the monomeric units of 2-prenyltryptamines by Diels–Alder type condensation (368). For the synthesis of 3-prenylquinolone (**402**), the required quinolone (**398**) would be obtained from anthranilic acid (**397**), which has greatest abundance in plants from the family Rutaceae. Anthranilic acid (**397**) is obtained from chorismic acid (**395**), a very important branch point compound in the shikimate pathway. A central intermediate in the shikimate pathway is shikimic acid (**394**), a compound which was isolated from plants of *Illicium* species (Japanese shikimi) many years before its role in metabolism had been discovered (366).

The shikimate pathway begins with a coupling of phosphoenolpyruvate (PEP) and D-erythrose 4-phosphate to give the seven-carbon 3-deoxy-D-arabino-heptulosonic acid 7-phosphate (DAHP) through an aldol-type condensation. Elimination of phosphoric acid from DAHP, followed by an intramolecular aldol reaction, generates the first carbocyclic intermediate, 3-dehydroquinic acid. Shikimic acid (**394**) is

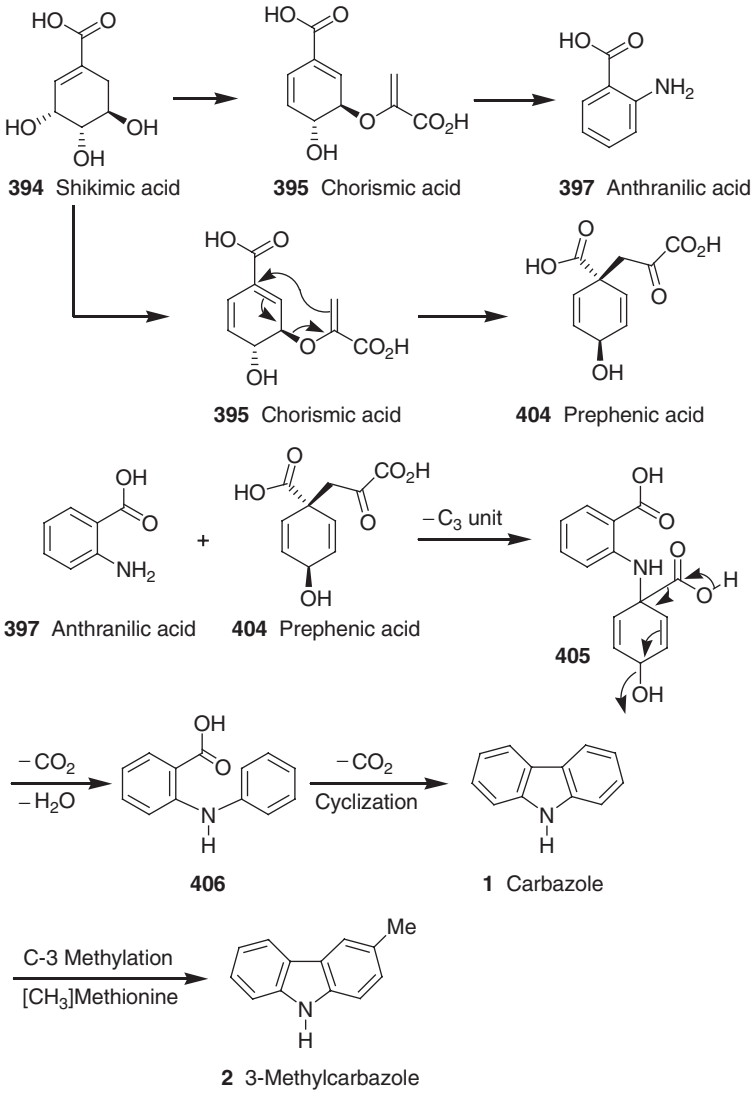

Scheme 3.2

formed from 3-dehydroquinic acid *via* 3-dehydroshikimic acid through a series of dehydration and reduction steps. Shikimic acid 3-phosphate, which is obtained by ATP-dependent phosphorylation of shikimic acid (**394**), combines with PEP *via* an addition–elimination reaction giving 3-enolpyruvylshikimic acid 3-phosphate (EPSP). This reaction is catalyzed by the enzyme EPSP synthase. Then, 1,4-elimination of phosphoric acid from EPSP leads to chorismic acid (**395**). Amination of chorismic acid (**395**) at C-2 from L-glutamine (Gln) with the elimination of water leads to 2-amino-2-deoxyisochorismic acid (**396**), and then 2-aminobenzoic acid (anthranilic acid) (**397**). Anthraniloyl-coenzyme A (CoA), obtained from anthranilic acid and acetyl-coenzyme A (CoA), undergoes a chain extension to afford quinoline (**398**) *via* the addition of one molecule of malonyl-CoA through amide formation. Alkylation

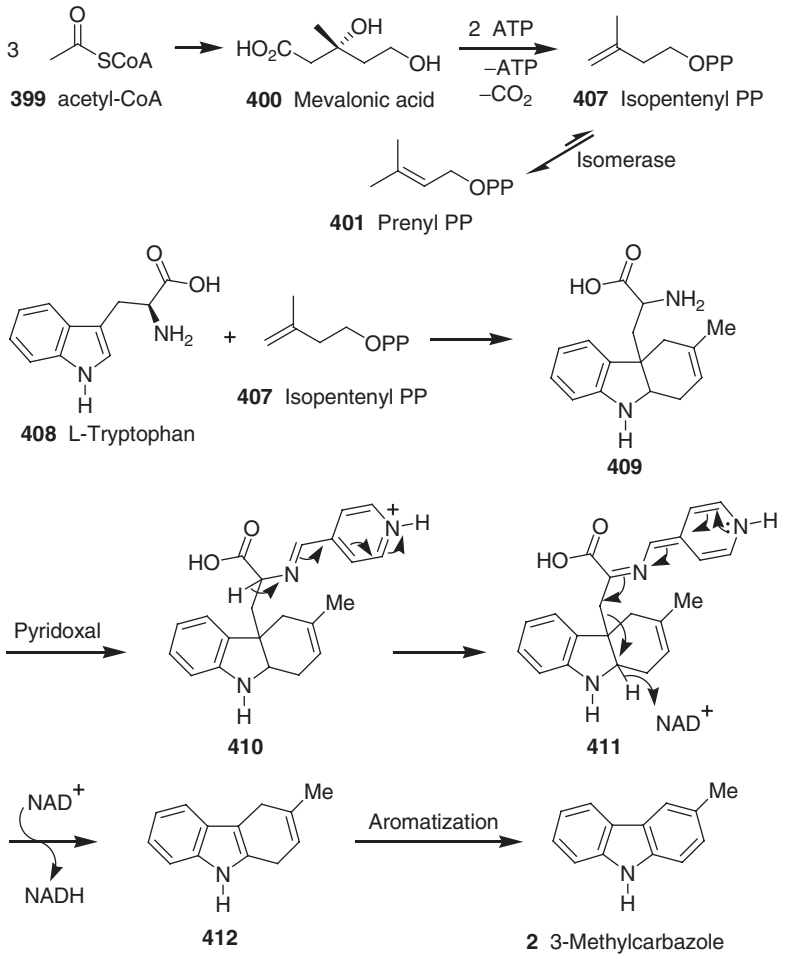

Scheme 3.3

of quinoline (**398**) at the nucleophilic C-3 position with prenyl diphosphate (DMAPP) affords 3-prenylquinolone (**402**). DMAPP is obtained from three molecules of acetyl-coenzyme A (**399**) *via* MVA (**400**) involving a series of reactions using β-hydroxy-β-methylglutaryl-CoA (HMG-CoA) reductase and ATP-dependent enzymes. The route for the transformation of 3-prenylquinolone (**402**) to 3-methylcarbazole lacks experimental support and is presumed to proceed through the 2-prenylindole **403** *via* elimination of carbon monoxide (CO) from 3-prenylquinolone (**402**) followed by oxidative cyclization of the 2-prenylindole **403** (362–366) (Scheme 3.1).

The biogenetic pathway proposed by Chakraborty for the formation of carbazole (**1**) and 3-methylcarbazole (**2**) proceeds through *N*-phenylated anthranilic acid (**406**). This hypothesis is based on aromatic C-methylation of aniline with methionine, and originates from anthranilic acid (**397**) and prephenic acid (**404**). Until now, there are no *N*-phenylated anthranilic acid derivatives known naturally, therefore, this hypothesis is lacking substantial biogenetic evidence. However, the isolation of carbazole (**1**), 3-methylcarbazole (**2**), and several derivatives of 3-methylcarbazole

from taxonomically related higher plants of the genera *Glycosmis*, *Clausena*, and *Murraya* (Rutaceae) supports this hypothesis. Based on this biogenetic pathway, *N*-phenylated anthranilic acid (**406**) could derive from anthranilic acid (**397**) and prephenic acid (**404**) with the elimination of a C_3 unit, followed by CO_2 and H_2O. *N*-Phenylated anthranilic acid (**406**) could be transformed to carbazole with the elimination of CO_2. The methyl group (or its equivalent) at the C-3 position, the most active center of electrophilic attack at the carbazole nucleus, could originate from *C*-methylation with methionine on carbazole (**1**). This could also happen prior to the formation of the carbazole nucleus (367) (Scheme 3.2).

In 1975, Narasimhan *et al*. described a biogenetic hypothesis for 3-methylcarbazole (**2**) starting from L-tryptophan (**408**). According to these authors, the A-ring of carbazole which shows an isopentane carbon skeleton could be of mevalonate origin. This was supported by the experiments of Kapil (1) by feeding 2-^{14}C- and 2-^{3}H-MVA lactone to *M. koenigii*, which resulted in the isolation of labeled koenimbin (**116**), koenigicine (**118**) (see Scheme 2.22), and mahanimbine (**139**) (see Schemes 2.27 and 3.7); though experiments establishing the location of the radioactivity are lacking. This experiment rules out Chakraborty's proposal that the methyl group at C-3 is part of a one-carbon unit (see Scheme 3.2).

Based on Narasimhan's approach, an initial introduction of the isopentenyl chain (**407**) at the 3-position of L-tryptophan (**408**), followed by the preferential migration of the isopentenyl chain to the 2-position, and subsequent cyclization, would give the tetrahydrocarbazole derivative (**409**). Loss of serine from **409** in the presence of pyridoxal co-enzyme, followed by dehydrogenation, would lead to 3-methylcarbazole (**2**) (133) (Scheme 3.3).

The isolation of murrayanine (**9**), the first member of the carbazole alkaloids, together with several members of this group, murrayafoline A (**7**), koenoline (**8**), mukoeic acid (**10**), mukonine (**11**), 1-hydroxy-3-methylcarbazole (**23**), *O*-demethylmurrayanine (**24**), clausine E (clauszoline-I) (**25**), 3-formylcarbazole (**3**), methyl carbazole-3-carboxylate (**4**), 2-methoxy-3-methylcarbazole (**37**), *O*-methylmukonal (glycosinine) (**38**), clausine L (*O*-methylmukonidine, methyl 2-methoxycarbazole-3-carboxylate) (**39**), 2-hydroxy-3-methylcarbazole (**52**), mukonal (**53**), mukonidine (**54**), and 3-methylcarbazole (**2**) from the taxonomically related genera *Murraya*, *Glycosmis*, and *Clausena* (Rutaceae) indicates the *in vivo* oxygenation and oxidation of 3-methylcarbazole (**2**).

The *in vivo* oxygenation of 3-methylcarbazole to hydroxy-3-methylcarbazoles is supported by biomimetic hydroxylation of 3-methylcarbazole with Fenton's reagent (Fe^{+2}/H_2O_2) under Udenfriend conditions (Fe^{+2}/EDTA/ascorbic acid/oxygen), a reaction prototype of mixed function oxidases. Under these conditions, 1-hydroxy-3-methylcarbazole and 2-hydroxy-3-methylcarbazole were isolated as the major products, along with other compounds (369). The *in vivo* oxidation of the C-3 methyl group to its oxidized functional variants, i.e., CH_2OH, CHO, and COOH, which have been found in various alkaloids was supported by the photochemical oxidation of the 3-methyl group of carbazole alkaloids (360) (Scheme 3.4).

The 3-methylcarbazole origin of the carbazole alkaloids of higher plants and the wider participation of 2-hydroxy-3-methylcarbazole in the formation of pyranocarbazoles, as well as furocarbazoles, has been further substantiated by the isolation of several derivatives of 3-methylcarbazoles, such as mukoenine-A (girinimbilol) (**55**), heptaphylline (**76**), furostifoline (**224**), furoclausine A (**225**), girinimbine (**115**), and murrayacine (**124**). Girinimbilol (**55**) could be considered the

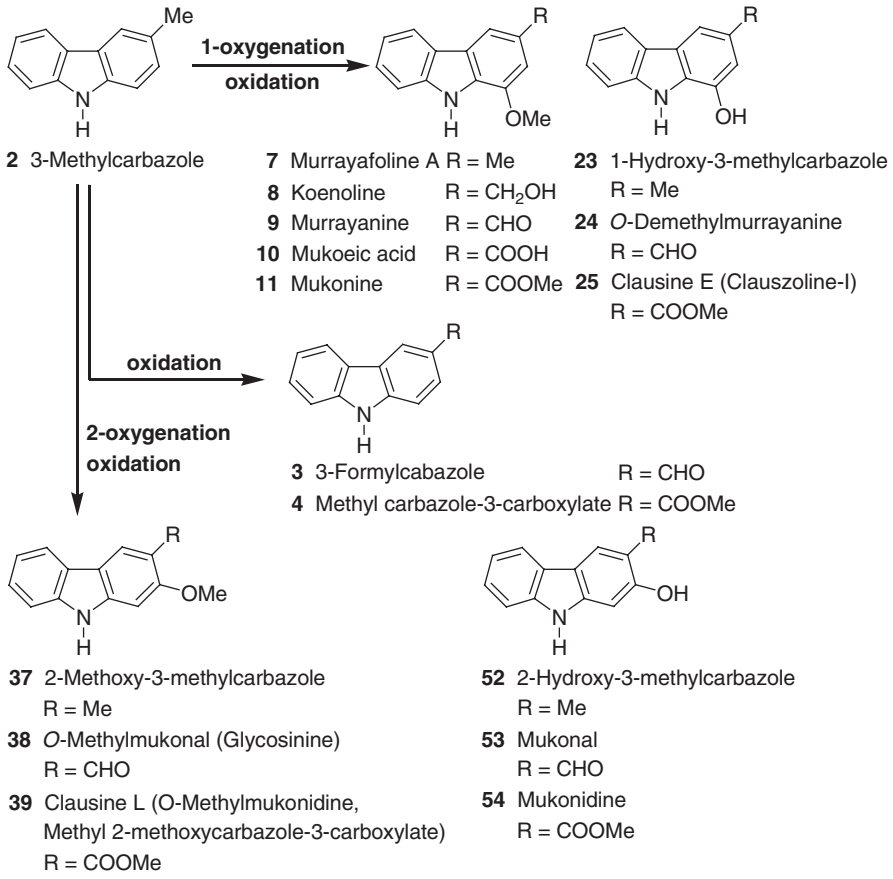

Scheme 3.4

precursor for furo- and pyrano[3,2-*a*]carbazole alkaloids. Moreover, the isolation of girinimbilol (**55**) and furostifoline (**224**) from *Murraya* species indicate the origin of the furan ring as shown through the cyclization pathway ''a'' from the prenylated congener. The occurrence of girinimbilol (**55**) and girinimbine (**115**) from *M. koenigii*, and heptaphylline (**76**) and murrayacine (**124**) in *Clausena heptaphylla*, may be considered circumstantial evidence in favor of the origin of the pyran ring as shown through the cyclization pathway ''b'' from the prenylated congeners (370) (Scheme 3.5).

2-Hydroxy-3-methylcarbazole (**52**) could also function as a precursor for the formation of carbazole alkaloids with a C_{23} skeleton as depicted in Scheme 3.6 (370). Insertion of a C_{10} unit, *viz*., geraniol at C-1 of 2-hydroxy-3-methylcarbazole (**52**) would yield mahanimbinol (mahanimbilol) (**56**). The geranyl monoterpene unit could undergo various transformations, thus giving rise to isomeric carbazole alkaloids with a C_{23} skeleton, such as mahanimbine (**139**), cyclomahanimbine (murrayazolidine, curryanin) (**151**), and bicyclomahanimbine (**160**). Therefore, mahanimbinol (mahanimbilol) could be considered as the representative member of the carbazoles with a C_{23} skeleton. The occurrence of 2-hydroxy-3-methylcarbazole (**52**),

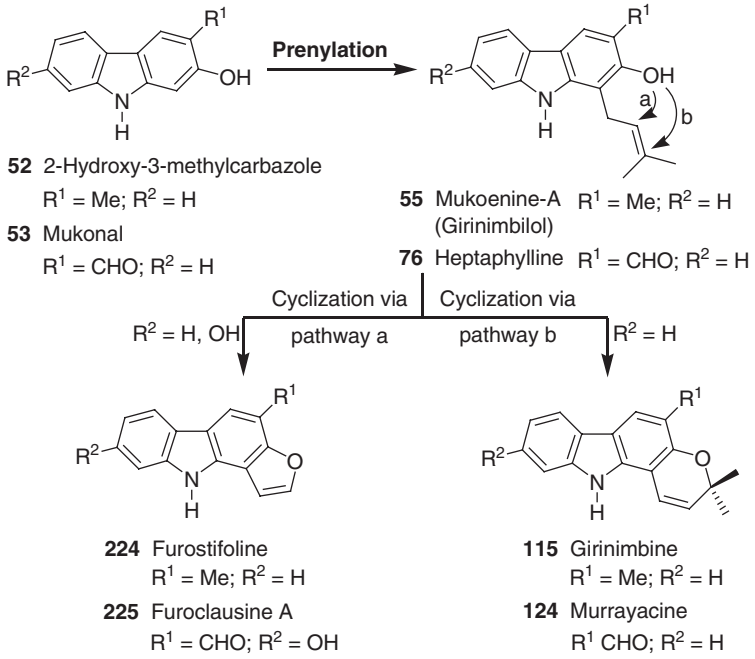

52 2-Hydroxy-3-methylcarbazole
R^1 = Me; R^2 = H

53 Mukonal
R^1 = CHO; R^2 = H

55 Mukoenine-A (Girinimbilol) R^1 = Me; R^2 = H

76 Heptaphylline R^1 = CHO; R^2 = H

224 Furostifoline
R^1 = Me; R^2 = H

225 Furoclausine A
R^1 = CHO; R^2 = OH

115 Girinimbine
R^1 = Me; R^2 = H

124 Murrayacine
R^1 CHO; R^2 = H

Scheme 3.5

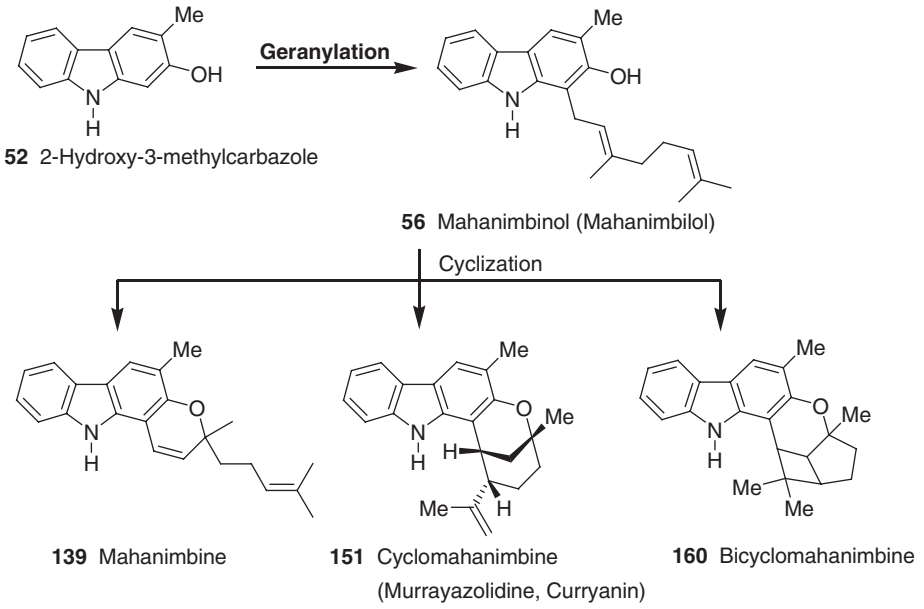

52 2-Hydroxy-3-methylcarbazole

56 Mahanimbinol (Mahanimbilol)

139 Mahanimbine

151 Cyclomahanimbine (Murrayazolidine, Curryanin)

160 Bicyclomahanimbine

Scheme 3.6

mahanimbinol (mahanimbilol) (**56**), mahanimbine (**139**), cyclomahanimbine (murrayazolidine, curryanin) (**151**), and bicyclomahanimbine (**160**) in *M. koenigii* may be considered circumstantial evidence in favor of the origin of the carbazole C_{23} skeleton from the geranylated congener, mahanimbinol (mahanimbilol) (**56**) (370) (Scheme 3.6).

Mukonal (**53**), an oxidation product of 2-hydroxy-3-methylcarbazole, could be further hydroxylated at the C-ring of the carbazole nucleus to give clauszoline-M (**73**), which could undergo insertion of a C_5 prenyl unit on either ring of the carbazole nucleus, to give the C-ring prenylated carbazole derivative **413** and heptazoline (**77**), which on cyclization would lead to clauszoline-B (**168**) and clauszoline-G (**126**), respectively. The isolation of mukonal (**53**), clauszoline-M (**73**), heptazoline (**77**), clauszoline-B (**168**), and clauszoline-G (**126**) from the taxonomically related genera *Murraya* and *Clausena* (Rutaceae) is in favor of the origin of the pyran ring from the prenylated congeners (76) (Scheme 3.7).

Chakraborty's biomimetic hydroxylation studies of 3-methylcarbazole (**2**) using Udenfriend conditions (Fe^{+2}/EDTA/ascorbic acid/oxygen) furnished a bis-carbazole, as a result of biomimetic dimerization of 3-methylcarbazole. This reaction, which is a prototype of hydroxylation followed by dimerization, provides circumstantial evidence for the existence of bis-carbazole alkaloids in higher plants (369,371).

Murrayafoline A (**7**) could undergo various oxidative dimerizations to give murrastifoline-A (**186**), murrastifoline-F (**191**), and bismurrayafoline-A (**197**) as

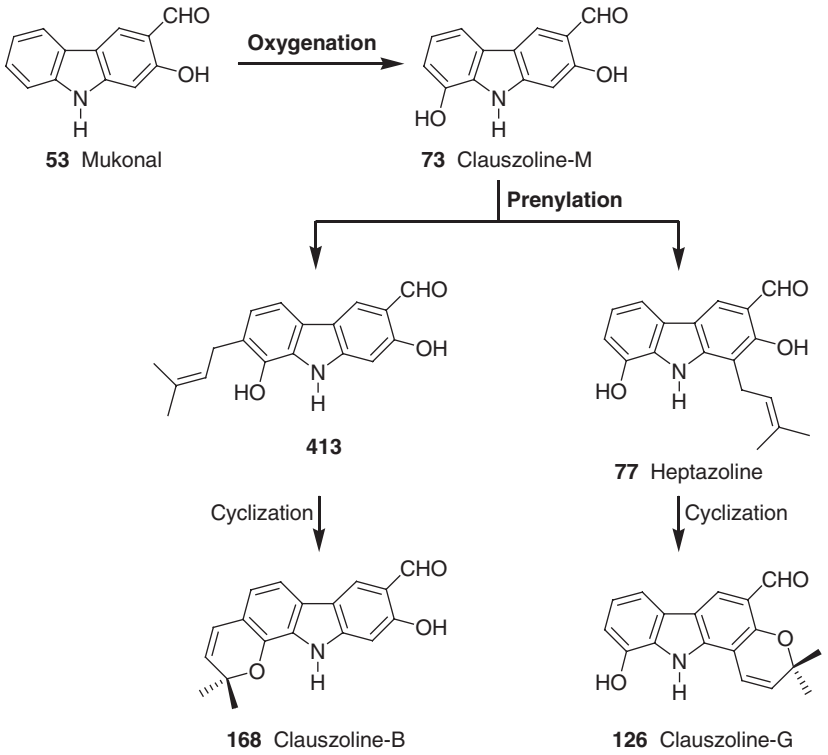

Scheme 3.7

depicted in Scheme 3.8. The occurrence of murrayafoline A (7), murrastifoline-A (**186**), murrastifoline-F (**191**), and bismurrayafoline-A (**197**) in *Murraya euchrestifolia* may be considered circumstantial evidence in favor of the oxidative dimerization of murrayafoline A (7) (Scheme 3.8).

Similarly, 1-hydroxy-3-methylcarbazole (**23**) and 2-hydroxy-3-methylcarbazole (**52**) could lead to bis(*O*-demethylmurrayafoline A) (**204**) and bis-2-hydroxy-3-methylcarbazole [1,1-bis(2-hydroxy-3-methylcarbazole)] (**213**), respectively, as shown in Scheme 3.9. Although bis(*O*-demethylmurrayafoline A) (**204**) is a non-natural carbazole derivative, the isolation of 2-hydroxy-3-methylcarbazole (**52**) and bis-2-hydroxy-3-methylcarbazole [1,1-bis(2-hydroxy-3-methylcarbazole)] (**213**) from *M. koenigii* supports the oxidative dimerization of 2-hydroxy-3-methylcarbazole (**52**) (Scheme 3.9).

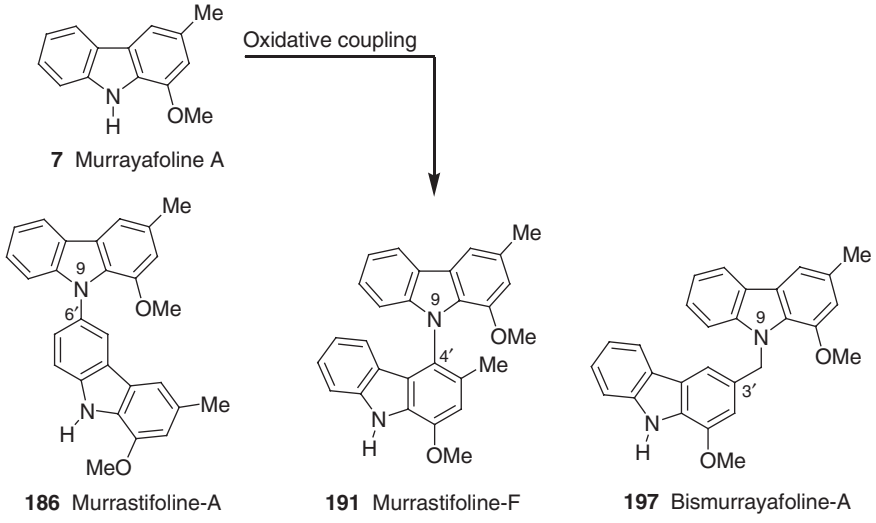

7 Murrayafoline A

186 Murrastifoline-A

191 Murrastifoline-F

197 Bismurrayafoline-A

Scheme 3.8

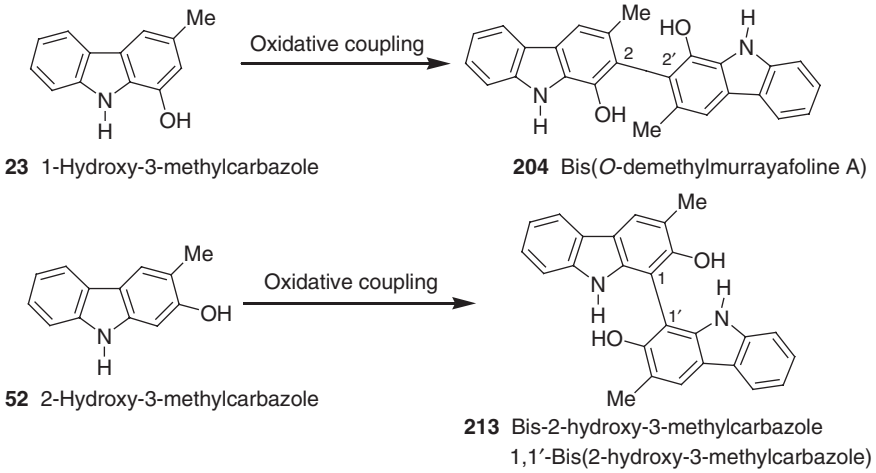

23 1-Hydroxy-3-methylcarbazole

204 Bis(*O*-demethylmurrayafoline A)

52 2-Hydroxy-3-methylcarbazole

213 Bis-2-hydroxy-3-methylcarbazole
1,1′-Bis(2-hydroxy-3-methylcarbazole)

Scheme 3.9

The biogenesis of ellipticine (**228**), as a representative member of the pyrido[4,3-*b*]carbazole alkaloids, lacks experimental support (372,373). However, for these alkaloids elegant and rational biogenetic pathways have been proposed (189,374–376). Because of this, their biosynthetic pathways remain an interesting enigma to be solved. Ellipticine (**228**) and its natural isomer olivacine (**238a**) are frequently present in the same plant, along with uleine. It is presumed, therefore, that all these *Aspidosperma* alkaloids have the same progenitor.

Prior to the first detailed biogenetic proposal of Wenkert for ellipticine (**228**) and related alkaloids (374), Woodward *et al*. had already mentioned a common biosynthetic relationship of ellipticine and uleine, two structurally different *Aspidosperma* alkaloids (178). Wenkert's non-tryptophan pathway was based on a common precursor **417**, derived from glycosylideneanthranilic acid (**414**), a tryptophan progenitor, and a *seco*-prephenate formaldehyde (SPF) unit or secologanin, as possible biogenetic intermediates for the *Aspidosperma* alkaloids. The α-oxidation of glycosylideneanthranilic acid (**414**) and Mannich condensation of the product with SPF or secologanin would be expected to produce the α-alkyl-β-glycosylindole **418**, an immediate precursor for the *Aspidosperma* alkaloids. This intermediate could undergo two modes of imine formation through the depicted pathways a and b to afford compounds, **419a** and **419b**, respectively. Finally, cyclization of **419a** and **419b** through the indolic β-position and extrusion (*via* retro-aldolization) of the β-glycosyl function would lead to the *Aspidosperma* alkaloids, ellipticine (**228**), and olivacine (**238a**) (374) (Scheme 3.10).

The biosynthetic pathway proposed by Potier and Janot involves both L-tryptophan (**408**) and stemmadenine (**420**) (375). Labeling experiments with both L-tryptophan (**408**) and stemmadenine (**420**) indicated a weak incorporation into uleine, and none at all for both ellipticine (**228**) and olivacine (**238a**) (373). In the light of these observations, this hypothesis needs further experimental support to show its validity, although, using this biogenetic model, Besselièvre and Husson achieved the syntheses of ellipticine (**228**) and olivacine (**238a**) (376). The conjugated iminium salt **426**, which is often invoked for the biogenesis of indole alkaloids (376), functions as a key intermediate in this hypothesis. Stemmadenine (**420**), which is formed from L-tryptophan (**408**), undergoes a whole series of transformations (377) as shown in Scheme 3.11 to afford the conjugated iminium salt **426**.

Intramolecular Mannich type reaction of the conjugated iminium salt **426** should lead to ellipticine (**228**) *via* an intermediate **427**. Alternatively, the conjugated iminium salt **426** could hydrolyze to afford the 2-vinylsubstituted indole **428**, which, on cyclization through an intermediate **429**, would lead to guatambuine (**233**). This alkaloid, on demethylation and dehydrogenation, should afford olivacine (**238a**) (375) (Scheme 3.11).

II. CARBAZOLE ALKALOIDS FROM OTHER SOURCES

Biogenetic considerations of the carbazole alkaloids isolated from other sources have led to a different view about the genesis of these alkaloids. Without exception, to date, all of the biogenetic proposals of the carbazole alkaloids isolated from other sources have indicated L-tryptophan has a progenitor.

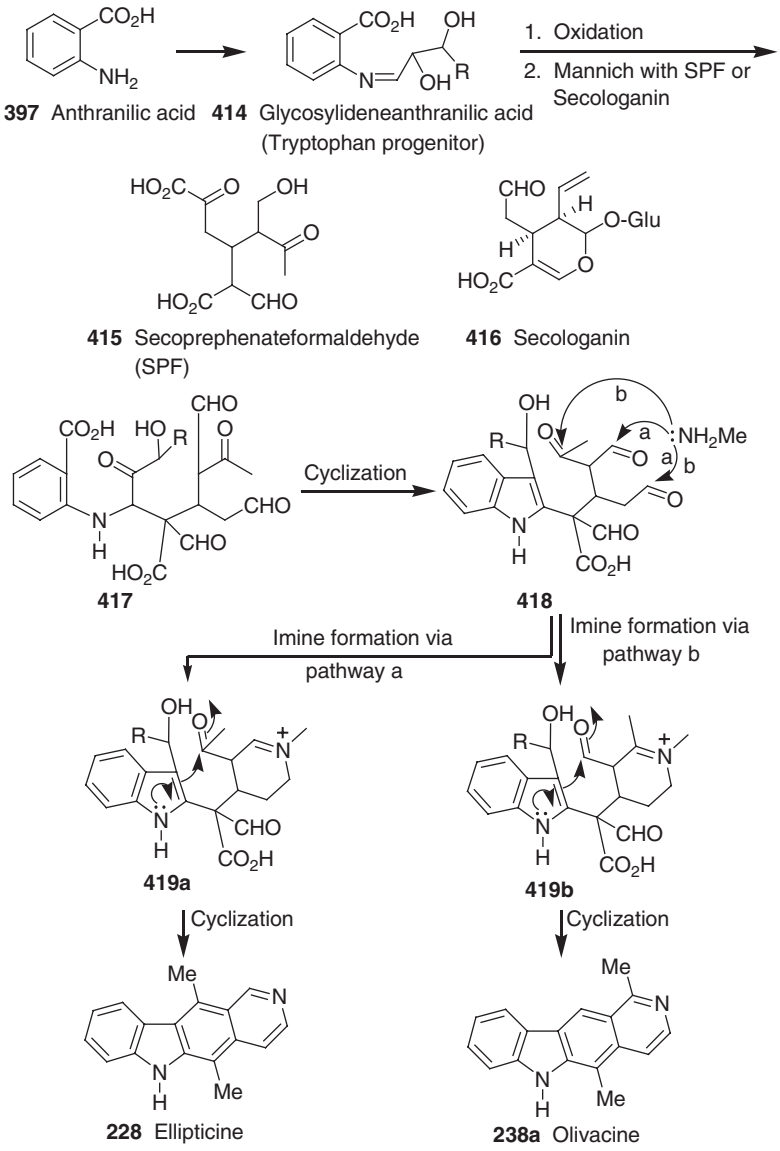

Scheme 3.10

In 1990, Nakamura *et al.* reported for the first time the complete biosynthetic origin of the whole carbon skeleton of carbazomycin B isolated from lower plants (378). Based on feeding experiments with ^{14}C- and ^{13}C-labeled compounds, followed by measurement of radioactivity and ^{13}C-NMR spectroscopy, it was shown that L-tryptophan (**408**) contributes to C-3 and C-4 of the hexasubstituted aromatic ring, in addition to the indole ring, indicating tryptophan as the progenitor of carbazomycin B (**261**), in contrast to Chakraborty's proposal of 2-methylcarbazole. The indole part of L-tryptophan (**408**) is formed by incorporation of two carbons from phosphoribosyl diphosphate (**430**), with loss of the anthranilic acid (**397**) carboxyl. The

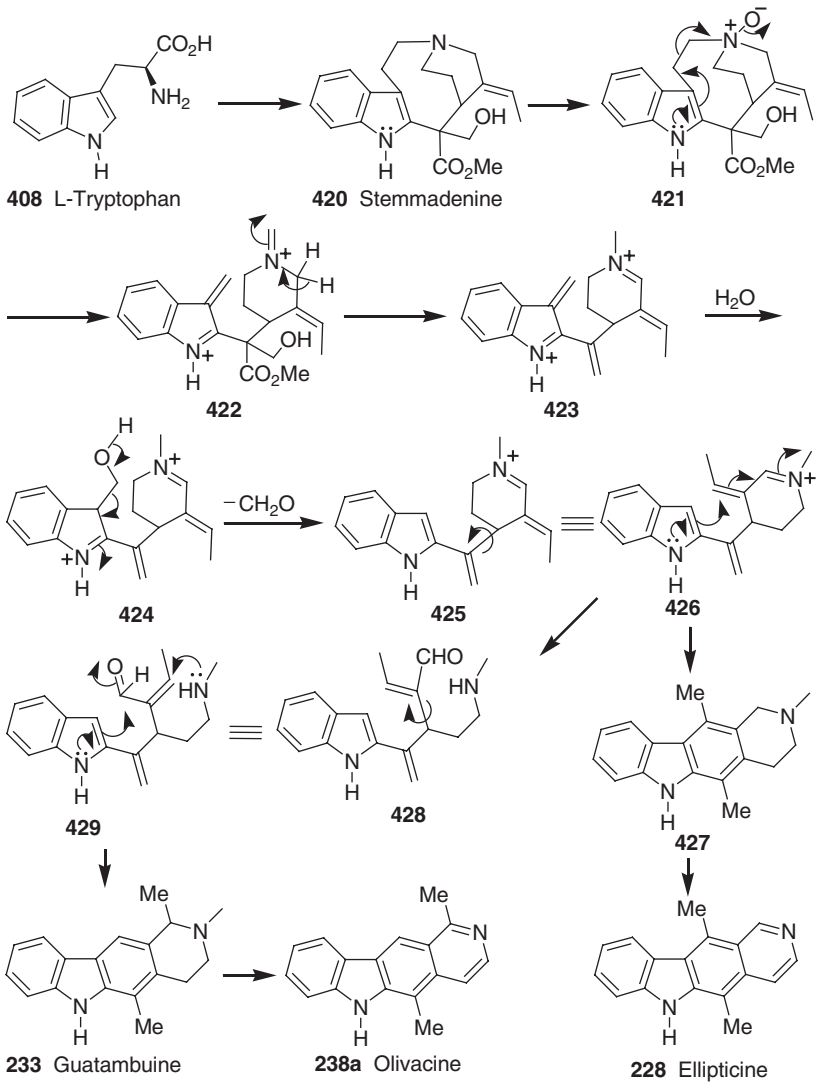

Scheme 3.11

remaining ribosyl carbons are removed by a reverse aldol reaction and replaced by L-serine (**434**), which becomes the side chain of L-tryptophan (**408**) (366). Further feeding experiments with ^{13}C-labeled alanine, which is known to be a biosynthetic equivalent for the two-carbon unit of pyruvate, followed by measurement of the ^{13}C-NMR spectra, indicated the origin of the C-1 and C-2 carbons and their methyl groups in the A-ring of the carbazole framework. Finally, a ^{13}C-labeled methionine experiment indicated the origin of the methyl of the methoxy group. All these experiments established that tryptophan (**408**), after decarboxylation and deamination, reacts with two molecules of sodium pyruvate (**436**), before methylation with methionine, to give the complete carbon skeleton of carbazomycin B (**261**) (234,378) (Scheme 3.12).

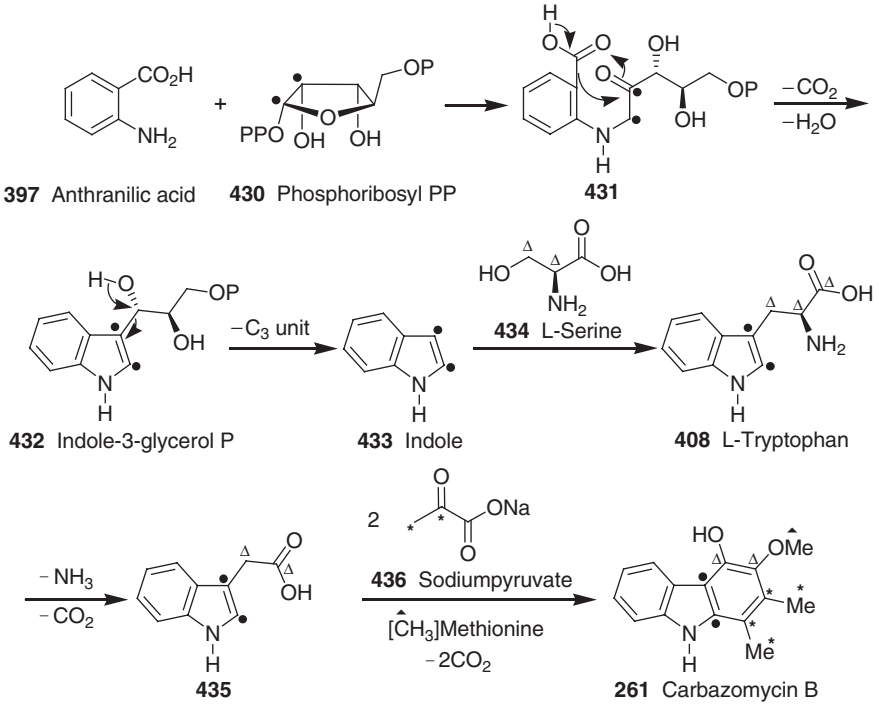

Scheme 3.12

Independently, in 1998, the Cordell (290,379,380) and Pearce (381) groups published some preliminary biosynthetic results on staurosporine and rebeccamycin, typical representative members of the indolo[2,3-*a*]pyrrolo[3,4-*c*]carbazole alkaloids. Cordell's biosynthetic studies on staurosporine were based on feeding experiments with L-tryptophan. These studies showed that two units of L-tryptophan, with the two carbon side-chains intact, were responsible for the biosynthesis of staurosporine aglycone. Further experimental studies are necessary to establish the nature of the intermediate in the biotransformation of L-tryptophan to staurosporine. Although these studies are not complete, they gave for the first time insight into the biosynthesis of staurosporine (379,380).

Pearce's biosynthetic model study for rebeccamycin, a halogenated natural product of the indolocarbazole family, demonstrated that this alkaloid is biosynthesized by *Lechevalieria aerocolonigenes* (322) (formerly *Saccharothrix aerocolonigenes*) from one unit of glucose, one unit of methionine, and two units of tryptophan. It was also shown that the α-amino group of neither tryptophan unit provides the nitrogen of the phthalimide function. From these studies it is presumed that D-glucose and L-methionine are probably incorporated *via* UDP-glucose and *S*-adenosylmethionine, respectively. Tryptophan is probably incorporated following deamination to yield indolepyruvic acid. In order to understand the complete biosynthetic pathway to rebeccamycin it is necessary to have experimental studies based on a corresponding chloro analogue of L-tryptophan (381).

Until the mid-1990s, knowledge on the biosynthesis of staurosporine (**295**), a pharmacologically interesting molecule was limited to the early steps, especially the

incorporation of tryptophan (290,379). In 1995, Hoehn *et al*. for the first time used a blocked mutant of *Streptomyces longisporoflavus* R19 for the demonstration of the biosynthetic path of staurosporine (**295**) by the isolation of *O*-demethylstaurosporine (3′-*O*-demethylstaurosporine) (**297**) in the last step of the biosynthetic pathway. In their studies, the staurosporine-producing strain *S. longisporoflavus* selected colony R 19/col 15 was taken as the parental strain, blocked mutant M13, responsible for the production of staurosporine aglycone (K-252c) (**293**) and M14, responsible for the production of *O*-demethylstaurosporine (**297**) from the staurosporine producer strain *S. longisporoflavus* R 19/col 15 were used for the mutation studies. The mutagenic treatment was performed by irradiation with a UV lamp (254 nm; 500 $\mu W/cm^2$). These studies led to the isolation of *O*-demethylstaurosporine (3′-*O*-demethylstaurosporine) (**297**), a direct precursor for staurosporine by blocked mutants of the staurosporine producer strain M14. By cofermentation and bioconversion experiments, the possibility that *O*-demethylstaurosporine (3′-*O*-demethylstaurosporine) (**297**) is produced by demethylation of staurosporine (**295**), by an enzyme which could be repressed in the parental strain, was excluded. Subsequent experiments have corroborated that *O*-methylation (382) is the final step in the biosynthetic pathway of staurosporine (**295**) and that the mutant M14 is lacking the *O*-methylase enzyme required for this step (294,383) (Scheme 3.13).

In 1996, Fredenhagen *et al.* proposed some plausible intermediates in the biosynthesis of K-252a (SF 2370) (**330**), based on the isolation of several, closely related, minor metabolites, either to staurosporine or to oxime TAN-1030A (**313**) (300), from the staurosporine-producing strain *S. longisporoflavus*. The absolute stereochemistry of TAN-1030A (**313**) was similar as K-252a (SF 2370) (**330**) at the bridging atoms 2′ and 5′. TAN-1030A might be formed by oxidation of the

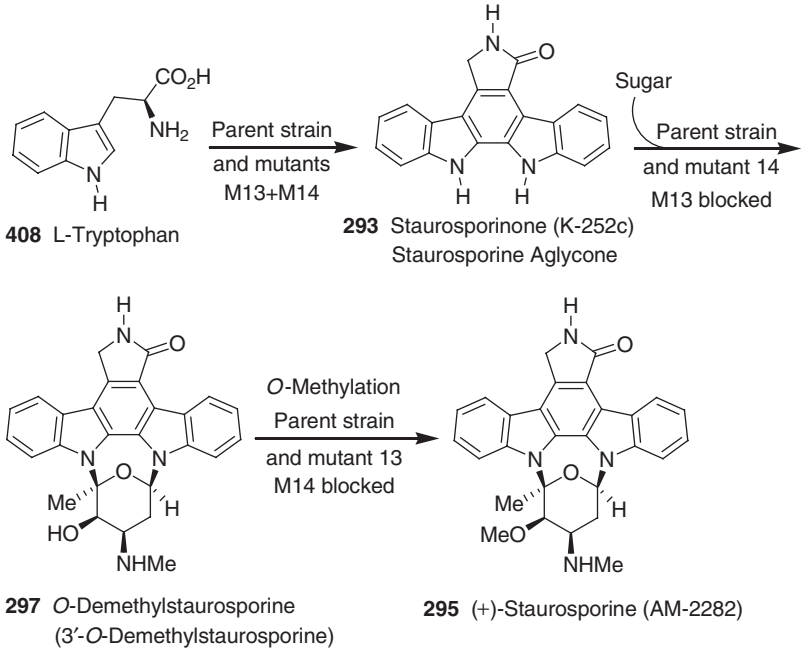

408 L-Tryptophan

293 Staurosporinone (K-252c)
Staurosporine Aglycone

297 *O*-Demethylstaurosporine
(3′-*O*-Demethylstaurosporine)

295 (+)-Staurosporine (AM-2282)

Scheme 3.13

corresponding ketone derivative, 4′-deoxime-4′-oxo-TAN-1030A (**316**) (see Scheme 2.80), another minor metabolite of strain *S. longisporoflavus* R 19, which could be easily formed by oxidation of a sugar hydroxy function. Ring contraction of TAN-1030A (**313**) under Beckmann conditions leads to **437** (384). It is therefore conceivable that TAN-1030A (**313**) is the biosynthetic precursor which is converted by the microorganism to the proposed intermediate **437**, which could not be isolated from fermentation broth; instead, the corresponding *N*-methyl derivative, 3′-methylamino-3′-deoxy-K-252a (**332**), was found. It could be presumed that the same enzyme which introduces the *N*-methyl group (382) into staurosporine might be responsible for this transformation and might be unable to discriminate between substrates with five- and six-membered ring systems. The free amino group of intermediate **437** could be converted to the hydroxy group of K-252a (SF-2370) (**330**). This metabolite was found to be co-produced in small amounts by the staurosporine-producing strain *S. longisporoflavus* R 19 (300) (Scheme 3.14).

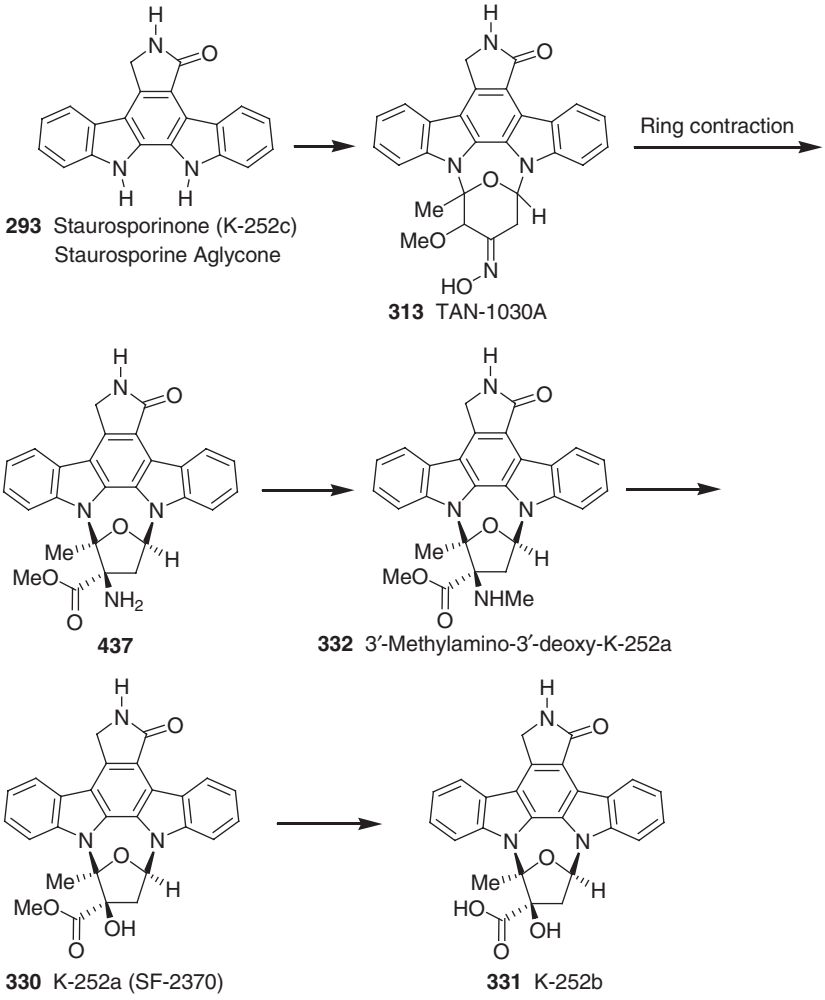

Scheme 3.14

Prior to these studies, the same authors isolated various minor metabolites related to staurosporine, and also staurosporine with a nitro function at C-4′. These studies suggest TAN-1030A (**313**) as a key intermediate for the degradation product of staurosporine and for the staurosporine congeners (301).

In 1994, Steglich *et al.* isolated lycogalic acid A (**443**) and staurosporinone (**293**), together with traces of arcyriaflavin A (**345**) and arcyriarubin A (**349**), from the slime mold (Myxomycetes) *Lycogala epidendrum* (385). The co-occurrence of these alkaloids points to a close biosynthetic relationship among them (252,255,385). Prior to this report on lycogalic acid A, Hoshino *et al.* reported the same alkaloid as a new metabolite of tryptophan from the mutant of *Chromobacterium violaceum* and named as chromopyrrolic acid (**443**). Tracer experiments with ^{13}C-tryptophan showed incorporation into chromopyrrolic acid, indicating the formation through the biosynthetic condensation of two molecules of tryptophan (386).

In 2006, Walsh *et al.* reported for the first time a complete enzyme-catalyzed biosynthetic pathway from L-tryptophan (**408**) [or 7-chloro-L-tryptophan (**438**)] to the staurosporine and rebeccamycin aglycons, K-252c (**293**) and 1,1-dichloroarcyriaflavin A (**446**) (387). These studies are in agreement with the previously reported biosynthetic pathways of staurosporine and rebeccamycin which are based on the isolation of putative intermediates of gene disruption studies from *Streptomyces* sp. TP-A0274 (388–390) and *L. aerocolonigenes* ATCC 39243 (391,392), respectively. Walsh's pathway uses a series of oxidative transformations (Scheme 3.15) involving the use of biosynthetic enzymes StaP, StaC, and RebC through an intermediate lycogalic acid (chromopyrrolic acid) (**443**) and dichlorolycogalic acid (dichlorodichlorochromopyrrolic acid) (**444**). The pathways to the two aglycons follow very similar routes, differing only by the chlorination at the 7-position of L-tryptophan *en route* to rebeccamycin, and the oxidation state of the pyrrole-derived five-membered ring, taking the form of a maleimide in rebeccamycin and a pyrrolinone in the staurosporine aglycone. Subsequent *N*-glycosylation (389) and tailoring modifications follow divergent pathways toward rebeccamycin (**337**) and staurosporine (**295**).

The formation of lycogalic acid (chromopyrrolic acid) (**443**), a key biosynthetic intermediate, through the joint action of RebO, an L-amino acid oxidase, and RebD (or StaD), a heme-containing oxidase, was shown to proceed *via* the condensation of two molecules of indole-3-pyruvic acid imine (**439**) (393). StaP and StaC (or RebP and RebC) are involved in aglycone ring construction. The overall reaction is catalyzed by StaP, a cytochrome P450 enzyme, and is intriguing, since it involves both aryl–aryl coupling to give the central six-membered ring of the indolocarbazole scaffold, as well as double oxidative decarboxylation to facilitate a net four- to eight-electron oxidation by converting lycogalic acid (chromopyrrolic acid) (**443**) into the three aglycone products, K-252c (**293**), arcyriaflavin A (**345**), and 7-hydroxy K-252c (**445**). It is pertinent to note that the ability of the StaP/StaC and StaP/RebC systems to transform possible biosynthetic intermediates to the final aglycon products showed that arcyriarubin A (**349**) is not a biosynthetic intermediate in the conversion of lycogalic acid (chromopyrrolic acid) (**443**) to the aglycon products, K-252c (**293**), arcyriaflavin A (**345**), and 7-hydroxy K-252c (**445**). Aglycons **293**, **345**, and **445** are not interconvertible, but appear to diverge from a common biosynthetic intermediate. Incorporation experiments with ^{18}O-labeled dioxygen or ^{18}O-labeled

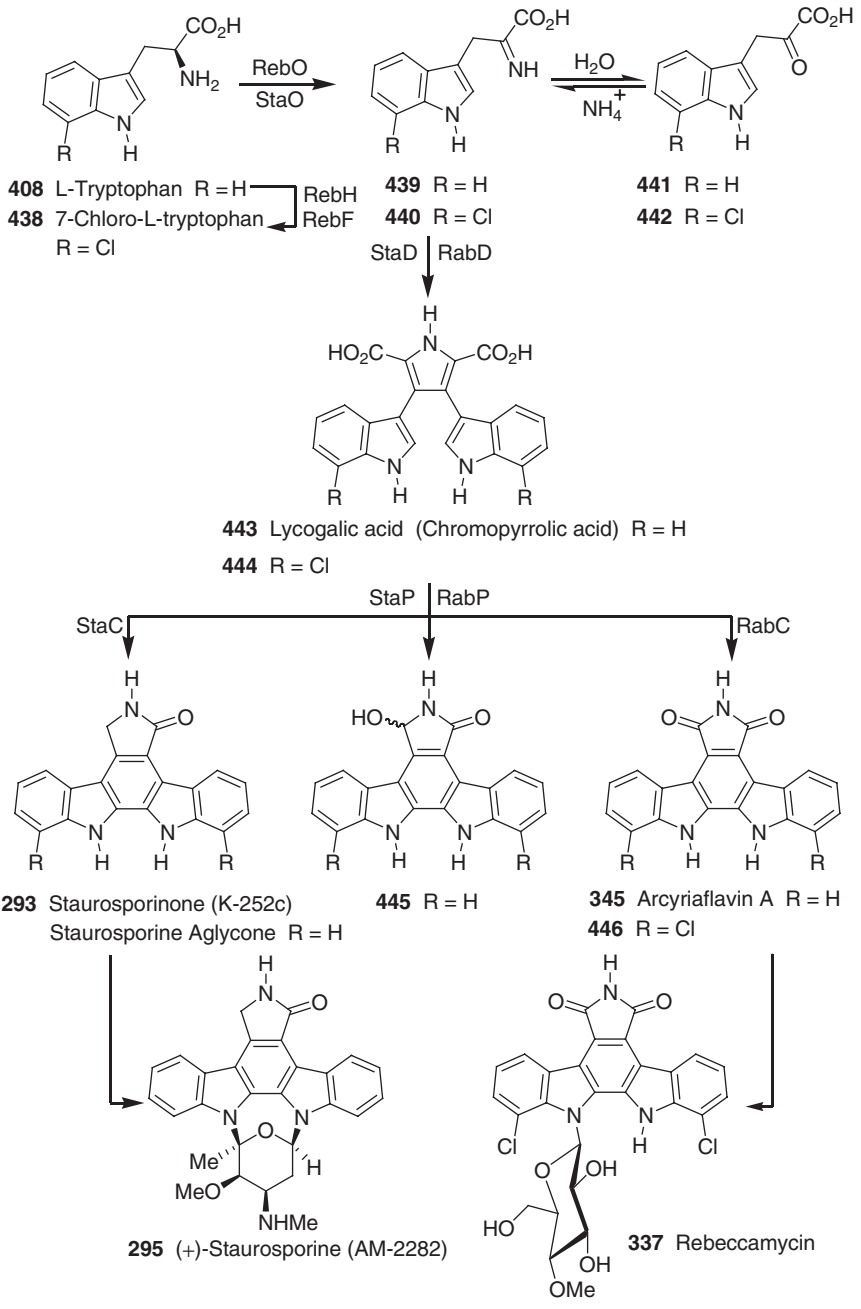

Scheme 3.15

water involving lycogalic acid (chromopyrrolic acid) (**443**) and the StaP/StaC and StaP/RebC systems demonstrated that the amide oxygen of K-252c (**293**) and both oxygens of arcyriaflavin A (**345**) are directly derived from dioxygen (387) (Scheme 3.15).

Examining the structures of the sesquiterpenoid carbazole alkaloids, tubingensins A (**379**), B (**380**), aflavazole (**381**), and dihydrotubingensins A (**382**) and B (**383**), it is likely that they are biogenetically related, and could have originated from a common intermediate, nominine (**448**) (394). This hypothesis was supported by the isolation of nominine (**448**) and 20,25-dihydrooxyaflavinine (**452**) from the sclerotia of the same *Aspergillus* spp. (347).

Although this biogenetic hypothesis is lacking experimental support, it is postulated that nominine (**448**), an indole diterpenoid alkaloid which functions as a key intermediate for the sesquiterpenoid carbazole alkaloids, tubingensins A (**379**) and B (**380**), aflavazole (**381**), and the dihydrotubingensins A (**382**) and B (**383**) arises from geranyl–geranylindole (**447**), a biogenetic precursor of the indole diterpenoid alkaloids (394).

Geranyl–geranylindole (**447**) would lead to dihydrotubingensin A (**382**) through nominine (**448**), with cyclization at the indole C-2, after the rotation around the indole C-3 bond. Dihydrotubingensin A (**382**), under dehydrogenation conditions, could form the aromatized analog, tubingensin A (**379**) (394). The co-occurrence of these two sesquiterpenoid carbazole alkaloids in *Aspergillus tubingensis* supports the

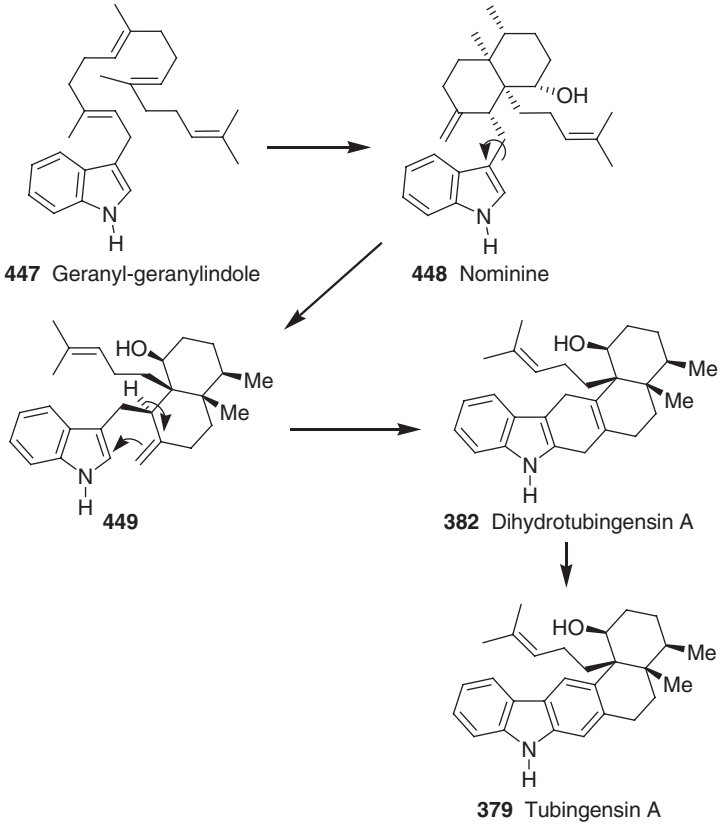

Scheme 3.16

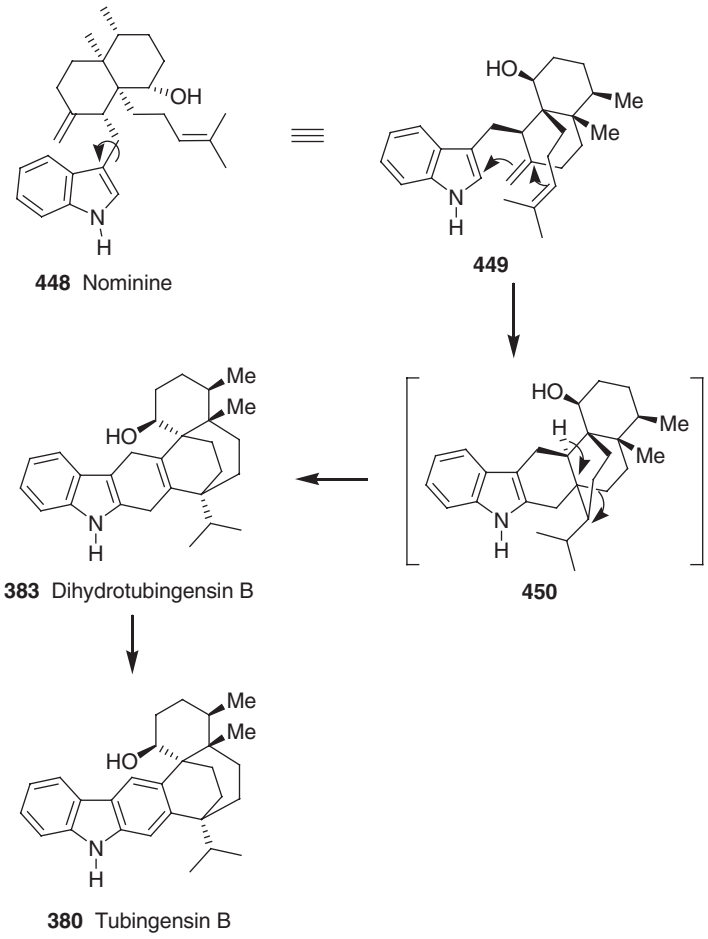

Scheme 3.17

oxidative transformation of the unstable dihydrocarbazole to tubingensin A (**379**) (349) (Scheme 3.16).

The formation of tubingensin B (**380**) starting from nominine (**448**) could be rationalized through dihydrotubingensin B (**383**), which is formed by cyclization at the indole C-2 of **449** involving the prenyl group and an exocyclic double bond, followed by ring expansion, as shown in intermediate **450**. The co-occurrence of dihydrotubingensin B (**383**) and tubingensin B (**380**) from *A. tubingensis* supports the oxidative transformation of the unstable dihydrocarbazole to tubingensin B (**380**) (349) (Scheme 3.17).

The formation of aflavazole (**381**) from the proposed common biosynthetic intermediate, nominine (**448**), could proceed through aflavinine (**451**) and 20,26-dihydrooxyaflavinine (**452**) by way of the transformations depicted in

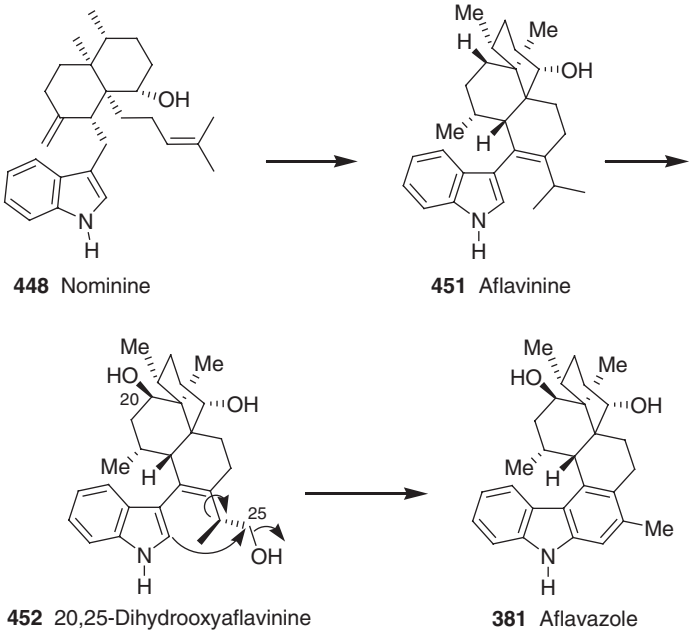

448 Nominine **451** Aflavinine

452 20,25-Dihydrooxyaflavinine **381** Aflavazole

Scheme 3.18

Scheme 3.18. The occurrence of nominine (**448**), aflavinine (**451**), 20,25-dihydrooxyaflavinine (**452**), and aflavazole (**381**) in the sclerotia of the same *Aspergillus* spp. may be considered circumstantial evidence in favor of this biogenetic proposal (347).

The occurrence of pityriazole (**389**), along with malasseziazoles A (**390**), B (**391**), and C (**392**), in the same source, namely, cultures of the human pathogenic yeast *Malassezia furfur*, indicates a common biogenesis among these structurally diverse carbazole derivatives. As proposed by Steglich *et al.*, pityriazole (**389**) and malasseziazole B (**391**) could be derived from a common biogenetic precursor **454** through the transformations shown in Scheme 3.19. Metabolite **454** in turn could be obtained by oxidative coupling of two indol-3-yl pyruvate (**441**) molecules at C-2 and C-3′, followed by thiamine pyrophosphate (TPP)-catalyzed decarboxylation of the resulting dimer **453** to the formyl derivative **454**. Dehydrogenation of **454**, followed by 6π-electrocyclization and aromatization, could lead to malasseziazole B (**391**), an indolo[2,3-*b*]carbazole. The formation of pityriazole (**389**), a structurally different 9*H*-carbazole derivative could be rationalized by a TPP-catalyzed C–C bond formation of **454**, followed by dehydration of the resulting hydroxy acid **455** (358) (Scheme 3.19).

In 1999, Rickards *et al.* proposed a rational biosynthetic approach for calothrixins A (**377**) and B (**378**), novel pentacyclic carbazole alkaloids with a quinolino[4,3-*b*] carbazole-1,4-quinone framework. This hypothesis uses a common metabolite **458**,

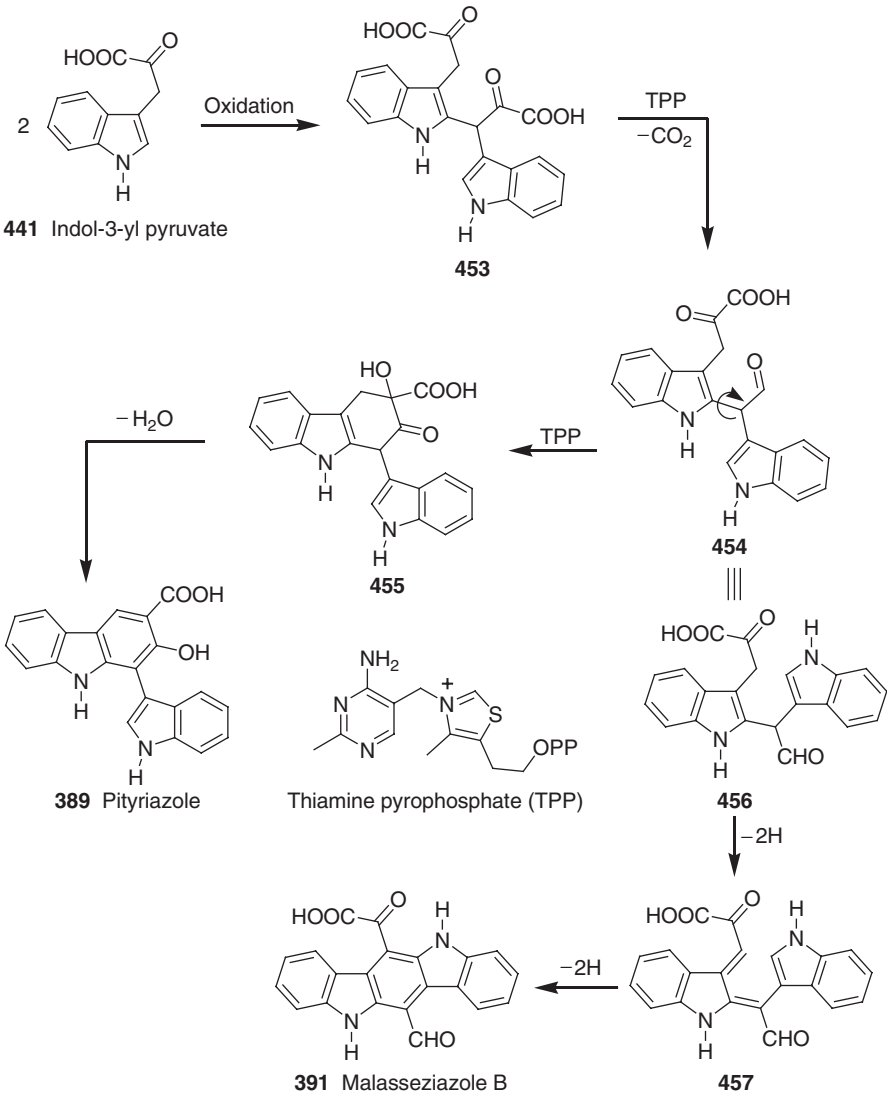

Scheme 3.19

which has an indolo[2,3-*a*]carbazole framework and is closely related to the known 5-cyano-6-methoxyindolo[2,3-*a*]carbazole (**358**) (see Scheme 2.93). Oxidation of the 4-aminophenol of the metabolite **458**, followed by hydrolytic cleavage of the corresponding quinone imine (**459**), would afford a 2-aminophenyl-substituted quinone **460**. Rotation around the biaryl bond and condensation of the amine with the formyl group or its equivalent would lead to calothrixin B (**378**). *N*-Oxidation of **378** would afford calothrixin A (**377**). Labeling studies with L-tryptophan (**408**), the established precursor of several indolo[2,3-*a*]carbazole metabolites (235), would also

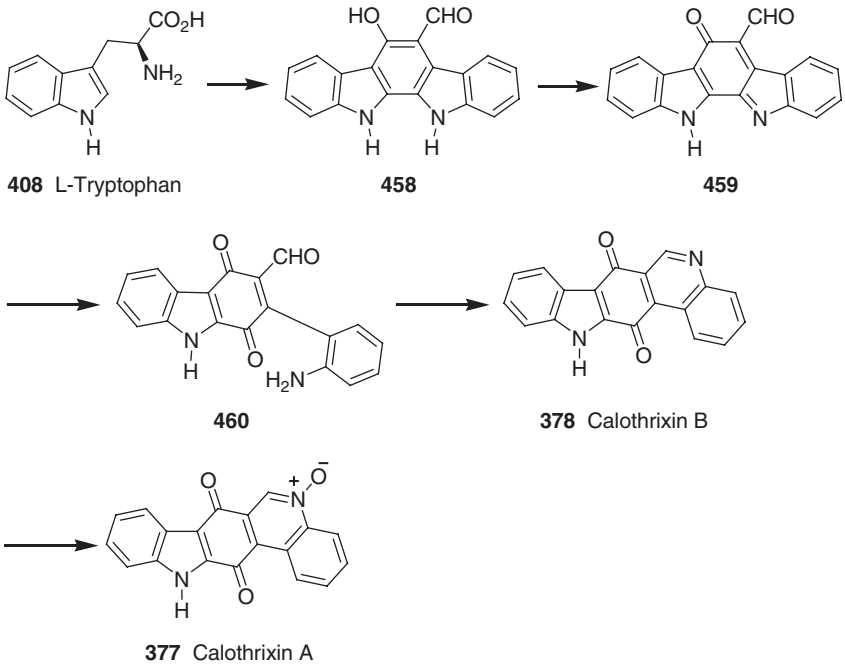

408 L-Tryptophan **458** **459**

460 **378** Calothrixin B

377 Calothrixin A

Scheme 3.20

support the formation of the common metabolite (**458**). The occurrence of the calothrixins A (**377**), B (**378**), and 5-cyano-6-methoxyindolo[2,3-*a*]carbazole (**358**) in cyanobacterial genera is circumstantial evidence in favor of this biogenetic pathway (345) (Scheme 3.20).

CHAPTER 4

Biological and Pharmacological Activities of Carbazole Alkaloids

Previously in this series, Kapil (1) and Chakraborty (3) described some of the biological properties of carbazole alkaloids. Since then, a great interest in this area has developed, as attested by some special reviews (7,8,190,192,194,195,255,256,259,260,395–397). In this section, we have summarized some of the important biological and pharmacological activities of this class of alkaloids.

I. ANTI-TUMOR ACTIVE CARBAZOLES

Cancer and related diseases represent one of the major causes of death for humankind. The etiology of cancer is multiple, but great progress has been made in recent times toward the understanding of these diseases with the discovery of oncogenes. Various natural products of plant and animal origin constitute the major sources for compounds affecting such oncogenes. With the passage of time, a wide range of synthetic analogs based on natural products emerged as therapeutically useful anti-tumor agents. Among these natural products, the carbazole alkaloids constitute one of the important classes of natural products. Within the carbazole alkaloids, natural and synthetic congeners of the pyrido[4,3-*b*]carbazole and the indolo[2,3-*a*]pyrrolo[3,4-*c*]carbazole alkaloids comprise a large group of therapeutically useful anti-tumor agents, either in current clinical use, or in the various stages of clinical development (190,192,194,195,255,256,259,260,395,396).

In addition to these classes of alkaloids, 7-methoxymukonal (3-formyl-2-hydroxy-7-methoxycarbazole) (**68**) (see Scheme 2.14) belongs to the 2-oxygenated, tricyclic carbazole alkaloid series and was more active in the brine shrimp lethality assay than 7-methoxyheptaphylline (**79**) (see Scheme 2.15), whereas against the human colon adenocarcinoma (HT-29), 7-methoxyheptaphylline (**79**) was more active than 7-methoxymukonal (3-formyl-2-hydroxy-7-methoxycarbazole) (**68**) (89). Koenoline (**8**) (see Scheme 2.4), which belongs to the 1-oxygenated tricyclic carbazole alkaloid series, has shown cytotoxic activity against cultured KB cells (32). Earlier than these reports, similar cytotoxic activity was also reported for girinimbine (**115**) (see Scheme 2.22) and mahanimbine (**139a**) (7) (see Scheme 2.27). Spurred by these results, further studies on *Murraya* species indicated that pyrayafoline D (isomahanine) (**138**)

(see Scheme 2.26) possessed brine shrimp lethality (398), and 9-formyl-3-methylcarbazole (**6**) (see Scheme 2.3) showed weak cytotoxicity against B16 mouse melanoma and adriamycin-resistant P388 mouse leukemia cell lines (17). Murrayaquinone A (**107**) (see Scheme 2.21) showed significant cytotoxicity against SK-MEL-5 and Colo-205 cells (399). Recently, pyrayafoline D (isomahanine) (**138**) (see Scheme 2.26) also showed significant cytotoxic activity against the human leukemia cell line HL-60. This cytotoxicity was mediated through apoptosis by activation of the caspase-9/caspase-3 pathway, through mitochondrial dysfunction (131). Similar activity was also shown by another pyrano[2,3-*a*]carbazole alkaloid, mahanine (**149**) (Scheme 2.29), and a bis-pyrano[2,3-*a*]carbazole alkaloid, murrafoline-I (**180b**) (see Scheme 2.39). This was the first report of the cytotoxic evaluation of bis-carbazole alkaloids (131).

In 1970, Rice *et al.* studied a diverse range of 3-substituted 1,2,3,4-tetrahydrocarbazole derivatives in a preliminary pharmacological screening for general stimulation, depression, and autonomic activity, and found that 3-carboethoxy-9-(3-dimethylaminopropyl)-1,2,3,4-tetrahydrocarbazole (**461**) exhibited growth inhibition at a concentration of 1 μg/mL in mammary carcinoma tissue (400). These studies were based on the carcinogenic activity observed for the bis-angular bis-benzocarbazoles reported by Buu-Hoï *et al.* (401).

Carbazole alkaloids with a benzo-annulated ring system are found very rarely in nature. However, a large structural variety of these ring systems was known as synthetic analogs due to their potential as anti-tumor agents. Among the various benzocarbazoles, a series of dihydrobenzo[*a*]carbazoles (**462**–**465**) with oxygen functions were shown to bind estrogen receptors and inhibit the growth of mammary tumors of rats (257,402,403). The benzo[*a*]carbazoles **466** and **467** exhibit pronounced cytotoxic activity against leukemia, renal tumor, colon cancer, and malignant melanoma tumor cell lines (257). Among the different 2-deazaellipticine derivatives, the benzo[*b*]carbazole **468** was found to have cytostatic activity against L1210 leukemia cells (194,404,405) (Scheme 4.1).

In 1984, Gribble *et al.* reported for the first time a novel 1,10-bis-(6-methyl-5*H*-benzo[*b*]carbazol-11-yl)decane (**469**) which has potential bifunctional nucleic acid intercalating properties (406). To function as anti-tumor active drugs, one of the most important cytostatic mechanisms of action of coplanar annelated polycyclic compounds is their intercalation with DNA (405). Ten years later, Kuckländer *et al.* studied a series of 5*H*-benzo[*b*]carbazole quinone derivatives for their cytotoxic activity against colon and lung cancer cells, and found that the heteroannelated 5*H*-benzo[*b*]carbazole quinone derivative **470** was the most active among the various analogs (407) (Scheme 4.2).

Ellipticine (**228**), a representative member of the pyrido[4,3-*b*]carbazole alkaloids and its analogs, was found to be highly active against various experimental tumors and leukemias. Although the parent alkaloid ellipticine is too toxic to be useful, an ellipticine analog, elliptinium (2-*N*-methyl-9-hydroxy ellipticine acetate-NMHE) (celiptium®, NSC 264-137) (**472**) was introduced in 1977 in cancer chemotherapy (197–201). Since then, pyridocarbazoles and related ring systems have made a tremendous development, both in the synthesis and in their biological evaluation. These were comprehensively reviewed by Suffness and Cordell in Volume 25 (408) and by Gribble in Volume 39 (192) of this series. In addition to these excellent reviews, there are several other important articles that provide coverage of the biological profile of the ellipticine alkaloids, together with their synthesis

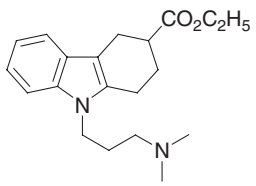

461

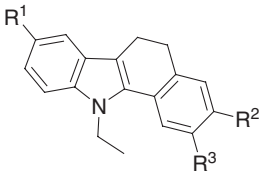

462 R^1,R^2 = OAc; R^3 = H
463 R^1,R^3 = OAc; R^2 = H

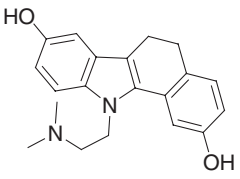

464

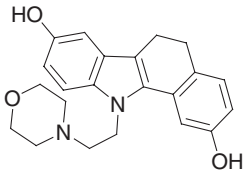

465

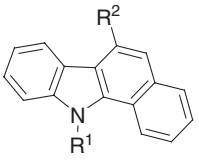

466 R^1 = SO_2Ph; R^2 = H
467 R^1,R^2 = Me

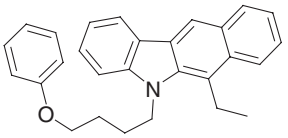

468

Scheme 4.1

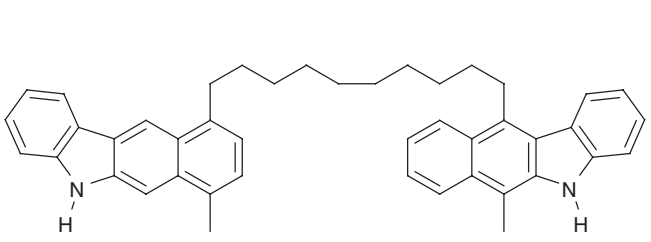

469

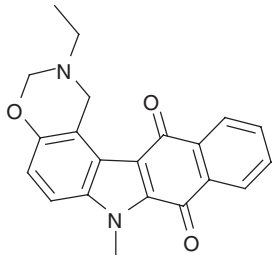

470

Scheme 4.2

(8,185,189,190,194,195). Besides the clinically active monointercalator elliptinium, ditercalinium® (NSC 335 153) (**471**), a bis-intercalator of DNA is also used in clinical trial for the treatment of cancer (409).

In the late 1980s, a second generation of ellipticine-derived anti-tumor agents was developed, including the new clinical candidates, datelliptium [2-(diethylamino-2-ethyl)-9-hydroxyellipticinium chloride-DHE] (**473**) (192,410), retellipticine (BD-84) (**474**) (192,411), and pazellipticine (PZE, BD-40) (**475**) (192,412) (Scheme 4.3). Datelliptium (**473**), which was obtained by simple modification of the *N*-2 methyl group of elliptinium (**472**), showed better *in vivo* activity than elliptinium in the L1210, P388, B16, colon 38, and M5076 reticulosarcoma test systems. The increased anti-tumor potency is believed to be due to increased diffusion across cellular membranes and a more favorable biodistribution *in vivo* (410). Similar to datelliptium, retellipticine (BD-84) (**474**) showed potent activity against P388, L1210, B16, M5076, and colon 38 systems *in vivo* (411). An azaellipticine derivative, pazellipticine (PZE, BD-40), has excellent *in vitro* activity against L1210 cells (412).

The complete *in vivo* anti-tumor mechanism of action of ellipticine and its derivatives is still not well understood. However, a tremendous amount of work has

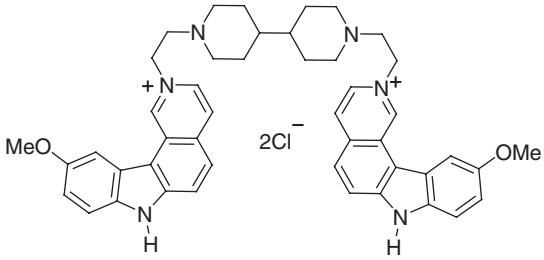

471 Ditercalinium,® (NSC 335153)

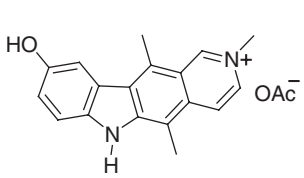

472 Elliptinium (Celiptium,® NMHE, NSC 264-137)

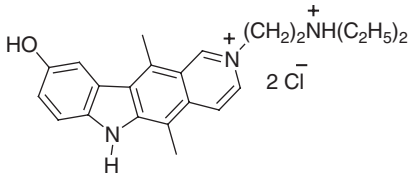

473 Datelliptium (DHE)

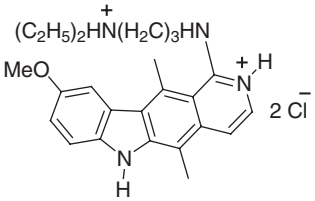

474 Retellipticine (BD-84)

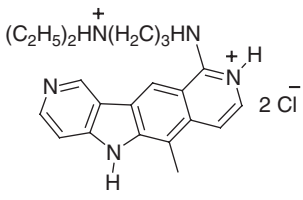

475 Pazellipticine (BD-40)

Scheme 4.3

been carried out to solve this enigma, and based on these studies it may be concluded that ellipticine and derivatives interact *in vivo* by more than one mechanism (189). Among these various mechanisms, one of the most widely supported mode of action of monointercalators, such as ellipticine and its derivatives, for the cytotoxic activity is DNA strand breakage associated with the enzyme topoisomerase II. In performing its role in the cleavage and rejoining of DNA strands (catenation, decatenation, relaxation, unknotting), topoisomerase II binds to the 5-phosphate on adjacent DNA strands four base pairs apart to form an enzyme–DNA complex. It is the interaction between this complex and certain drugs, such as ellipticine and derivatives, which results in the stabilization of the complex and the formation of a cleavable complex, leading eventually to the cleavage of double stranded DNA (189). Unlike ellipticine and its derivatives, detercalinium does not stimulate DNA cleavage by DNA topoisomerase II. In contrast, its anti-tumor activity is through a new mechanism characterized by a delayed toxicity on L1210 cell cultures (409).

In addition to the aforementioned drugs, clinical trials of several other natural pyrido[4,3-*b*]carbazole alkaloids and a number of synthetic analogs showed them to be potent inhibitors of several cancerous disorders, but pre-clinical toxicology indicated a number of side effects, including hemolysis and cardiovascular effects (192).

Although the indolo[2,3-*a*]pyrrolo[3,4-*c*]carbazole alkaloids were found to exhibit various biological activities, the greatest interest is focused on compounds that possess anti-tumor and neuroprotective properties. These activities may be due to different mechanisms of action, including DNA intercalation, inhibition of DNA topoisomerases, and inhibition of protein kinases. These efforts generated indolocarbazole derivatives with improved properties for the treatment of cancer, neurodegenerative disorders, and diabetes-associated pathologies; as a result, several analogs have entered clinical trials (255,256,259,260,270,395,396).

Based on their structural features and mechanism of anti-tumor activity, the indolo[2,3-*a*]pyrrolo[3,4-*c*]carbazole alkaloids are divided into two major groups. One group includes the inhibitors of DNA topoisomerase I, such as rebeccamycin and its congeners, without inhibitory properties toward kinases, such as CDK1/cyclinB, CDK5/p25, and PKC. Most of the members of this group contain a sugar moiety attached by a β-glycosidic linkage to one of the indole nitrogen atoms of the aglycon. Localized in the cell core, topoisomerase I controls the topology of DNA, and takes part in replication, transcription, and recombination processes. Topoisomerase I also relaxes the superstranded DNA through single-chain rupture and subsequent reunion of chains. Rebeccamycin and its derivatives were found to induce the cleavage of DNA with topomerase I due to stabilization of the DNA–enzyme complex. The stabilization of DNA with a single-chain rupture is fatal for rapidly dividing cells (by the mechanism of apoptosis). Rebeccamycin (**337**) (see Scheme 2.86) is undergoing phase III clinical testing as an anti-tumor agent. Other derivatives such as NSC 655649 (**476**) (413–415), bacatecarin® (BMY 27557, XL 119, BMS 181176) (**477**) (416), Edotecarin® (ED-749, J-107088) (**478**) (417,418), NB 506 (L-753000) (**479**) (419–421), and BMS-250749 (**480**) (422), a fluoro-glycosylated fluoroindolocarbazole are at various stages of development (270) (Schemes 4.4 and 4.5).

The second group of compounds includes the protein kinase C (PKC) inhibitors, such as staurosporine and its derivatives. Usually, they contain a sugar moiety linked

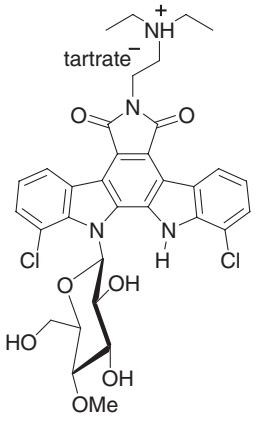

476 NSC 655649

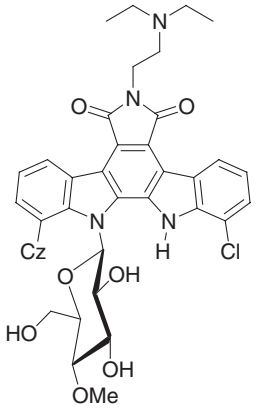

477 Bacatecarin®
(BMY 27557, XL 119
BMS 181176)

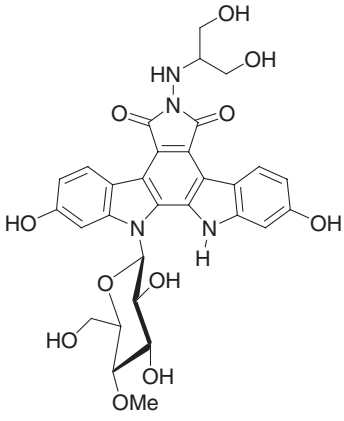

478 Edotecarin®
(ED-749, J-107088)

Scheme 4.4

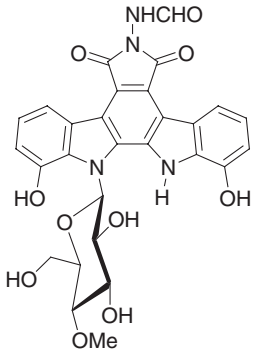

479 NB 506 (L-753000)

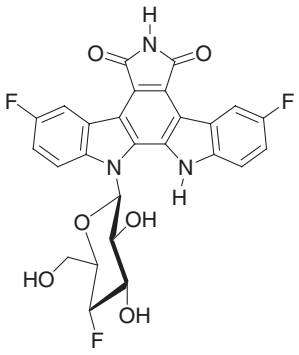

480 BMS-250749

Scheme 4.5

to both indole nitrogen atoms of the indolocarbazole core. Protein kinases play a key role in the transfer of information from the cell periphery to its nucleus, and to the apparatus of gene transcription. The activation of PKC upon coupling of a receptor with a ligand modulates the activity of the target proteins due to transfer of the phosphate group of ATP to the OH groups of serine or threonine in these proteins. Target proteins can act as regulators of gene differentiation, proliferation, expression, including the induction of multiple resistances of tumor cells to the action of drugs. PKC can also regulate the angiogenesis, invasiveness, and programmed cell death. Therefore, inhibitors of PKC can be regarded as potential anti-tumor agents. At least 12 different isoforms of PKC may be expected to occupy various positions in the cell and tissues. A basic problem in the development of PKC inhibitors is the selectivity with respect to other kinases, and also to different isoforms of PKC. Many derivatives of staurosporine, K-252a, and their analogs have been prepared in order to obtain more specific PKC inhibitors in both the indolocarbazole and 2,3-bis(indol-3-yl)maleimide series, based on structure activity relationship studies. These studies led to more efficient and more specific compounds which entered phase I and II clinical trials. UCN-01 (**325a**) (see Scheme 2.83), the C-7 hydroxy derivative of staurosporine, entered phase I and II clinical trials in combination with topotecan in ovarian cancers, and in combination with cisplatin or carboplatin in patients with advanced refractory solid tumors (423–426). CGP 41251 (PKC412, *N*-benzoyl staurosporine) (**481**) entered a phase I pharmacokinetic study (427,428). CEP-701 (**482**), a derivative of the bacterial metabolite K-252a, is a tyrosine kinase inhibitor and has entered phase II clinical trials for the treatment of acute myelogenous leukemia (429). CEP-1347 (KT-7515) (**483**), a 3,9-disubstituted (alkylthiomethyl)-K-252a derivative, has the ability to inhibit cell death and maintain the trophic status of neurons in culture by inhibiting the activation of the c-Jun *N*-terminal kinase (JNK) pathway (430). The possible importance of the JNK pathway in neurodegenerative diseases such as Alzheimer's and Parkinson's diseases provides a rationale for the use of CEP-1347 for the treatment of these diseases (431) (Scheme 4.6).

Gö 6976, a non-glycosidic/non-aminoalkyl substituted indolocarbazole lactam was shown to be a potent and selective PKC inhibitor with a remarkable

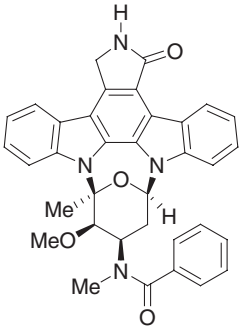

481 CGP 41251 (PKC412)

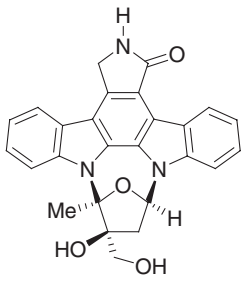

482 CEP-701

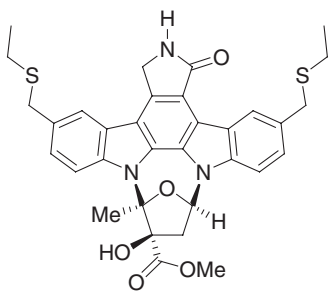

483 CEP-1347 (KT-7515)

Scheme 4.6

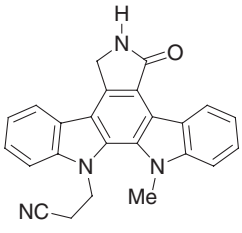

484 Gö 6976

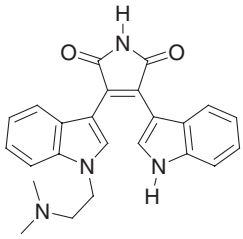

485 Gö 6850 (GF109203X)

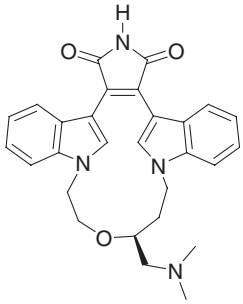

486 LY-333531

Scheme 4.7

discrimination between Ca^{2+}-dependent subtypes α and β1 and the Ca^{2+}-independent isoforms δ, ε, and ζ. Gö 6976 inhibits HIV-1 induction by bryostatin 1 (a PKC activator), tumor necrosis factor α, and interleukin 6 (256) (Scheme 4.7).

Gö 6850 (GF-109203X) (**485**), a dimethylaminoethyl analog of 2,3-bis(indol-3-yl) maleimide was shown to be a selective inhibitor of PKC with anti-inflammatory activity in several *in vivo* and *in vitro* murine models of acute inflammation (432) (Scheme 4.7).

Eli Lilly's LY-333531 (**486**), a new macrocyclic analog of staurosporine, was discovered to be a potent and specific inhibitor of the PKC β-isozymes, indicating it to be a clinically useful agent for PKC-mediated human diseases, such as the vascular dysfunctions associated with diabetes mellitus (433,434) (Scheme 4.7).

In addition to the aforementioned natural and synthetic analogs of staurosporine and rebeccamycin, a number of non-glycosidic indolocarbazoles and staurosporine-related bisindolylmaleimides, such as the arcyriaflavin derivatives (see Scheme 2.89), are currently being evaluated in human clinical trials as anti-tumor agents (256,396,435,436). In addition to this activity, these derivatives have shown antimicrobial activity against *Bacillus cereus* and anti-viral activity against human cytomegalovirus (HCMV) (437,438). Comparison of the D1/CDK4 inhibitory activity of arcyriaflavin derivatives (see Scheme 2.89) and their bis-indolylmaleimide

counterparts (see Scheme 2.90) indicated that arcyriaflavin derivatives are selective G1 blockers, while the bis-indolylmaleimides arrest cells in the G2/M phase (439). Cyclin–CDK complexes regulate the progression of cells through the cell cycle. To date, strong evidence suggests a G1-phase role for D-type cyclins through the association with CDK4 and CDK6. CDK2 complexes with cyclin E and participates in the G1/S transition, whereas association with cyclin A peaks at S phase and may have a profound effect on proliferation. Moreover, CDK1 (Cdc2) plays an essential role in mitosis by interaction with B-type cyclin in the G2/M transition (439,440).

The dictyodendrin class of carbazole alkaloids (see Schemes 2.70 and 2.71) completely inhibit telomerase activity (at a concentration of 50 μg/mL). It is known that 90% of human tumors show telomerase activity, which is absent in normal cells. Telemorase is a ribonucleoprotein enzyme that adds repeating known telomers to the DNA sequence (251).

II. ANTIBIOTIC CARBAZOLES

Among the various carbazole derivatives, murrayanine (3-formyl-1-methoxycarbazole) (**9**) (see Scheme 2.4) was the first carbazole alkaloid isolated from a natural source and it shows antimicrobial properties (35). In 1978, Das *et al.* studied the insecticidal and antimicrobial properties of some carbazole, tetrahydrocarbazole, and 1-oxotetrahydrocarbazole derivatives (352). The antibiotic properties of carbazomycin B (**261**) (see Scheme 2.64) and related alkaloids attracted wider attention. Carbazomycin B was active against *Glomerella cingulate* No. 3 and *Elsinoë fawcetti* at a MIC of 3 μg/mL, whereas against *Trichophyton asteroides* 429 and *Trichophyton mentagrophytes* 833 it was active at a concentration of 12.5 μg/mL (231). 4-Deoxycarbazomycin B (**487**), a degradation product of carbazomycin B, showed significant inhibitory activity against various Gram-positive and Gram-negative bacteria (441) (Scheme 4.8).

In 2003, Sunthitikawinsakul *et al.* described the anti-mycobacterial activity of various 3-methylcarbazole derivatives, including 3-formylcarbazole (**3**), methyl carbazole-3-carboxylate (**4**) (see Scheme 2.2), clausine K (clauszoline-J) (**51**) (see Scheme 2.11), and 7-methoxymukonal (**68**) (see Scheme 2.14) against *Mycobacterium tuberculosis* H37Ra. Except for clausine K (clauszoline-J) (**51**), all of these alkaloids also showed anti-fungal activity against *Candida albicans* (442). In 2005, Franzblau *et al.* reported the *in vitro* anti-TB activity of various carbazole derivatives such as 3-formylcarbazole (**3**), methyl carbazole-3-carboxylate (**4**) (see Scheme 2.2), lansine

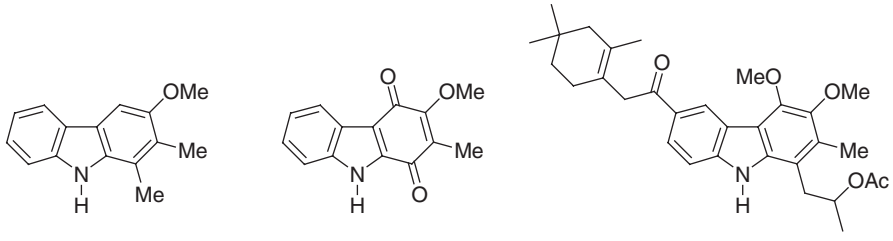

487 4-Deoxycarbazomycin B **488** **489**

Scheme 4.8

(**69**) (see Scheme 2.14), 3-formyl-6-methoxycarbazole (**97**), and micromeline (**100**) (see Scheme 2.19) against *M. tuberculosis* (H37Rv) (103).

Recently, in the screening of carbazole derivatives for inhibition of *M. tuberculosis* growth, two synthetic analogs, the carbazole-1,4-quinone **488** and the 6-acylcarbazole **489**, with MIC values of 2.2 and 4.0 μg/mL against *M. tuberculosis* were identified; these compounds were relatively non-toxic for the mammalian cell line (443–445) (Scheme 4.8).

The alkaloid K-252a (**330**) (see Scheme 2.85) was examined against several microbes and found to be active against *Micrococcus luteus*, *Micrococcus flavus* FDA16, and *Corynebacterium bovis 1810* with a MIC of 6.25 μg/mL (314).

In 1986, researchers at Bristol-Myers and Schering Plough reported the antimicrobial properties of AT2433-A1 (**339**), AT2433-A2 (**340**), AT2433-B1 (**341**), and AT2433-B2 (**342**) (see Scheme 2.87). All these derivatives are active against Gram-positive bacteria, such as *M. luteus* (ATCC 9341), *Bacillus subtilis* (ATCC 6633), *Staphylococcus aureus* (A 9537), *Streptococcus faecalis* (A 20688), and *Streptococcus faecium* (ATCC 9790). AT2433-B2 (**342**) has shown activity against the Gram-negative bacterium *Escherichia coli* SS 1431 (326,327).

In addition to these carbazole alkaloids, isomers of glycozoline and girinimbine were tested against various microbes and found to be active against *S. aureus* (446). Some aminoacyl carbazoles were found to be active against *B. subtilis* (ICC-Strain) and *B. cereus* (NRRL-B-569) (447).

III. ANTI-VIRAL CARBAZOLES

The tubingensins A (**379**) and B (**380**) showed activity against the widespread crop pest *Heliothis zea*, and display *in vitro* anti-viral activity against herpes simplex virus type 1 with IC_{50} values of 8 and 9 μg/mL, respectively (346) (see Scheme 2.100). Some bis-basic ethers of carbazoles are anti-viral. When tested against *Encephalo myocarditis* viral infection, several *N*-ethyl substituted bis-basic carbazoles of the general formula **490** were shown to be active (448) (Scheme 4.9).

In 2000, Boyd *et al.* reported for the first time an anti-HIV active carbazole alkaloid, siamenol (**89**) (see Scheme 2.17). This prenylated carbazole alkaloid inhibited HIV-1 induced cytopathic inhibitor activity in an XTT-tetrazolium assay with EC_{50} 2.6 μg/mL (85,449). Recently, Kongkathip *et al.* reported anti-HIV-1 activity for *O*-methylmukonal (glycosinine) (**38**) (see Scheme 2.9), 7-methoxy-*O*-methylmukonal (2,7-dimethoxy-3-formylcarbazole) (**48**) (see Scheme 2.10), and clausine K (clausazoline-J) (**51**). These studies showed strong anti-HIV-1 activity for

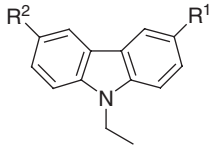

490 R^1 = COOR, $CONMe_2$
R^2 = Et, Bu, Hexyl

Scheme 4.9

O-methylmukonal (glycosinine) (**38**) with an EC_{50} value of 12 μM, and an IC_{50} of 680 μM for inhibition of tetrazolium conversion to formazan. Therefore, it had a potential therapeutic index (PTI) of 56.7, while 7-methoxy-*O*-methylmukonal (3-formyl-2,7-dimethoxycarbazole) (**48**) and clausine K (clauszoline-J) (**51**) exhibited anti-HIV-1 activity with EC_{50} values of 29.1 and 34.2 μM, respectively. These alkaloids did not exert reverse transcriptase (RT) inhibitory activity, indicating interaction at another stage(s) in the replication cycle of HIV-1 (58). Likewise, the carbazole alkaloids, glybomine B (**60**) (see Scheme 2.12) and glycoborinine (**174**) (see Scheme 2.36) indicated weak to moderate anti-HIV activity with IC_{50} values of 9.73 and 4.47 μg/mL, respectively (450).

IV. ANTI-INFLAMMATORY CARBAZOLES

The anti-inflammatory properties of several carbazole derivatives have attracted widespread attention. Some acidic tetrahydrocarbazoles have been shown to have anti-inflammatory activity (451). Among these derivatives, 1-ethyl-8-*n*-propyl-1,2,3,4-tetrahydrocarbazole-1-acetic acid (**491**) was found to be a novel anti-inflammatory agent (451), and 6-chloro-1,2,3,4-tetrahydrocarbazole-2-carboxylic acid (**492**) was clinically active in the treatment of acute gout (452).

Carprofen (**493**), a COX-2 (cyclooxygenase) inhibitor, has received significant attention as a substitute for non-steroidal anti-inflammatory drugs (453). Its activity is comparable to indomethacin, with less toxic side effects (production of gastric ulcers and blockade of diarrhea). *In vitro* cellular effects of carprofen (**493**) were found to be higher than those of ibuprofen, and were almost comparable to those of hydrocortisone. The anti-inflammatory activity of carprofen is probably dependent on inhibition of some neutrophil–macrophage function (454). It stimulates acid secretion without effecting basal acid secretion. The enhancement of secretagogue-stimulated acid secretion was dependent on extracellular calcium. It was suggested that the compound acts at a post-receptor site between adenylate cyclase and a protein pump. The drug probably increases calcium efflux through the plasma membrane and decreases the endogenous prostaglandin E_2 content. Carprofen was approved for use in dogs, cows, and horses as Imadyl® or Rimadyl® as an anti-inflammatory drug with weak ulcerogencity activity and fecal occult bleeding (455) (Scheme 4.10).

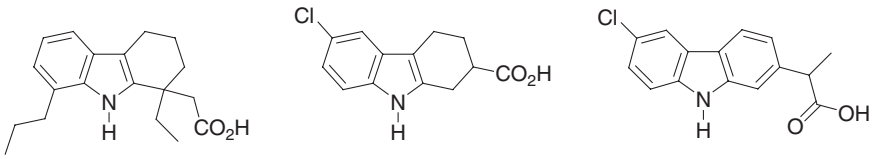

491 **492** **493** Carprofen (Imadyl®, Rimadyl®)

Scheme 4.10

V. ANTI-MALARIAL CARBAZOLES

In 1998, Bringmann *et al.* reported the anti-plasmodial activity of a series of mono- and bis-natural and structurally modified carbazoles and found that the synthetic compound 1,4-diacetoxy-3-methylcarbazole (168) showed higher activity (IC_{50} 1.79 μg/mL) against *Plasmodium falciparum* than natural 1-hydroxy-3-methylcarbazole (**23**) (see Scheme 2.6) (166). In the following year, Rickards *et al.* reported the anti-malarial active quinolino[4,3-*b*]carbazole-1,4-quinone alkaloids, calothrixins A (**377**) and B (**378**) (see Scheme 2.99) from photoautrophic cultures of *Calothrix* cyanobacteria. These carbazole alkaloids inhibited the growth *in vitro* of a chloroquine-resistant strain of the malaria parasite, *P. falciparum* at nanomolar concentrations (345).

In 2000, Yenjai *et al.* reported the anti-plasmodial activity of 2-oxygenated carbazole alkaloids against *P. falciparum*. In their studies, clausine H (clauszoline-C) (**50**) (see Scheme 2.11) and heptaphylline (**76**) (see Scheme 2.15) showed activity with IC_{50} values of 3.2–6.4 and 5.5–10.7 μg/mL, respectively (456). Prior to these studies, a report on the anti-plasmodial activity of 3- and 4-carbazole dialkylaminocarbinols had appeared (457).

VI. DIVERSE PHARMACOLOGICALLY ACTIVE CARBAZOLES

N-Alkylamino carbazoles (e.g., **494** and **495**) possess significant anti-convulsant and diuretic activity. Introduction of an aminopropyl chain at the *N*-atom seems to enhance the anti-convulsant activity in combination with methoxy groups at positions 2, 3, and 4, or a chlorine atom at the C-2 and C-3 positions (458).

Rimcazole® (BW 234U) (**496**) is a novel anti-pyretic, neuroleptic agent. It was found to be a specific competitive antagonist of σ-sites in the brain. It reverses psychotic conditions induced in humans by phencyclidine and/or σ-opiod antagonists, probably by binding to receptors in the brain (459–461). Rimcazole has an indirect effect on dopamine neurons with relative selectivity for A10 dopamine cells (462).

Some neuroleptic agents, like cycloindole (**497**), which has a modified tryptamine structure, and flucindole (**498**), a difluoro analog of cycloindole, have found use in therapy because of their anti-depressant and anti-psychotic activity (463,464) (Scheme 4.11). 3-Chlorocarbazole (**385**) (see Scheme 2.102), isolated from female bovine urine, has Diazepam-like activity (354).

In 1997, carvedilol (Coreg®, Kredex®) (**499**), a vasodilating β-adrenergic blocking agent, was approved for the treatment of hypertension and heart failure (465). In addition, carvedilol is also approved for the treatment of angina (465). Carvedilol is a multiple action, non-specific β- and α_1-adrenergic receptor blocker (465–468) and a potent anti-oxidant agent (469) (Scheme 4.12).

Carazolol (BM 51.052) (**500**), a further β-adrenergic blocking carbazole derivative, was prescribed as a veterinary medicine for use in pigs to relieve the stress of parturition, reduce the incidence of the mastitis, metritis, agalactia syndrome, prevent frenzy during mating, and alleviate tachycardia. However, it is most widely used to reduce stress during transportation from farm to slaughterhouse, and the subsequent incidence of pale, soft, and exudative (PSE) meat caused by stress-induced accelerated glycogen metabolism in muscle. Unlike other clinically

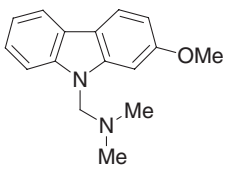

494

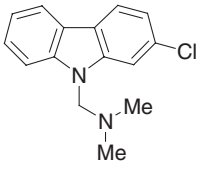

495

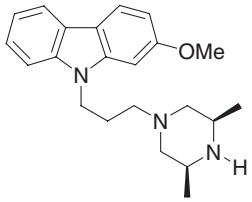

496 Rimcazole® (BW 234U)

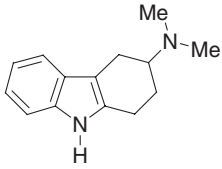

497 Cycloindole

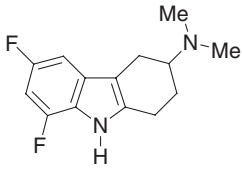

498 Flucindole

Scheme 4.11

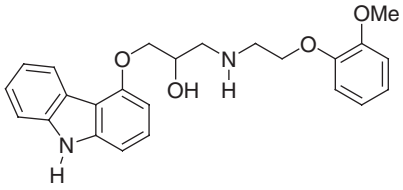

499 Carvedilol (Coreg®, Kredex®)

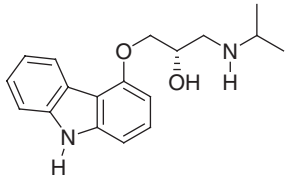

500 Carazolol®(BM 51.052)

Scheme 4.12

employed β-blockers, carazolol is largely devoid of intrinsic sympathomimetic activity (470–472) (Scheme 4.12).

Murrayaquinone A (**107**) (see Scheme 2.21) was found to produce a triphasic inotropic response of guinea-pig papillary muscle. This triphasic inotropic response is not mediated through a receptor mechanism, but through a mechanism involving ATP production (473).

Ramatroban (BAY U 3405) (**501**) functions as a novel, dual antagonist of the thromboxane A_2 (TXA_2) receptor and chemoattractant receptor-homologous molecule expressed on Th2 cells (CRTh2), a newly identified prostaglandin D_2 (PGD_2) receptor (474,475). It is known that TXA_2 contributes to various diseases such as bronchial asthma, ischemic heart disease, cerebrovascular disorders, and allergic rhinitis (475). In rabbits, the sudden death produced by arachidonic acid was antagonized by pretreatment with Bay U 3405 (**502**), showing it to be a thromboxane A_2 antagonist with anti-thrombotic activity (3). Therefore, ramatroban (BAY U 3405) may be beneficial in the treatment of atherosclerosis (Scheme 4.13).

Wu *et al.* studied a range of natural carbazole alkaloids isolated from *Murraya euchrestifolia* for platelet aggregation inhibitory activity, and found that murrayamine A (7-hydroxygirinimbine, mukoenine-C) (**120**) (see Scheme 2.22) and murrayamine-M

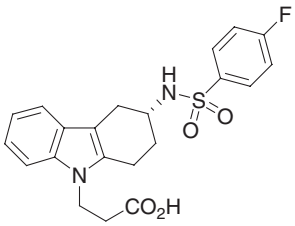

501 Ramatroban®(BAY u 3405)

Scheme 4.13

(**162**) (see Scheme 2.32) showed potent inhibitory activity on rabbit platelet aggregation with an IC_{50} of 2 μg/mL induced by collagen and platelet activation factor (PAF), respectively (18).

Pyrrolo[2,3-*c*]carbazole alkaloids (see Schemes 2.70–2.72) isolated from the dark green marine sponge, *Dictyodendrilla* sp., showed inhibitory activity against bovine lens aldose reductase catalyzing the reduction of aldoses to polyols which, on accumulation in cells, may result in diabetes. These alkaloids could provide prevention from such ailments (250).

The inhibition of lipid peroxidation induced by free radicals generated in the presence of Fe^{2+} and ascorbic acid by carazostatin (**247**) (see Scheme 2.61) is higher than that with the brain-protective agent, flunarizine or α-tocopherol, which has free-radical-scavenging activity. Carazostatin may be helpful for the alleviation of tissue damage due to the action of superoxide radicals and subsequent peroxidative disintegration of cell membranes (476,477). Carbazomycin B (**261**) (see Scheme 2.64) was also found to inhibit lipoxygenase activity, which could be related to free-radical-scavenging effects (476,477). In the 1990s, a range of functionally different carbazole alkaloids, such as the neocarazostatins A (**266**), B (**268**), and C (**267**) (see Scheme 2.65) (239) and the carbazoquinocins A (**272**), B (**273**), C (**274**), D (**275**), E (**276**), and F (**277**) (see Scheme 2.67) (246), and carquinostatin A (**278**) (241) (Scheme 2.68) were isolated from different *Streptomyces* sp. which have shown strong inhibitory activity against lipid peroxidation. In addition to these natural carbazoles, some semi-synthetic carbazoles have shown lipid peroxidation inhibitor activity. These results suggest that these natural and semi-synthetic carbazole alkaloids may be useful as a new class of therapeutic agents for various diseases, such as myocardial and cerebral ischemia, arteriosclerosis, renal failure, inflammation, and rheumatoid arthritis, which might be caused by tissue damage due to the generation of free radicals and subsequent peroxidative disintegration of cell membranes (476,477).

Recently, some *N*-substituted carbazolyloxyacetic acid derivatives were investigated for the inhibition and modulation of Alzheimer's disease (AD) associated γ-secretase, and it was found that selective reduction of $A\beta_{42}$ and an increase of the less aggregatory $A\beta_{38}$ fragment occurred (478).

Various 9-*N*,*N*-diethylaminopropyl-1,2,3,4-tetrahydrocarbazoles have been tested against Chagas' disease (American trypanosomiasis), a human tropical parasitic disease. It was found that 8-chloro- and/or 8-methoxy-substituted analogs may have promise as trypanocidal substances (479).

CHAPTER 5

Chemistry of Carbazole Alkaloids

I. GENERAL METHODS FOR CARBAZOLE CONSTRUCTION

From the initial discovery till today, biologically active carbazole alkaloids isolated from nature may have quite simple but in some cases also structurally complex substitution patterns. Therefore, a large number of classical and non-classical methods has been developed for the synthesis of the carbazole framework.

In earlier times, the method that was most utilized for the preparation of aromatic carbazoles was the dehydrogenation of a 1,2,3,4-tetrahydrocarbazole. The next most used precursors are biphenyls with an *ortho* nitrogen substituent and diphenylamines. In the progress of time, a large number of synthetic methods has been developed which can be regarded as general procedures. Most of these methods offer carbazoles in good to excellent yields and use starting materials which are either commercially available or accessible by short synthetic routes. Some of these methods were covered in various reviews (4–8,480,481), as well as in the chapters by Kapil (1), Husson (2), and Chakraborty (3) in Volumes 13, 26, and 44 of this series. In the following section, we summarize the different synthetic methods. Additionally, the application of these procedures to the total synthesis of natural products will be covered in the appropriate sections.

A. Synthesis of Carbazoles by Deoxygenation of Nitrobiphenyls

1 Watermann and Vivian's Method

Deoxygenation of *o*-nitrobiphenyl (**502**) to carbazole (**1**) was realized first by Waterman and Vivian using stoichiometric iron oxalate at 200°C (482,483) (Scheme 5.1).

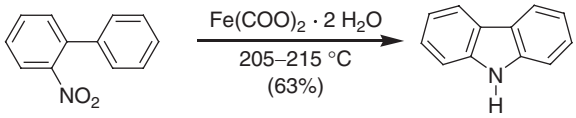

502 **1**

Scheme 5.1

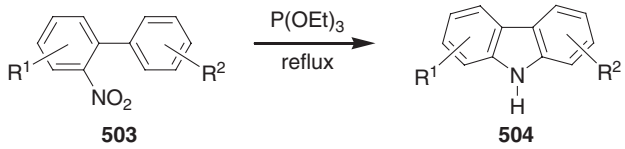

503 504

Scheme 5.2

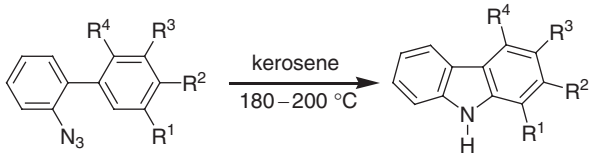

505 506

Scheme 5.3

2 Cadogan's Method

Later, Cadogan developed a similar deoxygenative cyclization using refluxing triethylphosphite as solvent. Subsequently, this method remained as the most common procedure for this conversion which tolerates a variety of substituents on the *o*-nitrobiphenyls (**503**) to afford diverse, functionalized carbazole derivatives (**504**) (484). The widely accepted mechanism for this transformation involves exhaustive deoxygenation to a singlet nitrene that undergoes a downstream C–H insertion (485,486). In the initial studies by Cadogan, alternative deoxygenation reagents (triphenylphosphine, phosphorus trichloride) were investigated, but triethyl phosphite was the reagent of choice. While broad in scope, the generation of a large amount of phosphorus waste represents a disadvantage of this approach (484) (Scheme 5.2). Recently, transition metal catalyzed variants of this reaction with CO as the stoichiometric reductant have been developed (487).

B. Synthesis of Carbazoles from Azidobiphenyls

An important route to the carbazoles is the thermal or photolytic decomposition of *ortho*-azidobiphenyls. Of the two procedures, thermolysis proceeds in higher yields. One advantage of photolysis is that it proceeds at room temperature and would therefore be compatible with thermally labile functional groups.

1 Thermal Decomposition

In 1951, Smith and Brown reported the synthesis of carbazole **506** by thermal decomposition of *ortho*-azidobiphenyl (**505**) in kerosene at 180°C (488). The reaction is believed to proceed *via* loss of nitrogen gas forming a nitrene, followed by cyclization to 9a-hydro-9*H*-carbazole. A rapid [1,5]sigmatropic rearrangement restores the aromaticity of the intercepting aromatic ring producing carbazole (485,486). This was the first application of a nitrene intermediate in the synthesis of nitrogen-containing heterocycles (486). A variety of functional groups are tolerated under the reaction conditions (488,489) (Scheme 5.3).

2 Photolytic Decomposition

The photolytic decomposition of *ortho*-azidobiphenyls **507** to carbazoles **508** is not as high yielding as the thermolytic procedure, and the reaction times are longer. However, the reaction proceeds under milder conditions (488,489). The reaction mechanism has been studied, and it was concluded that two intermediates were present in the reaction, both of which were capable of rearranging to carbazole (490) (Scheme 5.4).

C. Synthesis of Carbazoles by Cyclization of 2,2′-Diaminobiphenyls

Among the two cyclization procedures that utilize 2,2′-diaminobiphenyls, the Täuber synthesis has been most widely used and proceeds in higher yields than the diazotization reaction. The application of this method to the synthesis of carbazoles is limited by the availability of 2,2′-diaminobiphenyls.

1 Täuber's Method

In 1892, Täuber reported the synthesis of carbazole (**1**) by the cyclization of 2,2′-diaminobiphenyl (**509**). This reaction relies on high temperatures and acidic conditions involving cyclization with the elimination of ammonia (491,492). This method works well with chloro- and nitro-substituted 2,2′-diaminobiphenyls. However, the general application of this methodology to the synthesis of carbazoles is limited by the limited availability of 2,2′-diaminobiphenyls (493) (Scheme 5.5).

2 Diazotization of 2,2′-Diaminobiphenyls

As an alternative to the Täuber method, 2,2′-diaminobiphenyl (**509**) was transformed to carbazole (**1**) using diazotization conditions. This reaction proceeds intramolecularly by displacement of nitrogen. With this procedure, only moderate yields of carbazoles were obtained. The reaction is mechanistically similar to the Graebe–Ullmann synthesis (494) (Scheme 5.6).

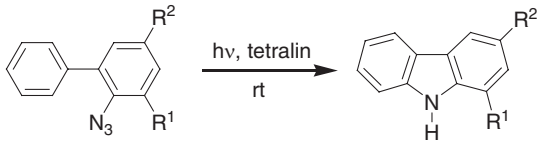

507 **508**

Scheme 5.4

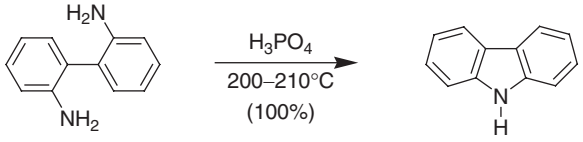

509 **1**

Scheme 5.5

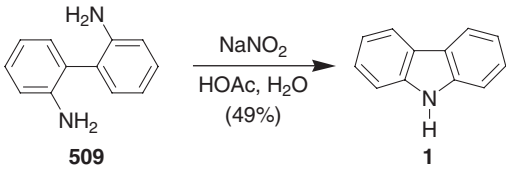

509 1

Scheme 5.6

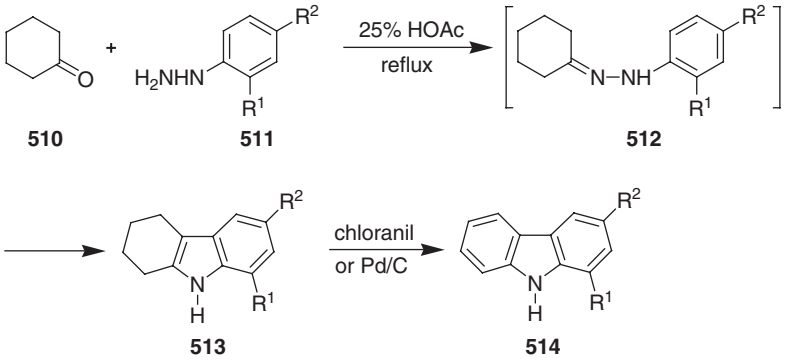

510 511 512 513 514

Scheme 5.7

D. Synthesis of Carbazoles by Cyclization of Arylhydrazones

A large number of carbazole syntheses involve the preparation and dehydrogenation of hydrocarbazoles, mainly 1,2,3,4-tetrahydrocarbazoles. They are usually prepared by either the Fischer–Borsche synthesis or the Japp–Klingemann reaction. The most commonly used dehydrogenating agents are palladium on charcoal or chloranil (495,496).

1 Fischer–Borsche Synthesis

The Fischer method (497) of indole synthesis by the indolization of an arylhydrazone by treatment with an acid catalyst was applied to the synthesis of tetrahydrocarbazoles by Borsche (498).

The cyclohexanone phenylhydrazone (**512**), obtained by reacting cyclohexanone (**510**) with phenylhydrazine (**511**), on indolization, furnished tetrahydrocarbazole **513** which, on dehydrogenation, afforded carbazole **514**. The success of the reaction is dependent on the reagent used for indolization and the dehydrogenating agent. The mechanism for the formation of the tetrahydrocarbazole involves a tautomeric equilibrium and the formation of a new C–C bond *via* a [3,3]-sigmatropic rearrangement followed by elimination of ammonia (495,496,498) (Scheme 5.7).

2 Japp–Klingemann Reaction

The preparation of the hydrazone required in the Borsche method was accomplished very conveniently using the Japp–Klingemann reaction (499,500). The reaction uses formylcyclohexanone (**515**) and a diazotized aromatic amine (**516**) for the synthesis

of hydrazone **517**. Using this method, better yields of the hydrazones were achieved. Mechanistically, this reaction proceeds *via* the electrophilic attack of an aryldiazonium cation at the anionic carbon atom of an active methinyl compound to give an intermediate azo compound, which undergoes hydrolysis under the reaction conditions with expulsion of the carbon substituent, to give an aryl hydrazone (495,496,501) (Scheme 5.8).

E. Syntheses of Carbazoles by Diverse Annulation Methods

1 Graebe–Ullmann Synthesis

Transformation of 1-arylbenzotriazole (**520**) to carbazole (**1**) under thermal conditions is known as the Graebe–Ullmann synthesis (502). This transformation is very sensitive to the nature of the substituents on the benzotriazole. However, unsubstituted 1-arylbenzotriazole (**520**) affords carbazole in nearly quantitative yield. The required starting material, 1-arylbenzotriazole (**520**), is prepared by the diazotization of *N*-(2-aminophenyl)aniline (**519**) (503,504). Limited reports on the mechanism of the Graebe–Ullmann reaction have appeared. Presumably, a diradical intermediate is involved in the thermolysis of the triazole (505) (Scheme 5.9).

2 Nenitzescu Carbazole Synthesis

As an extension of the Nenitzescu indole synthesis, *p*-benzoquinone (**521**) was condensed with various electron-withdrawing anilines **522** in the presence of trifluoroacetic acid (TFA) to give 6-hydroxycarbazoles **523**. Besides the low yield of

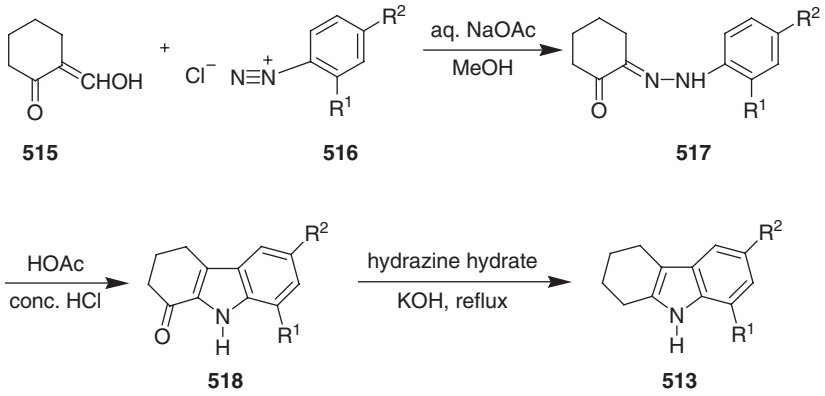

Scheme 5.8

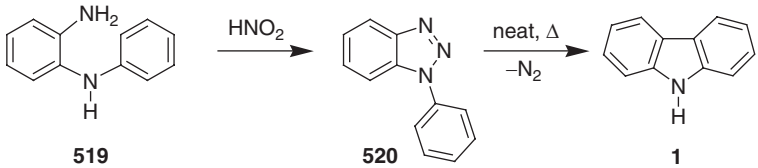

Scheme 5.9

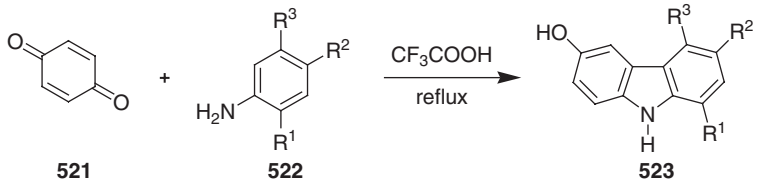

521 **522** **523**

Scheme 5.10

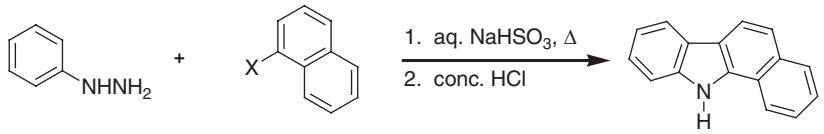

524 **525** X = OH **526** X = NH_2 **527**

Scheme 5.11

the 6-hydroxycarbazoles, this reaction suffers from the formation of many by-products (506). Mechanistically, this reaction proceeds with the 1,4-addition of the aniline reacting as an enamine, followed by condensation of the aniline to the benzoquinone. This mechanism is supported by the by-product formation (506,507) (Scheme 5.10).

3 Bucherer Synthesis of Benzocarbazoles

The Bucherer carbazole synthesis involves the treatment of a naphthyl alcohol (**525**) or a naphthylamine (**526**) with phenylhydrazine (**524**) in the presence of aqueous sodium bisulfite to afford, after work-up, benzocarbazole (**527**) (508).

Mechanistically, this reaction resembles the Fischer indole synthesis and is based on the condensation of the naphthyl alcohol or naphthylamine in its oxo form with phenylhydrazine, and subsequent rearrangement (496,505,508–510) (Scheme 5.11).

4 Cyclization of β-Keto Sulfoxides

Oikawa and Yonemitsu reported a general method for the synthesis of 2-hydroxycarbazoles (**529**) by the acid-catalyzed cyclization of the β-keto sulfoxide **528** (511). The required β-keto sulfoxide was derived from nucleophilic attack of dimethyl sulfoxide on methyl 3-indolepropionate.

The key step in this synthesis is an intramolecular nucleophilic attack on the electron-rich indole nucleus by the carbocation derived from the β-keto sulfoxide in the presence of acid. Finally, the intermediate tetrahydrocarbazole aromatizes by elimination of methanethiol under the conditions of the reaction to produce the hydroxycarbazole (511) (Scheme 5.12).

5 Annulation of a 2,3-Disubstituted Indole

Takano *et al.* reported an efficient synthesis of the carbazole framework using the annulation of a 2,3-disubstituted indole (512,513). This method involves the condensation of 2-benzyltryptamine (**530**) with ethoxymethylene acetoacetate (**531**) to give the enamine **532**, which, on treatment with acetic anhydride/acetic acid (3:2),

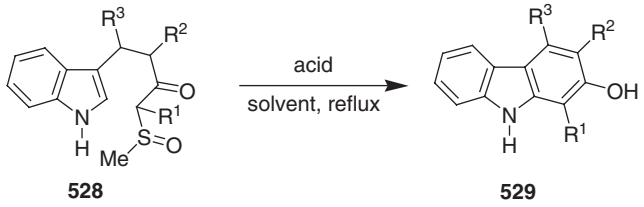

Scheme 5.12

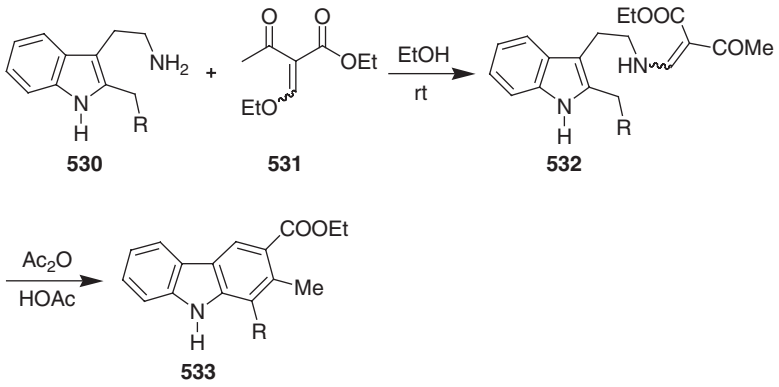

Scheme 5.13

cyclizes to the carbazole **533**. This one-pot transformation is believed to proceed *via* a Fischer-base-type intermediate which promotes the crucial cyclization and the removal of the ethylamine side chain (512,513) (Scheme 5.13).

6 Diels–Alder Reaction of Indolo-2,3-quinodimethanes

The application of indolo-2,3-quinodimethanes and their cyclic analogs in the synthesis of carbazole alkaloids has attracted wide interest since they could undergo Diels–Alder reactions with a wide variety of dienophiles to afford functionalized carbazole derivatives. This represents the shortest and most elegant method for the preparation of selectively functionalized carbazole derivatives (514).

The reactive indolo-2,3-quinodimethanes are generated *in situ* generally from *N*-protected 2,3-disubstituted indoles (514,515). Generation of reactive indolo-2,3-quinodimethanes was achieved by fluoride-induced, 1,4-elimination of silylated indolyl ammonium salts, and was applied in the synthesis of substituted tetrahydrocarbazoles (516). Subsequently, the iodide-induced 1,4-elimination of *N*-benzoyl-2,3-bis(bromomethyl)indole (**534**) methodology was developed for the synthesis of reactive indolo-2,3-quinodimethanes and was applied for the first time in the synthesis of substituted carbazoles (e.g., **536**) (517) (Scheme 5.14).

Later, independently, different anionic indolo-2,3-quinodimethanes which exhibit pronounced diene reactivity were developed from 2-cyano-1-methylindole-3-acetonitrile (**537**) (518,519) and 1,2-dimethylindole-3-carboxaldehyde (**539**) (520) by reacting with strong base. These quinodimethanes were used in the synthesis of polyfunctionalized carbazole derivatives (**538** and **541**) (Scheme 5.15).

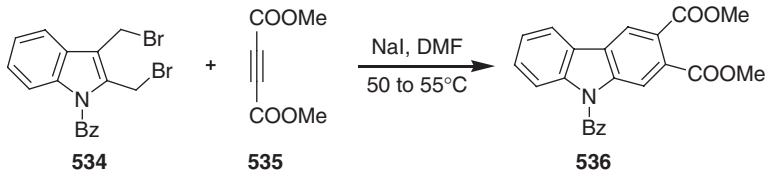

534 535 536

Scheme 5.14

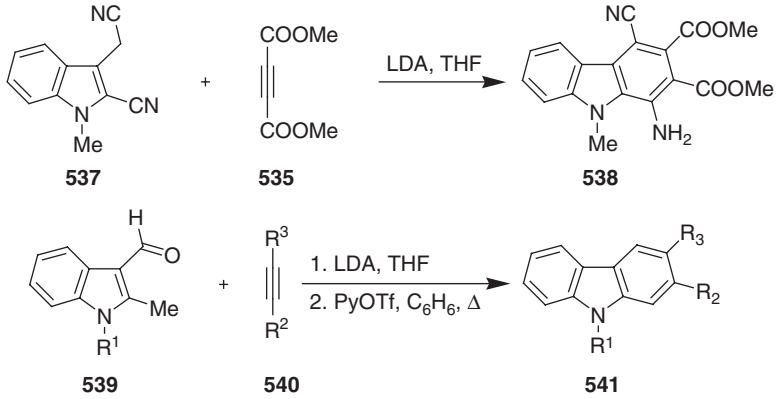

537 535 538

539 540 541

Scheme 5.15

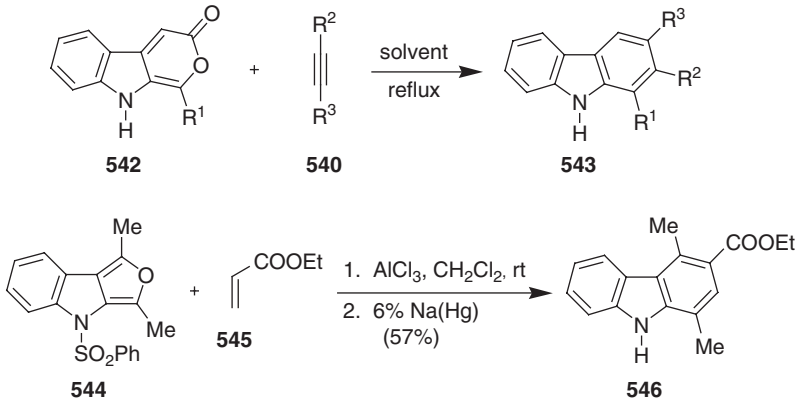

542 540 543

544 545 546

Scheme 5.16

Stable, cyclic analogs of indolo-2,3-quinodimethane derivatives were generated from pyrano[3,4-*b*] (**542**) (521–525) or furo[3,4-*b*] (**544**) (193,526–528) indole derivatives. Later, this strategy has been extended to pyrrolo[3,4-*b*], thieno[3,4-*b*] and selenolo[3,4-*b*]indole derivatives (193,514,528). In all these cases, the 2,3-bis(methylene)-2,3-dihydroindole structure is stabilized by the presence of a heteroatom capable of conjugation in the ring. Even so, such compounds are still reactive and afford cycloadducts useful for subsequent transformations. In accord with the Diels–Alder/bridge extrusion methodology, they react initially with dienophiles to form the bridged adducts. Finally, the bridging unit is removed from these adducts to form selectively functionalized carbazole derivatives (193,514,528) (Scheme 5.16).

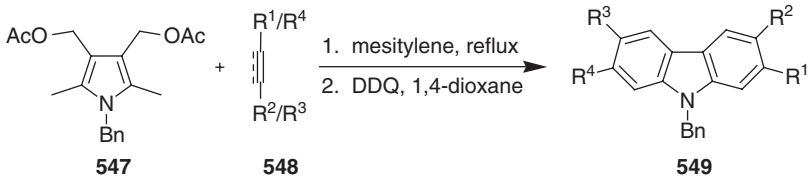

Scheme 5.17

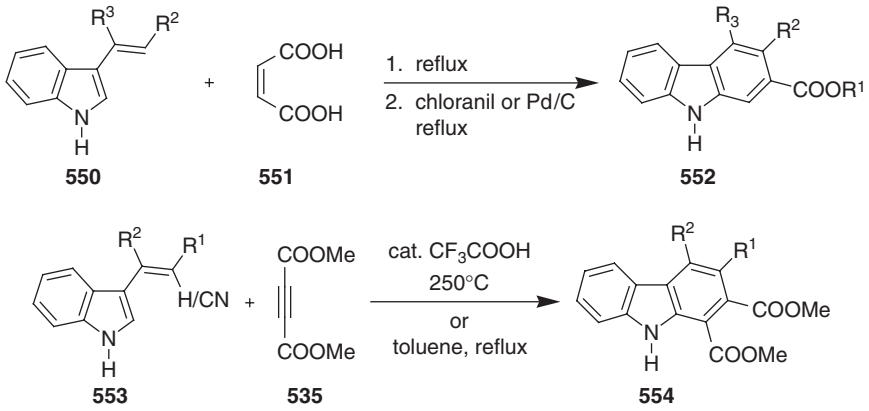

Scheme 5.18

This methodology was efficiently applied to a wide variety of natural and non-natural carbazole alkaloids.

For the first time, application of sequential Diels–Alder reactions to an *in situ*-generated 2,3-dimethylenepyrrole was shown with various dienophiles **548** to afford 2,3,6,7-tetrasubstituted carbazoles (**549**). This novel tandem Diels–Alder reaction leads to carbazole derivatives in two steps, starting from pyrrole **547** and 2 equivalents of a dienophile, and is followed by 2,3-dichloro-5,6-dicyano-1,4-benzoquinone (DDQ) oxidation of the intermediate octahydrocarbazole. Mechanistically, the formation of the intermediate octahydrocarbazole appears to involve two sequential [4+2] cycloadditions between the exocyclic diene generated by the thermal elimination of acetic acid and a dienophile (529) (Scheme 5.17).

7 Diels–Alder Cycloaddition of Vinylindoles

Diels–Alder reaction of vinylindoles with dienophiles has been established as a versatile and flexible methodology for the synthesis of carbazole alkaloids. Among the two different vinylindoles, 3-vinylindoles were the first to be explored for the Diels–Alder cycloaddition methodology with a range of dienophiles to give polyfunctionalized carbazole derivatives. This reaction is catalyzed by trifluoroacetic acid, and the yield in the absence of the acidic catalyst is very low. The reaction of substituted 3-vinylindoles **550** and **553** with ethylenic dienophiles **551** and acetylenic dienophiles **535** leads, *via* a tetrahydrocarbazole and a dihydrocarbazole, to the corresponding carbazoles (**552** and **554**), respectively (530,531) (Scheme 5.18).

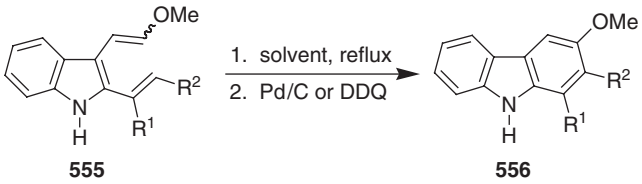

555 556

Scheme 5.19

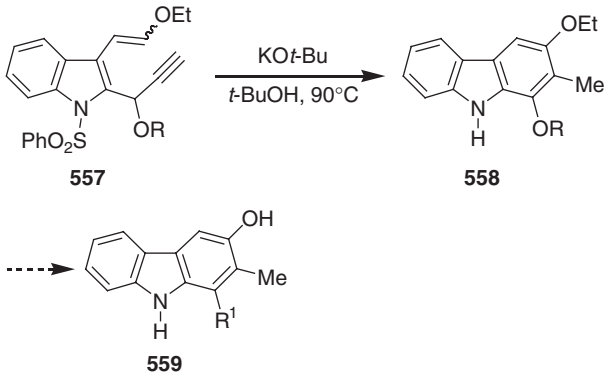

557 558 559

Scheme 5.20

Later, Pindur *et al.* developed an easy route to 2-vinylindoles with an unsubstituted 3-position, and these were efficiently employed as heterocyclic dienes for the synthesis of a diverse range of carbazole derivatives (532,533).

8 Electrocyclic Reactions to Carbazoles

The electrocyclic reaction of divinylindoles to functionalized carbazole derivatives has emerged as an efficient method for the synthesis of a diverse range of carbazole derivatives. This reaction has been achieved at high temperatures in the presence of palladium on charcoal or DDQ. The palladium catalyst or DDQ act as dehydrogenating agent (534,535) (Scheme 5.19).

A new benzannulation methodology was developed in order to overcome the limitations of electrocyclic ring closure of divinylindoles. The cyclization is achieved *via* an allene-mediated electrocyclic reaction of 2,3-difunctionalized indoles. This method is more efficient for the synthesis of highly substituted 2-methyl carbazole alkaloids (**559**). The 3-alkenyl-2-propargylindole **557**, a precursor for the allene intermediate, was prepared from 2-formylindole over several steps using simple functional group transformations (536,537) (Scheme 5.20).

A new method for the benzannulation of indole involving the thermal cyclization of 3-buta-1,3-dienylindoles (**560** and **561**) was described for the synthesis of 3-methoxycarbazole alkaloids **562** (538–540). Contrary to earlier benzannulation procedures, this method involves the ring closure of a 3-buta-1,3-dienylindole without the loss of the methoxy group at the 3-position of the carbazole nucleus. The 3-buta-1,3-dienylindole required for this method was obtained by Sakamoto's procedure (538,539) starting from 1-acetyl-2-methoxy-1,2-dihydroindole-3-one by

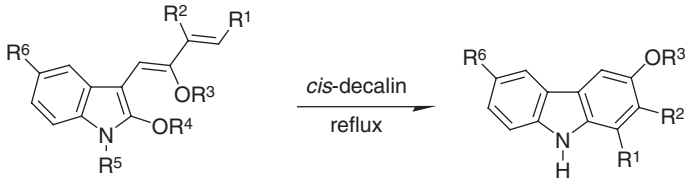

560 R^3 = TMS; R^4 = Me; R^5 = Ac
561 R^3, R^4, R^5 = COOEt
562

Scheme 5.21

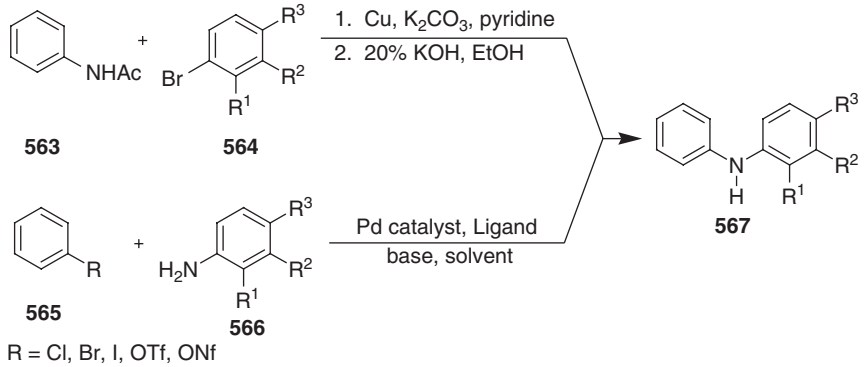

563 **564** **567**
565 **566**
R = Cl, Br, I, OTf, ONf

Scheme 5.22

a Wittig reaction, followed by silylation, as well as Beccalli's procedure (540) by condensation of indole-2,3-dione with the 3-methyl-4-phenylbut-3-en-2-one (Scheme 5.21).

9 Cyclization of Diarylamines

Intramolecular cyclization of diphenylamines to carbazoles is one of the most versatile and practical methods. This has been achieved photochemically, thermally in the presence of elemental iodine at 350°C, or with platinum at 450–540°C, *via* free radicals with benzoyl peroxide in chloroform, or by using activated metals such as Raney nickel or palladium on charcoal. Most of these methods suffer from low to moderate yields, and, in some cases, harsh reaction conditions (8,480).

Formerly, the diphenylamines **567** required for the synthesis of carbazole alkaloids were obtained through the Ullmann–Goldberg procedure using acetanilide (**563**) and a bromobenzene derivative **564** as coupling partners, followed by alkaline hydrolysis (541). Alternatively, the palladium(0)-catalyzed Buchwald–Hartwig amination protocol also provides diphenylamines. This method is superior to the Ullmann–Goldberg procedure since it uses only catalytic amounts of palladium(0) and proceeds in high yield under mild reaction conditions. In addition, this procedure works for aromatic halides and for aryl triflates and their structural analogs (542,543) (Scheme 5.22).

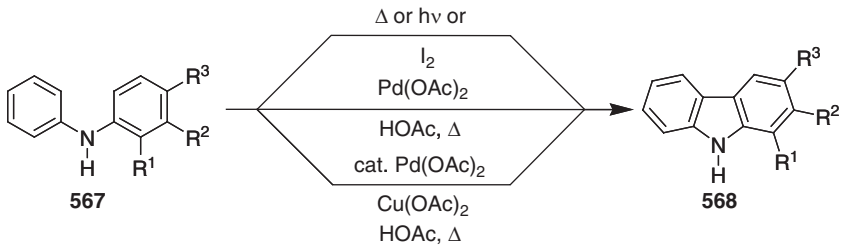

Scheme 5.23

Åkermark *et al.* reported the palladium(II)-mediated intramolecular oxidative cyclization of diphenylamines **567** to carbazoles **568** (355). Many substituents are tolerated in this oxidative cyclization, which represents the best procedure for the cyclization of the diphenylamines to carbazole derivatives. However, stoichiometric amounts of palladium(II) acetate are required for the cyclization of diphenylamines containing electron-releasing or moderately electron-attracting substituents. For the cyclization of diphenylamines containing electron-attracting substituents an over-stoichiometric amount of palladium(II) acetate is required. Moreover, the cyclization is catalyzed by TFA or methanesulfonic acid (355). We demonstrated that this reaction becomes catalytic with palladium through a reoxidation of palladium(0) to palladium(II) using cupric acetate (10,544–547). Since then, several alternative palladium-catalyzed carbazole constructions have been reported (548–556) (Scheme 5.23).

10 Iron-Mediated Synthesis of Carbazoles

Tricarbonyliron-coordinated cyclohexadienylium ions **569** were shown to be useful electrophiles for the electrophilic aromatic substitution of functionally diverse electron-rich arylamines **570**. This reaction combined with the oxidative cyclization of the arylamine-substituted tricarbonyl(η^4-cyclohexadiene)iron complexes **571**, leads to a convergent total synthesis of a broad range of carbazole alkaloids. The overall transformation involves consecutive iron-mediated C–C and C–N bond formation followed by aromatization (8,10) (Schemes 5.24 and 5.25).

Over the past 15 years, we developed three procedures for the iron-mediated carbazole synthesis, which differ in the mode of oxidative cyclization: arylamine cyclization, quinone imine cyclization, and oxidative cyclization by air (8,10,557,558). The one-pot transformation of the arylamine-substituted tricarbonyl(η^4-cyclohexadiene) iron complexes **571** to the 9*H*-carbazoles **573** proceeds *via* a sequence of cyclization, aromatization, and demetalation. This iron-mediated arylamine cyclization has been widely applied to the total synthesis of a broad range of 1-oxygenated, 3-oxygenated, and 3,4-dioxygenated carbazole alkaloids (Scheme 5.24).

In the quinone imine cyclization of iron complexes to carbazoles, the arylamine-substituted tricarbonyl(η^4-cyclohexadiene)iron complexes **571** are chemoselectively oxidized to a quinone imine **574** prior to cyclodehydrogenation. This mode of cyclization is particularly applicable for the total synthesis of 3-oxygenated tricyclic carbazole alkaloids (Scheme 5.25).

More recently, an environmentally benign method using air as an oxidant has been developed. Following this approach, in the presence of air the

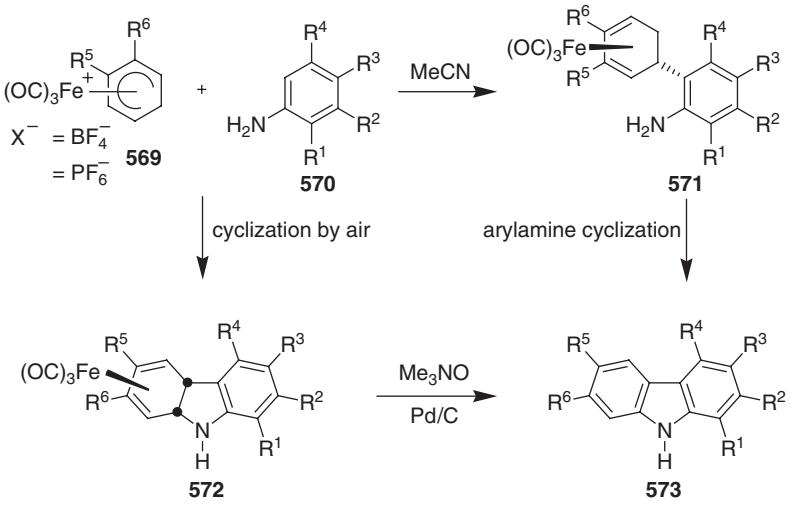

Scheme 5.24

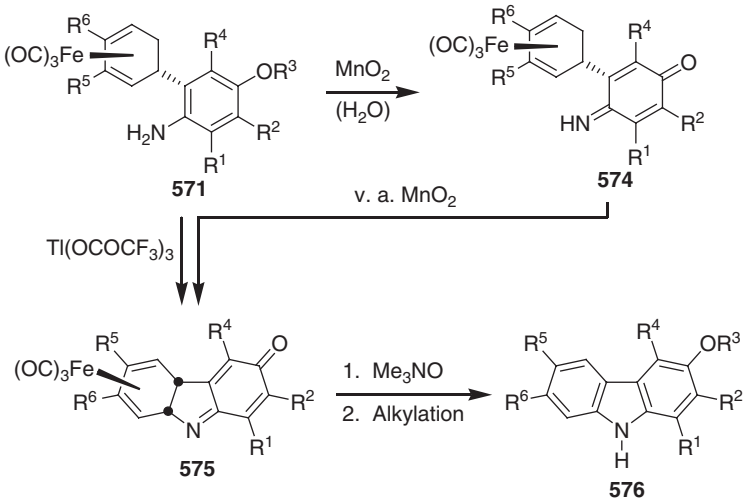

Scheme 5.25

tricarbonyliron-complexed cyclohexadienylium ions **569** and the arylamines **570** are directly transformed to tricarbonyliron-complexed 4a,9a-dihydrocarbazoles **572**. These, on demetalation and subsequent aromatization, lead to 9*H*-carbazoles **573**. This eco-friendly method offers an excellent alternative to the previous cyclization procedures (Scheme 5.24).

11 Molybdenum-Mediated Synthesis of Carbazoles

Despite many applications of the iron-mediated synthesis of carbazoles, this method offers limited access to 2-oxygenated tricyclic carbazoles due to the moderate yield

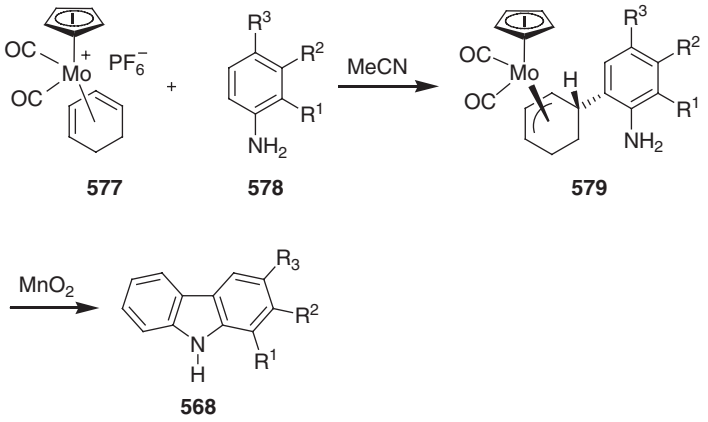

Scheme 5.26

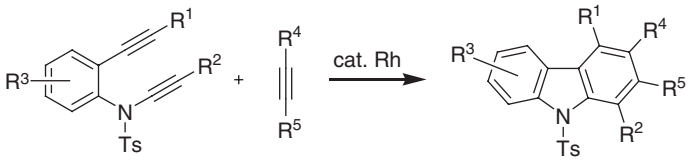

Scheme 5.27

for the oxidative cyclization (81,559). To overcome this limitation, and as a complementary method, we developed an alternative, molybdenum-mediated approach.

Using this method, the electrophilic aromatic substitution of the electron-rich arylamine **578** by the molybdenum-complexed cation **577** affords regio- and stereoselectively the molybdenum complexes **579**. Cyclization with concomitant aromatization and demetalation using activated manganese dioxide leads to the carbazole derivatives **568** (8,10,560) (Scheme 5.26).

12 Rhodium-Catalyzed Synthesis of Carbazoles

Intermolecular cyclotrimerization of alkynes using Wilkinson's catalyst has also afforded substituted carbazole derivatives. This reaction was extended to an intramolecular version by offering the possibility for a six-membered ring annulation that cannot be achieved easily in the corresponding intermolecular version. Intramolecular cyclotrimerization is completely regioselective due to an additional tether.

Crossed-alkyne cyclotrimerizations between the diynes **580** and the monoalkynes **581** with a catalytic amount of $RhCl(PPh_3)_3$ afforded substituted carbazoles **582**. The high efficiency of the carbazole formation could be rationalized by the conformational restrictions present in the diynes **580** (561) (Scheme 5.27).

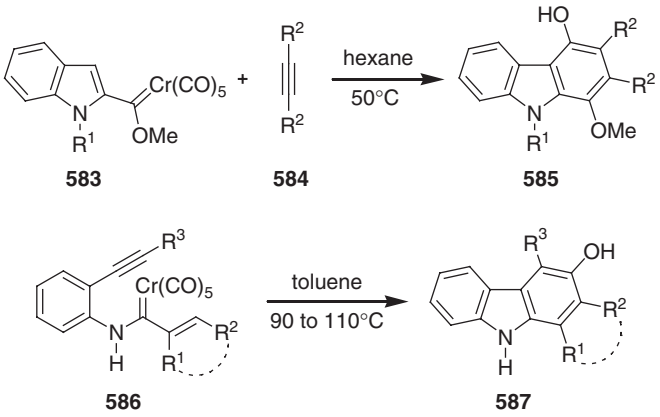

Scheme 5.28

13 Annulations of Chromium–Carbene Complexes

The Dötz benzannulation reaction, based on the alkyne cycloaddition to chromium carbene complexes, is the most important application of Fischer carbene complexes. Among the various Fischer carbene complexes, alkoxy and aminocarbene complexes of chromium undergo a novel inter- and intramolecular tandem alkyne insertion/carbene annulation sequence to give 9*H*-carbazoles and 11*H*-benzo[*a*]carbazoles.

The annulation of indole carbene complexes **583** with acetylene derivatives **584** affords hydroxycarbazole derivatives **585**. In this reaction, the indole carbene complexes **583** undergo intermolecular acetylene **584** insertion followed by carbene annulation (562). Recently, an intramolecular version of this method was reported by using 3-(2-vinyl)indolylcarbene complexes in the total synthesis of carbazole-3,4-quinone alkaloids (563). The (alkylanilino)carbene chromium complexes **586**, under thermal conditions, undergo a tandem insertion–cyclization sequence to give 11*H*-benzo[*a*]carbazoles **587**. This reaction is known to occur through a tandem alkyne insertion–carbonylation to give the indolylketene intermediate, which, on electrocyclic ring closure involving the π-system, results in the formation of oxygenated 11*H*-benzo[*a*]carbazoles (564,565) (Scheme 5.28).

14 Palladium-Catalyzed Annulation of Internal Alkynes

An efficient synthesis of functionalized carbazoles was developed by the palladium-catalyzed annulation of a variety of internal alkynes. This reaction involves arylpalladation of the alkyne, followed by intramolecular Heck olefination, and double bond isomerization. The iodoindole **588** reacts with the alkyne **589** in the presence of a catalytic amount of palladium(0) to give substituted carbazoles **590**. In this reaction two new C–C bonds are formed in a single step. Higher reaction temperatures were necessary due to the low reactivity of the iodoindole (566) (Scheme 5.29).

15 Double *N*-arylation of Primary Amines

The double *N*-arylation of primary amines or ammonia equivalents **592** with 2,2′-biphenylylene ditriflate (**591**) under Buchwald–Hartwig *N*-arylation conditions gave the unsymmetrically multi-substituted carbazoles **593**. Among the various

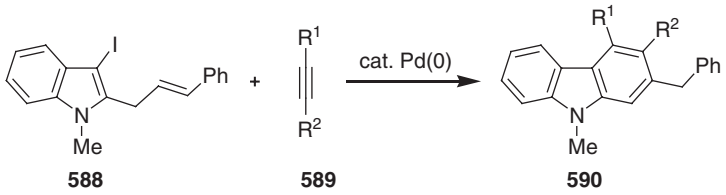

Scheme 5.29

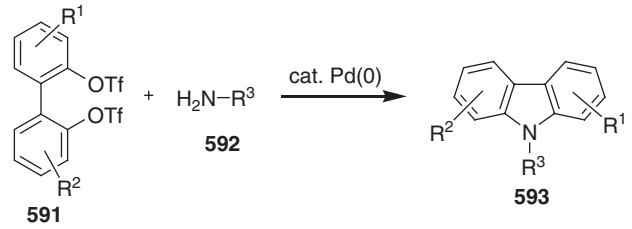

Scheme 5.30

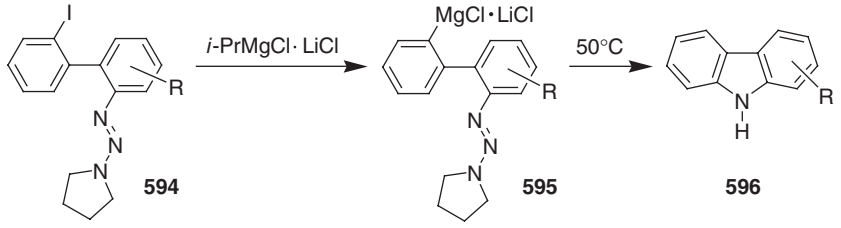

Scheme 5.31

ammonia equivalents, *O-tert*-butyl carbamate served as the best nitrogen source. The required 2,2′-biphenylylene ditriflate **591** was easily prepared by the Suzuki–Miyaura coupling of *o*-halophenols with *o*-hydroxyphenylboronic acids (567,568) (Scheme 5.30).

16 Carbazole Synthesis Using Arylmagnesium Reagents

The reaction of iodo-substituted aryltriazenes **594** with *i*-PrMgCl · LiCl afforded functionalized carbazoles **596**. In this reaction, evaporation of *i*-PrI resulting from the I/Mg-exchange is important before heating; otherwise, unwanted cross-coupling products with *i*-PrI are observed. Mechanistically, this reaction could proceed with the formation of an arylmagnesium derivative **595** followed by intramolecular addition of the triazene onto nitrogen with the elimination of hydroxylamine (569) (Scheme 5.31).

II. TOTAL SYNTHESES OF CARBAZOLE ALKALOIDS

This part of the review covers only the total synthesis of biologically active natural carbazole alkaloids. In the following sections, all of the total syntheses since 1990 are

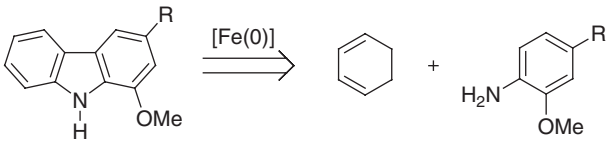

7 Murrayafoline A
R = Me

8 Koenoline
R = CH_2OH

9 Murrayanine
R = CHO

10 Mukoeic acid
R = COOH

11 Mukonine
R = COOMe

597

598 R = Me
599 R = OMe
600 R = COOMe

Scheme 5.32

covered, although this is an update of the treatise which appeared in 1993 by Chakraborty (3) in Volume 44 of this series. Recently, a large number of total syntheses has appeared for this class of natural products.

A. Tricyclic Carbazole Alkaloids

This section includes the carbazole alkaloids that have substitutions and functionalizations without any further heterocyclic fusions and annulations on the 9*H*-carbazole nucleus. Further, irrespective of their natural sources, based on the oxygenated substitution pattern, these tricyclic carbazole alkaloids were classified into the following sub-sections.

1 1-Oxygenated Tricyclic Carbazole Alkaloids

Among the several strategies developed for carbazole syntheses, organometallic approaches to carbazoles have received special attention, since they have led, in many cases, to highly convergent total syntheses of carbazole alkaloids (8,10, 570–572). The iron-mediated retrosynthesis of 1-oxygenated carbazoles **7**–**11** leads to cyclohexadiene (**597**) and the corresponding arylamines **598**–**600** as synthetic precursors (Scheme 5.32).

The two key steps for the construction of the carbazole framework by the iron-mediated approach are, first, C–C bond formation by electrophilic aromatic substitution of the arylamine with the tricarbonyliron-complexed cyclohexadienyl cation and, second, C–N bond formation and aromatization by an oxidative cyclization. Application of this methodology provides murrayanine (**9**) and koenoline (**8**) in three steps and 15%, and in four steps and 14% overall yield, respectively, starting from the commercial nitroaryl derivative **601** (573,574) (Scheme 5.33).

Catalytic hydrogenation of the nitroarene **601** afforded the corresponding arylamine **598**. An electrophilic aromatic substitution of the arylamine **598** by

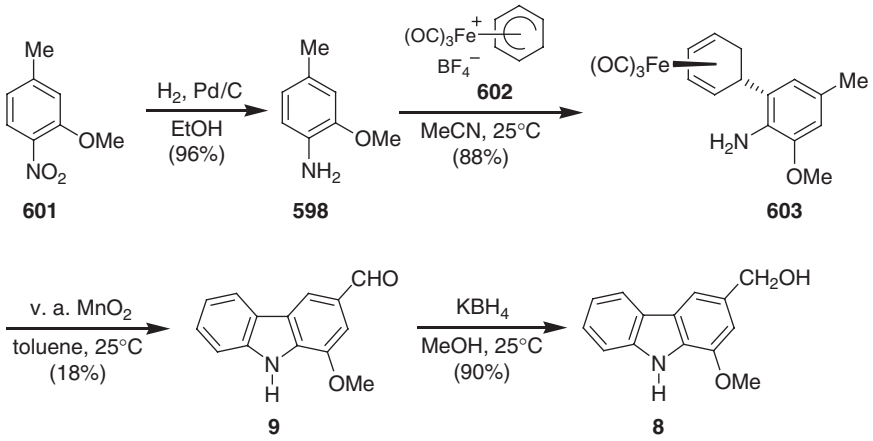

Scheme 5.33

reaction with tricarbonyl(η^5-cyclohexadienylium)iron tetrafluoroborate (**602**) afforded the tricarbonyl iron complex **603**. The iron complex salt **602** is readily available by 1-aza-1,3-butadiene-catalyzed complexation of 1,3-cyclohexadiene with pentacarbonyliron, followed by hydride abstraction using triphenylcarbenium tetrafluoroborate. The oxidative cyclization of the iron complex **603** with very active manganese dioxide in toluene at room temperature led directly to murrayanine (**9**). This one-pot conversion is rationalized by a four-step sequence. First, oxidation of the methyl group to the formyl group. Second, a cyclizing dehydrogenation to the 4b,8a-dihydro-9*H*-carbazole. Third, aromatization to a 20-electron complex, and fourth, spontaneous demetalation to murrayanine (**9**). Murrayanine (**9**) was transformed to the cytotoxic carbazole alkaloid koenoline (**8**) by borohydride reduction (573,574) (Scheme 5.33).

As shown above, a direct synthesis of murrayafoline A by the iron-mediated arylamine cyclization using the arylamine **598** is not feasible due to unavoidable concomitant oxidation of the methyl group on cyclization of the complex **603** (see Scheme 5.33). In order to overcome this problem, the iron-mediated iminoquinone cyclization was applied for the total synthesis of murrayafoline A (**7**) (Scheme 5.34). The methyl group of murrayafoline A (**7**) was introduced by nucleophilic addition of methyllithium to the carbonyl group of the resulting tricarbonyl-complexed 4b,8a-dihydrocarbazol-3-one (**606**). The iron complex **604** required for the synthesis of the quinone imine complex **606** was obtained by electrophilic substitution of 2,4-dimethoxyaniline (**599**) with the iron complex cation **602**. A direct, iron-mediated, iminoquinone cyclization of **604** failed to give the desired cyclized quinone imine complex **606**. Therefore, the two-step procedure with isolation of the intermediate non-cyclized quinone imine **605** was applied. Oxidation of complex **604** using commercial manganese dioxide afforded the non-cyclized iminoquinone **605** in 77% yield. All attempts to cyclize the complex **605** with very active manganese dioxide led only to decomposition. However, oxidative cyclization of **605** with thallium(III) trifluoroacetate furnished the required cyclized iminoquinone complex **606** in 40% yield. Addition of methyllithium to the complex **606** provided the corresponding tertiary carbinol **607** as a 1:1 diastereomeric mixture. Treatment of the complex **607**

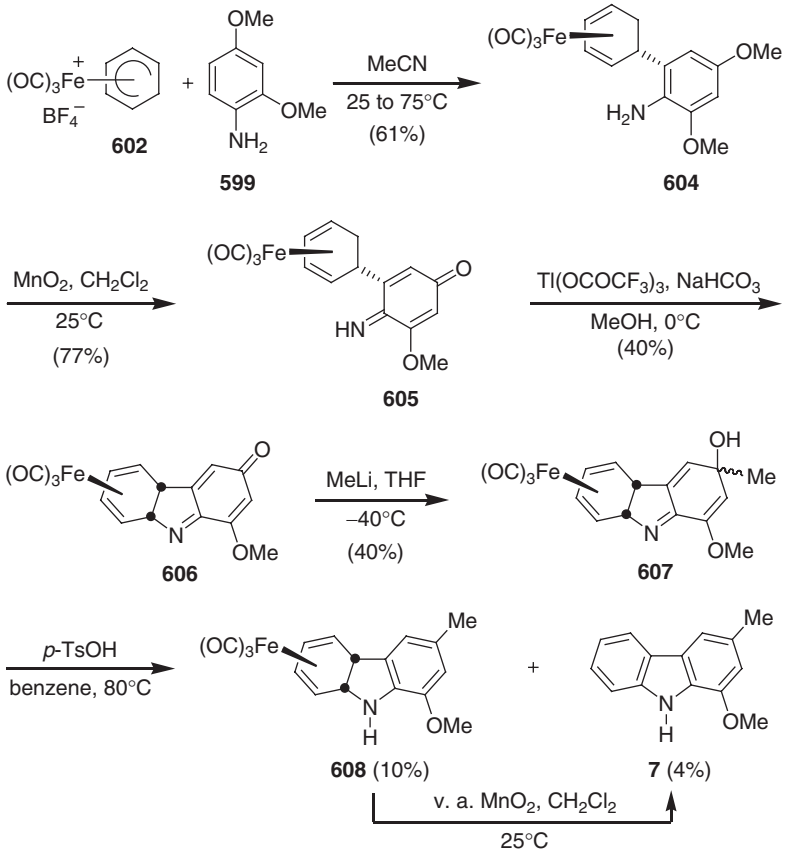

Scheme 5.34

with *p*-toluenesulfonic acid (*p*-TsOH) in refluxing benzene afforded murrayafoline A (**7**) directly by elimination of water with concomitant aromatization and demetalation. However, the yield of murrayafoline A (**7**) was only 4%, along with the corresponding 4b,8a-dihydro-9*H*-carbazole **608** in 10% yield. Complex **608** was smoothly converted to murrayafoline A (**7**) with very active manganese dioxide (574) (Scheme 5.34).

The total synthesis of mukonine (**11**) and mukoeic acid (**10**) starts from the arylamine **600**. An optimized procedure for the reaction of the complex salt **602** with the arylamine **600** in refluxing acetonitrile provided the iron complex **609** in 61% yield. The iron complex **609** is subjected to smooth cyclodehydrogenation by reacting with air in TFA to afford the 4b,8a-dihydro-9*H*-carbazole **610**. Aromatization of **610** with concomitant demetalation with ferricenium hexafluorophosphate in the presence of sodium bicarbonate provided mukonine (**11**) in 50% yield (route A: three steps, 15% overall yield) (80). An alternative method for the aromatization of the intermediate dihydro-9*H*-carbazole **610** to mukonine (**11**) was provided by demetalation and subsequent catalytic dehydrogenation, albeit in low yield (81). Alternatively, in a one-pot operation, **609** was transformed to mukonine (**11**) by the iron-mediated arylamine cyclization with very active manganese dioxide

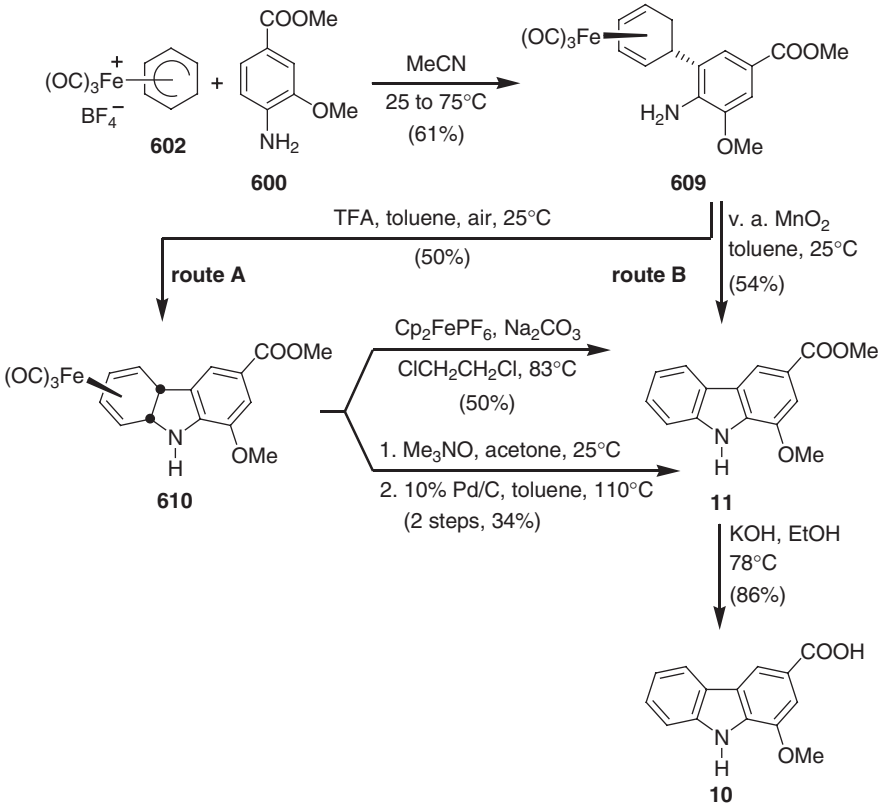

Scheme 5.35

in 54% yield (route B: two steps, 33% overall yield). Finally, ester cleavage of mukonine (**11**) provided mukoeic acid (**10**) in 86% yield (574) (Scheme 5.35).

An alternative access to murrayanine (**9**) was developed starting from the mukonine precursor **609**. The reduction of the ester group of **609** using diisobutylaluminum hydride (DIBAL) afforded the benzylic alcohol **611**. In a one-pot reaction, using very active manganese dioxide, **611** was transformed to murrayanine (**9**) (574) (Scheme 5.36).

Chowdhury *et al*. reported the syntheses of clausenol (**28**) and clausenine (**14**) by Fischer–Borsche indolization of the hydrazone **517a** (40). Under Japp–Klingemann conditions, the required hydrazone **517a** was obtained by condensation of 2-hydroxymethylene-5-methylcyclohexanone (**515a**) with 4-methoxybenzene diazonium chloride (**516a**). Indolization of the hydrazone **517a** with concentrated HCl and acetic acid furnished the oxotetrahydrocarbazole **518a**. Palladium-catalyzed dehydrogenative aromatization of **518a** led to clausenol (**28**). Finally, methylation of **28** with diazomethane afforded clausenine (**14**) (40) (Scheme 5.37).

Murakami *et al.* reported the total synthesis of 1-hydroxy-3-methylcarbazole (**23**) and murrayafoline A (**7**) by classical Fischer indolization of the *O*-methanesulfonyl phenylhydrazone derivative **614** (575). The compound **614** was prepared from the corresponding aminophenol **612** *via* 2-hydrazino-5-methylphenol *p*-toluenesulfonate

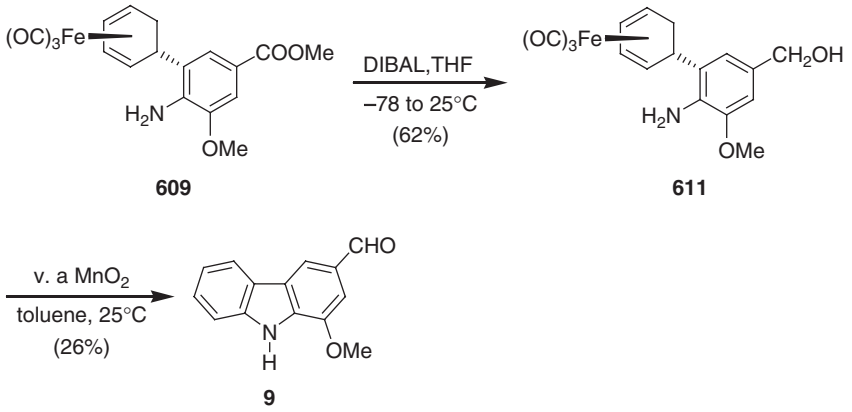

Scheme 5.36

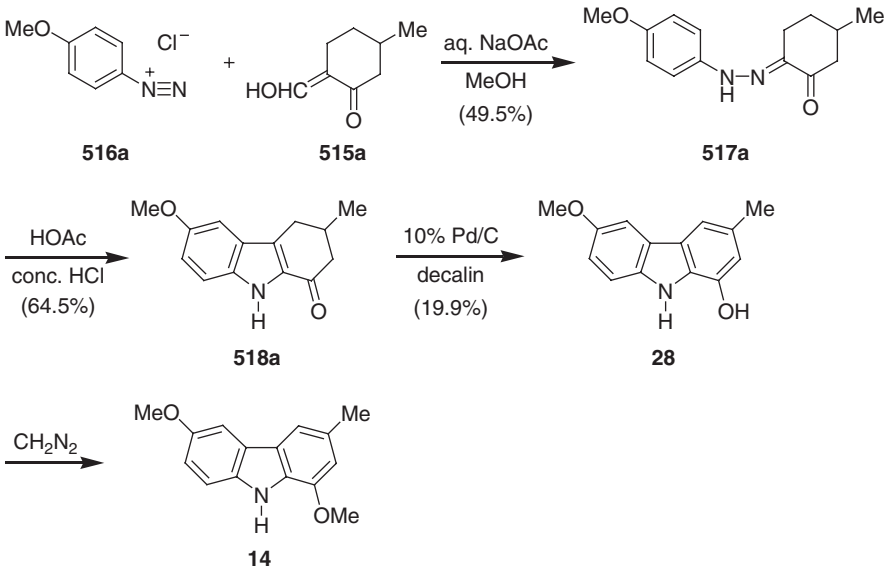

Scheme 5.37

(**613**) by reacting with cyclohexanone (**510**). Under Fischer indolization conditions (TsOH/benzene), the *O*-mesylphenylhydrazone **614** was transformed to the tetrahydrocarbazoles **615** and **616** in 63% and 3% yield, respectively. The mesyloxy compound **615** was dehydrogenated with 10% Pd/C in nitrobenzene to afford 1-mesyloxy-3-methylcarbazole (**617**). Hydrolysis of the mesyl group of **617** with potassium hydroxide in diethylene glycol afforded 1-hydroxy-3-methylcarbazole (**23**). Finally, *O*-methylation of **23** gave murrayafoline A (**7**). This synthesis provides 1-hydroxy-3-methylcarbazole (**23**) and murrayafoline A (**7**) in 48% and 40% overall yield and five and six steps, respectively, based on the aminophenol **612** (575) (Scheme 5.38).

Brenna *et al*. reported the synthesis of mukonine (**11**) from 3-formylindole (**618**) *via* a base-promoted cyclization of a mixed anhydride of mono-ester mono-acid **619** (576).

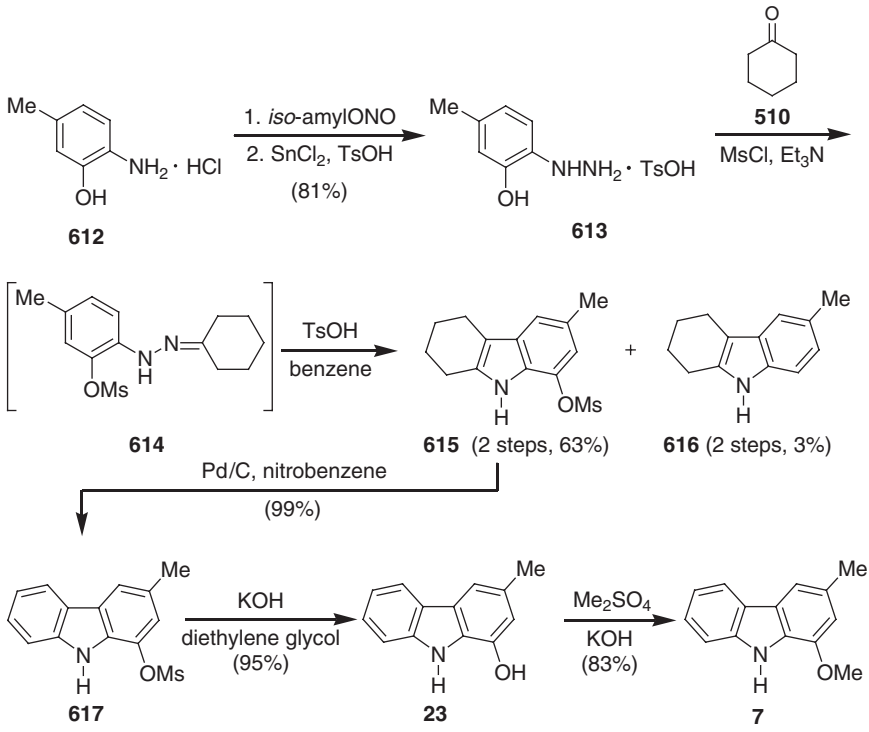

Scheme 5.38

The key step in this annulation methodology is assumed to proceed through a 1,6-electrocyclic reaction involving a ketene intermediate **620**. The mono-acid **619** required for the key cyclization step was prepared through Stobbe condensation of 3-formylindole (**618**) and dimethyl succinate. In a one-pot procedure, compound **619** was transformed to the aromatic derivative **621** by reacting with ethyl chloroformate in the presence of triethylamine. After base-promoted cleavage of the carbonic ester, **621** was transformed to clausine E (clauszoline-I) (**25**). Methylation of **25** with diazomethane gave mukonine (**11**). Finally, saponification of **11** in ethanolic sodium hydroxide afforded mukoeic acid (**10**). This method provides clausine E (clauszoline-I) (**25**) (three steps, 34% yield), mukonine (**11**) (four steps, 33% yield), and mukoeic acid (**10**) (five steps, 30% yield) based on 3-formylindole (**618**), and is formally complementary to Moody's electrophilic substitution of a 2-substituted indole. So far, this is the best method for the synthesis of clausine E (clauszoline-I) (**25**), mukonine (**11**), and mukoeic acid (**10**) because of the experimental simplicity and easy availability of the reagents (576) (Scheme 5.39).

Bringmann *et al*. reported the total synthesis of mukonine (**11**) and its transformation into seven further oxygenated carbazole alkaloids: murrayafoline A (**7**), koenoline (**8**), murrayanine (**9**), mukoeic acid (**10**), 1-hydroxy-3-methylcarbazole (**23**), *O*-demethylmurrayanine (**24**), and clausine E (clauszoline-I) (**25**) (577). The relay compound, mukonine (**11**) was prepared starting from 3-formylindole (**618**) through a sodium acetate in acetic anhydride-promoted cyclization of the intermediate mono-acid obtained by TFA-mediated cleavage of the *tert*-butoxycarbonyl (Boc) and

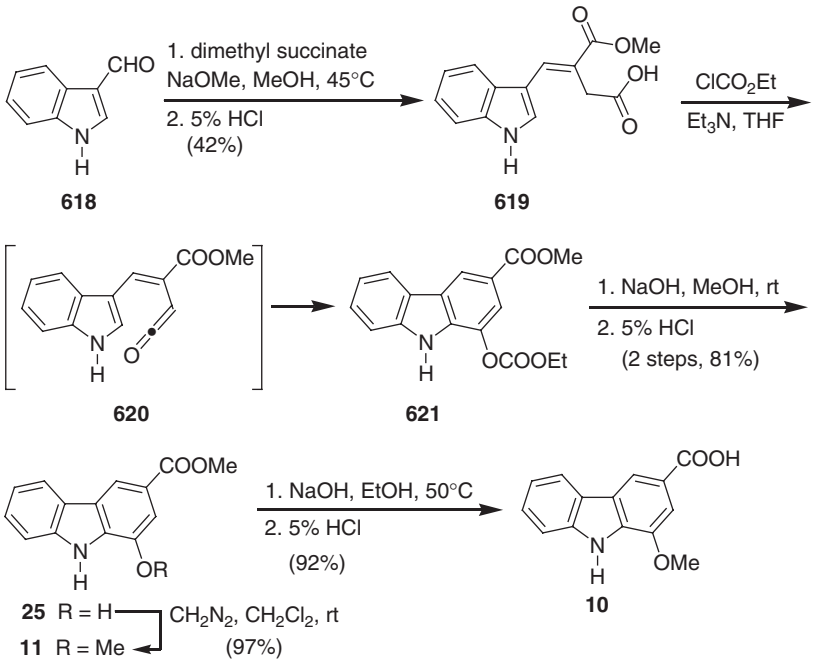

Scheme 5.39

tert-butyl ester of the mixed ester **624**. After protection of 3-formylindole (**618**) as the *N*-Boc derivative **622**, the mixed ester **624** was prepared *via* Horner–Emmons reaction of **622** with the phosphonate **623**. Compound **624** was transformed to mukonine (**11**) in 69% overall yield in a four-step sequence: removal of the Boc group with concomitant cleavage of the *tert*-butyl ester, cyclization with sodium acetate in acetic anhydride, methanolysis, and *O*-methylation. This method is an extension of Brenna's methodology.

Using the following common functional group manipulations, mukonine (**11**) was transformed into further oxygenated carbazole alkaloids. The reduction of mukonine with lithium aluminum hydride, led to murrayafoline A (**7**), which, on further *O*-demethylation with boron tribromide, afforded 1-hydroxy-3-methylcarbazole (**23**). Reduction of mukonine (**11**) with DIBAL gave koenoline (**8**). Oxidation of **8** with activated manganese dioxide led to murrayanine (**9**), and subsequent treatment with boron tribromide, provided *O*-demethylmurrayanine (**24**). Saponification of mukonine (**11**) with potassium hydroxide in ethanol afforded mukoeic acid (**10**). *O*-Demethylation of mukonine (**11**) with boron tribromide afforded clausine E (clauszoline-I) (**25**) (577) (Scheme 5.40).

Lin and Zhang reported the synthesis of 1-hydroxy-3-methylcarbazole (**23**) starting from the nitro derivative **625** (578). This synthesis uses a Buchwald–Hartwig amination for the synthesis of the diphenylamine **628**. After protection of the hydroxy group in the nitrophenol **625** as a benzyl ether, the nitro group was reduced to the corresponding amino derivative **627**. Amination of **627** with iodobenzene under Buchwald–Hartwig conditions afforded the diarylamine **628**. Palladium(II)-mediated cyclization of **628** led to the carbazole derivative **629**, albeit in low

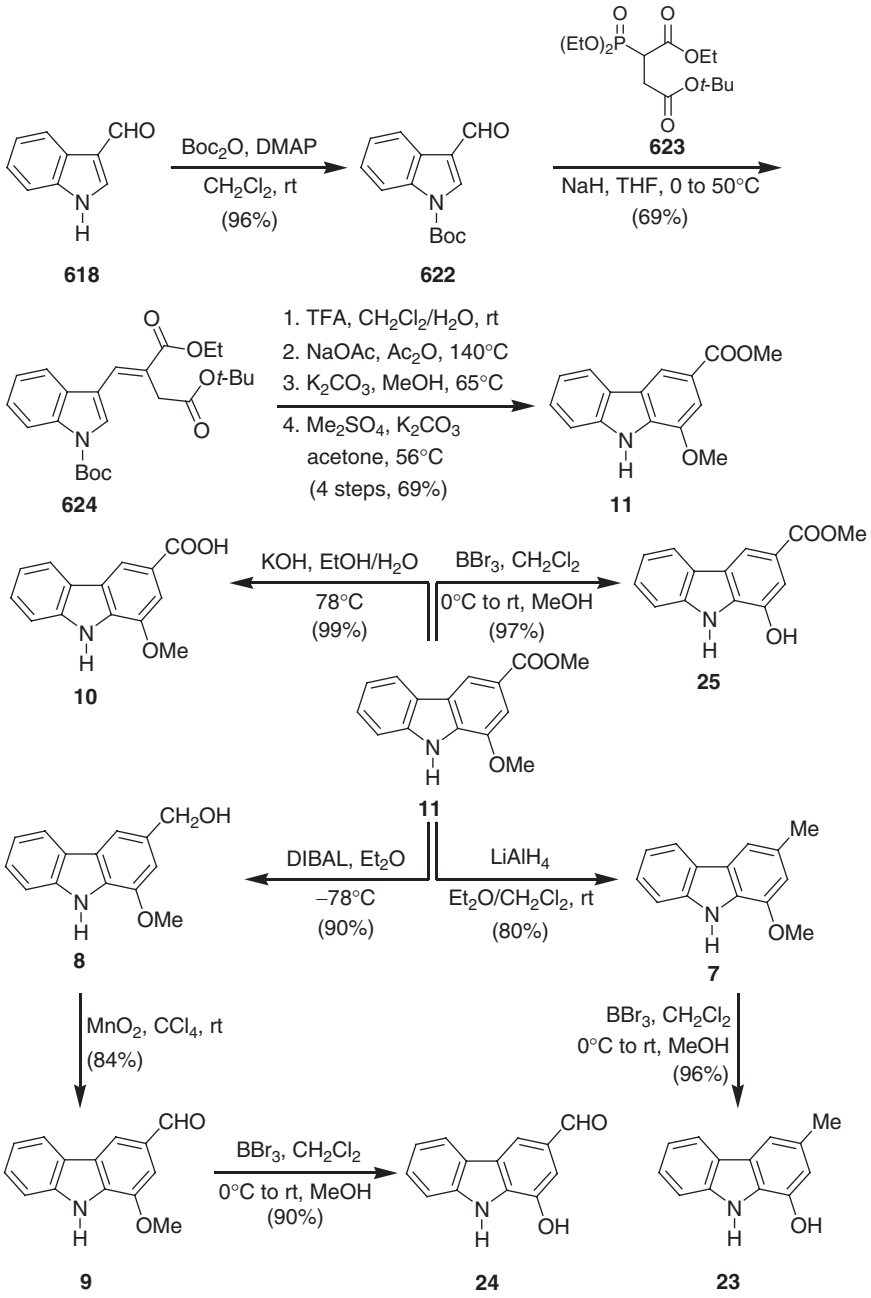

Scheme 5.40

yield. Finally, debenzylation using catalytic hydrogenation conditions furnished 1-hydroxy-3-methylcarbazole (**23**) (578) (Scheme 5.41).

Kikugawa *et al.* reported the synthesis of murrayafoline A (**7**) starting from the *N*-(*N*,*N*-diarylamino)phthalimide derivative **630** by reaction with $AlCl_3$ in benzene

(579). Under these conditions, 1-bromo-3-methylcarbazole **631** was formed *via* an intramolecular C–C bond formation by trapping of the diphenylnitrenium ion. In this reaction, the phthalimido group plays an important role for the generation and stabilization of a diphenylnitrenium ion. Finally, direct methoxide displacement of bromine from **631** led to murrayafoline A (**7**) (579) (Scheme 5.42).

Tamariz *et al.* reported the synthesis of mukonine (**11**) based on a regioselective Diels–Alder reaction of *N*-phenyl-4,5-dimethylidene-2-oxazolidinone (**634**) with methyl propiolate (**635**). The diene **634** was prepared in moderate yield from the condensation reaction of 2,3-butanedione (**632**) with phenyl isocyanate (**633**). In an optimized reaction procedure using drastic basic hydrolytic conditions (KOH/MeOH), followed by methylation with dimethyl sulfate, the adduct **636**, was

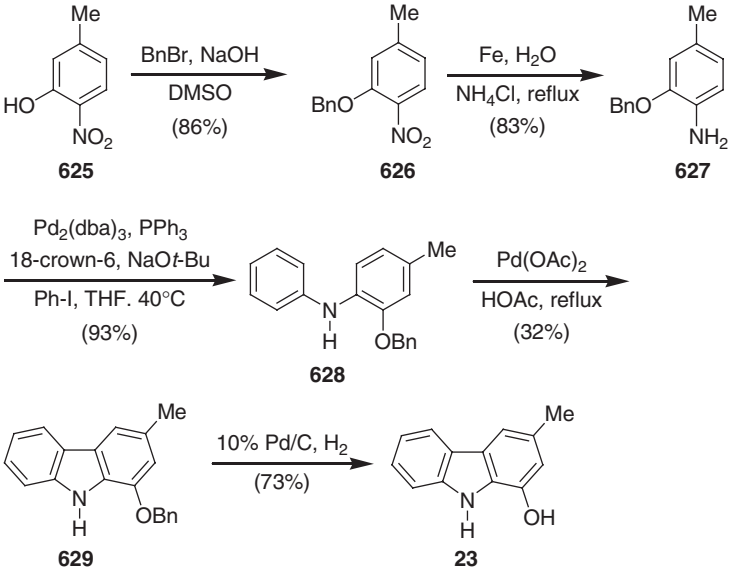

Scheme 5.41

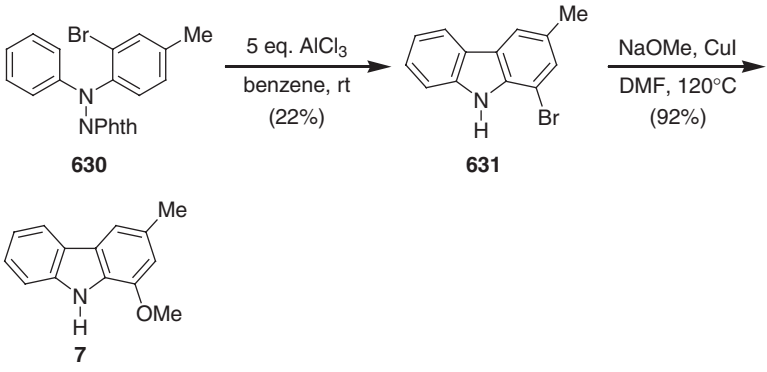

Scheme 5.42

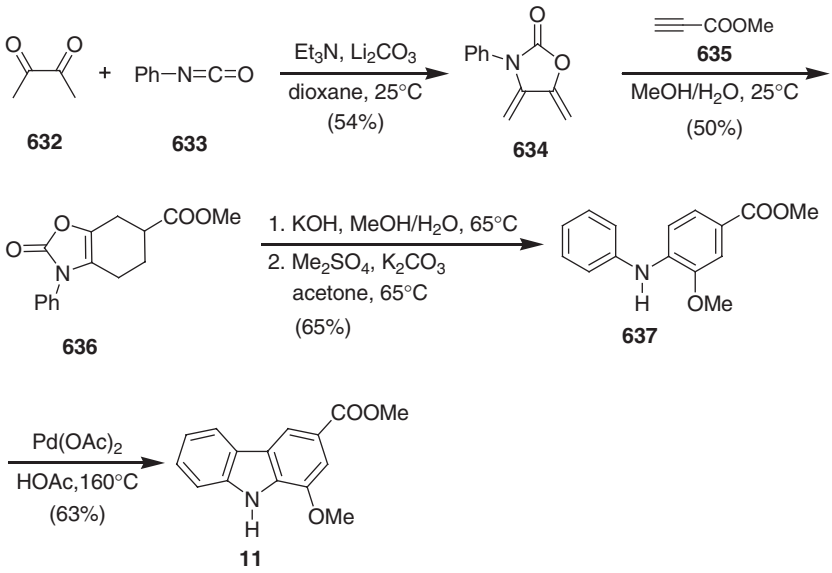

Scheme 5.43

transformed to the diphenylamine **637**. Finally, cyclization of **637** using stoichiometric $Pd(OAc)_2$ in acetic acid furnished mukonine (**11**) (580) (Scheme 5.43).

Two years later, this methodology was extended to the 1-oxygenated carbazole alkaloids, murrayanine (**9**) and murrayafoline A (**7**). For this total synthesis, the required key cycloadduct **639** was obtained by Lewis acid-catalyzed regioselective cycloaddition of the diene **634** to acrolein (**638**). Contrary to the synthesis of mukonine (**11**) (see Scheme 5.43), prior to basic hydrolysis, the Diels–Alder adduct **639** was aromatized with DDQ in refluxing benzene to furnish the corresponding aromatic derivative **640**. Hydrolysis of **640** under mild basic conditions gave the diphenylamine **642**. Then, methylation using MeI followed by palladium(II)-promoted cyclization of **643** furnished murrayanine (**9**). Following this pathway, murrayafoline A (**7**) was also synthesized. For this synthesis, the required aromatic cycloadduct **641** was obtained in quantitative yield by palladium-catalyzed hydrogenation of **640** (581) (Scheme 5.44).

Fagnou *et al*. reported the synthesis of mukonine (**11**) starting from methyl vanillate (**644**). This synthesis uses both a palladium(0)-catalyzed intermolecular direct arylation and an intramolecular cyclization reaction. Triflation of methyl vanillate (**644**) afforded the aryl triflate **645**. Using a Buchwald–Hartwig amination protocol, the latter was subjected to direct arylation with 2-chloroaniline (**646**) to furnish the corresponding diarylamine **647**. Finally, intramolecular cyclization of **647** afforded mukonine (**11**). To date, this is the best synthesis (three steps, 75% overall yield) available for mukonine based on commercially available methyl vanillate (**644**) (582) (Scheme 5.45).

Mal *et al*. reported a new benzannulation strategy for the synthesis of murrayafoline A (**7**) *via* anionic [4+2] cycloaddition of the furoindolone **650** (583,584). Using a literature procedure, Fischer indolization of 3-(2-phenylhydrazono)-dihydrofuran-2(3*H*)-one (**648**) afforded the furoindolone **649** (583). This was

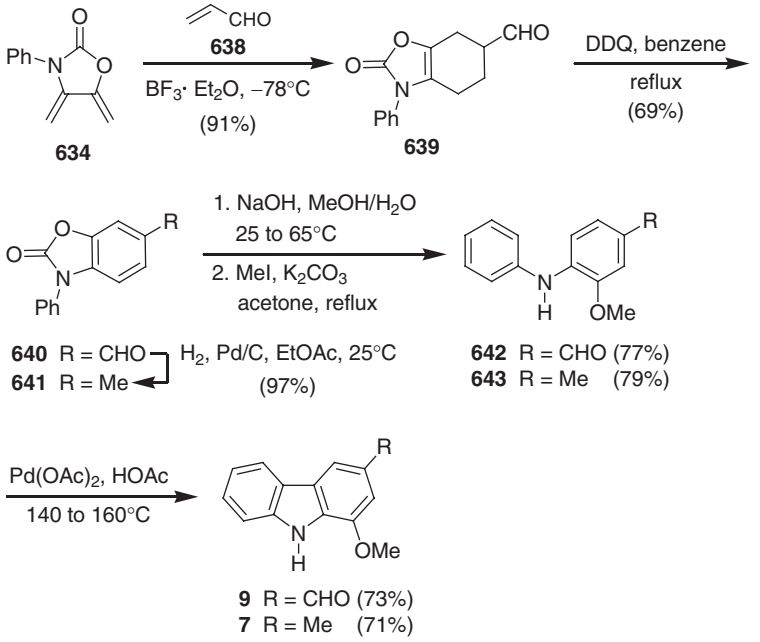

Scheme 5.44

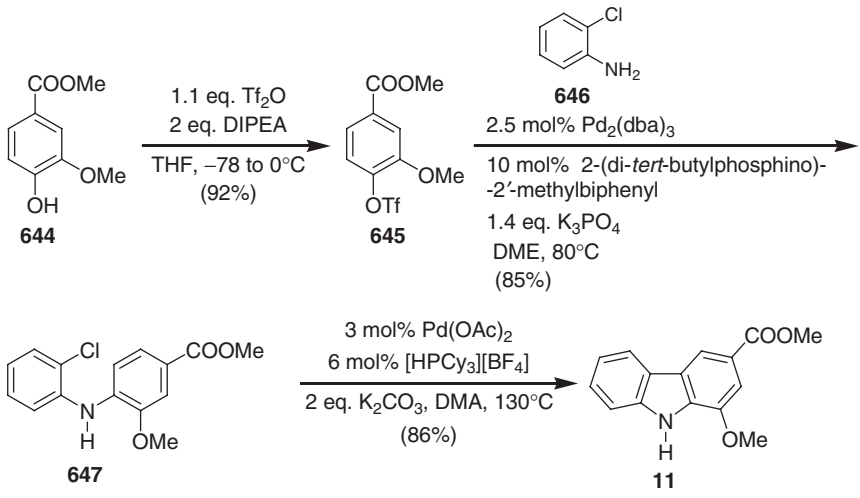

Scheme 5.45

derivatized to the *N*-benzyl derivative **650**. Annulation of compound **650** with methyl crotonate in the presence of lithium diisopropylamide (LDA) gave compound **651**. Demethoxycarbonylation of **651** with concentrated KOH in methanol, followed by *O*-methylation of the intermediate 1-hydroxycarbazole **652** using dimethyl sulfate, and finally debenzylation of **652** by refluxing in TFA with a catalytic amount of trifluoromethanesulfonic acid (TfOH), furnished murrayafoline A (**7**) (584) (Scheme 5.46).

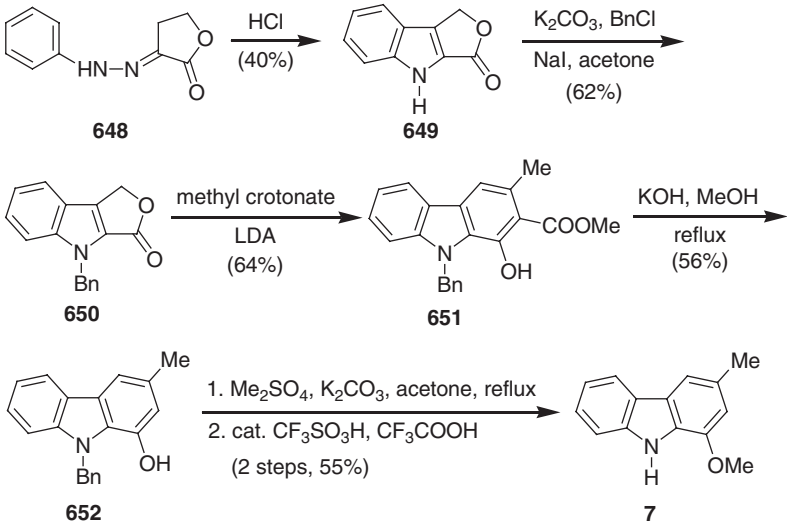

648 **649** **650** **651** **652** **7**

Scheme 5.46

Menéndez *et al.* reported the synthesis of murrayafoline A (**7**) by palladium(II)-mediated oxidative double C–H activation of a diarylamine assisted by microwave irradiation (585). The aniline derivative **598** was obtained by *O*-methylation of 5-methyl-2-nitrophenol (**625**) followed by catalytic hydrogenation. The required diarylamine **654** was obtained by *N*-arylation of the aniline derivative **598** with phenyllead triacetate (**653**) in the presence of copper(II) acetate. Under microwave-assisted conditions, in the presence of more than the stoichiometric amount of palladium(II) acetate and a trace of dimethylformamide, the diarylamine **654** was cyclodehydrogenated to murrayafoline A (**7**) (585) (Scheme 5.47).

2 2-Oxygenated Tricyclic Carbazole Alkaloids

Although a large number of 2-oxygenated tricyclic carbazole alkaloids have been isolated from different natural sources, only a few syntheses of this class of alkaloids were reported. This is mainly due to the lack of general methods, as well as the difficulty associated with the known synthetic methods, to build up the required substitution pattern. Prior to 1990, some total syntheses of 2-oxygenated carbazoles were reported and were covered in the earlier treatises by Kapil (1), Husson (2), and Chakraborty (3) in Volumes 13, 26, and 44 of this series. Since 1990, the only total syntheses which appeared in the literature for this class of carbazole alkaloids were transition metal-mediated or -catalyzed approaches, respectively. These general approaches offered a series of 2-oxygenated carbazole alkaloids (8,10).

The retrosynthetic analysis of the 2-oxygenated carbazole alkaloids, 2-methoxy-3-methylcarbazole (**37**) and mukonidine (**54**), based on an iron-mediated approach, led to the iron-complexed cation **602** and the arylamines **655** and **656** as precursors (Scheme 5.48).

The electrophilic aromatic substitution of **655** with the iron-complexed cation **602** afforded the iron complex **657** in almost quantitative yield. Treatment of **657** with

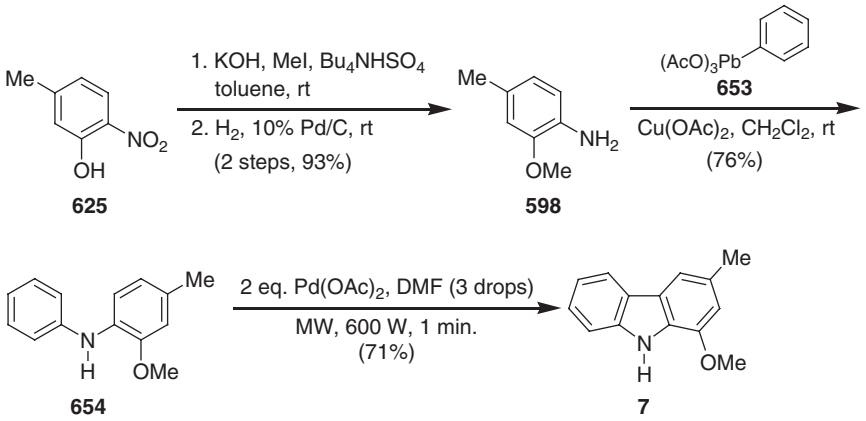

Scheme 5.47

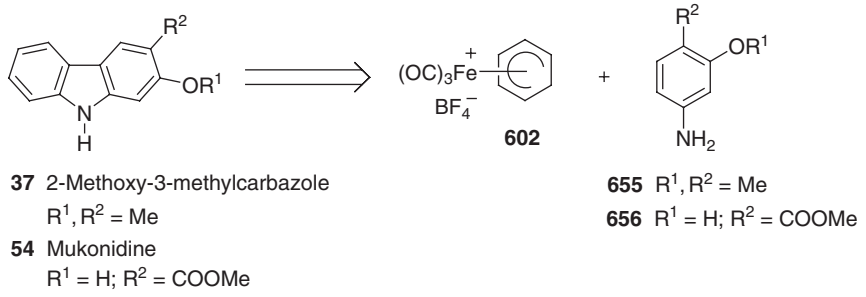

37 2-Methoxy-3-methylcarbazole
R^1, R^2 = Me

54 Mukonidine
R^1 = H; R^2 = COOMe

655 R^1, R^2 = Me

656 R^1 = H; R^2 = COOMe

Scheme 5.48

very active manganese dioxide led only to slow decomposition. However, reaction of complex **657** with iodine in pyridine furnished 2-methoxy-3-methylcarbazole (**37**) in 11% yield, along with the diene **658** in 44% yield (559) (Scheme 5.49).

For the total synthesis of mukonidine (**54**), the required arylamine **656** was obtained quantitatively from commercial 4-aminosalicylic acid (**659**) using diazomethane (559). However, for large-scale preparation, this transformation was better achieved with sulfuric acid and methanol (81). The reaction of the arylamine **656** with the iron-complex salt **602** provided the iron complex **660** in 87% yield. The high yield of C–C bond formation was ascribed to the high nucleophilicity of the *ortho*-amino position of the aromatic nucleus arising from the hydroxy group in the 3-position of the arylamine. The iron-mediated arylamine cyclization of the complex **660** using very active manganese dioxide, iodine in pyridine (559), or ferricenium hexafluorophosphate (81) failed, which was ascribed to the known problem caused by free hydroxy groups in these reactions. However, the oxidative cyclization of complex **660** in toluene, in the presence of air at room temperature, provided the iron-complexed dihydrocarbazole **661** (80,81). Various attempts to transform complex **661** to mukonidine (**54**) using very active manganese dioxide or ferricenium hexafluorophosphate in the presence of sodium carbonate led to complete decomposition. However, oxidation of complex **661** with *p*-chloranil (tetrachloro-1,4-benzoquinone) in toluene by aromatization and demetalation afforded mukonidine

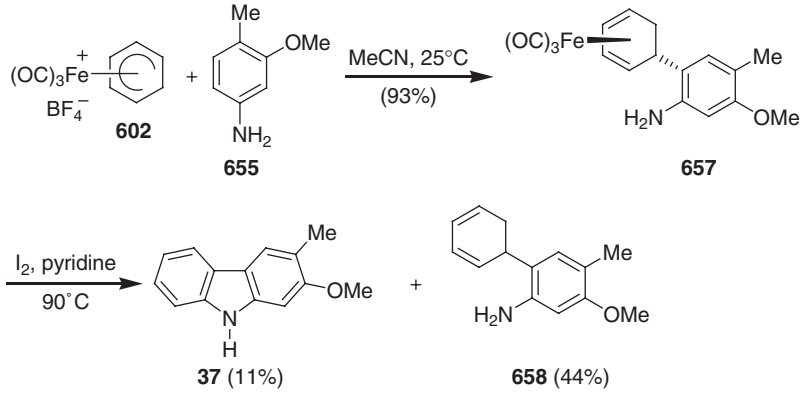

Scheme 5.49

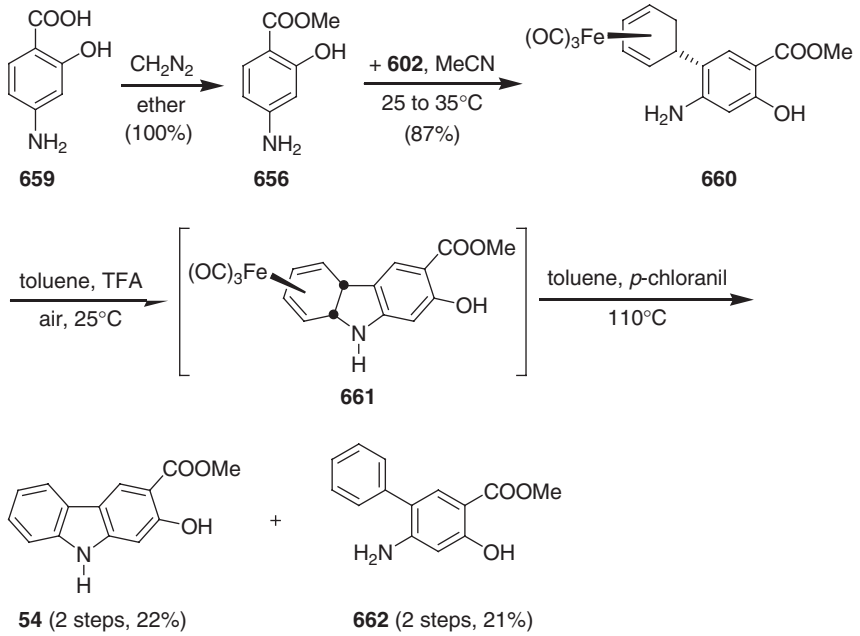

Scheme 5.50

(**54**) in 22% yield based on complex **602**, along with the biphenyl derivative **662** (21% yield). Alternatively, the final transformation of complex **661** to mukonidine (**54**) was achieved by demetalation with trimethylamine *N*-oxide in acetone, followed by catalytic dehydrogenation with palladium on activated carbon in toluene under reflux (11% yield based on the complex **602**) (80,81) (Scheme 5.50).

Despite many applications of the iron-mediated carbazole synthesis, the access to 2-oxygenated tricyclic carbazole alkaloids is limited due to the moderate yields for the oxidative cyclization. To overcome this problem, a molybdenum-mediated approach was developed as a complementary method. This alternative synthesis of

carbazole derivatives involves the oxidative cyclization of an arylamine at a dicarbonyl[η^5-cyclopentadienyl]molybdenum-coordinated η^3-cyclohexenyl ligand.

The retrosynthetic analysis of the 2-oxygenated carbazole alkaloids, 2-methoxy-3-methylcarbazole (**37**), *O*-methylmukonal (glycosinine) (**38**), 2-hydroxy-3-methylcarbazole (**52**), and mukonal (**53**) based on the molybdenum-mediated approach led to the molybdenum-complexed cation (**663**) and 3-methoxy-4-methylaniline (**655**) as precursors (Scheme 5.51). The cationic molybdenum complex, dicarbonyl (η^4-cyclohexadiene)(η^5-cyclopentadienyl)molybdenum hexafluorophosphate (**663**), required for the electrophilic substitution, was easily prepared quantitatively through known literature procedures (586,587).

Electrophilic substitution of 3-methoxy-4-methylaniline (**655**) by the complex **663** leads to the molybdenum complex **664**. Oxidative cyclization of complex **664** with concomitant aromatization using activated commercial manganese dioxide provides 2-methoxy-3-methylcarbazole (**37**) in 53% yield (560). In contrast, cyclization of the corresponding tricarbonyliron complex to **37** was achieved in a maximum yield of 11% on a small scale using iodine in pyridine as the oxidizing agent (see Scheme 5.49).

2-Methoxy-3-methylcarbazole (**37**) serves as a relay compound for the synthesis of further 2-oxygenated tricyclic carbazole alkaloids. Oxidation of the methyl group using DDQ gave *O*-methylmukonal (glycosinine) (**38**), which, on demethylation with boron tribromide, provided mukonal (**53**). Ether cleavage of **37** with hydrogen bromide/acetic acid gave 2-hydroxy-3-methylcarbazole (**53**) (560) (Scheme 5.52).

Retrosynthetic analysis of the 2,7-dioxygenated carbazole alkaloids, 7-methoxy-*O*-methylmukonal (**48**), clausine H (clauszoline-C) (**50**), clausine K (clauszoline-J) (**51**), and clausine O (**72**), based on an iron-mediated approach, led to 2-methoxy-substituted iron complex salt **665** and 3-methoxy-4-methylaniline (**655**) as precursors (588) (Scheme 5.53).

Electrophilic aromatic substitution of 3-methoxy-4-methylaniline (**655**) using the 2-methoxy-substituted iron complex salt **665**, followed by oxidative cyclization with concomitant aromatization of the resulting iron complex salt **666**, affords 2,7-dimethoxy-3-methylcarbazole (**667**). Oxidation of the carbazole **667** with DDQ

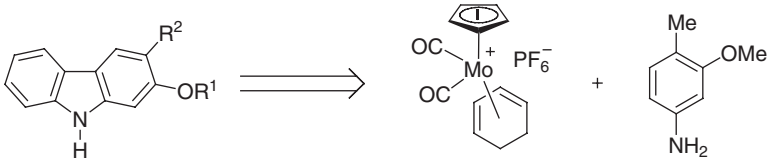

37 2-Methoxy-3-methylcarbazole
R^1, R^2 = Me

38 *O*-Methylmukonal (Glycosinine)
R^1 = Me; R^2 = CHO

52 2-hydroxy-3-methylcarbazole
R^1 = H; R^2 = Me

53 Mukonal
R^1 = H; R^2 = CHO

663 **655**

Scheme 5.51

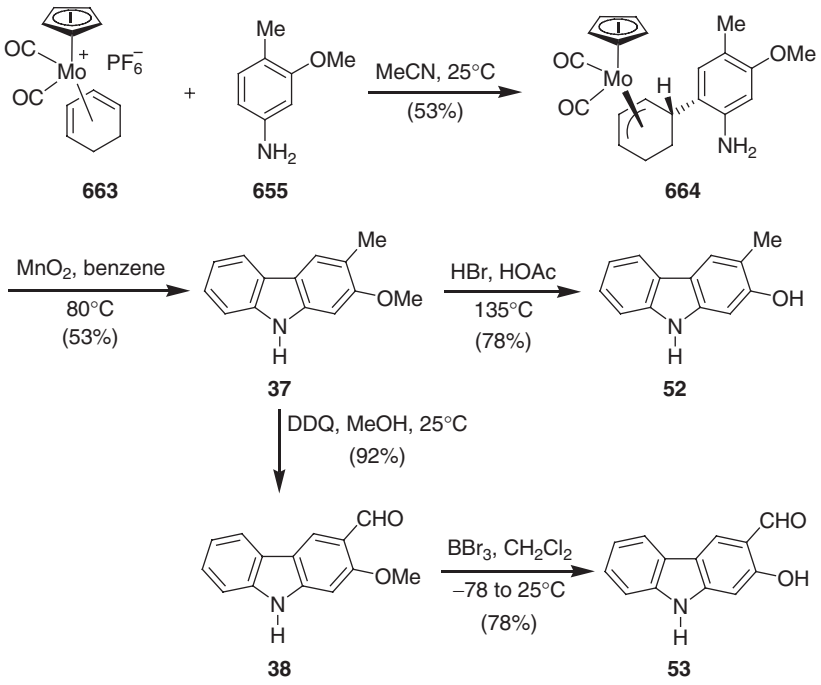

Scheme 5.52

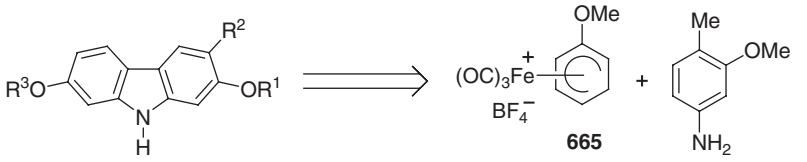

48 7-Methoxy-*O*-methylmukonal
R^1 = Me; R^2 = CHO; R^3 = H

50 Clausine H (Clauszoline-C)
R^1,R^3 = Me; R^2 = COOMe

51 Clausine K (Clauszoline-J)
R^1,R^3 = Me; R^2 = COOH

72 Clausine O
R^1,R^3 = H; R^2 = CHO

Scheme 5.53

leads to 7-methoxy-*O*-methylmukonal (**48**), which subsequently can be used as a relay compound to the other 2,7-dioxygenated carbazole alkaloids (Scheme 5.54).

Oxidation of **48** using manganese dioxide in methanol in the presence of potassium cyanide provides clausine H (clauszoline-C) (**50**) quantitatively, which on ester cleavage affords clausine K (clauszoline-J) (**51**). Cleavage of both methyl ethers of **51** on treatment with boron tribromide led to clausine O (**72**) (588).

Bedford *et al.* reported the total synthesis of glycozolidine (**40**) and clausine P (**46**) using the palladium(0)-catalyzed sequential amination and C–H activation reactions

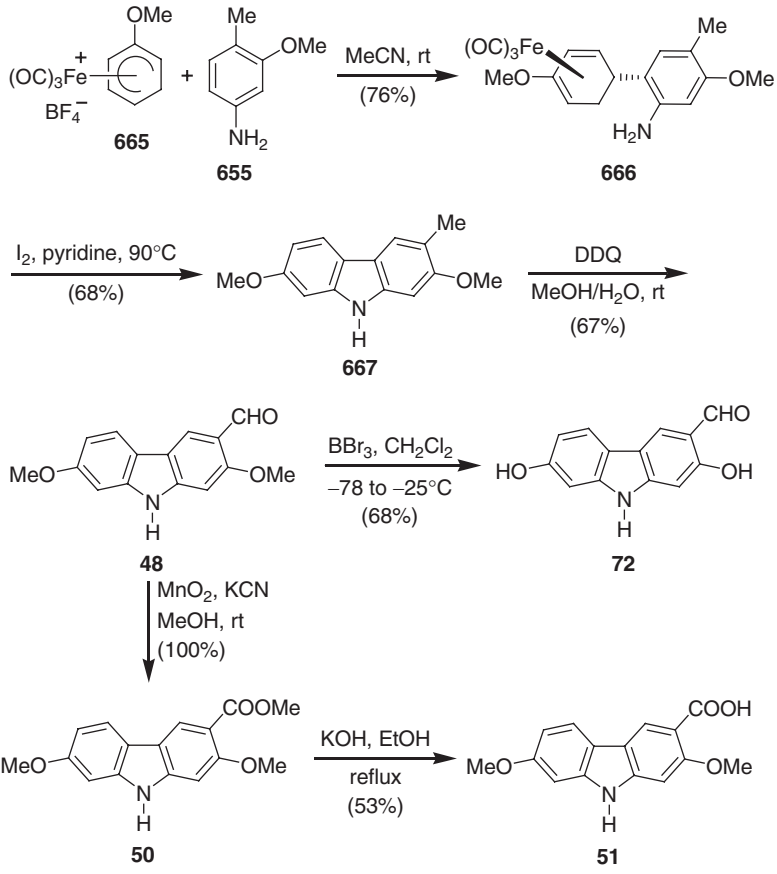

Scheme 5.54

of 2-chloroaniline **669** with arylbromides **670** and **671** (589). Buchwald–Hartwig amination of 2-chloroaniline **669** with 4-bromoanisole (**670**) led to the formation of the intermediate diarylamine **672**. Subsequent ring closure under palladium(0)-catalyzed thermal conditions in 1,4-dioxane yielded glycozolidine (**40**). Similarly, the two-step methodology was applied to the total synthesis of clausine P (**46**) starting from the same chloroaniline **669** and 2-bromoanisole (**671**). This two-step process was achieved in a microwave-assisted one-pot procedure involving two, sequential catalytic transformations (589) (Scheme 5.55).

3 3-Oxygenated Tricyclic Carbazole Alkaloids

Danheiser *et al.* developed a new aromatic annulation methodology for the total synthesis of hyellazole (**245**) by irradiation of the heteroaryl α-diazo ketone **675** in the presence of 1-methoxypropyne (590). This reaction proceeds *via* the photochemical Wolff rearrangement of the heteroaryl α-diazo ketone **675** to generate a vinylketene, followed by a cascade of three pericyclic reactions.

A diazo transfer to *N*-Boc-3-acetylindole (**674**) provided the corresponding α-diazo ketone **675**. Irradiation of a 1,2-dichloroethane solution of **675** and

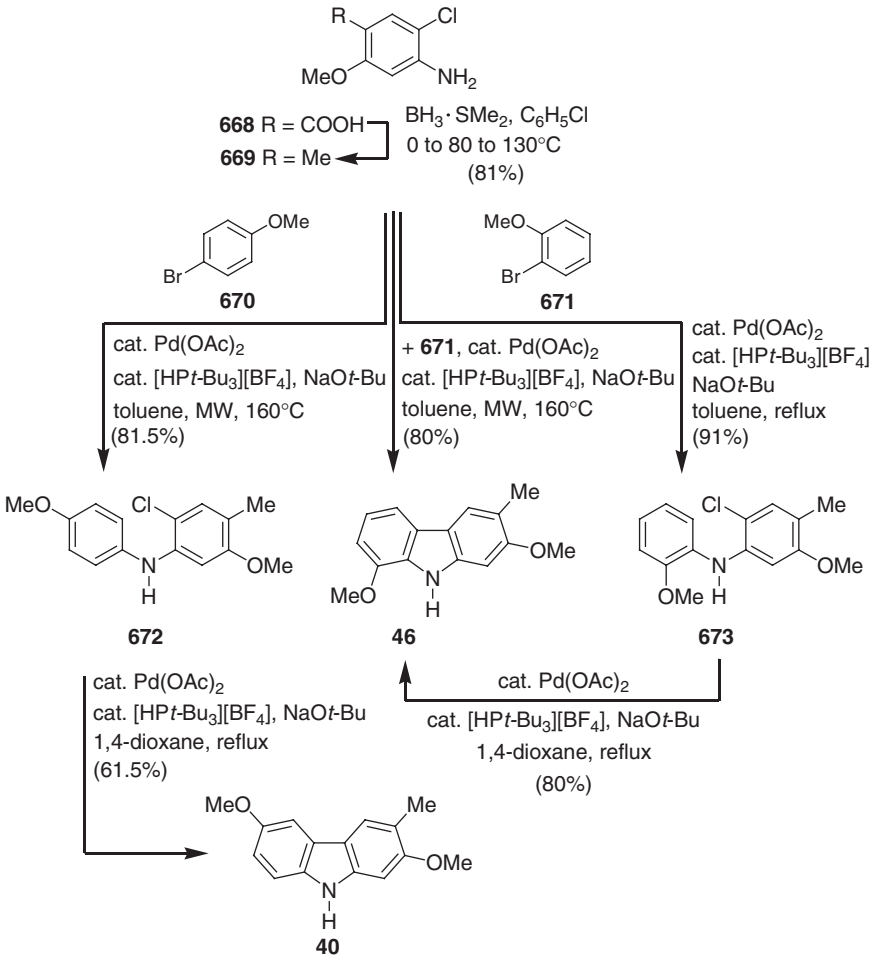

Scheme 5.55

1-methoxypropyne gave the 1-hydroxycarbazole **678**. Mechanistically, this annulation involves a photochemical Wolff rearrangement of the α-diazo ketone **675** to generate a vinylketene intermediate, which combines with 1-methoxypropyne in a regiospecific [2+2] cycloaddition. Further irradiation results in a 4π-electrocyclic ring opening of the cyclobutenone **676** to the dienylketene **677**, and subsequent 6π electrocyclization to afford a 2,4-cyclohexadienone, which, on tautomerization, furnishes the hydroxycarbazole **678**. After conversion of the hydroxycarbazole **678** to the corresponding triflate **679**, the phenyl group was introduced at C-1 by a Stille cross-coupling reaction with trimethylphenylstannane in the presence of a catalytic amount of tetrakis(triphenylphosphane)palladium to afford hyellazole (**245**) (590) (Scheme 5.56).

Moody *et al.* reported the synthesis of the 3-oxygenated carbazole alkaloids, hyellazole (**245**) (591,592) and carazostatin (**247**) (593,594) based on their pyrano[3,4-*b*]indol-3-one methodology (Scheme 5.57). This synthetic strategy involves the use of a 1-substituted pyrano[3,4-*b*]indol-3-one **542** as a stable

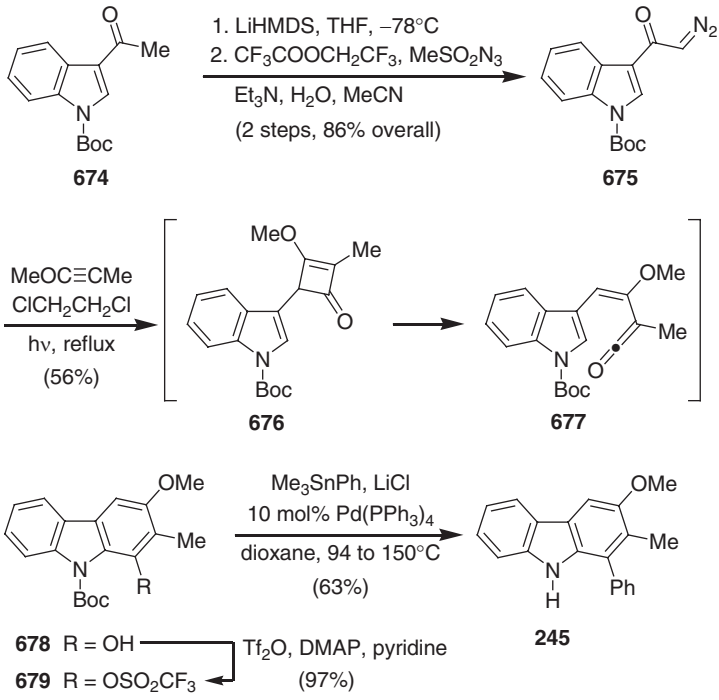

Scheme 5.56

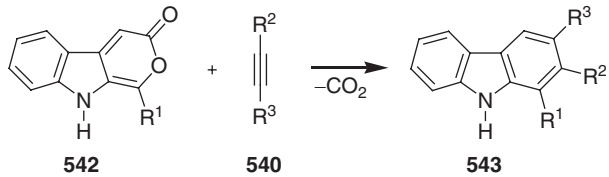

Scheme 5.57

equivalent of indolo-2,3-quinodimethanes in the Diels–Alder reaction with the alkyne **540** to afford carbazole derivatives **543** by concomitant loss of carbon dioxide.

For the synthesis of carazostatin (**247**) the required 1-heptylpyrano[3,4-*b*]indol-3-one (**681**) was obtained from indol-3-ylacetic acid (**680**) by reaction with octanoic anhydride in the presence of boron trifluoride etherate. Diels–Alder reaction of the pyrone **681** with ethyl 3-trimethylsilylpropynoate (**682**) afforded the desired carbazole **683** with complete regioselectivity, following the loss of carbon dioxide. The ester group in carbazole **683** was directly reduced to a methyl group by reacting with an excess of lithium aluminum hydride. Transformation of the trimethylsilyl group of the carbazole **684** into a hydroxy group was achieved by a three-step sequence employing mild oxidizing conditions. Thus, the 1,2-dialkyl-3-trimethylsilylcarbazole **684** was converted into carazostatin (**247**) in 44% overall yield by mercuriodesilylation, followed by hydroboration and oxidation (593,594) (Scheme 5.58).

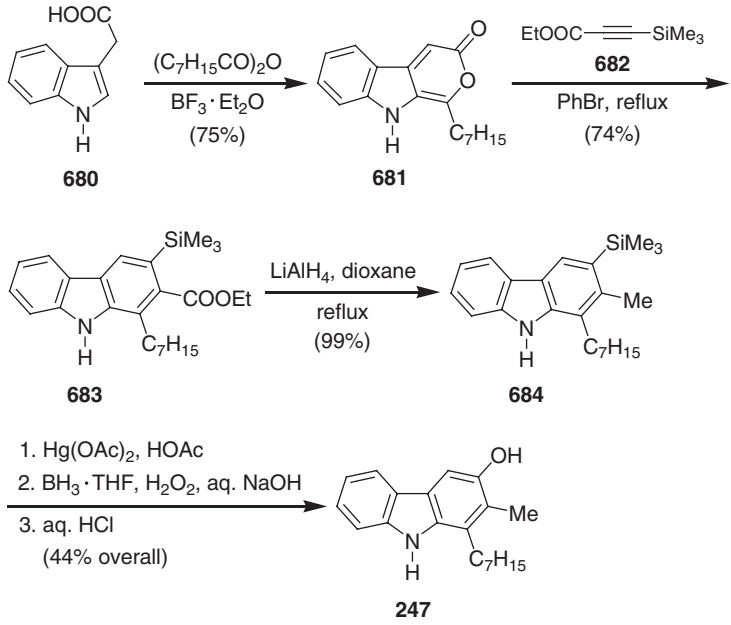

Scheme 5.58

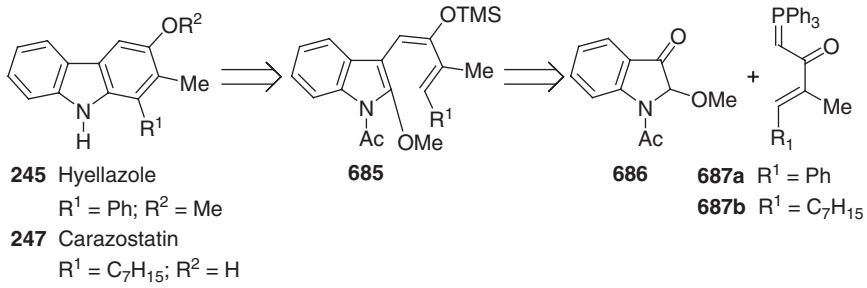

Scheme 5.59

Sakamoto *et al.* reported the synthesis of hyellazole (**245**) and carazostatin (**247**) based on the benzannulation of indoles. This method involves an electrocyclization of the 3-(1,3-butadienyl)indoles **685**, which derive from the indolin-3-one **686** and the phosphorus ylides **687** (Scheme 5.59).

Wittig reaction of the readily available 1,2-dihydroindol-3-one (**686**) with phosphoranes **687** afforded the enones **688**, which were treated with trimethylsilyl iodide (TMSI) in the presence of 1,1,1,3,3,3-hexamethyldisilazane (HMDS) to give the corresponding trimethylsilyl enol ethers **685**. The electrocyclic reaction of the enol ethers **685** in boiling *cis*-decalin (bp 195°C) gave the 3-silyloxycarbazoles **690**. The reaction sequence probably involves the isomerization of the enol ethers **685**, followed by electrocyclization and aromatization of the intermediate dihydrocarbazoles **689** by elimination of methanol. Removal of the silyl group from the 3-silyloxycarbazoles **690** with tetrabutylammonium fluoride (TBAF) afforded the 3-hydroxycarbazoles **691**. The 3-hydroxycarbazole **691a** was methylated to give

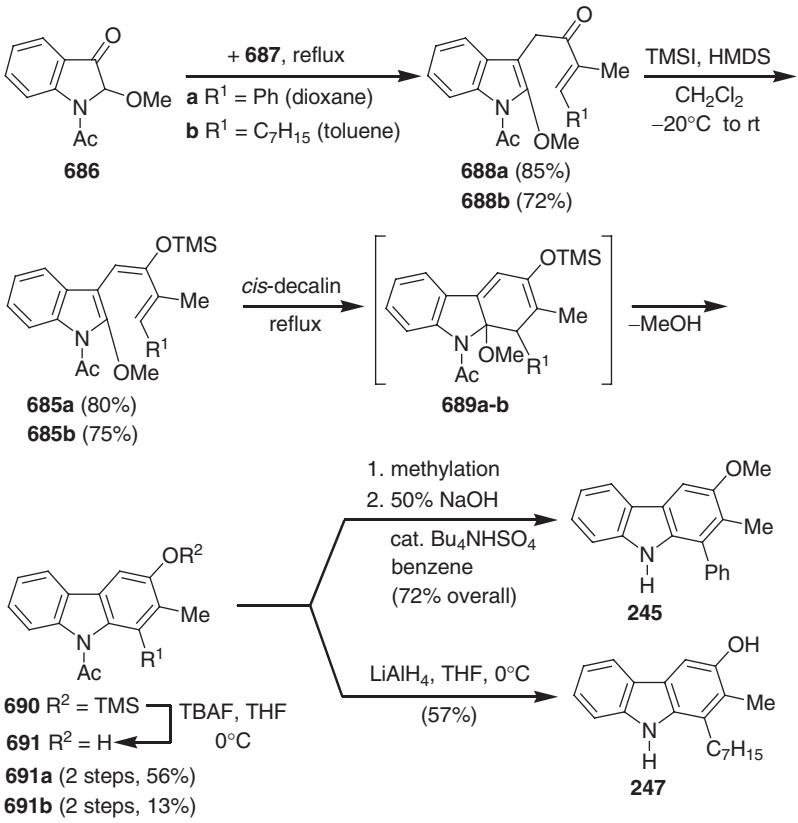

Scheme 5.60

N-acetylhyellazole, which on deacetylation with sodium hydroxide under phase transfer conditions afforded hyellazole (**245**) (538,539). Removal of the acetyl group from *N*-acetylcarazostatin (**691b**), by reduction with lithium aluminum hydride, provided carazostatin (**247**) (595) (Scheme 5.60).

Using a modification of Sakamoto's indole benzannulation protocol (see Scheme 5.59), Beccalli *et al.* reported the synthesis of the 3-methoxycarbazole alkaloids hyellazole (**245**) and 6-chlorohyellazole (**246**) (540) (Scheme 5.61). Unlike Sakamoto's methodology, this method requires a good leaving group at the 2-position of the indole moiety of the 3-(1,3-butadienyl)indoles **692** to facilitate the aromatization of the intermediate dihydrocarbazole by eliminating the dehydrogenation step.

The key intermediates **692** required for the thermal cyclization were prepared from the readily available indole-2,3-diones **693**. The condensation of **693** with 3-methyl-4-phenylbut-3-en-2-one (**694**) afforded the 3-hydroxy derivatives **695**. The dehydration of **695**, followed by selective reduction of the 3,1′-double bond of compounds **696**, provided the 3-alkyl derivative **697**. Finally, the compounds **697** were transformed to the 3-(1,3-butadienyl)indoles **692** by reaction with an excess of ethyl chloroformate (Scheme 5.62).

The thermal cyclization of 3-(1,3-butadienyl)indoles **692** in refluxing *cis*-decalin afforded the carbazoles **698**. Selective hydrolysis of the 3-carbonate ester, methylation of the corresponding 3-hydroxycarbazoles **699** with methyl iodide in the presence of

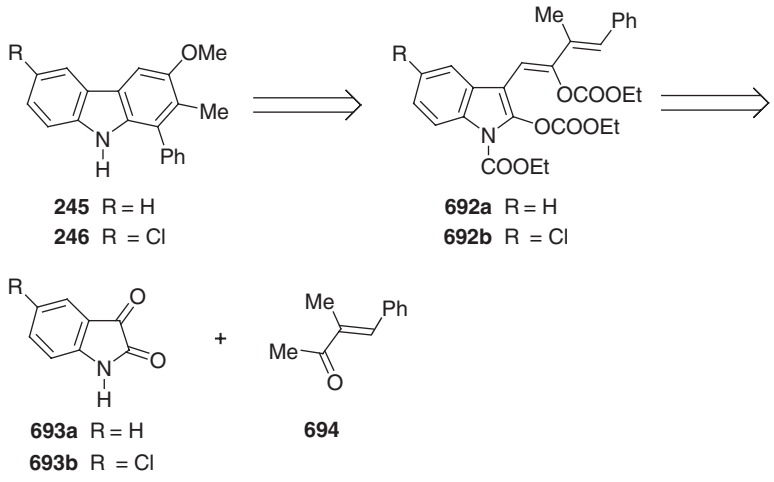

Scheme 5.61

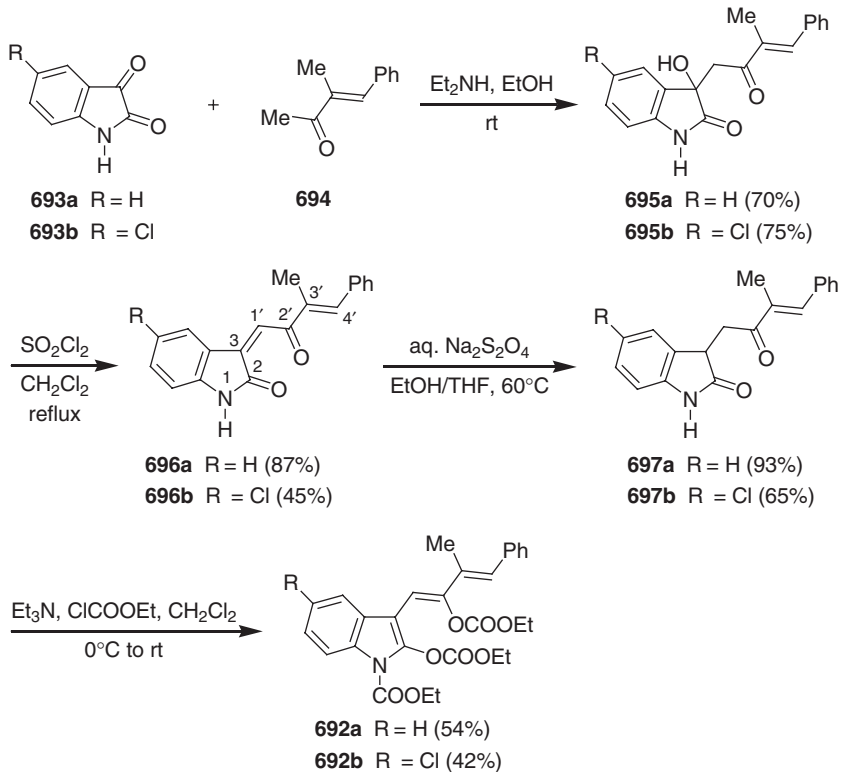

Scheme 5.62

sodium hydride, and subsequent alkaline hydrolysis under reflux gave hyellazole (**245**) and 6-chlorohyellazole (**246**) (540) (Scheme 5.63).

Shin and Ogasawara reported a new total synthesis of carazostatin (**247**) from *N*-carbethoxy-2-iodoaniline (**700**) and 1-decyne involving two aromatic annulation

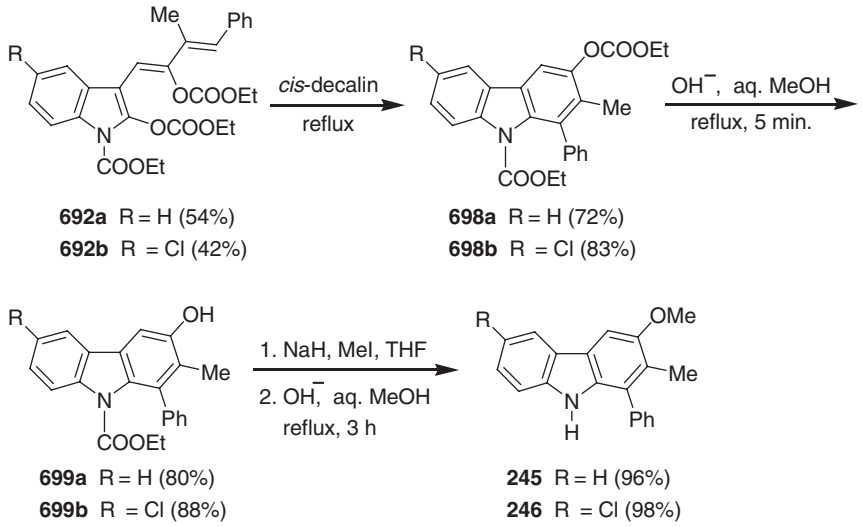

Scheme 5.63

reactions as key steps (596). The palladium-catalyzed cross-coupling of *N*-carbethoxy-2-iodoaniline (**700**) and 1-decyne afforded the arylacetylene **701**. The first aromatic annulation of the arylacetylene **701** by a base-induced indolization provided 2-octylindole (**702**). Following a standard procedure, 2-octylindole (**702**) was transformed to 2-octyltryptamine (**704**) in four steps. The condensation of 2-octyltryptamine (**704**) with ethyl(2-ethoxymethylene)acetoacetate (**705**) provided the conjugated enamine **706** required for the second aromatic annulation. In a one-pot operation, compound **706** was transformed to the carbazole **707** by refluxing in a 5:3 mixture of acetic anhydride and acetic acid. Finally, using the indicated four-step sequence (–COOEt→–CH_2OH→–CHO→–OCHO→–OH), the carbazole **707** was converted to carazostatin (**247**) (596) (Scheme 5.64).

The total syntheses of carazostatin (**247**), hyellazole (**245**), and 6-chlorohyellazole (**246**) based on our iron-mediated annulation require 1,3-cyclohexadiene (**597**) and the corresponding arylamines **708** and **709** as precursors (597–600) (Scheme 5.65).

For the synthesis of carazostatin (**247**), the required arylamine **708** was synthesized starting from 1-methoxycyclohexa-1,3-diene (**710**) and methyl 2-decynoate (**711**). The key step in this route is the Diels–Alder cycloaddition of **710** and **711**, followed by retro-Diels–Alder reaction with extrusion of ethylene to give 2-heptyl-6-methoxybenzoate (**712**). Using a three-step sequence, the methoxycarbonyl group of compound **712** was transformed to the methyl group present in the natural product. 3-Heptyl-3-methylanisole (**713**) was obtained in 85% overall yield. Finally, the anisole **713** was transformed to the arylamine **708** by nitration and subsequent catalytic hydrogenation. This simple sequence provides the arylamine **708** in six steps and with 26% overall yield (597,598) (Scheme 5.66).

Electrophilic aromatic substitution of **708** with the iron-coordinated cation **602** afforded the iron-complex **714** quantitatively. The iron-mediated quinone imine cyclization of complex **714**, by sequential application of two, differently activated, manganese dioxide reagents, provided the iron-coordinated 4b,8a-dihydrocarbazole-3-one **716**. Demetalation of the iron complex **716** with concomitant

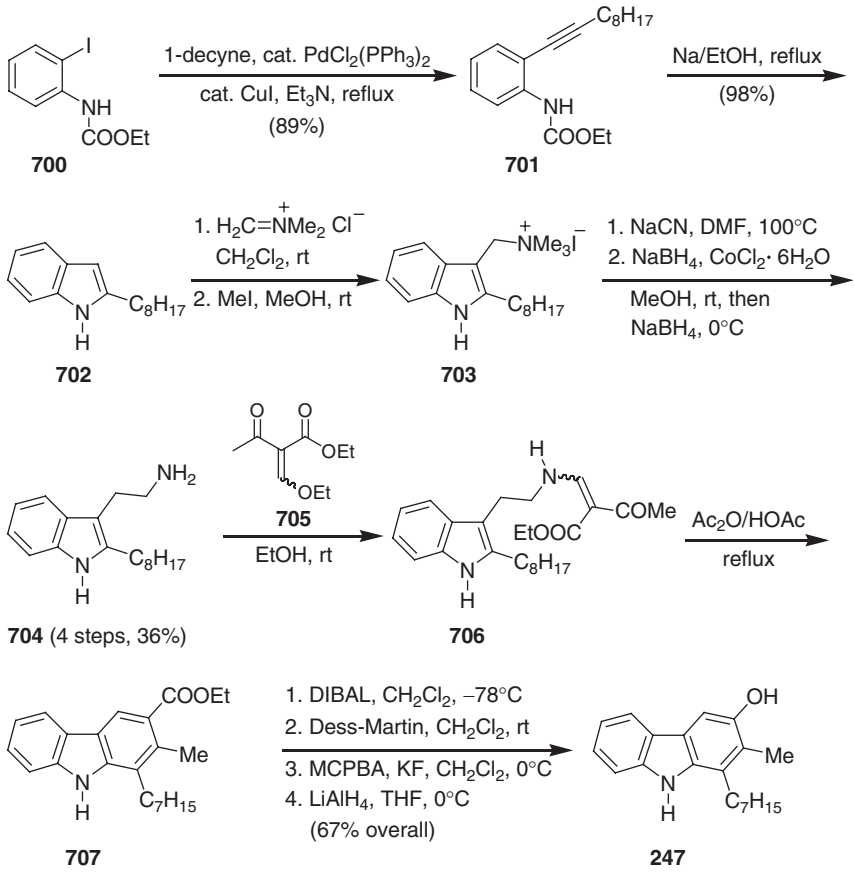

Scheme 5.64

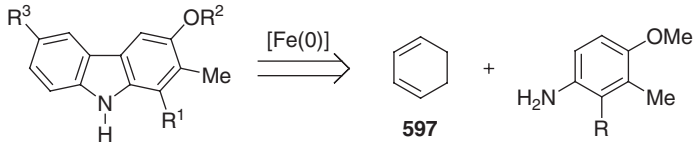

247 Carazostatin
$R^1 = C_7H_{15}$; R^2,R^3 = H

245 Hyellazole
R^1 = Ph; R^2 = Me; R^3 = H

246 6-Chlorohyellazole
R^1 = Ph; R^2 = Me; R^3 = Cl

Scheme 5.65

tautomerization using trimethylamine *N*-oxide afforded carazostatin (**247**) (597,598) (Scheme 5.67).

Alternatively, using the iron-mediated arylamine cyclization, a short access to carazostatin (**247**), albeit in lower yield, was achieved. The oxidation of the complex **714** with ferricenium hexafluorophosphate in the presence of sodium carbonate

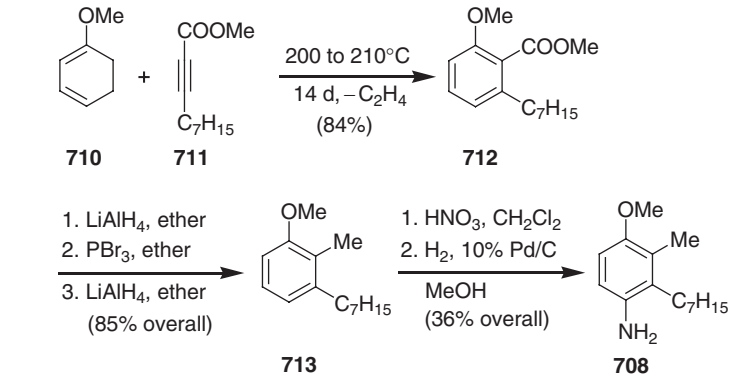

Scheme 5.66

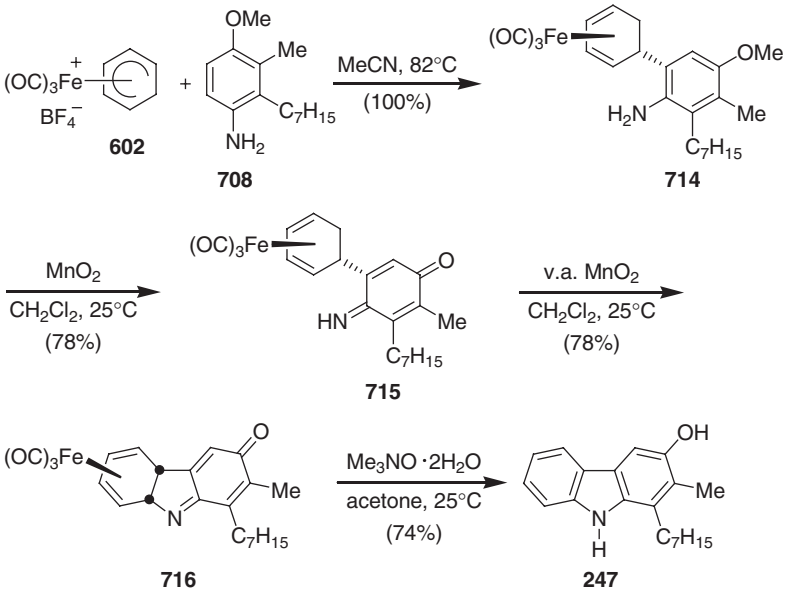

Scheme 5.67

followed by demetalation with concomitant tautomerization of the intermediate iron-coordinated 4b,8a-dihydrocarbazol-3-one **716** using trimethylamine *N*-oxide led to carazostatin (**247**) (598).

The arylamine **709** required for the total synthesis of hyellazole (**245**) was synthesized by Diels–Alder reaction of 1-methoxycyclohexa-1,3-diene (**710**) and ethyl phenylpropynoate **711**. The biphenyl derivative **719** thus obtained was transformed to the arylamine **709** by excecuting a similar reaction sequence as shown in Scheme 5.66. The arylamine **709** was obtained in six steps and 7% overall yield based on 1-methoxycyclohexa-1,3-diene (**710**) (599,600) (Scheme 5.68).

The drawback of the aforementioned sequence is the low yield (30%) of the desired regioisomer **719** in the Diels–Alder reaction. Therefore, the overall yield of the intermediate biphenyl derivative **720** by the route shown in Scheme 5.68 was

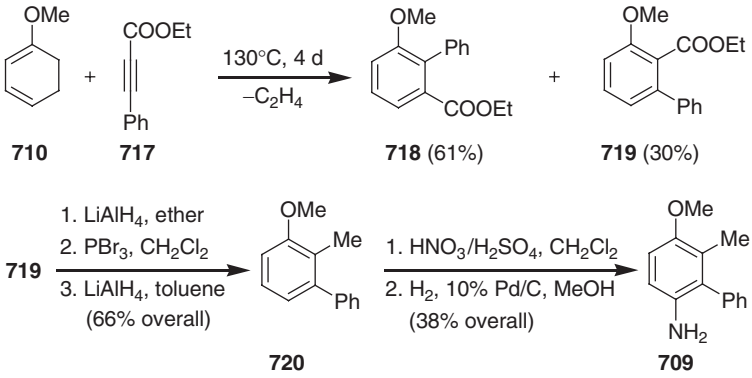

Scheme 5.68

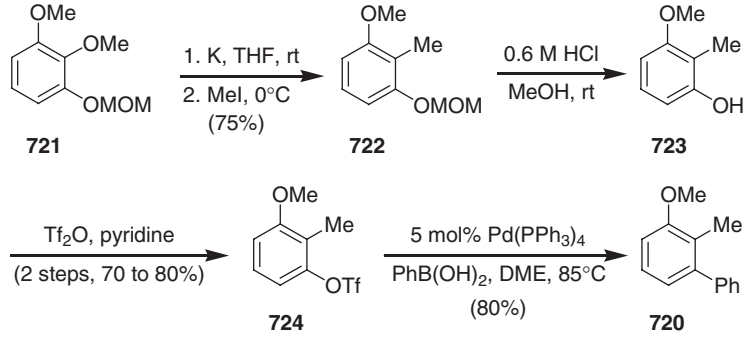

Scheme 5.69

limited to 20%. However, Azzena *et al.* reported a new synthesis of the biphenyl derivative **720** starting from 1,2-dimethoxy-3-methoxymethoxybenzene (**721**) (601). The key step in this approach is a Suzuki-Miyaura cross-coupling of the triflate **724** with phenylboronic acid using 5 mol% $Pd(PPh_3)_4$. This alternative method provides the biphenyl derivative **720** in four steps and 48% overall yield based on compound **721** (600) (Scheme 5.69).

Electrophilic substitution at the arylamine **709** using the complex salt **602**, provided the iron complex **725** quantitatively. Sequential, highly chemoselective oxidation of the iron complex **725** with two, differently activated, manganese dioxide reagents provided the tricarbonyliron-complexed 4b,8a-dihydrocarbazol-3-one (**727**) *via* the non-cyclized quinone imine **726**. Demetalation of the tricarbonyliron-complexed 4b,8a-dihydrocarbazol-3-one (**727**), followed by selective *O*-methylation, provided hyellazole (**245**) (599,600) (Scheme 5.70).

An alternative method for the oxidative cyclization of the arylamine-substituted tricarbonyl(η^4-cyclohexa-1,3-diene)iron complex (**725**) is the iron-mediated arylamine cyclization. Using ferricenium hexafluorophosphate in the presence of sodium carbonate provided hyellazole (**245**) directly, along with the complex **727**, which was also converted to the natural product (599,600) (Scheme 5.71).

For the synthesis of 6-chlorohyellazole (**246**), the required arylamine **709** was prepared in very good overall yield starting from commercially available

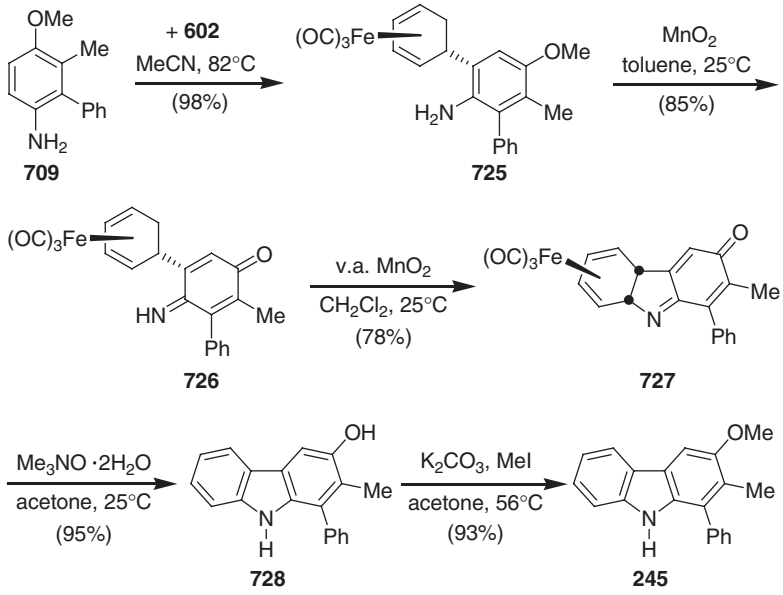

Scheme 5.70

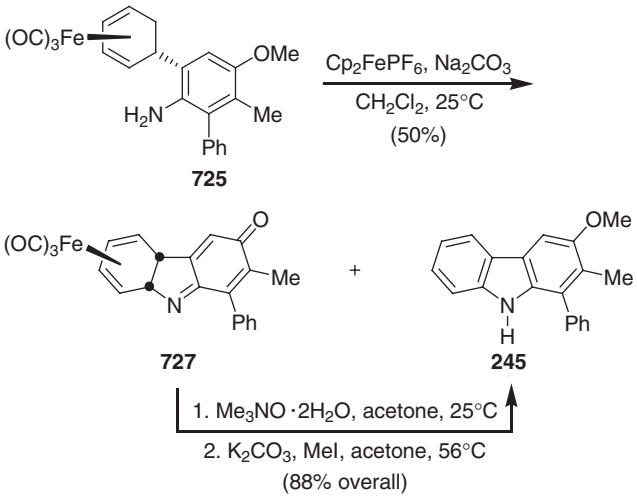

Scheme 5.71

2,6-dimethoxytoluene (**729**). Nitration of **729** using claycop afforded selectively the desired nitro derivative **730**. After demethylation, the corresponding hydroxy derivative **731a** was transformed to the triflate **731b**, which, on Suzuki–Miyaura cross-coupling with phenylboronic acid, led to the biphenyl derivative **732**. Finally, catalytic hydrogenation of **732** afforded the corresponding arylamine **709**. This improved route affords the arylamine **709** in five steps and 76% overall yield (previous route: six steps, 18%) (602) (Scheme 5.72).

Electrophilic substitution of the arylamine **709** with the complex salt **602** gave the iron complex **725** quantitatively. The iron-mediated arylamine cyclization, by

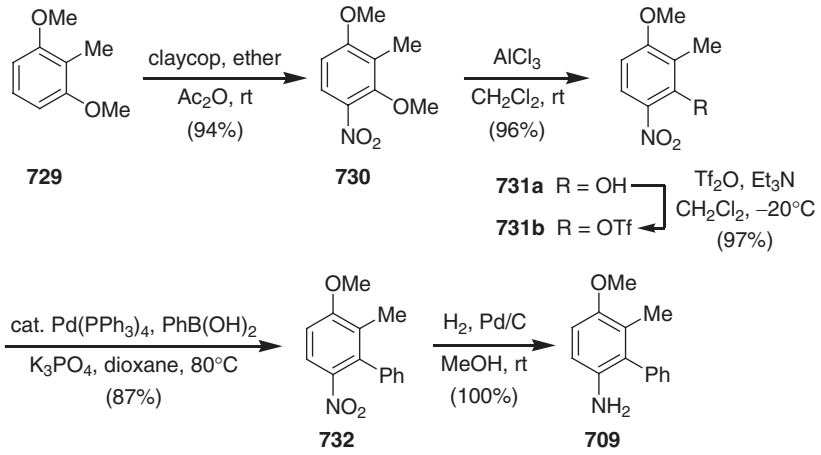

Scheme 5.72

oxidation with ferricenium hexafluorophosphate in the presence of sodium carbonate, transformed the complex **725** into hyellazole (**245**) in two steps and 84% yield. Alternatively, in a one-pot operation, the iron complex **725** was directly transformed into hyellazole (**245**) in 69% yield by reacting with 3 equivalents of *N*-bromosuccinimide (NBS) in the presence of an excess of sodium carbonate. Taking the improved synthesis of the arylamine **709** into account, hyellazole (**245**) was obtained in eight steps and 63% overall yield (602).

An attempt to directly convert hyellazole (**245**) to 6-chlorohyellazole (**246**) by reaction with *N*-chlorosuccinimide in the presence of a catalytic amount of hydrochloric acid led exclusively to 4-chlorohyellazole. On the other hand, bromination of **245** using NBS and a catalytic amount of hydrobromic acid gave only the expected 6-bromohyellazole (**733**). Alternatively, a direct one-pot transformation of the iron complex **725** to 6-bromohyellazole (**733**) was achieved by reaction with an excess of NBS and switching from oxidative cyclization conditions (basic reaction medium) to electrophilic substitution conditions (acidic reaction medium). Finally, a halogen exchange reaction with 4 equivalents of cuprous chloride in *N*,*N*-dimethylformamide (DMF) at reflux, transformed 6-bromohyellazole (**733**) into 6-chlorohyellazole (**246**) (602) (Scheme 5.73).

Hibino *et al*. reported the total synthesis of carazostatin (**247**) and hyellazole (**245**) using a benzannulation method based on the electrocyclization of a 2,3-difunctionalized indole *via* an allene intermediate (536,537). The 3-alkenyl-2-propargylindole **736**, used as common precursor for the total synthesis of carazostatin (**247**) and hyellazole (**245**), was prepared in five steps and 51% overall yield starting from 2-formylindole (**734**). The thermal electrocyclization of **736** *via* the intermediate allene **737** was achieved by heating at 90°C in *tert*-butyl alcohol in the presence of potassium *tert*-butoxide to afford the desired carbazole **738** (43% yield), along with the *N*-deprotected carbazole **739** (41% yield). However, using alkaline hydrolytic conditions, **738** was transformed to the carbazole **739** as the sole product. Subsequent cleavage of the MOM ether of **739** using trimethylsilyl chloride (TMSCl) and sodium iodide, followed by treatment with trifluoromethane sulfonic anhydride (Tf_2O) and pyridine, afforded the triflate **740**. The introduction of either the heptyl side chain or

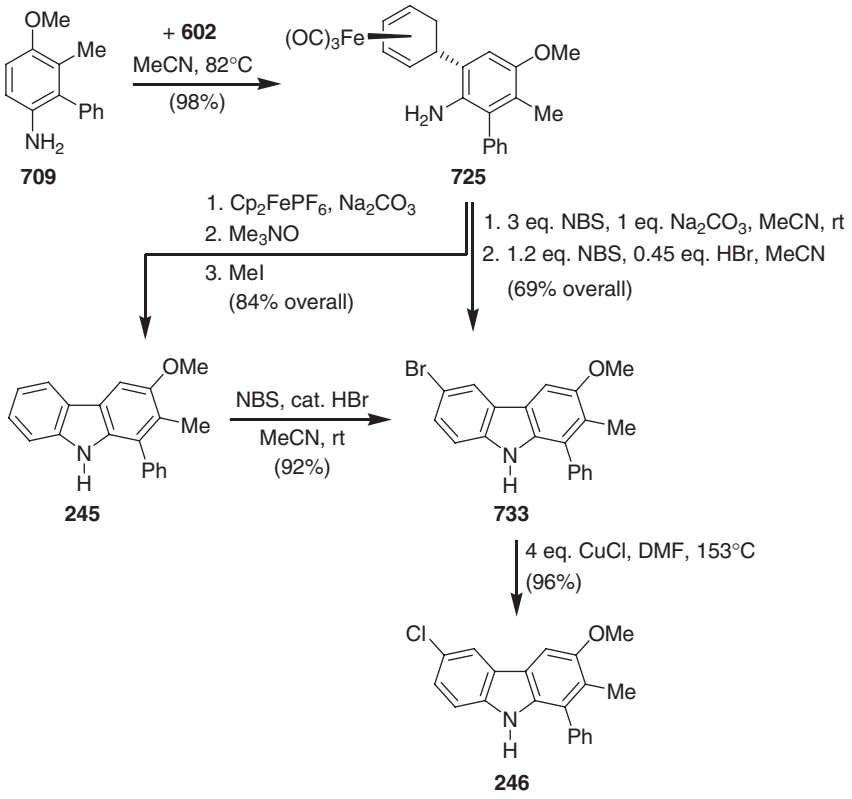

Scheme 5.73

the phenyl group at C-1 by Suzuki cross-coupling reaction transformed the triflate **740** to the carbazoles **741** and **742**, respectively.

Finally, cleavage of the ethyl ether of **741** using boron tribromide afforded carazostatin (**247**). Similarly, cleavage of the ethyl ether of **742** led to the hydroxycarbazole **728**, which, on *O*-methylation, provided hyellazole (**245**) (536,537) (Scheme 5.74).

Witulski and Alayrac reported the synthesis of hyellazole (**245**) using a rhodium-catalyzed alkyne cyclotrimerization (561). The key diyne **746** precursor required for cyclotrimerization with 1-methoxy propyne (**747**) was obtained in three steps starting from readily available 2-iodoaniline (**743**). Using Sonogashira reaction conditions, 2-iodoaniline (**743**) was reacted with trimethylsilylacetylene followed by *N*-tosylation and protodesilylation to afford the alkyne **744**. The alkyne **744** underwent *N*-ethynylation with alkynyliodinium triflate **745** to furnish the diyne **746**. Using Wilkinson's catalyst, $[RhCl(PPh_3)_3]$, crossed alkyne cyclotrimerization between diyne **746** and 1-methoxy propyne (**747**) led to *N*-tosylhyellazole (**748**) in 89% yield and an isomeric ratio of 30:1. Isomerically pure hyellazole was obtained by deprotection of the tosyl group with TBAF in refluxing tetrahydrofuran (THF), followed by crystallization (561) (Scheme 5.75).

Our total syntheses of the carbazomadurins A (**253**) (603) and B (**254**) (604) use the palladium-catalyzed fusion of three building blocks **749**, **750**, and **751**, and a

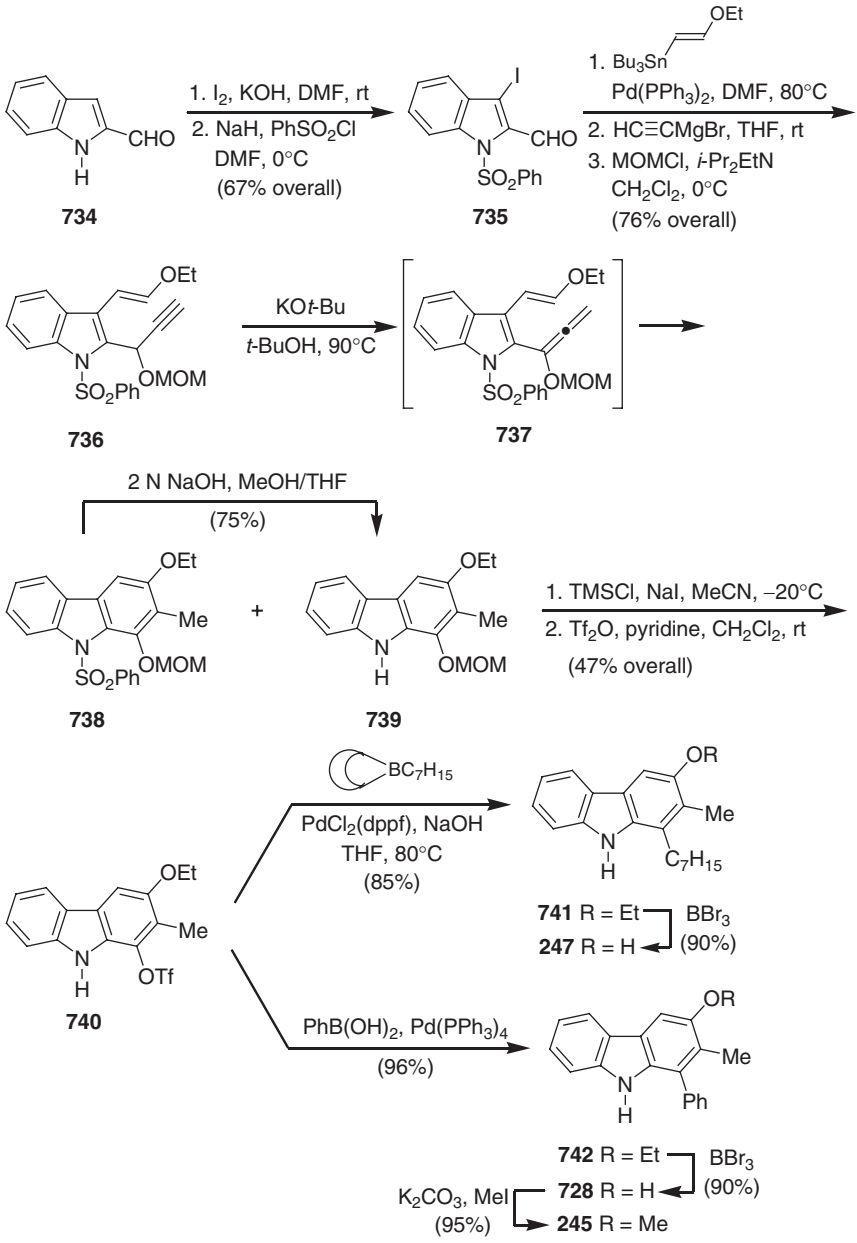

Scheme 5.74

zirconium-catalyzed generation of the *E*-configured double bond (Scheme 5.76). One of the three building blocks, the aryl triflate **749**, was easily prepared in 91% overall yield in two steps starting from isovanillic acid (**752**). After esterification of **752**, the corresponding methyl ester **753** was reacted with triflic anhydride using 2,6-lutidine as base to give the corresponding triflate **749** (Scheme 5.77).

Another building block, the arylamine **750**, was prepared from 2-bromo-6-nitrotoluene (**754**) in 44% overall yield in five simple steps. Transfer hydrogenation of

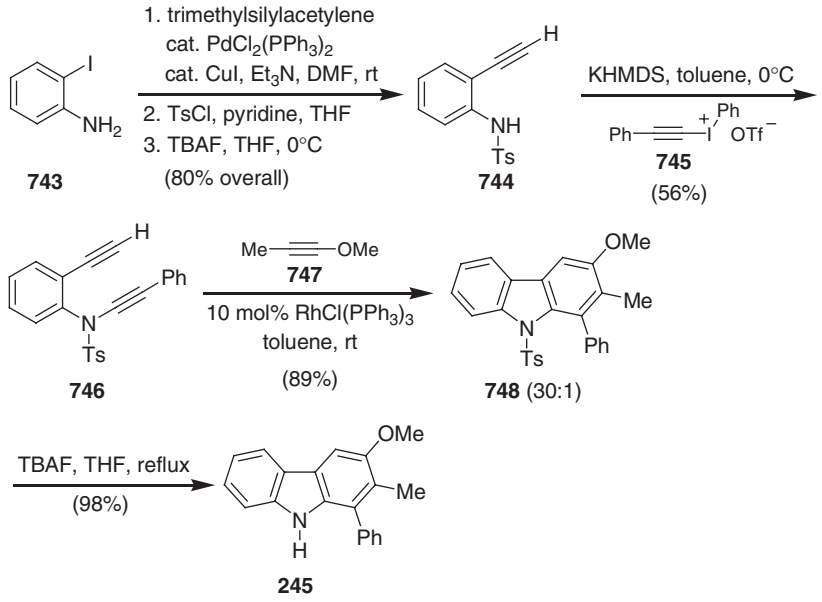

Scheme 5.75

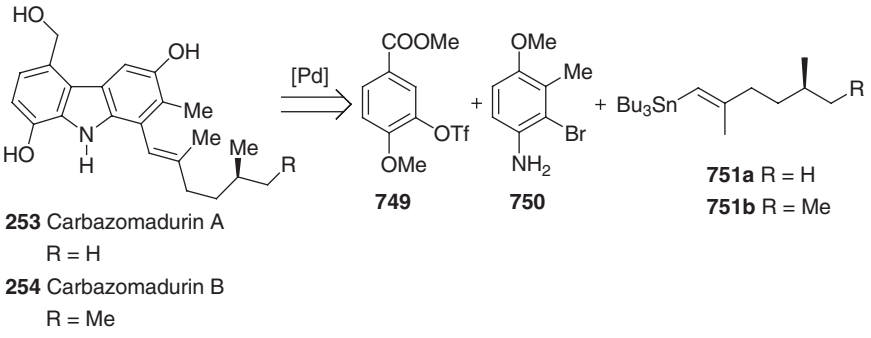

Scheme 5.76

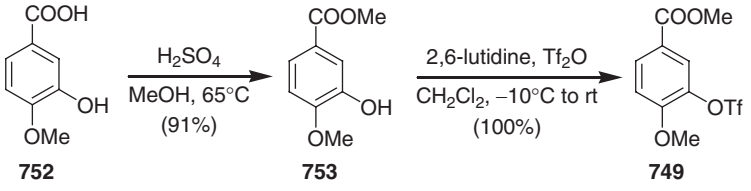

Scheme 5.77

754 using hydrazine hydrate afforded 3-bromo-2-methylaniline (**755**), which was converted to the corresponding phenol **756** *via* diazotization. After methylation of **756**, the corresponding anisole **757** was subjected to nitration using claycop, followed by reduction, which led to the arylamine **750** (603) (Scheme 5.78).

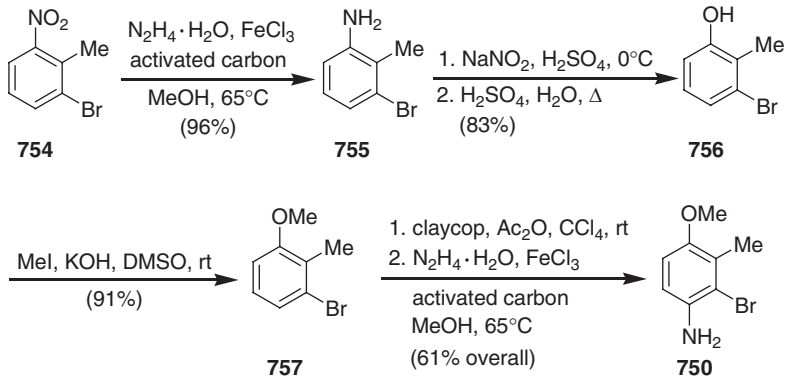

Scheme 5.78

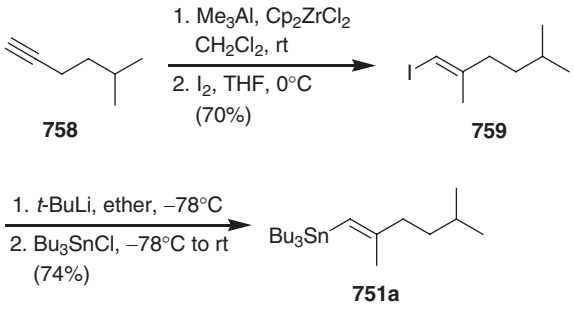

Scheme 5.79

The stereospecific construction of the trisubstituted double bond of the side chain at C-1 of carbazomadurins A (**253**) and B (**254**) was achieved using Negishi's zirconium-catalyzed carboalumination of alkynes **758** and **763**, respectively. Reaction of 5-methyl-1-hexyne (**758**) with trimethylalane in the presence of zirconocene dichloride, followed by the addition of iodine, afforded the vinyl iodide **759** with the desired *E*-configuration of the double bond. Halogen–metal exchange with *tert*-butyllithium, and reaction of the intermediate vinyllithium compound with tributyltin chloride, provided the vinylstannane **751a** (603) (Scheme 5.79).

Assuming an *S* configuration for carbazomadurin B (**254**), the synthesis of the chiral alkenylstannane **751b** was achieved in six steps and 11% overall yield from commercial (*S*)-(−)-2-methyl-1-butanol (**760**). After confirming an enantiomeric purity of >99% ee for **760**, it was transformed to the corresponding bromo derivative **761**. Conversion of **761** to the Grignard reagent and Wurtz coupling with allyl bromide led to the alkene derivative **762**. Subsequent bromination, followed by double dehydrobromination with potassium *tert*-butoxide in the presence of catalytic amounts of [18]-crown-6, provided (*S*)-(+)-5-methyl-1-heptyne (**763**). Executing the similar reaction sequence of the transformation of 5-methyl-1-hexyne (**758**) to the *E*-configured vinylstannane **751a** (see Scheme 5.79), the 1-heptyne **763** was transformed to the *E*-alkenylstannane **751b** (604) (Scheme 5.80).

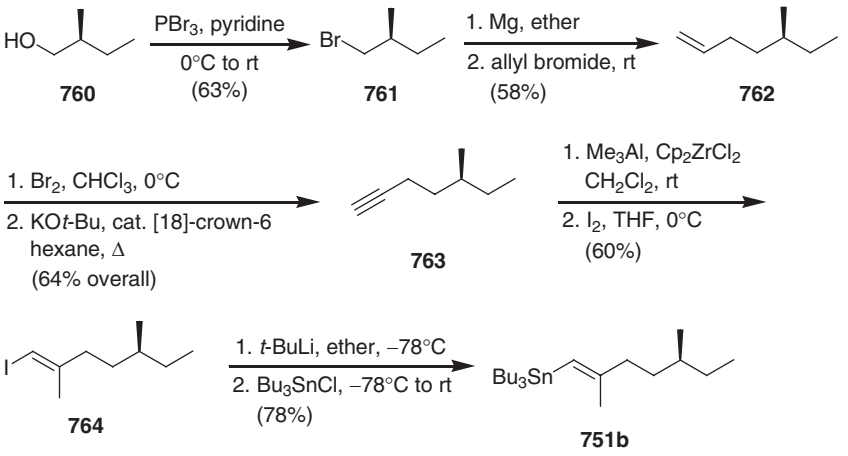

Scheme 5.80

Using Buchwald–Hartwig amination conditions, the aryl triflate **749** and the arylamine **750** were coupled to afford the *N*,*N*-diarylamine **765**. Subsequent palladium(II)-mediated oxidative cyclization of **765** led to the carbazole **766**. Cleavage of both methyl ethers, followed by double silylation, afforded the bis(*tert*-butyldiphenylsilyl) (TPS) ether **767** with a switch of the protecting group. Palladium(0)-catalyzed Stille coupling of the 1-bromocarbazole **767** and the alkenylstannanes **751a** and **751b** furnished the 1-alkenylcarbazoles **768a** and **768b**, respectively. Reduction of the methyl ester using DIBAL-H led to the corresponding benzylic alcohols **769a** and **769b** which served as common precursors for the carbazomadurins and epocarbazolines. Finally, removal of both silyl protecting groups from the disilyl-protected precursors **769** with TBAF provided the carbazomadurins A (**253**) (603) and B (**254**) (604) (Scheme 5.81).

All attempts to achieve a direct transformation of the carbazomadurins A (**253**) and B (**254**), as well as the disilyl-protected carbazomadurins A (**769a**) and B (**769b**), into the epocarbazolins A (**258**) and B (**259**) were unsuccessful and resulted in complete decomposition. Therefore, prior to the epoxidation, the disilyl-protected carbazomadurins A (**769a**) and B (**769b**) were transformed to the corresponding trisilyl-protected carbazomadurins A (**770**) and B (**771**) by treatment with TPS chloride in the presence of stoichiometric amounts of 4-(dimethylamino)pyridine (DMAP). Epoxidation of the fully protected carbazomadurins A (**770**) and B (**771**) with dimethyldioxirane at −20°C, followed by desilylation, provided racemic epocarbazolin A (**258**) and epocarbazolin B (**259**) (605) (Scheme 5.82).

Duval and Cuny reported the total syntheses of hyellazole (**245**) and 6-chlorohyellazole (**246**) starting from diketoindoles **777a** and **777b** (606). In this methodology, the key step is the base-catalyzed intramolecular aldol condensation of the ketoindoles to fully functionalized 3-hydroxycarbazoles.

The diketoindoles **777** were prepared in three steps starting from indol-3-ylacetic acid (**680**) and 5-chloro indol-3-ylacetic acid (**774**) in 75% and 66% overall yield, respectively. The indole acids **680** and **774** were converted into Weinreb amides **775**, followed by reaction with ethyl Grignard reagent to afford the corresponding indol-3-yl ketones **776**. In order to introduce the second carbonyl moiety, the 3-substituted

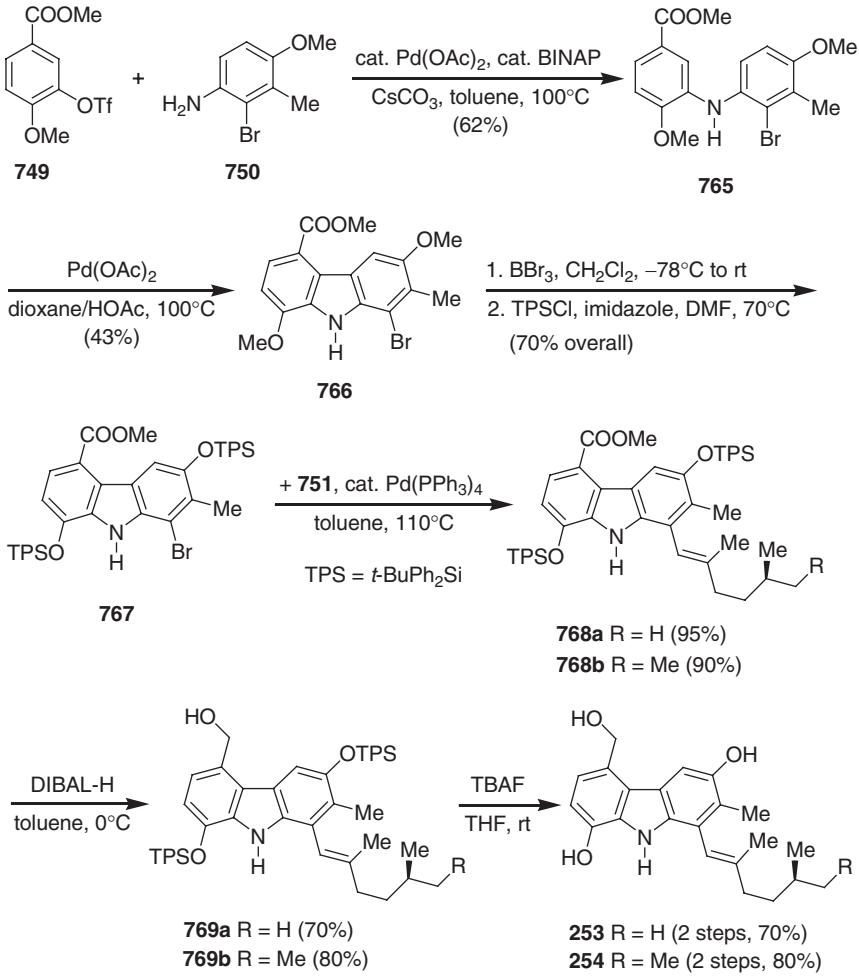

Scheme 5.81

indoles **776** were subjected to Friedel–Crafts benzoylation with benzoyl chloride in the presence of an excess of zinc chloride to give the diketoindoles **777**. The base-catalyzed intramolecular cyclization of diketoindoles **777** with sodium hydroxide led to the 3-hydroxycarbazoles **728** and **778** in 85% and 74% yield, respectively. Finally, *O*-methylation with methyl iodide in the presence of potassium carbonate in refluxing acetone afforded hyellazole (**245**) and 6-chlorohyellazole (**246**) (606) (Scheme 5.83).

4 3,4-Dioxygenated Tricyclic Carbazole Alkaloids

Our approach for the total syntheses of carbazomycins A (**260**), B (**261**), C (**262**), D (**263**), and E (**264**), based on the iron-mediated construction of the carbazole framework by consecutive C–C and C–N bond formation, leads to the iron complex salts **602** and **779** and the fully functionalized arylamines **780a–c** (607–610) (Scheme 5.84).

The arylamine **780a** required for the total synthesis of carbazomycin A (**260**) was prepared from commercially available 2,3-dimethylphenol (**781**). The regioselective

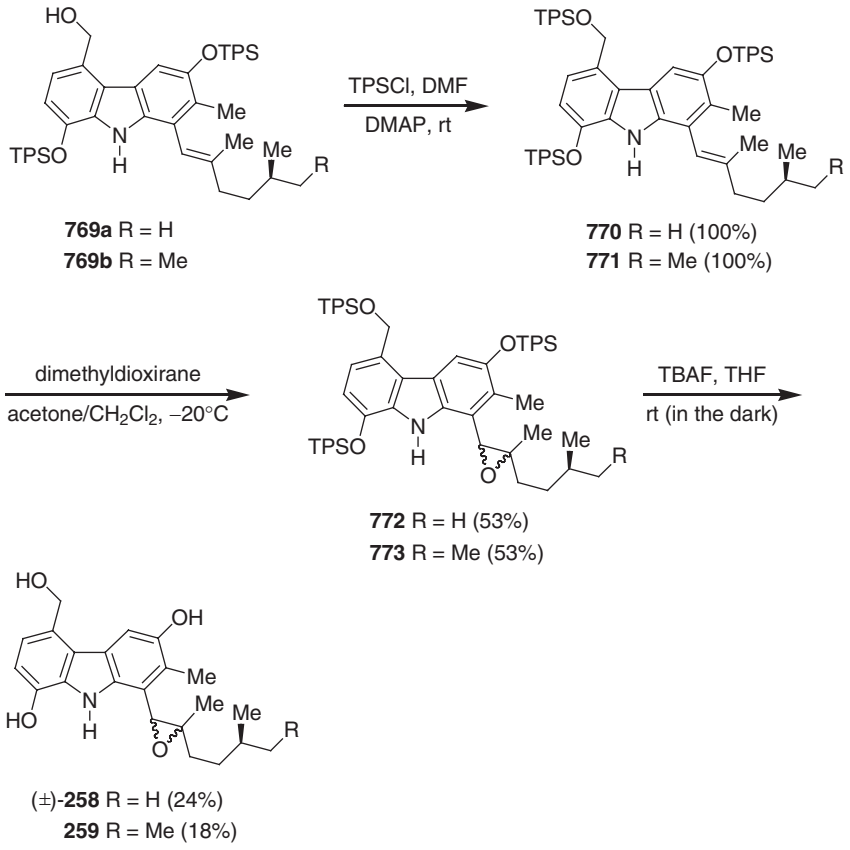

Scheme 5.82

introduction of the second oxy substituent in the *ortho*-position to the hydroxy group was achieved by acetylation of **781** and subsequent *ortho*-selective Fries rearrangement of the intermediate acetoxy derivative to the desired acetophenone **782**. Methylation of **782** followed by a regioselective Baeyer–Villiger oxidation afforded the acetoxy compound **783**. Regioselective nitration of **783** using the preformed complex of fuming nitric acid and $SnCl_4$ at −78°C afforded the desired nitro derivative which, on deacetylation, led to the corresponding nitro phenol **784**. Finally, methylation of **784**, followed by palladium-catalyzed hydrogenation, furnished the arylamine **780a** (609) (Scheme 5.85).

Electrophilic aromatic substitution of the arylamine **780a** using the iron-complex salt **602** afforded the iron-complex **785**. Oxidative cyclization of complex **785** in toluene at room temperature with very active manganese dioxide afforded carbazomycin A (**260**) in 25% yield, along with the tricarbonyliron-complexed 4b,8a-dihydro-3*H*-carbazol-3-one (**786**) (17% yield). The quinone imine **786** was also converted to carbazomycin A (**260**) by a sequence of demetalation and *O*-methylation (Scheme 5.86). The synthesis *via* the iron-mediated arylamine cyclization provides carbazomycin A (**260**) in two steps and 21% overall yield based on **602** (607–609) (Scheme 5.86).

Selective oxidation of the iron complex **785** with commercial manganese dioxide in dichloromethane at room temperature afforded the iron-complexed

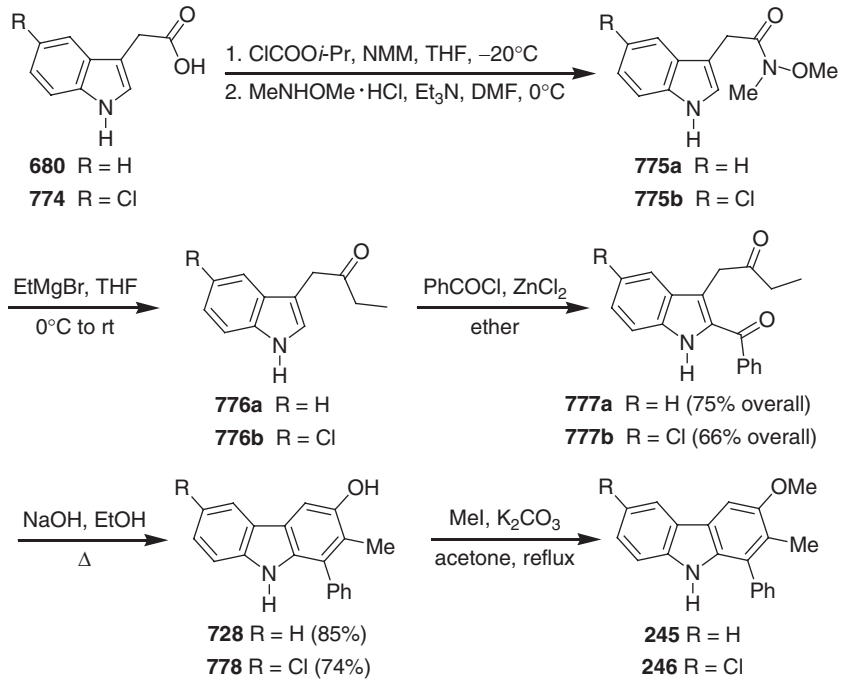

680 R = H
774 R = Cl

775a R = H
775b R = Cl

776a R = H
776b R = Cl

777a R = H (75% overall)
777b R = Cl (66% overall)

728 R = H (85%)
778 R = Cl (74%)

245 R = H
246 R = Cl

Scheme 5.83

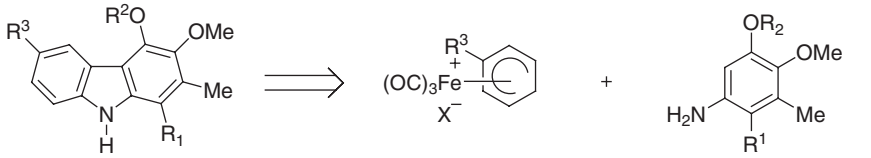

260 Carbazomycin A
R^1,R^2 = Me; R^3 = H
261 Carbazomycin B
R^1 = Me; R^2,R^3 = H
262 Carbazomycin C
R^1= Me; R^2 = H; R^3 = OMe
263 Carbazomycin D
R^1,R^2 = Me; R^3 = OMe
264 Carbazomycin E
R^1 = CHO; R^2,R^3 = H

602 R^3 = H; X = BF_4
779 R^3 = OMe; X = PF_6

780a R^1,R^2 = Me
780b R^1 = Me; R^2 = H
780c R^1 = CHO; R^2 = H

Scheme 5.84

4b,8a-dihydro-3*H*-carbazol-3-one (**786**) in 63% yield. Finally, demetalation of the quinone imine **786**, followed by *O*-methylation of the intermediate 3-hydroxycarbazole using NaH/Me_2SO_4, gave carbazomycin A (**260**). The iron-mediated quinone imine cyclization provides carbazomycin A (**260**) in four steps and 35% overall yield based on **602** (608,609) (Scheme 5.86).

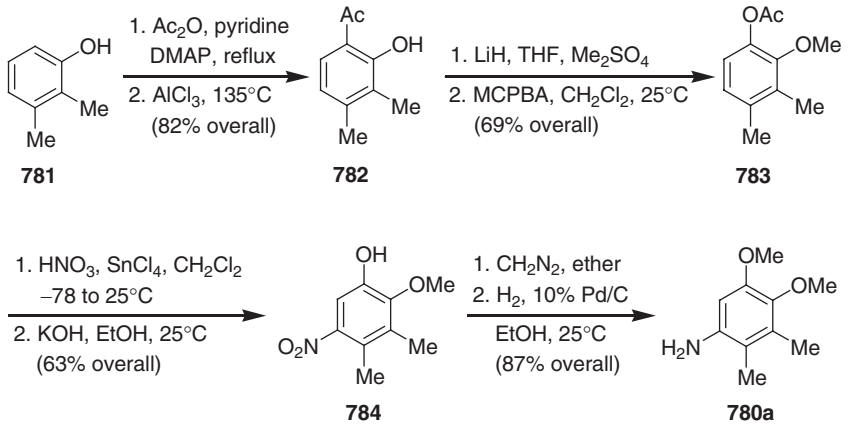

Scheme 5.85

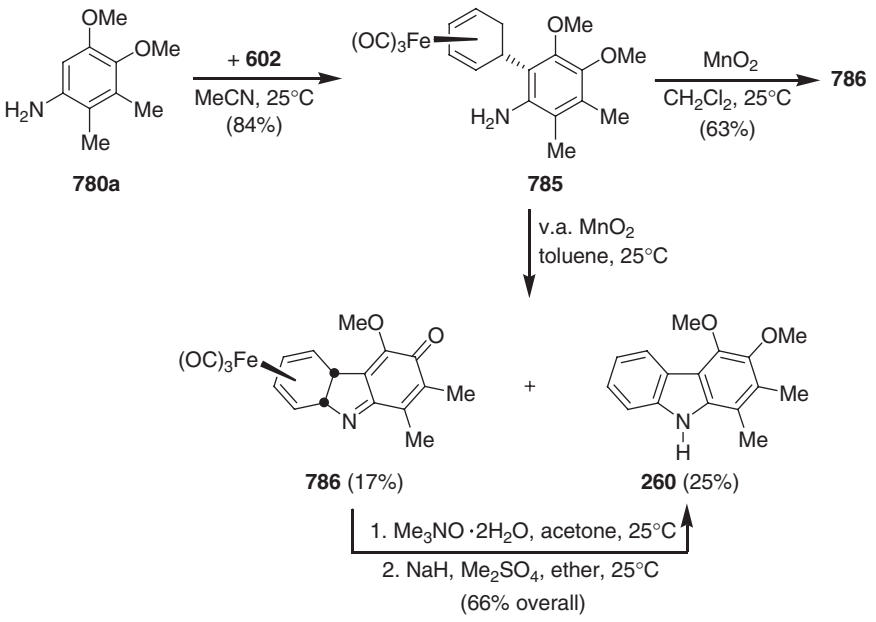

Scheme 5.86

The arylamine **780b** required for the total synthesis of carbazomycin B (**261**) was obtained by catalytic hydrogenation, using 10% palladium on activated carbon, of the nitroaryl derivative **784** which was obtained in six steps and 33% overall yield starting from 2,3-dimethylphenol **781** (see Scheme 5.85). Electrophilic substitution of the arylamine **780b** with the iron-complex salt **602** provided the iron complex **787** in quantitative yield. The direct, one-pot transformation of the iron complex **787** to carbazomycin B **261** by an iron-mediated arylamine cyclization was unsuccessful, probably because the unprotected hydroxyarylamine moiety is too sensitive towards the oxidizing reaction conditions. However, the corresponding *O*-acetyl derivative

788 was transformed to carbazomycin B by oxidative cyclization with very active MnO_2, followed by cleavage of the ester. The total synthesis of carbazomycin B (**261**) *via* the iron-mediated arylamine cyclization was completed in four steps and 33% overall yield based on the iron-complexed cation **602** (608,609) (Scheme 5.87).

Six years later, we described a considerably improved total synthesis of the carbazomycins A (**260**) and B (**261**) using highly efficient synthetic routes to the arylamines **780a** and **794** (610). Moreover, this methodology uses air as an oxidant for the construction of the carbazole framework by oxidative coupling of the iron-complexed cation **602** with the arylamines **780a** and **794**.

The optimized procedure for the synthesis of the arylamine **780a** started from commercially available 3-methylveratrole (**789**). The electrophilic bromination of **789** led to the corresponding 4-bromo derivative **790**. Halogen–metal exchange of **790** with butyllithium, and subsequent methylation by iodomethane, afforded 3,4-dimethylveratrole. Regioselective nitration of 3,4-dimethylveratrole using fuming nitric acid in a 3:1 mixture of acetic anhydride and glacial acetic acid provided the 5-nitro derivative **791**. Finally, catalytic hydrogenation of **791** using 10% palladium on activated carbon provided the arylamine **780a**. This novel route provides the arylamine **780a** in four steps and 55% overall yield based on 3-methylveratrole (**789**) (610) (Scheme 5.88).

Using a one-pot process of oxidative cyclization in air, the arylamine **780a** was transformed to the tricarbonyl(η^4-4b,8a-dihydro-9*H*-carbazole)iron complex **792**. Finally, demetalation of **792** and subsequent aromatization gave carbazomycin A (**260**). This synthesis provided carbazomycin A (**260**) in three steps and 65% overall yield based on **602** (previous route: four steps and 35% yield based on **602**) (610) (Scheme 5.88).

The arylamine **794** required for the improved total synthesis of carbazomycin B (**261**) was prepared in quantitative yield by hydrogenation of the nitroaryl derivative **793** (see Scheme 5.85). Oxidative coupling of the iron complex salt **602** and the arylamine **794** in air afforded the tricarbonyl(η^4-4b,8a-dihydro-9*H*-carbazole)iron complex (**795**). Demetalation of **795**, followed by aromatization, led to *O*-acetylcarbazomycin B (**796**).

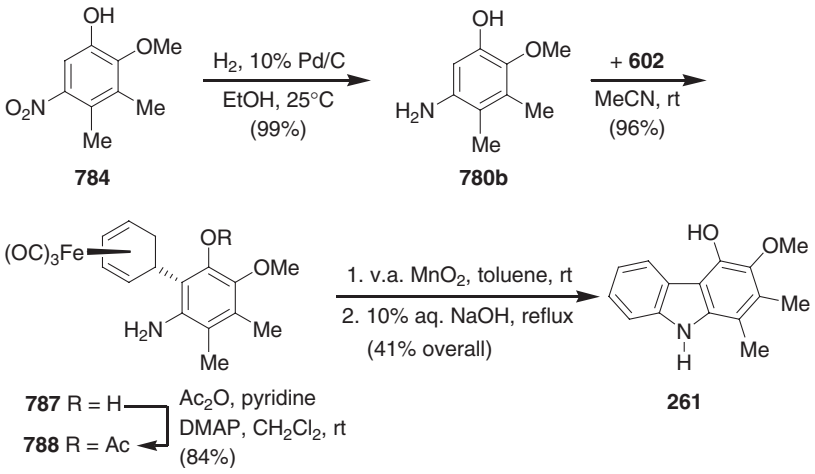

Scheme 5.87

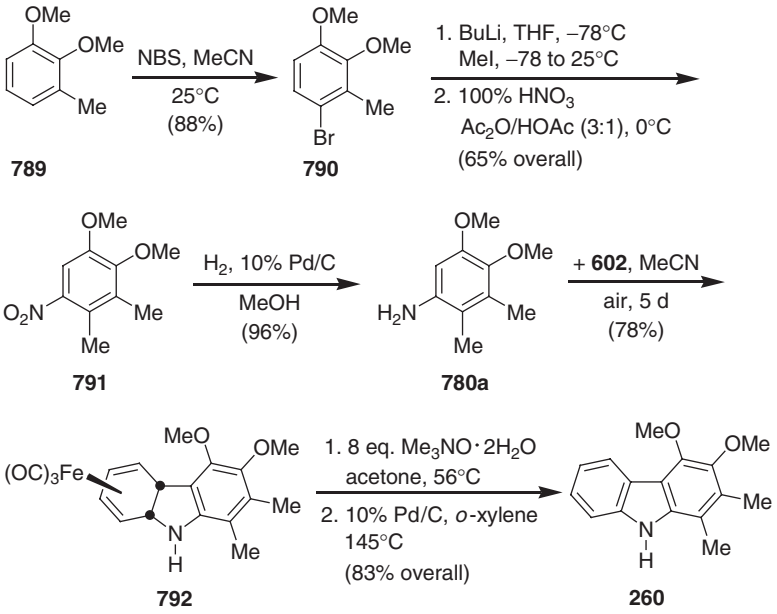

Scheme 5.88

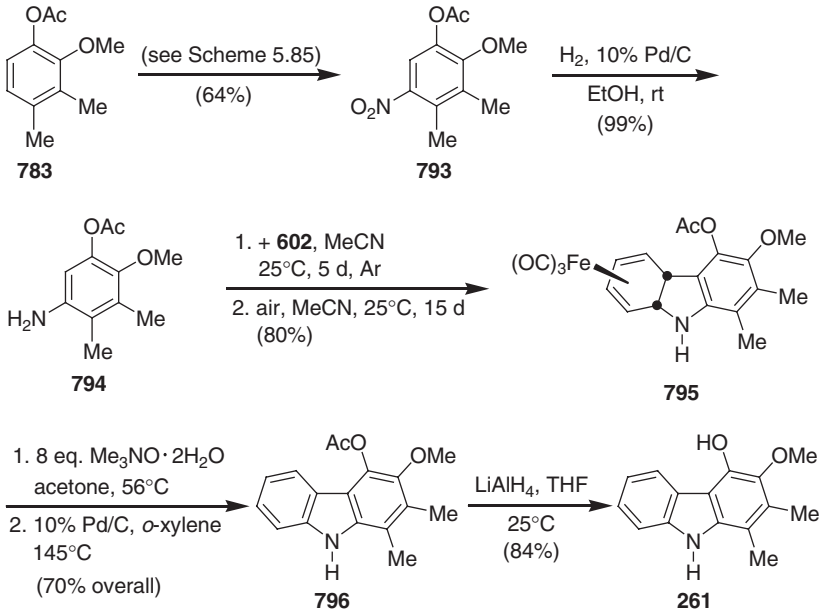

Scheme 5.89

Finally, cleavage of the ester group afforded carbazomycin B (**261**). This synthesis offers carbazomycin B (**261**) in four steps and 55% overall yield based on **602** (previous synthesis: four steps and 30% overall yield based on **602**) (610) (Scheme 5.89).

Retrosynthetic analysis of the carbazomycins C (**263**) and D (**264**) based on the iron-mediated construction of the carbazole framework leads to tricarbonyl [3-methoxy-(1–5-η)-cyclohexadienyl]iron hexafluorophosphate (**779**) and the arylamines **780a** and **780b** (see Scheme 5.84) as synthetic precursors (611). The arylamines **780a** and **780b** have been used previously as precursors for the total syntheses of carbazomycin A (**260**) and B (**261**) (see Schemes 5.86, 5.87 and 5.88).

The total synthesis of carbazomycin C (**262**) was achieved by executing similar reaction sequences as in the iron-mediated arylamine cyclization route described for the synthesis of carbazomycin B (**261**) (see Scheme 5.87). The electrophilic substitution of the arylamine **780b** using the complex salt **779** afforded the iron complex **797**, which was transformed to the corresponding acetate **798**. Using very active manganese dioxide, compound **798** was cyclized to *O*-acetylcarbazomycin C (**799**). Finally, saponification of the ester afforded carbazomycin C (**262**) (four steps and 25% overall yield based on **779**) (611) (Scheme 5.90).

The total synthesis of carbazomycin D (**263**) was completed using the quinone imine cyclization route as described for the total synthesis of carbazomycin A (**261**) (see Scheme 5.86). Electrophilic substitution of the arylamine **780a** by reaction with the complex salt **779** provided the iron complex **800**. Using different grades of manganese dioxide, the oxidative cyclization of complex **800** was achieved in a two-step sequence to afford the tricarbonyliron complexes **801** (38%) and **802** (4%). By a subsequent proton-catalyzed isomerization, the 8-methoxy isomer **802** could be quantitatively transformed to the 6-methoxy isomer **801** due to the regio-directing effect of the 2-methoxy substituent of the intermediate cyclohexadienyl cation. Demetalation of complex **801** with trimethylamine *N*-oxide, followed by *O*-methylation of the intermediate 3-hydroxycarbazole derivative, provided carbazomycin D (**263**) (five steps and 23% overall yield based on **779**) (611) (Scheme 5.91).

The arylamine **780c** required for the total synthesis of carbazomycin E (**264**) was prepared in seven steps starting from vanillyl alcohol (**803**). Vanillyl alcohol (**803**) was transformed to the tetrasubstituted aryl derivative **804** *via* generation of the benzyl methyl ether followed by *ortho*-directed lithiation and subsequent

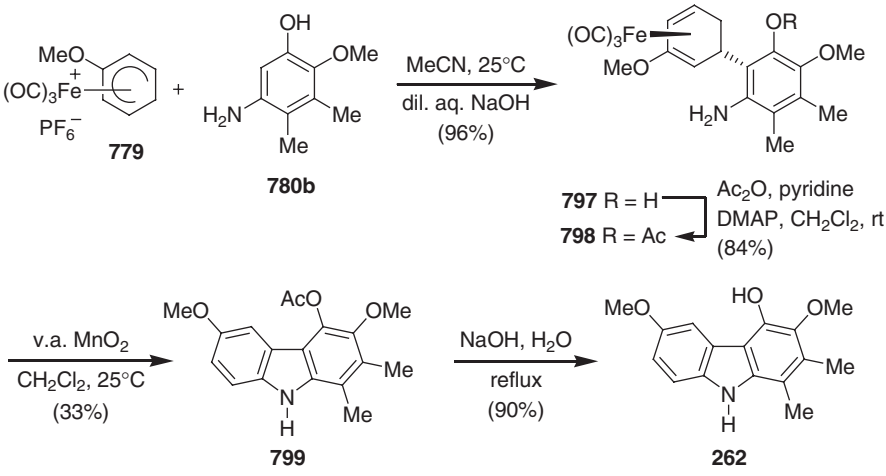

Scheme 5.90

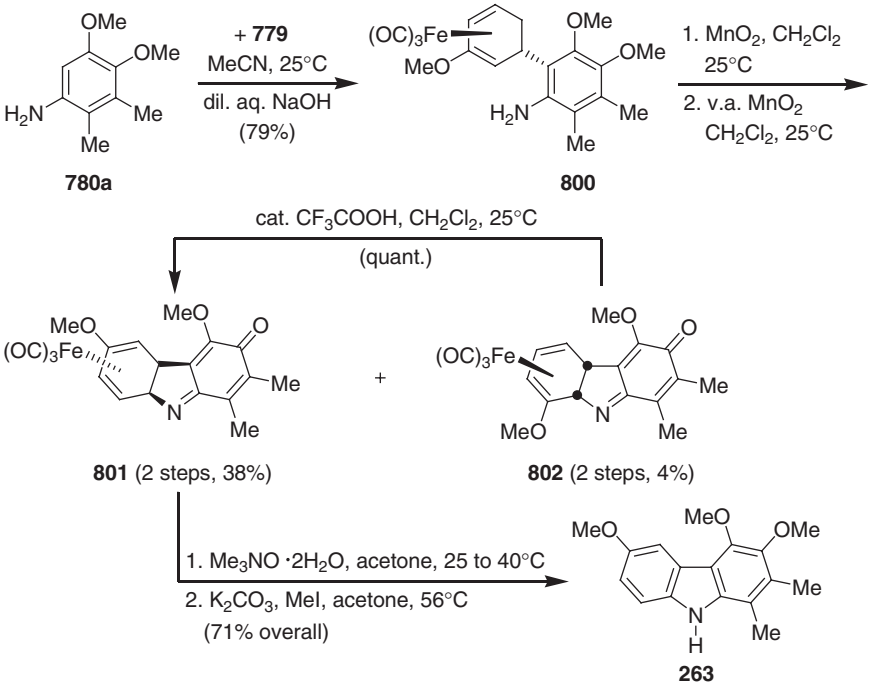

Scheme 5.91

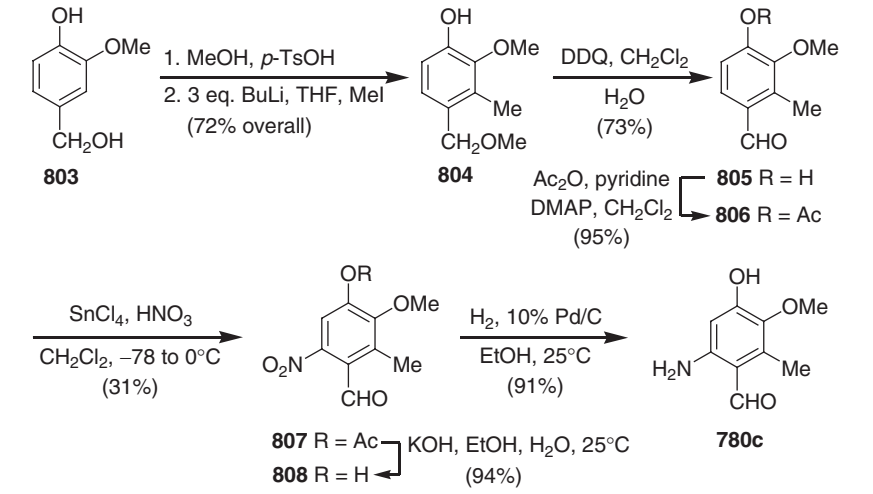

Scheme 5.92

methylation. After DDQ oxidation of the benzyl methyl ether **804**, the corresponding aldehyde **805** was converted to the *O*-acetyl derivative **806**. Nitration of **806** to the nitrobenzaldehyde **807** was achieved using the complex of tin tetrachloride and fuming nitric acid. Ester cleavage to the nitrophenol **808** with potassium hydroxide and subsequent catalytic hydrogenation afforded the desired arylamine **780c** (612) (Scheme 5.92).

Electrophilic aromatic substitution of the arylamine **780c** using the iron-complex salt **602** provided the iron complex **809** in 26% yield. The low yield of complex **809** was ascribed to the strong electron-withdrawing effect of the formyl group. After acetylation of complex **809**, the resulting *O*-acetyl derivative **810** was subjected to iron-mediated arylamine cyclization with very active manganese dioxide to give *O*-acetylcarbazomycin E (**811**). Finally, base-mediated saponification of **811** afforded carbazomycin E (**264**). The overall yield for the iron-mediated total synthesis of carbazomycin E (**264**) is low (four steps and 4% overall yield based on **602**) (612) (Scheme 5.93). However, to date it represents the only total synthesis reported for this natural product.

By analogy with carquinostatin A (**275**) (see Scheme 2.68) we assumed an *R*-configuration of the stereogenic center for neocarazostatin B (**268**). Based on this assumption, the retrosynthetic analysis of neocarazostatin B (**268**) leads to the protected 6-bromocarbazole **813** as the key intermediate. For the regioselective introduction of the prenyl group, a reaction of the 6-bromocarbazole **813** with the dimeric π-prenylnickel bromide complex **812** was envisaged (613) (Scheme 5.94).

The fully functionalized chiral arylamine **814** with the required *R*-configuration of the stereogenic center for the total synthesis of neocarazostatin B (**268**) was obtained from commercial guaiacol (**815**) over eight steps in 65% overall yield (613). The same racemic arylamine (±)-**814** was previously used for the racemic synthesis of neocarazostatin B and was available in 10 steps and 14% overall yield based on *o*-cresol, a different commercial starting material (614).

Protection of **815** as a TPS ether, subsequent *ortho*-directed lithiation, followed by methylation of the intermediate lithio derivative, afforded the 2,3-dioxygenated toluene **816**. For an *R*-configuration of neocarazostatin B (**268**), the required chiral side chain was planned to be derived from (*R*)-propene oxide. Hydrolytic kinetic resolution (HKR) of racemic propene oxide using Jacobsen's (*R,R*)-(salen)cobalt(II) complex provided (*R*)-propene oxide in 99% ee (615–617). Regioselective bromination of **816**, followed by halogen–metal exchange and ring opening of the (*R*)-propene oxide by the intermediate aryllithium, provided the (*R*)-2-hydroxypropylarene **817**.

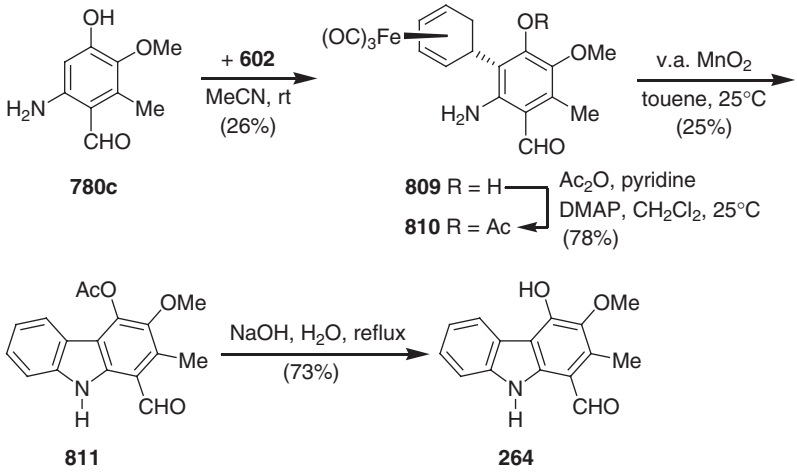

Scheme 5.93

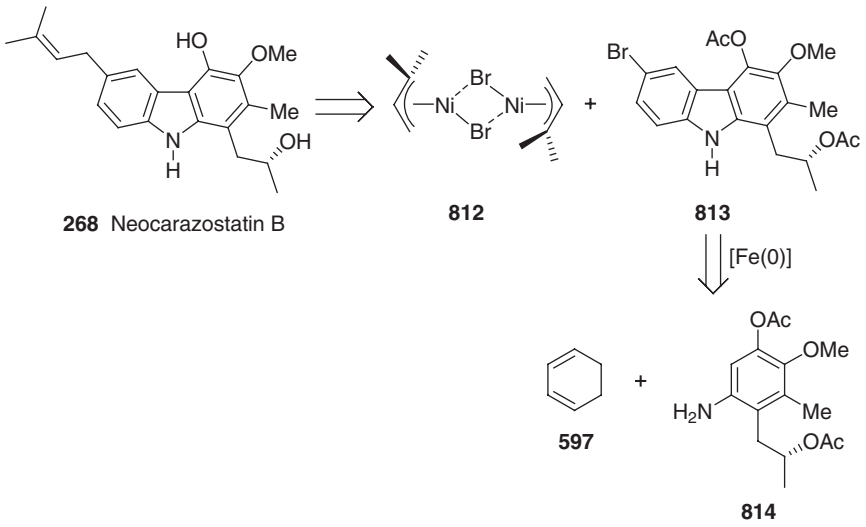

Scheme 5.94

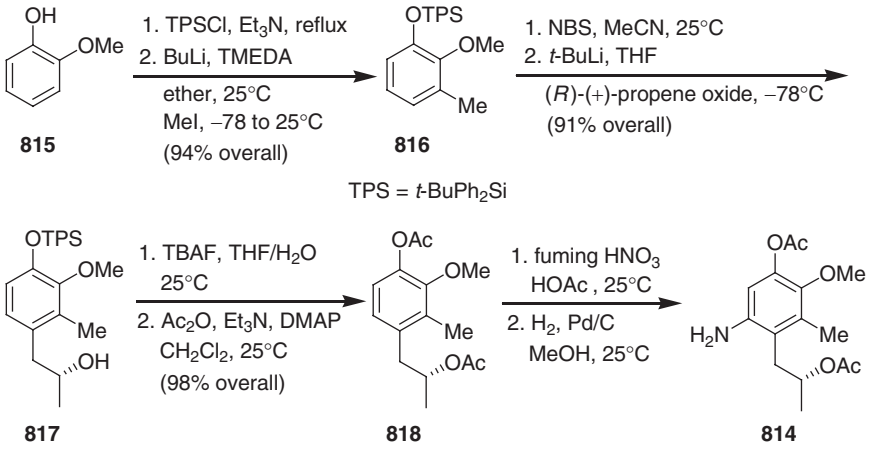

Scheme 5.95

Removal of the silyl protecting group using TBAF, and subsequent acetylation, led to the diacetate **818**. Regioselective nitration and catalytic hydrogenation provided the (*R*)-arylamine **814** (613) (Scheme 5.95).

The construction of the carbazole framework was achieved by slightly modifying the reaction conditions previously reported for the racemic synthesis (614). Reaction of the iron complex salt **602** with the fully functionalized arylamine **814** in air provided the tricarbonyliron-coordinated 4b,8a-dihydrocarbazole complex **819** *via* sequential C–C and C–N bond formation. This one-pot annulation is the result of an electrophilic aromatic substitution and a subsequent iron-mediated oxidative cyclization by air as the oxidizing agent. The aromatization with concomitant demetalation of complex **819** using NBS under basic reaction conditions, led to the carbazole. Using the same reagent under acidic reaction conditions the carbazole was

transformed to the 6-bromocarbazole **820** as a result of electrophilic bromination. Prenyl coupling of the 6-bromocarbazole **820** with 2 equivalents of the *in situ*-prepared dimeric π-prenylnickel bromide complex **812** from prenyl bromide and tetra carbonylnickel(0) afforded di(*O*-acetyl)neocarazostatin B (**821**) in 66% yield, along with some hydrodebrominated product. Finally, reductive cleavage of both ester groups by treatment with lithium aluminum hydride provided (*R*)-(−)-neocarazostatin B (**268**). This synthesis provides enantiopure neocarazostatin B in five steps and 36% overall yield based on the iron complex salt **602** (613) (Scheme 5.96).

Smooth conversion of (*R*)-(−)-neocarazostatin B (**268**) to carquinostatin A (**278**) was achieved by oxidation using cerium(IV) ammonium nitrate (CAN). The identity of the absolute configuration of both alkaloids, and also the enantiopurity of neocarazostatin B (>99% ee), has been additionally confirmed by the transformation of carquinostatin A (**278**) to the (*R,R*)-Mosher ester **822** by reaction with (S)-(+)-α-methoxy-α-(trifluoromethyl)phenylacetyl (MTPA) chloride (613) (Scheme 5.97).

Clive *et al.* reported the total synthesis of carbazomycin B (**261**) by radical cyclization of the sulfonamide **827**, followed by deprotection and dehydrogenation. The bromo sulfonamide **824** required for the preparation of the key intermediate **827** was obtained from the arylamine **794** (609) (see Schemes 5.85 and 5.89). Alkylation of **824** with 3-bromo-1-cyclohexene (**825**) gave two conformational isomers of **826** (ratio 3:2). Hydrolysis, followed by benzylation of **826**, led to the corresponding *O*-benzyl derivative **827**. The inseparable isomers of **827** were subjected to radical cyclization with triphenyltin hydride in refluxing benzene to afford the hexahydrocarbazole **828** in only 39% yield along with the major by-product **829**. Treatment of the hexahydrocarbazole **828** with sodium-naphthalene gave the corresponding hydroxy derivative as a result of deprotection of the *N*-tolylsulfonyl and *O*-benzyl groups, and finally, dehydrogenation with 10% Pd/C in triglyme, provided carbazomycin B **261** (618) (Scheme 5.98).

Beccalli *et al.* reported a synthesis of carbazomycin B (**261**) by a Diels–Alder cycloaddition using the 3-vinylindole **831** as diene, analogous to Pindur's synthesis of 4-deoxycarbazomycin B (619). The required 3-vinylindole, (*Z*)-ethyl 3-[(1-ethoxy-carbonyloxy-2-methoxy)ethenyl]-2-(ethoxy-carbonyloxy)indole-1-carboxylate (**831**), was synthesized starting from indol-2(3*H*)one (**830**) (620). The Diels–Alder reaction of the diene **831** with dimethyl acetylene dicarboxylate (DMAD) (**535**) gave the tetrasubstituted carbazole **832**. Compound **832** was transformed to the acid **833** by alkaline hydrolysis. Finally, reduction of **833** with Red-Al® afforded carbazomycin B (**261**) (621) (Scheme 5.99).

Crich and Rumthao reported a new synthesis of carbazomycin B using a benzeneselenol-catalyzed, stannane-mediated addition of an aryl radical to the functionalized iodocarbamate **835**, followed by cyclization and dehydrogenative aromatization (622). The iodocarbamate **835** required for the key radical reaction was obtained from the nitrophenol **784** (609) (see Scheme 5.85). Iodination of **784**, followed by acetylation, afforded 3,4-dimethyl-6-iodo-2-methoxy-5-nitrophenyl acetate **834**. Reduction of **834** with iron and ferric chloride in acetic acid, followed by reaction with methyl chloroformate, led to the iodocarbamate **835**. Reaction of **835** and diphenyl diselenide in refluxing benzene with tributyltin hydride and azobisisobutyronitrile (AIBN) gave the adduct **836** in 40% yield, along with 8% of the recovered substrate and 12% of the deiodinated carbamate **837**. Treatment of **836** with phenylselenenyl bromide in dichloromethane afforded the phenylselenenyltetrahydrocarbazole **838**. Oxidative

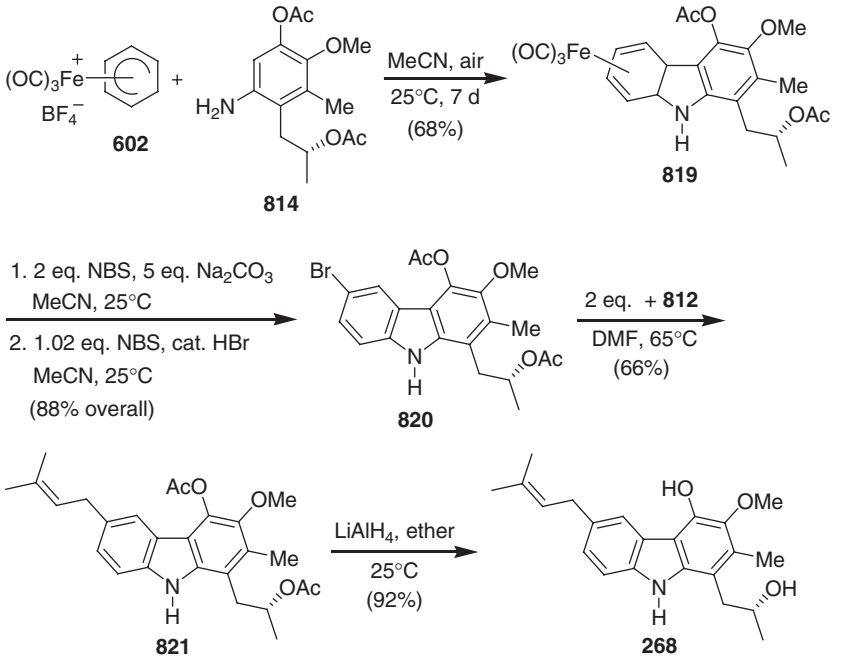

Scheme 5.96

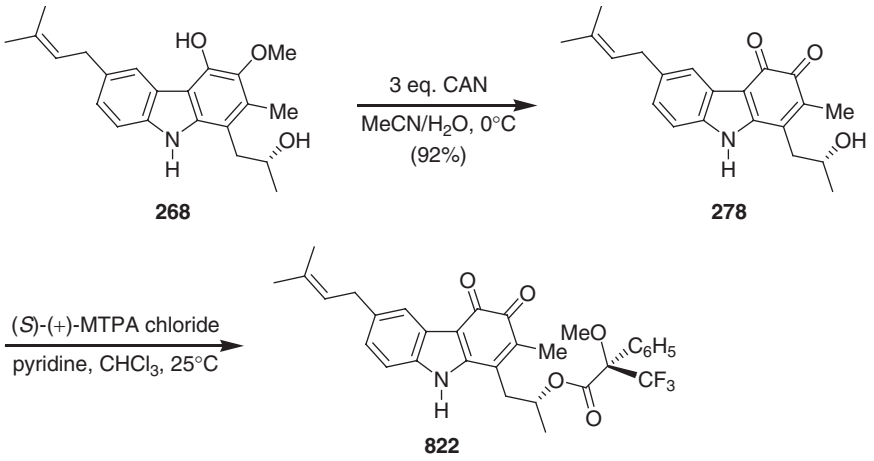

Scheme 5.97

deselenation and rearomatization of **838** with *tert*-butylhydroperoxide (TBHP) afforded the fully aromatized carbazole, which, on base-mediated saponification, led to carbazomycin B (**261**) (622) (Scheme 5.100).

5 Tricyclic Carbazolequinone and Carbazole-1,4-quinol Alkaloids

The tricyclic carbazolequinones represent an important class of carbazole alkaloids with a quinone moiety in the A-ring of the carbazole nucleus. This family of

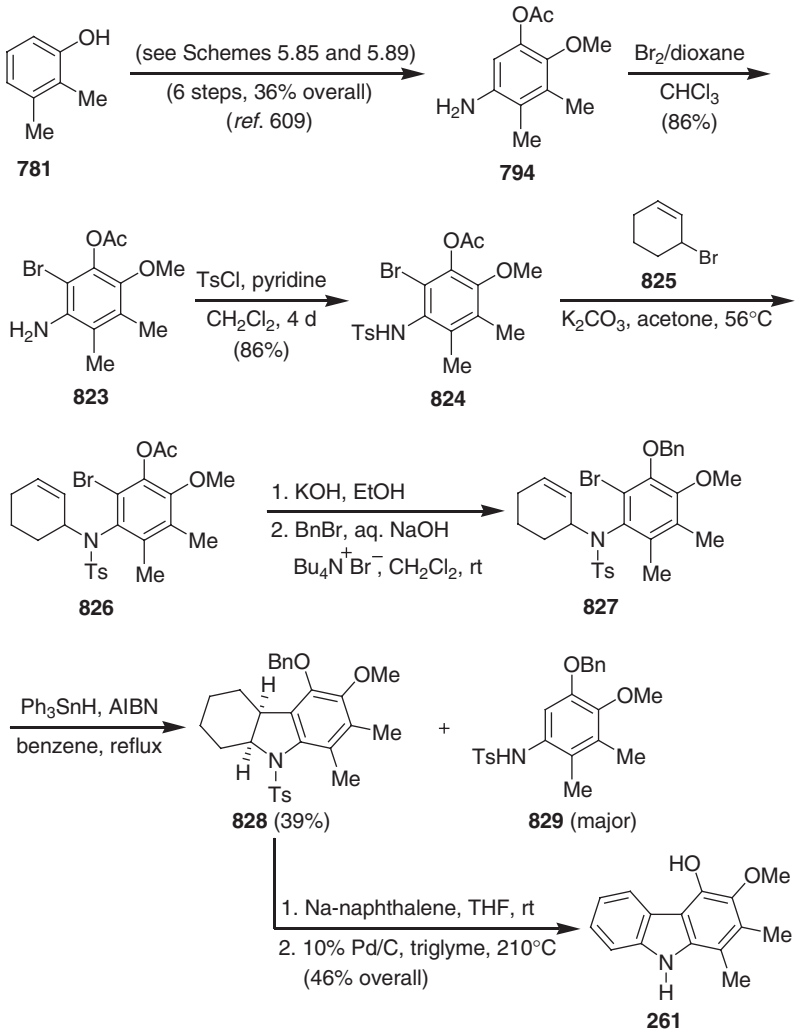

Scheme 5.98

carbazole alkaloids is divided into two groups, depending on the position of the quinone moiety in the A-ring of the carbazole nucleus: the carbazole-1,4-quinones and the carbazole-3,4-quinones. In addition to these two subfamilies, this section also includes the carbazole-1,4-quinol alkaloids.

To date, several syntheses have been reported for the natural 1,4-quinone alkaloids and their analogs. In 1994, Furukawa published a review on the isolation and synthesis of natural carbazole-1,4-quinones (105). Six years later, Fillion *et al.* published a comprehensive review with the coverage of various synthetic approaches towards natural and non-natural carbazole-1,4-quinones (106). In this section, we cover only the total syntheses of the natural carbazole-1,4-quinone alkaloids which have appeared since 1990. In contrast to other sections, this section also includes the formal total syntheses.

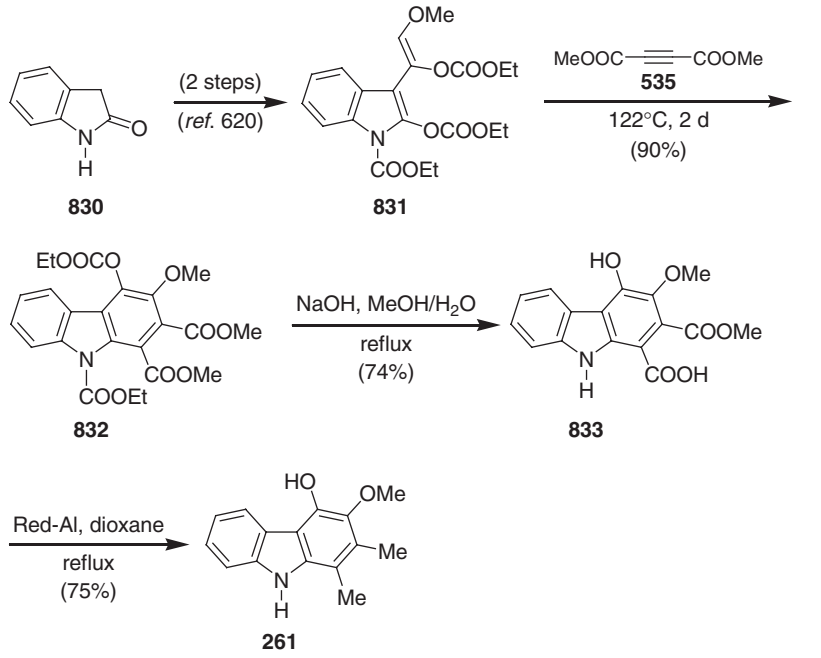

Scheme 5.99

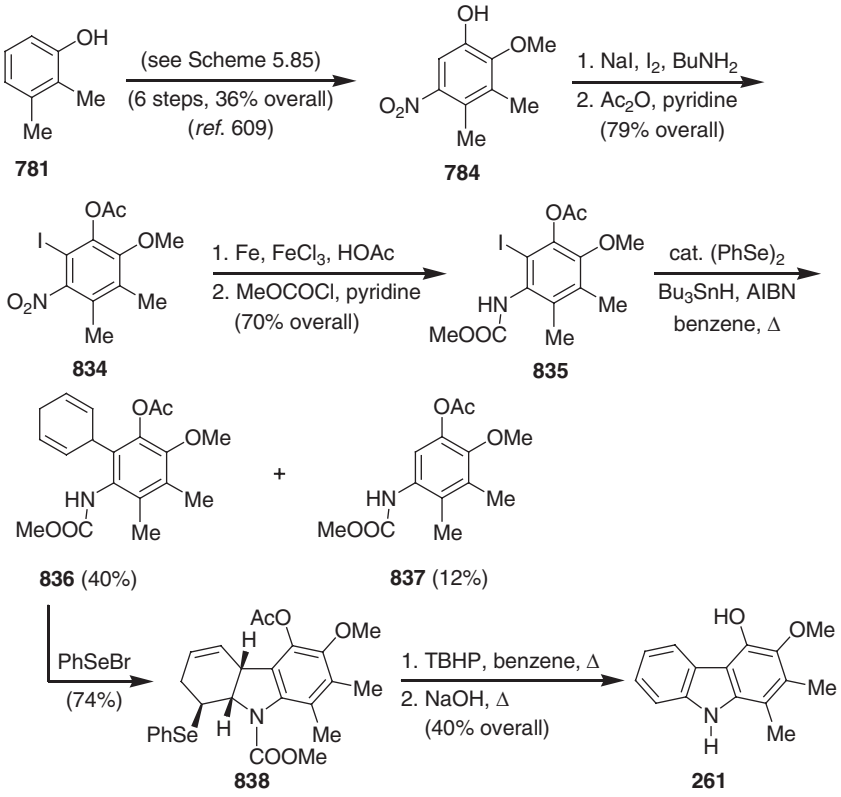

Scheme 5.100

Furukawa *et al*. reported the total synthesis of murrayaquinone A (**107**) by a palladium(II)-mediated oxidative cyclization of the corresponding 2-arylamino-5-methyl-1,4-benzoquinones. 2-Anilino-5-methyl-1,4-benzoquinone (**842**) was prepared starting from 2-methyl-1,4-benzoquinone **841** and aniline **839**, along with the regioisomeric 2-anilino-6-methyl-1,4-benzoquinone (**844**). The oxidative cyclization of 2-anilino-5-methyl-1,4-benzoquinone (**842**) with stoichiometric amounts of palladium(II) acetate provided murrayaquinone A (**107**) in 64% yield. This method was also applied to the synthesis of 7-methoxy-3-methylcarbazole-1,4-quinone (**113**) starting from 3-methoxyaniline (**840**) (623). Seven years later, Chowdhury *et al*. reported the isolation of 7-methoxy-3-methylcarbazole-1,4-quinone (**113**) from the stem bark of *Murraya koenigii* and named it koeniginequinone A (**113**) (49) (Scheme 5.101).

An alternative regioselective synthesis of 2-anilino-5-methyl-1,4-benzoquinone (**842**) was developed using 2-bromo-6-methyl-1,4-benzoquinone (**846**) (route A) and 4,4-dimethoxy-2-methylcyclohexa-2,5-dienone (**849**) (route B) as synthetic equivalents for methyl-1,4-benzoquinone (**841**) (623) (Scheme 5.102).

Miki and Hachiken reported a total synthesis of murrayaquinone A (**107**) using 4-benzyl-1-*tert*-butyldimethylsiloxy-4*H*-furo[3,4-*b*]indole (**854**) as an indolo-2,3-quinodimethane equivalent for the Diels–Alder reaction with methyl acrylate (624). 4-Benzyl-3,4-dihydro-1*H*-furo[3,4-*b*]indol-1-one (**853**), the precursor for the 4*H*-furo[3,4-*b*]indole (**854**), was prepared in five steps and 30% overall yield starting from dimethyl indole-2,3-dicarboxylate (**851**). Alkaline hydrolysis of **851** followed by *N*-benzylation of the dicarboxylic acid with benzyl bromide and sodium hydride in DMF, and treatment of the corresponding 1-benzylindole-2,3-dicarboxylic acid with trifluoroacetic anhydride (TFAA) gave the anhydride **852**. Reduction of **852** with sodium borohydride, followed by lactonization of the intermediate 2-hydroxymethylindole-3-carboxylic acid with 1-methyl-2-chloropyridinium iodide, led to the lactone **853**. The lactone **853** was transformed to 4-benzyl-1-*tert*-butyldimethylsiloxy-4*H*-furo[3,4-*b*]indole **854** by a base-induced silylation. Without isolation, the

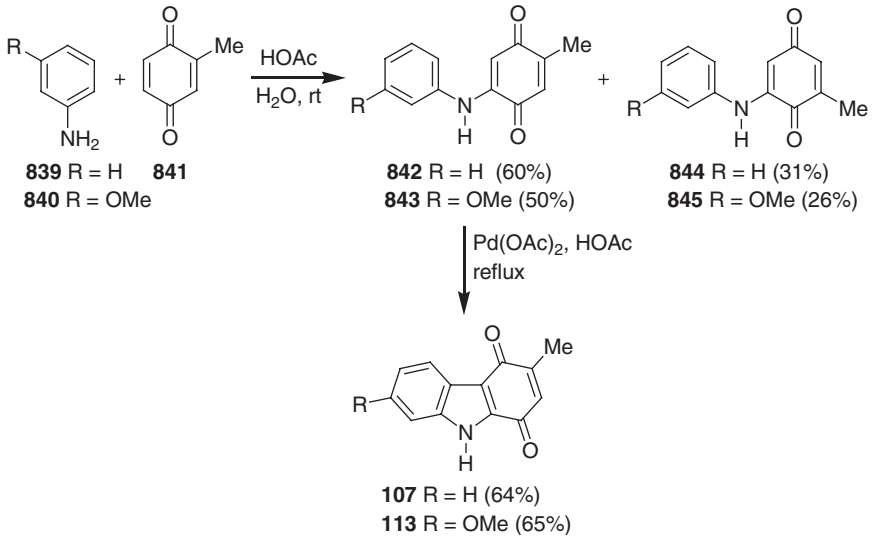

Scheme 5.101

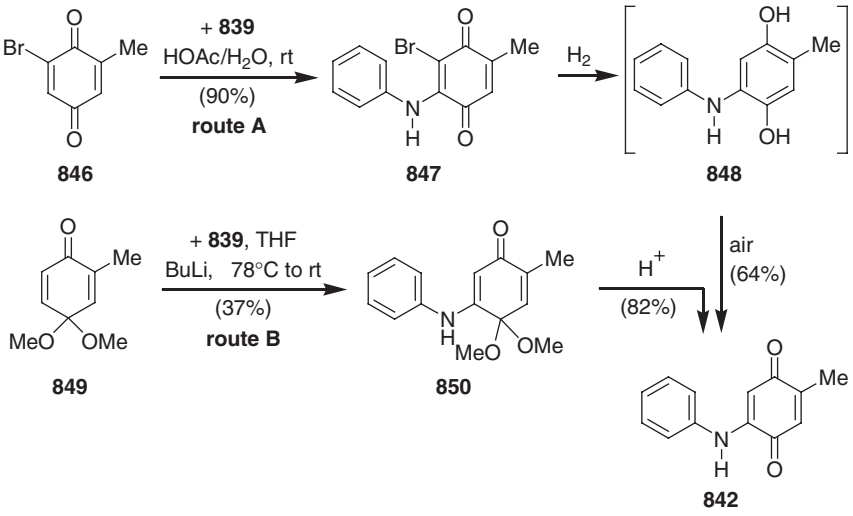

Scheme 5.102

furoindole **854** was reacted with methyl acrylate to afford the carbazole **855** with the desired regioselectivity. After reduction of the carbazole **855** with lithium aluminum hydride, the corresponding 3-methylcarbazole was acetylated to give 4-acetoxy-9-benzyl-3-methylcarbazole (**856**). Treatment of **856** with aluminum trichloride in anisole furnished a mixture of the debenzylated carbazoles **857** and **858** in 43% and 37% yield, respectively. However, by deacetylation with 10% hydrochloric acid, compound **857** was transformed to 4-hydroxy-3-methylcarbazole **858**. Finally, the oxidation of **858** with Fremy's salt (potassium nitrosodisulfonate) afforded murrayaquinone A (**107**) (624) (Scheme 5.103).

Starting from the known 1,2,3,4-tetrahydrocarbazol-4(9*H*)-one (**859**) (625–628), Matsuo and Ishida reported a total synthesis of murrayaquinone A (**107**) (629,630). After protection of the NH group of tetrahydrocarbazolone **859** with 4-methoxybenzyl chloride (PMBCl), methylation at C−3 was achieved by deprotonation with lithium cyclohexylisopropylamide (LCIA). In order to introduce the 2,3-double bond, the enone **860** was successively treated with LCIA and phenylselenenyl chloride in the presence of HMPA to give a mixture of the phenylselenenylated compound **861** and the aromatized product **862** in 38% and 30% yield, respectively. Further, **861** was converted to the fully aromatic compound **862** by treatment with peracetic acid. Oxidation of **862** with Fremy's salt led to the corresponding quinone in good yield. However, all attempts to remove the *N*-protecting group of this quinone intermediate failed. Therefore, prior to deprotection of the nitrogen atom, the 4-hydroxy group was protected by acetylation to afford the 4-acetoxycarbazole **863**. After deprotection of the *N*-atom in **863**, the ester group was hydrolyzed to give the corresponding 4-hydroxycarbazole **858**. Finally, oxidation with Fremy's salt transformed the compound **858** to murrayaquinone A (**107**) (629,630) (Scheme 5.104).

Hanaoka *et al.* reported a total synthesis of murrayaquinone A (**107**) based on an anionic [4+2] cycloaddition of the indole ester **864** with phenyl β-trimethylsilylvinyl sulfone (**865**) (631). The reaction of the MOM-protected indole **864** with phenyl

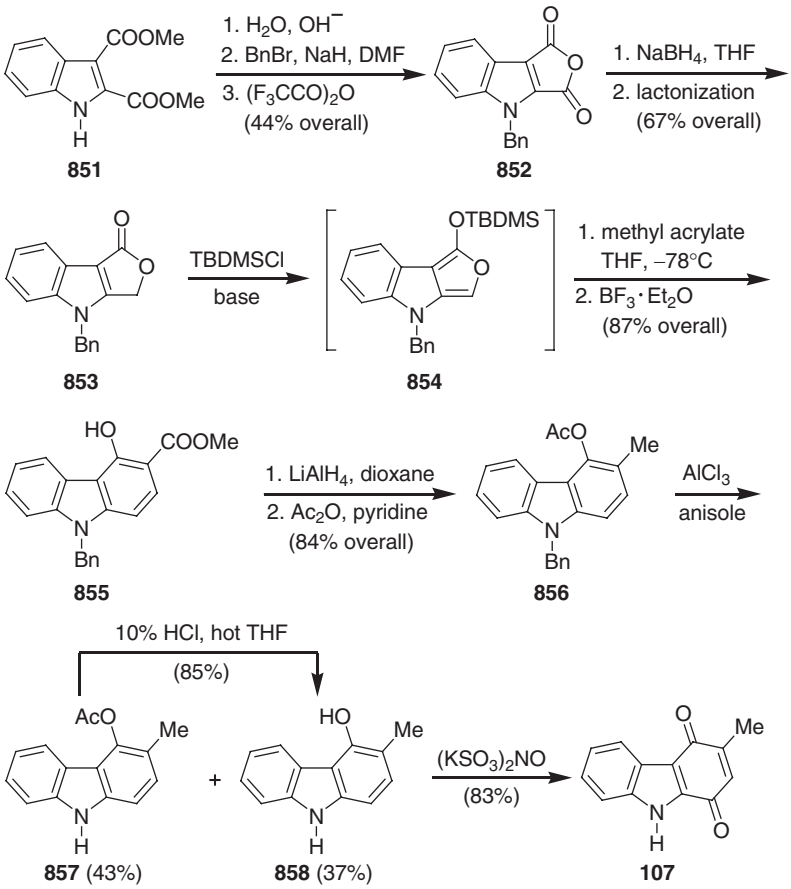

Scheme 5.103

β-trimethylsilylvinyl sulfone (**865**) in the presence of LDA afforded the cycloadduct **866** with the required regioselectivity. Methylation of **866** with methyl iodide in the presence of potassium *tert*-butoxide gave the two diastereoisomers **867** and **868** in 31% and 25% yield, respectively. This mixture was treated with TBAF in THF to afford the 4-hydroxycarbazole **869**. Oxidation of **869** with [bis(trifluoroacetoxy) iodo]benzene gave *N*-MOM-murrayaquinone A (**870**). Finally, removal of the methoxymethyl group with hydrochloric acid in methanol provided murrayaquinone A (**107**) (631) (Scheme 5.105).

Wu *et al.* reported the total synthesis of clausenaquinone A (**112**) using a palladium(II)-mediated oxidative cyclization of the 2-arylamino-5-methoxy-1,4-benzoquinone **874** (107). This total synthesis was undertaken to establish the structure of natural clausenaquinone A (**112**). The key intermediate, 2-(3-hydroxy-4-methylanilino)-5-methoxy-1,4-benzoquinone (**874**), required for this synthesis, was obtained by the reaction of 5-amino-*o*-cresol (**873**) with 2-methoxy-1,4-benzoquinone (**872**) which was readily obtained by oxidation of methoxyhydroquinone (**871**). The palladium(II)-mediated oxidative cyclization is non-regioselective. Thus, the cyclization of the 2-arylamino-5-methoxy-1,4-benzoquinone **874** with palladium(II)

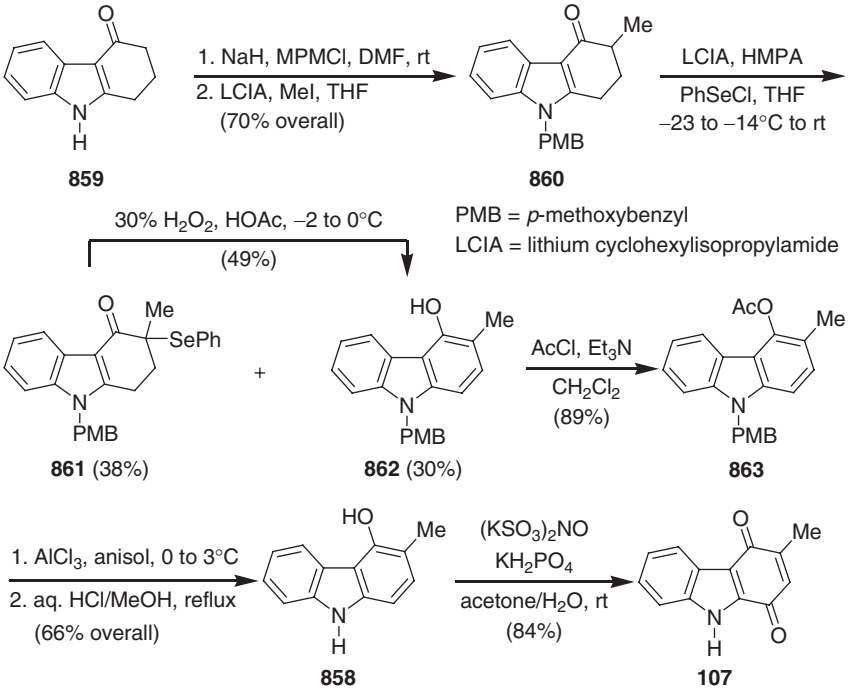

Scheme 5.104

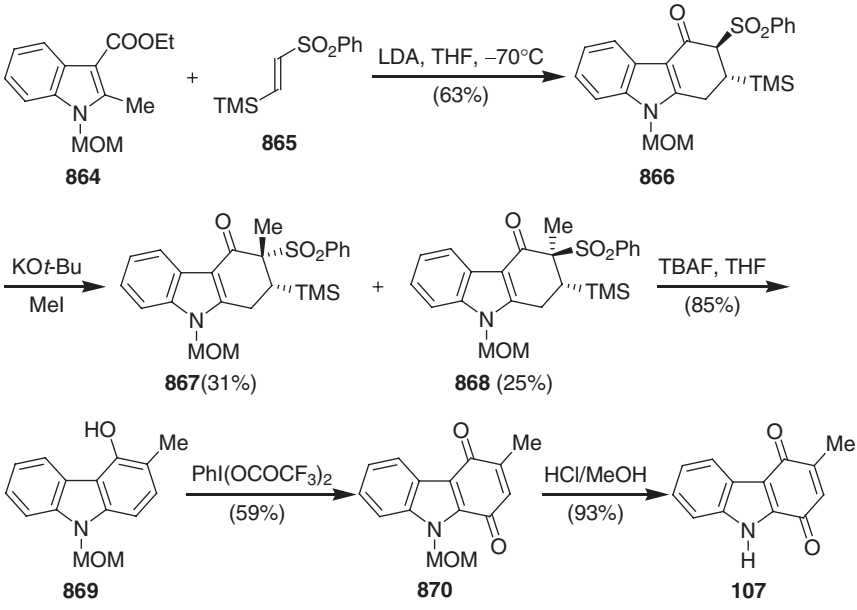

Scheme 5.105

acetate in acetic acid under reflux provided clausenaquinone A (**112**) and the regioisomeric product **875** in a 1:1 ratio (107) (Scheme 5.106).

Åkermark *et al.* applied (548) a catalytic version of Furukawa's palladium-mediated (stoichiometric) cyclization of 2-anilino-5-methyl-1,4-benzoquinone (**842**) to a total synthesis of murrayaquinone A (**107**) (see Scheme 5.101) (623). In this cyclization, only 5 mol% of palladium(II) acetate and an excess of TBHP as reoxidant were used (548). Subsequently, a catalytic cyclization of **842** to murrayaquinone A (**107**), using oxygen for the reoxidation of palladium, was reported (549) (Scheme 5.107).

Murakami *et al.* reported (575) a total synthesis of murrayaquinone A (**107**) by oxidation of 1-hydroxy-3-methylcarbazole (**23**) with Fremy's salt, as previously described by Martin and Moody (632). The hydroxycarbazole **23** required for this synthesis was obtained *via* the Fischer indolization of the *O*-methanesulfonyl phenylhydrazone **614** (575) (see Scheme 5.38). The oxidation of 1-hydroxy-3-methylcarbazole (23) with Fremy's salt afforded murrayaquinone A (**107**) as the major product, along with a 5% yield of isomeric carbazole-1,2-quinone **876** (575) (Scheme 5.108).

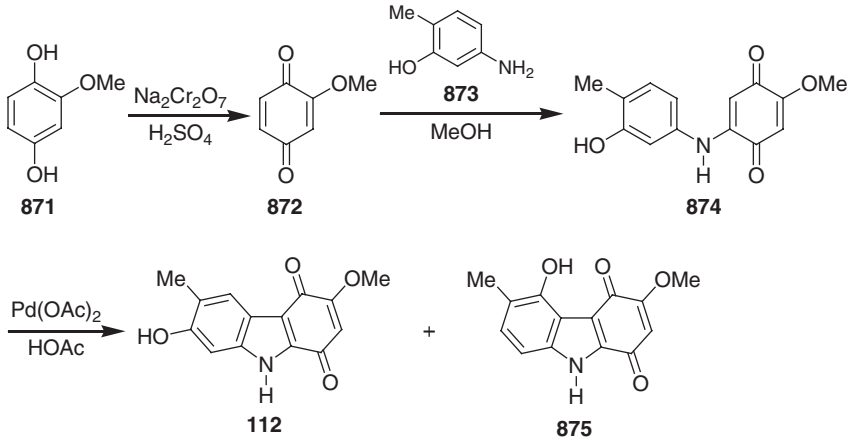

Scheme 5.106

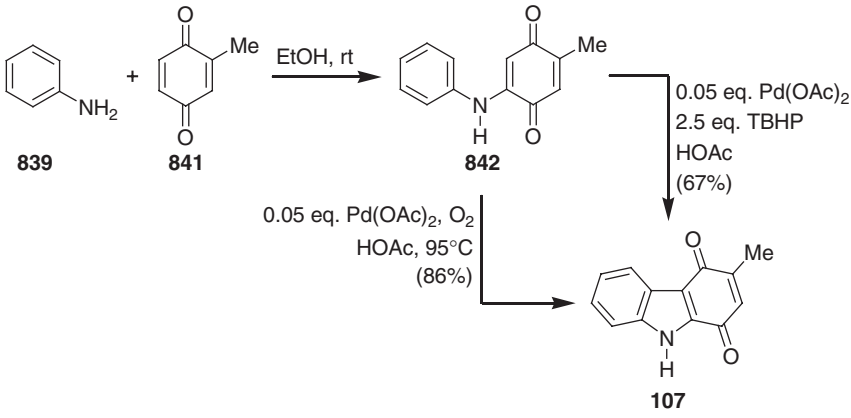

Scheme 5.107

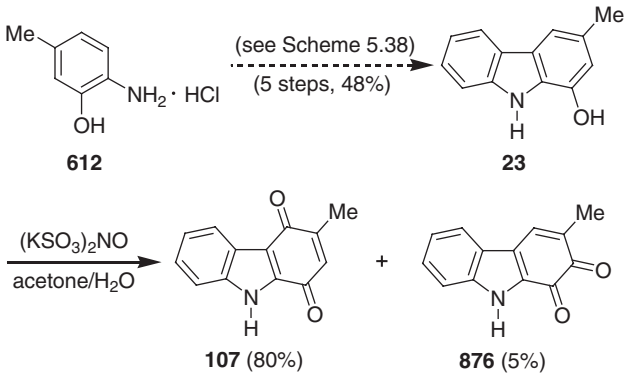

Scheme 5.108

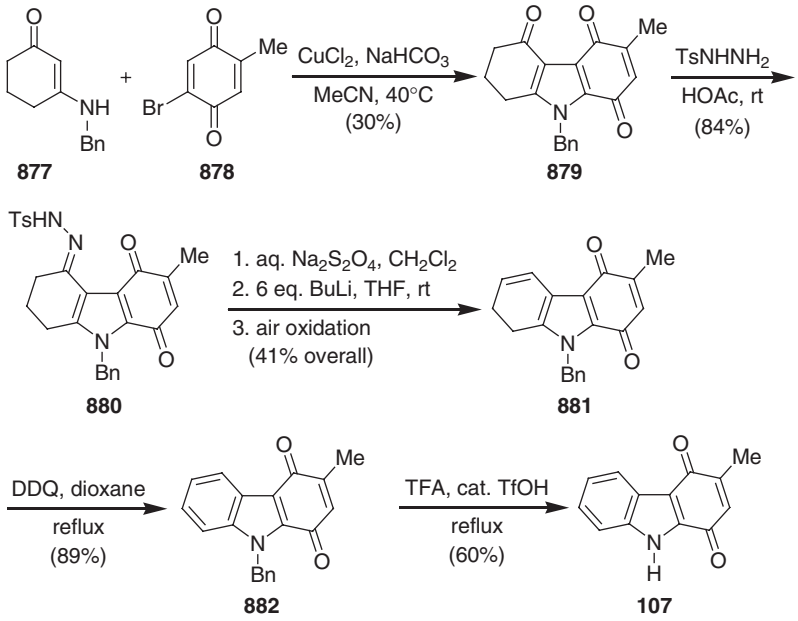

Scheme 5.109

Murphy and Bertrand reported a total synthesis of murrayaquinone A (**107**) based on his bromo-enamino ketone/enamino ester annulation route (633). This annulation methodology starts from the *N*-benzylenaminone (**877**) and 5-bromo-2-methyl-1,4-benzoquinone (**878**). Reaction of **877** and **878** led to the desired regioselective annulation product **879** involving Michael addition, followed by *in situ* reoxidation and dehalocyclization. The hexahydrocarbazoletrione **879** was transformed to *N*-benzylmurrayaquinone A (**882**) using Shapiro's deoxygenation–olefination and subsequent dehydrogenation with DDQ. Finally, debenzylation of **882** in TFA with a catalytic amount of TfOH afforded murrayaquinone A (**107**) (633) (Scheme 5.109).

Saha and Chowdhury reported the total synthesis of koeniginequinones A (**113**) and B (**114**) to confirm the assigned structures for these natural 3-methylcarbazole-

1,4-quinone alkaloids (49). This synthesis uses a Fischer indolization as a key step involving the corresponding phenylhydrazones **517b** and **884**. The required phenylhydrazones **517b** and **884** were obtained by a Japp–Klingemann reaction of 2-hydroxymethylene-5-methylcyclohexanone **515a** and the aryldiazonium chlorides **516b** and **883**, respectively. Aromatization of the 1-oxotetrahydrocarbazoles **518b** and **885** with 5% palladium on charcoal at 170–180°C in a sealed tube afforded the 1-hydroxycarbazoles **886** and **887**. Finally, oxidation of **886** and **887** with Fremy's salt provided koeniginequinone A (**113**) and B (**114**) in 65.5% and 72% yield, respectively (49) (Scheme 5.110).

Chowdhury *et al*. reported a synthesis of murrayaquinone A (**107**) starting from 3-methylcarbazole (**2**) (634). In a one-pot operation, direct, photochemical oxidation of 3-methylcarbazole (**2**) in a solution of methanol using UV light at 254 nm led to murrayaquinone A (**107**) in 24% yield. This reaction is assumed to proceed *via* photoperoxidation involving the intermediates **888a** and **888b** (634) (Scheme 5.111). This transformation supports the biogenetic relationship between the carbazoloquinones and the corresponding carbazoles.

Recently, we reported two-step total syntheses of murrayaquinone A (**107**), koeniginequinone A (**113**), and koeniginequinone B (**114**) starting from the commercially available arylamines **839**, **840**, and **889**, respectively (635). In these syntheses, catalytic amounts of palladium(II) acetate were used for the key transformations of the 2-arylamino-5-methyl-1,4-benzoquinones **842**, **843**, and **890** to the corresponding 3-methylcarbazole-1,4-quinones **107**, **113**, and **114**. The required 2-arylamino-5-methyl-1,4-benzoquinones **842**, **843**, and **890** were obtained in improved yield by the addition of the arylamines **839**, **840**, and **889** to 2-methyl-1,4-benzoquinone (**841**) using Musso's conditions. Finally, palladium(II)-catalyzed

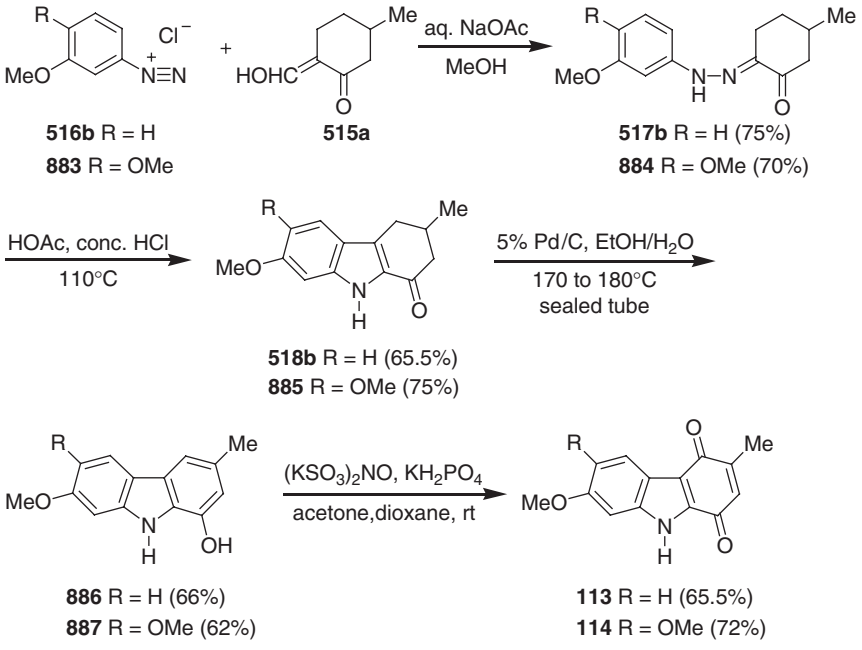

516b R = H
883 R = OMe

515a

517b R = H (75%)
884 R = OMe (70%)

518b R = H (65.5%)
885 R = OMe (75%)

886 R = H (66%)
887 R = OMe (62%)

113 R = H (65.5%)
114 R = OMe (72%)

Scheme 5.110

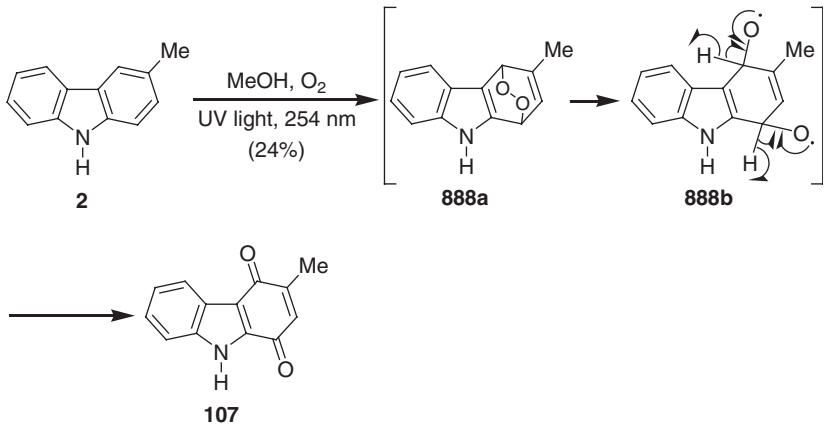

Scheme 5.111

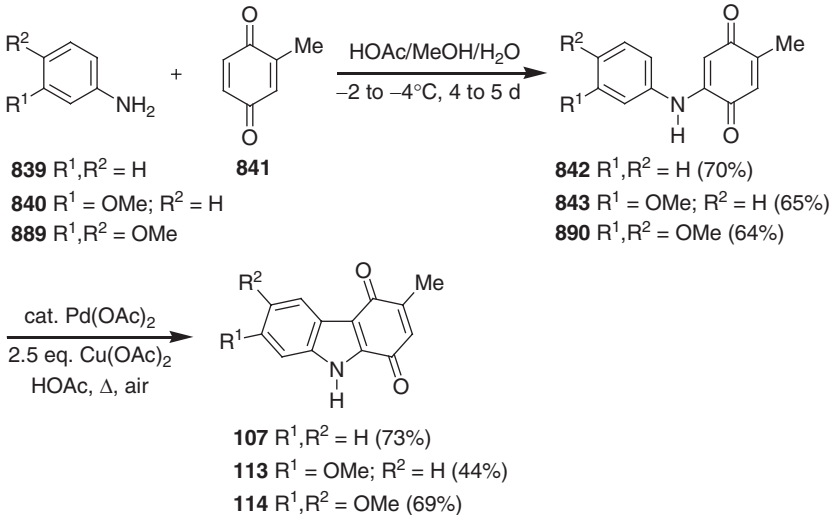

Scheme 5.112

oxidative cyclization of **842**, **843**, and **890** afforded the 3-methylcarbazole-1,4-quinone alkaloids murrayaquinone A (**107**), koeniginequinone A (**113**), and koeniginequinone B (**114**), respectively (635) (Scheme 5.112).

In addition to the aforementioned syntheses of various carbazole-1,4-quinone alkaloids, many formal syntheses for this class of carbazole alkaloids were also reported. These syntheses involve the oxidation of the appropriate 1- or 4-oxygenated-3-methylcarbazoles using Fremy's salt (potassium nitrosodisulfonate), or PCC (pyridinium chlorochromate), or $PhI(OCOCF_3)_2$ [bis(trifluoroacetoxy)iodo]-benzene. Our iron-mediated formal synthesis of murrayaquinone A (**107**) was achieved starting from murrayafoline A (**7**) (see Scheme 5.34). Cleavage of the methyl ether in murrayafoline A (**7**) and subsequent oxidation of the resulting intermediate hydroxycarbazole with Fremy's salt provided murrayaquinone A (**107**) (574,632) (Scheme 5.113).

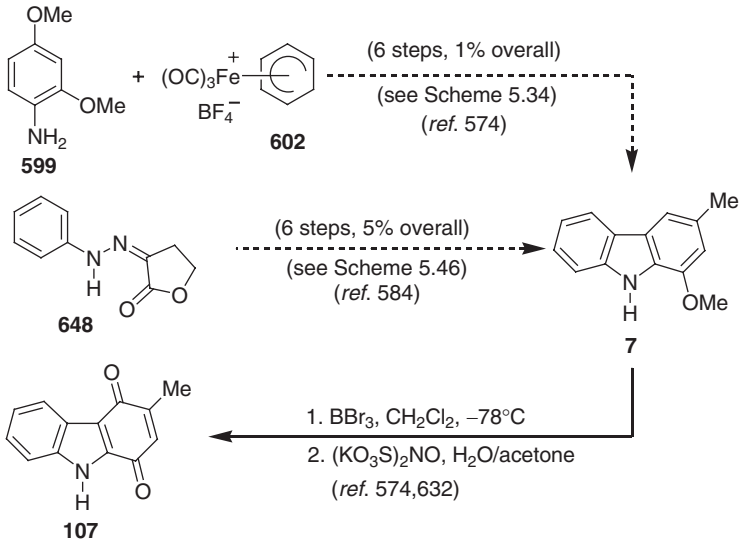

Scheme 5.113

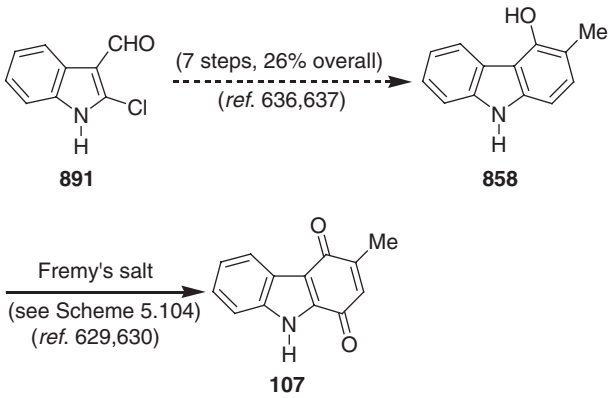

Scheme 5.114

Mal *et al.* also reported a formal synthesis of murrayaquinone A (**107**) starting from murrayafoline A (**7**). However, the required murrayafoline A (**7**) was obtained by the benzannulation of furoindolone, which was prepared by Fischer indolization of 3-(2-phenylhydrazono)dihydrofuran-2(3*H*)-one (**648**) (see Scheme 5.46) (584) (Scheme 5.113).

Hibino *et al.* reported a formal synthesis of murrayaquinone A (**107**) starting from 2-chloro-3-formylindole (**891**) by an allene-mediated electrocyclic reaction involving the indole 2,3-bond. The 4-hydroxy-3-methylcarbazole (**858**), a known precursor for murrayaquinone A (**107**), and required for this formal synthesis was obtained in seven steps, and 26% overall yield, starting from the 2-chloro-3-formylindole (**891**) (636,637) (Scheme 5.114).

Scott and Söderberg also reported a formal synthesis of murrayaquinone A (**107**) starting from 4-hydroxy-3-methylcarbazole (**858**) which was obtained from the

1,2-dihydro-4-(3*H*)-carbazolone **896** (638). This synthesis starts from 6-methyl-2-cyclohexenone (**892**) and uses two, sequential, palladium-catalyzed, intermolecular Stille cross-coupling and reductive *N*-heteroannulation steps. Iodination of **892** followed by Stille cross-coupling of the corresponding iodo derivative **893** with the arylstannane **894** gave the annulation precursor **895**. Reductive cyclization of **895** afforded the carbazolone **896**. Dehydrogenation of the carbazolone **896** using Pd/C in a mixture of diphenyl ether and 1,2,4-trimethylbenzene at 230°C led to 4-hydroxy-3-methylcarbazole (**858**). Finally, the literature-known oxidation of **858** using Fremy's salt (629,630) leads to murrayaquinone (**107**) (638) (Scheme 5.115).

On the basis of their earlier aromatic annulation strategy (see Scheme 5.64) (596), Shin and Ogasawara reported the first enantioselective total synthesis of carbazoquinocins A (**272**) and D (**275**) (639). The required methyl-substituted secondary chiral stereogenic center of the alkyl side chain at C-1 of carbazoquinocins A and D was introduced starting from the *O*-benzyl (*R*)-glycidol (*R*)-**897**.

Thus, the (*R*)-glycidol (*R*)-**897** was transformed to ethyl (*S*)-6-benzyloxy-3-methyl-4(*E*)-hexenoate (*S*)-**899** *via* addition of acetylide followed by spontaneous isomerization, stereoselective reduction, and Claisen–Johnson rearrangement. The chiral ester (*S*)-**899** was converted to (*R*)-4-methyl-6-phenylthiohexanol (*R*)-**902**. The primary alcohol (*R*)-**902** was then transformed to the terminal acetylene (*R*)-**904**, a common intermediate for the synthesis of carbazoquinocins A (**272**) and D (**275**). Chain elongation of (*R*)-**904** by two carbon atoms led to (*R*)-**905**, the chiral precursor for carbazoquinocin D (**275**) (639) (Scheme 5.116).

Using Sonogashira conditions, the (*R*)-acetylenes (*R*)-**904** and (*R*)-**905** were coupled with *N*-carbethoxy-2-iodoaniline **700** to afford the aryl acetylenes (*R*)-**906** and (*R*)-**907**. Executing similar functional group transformations as reported

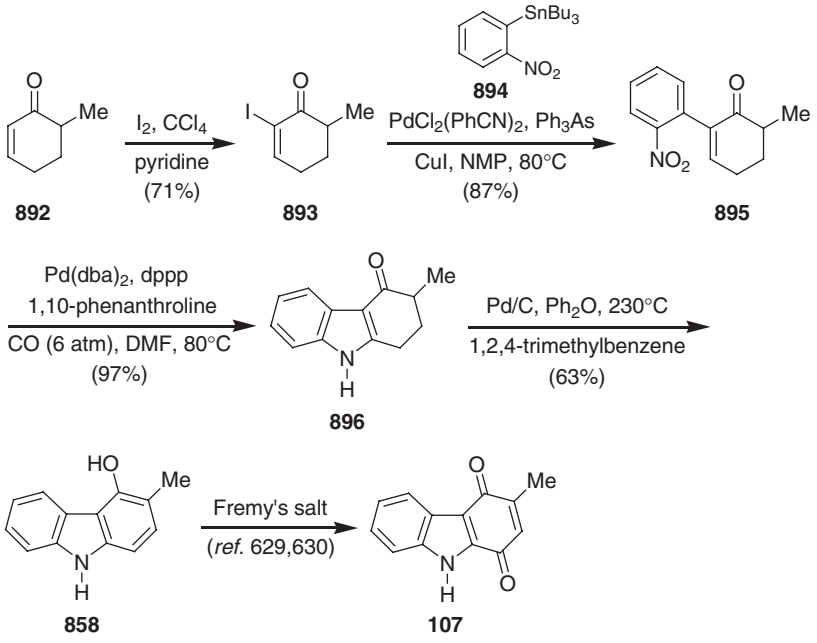

Scheme 5.115

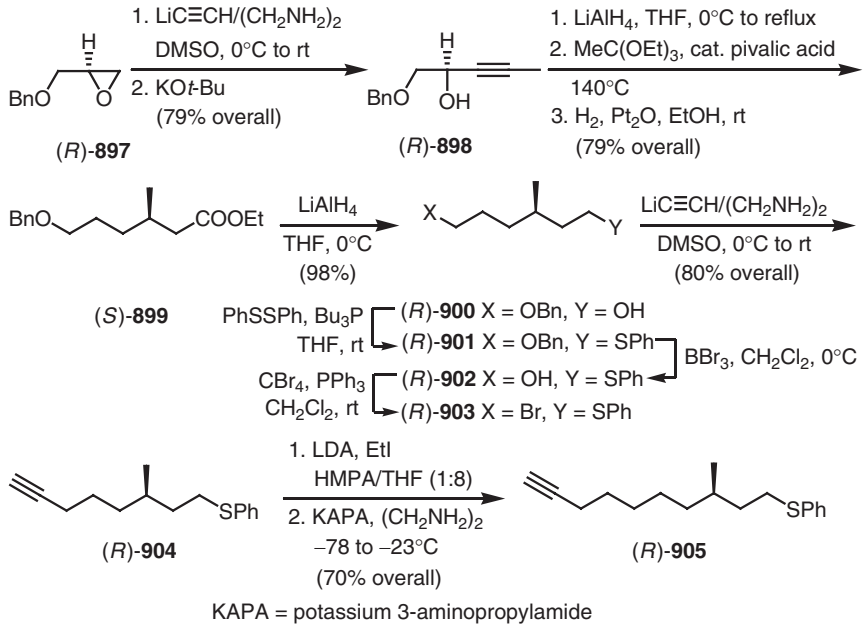

Scheme 5.116

previously for the total synthesis of carazostatin (**247**) (see Scheme 5.64) (596), the aryl acetylenes (*R*)-**906** and (*R*)-**907** were transformed to the 3-ethoxycarbonyl-2-methylcarbazoles (*S*)-**908** and (*S*)-**909**, and subsequently to the 3-hydroxy-2-methylcarbazoles (*S*)-**910** and (*S*)-**911**. Finally, oxidation of the 3-hydroxycarbazoles (*S*)-**910** and (*S*)-**911** with benzeneseleninic anhydride [$(PhSeO)_2O$] yielded quantitatively (*S*)-(−)-carbazoquinocin A (**272**) and (*S*)-(−)-carbazoquinocin D (**275**), respectively (639) (Scheme 5.117).

Hibino *et al*. reported the total synthesis of the carbazoquinocins B (**273**), C (**274**), D (**275**), E (**276**), and F (**277**) by his previously reported benzannulation method involving an allene-mediated, electrocyclic reaction of 2,3-functionalized indoles (536,537). The carbazole triflate **740**, a key-intermediate in the total synthesis of carazostatin (**247**) and hyellazole (**245**) (see Scheme 5.74) (536,537), also served as a common precursor for the total synthesis of the carbazoquinocins B–F (**273**–**277**). A Suzuki cross-coupling reaction of the carbazole triflate **740** with 9-alkyl-9-borabicyclo[3.3.1]nonane (9-alkyl-9-BBN) **912a–e** afforded the 1-alkylcarbazoles **913**, **741**, and **914**–**916** (56–85% yield). Cleavage of the ether by treatment of **913**, **741**, and **914**–**916** with boron tribromide gave the corresponding 3-hydroxycarbazoles **917**, **247**, and **918**–**920** (64–97% yield). Finally, the 3-hydroxycarbazoles **917**, **247**, and **918**–**920** were transformed to carbazoquinocin B (**273**), C (**274**), D (**275**), E (**276**), and F (**277**) in 70–95% yield, respectively, by oxidation with benzeneseleninic anhydride (537) (Scheme 5.118).

Our total synthesis of carbazoquinocin C (**274**) based on the iron-mediated construction of the carbazole framework as a key step uses the fully functionalized arylamine **921** and cyclohexadiene (**597**) as precursors (640) (Scheme 5.119).

The required arylamine **921** was prepared in a straightforward manner starting from commercial 3-methylveratrole (**789**). Regioselective bromination of the veratrole **789** afforded the 4-bromo derivative **790** in 88% yield. Halogen–metal

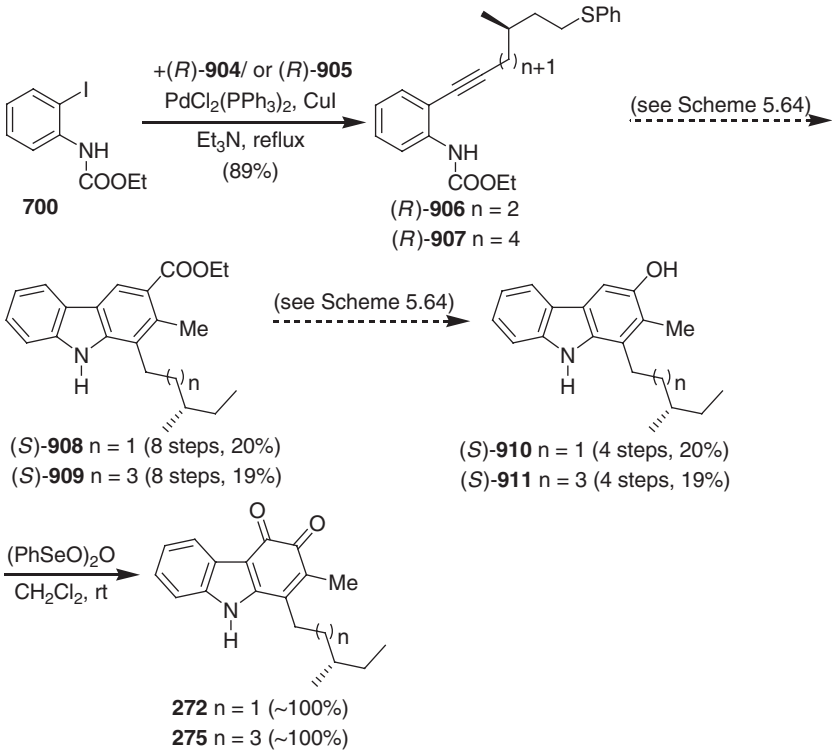

Scheme 5.117

exchange of **790** using butyllithium, followed by alkylation with 1-bromoheptane and subsequent regioselective nitration of the intermediate 4-heptyl derivative with fuming nitric acid in a mixture of acetic anhydride and glacial acetic acid (3:1), gave the 5-nitro derivative **922** in 50% overall yield. Finally, catalytic hydrogenation of the nitro derivative **922** led to the arylamine **921** in 83% yield (640).

Reaction of the iron complex salt **602** with the arylamine **921** in the presence of air led directly to the tricarbonyl(η^4-4b,8a-dihydro-9*H*-carbazole)iron complex (**923**) by a one-pot C–C and C–N bond formation. Demetalation of complex **923** and subsequent aromatization by catalytic dehydrogenation afforded 3,4-dimethoxy-1-heptyl-2-methylcarbazole (**924**), a protected carbazoquinocin C. Finally, ether cleavage of **924** with boron tribromide followed by oxidation in air provided carbazoquinocin C (**274**) (640) (Scheme 5.120).

A common precursor, the 6-bromocarbazole derivative **927**, required for the total synthesis of the carbazole-3,4-quinone alkaloids (±)-carquinostatin A [(±)-**278**] (641) and (±)-lavanduquinocin [(±)-**280**] (642), was prepared by iron-mediated one-pot C–C and C–N bond formation. Recently, the same methodology was adopted for the first enantioselective total synthesis of carquinostatin A (**278**) (643) and lavanduquinocin (**280**) (644).

The key intermediate, 6-bromocarbazole **927**, required for the first enantioselective total synthesis of carquinostatin A (**278**) and lavanduquinocin (**280**) arises from the (*R*)-arylamine **928** and the iron complex salt **602** (Scheme 5.121).

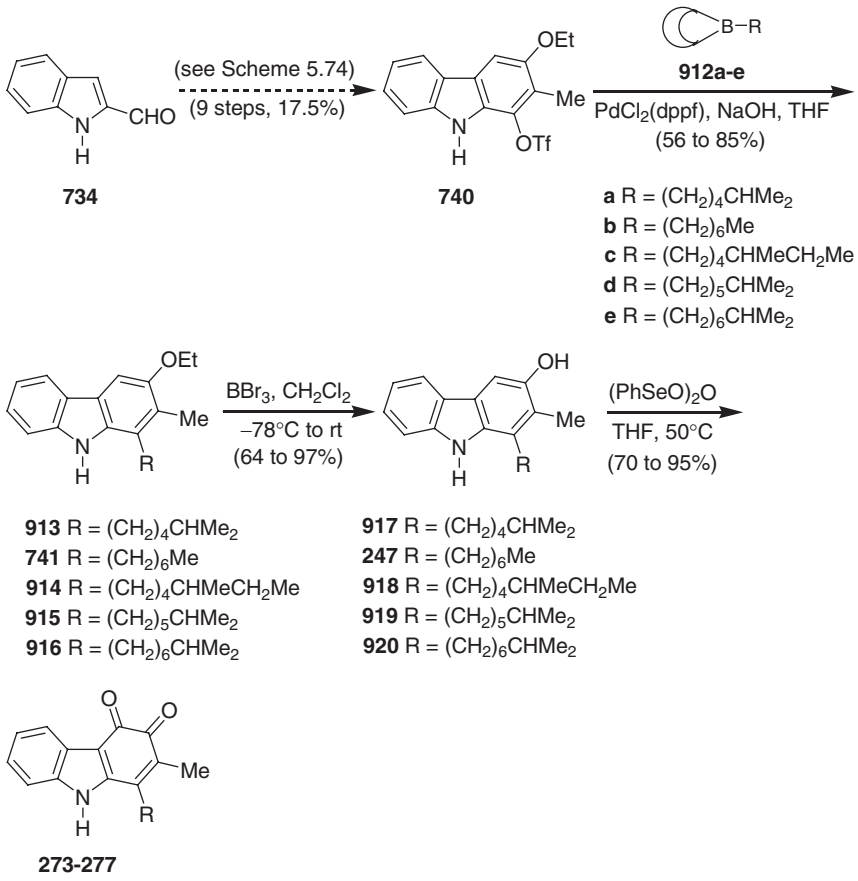

Scheme 5.118

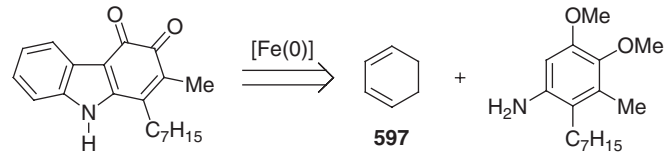

Scheme 5.119

The chiral side chain of the (*R*)-arylamine (**928**) derived from (*R*)-propene oxide and was obtained in 99% ee by Jacobsen's HKR of racemic propene oxide using (*R,R*)-(salen)cobalt(II) complex (615–617). The regioselective bromination of 3-methylveratrole (**789**) afforded the corresponding 4-bromo derivative **790** in almost quantitative yield. Halogen–metal exchange using butyllithium, followed by reaction with the (*R*)-propene oxide, afforded the (*R*)-carbinol **929**. Protection of **929** as the (*R*)-acetate **930** and subsequent regioselective nitration, followed by catalytic hydrogenation of the intermediate 5-nitro derivative, led to the (*R*)-arylamine **928** (643) (Scheme 5.122).

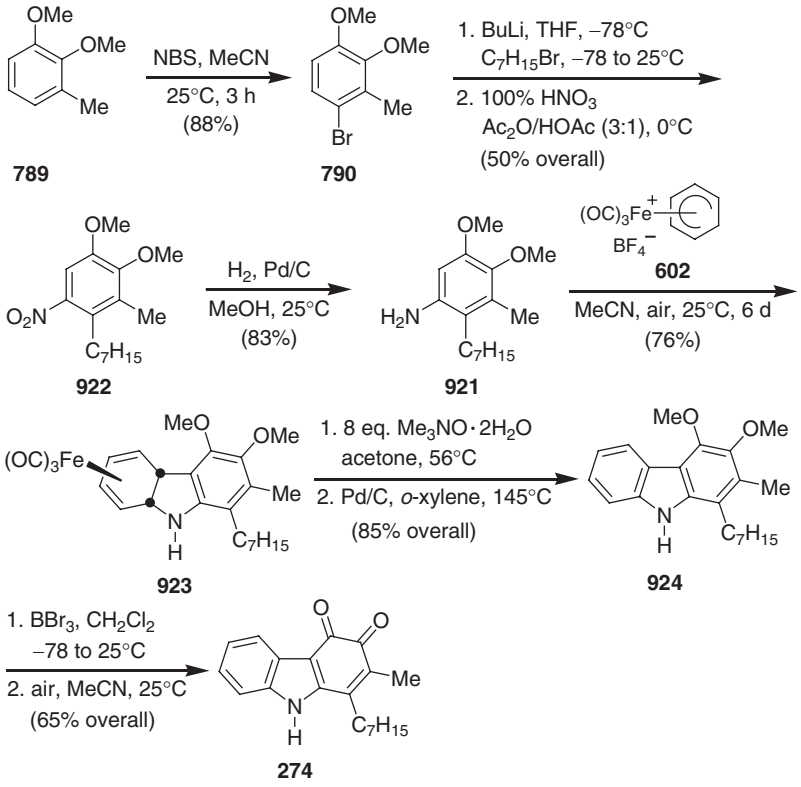

Scheme 5.120

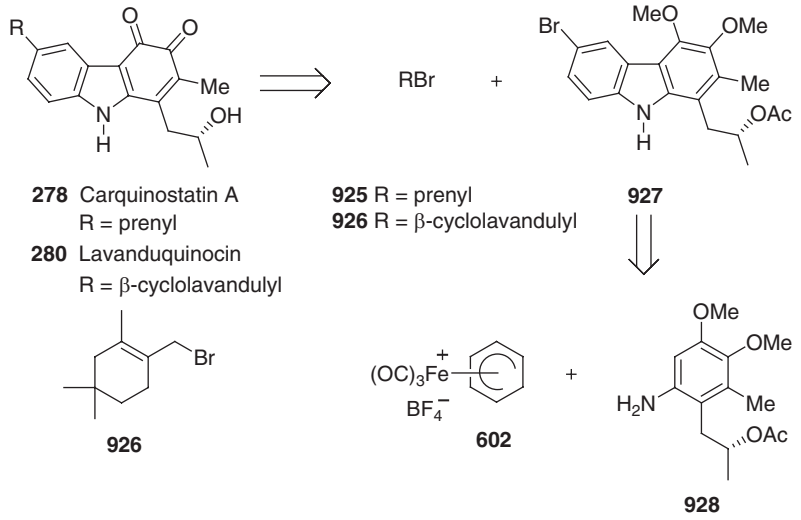

Scheme 5.121

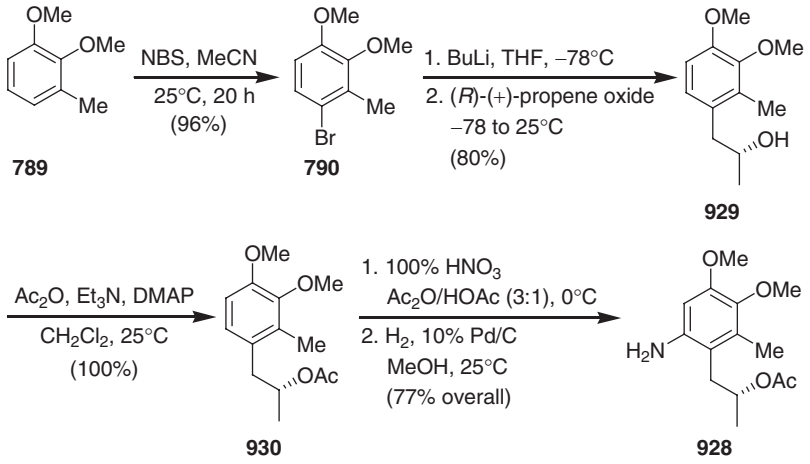

Scheme 5.122

Construction of the carbazole framework was achieved by slightly modifying the reaction conditions previously reported for the racemic synthesis (641,642). The reaction of the (*R*)-arylamine **928** with the iron complex salt **602** in air provided by concomitant oxidative cyclization the tricarbonyliron-complexed 4b,8a-dihydro-9*H*-carbazole (**931**). Demetalation of the complex **931**, followed by aromatization and regioselective electrophilic bromination, afforded the 6-bromocarbazole **927**, which represents a crucial precursor for the synthesis of the 6-substituted carbazole 3,4-quinone alkaloids. A nickel-mediated cross-coupling of the 6-bromocarbazole **927** with prenyl bromide (**925**) and β-cyclolavandulyl bromide (**926**), followed by ester cleavage and oxidation with either cobalt(III) fluoride or CAN, afforded carquinostatin A (**278**) (643) and lavanduquinocin (**280**) (644), respectively (Scheme 5.123).

Our second approach for the total synthesis of carbazoquinocin C (**274**) uses the palladium(II)-catalyzed oxidative coupling of aniline (**839**) and 2-methoxy-3-methyl-1,4-benzoquinone (**939**), followed by regioselective introduction of the heptyl side chain onto the carbazole-1,4-quinone **941** (645). The required 1,4-benzoquinone **939** was prepared starting from commercial 2,6-dimethoxytoluene (**935**). The titanium tetrachloride-promoted Friedel–Crafts acylation of **935** led to the acetophenone **936**, which was further transformed into the aryl acetate **937** by a proton-catalyzed Baeyer–Villiger oxidation. Ester cleavage of **937** to the phenol **938** and oxidation with CAN, $[(NH_4)_2Ce(NO_3)_6]$, afforded 2-methoxy-3-methyl-1,4-benzoquinone (**939**). Addition of aniline (**839**) to 2 equivalents of 1,4-benzoquinone **939** provided the corresponding 5-anilino-2-methoxy-3-methylbenzoquinone (**940**) in 84% yield with the expected regioselectivity (545,645) (Scheme 5.124).

The intramolecular oxidative cyclization of the anilinobenzoquinone **940** with a catalytic amount of palladium(II) acetate in the presence of copper(II) acetate in air afforded the carbazole-1,4-quinone **941** in almost quantitative yield. The regioselective introduction of the heptyl side chain at C-1 of the carbazole-1,4-quinone **941** was achieved by a 1,2-addition of the corresponding Grignard reagent to give the carbazole-1,4-quinol **942** in 55% yield. However, 1,4-addition at C-3 and 1,2-addition at C-4 led to the regioisomeric products **943** and **944** as well. Finally, under acidic reaction conditions, the carbazole-1,4-quinol **942** was smoothly transformed to

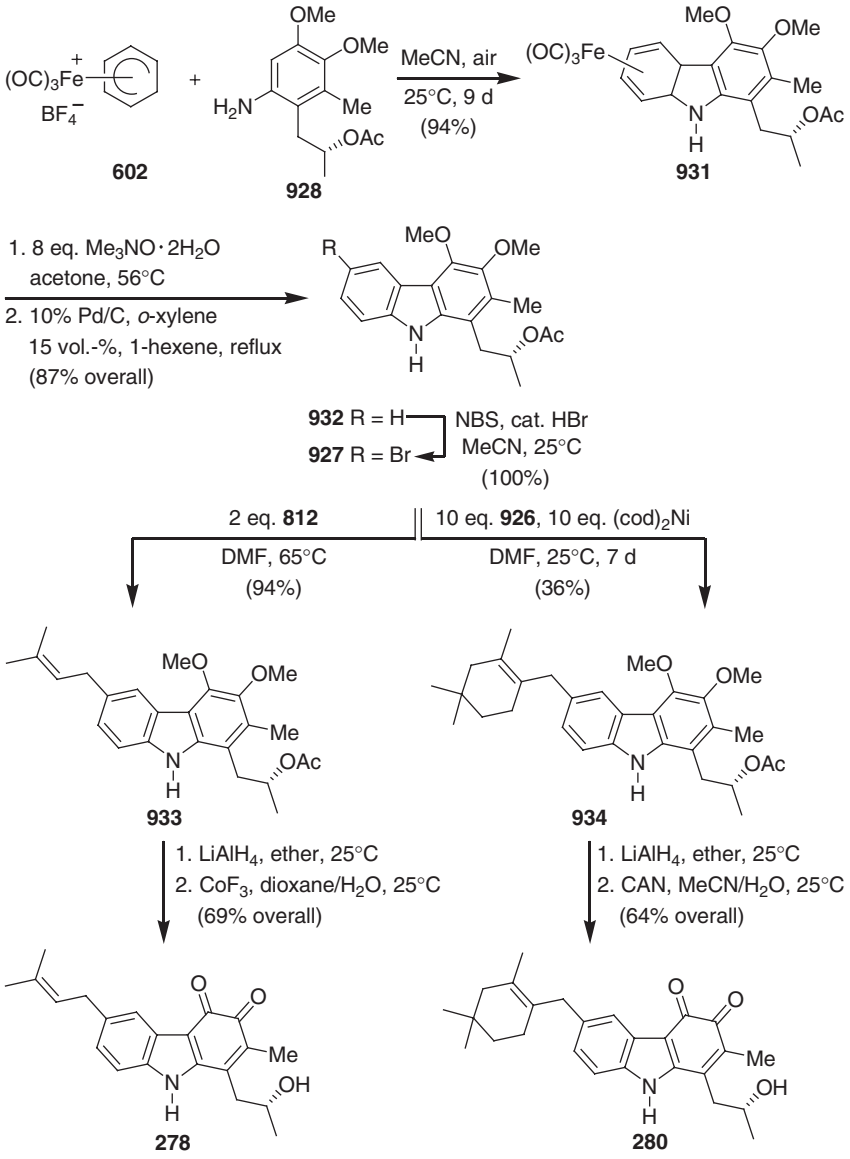

Scheme 5.123

carbazoquinocin C (**274**) by cleavage of the methyl ether, followed by elimination of water (545,645) (Scheme 5.125).

Retrosynthetic analysis of carbazoquinocin C (**274**) and (±)-carquinostatin A (±)-**278** based on our highly convergent palladium(II)-mediated intramolecular oxidative coupling of arylamino-1,2-benzoquinones provides aniline (**839**) and 4-heptyl-3-methyl-1,2-benzoquinone (**946**) as precursors for **274**, and 4-prenylaniline (**945**) and 4-(2-hydroxypropyl)-3-methyl-1,2-benzoquinone (**947**) as precursors for (±)-**278** (646) (Scheme 5.126).

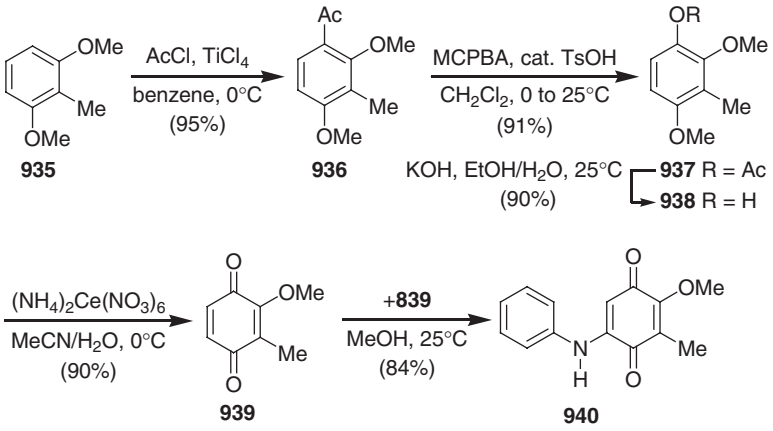

Scheme 5.124

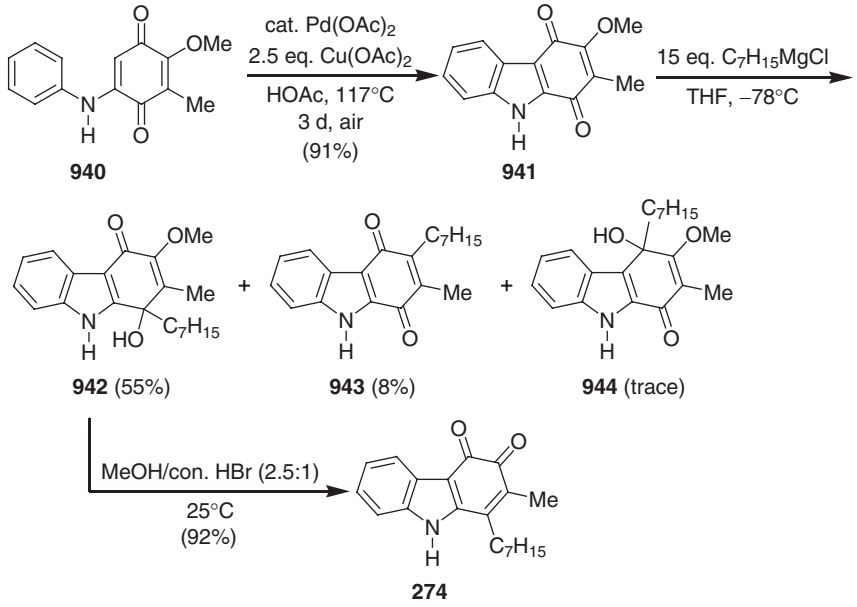

Scheme 5.125

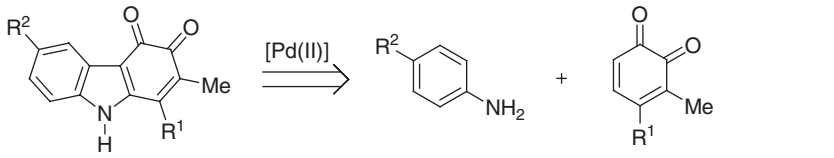

274 Carbazoquinocin C
$R^1 = C_7H_{15}$; R^2 = H

(±)-**278** (±)-Carquinostatin A
$R^1 = CH_2CH(OH)Me$; R^2 = prenyl

839 R^2 = H
945 R^2 = prenyl

946 $R^1 = C_7H_{15}$
947 $R^1 = CH_2CH(OH)Me$

Scheme 5.126

The veratrole **948**, required for the preparation of the 5-anilino-4-heptyl-3-methyl-1,2-benzoquinone (**950**), was already used as a precursor for the iron-mediated synthesis of carbazoquinocin C (**274**) (see Scheme 5.120). Ether cleavage of the veratrole **948** using boron tribromide afforded the corresponding catechol **949**. Oxidation of **949** with *o*-chloranil gave the required 1,2-benzoquinone **946** (see Scheme 5.126). The 1,2-benzoquinone **946** proved to be very labile. Therefore, it was transformed *in situ* to the anilino-1,2-benzoquinone **950** by addition of 0.5 equivalents of aniline (**839**) in methanol at low temperature. The oxidative cyclization using palladium(II) acetate in glacial acetic acid at 55°C transformed compound **950** directly to carbazoquinocin C (**274**). Using this approach, carbazoquinocin C (**274**) is available in three steps and 29% overall yield based on the veratrole **948** (646) (Scheme 5.127). Among the three known methods of our total syntheses of carbazoquinocin C (**274**) this palladium(II)-mediated *o*-quinone approach combines the advantages of both previous approaches (see Schemes 5.120 and 5.125) by using a fully functionalized 1,2-benzoquinone as a building block.

4-Prenylaniline (**945**) required for the synthesis of (±)-carquinostatin A [(±)-**278**] (see retrosynthesis in Scheme 5.126) was obtained by a nickel-mediated cross-coupling reaction of the *N*-protected 4-bromoaniline **952** with bis[μ-bromo(η^3-prenyl)nickel] (**825**) (646) (Scheme 5.128).

Following a synthetic pathway similar to the one reported for carbazoquinocin C (**274**) (see Scheme 5.127), the veratrole (±)-**818** was transformed to the arylamino-1,2-benzoquinone (±)-**954**. By palladium(II)-mediated oxidative cyclization, compound

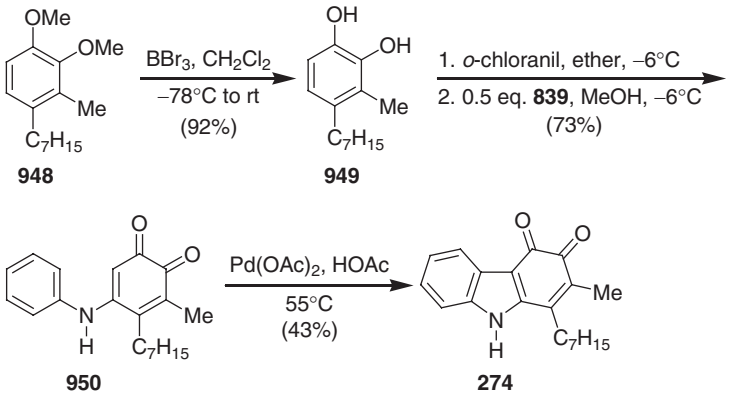

Scheme 5.127

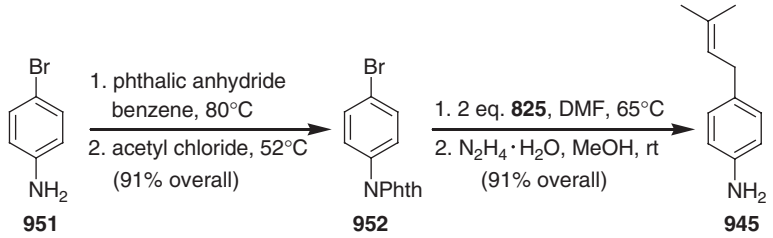

Scheme 5.128

(±)-**954** was transformed to *O*-acetylcarquinostatin A (±)-**955**. Finally, removal of the acetyl protecting group by reduction with lithium aluminum hydride provided (±)-carquinostatin A [(±)-**278**] in 62% yield (Scheme 5.129). Using this methodology, (±)-carquinostatin A [(±)-**278**] is available in four steps, and 33% overall yield, based on the veratrole (±)-**818** (646) (Scheme 5.129).

Aygün and Pindur reported the total synthesis of carbazoquinocin C (**274**) starting from *N*-(phenylsulfonyl)indole (**956**) (647). The key step in this methodology involves a polar cyclization of the 2-vinylindole **958** with oxalyl chloride. Regioselective 2-lithiation of *N*-(phenylsulfonyl)indole (**956**), followed by addition of 3-decanone, led to the carbinol **957**. Elimination of water with TFA/triethylamine in chloroform, followed by removal of the protecting group with sodium hydroxide in ethanol, afforded the 2-vinylindole **958**, along with an undesired double bond regioisomer (ratio 2:1, no yield given). The reaction of compound **958** with oxalyl chloride led to the corresponding indole-3-glyoxyl chloride, which on treatment with aluminum(III) chloride provided carbazoquinocin C (**274**) in 59% yield (647) (Scheme 5.130). This three-step synthesis was applied to a wide range of carbazole-3,4-quinones (648,649).

Rawat and Wulff reported the total synthesis of carbazoquinocin C (**274**) starting from indole 2-carboxylic acid (**959**) (563). This methodology uses the application of *o*-benzannulation of the Fischer carbene complexes **964** and **965**. The fully functionalized carbene complexes **964** and **965** required for the synthesis of carbazoquinocin C (**274**) were prepared from commercially available indole 2-carboxylic acid (**959**). The heptyl-2-indolyl ketone (**960**) was obtained from the acid **959** through Grignard addition to Weinreb's amide. After protection of the indole nitrogen, the corresponding *N*-benzyl derivative **962** was brominated to the corresponding 3-bromo derivative **963**, the precursor required for the carbene complexes **964** and **965**. Using the standard Fischer procedure, the 3-bromo

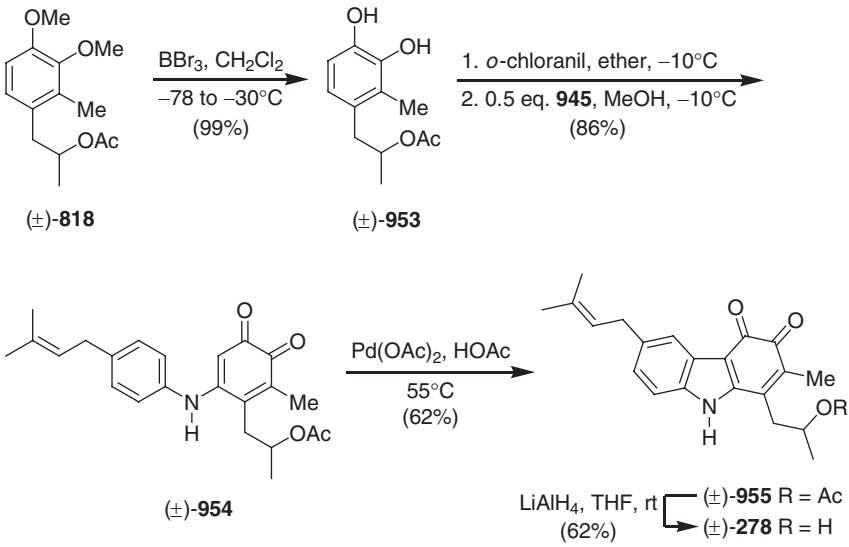

Scheme 5.129

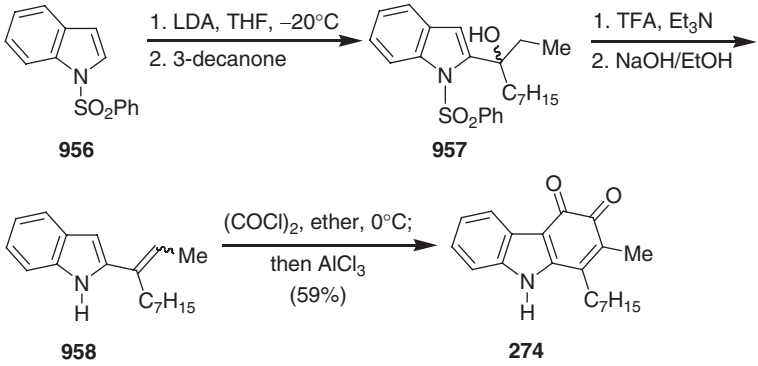

956 **957** **958** **274**

Scheme 5.130

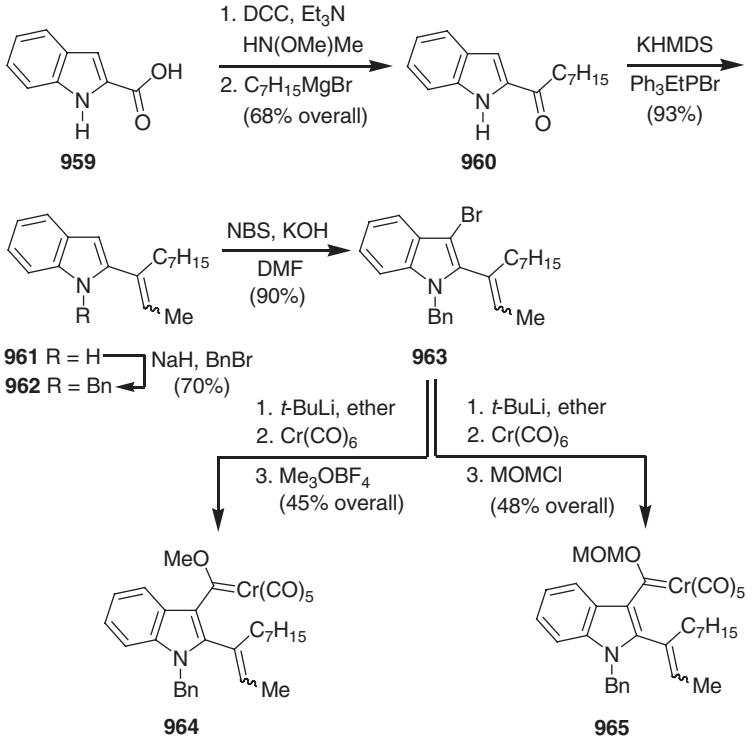

959 **960** **961** R = H **962** R = Bn **963** **964** **965**

Scheme 5.131

derivative **963** was transformed to the carbene complexes **964** and **965** in moderate yields along with hydrodebrominated by-products. Without purification, the carbene complex **964** was subjected to *o*-benzannulation by photolysis under an atmosphere of carbon monoxide to the *N*-benzylcarbazole **967**. After *O*-methylation, the benzyl group was cleaved with potassium *tert*-butoxide in DMSO in the presence of oxygen. Finally, following a two-step sequence of demethylation with boron tribromide and oxidation with sodium *meta*-periodate, the 3,4-dimethoxycarbazole **968** was transformed to carbazoquinocin C (**274**) (563) (Schemes 5.131 and 5.132).

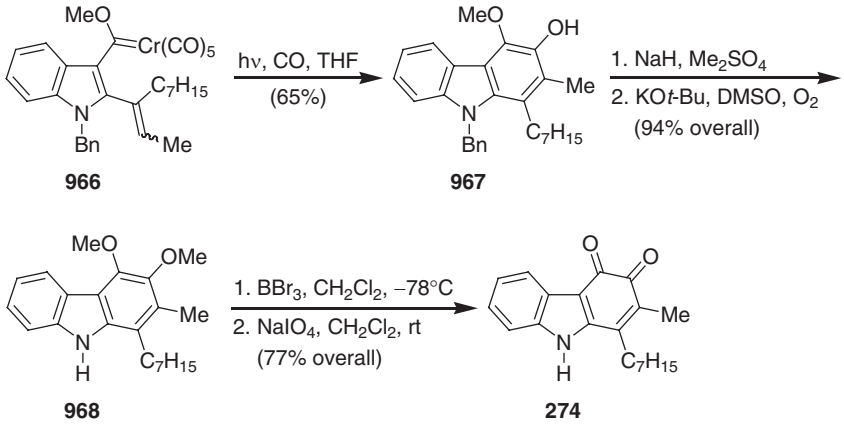

Scheme 5.132

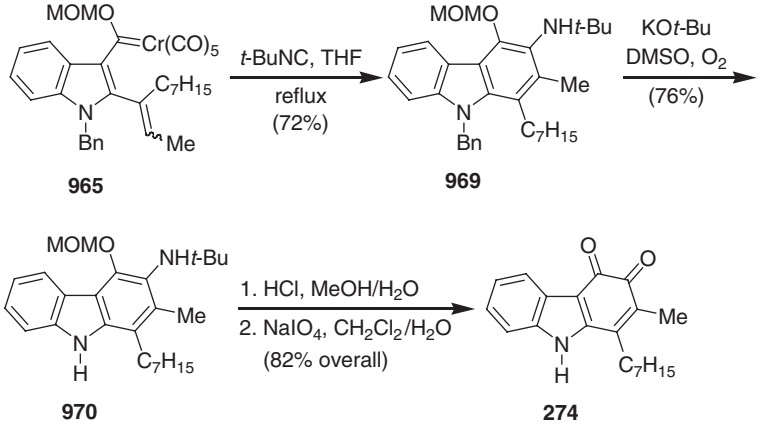

Scheme 5.133

An alternative short synthesis of carbazoquinocin C (**274**) was achieved by thermal *o*-benzannulation of a different carbene complex **965** with isonitrile. Thus, the reaction of carbene complex **965** with *tert*-butylisonitrile in refluxing THF gave the *N*-benzyl carbazole **969** in 72% yield. After debenzylation, the corresponding 3-aminocarbazole **970** was subjected to cleavage of the MOM group to afford the intermediate 4-hydroxycarbazole, which, on oxidation with sodium *meta*-periodate, led to carbazoquinocin C (563) (**274**) (Scheme 5.133).

The total synthesis of the carbazomycins G (**269**) and H (**270**) based on our iron-mediated approach uses the *O*-acetylcarbazoles **971** and **972** as precursors, which are derived from the the iron-complex salts **602** and **779** and the arylamine **973** (650,651) (Scheme 5.134).

The required arylamine **973** was prepared starting from the aryl acetate **937**. The compound **937** was also used for the palladium(II)-catalyzed total synthesis of carbazoquinocin C (**274**) (545) (see Scheme 5.124) and carbazomycin G (**269**) (652). The acetate **937** was transformed to the corresponding 5-nitro derivative **974** by reacting with fuming nitric acid in a mixture of acetic anhydride and glacial acetic

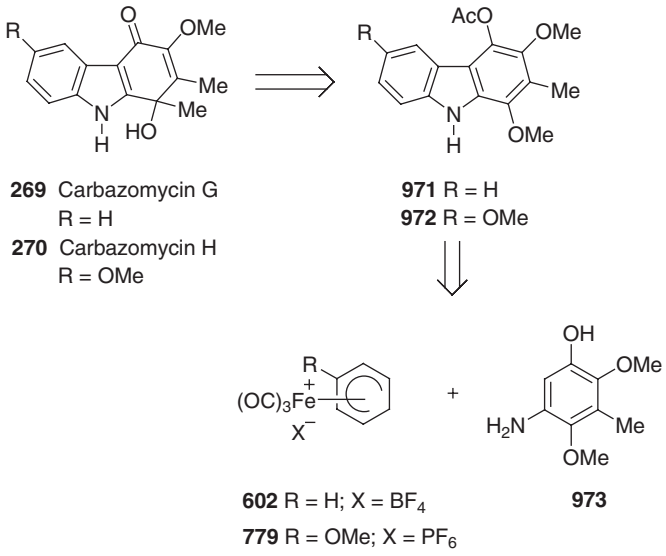

Scheme 5.134

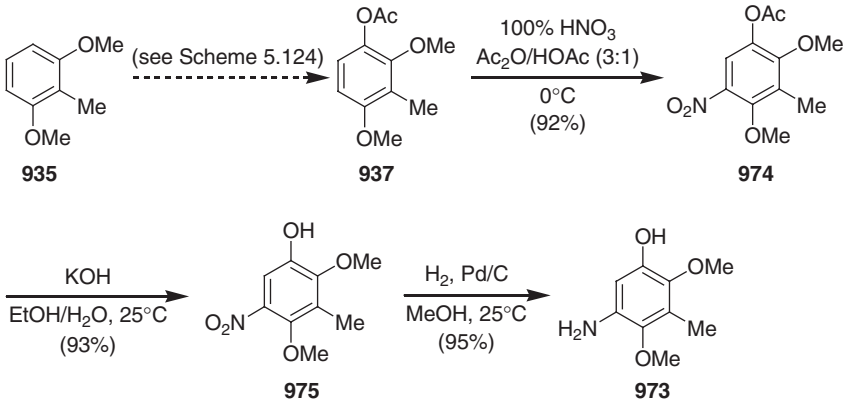

Scheme 5.135

acid (3:1). Finally, ester cleavage to the phenol **975** and catalytic hydrogenation afforded the arylamine **973** (Scheme 5.135). This route provides the arylamine **973** in three steps, and 81% overall yield, on a multigram scale starting from the aryl acetate **937** (650,651) (Scheme 5.135).

The reaction of the iron-complex salts **602** and **779** with the arylamine **973** afforded the iron complexes **976** and **977**, both in 96% yield. Subsequent *O*-acetylation provided the corresponding acetates **978** and **979** in almost quantitative yield. The iron-mediated arylamine cyclization of the *O*-acetyl derivative **978** using very active manganese dioxide provided the carbazole **971** in 72% yield. Under similar reaction conditions, the *O*-acetyl derivative **979** gave a mixture of the carbazoles **972** and **980** in 35% and 17% yield, respectively (650,651) (Scheme 5.136).

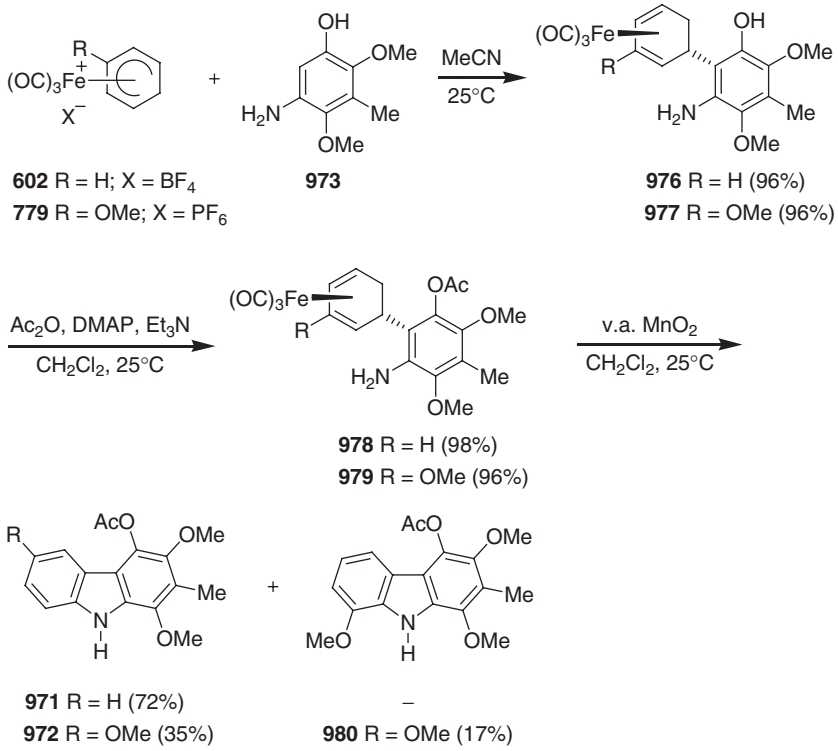

Scheme 5.136

The oxidation of the *O*-acetylcarbazole derivatives **971** and **972** with CAN, $[(NH_4)_2Ce(NO_3)_6]$, led to the carbazole-1,4-diones **941** and **981**, the immediate precursors for carbazomycin G (**269**) and H (**270**). The carbazole-1,4-quinone **941** also served as precursor for the palladium(II)-catalyzed total synthesis of carbazoquinocin C (**274**) (545,645). Finally, addition of an excess of methyllithium to **941** and **981** afforded carbazomycins G **269** and H **270** (the products of 1,2-addition at C-1) in 71% and 42% yield, along with the corresponding 2,3-dimethylcarbazole-1,4-quinones **982** and **983** in 12% and 14% yield (the products of 1,4-addition at C-3 followed by elimination) (650,651) (Scheme 5.137).

Our palladium(II)-catalyzed approach for the carbazomycins G (**269**) and H (**270**) requires the carbazole-1,4-quinones **941** and **981** as precursors (compare the iron-mediated synthesis, see Scheme 5.137). These intermediates should result from oxidative cyclization of the arylamino-1,4-benzoquinones, which in turn are prepared from the arylamines **839** and **984** and 2-methoxy-3-methyl-1,4-benzoquinone (**939**) (652) (Scheme 5.138).

One of the carbazole-1,4-quinones, 3-methoxy-2-methylcarbazole-1,4-quinone (**941**), required for the total synthesis of carbazomycin G (**269**), was already used as a key intermediate for the total synthesis of carbazoquinocin C, and was obtained by the addition of aniline (**839**) to 2-methoxy-3-methyl-1,4-benzoquinone (**939**), followed by oxidative cyclization with catalytic amounts of palladium(II) acetate (545,645) (see Schemes 5.124 and 5.125). Similarly, in a two-pot operation, 4-methoxyaniline (**984**) was transformed to 3,6-dimethoxy-2-methylcarbazole-1,4-quinone

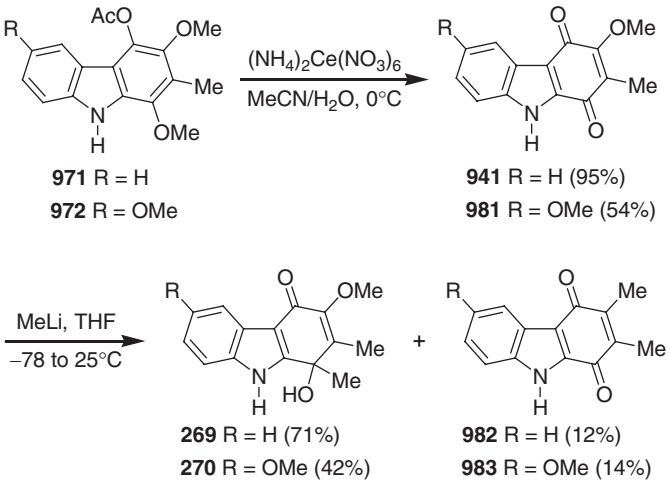

971 R = H
972 R = OMe

941 R = H (95%)
981 R = OMe (54%)

269 R = H (71%)
270 R = OMe (42%)

982 R = H (12%)
983 R = OMe (14%)

Scheme 5.137

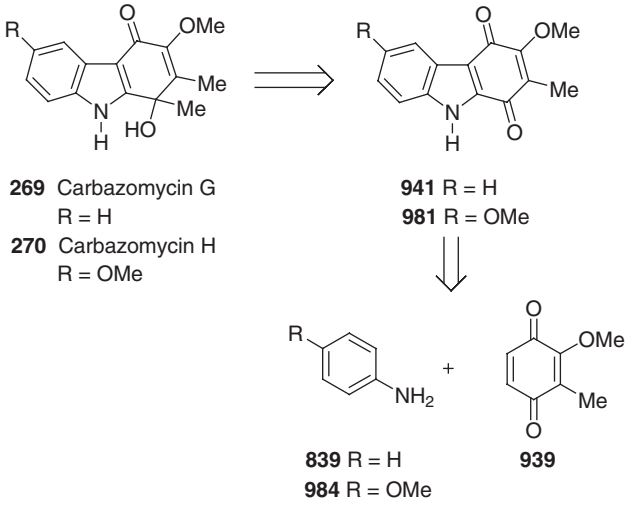

269 Carbazomycin G
R = H
270 Carbazomycin H
R = OMe

941 R = H
981 R = OMe

839 R = H
984 R = OMe

939

Scheme 5.138

(**981**) in 61% overall yield (Schemes 5.139 and 5.140). Finally, regioselective addition of methyllithium to the carbazole-1,4-quinones **941** and **981** afforded carbazomycins G (**269**) and H (**270**), respectively (652) (Scheme 5.140).

Hibino *et al.* reported the total synthesis of carbazomycin G (**269**) by the regioselective addition of methyllithium onto 3-methoxy-2-methylcarbazole-1,4-quinone (**941**) (653). The required immediate precursor of carbazomycin G, carbazole-1,4-quinone **941**, was obtained from 3-(2-methoxyethenyl)-*N*-(phenylsulfonyl)indole (**986**). The benzannulation involves an allene-mediated electrocyclic reaction of a 6π-electron system generated from the 2-propargylindole **989**, which was derived from the 3-vinylindole **986** in three steps.

Thus, reaction of a mixture of the *E*- and *Z*-isomers **986** with LDA, followed by addition of DMF, afforded the 3-[(*E*)-2-methoxyethenyl]indole-2-carbaldehyde (**987**)

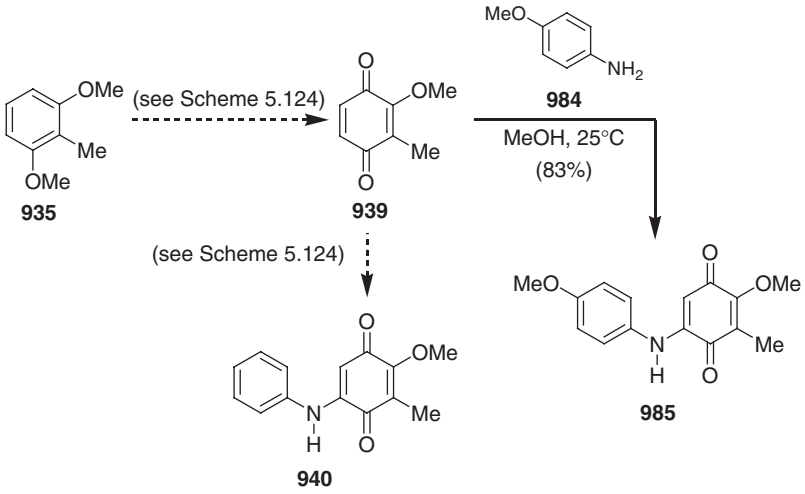

Scheme 5.139

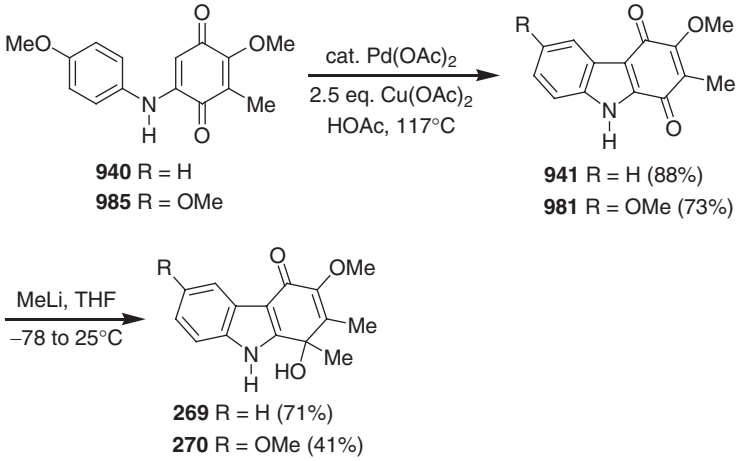

Scheme 5.140

in 41% yield, along with the unreactive *Z*-isomer **986** (14% yield). The lower reactivity of the lithiated *Z*-isomer towards DMF was explained by the formation of a more stable six-membered ring chelate. Addition of ethynylmagnesium bromide to **987** afforded the propargyl alcohol **988**. After protection as the MOM ether, the compound **989** was subjected to electrocyclic reaction by treatment with potassium *tert*-butoxide in *tert*-butanol and THF at 90°C to afford the 1,3-dioxygenated carbazole **990** *via* an allene intermediate. Cleavage of the MOM ether with chlorotrimethylsilane and sodium iodide gave the corresponding 1-hydroxycarbazole **991**. Oxidation of **991** with [bis(trifluoroacetoxy)iodo]benzene in aqueous acetonitrile provided the carbazole-1,4-quinone **941**. Using our previously developed regioselective methyllithium addition protocol (650–652), the compound **941** was transformed to carbazomycin G (**269**) (653) (Scheme 5.141).

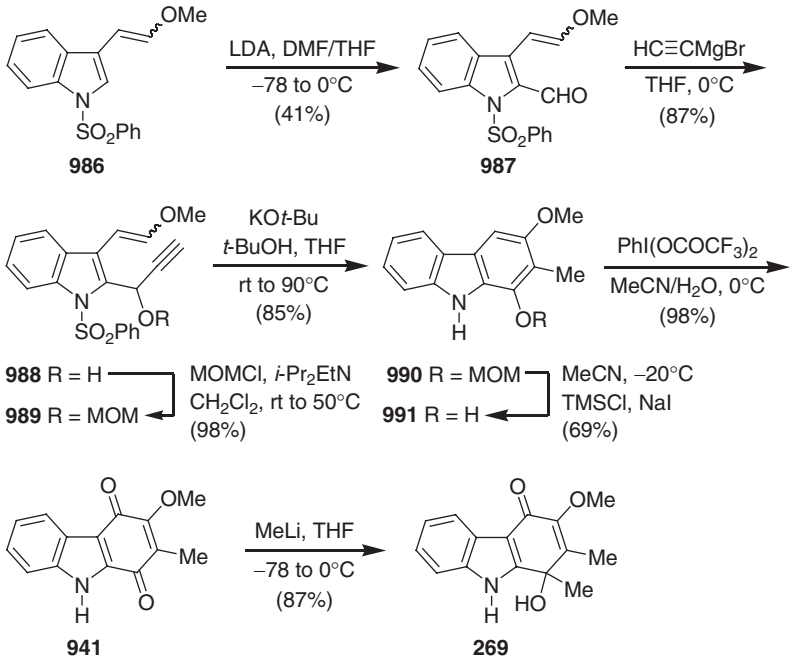

Scheme 5.141

6 Other Tricyclic Alkaloids

This section covers the total synthesis of simple tricyclic carbazoles which are not covered in Sections II.A.1–II.A.5, and includes the tricyclic carbazoles substituted either at the C-ring or at the 9(*N*)- of the carbazole nucleus.

Kawasaki and Somei reported the first total synthesis of 3-formyl-9-methoxycarbazole (**105**) starting from the hexahydrocarbazole **992** (654). Prior to regioselective iodination, **992** was transformed to the 9-methoxycarbonyl derivative **993** by reaction with methyl chloroformate. After regioselective iodination of **993** with iodine and sodium periodate ($NaIO_4$), the corresponding 3-iodocarbazole **994** was subjected to alkaline hydrolysis to afford 4b,8a-*cis*-hexahydro-3-iodocarbazole **995** in 85% yield. Using a literature procedure (655), the hexahydrocarbazole **995** was transformed to 3-iodo-9-methoxy-tetrahydrocarbazole (**996**) in two steps and 37% overall yield. Halogen–metal exchange of **996** using butyllithium, followed by reaction with DMF led to 3-formyl-9-methoxy-tetrahydrocarbazole (**997**). Finally, dehydrogenation of the tetrahydrocarbazole **997** with DDQ furnished 3-formyl-9-methoxycarbazole (**105**) (654) (Scheme 5.142).

Bhattacharyya *et al.* reported the first total synthesis of clausenalene (**90**) to establish its structure (99). This total synthesis uses Japp–Klingemann and Fischer–Borsche reactions as key steps. The phenyl hydrazone **1000** required for the transformation to 1-oxo-tetrahydrocarbazole **1001** under Fischer–Borsche conditions was obtained by condensation of 2-hydroxymethylene-5-methylcyclohexanone (**999**) with diazotized 3,4-methylenedioxyaniline (**998**) using Japp–Klingemann conditions. Wolff–Kishner reduction of **1001** furnished 3-methyl-6,7-methylenedioxy-1,2,3,4-tetrahydrocarbazole (**1002**), which, on aromatization with 10% Pd/C in decalin, afforded clausenalene (**90**) (99) (Scheme 5.143).

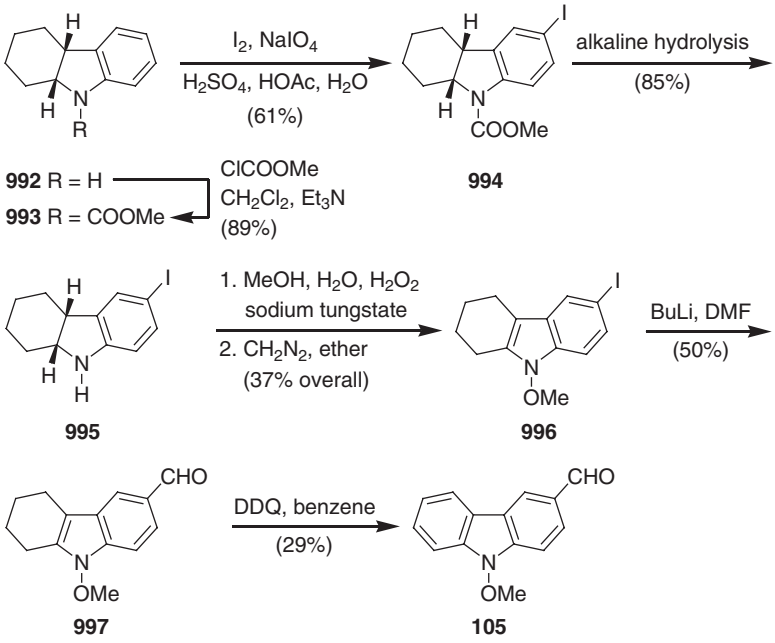

Scheme 5.142

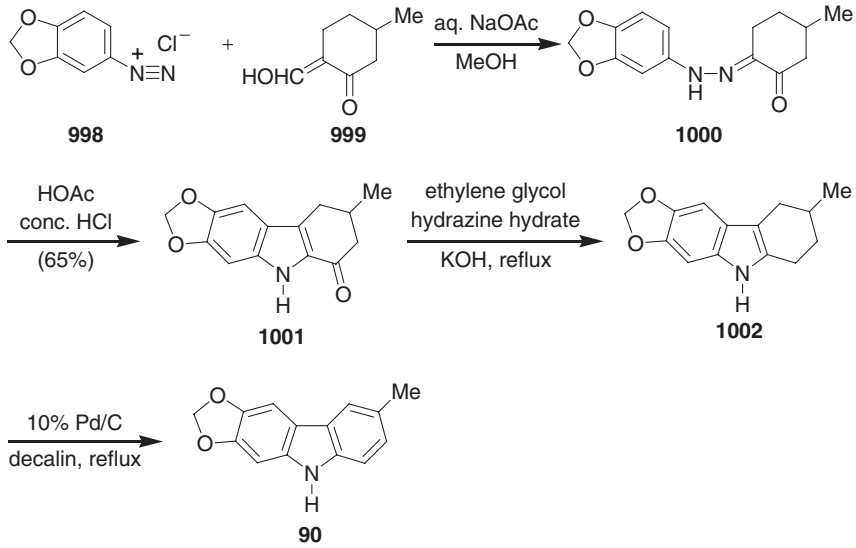

Scheme 5.143

During the course of photoformylation studies on methoxycarbazoles with chloroform, Chowdhury and Saha reported the synthesis of 3-formyl-6-methoxycarbazole (**97**) starting from 3-methoxycarbazole (**1003**) (656). In this transformation, the desired 3-formyl-6-methoxycarbazole (**97**) was obtained in only 10% yield, along with the other major regioisomeric formyl carbazoles, **1004** (14%)

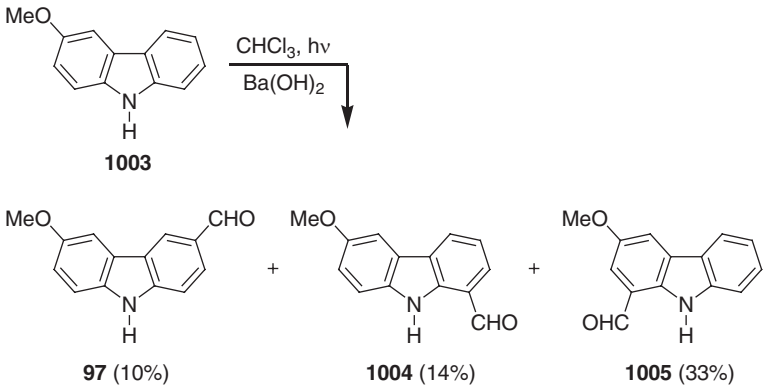

Scheme 5.144

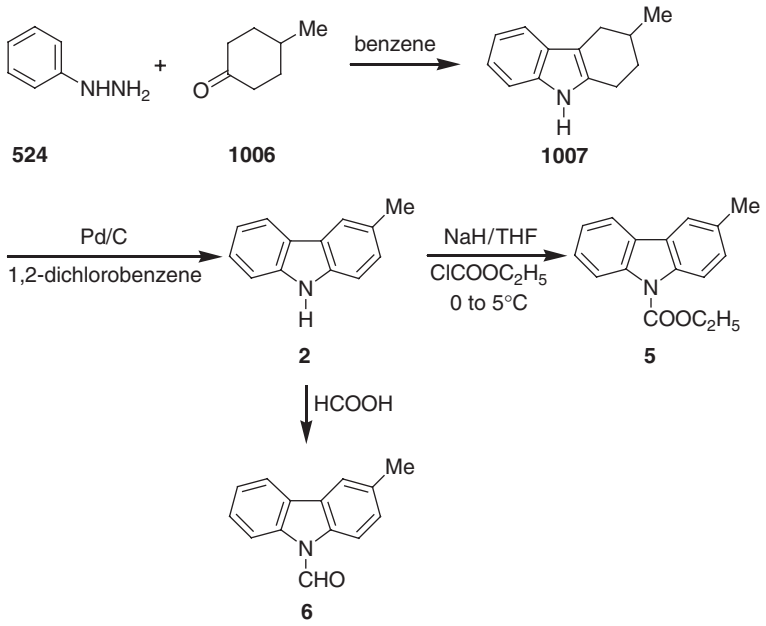

Scheme 5.145

and **1005** (33%). The high yield of 1-formyl-3-methoxycarbazole (**1005**) suggests that the methoxy group activates the nucleus during photoformylation (656) (Scheme 5.144).

Chakrabarty *et al*. reported the syntheses of 9-carbethoxy-3-methylcarbazole (**5**) and 9-formyl-3-methylcarbazole (**6**) to confirm the assigned structures (17). The syntheses use 3-methylcarbazole (**2**) as a common intermediate, which was obtained under Fischer–Borsche conditions starting from phenylhydrazine (**524**) and 4-methylcyclohexanone (**1006**). Reaction of 3-methylcarbazole (**2**) with sodium hydride (NaH), followed by addition of ethyl chloroformate, afforded 9-carbethoxy-3-methylcarbazole (**5**). 9-Formyl-3-methylcarbazole (**6**) was obtained by reaction of 3-methylcarbazole (**2**) with formic acid (17) (Scheme 5.145).

Chakravarty *et al.* reported the synthesis of glycoborine (**87**) to confirm the assigned structure (98). This synthesis also led to the reassignment of the structure of glycozolicine (**88**) as 8-methoxy-3-methylcarbazole, which was supported by synthesis. Both these syntheses involve the Fischer–Borsche reaction as the key step. The hydrazones **1010** and **1011**, required for these syntheses, were obtained by condensation of hydrazines **1008** and **1009** with 4-methylcyclohexanone (**1006**), respectively. Under Fischer–Borsche conditions, the hydrazone **1010** was transformed to the desired 5-methoxytetrahydrocarbazole **1012** in only 6% yield, along with 54% of the regioisomeric 7-methoxytetrahydrocarbazole **1013**. The high yield of the wrong regioisomeric product is explained by the electronic and steric effects of the methoxy group. Finally, dehydrogenation of **1012** in the presence of chloranil in xylene led to glycoborine (**87**). Using a similar reaction sequence, the hydrazone **1011** was transformed to glycozolicine (**88**) in 15% overall yield (98) (Scheme 5.146).

Witulski and Alayrac reported the synthesis of clausine C (clauszoline-L) (**101**) by a rhodium-catalyzed alkyne cyclotrimerization of diyne **1014** and propiolic ester **635** (561). Analogous to the hyellazole (**245**) synthesis (see Scheme 5.75), the diyne precursor **1014** required for this key cyclotrimerization reaction was obtained starting from readily available 2-iodo-5-methoxyaniline. Using Wilkinson's catalyst, $[RhCl(PPh_3)_3]$, crossed-alkyne cyclotrimerization of **1014** and **635** led to *N*-tosylclausine C (**1015**) in 78% yield in an isomeric ratio of 3.8:1. Finally, deprotection of the tosyl group with TBAF in refluxing THF afforded clausine C (clauszoline-L) (**101**) (561) (Scheme 5.147).

Selvakumar *et al.* reported the total synthesis of 3-formyl-9-methoxycarbazole (**105**) starting from 3-fluoro-4-nitrotoluene (**1016**) (657). This methodology uses a novel benzannulation strategy involving ring closing metathesis (RCM) as key step. Nucleophilic aromatic substitution of methyl cyanoacetate and 3-fluoro-4-nitrotoluene (**1016**) led to the cyanoester **1017** in almost quantitative yield. The alkylation of **1017** with allyl bromide, followed by rearrangement (658) of **1018** in a solution of NaCl and DMSO at 155°C, led to the required 1-methoxyindole **1019**. Reaction of the nitrile

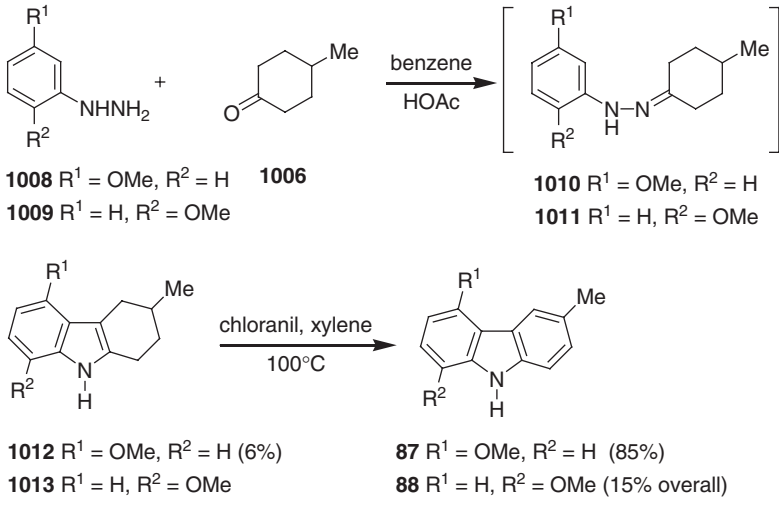

Scheme 5.146

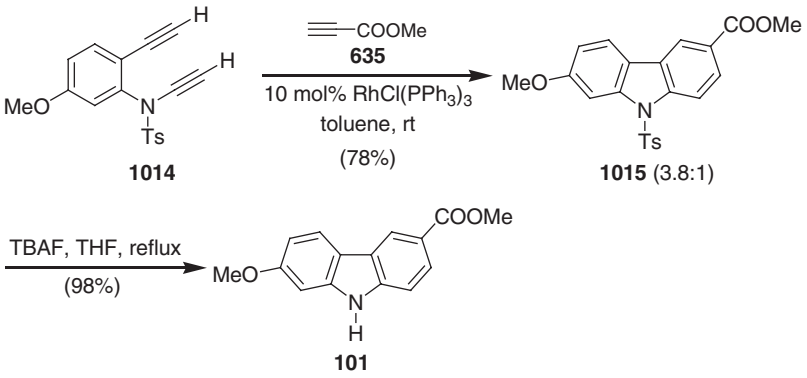

Scheme 5.147

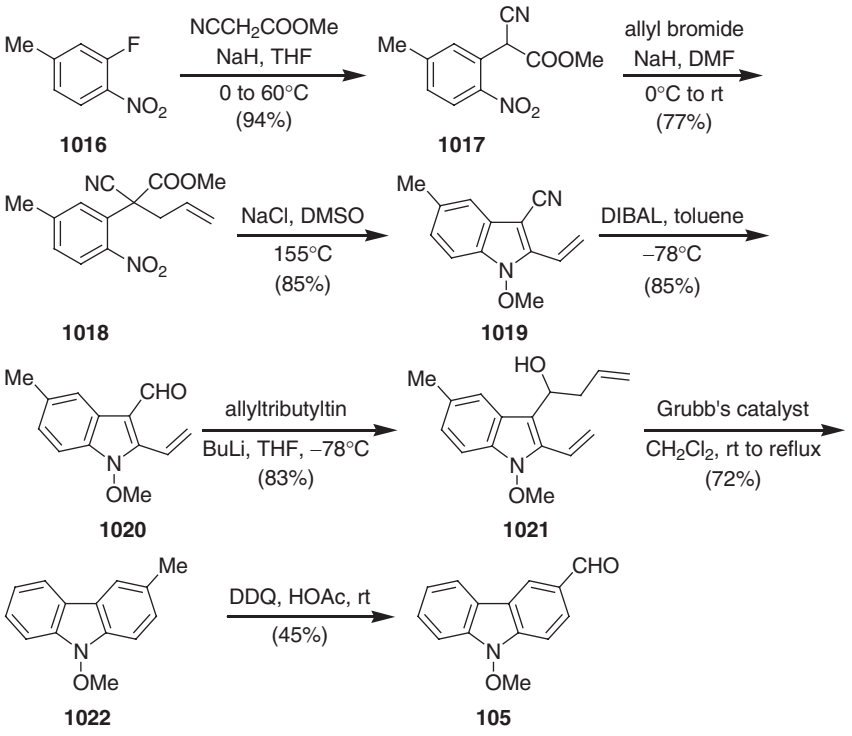

Scheme 5.148

1019 with DIBAL, followed by transmetalation of the resulting aldehyde **1020** with allyltributyltin, cleanly afforded the alcohol **1021**. Treatment of the alcohol **1021** with Grubbs' catalyst resulted in the 9-methoxycarbazole **1022** by cyclization with concomitant dehydration. Finally, reaction of **1022** with DDQ in acetic acid afforded 3-formyl-9-methoxycarbazole (**106**) (657) (Scheme 5.148).

Using our palladium(II)-catalyzed approach, we reported the total syntheses of a wide range of 7-oxygenated carbazole alkaloids, including siamenol (**89**),

clauszoline-K (**98**), 3-formyl-7-hydroxycarbazole (**99**), clausine C (clauszoline-L) (**101**), clausine M (**102**), and clausine N (**103**) (546).

The relay compound **1025** required for the synthesis of all of these 7-oxygenated carbazole alkaloids was obtained starting from commercially available 4-bromotoluene (**1023**) and *m*-anisidine (**840**) in two steps and 72% overall yield. Buchwald–Hartwig amination of 4-bromotoluene (**1023**) with *m*-anisidine (**840**) furnished quantitatively the corresponding diarylamine **1024**. Oxidative cyclization of **1024** using catalytic amounts of palladium(II) acetate afforded 3-methyl-7-methoxycarbazole (**1025**). Oxidation of **1025** with DDQ led to clauszoline-K (**98**), which, on cleavage of the methyl ether using boron tribromide, afforded 3-formyl-7-hydroxycarbazole (**99**) (546) (Scheme 5.149).

Clauszoline-K (**98**) was transformed quantitatively to clausine C (clauszoline-L) (**101**) by treatment with manganese dioxide and potassium cyanide in methanol. Ether cleavage of clausine C (**101**) gave clausine M (**102**), while saponification of the ester led to clausine N (**103**) (Scheme 5.150).

Regioselective electrophilic bromination of the carbazole **1025** afforded the 6-bromocarbazole **1026**. Cleavage of the methyl ether to **1027** and subsequent nickel-mediated coupling using a dimeric π-prenylnickel bromide complex prepared *in situ* from prenyl bromide **925** and bis(1,5-cyclooctadiene)nickel(0) led directly to siamenol (**89**) (546) (Scheme 5.151).

One year later, we extended the aforementioned palladium(II)-catalyzed approach to a series of 6-oxygenated carbazole alkaloids, glycozoline (**86**), glycozolinine (glycozolinol) (**91**), glycomaurrol (**92**), micromeline (**100**), and methyl 6-methoxycarbazole-3-carboxylate (**104**) (547). The palladium(0)-catalyzed coupling of 4-bromoanisole (**670**) and *p*-toluidine (**1028**), followed by palladium(II)-catalyzed oxidative cyclization, afforded directly glycozoline (**86**).

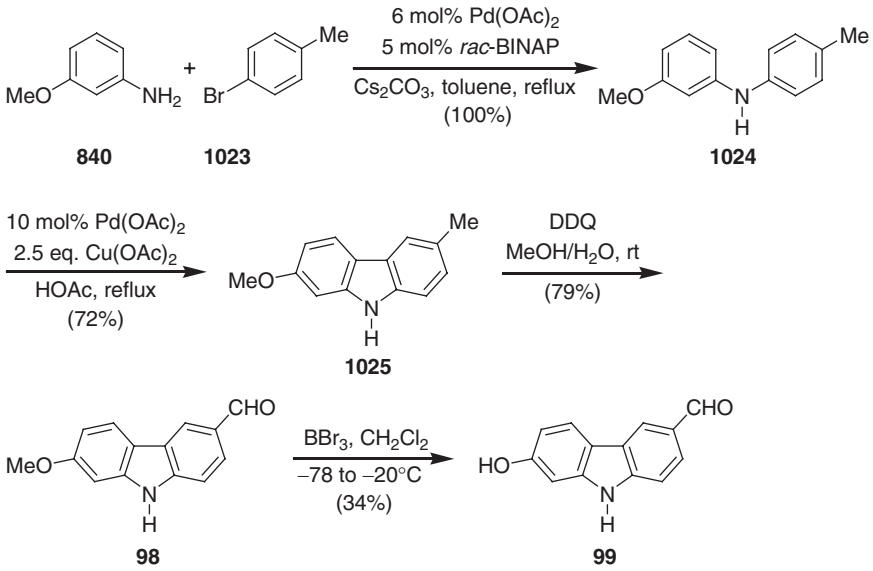

Scheme 5.149

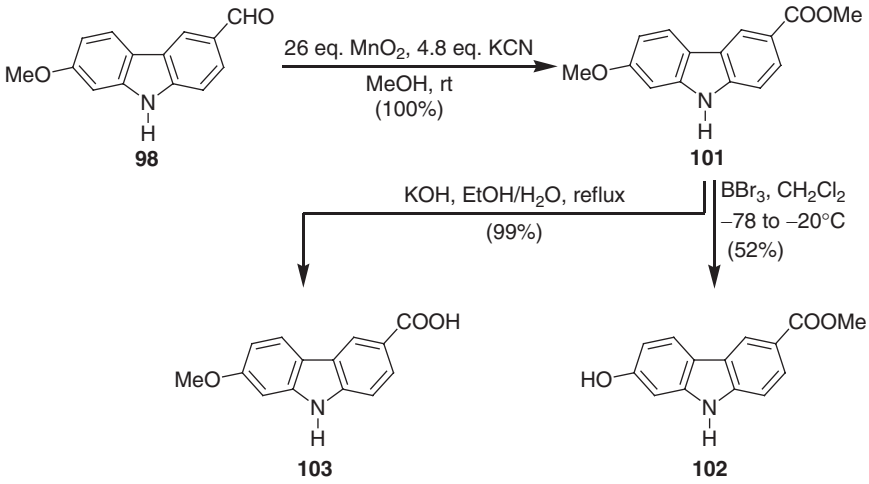

Scheme 5.150

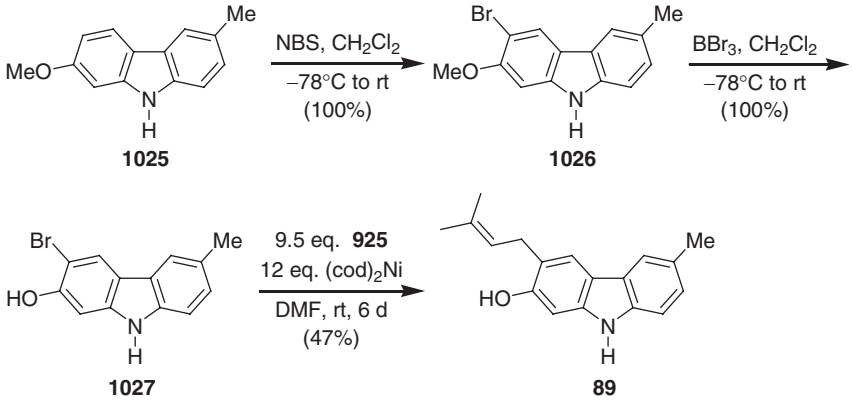

Scheme 5.151

For the syntheses of further 6-oxygenated carbazole alkaloids, glycozoline (**86**) was used as relay compound (Schemes 5.152–5.154). Cleavage of the ether with boron tribromide transformed glycozoline (**86**) into glycozolinine (glycozolinol) (**91**). Further, oxidation of **86** with DDQ gave 3-formyl-6-methoxycarbazole (**97**) (Scheme 5.152). Regioselective bromination of glycozolinine (**91**) at C-5 and subsequent nickel-mediated prenylation provided glycomaurrol (**92**) (547) (Scheme 5.153).

Oxidation of 3-formyl-6-methoxycarbazole (**97**) with manganese dioxide and potassium cyanide in methanol afforded methyl 6-methoxycarbazole-3-carboxylate (**104**). Regioselective bromination of **97** afforded the 5-bromocarbazole **1031**. Cleavage of the methyl ether to **1032**, followed by nickel-mediated prenylation, provided micromeline (**100**) (547) (Scheme 5.154).

Söderberg *et al.* reported a formal synthesis of clausenalene (**90**) starting from 3-methyl-6,7-methylenedioxy-1-oxo-1,2,3,4-tetrahydrocarbazole (**1001**) (659). The required tetrahydrocarbazole **1001** was obtained starting from 5-methyl-1,3-cyclohexadione (**1033**) using two sequential palladium-catalyzed intermolecular

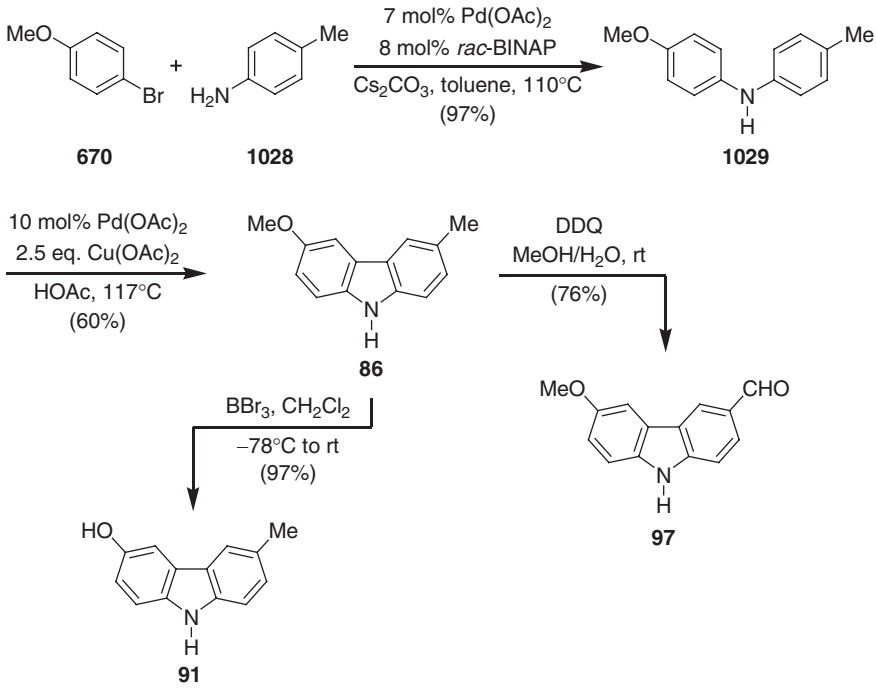

Scheme 5.152

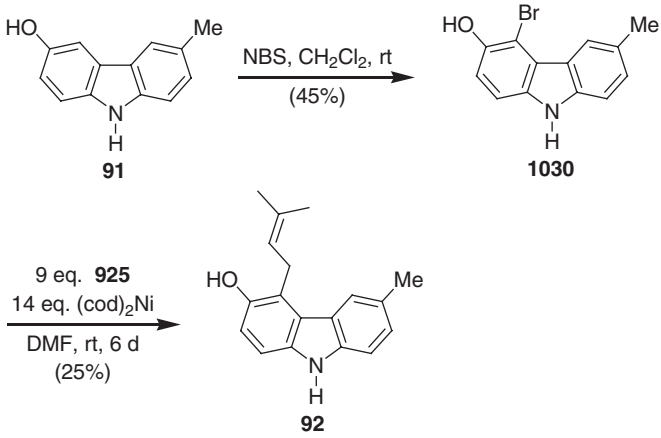

Scheme 5.153

Stille cross-coupling and reductive *N*-heteroannulation steps. Iodination of **1033**, followed by Stille cross-coupling of the corresponding iodo derivative **1034** with the arylstannane **1035**, gave the annulation precursor **1036**. Reductive *N*-heteroannulation of **1036** afforded the carbazolone **1001**, which was previously (99) (see Scheme 5.143) used to prepare clausenalene (**90**) *via* a Wolff–Kishner reduction followed by aromatization (659) (Scheme 5.155).

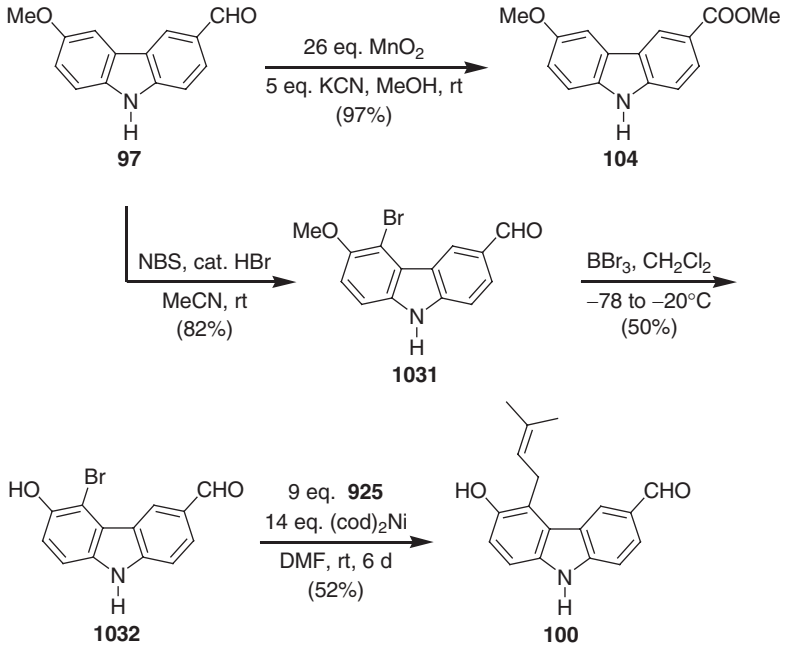

Scheme 5.154

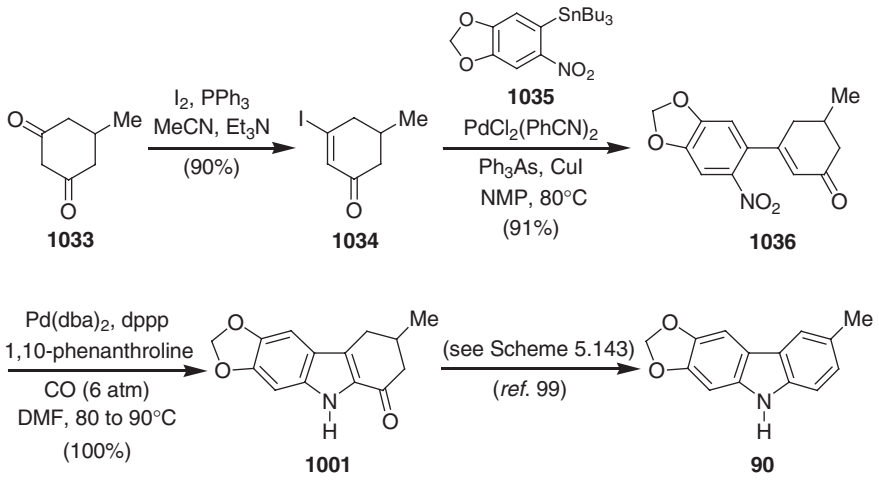

Scheme 5.155

B. Pyranocarbazole Alkaloids

Furukawa *et al.* reported a palladium(II)-mediated intramolecular cyclization of arylamino-1,4-benzoquinones to carbazole-1,4-quinones (623). Previously, this facile synthetic approach was applied to various 3-methylcarbazole-1,4-quinone alkaloids (623) (see Schemes 5.101 and 5.102). As an extension, this methodology was further

applied to the total synthesis of the pyrayaquinones A (**175**) and B (**176**). The required starting materials, 7-amino- (**1039**) and 5-amino-2,2-dimethyl-2*H*-chromene (**1041**) were prepared from acetamidophenol (**1037**) and 3-chloro-3,3-dimethyl-1-butyne *via* etherification and a Claisen rearrangement, followed by hydrolysis (Scheme 5.156).

Condensation of the aminochromenes **1039** and **1041** with 2-methyl-1,4-benzoquinone (**841**) afforded 2-(2,2-dimethyl-2*H*-chromen-7-ylamino)- (**1042**) and 2-(2,2-dimethyl-2*H*-chromen-5-ylamino)-5-methyl-1,4-benzoquinone (**1043**), along with the corresponding 6-methyl isomers. Finally, reaction of the benzoquinones **1042** and **1043** with stoichiometric amounts of palladium(II) acetate in acetic acid under reflux furnished pyrayaquinone A (**175**) and B (**176**) in 78% and 50% yield, respectively (623) (Schemes 5.157 and 5.158).

Retrosynthetic analysis of girinimbine (**115**) and murrayacine (**124**), based on our molybdenum-mediated approach, provides the molybdenum complex salt **577** and the 5-aminochromene **1044** as potential precursors (660) (Scheme 5.159).

Starting from commercially available 2-methyl-5-nitroaniline (**1045**), the required 5-amino-2,2,8-trimethylchromene (**1044**) was obtained in four steps and 52% overall

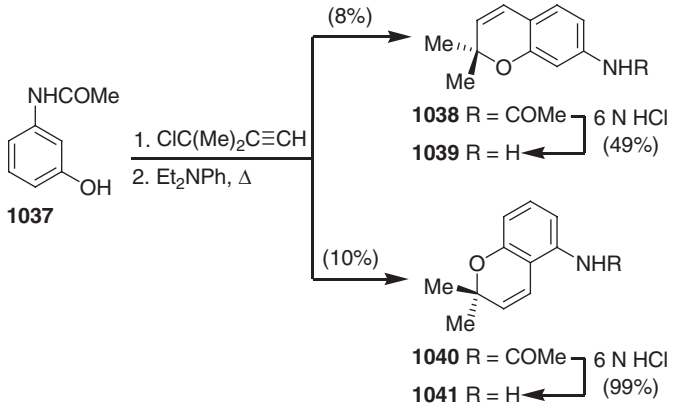

Scheme 5.156

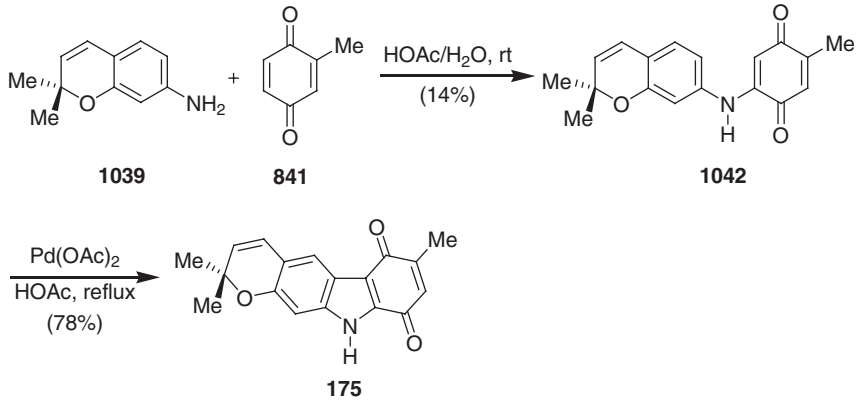

Scheme 5.157

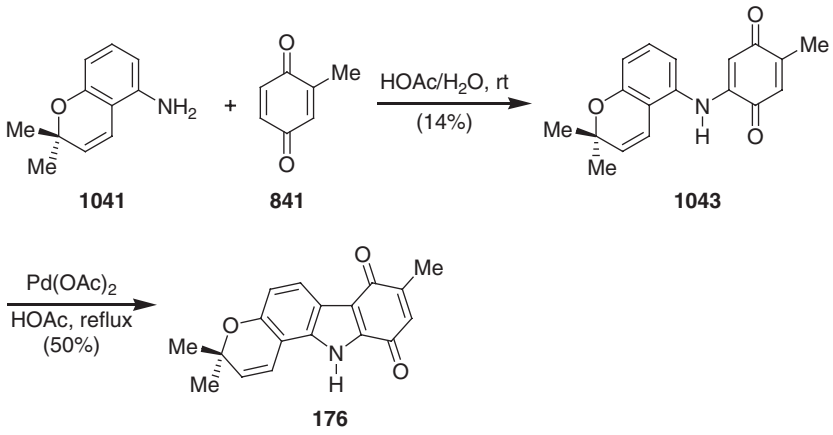

1041 **841** **1043** **176**

Scheme 5.158

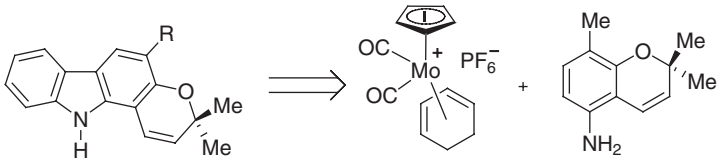

115 Girinimbine
R = Me

124 Murrayacine
R = CHO

577 **1044**

Scheme 5.159

yield. The reaction of **1045** with nitrous acid afforded the phenol **1046**, which was alkylated by 3-chloro-3-methylbut-1-yne (**1047**) to the aryl propargyl ether **1048**. The key step of this synthesis is the transformation of the aryl propargyl ether **1048** to the 5-nitrochromene **1049** by a [3,3]-sigmatropic rearrangement and subsequent cyclization. Heating of **1048** in *o*-xylene at reflux for 14 h provided the 5-nitrochromene **1049** in 93% yield. Finally, reduction of the 5-nitrochromene **1049** with tin in methanolic hydrochloric acid afforded the 5-aminochromene **1044** (Scheme 5.160).

Reaction of the 5-aminochromene **1044** with the complex salt **577** provided *via* an electrophilic aromatic substitution regio- and diastereoselectively the molybdenum complex **1050**. The oxidative cyclization of complex **1050** with concomitant aromatization and demetalation using activated manganese dioxide led directly to girinimbine (**115**) in 50% yield. Oxidation of girinimbine (**115**) with DDQ in methanol afforded murrayacine (**124**) in 64% yield (660) (Scheme 5.161).

For the transformation of girinimbine (**115**) to dihydroxygirinimbine (**133**), girinimbine was oxidized by *m*-chloroperbenzoic acid (MCPBA) to give a mixture of the two regioisomeric 3-chlorobenzoic acid esters **1051** and **1052** in 82% yield (ratio 1.5:1). The hydrolysis of the 3-chlorobenzoates **1051** and **1052** with methanolic sodium hydroxide provided dihydroxygirinimbine **133** in 43% yield, along with 53% of the corresponding *cis*-diol **1053** (660) (Scheme 5.162).

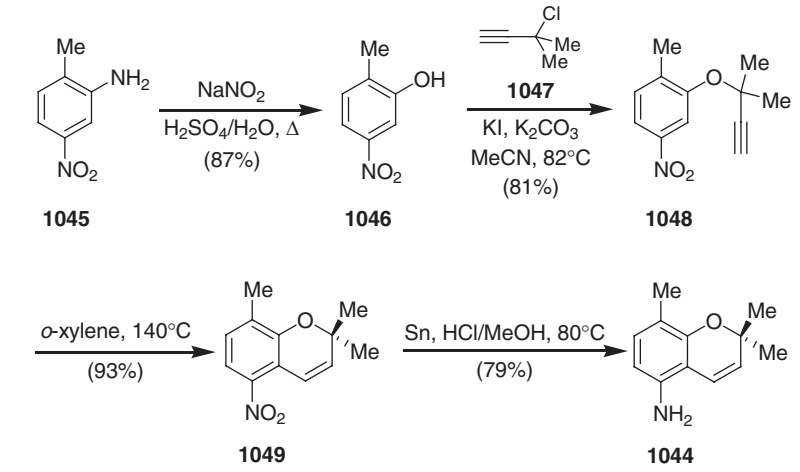

Scheme 5.160

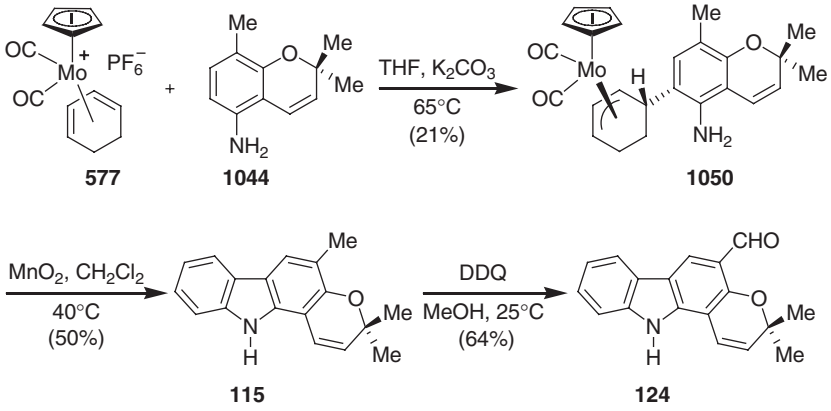

Scheme 5.161

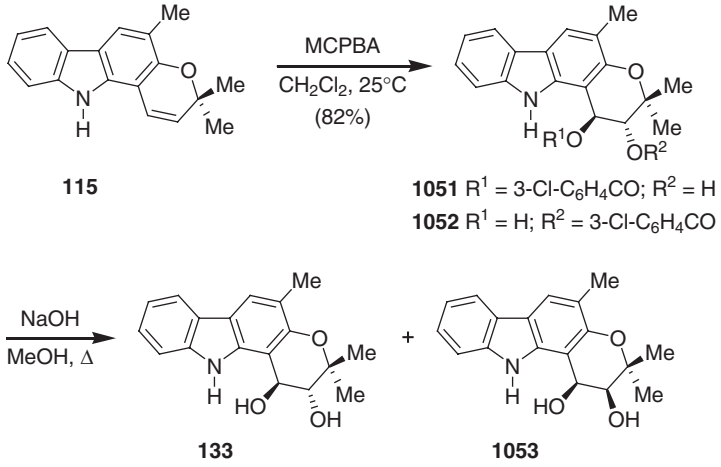

Scheme 5.162

C. Bis-Carbazole Alkaloids

The bis-carbazole alkaloids typically contain previously known monomeric carbazoles as structural subunits. To date, bis-carbazole alkaloids have been isolated from plants of two genera of the family Rutaceae, *Murraya* and *Clausena*, and are linked either by a methylene unit, a bisbenzylic ether bridge, a bond joining one aromatic portion directly to an annelated dihydropyran unit, or by a biaryl bond. Many reviews have appeared on the monomeric carbazole alkaloids. However, in these articles only a few bis-carbazole alkaloids were listed (3,5–7). For the first time, in 1992, Furukawa *et al.* compiled all of the bis-carbazole alkaloids that were known to the end of 1992 (158). Tasler and Bringmann summarized to the end of 2001, the occurrence, stereochemistry, synthesis, and biological activity of the bis-carbazoles linked through a biaryl bond (159). We compiled to the mid of 2002, the occurrence, stereochemistry, synthesis, and the biological activity of all classes of bis-carbazoles (8). In this section, we cover the total syntheses of the natural bis-carbazole alkaloids reported since 1990.

Furukawa *et al.* reported the syntheses of the murrafolines-D (**181**), -G (**182**), and -H (**183**) starting from murrayafoline A (**7**) and girinimbine (**115**) (146). This synthetic effort was undertaken to confirm the assigned structures of murrafolines -D (**181**), -G (**182**), and -H (**183**) isolated from *Murraya euchrestifolia* (146). Reaction of murrayafoline A (**7**) and girinimbine (**115**) in the presence of an ion-exchange resin (Nafion 117) in refluxing aqueous methanol for 27 h afforded the murrafolines -D (**181**), -G (**182**), and -H (**183**). For this synthesis no yields were given, moreover, this reaction was non-regioselective. When the reaction was extended to longer reaction times, several oligomers of girinimbine (**115**) were formed (146) (Scheme 5.163).

Bringmann *et al.* reported the first total synthesis and stereoanalysis of bismurrayaquinone-A (**215**) by oxidation of bis(*O*-demethylmurrayafoline A) (**204**) (661). The required monomer, 1-hydroxy-3-methylcarbazole (*O*-demethylmurrayafoline

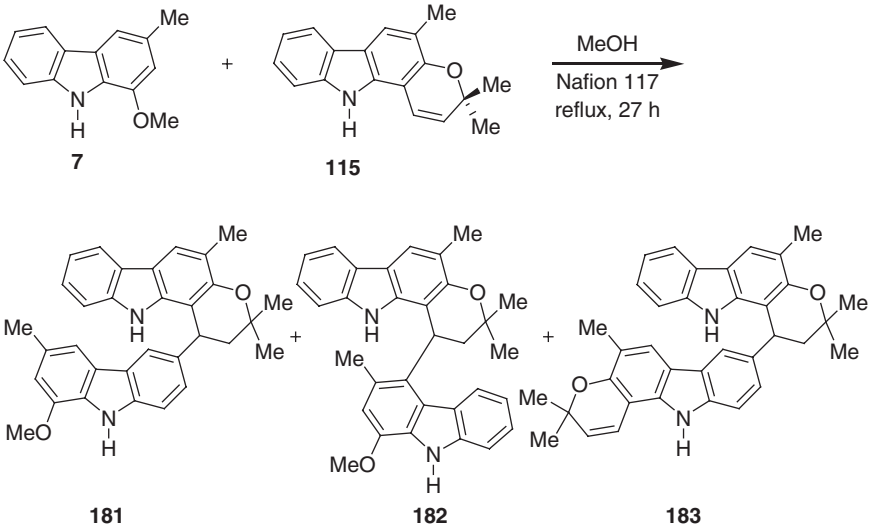

Scheme 5.163

A) (**23**), was obtained in an improved yield using the modified literature procedure (28) starting from benzene diazonium chloride (**1054**) and hydroxymethylene-5-methylcyclohexanone (**1055**). A biomimetic coupling of 1-hydroxy-3-methylcarbazole (*O*-demethylmurrayafoline A) (**23**) by reaction with di-*tert*-butyl peroxide [(*t*-BuO)$_2$] afforded the dimer of *O*-demethylmurrayafoline A (**204**). Finally, oxidation of **204** with PCC afforded (±)-bismurrayaquinone-A (**215**). The resolution of atropoenantiomers was achieved by chiral HPLC using Chiracel OF. The assignment of the absolute configuration of the two enantiomers (*S*)-**215** and (*R*)-**215** was achieved by comparison of their theoretical and experimental circular dichroism (CD) spectra (166,167,661) (Scheme 5.164).

In the following year, Bringmann *et al.* showed a further application of a biomimetic oxidative coupling of murrayafoline A (**7**) to the first total synthesis of murrastifoline F (**191**) (162). This work also includes the resolution of (±)-murrastifoline F (**191**), the stereochemical assignment of its atropisomers, and the determination of the enantiomeric ratio present in an authentic root extract of *M. koenigii*.

Murrayafoline A (**7**) required for this total synthesis was obtained starting from 3-formylindole (**618**) (577) (see Scheme 5.40). Lead tetraacetate-mediated oxidative non-phenolic biaryl coupling of **7** led to murrastifoline F (**191**) in 60% yield. The

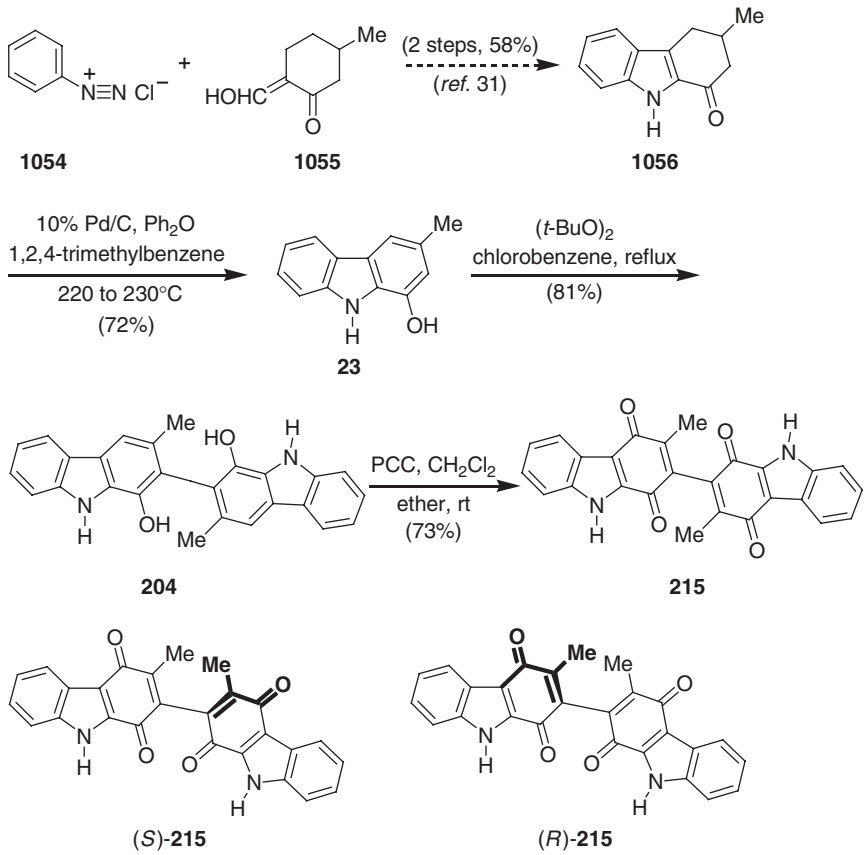

1054 **1055** **1056** **23** **204** **215** (*S*)-**215** (*R*)-**215**

Scheme 5.164

resolution of racemic **191** was performed by *O*-demethylation, derivatization with Mosher's reagent, and chromatographic resolution of the resulting diastereomers. The assignment of the absolute configuration of the atropisomers (*S*)-**191** and (*R*)-**191** was based on CD spectroscopy in combination with quantum chemical CD, as well as ROESY experiments of the diastereomeric Mosher derivatives (162) (Scheme 5.165).

In the same year, Bringmann *et al.* reported the first total synthesis of the methylene-bridged dimeric carbazole alkaloids, chrestifoline A (**192**) and bismurrayafoline-A (**197**) starting from their monomeric halfs, murrayafoline A (**7**) and koenoline (**8**) and the carbazole ester **1057**, respectively (662).

Acid treatment of a 3:1 mixture of murrayafoline A (**7**) and koenoline (**8**) led to chrestifoline A (**192**) in 70% yield. Addition of murrayafoline A (**7**) to a mixture of **1057** and lithium aluminum hydride in ether and dichloromethane afforded bismurrayafoline-A (**197**) in 19% yield (662) (Scheme 5.166). In addition to the aforementioned methods, the same group also reported a stereoselective synthesis of axially chiral bis-carbazole alkaloids by application of their ''lactone concept'' (663) and a reductive biaryl coupling leading to 2,2′-bis-carbazoles (664).

We reported the first total synthesis of 1,1′-bis(2-hydroxy-3-methylcarbazole) (**213**) using our molybdenum-mediated construction of the carbazole framework (560). The required monomer, 2-hydroxy-3-methylcarbazole (**52**), was obtained in three steps, and 22% overall yield, starting from dicarbonyl(η^4-cyclohexa-1,3-diene)(η^5-cyclopentadienyl)molybdenum hexafluorophosphate (**663**) and 3-methoxy-4-methylaniline (**655**) (560) (see Scheme 5.52). Finally, oxidative coupling of the monomer **52** using *p*-chloranil afforded 1,1′-bis(2-hydroxy-3-methylcarbazole) (**213**) in 38% yield (560) (Scheme 5.167).

Murphy and Bertrand reported a second total synthesis (±)-bismurrayaquinone-A (**215**) *via* the bromoquinone-enaminone annulation (633). Reaction of the 4-methoxybenzyl-protected enamino ketone **1058** and 5-bromo-2-methyl-1,4-benzoquinone (**878**) with copper(II) chloride in the presence of sodium bicarbonate and 3 Å molecular sieves (MS) afforded, in low yield, the dimer **1059**. Mechanistically, the

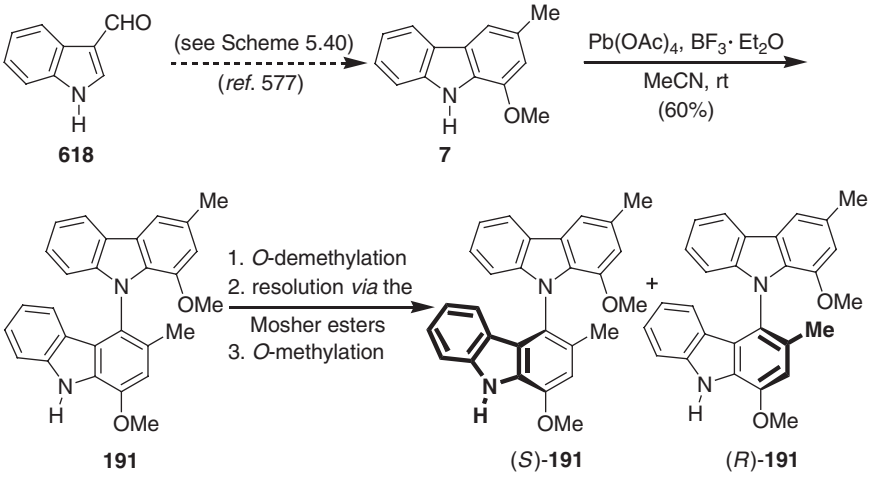

Scheme 5.165

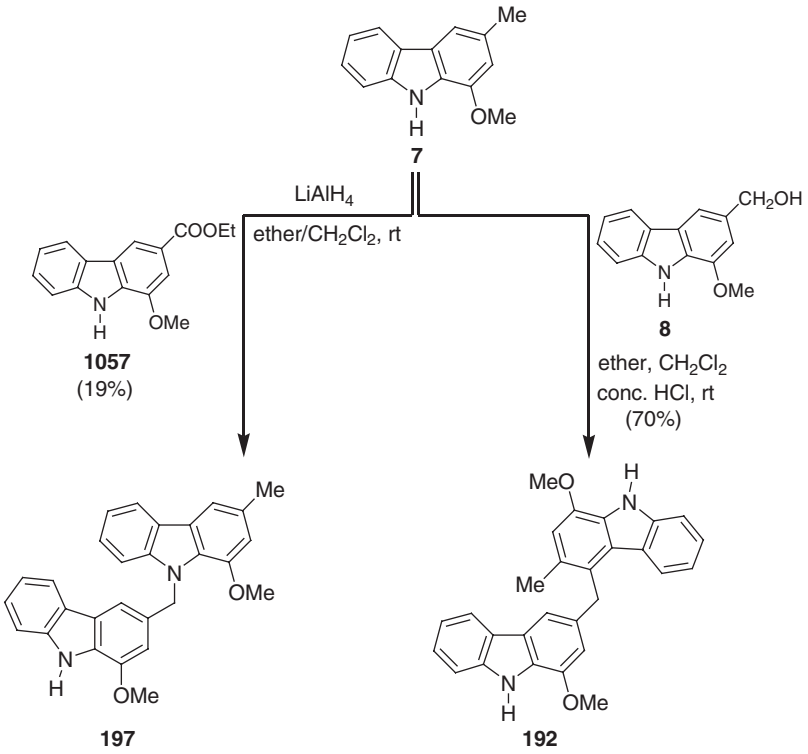

Scheme 5.166

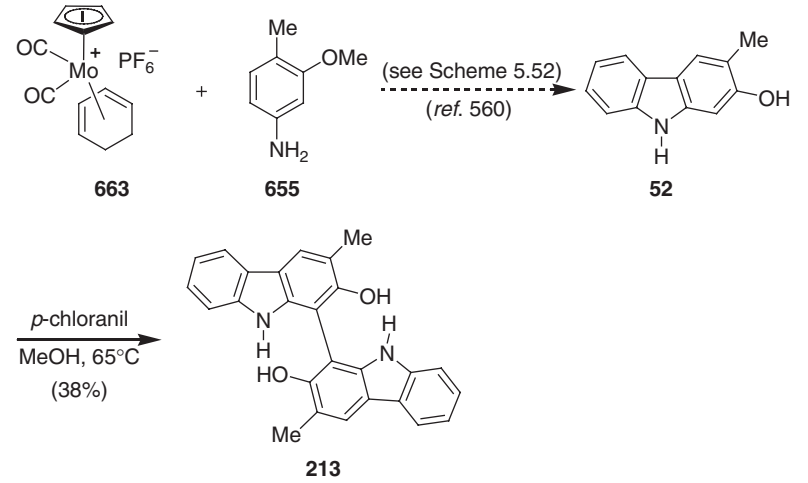

Scheme 5.167

dimer **1059** might have formed by dimerization of free radicals of the first-formed annulation product. Compound **1059** was transformed to the bis(tosylhydrazone) **1060**, followed by Shapiro deoxygenation–olefination and aromatization with DDQ in dioxane, to afford the bis-*N*-protected murrayaquinone-A **1061**. Finally,

deprotection in TFA with catalytic amounts of TfOH provided (±)-bismurrayaquinone-A (**215**) in 60% yield (633) (Scheme 5.168).

Lin and Zhang reported the first total synthesis and resolution of (±)-clausenamine-A (**203**) involving Suzuki cross-coupling and oxidative coupling as key steps (165,665). This synthesis starts from the commercially available 2-amino-5-methylphenol (**1062**) as shown in Scheme 5.169. After protection of the free hydroxy group in **1062** as a tosylate, **1063** was subjected to regioselective electrophilic bromination *ortho* to the amino group using bromo-dimethylsulfonium bromide generated *in situ* to afford the bromoaniline **1064**. The required biphenyl **1066** was prepared quantitatively by Suzuki cross-coupling of 3,5-dimethoxyphenylboronic acid (**1065**) and **1064** using 5% $Pd(PPh_3)_4$ and aqueous sodium carbonate in benzene. Bromination of **1066** using 48% HBr in DMSO afforded the corresponding bromo derivative **1067**. A palladium(0)-mediated oxidative cyclization of **1067** led to the carbazole **1068** in almost quantitative yield. After detosylation, the corresponding hydroxycarbazole **1069** was subjected to oxidative coupling using di-*tert*-butyl peroxide [$(t\text{-BuO})_2$] in chlorobenzene to afford (±)-clausenamine-A (**203**) in 90% yield (165,665) (Scheme 5.169).

The resolution of racemic clausenamine-A (**203**) was accomplished by silica gel column chromatography of the corresponding (+)-camphorsulfonates **203a** and **203b** using dichloromethane/chloroform/diethyl ether (50:1:2) as the eluent. Alkaline hydrolysis of **203a** and **203b** provided optically pure clausenamine-A (*R*)-(+)-**203** and (*S*)-(−)-**203** (165,665) (Scheme 5.170). The assignment of the absolute configuration was based on an X-ray analysis and the CD spectra. The same method was applied to

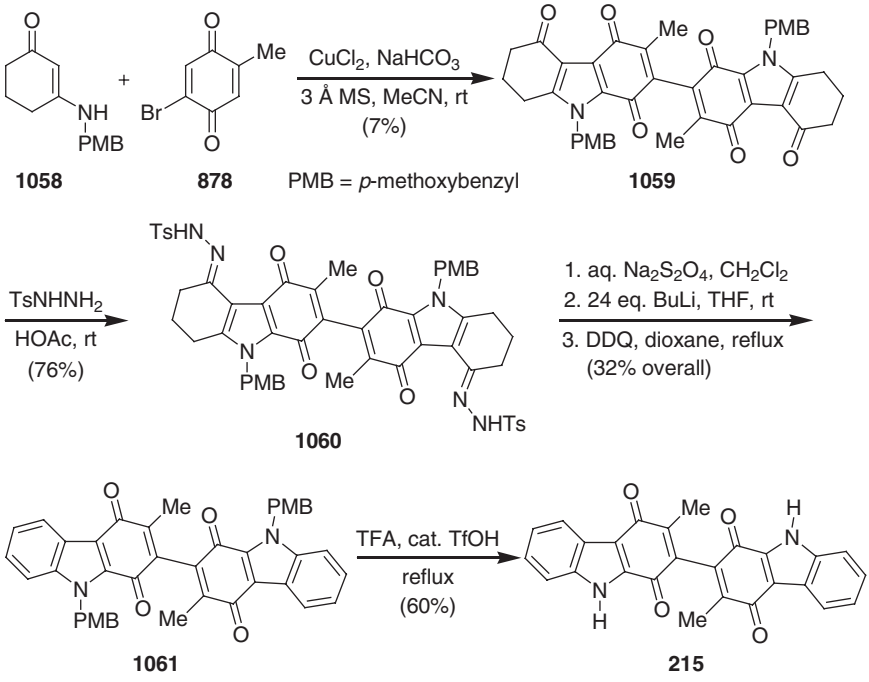

Scheme 5.168

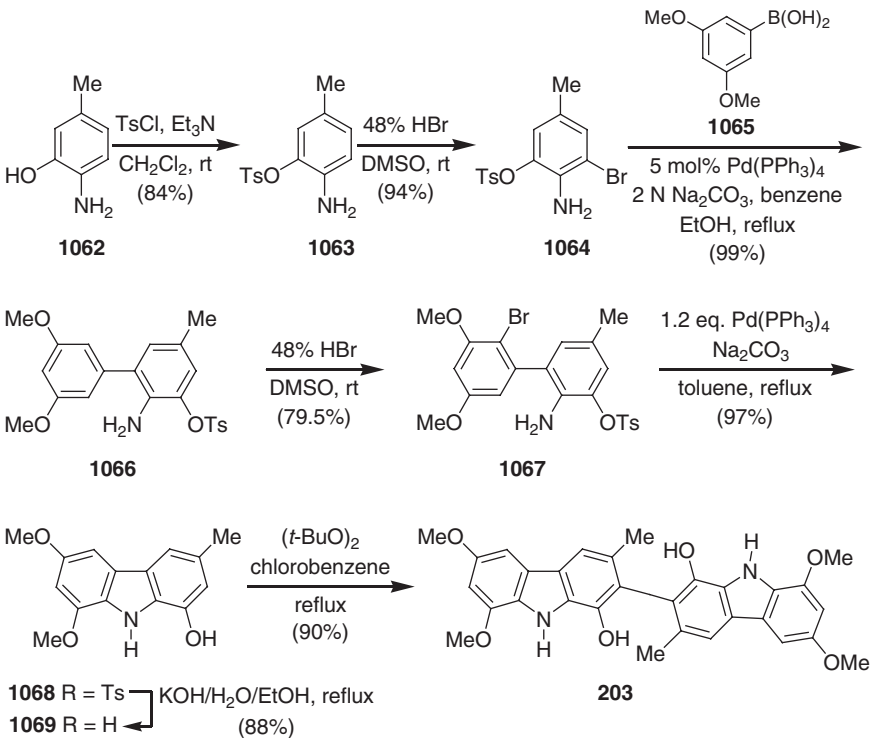

Scheme 5.169

the synthesis and resolution of the demethoxylated analogs of clausenamine-A (**203**), including bis(*O*-demethylmurrayafoline A) (**204**) (665) (Scheme 5.170).

Hao *et al*. reported the synthesis of 8,8″-biskoenigine (**205**) through oxidative coupling of its monomeric half koenigine (**119**). This synthesis was undertaken to confirm the assigned structure of 8,8″-biskoenigine (**205**) isolated from *M. koenigii*. Reaction of koenigine (**119**) with iron(III) chloride ($FeCl_3$) in solid state at room temperature for 30 days afforded 8,8″-biskoenigine (**205**) in 30% yield (119) (Scheme 5.171).

Chida *et al*. reported the first total synthesis of murrastifoline-A (**186**) starting from 2-amino-5-methylphenol (**1062**) (666,667). This synthesis involves a palladium(0)-catalyzed double *N*-arylation of the arylamine (**1082**) with 2,2′-dibromobiphenyl **1075** as a key step.

The synthesis of dibromobiphenyl **1075** starts from the known *O*-tosylate **1063** (165,665), which was prepared from commercially available 2-amino-5-methylphenol (**1062**). Regioselective electrophilic iodination of **1063** using *N*-iodosuccinimide (NIS) afforded the iodoaniline **1070**. The biphenyl **1072** was prepared quantitatively by Suzuki–Miyaura cross-coupling of 2-bromophenylboronic acid (**1071**) and **1070** using $Pd(PPh_3)_4$ and 2 M aqueous sodium carbonate in ethanol and benzene. Sandmeyer reaction of **1072** gave dibromobiphenyl (**1073**). After de-*O*-tosylation using alkaline hydrolytic conditions, the corresponding hydroxy derivative **1074** was *O*-methylated to afford the required dibromobiphenyl **1075** (Scheme 5.172).

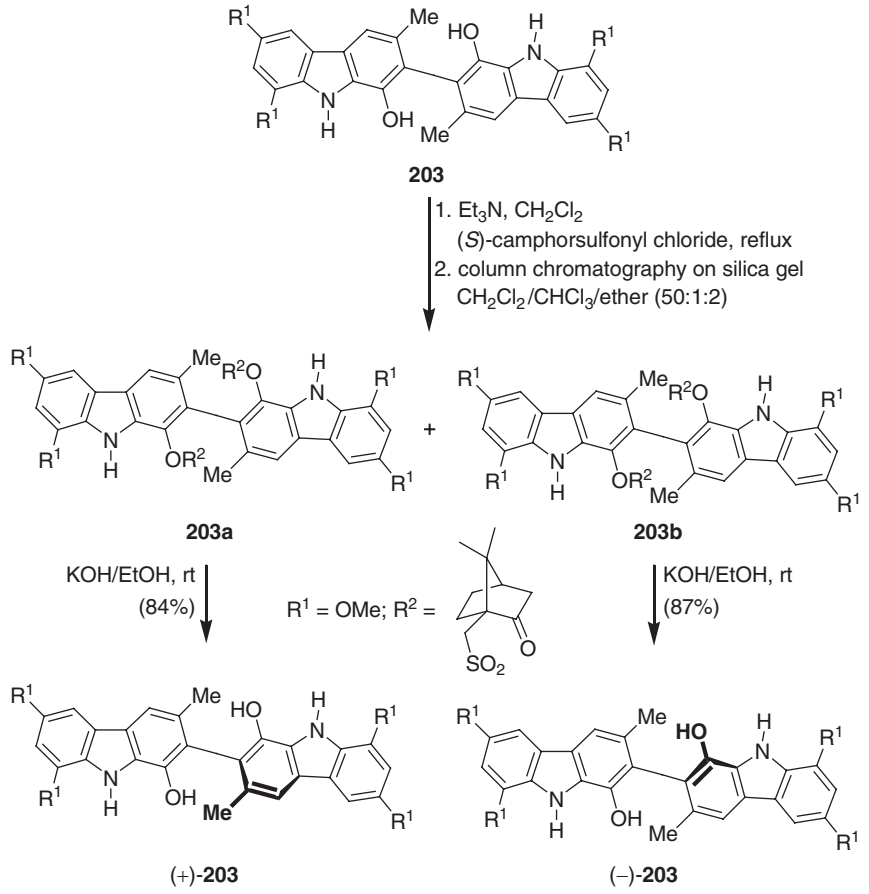

Scheme 5.170

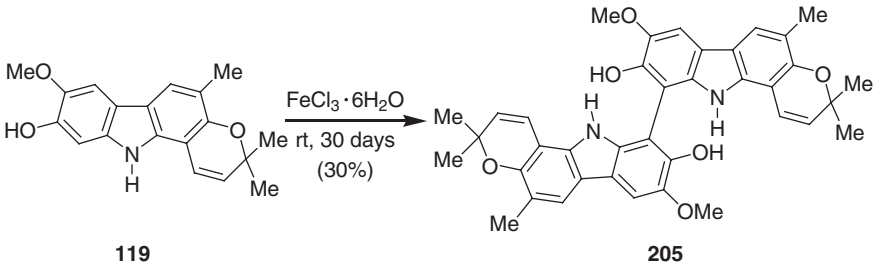

Scheme 5.171

The second coupling component, 6-aminocarbazole **1082**, was prepared starting from the same known *O*-tosylate **1063** (165,665). Thus, Buchwald–Hartwig palladium-catalyzed amination of 4-bromonitrobenzene (**1076**) with **1063** afforded the diarylamine **1077**. Treatment of **1077** with an excess of $Pd(OAc)_2$ in acetic acid led to the carbazole **1078** in 53% yield. After protection of the carbazole nitrogen with a 2-trimethylsilylethoxymethyl (SEM) group, the product **1079** was subjected to alkaline

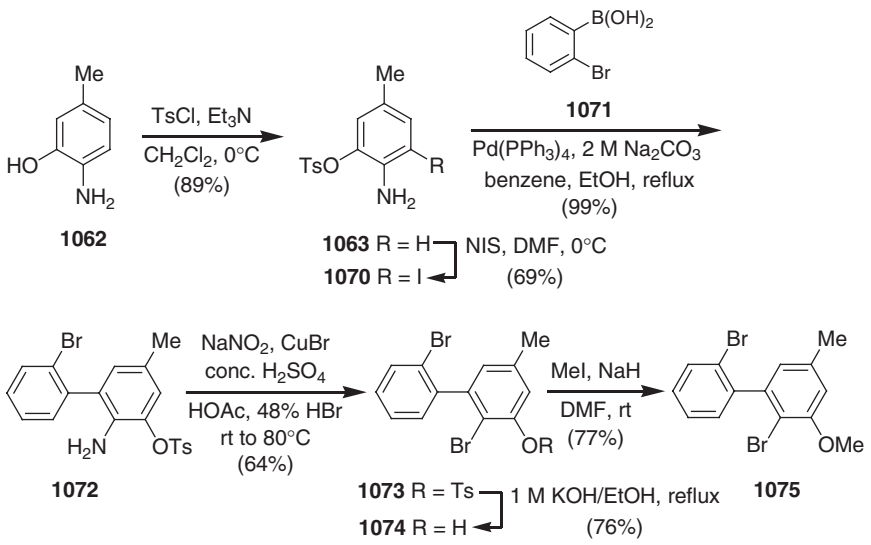

Scheme 5.172

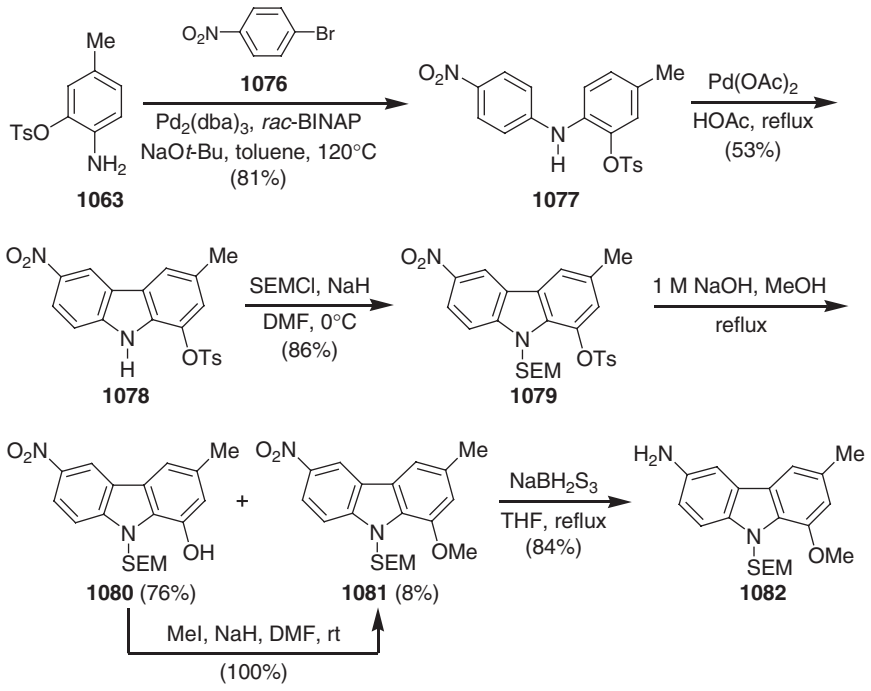

Scheme 5.173

hydrolytic conditions to provide the de-*O*-tosyl derivative **1080**, along with its methyl ether **1081**, in 76% and 8% yield, respectively. *O*-Methylation of **1080** transformed it to **1081** quantitatively. Finally, reduction of the 6-nitrocarbazole **1081** with $NaBH_2S_3$ furnished the required 6-aminocarbazole **1082** in 84% yield (666,667) (Scheme 5.173).

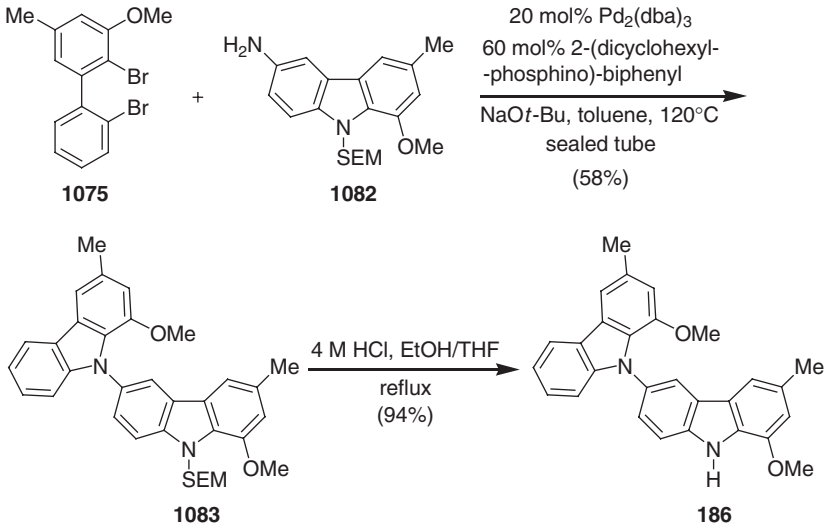

Scheme 5.174

The double *N*-arylation of the 6-aminocarbazole **1082** with the dibromobiphenyl derivative **1075** under Buchwald–Hartwig *N*-arylation conditions afforded *N*-SEM-murrastifoline-A (**1083**) in 58% yield. Finally, the *N*-SEM group was removed under acidic conditions to furnish murrastifoline-A (**186**) in 94% yield (666,667) (Scheme 5.174).

In addition to the aforementioned total syntheses, Shannon *et al*. observed the formation of an N–C3-linked dimer during the transformation of a 3-bromocarbazole to a 3-cyanocarbazole by reaction with copper(I) cyanide in DMF under reflux (668). Harrity *et al*. reported the synthesis of non-natural (±)-*N*,*N*′-dimethylbismurrayafoline A *via* a chromium-mediated benzannulation, followed by a palladium-catalyzed oxidative coupling reaction (669).

D. Benzocarbazole Alkaloids

Prior to the isolation of the natural benzocarbazole alkaloids, purpurone (**281**) and ningaline D (**282**), a wide range of different isomeric benzocarbazoles was synthesized. This widespread synthetic activity on the non-natural benzocarbazoles was justified because of their useful pharmacological properties (194,257,400–407). The methods that were often employed for the synthesis of the various benzocarbazole derivatives range from polar (ionic) over radical to pericyclic type reactions. Complementary to these more classical synthetic strategies, various transition metal-mediated reactions have been applied. We previously compiled all of these methods that were known to the middle of 2002 (8). In this section, we cover only the total synthesis of natural benzocarbazole alkaloids, although some new methods were used for the synthesis of the functionally diverse non-natural benzocarbazoles (670–685).

Peschko and Steglich reported the first biomimetic total synthesis of purpurone (**281**) starting from 3-(3,4-dimethoxyphenyl)pyruvic acid (**1084**), 2-(4-methoxyphenyl) ethylamine (**1085**) and 2′,2′,2′-trichloroethyl-2-bromo-2-(3,4-dimethoxyphenyl)acetate

(**1088**) (686). Oxidative dimerization of two molecules of 3-(3,4-dimethoxyphenyl)pyruvic acid (**1084**), followed by subsequent condensation with 2-(4-methoxyphenyl)ethylamine (**1085**), led to the formation of the pyrrolo dicarboxylic acid **1086**. Decarboxylation of **1086** by treatment with TFA afforded the pyrrole **1087** in almost quantitative yield. The two-fold Friedel–Crafts alkylation of **1087** with the bromoester **1088** led to the key intermediate **1089**. Cleavage of the ester groups in **1089** under mild conditions by reacting with Zn and aqueous NH_4OAc in THF, followed by regioselective cyclization of the diacid **1090** on heating with Ac_2O/KOAc led to the diacetate **1091**. Saponification of **1091** with aqueous sodium hydroxide, followed by demethylation of the intermediate purpurone nonamethyl ether with an excess of boron tribromide in dichloromethane under addition of cyclohexene as a bromine scavenger led to purpurone (**281**) (686) (Scheme 5.175).

Boger *et al.* reported the first total synthesis of ningaline D (**282**) starting from the diphenylacetylene **1092** and dimethyl 1,2,3,4-tetrazine-3,6-dicarboxylate (**1093**) (687). In this synthesis, the key step is the formation of the fully substituted pyrrole core using an inverse electron demand heterocyclic azadiene Diels–Alder reaction followed by a reductive ring contraction of the resultant 1,2-diazine.

The key [4+2] cycloaddition reaction of **1092** with dimethyl 1,2,3,4-tetrazine-3,6-dicarboxylate (**1093**) in refluxing toluene led to the symmetrical 1,2-diazine **1094**. Reductive ring contraction of **1094** by treatment with Zn/TFA, followed by *N*-alkylation of the resulting pyrrole with the phenylethyl iodide **1095** afforded the corresponding *N*-alkyl pyrrole **1096**. A double Dieckmann condensation of **1096** by treatment with NaH cleanly afforded the bisphenol **1097**. Conversion of the bisphenol **1097** to the corresponding bistriflate **1098**, followed by double Suzuki coupling with 3,4-dimethoxyphenylboronic acid (**1099**), provided the diester **1100**. Hydrolysis of the diester **1100** to the dicarboxylic acid **1101** was affected by treatment with potassium *tert*-butoxide. Using modified Curtius rearrangement conditions [diphenyl phosphorazidate (DPPA) and triethylamine], the dicarboxylic acid **1101** was transformed to the corresponding diisocyanate, which, on *in situ* hydrolysis, afforded permethylningaline D (**1102**) in 70% yield. Demethylation of **1102** with an excess of boron tribromide led to ningaline D (**282**) in almost quantitative yield (687) (Scheme 5.176).

E. Furocarbazole Alkaloids

Carbazole alkaloids condensed to a furan ring represent a relatively new class of natural products. Until now, only four, natural furocarbazole alkaloids were isolated. Recently, we summarized the occurrence, biological activities, and total synthesis of these heteroarylcarbazoles (175,176).

Six years after the original isolation, we reported the first total synthesis of furostifoline (**224**) (688). This synthesis is based on an iron-mediated construction of the carbazole nucleus using 1,3-cyclohexadiene (**597**) and the 4-amino-7-methylbenzofuran (**1103**) as precursors (Scheme 5.177).

The required 4-amino-7-methylbenzofuran (**1103**) was prepared starting from the commercial 2-methyl-3-nitrophenol (**1104**) over five steps in 52% overall yield. In this sequence, the key step is the annulation of the furan ring using bromoacetaldehyde

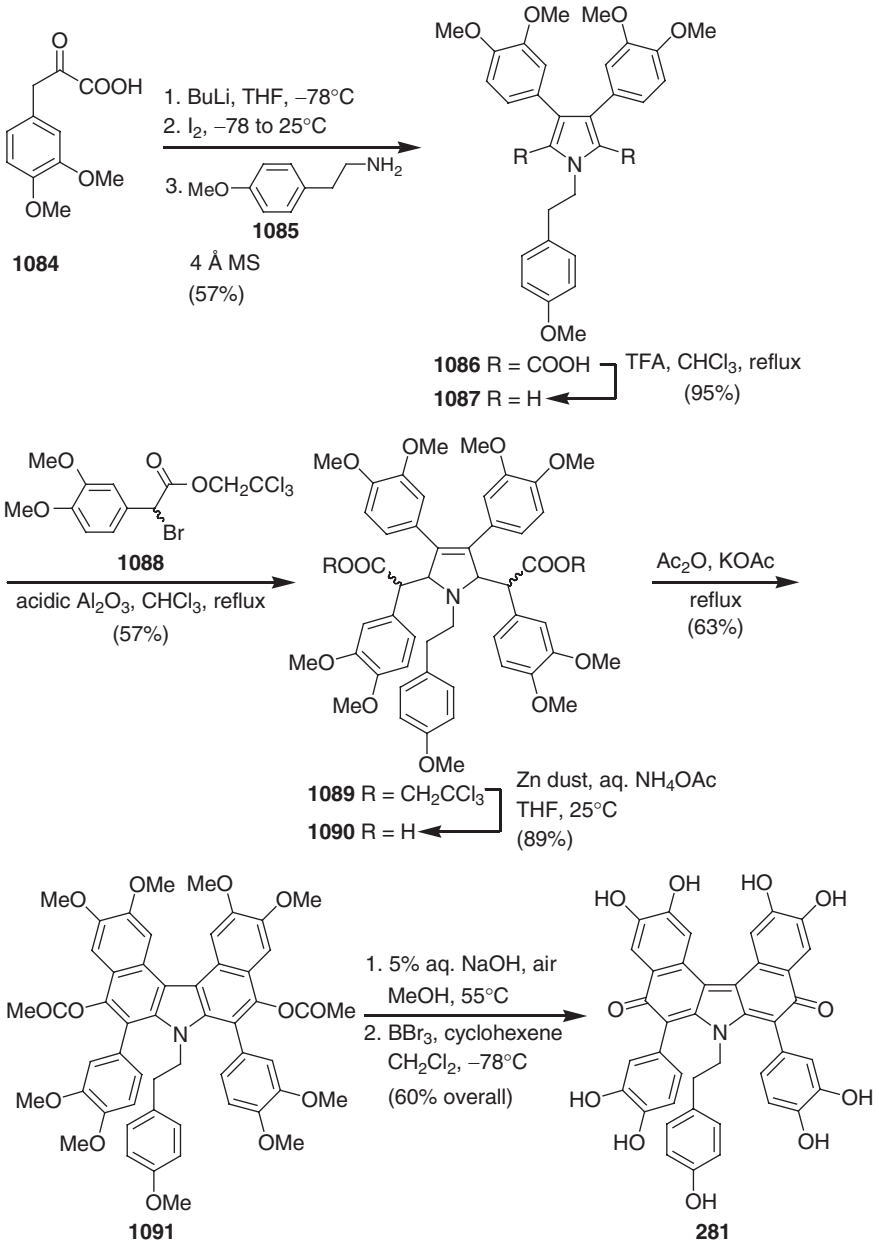

Scheme 5.175

diethyl acetal as a C_2-building block. The alkylation of **1104** with bromoacetaldehyde diethyl acetal afforded the ether **1105**, which was hydrogenated to the corresponding arylamine **1106**. After protection of the amino group to the phthalimide **1107**, an Amberlyst 15-catalyzed cyclization provided 7-methyl-4-phthalimidobenzofuran (**1108**). Finally, deprotection of the phthalimido group afforded the required 4-amino-7-methylbenzofuran (**1103**) in 79% yield (Scheme 5.178).

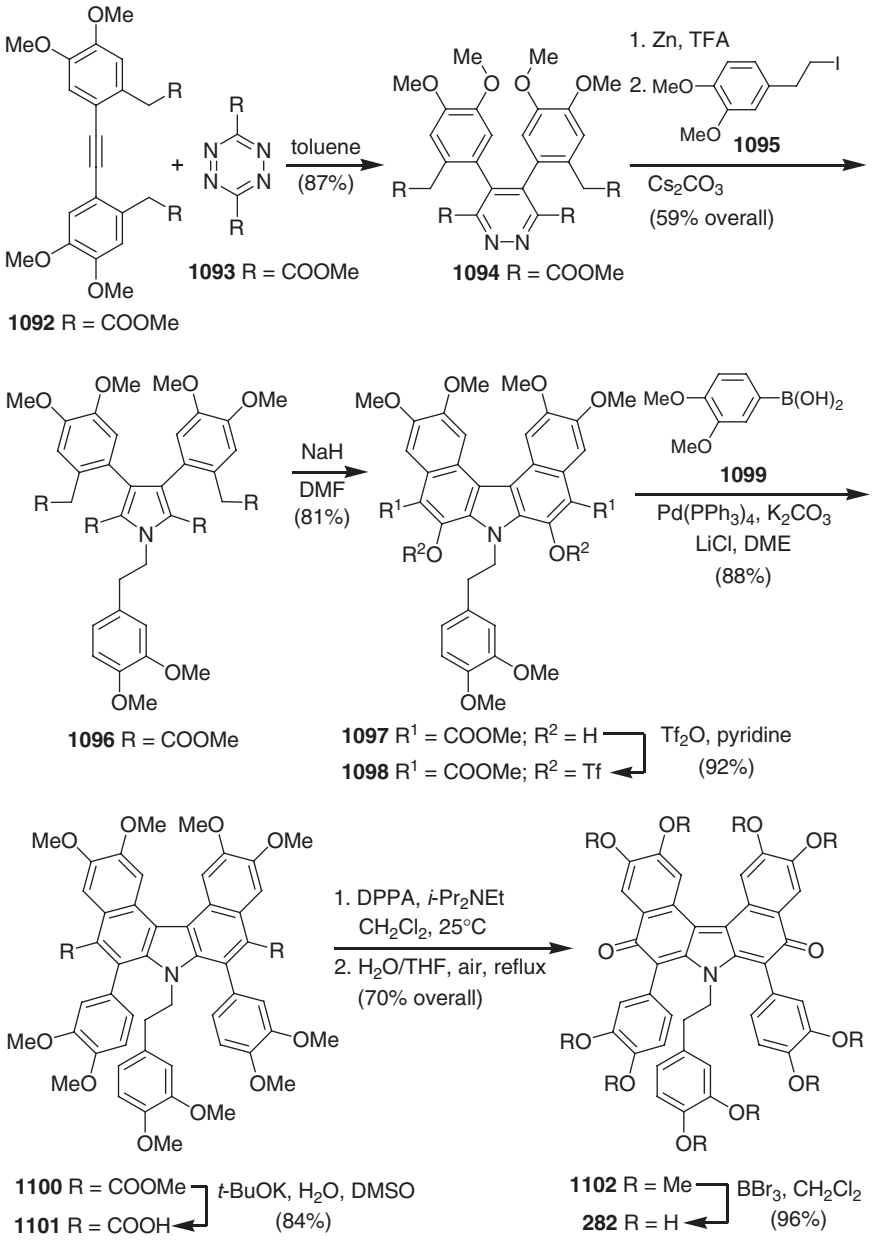

Scheme 5.176

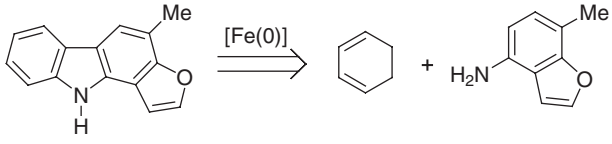

Scheme 5.177

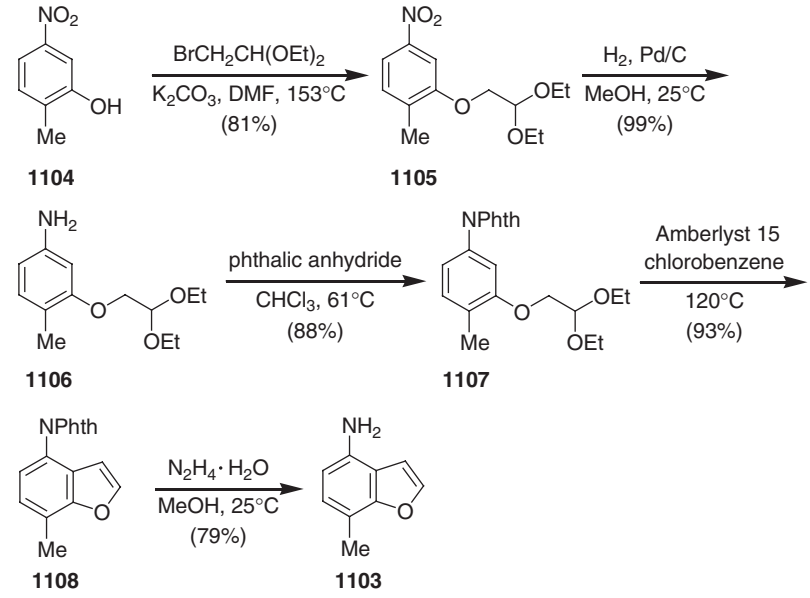

Scheme 5.178

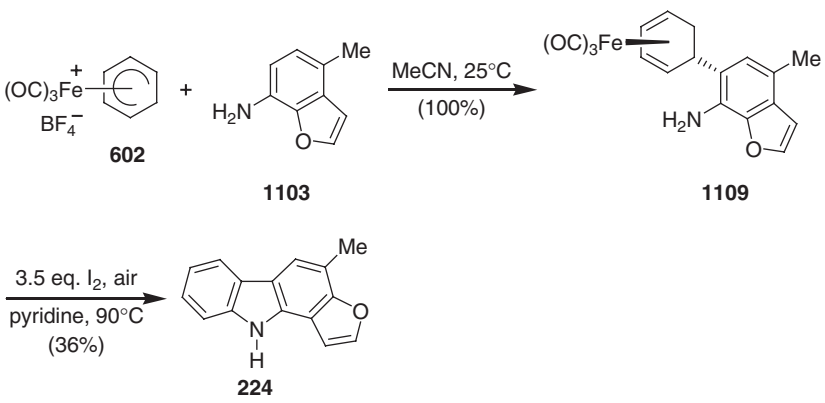

Scheme 5.179

Electrophilic aromatic substitution of the 4-aminobenzofuran **1103** with the complex salt **602** afforded the iron complex **1109** in quantitative yield. Cyclization of the complex **1109** with concomitant aromatization was achieved by oxidation with an excess of iodine in pyridine at 90°C in air to afford directly furostifoline (**224**) (688,689) (Scheme 5.179).

Four years later, we reported an improved iron-mediated total synthesis of furostifoline (**224**) (689). This approach features a reverse order of the two cyclization reactions by first forming the carbazole nucleus, then annulation of the furan ring. As a consequence, in this synthesis the intermediate protection of the amino function is not necessary (*cf*. Schemes 5.178 and 5.179). The electrophilic aromatic substitution at the arylamine **1106** by reaction with the iron complex salt **602** afforded the iron

complex **1110**. The iron-mediated arylamine cyclization of complex **1110** with iodine in pyridine led to the carbazole **1111**. Annulation of the furan ring by reaction of the carbazole **1111** with catalytic amounts of Amberlyst 15 in chlorobenzene at 120°C afforded directly furostifoline (**224**) This synthesis provides furostifoline in only five steps and 21% overall yield based on the nitrophenol **1104** (689) (Scheme 5.180). The first synthesis required seven steps to achieve a 19% overall yield based on the same starting material (688,689) (see Schemes 5.178 and 5.179).

Recently, we reported the first total synthesis of furoclausine A (**225**) following the improved protocol developed for the synthesis of furostifoline (**224**) (see Scheme 5.180). This strategy to furoclausine A (**225**) suggested tricarbonyl(η^5-2-methoxycyclohexadienylium)iron tetrafluoroborate (**1112**) and the arylamine **1106** as precursors (Scheme 5.181). The arylamine **1106** previously served as the starting material for our improved total synthesis of furostifoline (**224**) and was obtained in two steps and 80% overall yield from 2-methyl-3-nitrophenol (**1104**) (see Scheme 5.178). Electrophilic substitution of the arylamine **1106** by reaction with the iron complex salt **1112** led regioselectively to the iron complex **1113**. Oxidative cyclization of complex **1113** with iodine in pyridine provided the carbazole **1114**. Annulation of the furan ring by reaction of the carbazole **1114** with catalytic amounts of Amberlyst 15 in chlorobenzene at 120°C afforded 8-methoxyfurostifoline (**1115**). Oxidation of **1115** with DDQ, followed by cleavage of the methyl ether using boron tribromide (BBr_3), afforded furoclausine A (**225**) (690) (Scheme 5.182).

Beccalli *et al.* reported a total synthesis of furostifoline (**224**) starting from indole-3-acetic acid (**680**) (691). The key step of this strategy is the oxidative

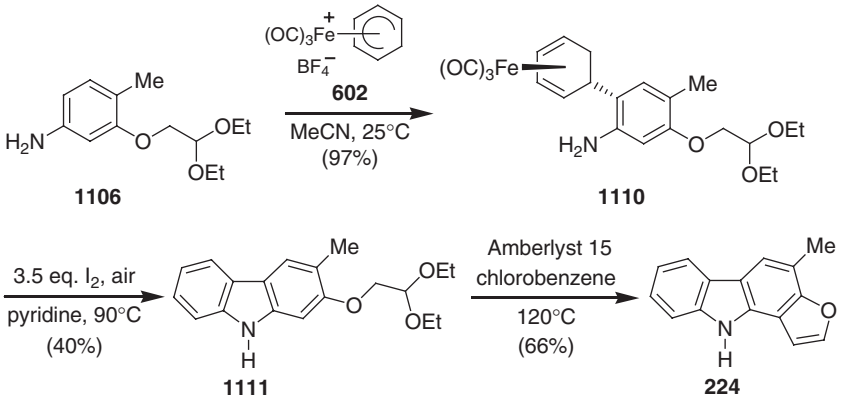

Scheme 5.180

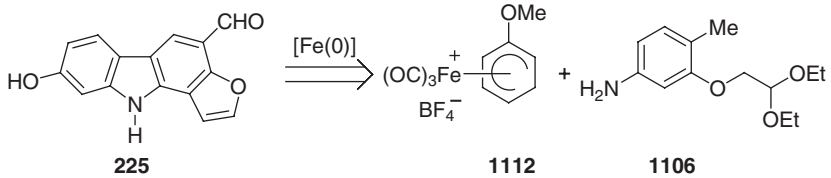

Scheme 5.181

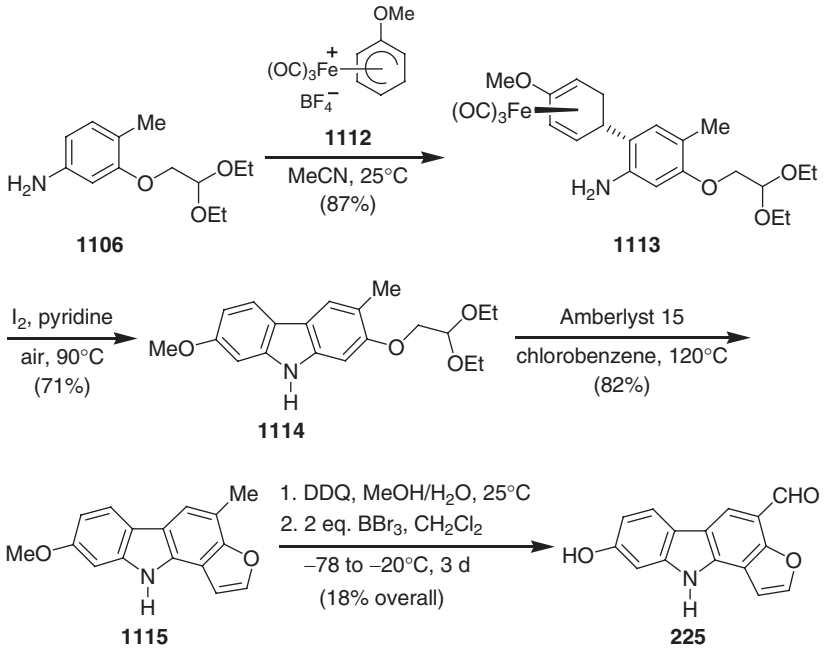

Scheme 5.182

photocyclization of the 3-substituted indole **1121**. Reaction of indole-3-acetic acid (**680**) with diethyl dicarbonate in the presence of DMAP led to the 1-ethoxycarbonyl derivative **1116**. Deprotonation of **1116** with sodium bis(trimethylsilyl)amide (NaHMDS), followed by quenching of the resulting anion with acetic anhydride, afforded a 3.5:1 ratio of the enol acetate **1117** and enol **1118** in 89% total yield. Additionally, the enol acetate **1117** was converted to the desired enol **1118** in 93% yield by treatment with dimethylamine in dichloromethane (two steps, 84% overall yield of **1118**). Alternatively, deprotonation of **1116** with LDA, and reaction of the corresponding lithioanion with acetic anhydride, led to the enol **1118** as the sole product in 68% yield. The enol **1118** was transformed to an inseparable, diastereoisomeric 1:1 mixture of the vinyl triflate **1119**. The palladium(0)-catalyzed cross-coupling of the triflate **1119** with 2-(tributylstannyl)furan (**1120**) afforded the vinylfuran **1121** as a 1:1 mixture of diastereoisomers. Photocyclization of the vinylfuran **1121** in the presence of iodine as the oxidizing agent provided the furo[3,2-*a*]carbazole **1122** in 69% yield. Alkaline hydrolysis of **1122** gave the acid **1123** *via* the *N*-deprotected furo[3,2-*a*]carbazole. Finally, decarboxylation of **1123** afforded furostifoline (**224**) (691) (Scheme 5.183).

In the same year, Hibino *et al.* reported a total synthesis of furostifoline (**224**) employing a new type of electrocyclic reaction (636). This cyclization proceeds through a 2-alkenyl-3-allenylindole intermediate, which is derived from 2-(fur-3-yl)-3-propargylindole **1128**. Compound **1128** was prepared starting from 2-chloroindole-3-carbaldehyde (**891**), furan-3-boronic acid (**1124**), and ethynylmagnesium bromide.

Vilsmeier reaction of 2-oxindole (**830**) afforded 2-chloroindole-3-carbaldehyde (**891**). Suzuki cross-coupling of **891** with furan-3-boronic acid (**1124**), followed by protection of the indole nitrogen with benzyloxymethyl (BOM) chloride, led to

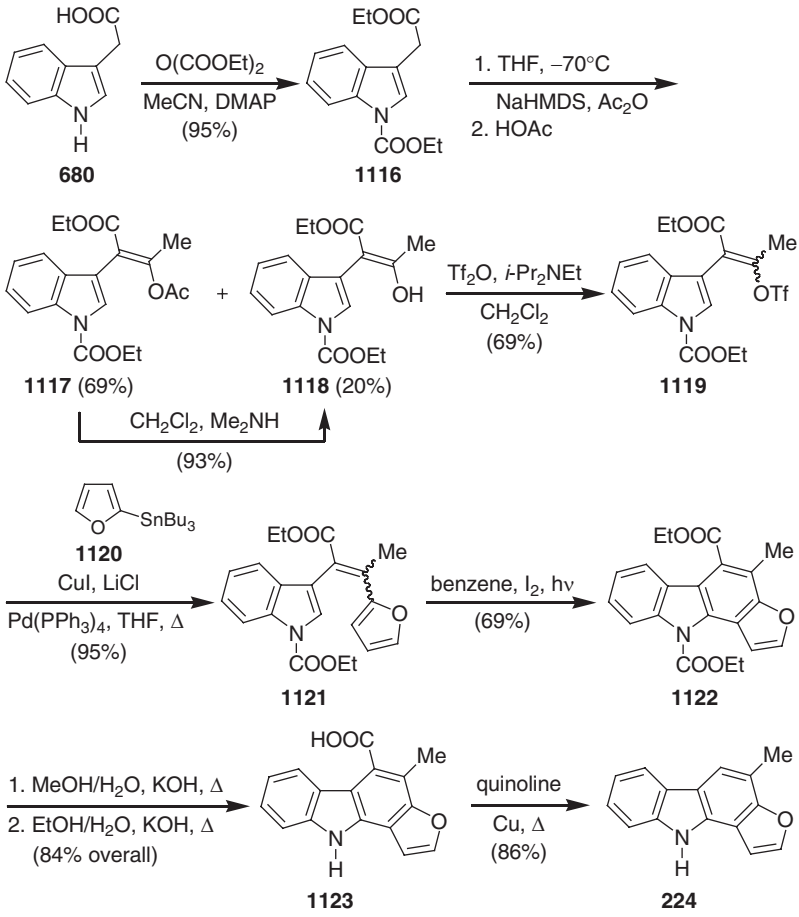

Scheme 5.183

N-BOM-protected 2-(fur-3-yl)indole-3-carbaldehyde (**1126**). Grignard reaction of **1126** with ethynylmagnesium bromide afforded the propargyl alcohol **1127**, which, on BOM protection, afforded 2-(3-furyl)-3-propargyl indole **1128**. Thermal electrocyclic reaction of **1128** in the presence of potassium *tert*-butoxide gave the 4-oxygenated furo[3,2-*a*]carbazole **1129**. Removal of the *N*,*O*-BOM groups of the furo[3,2-*a*]carbazole **1129** under Birch conditions led to a separable mixture of the *N*-(hydroxymethyl)furo[3,2-*a*]carbazole **1130** (41%) and the furo[3,2-*a*]carbazole **1131** (51%). Compound **1130** was converted to **1131** in 93% yield by treatment with Triton B. For the final transformation of the furocarbazole **1131** to furostifoline (**224**), the hydroxy group was removed *via* reductive elimination of the intermediate triflate **1132** (636,637) (Scheme 5.184).

Timári *et al.* described a total synthesis of furostifoline (**224**) starting from commercial *o*-cresol (**1133**). The key steps in this approach are the Suzuki coupling to the *o*-nitrobiaryl **1139** and subsequent Cadogan's reductive cyclization *via* a nitrene intermediate (692).

Bromination of *o*-cresol (**1133**) led to 5-bromocresol (**1134**), which, on alkylation with bromoacetaldehyde diethyl acetal, followed by P_2O_5-promoted cyclization in

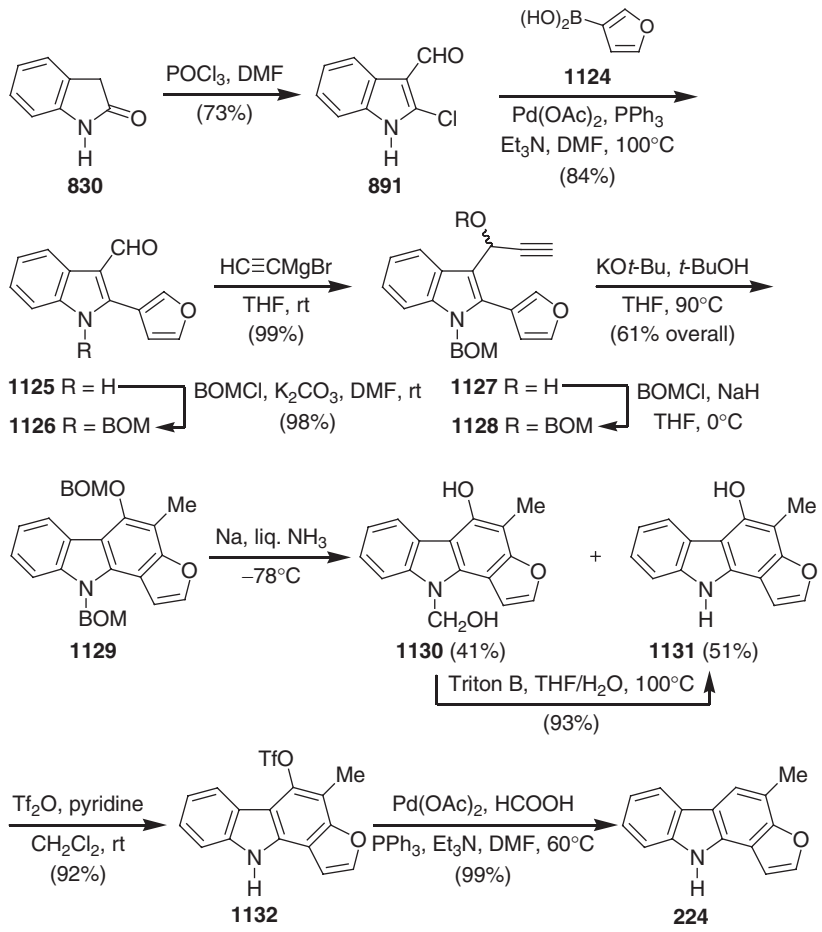

Scheme 5.184

85% H_3PO_4 at 140°C, afforded 5-bromo-7-methylbenzofuran (**1136**). A halogen–metal exchange reaction of **1136** with butyllithium, and subsequent treatment with tributyl borate, gave the boronic acid **1137**. The palladium(0)-catalyzed cross-coupling of the boronic acid **1137** with 2-bromonitrobenzene (**1138**) provided the *o*-nitrobiaryl **1139** in 72% yield. Using Cadogan's method, by reductive cyclization with triethyl phosphite, the *o*-nitrobiaryl **1139** was directly transformed to furostifoline (**224**) in 42% yield (692) (Scheme 5.185).

Yasuhara *et al.* reported a total synthesis of furostifoline (**224**) by the oxidative photocyclization of 3-(indol-2-yl)-2-(isopropenyl)furan (**1146**), which was obtained by Sonogashira coupling of ethyl 2-ethynylphenylcarbamate (**1143**) with 3-bromo-2-propenylfuran (**1142**) (693).

2-Acetyl-3-bromofuran (**1141**) was prepared by Friedel–Crafts acylation of 3-bromofuran (**1140**). Wittig reaction of **1141** with methyltriphenylphosphonium bromide and butyllithium led to 3-bromo-2-propenylfuran (**1142**), which, on Sonogashira coupling with ethyl 2-ethynylphenylcarbamate (**1143**), provided *N*-protected (2-isopropenylfur-3-yl)ethynylaniline **1144**. The TBAF-promoted

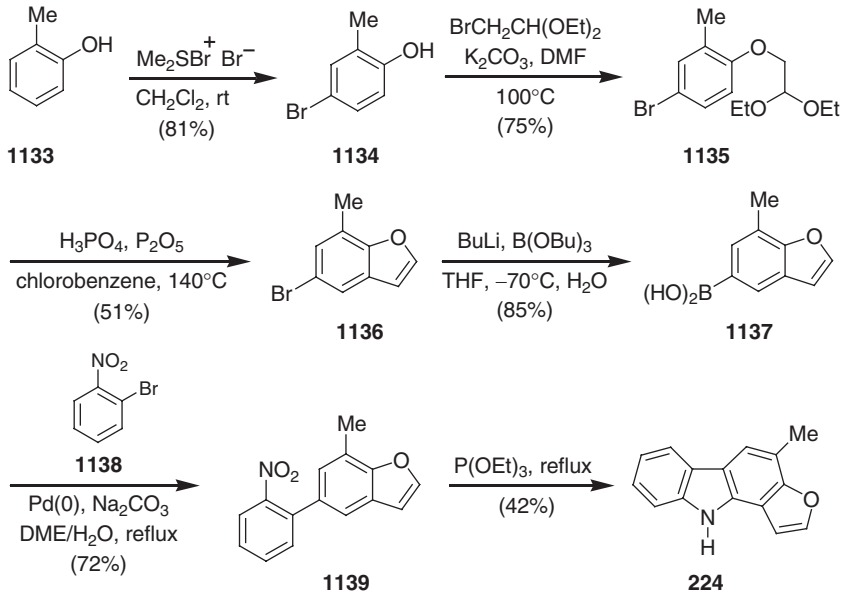

Scheme 5.185

cyclization of **1144** provided 3-(indol-2-yl)-2-(isopropenyl)furan (**1146**) in 47% yield, along with the deprotected aniline **1145** in 33% yield. Compound **1145** was recycled to the *N*-ethoxycarbonyl derivative **1144** in 76% yield by protection of the amino group. Finally, oxidative photocyclization of the 2-substituted indole **1146** in the presence of catalytic amounts of iodine afforded furostifoline (**224**) (693) (Scheme 5.186).

In 2007, we reported the first total synthesis of the furo[2,3-*c*]carbazole eustifoline-D (**227**) starting from glycozolinine (**91**), which was obtained in three steps and 56% overall yield starting from 4-bromoanisole (**670**) and *p*-toluidine (**1028**) (see Scheme 5.152). Williamson ether synthesis by alkylation of glycozolinine (**91**) with 2-bromo-1,1-diethoxyethane, and subsequent annulation of the furan ring with catalytic amounts of Amberlyst 15 in chlorobenzene at reflux, provided eustifoline-D (**227**), along with isoeustifoline-D (**1148**), in a ratio of 4.3:1. This method provides eustifoline-D (**227**) in five steps and 20% overall yield based on 4-bromoanisole (**670**) (547) (Scheme 5.187).

F. Pyrrolo[2,3-*c*]carbazole Alkaloids

Recently, Fürstner *et al*. reported the first total synthesis of the pyrrolo[2,3-*c*]carbazole alkaloids dictyodendrin B (**284a**) (694,695), C (**286a**) (695), and E (**288a**) (695) in the form of their ammonium salts starting from the common intermediate **1157**. This relay compound **1157** was prepared on a multigram scale starting from commercial 3-hydroxy-2-nitroacetophenone (**1149**) over seven steps. This sequence comprises a toluenesulfonylmethyl isocyanide (TosMIC) cycloaddition, a low valent titanium-induced reductive oxamide coupling, and a photochemical tandem 6π-electrocyclization/aromatization as key steps for the generation of pyrrole, indole, and pyrrolocarbazole frameworks, respectively.

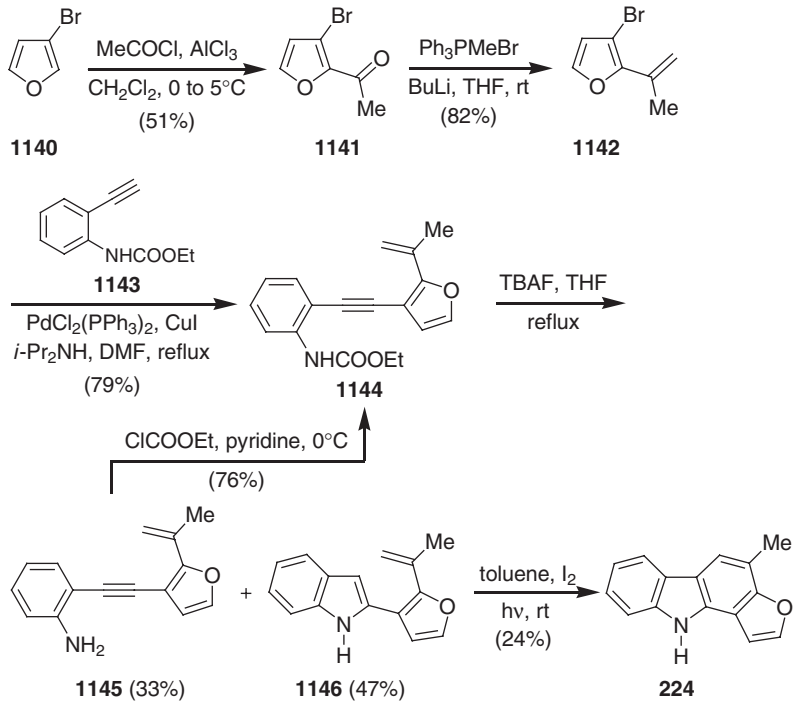

Scheme 5.186

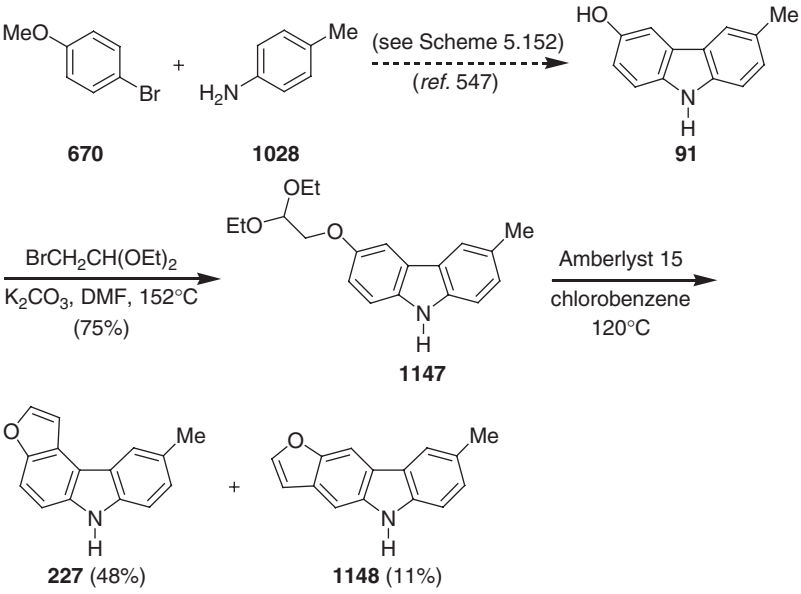

Scheme 5.187

Prior to base-induced condensation with 4-methoxybenzaldehyde, the free hydroxy group in 3-hydroxy-2-nitroacetophenone (**1149**) was protected as an isopropyl ether **1150**. The resulting chalcone **1151** was treated with TosMIC in the presence of NaH at low temperature to afford a pyrrole, which, on *in situ* *N*-alkylation with 4-$MeOC_6H_4(CH_2)_2Br$, led to the corresponding *N*-alkyl derivative **1152**. Reduction of the nitro group in **1152** with Fe/HCl furnished the aniline **1153** in almost quantitative yield. Compound **1153** was acylated by the acid chloride **1154** to give the amide **1155**. Reaction of the ketoamide **1155** with titanium on graphite, prepared from $TiCl_3$ and 2 equivalents KC_8 in refluxing DME, led to the desired indole **1156** in up to 93% yield. In a single operation, irradiation of **1156** with UV light (Hanovia Hg lamp, 250 W) in MeCN, followed by addition of Pd/C in nitrobenzene, led to the desired pyrrolocarbazole **1157** in 81% yield as result of a 6π-electrocyclization with concomitant aromatization (Schemes 5.188 and 5.189).

Regioselective bromination of the pyrrolocarbazole **1157** with NBS led to the bromocarbazole **1158**, which, on halogen–metal exchange with butyllithium and

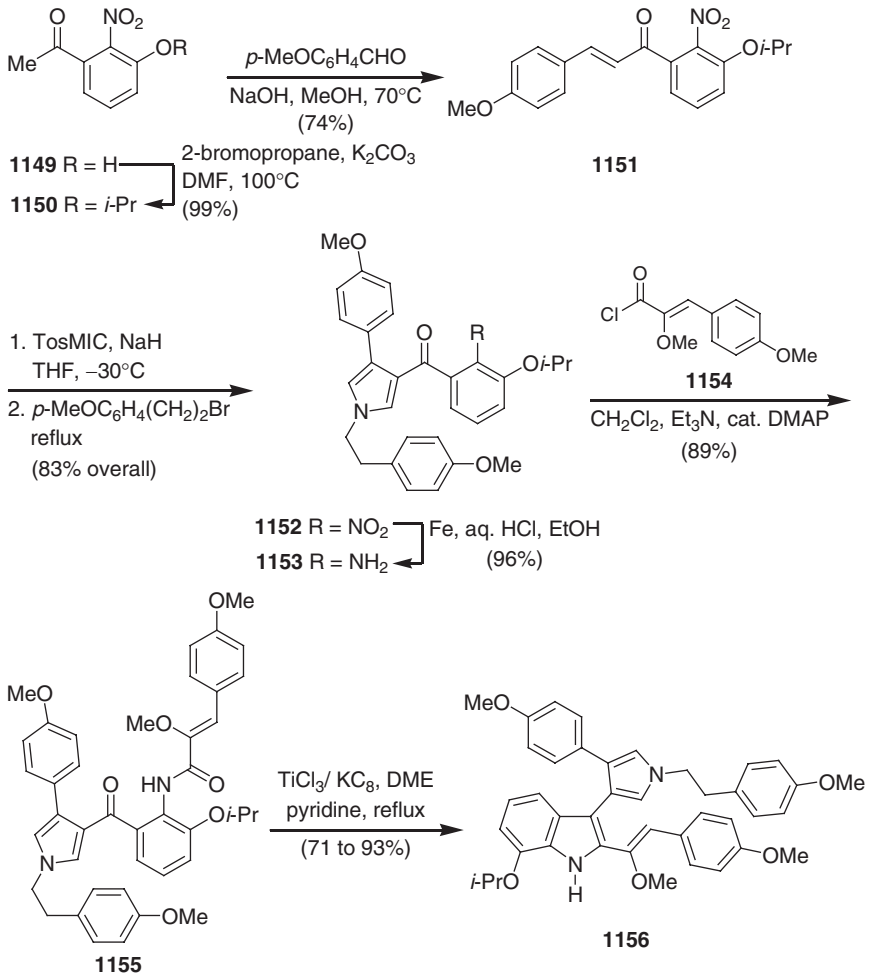

Scheme 5.188

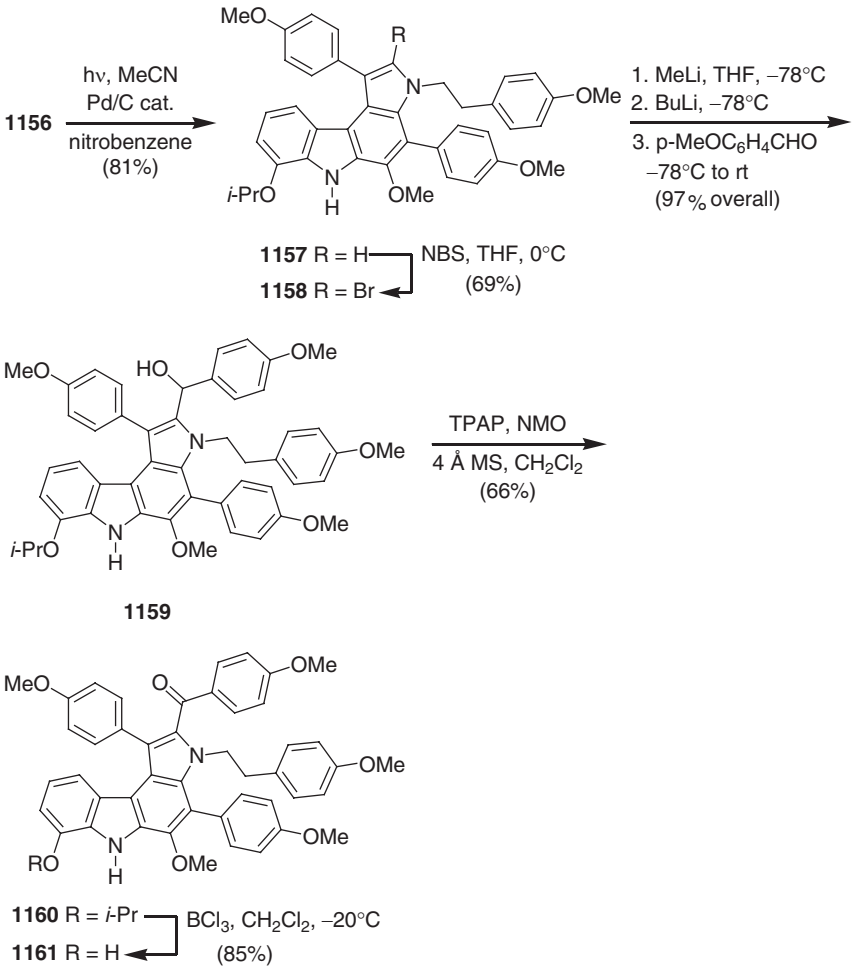

Scheme 5.189

subsequent quenching of the intermediate lithio species with 4-methoxybenzaldehyde, led to **1159**. Oxidation of the benzylic alcohol **1159** to the corresponding ketone **1160** was achieved in dilute CH_2Cl_2 solution with tetra-*n*-propylammonium perruthenate (TPAP) and *N*-methylmorpholine *N*-oxide (NMO). Selective cleavage of the isopropyl ether in **1160** with BCl_3, followed by reaction of the resulting phenol **1161** with trichloroethyl chlorosulfuric acid ester, gave the aryl sulfate **1162** in 92% yield. Exhaustive demethylation of **1162** with BCl_3 under phase transfer conditions, followed by reductive cleavage of the remaining trichloroethyl moiety with $Zn/HCOONH_4$, led to dictyodendrin B (**284a**) (694,695) (Schemes 5.189 and 5.190).

Selective cleavage of the isopropyl ether in **1157** with BCl_3, followed by reaction of the resulting phenol **1163** with trichloroethyl chlorosulfuric acid ester gave the aryl sulfate **1164**. After complete demethylation of **1164** with BCl_3, the resulting phenol was reacted with H_2O_2 in MeCN to give the quinone **1165**. Finally, reductive cleavage of the trichloroethyl ester moiety in **1165** with excess zinc dust and ammonium formate in MeOH, followed by stirring of the crude reaction mixture under an

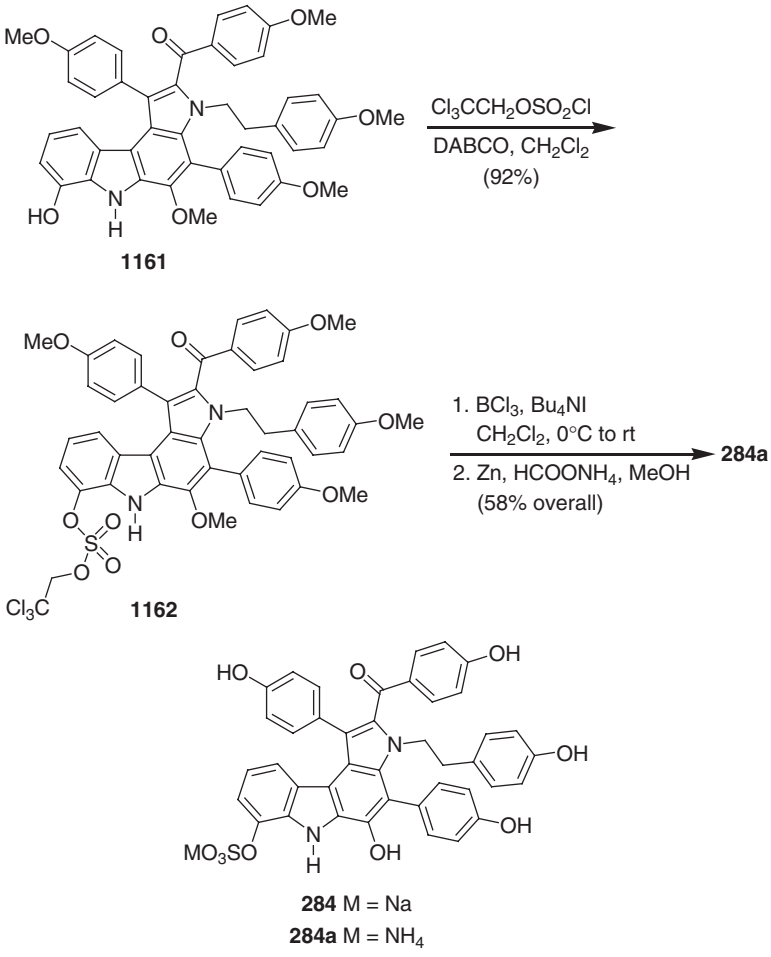

Scheme 5.190

oxygen atmosphere, led to dictyodendrin C (**286a**) in 76% yield over two steps (695) (Scheme 5.191).

For the total synthesis of dictyodendrin E (**288a**), the required benzylidene substituent at C-2 (see Scheme 2.71) was introduced almost quantitatively by palladium-catalyzed benzylation of the bromide **1156** with the borate complex **1166**. Thus, reaction of **1156** with borate complex **1166**, which was generated *in situ* from 9-methoxy-9-borabicyclo[3.3.1]nonane (9-MeO-9-BBN) and 4-methoxybenzylmagnesium chloride with $Pd(OAc)_2$ and Buchwald's sterically encumbered S-PHOS ligand, led to the coupling product **1167** in 90% yield. Selective removal of the isopropyl ether in **1167** with BCl_3, followed by reaction of the resulting phenol with trichloroethyl chlorosulfuric acid ester, gave the aryl sulfate **1168**. After cleavage of the methyl ethers with BCl_3, the sensitive hydroxy derivative **1169** was subjected to immediate reductive cleavage of the trichloroethyl group followed by DDQ oxidation to afford dictyodendrin E (**288a**) in its ammonium salt form (695) (Scheme 5.192).

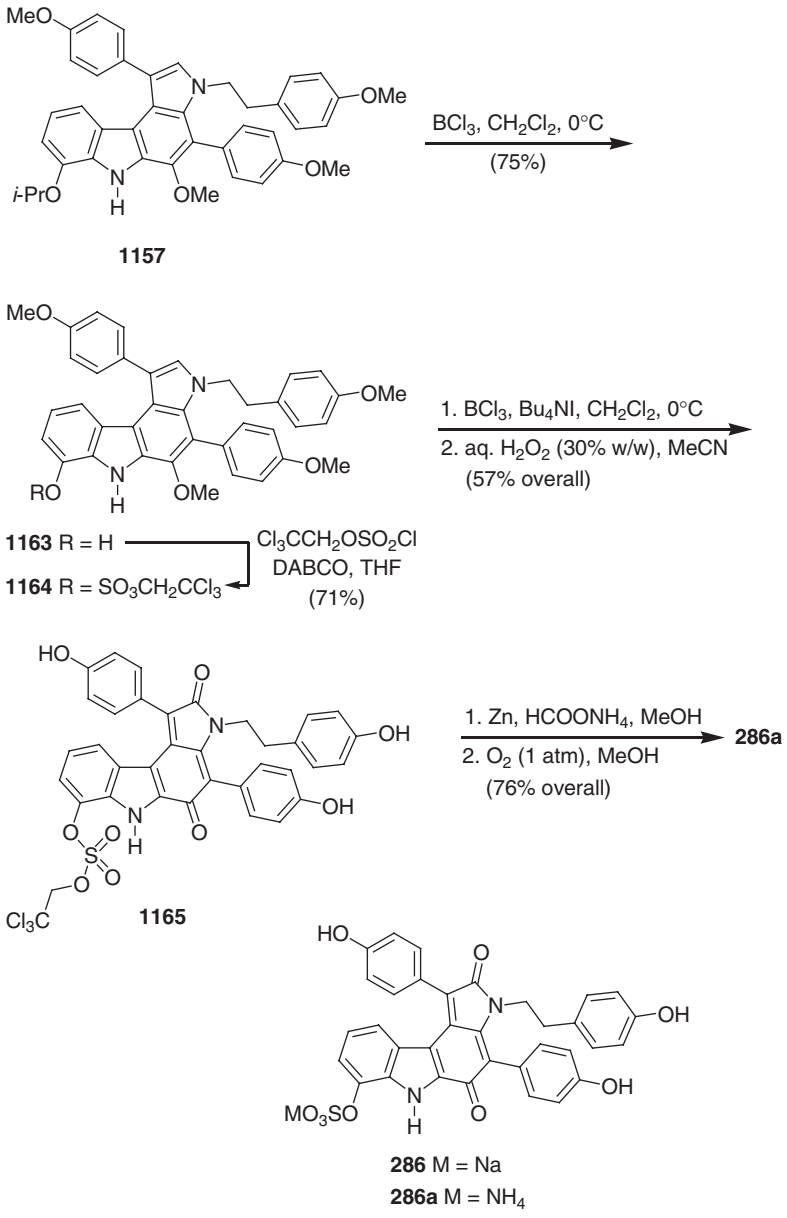

Scheme 5.191

G. Pyrido[4,3-*b*]carbazole Alkaloids

The strong interest in the synthesis of pyrido[4,3-*b*]carbazole alkaloids started in the late 1960s with the disclosure of the antitumor activity of ellipticine (**228**) and 9-methoxyellipticine (**229**) (see Scheme 2.56) in several animal and human tumor systems. This discovery made these alkaloids to important synthetic targets and induced extensive studies of structure modification. These synthetic efforts have

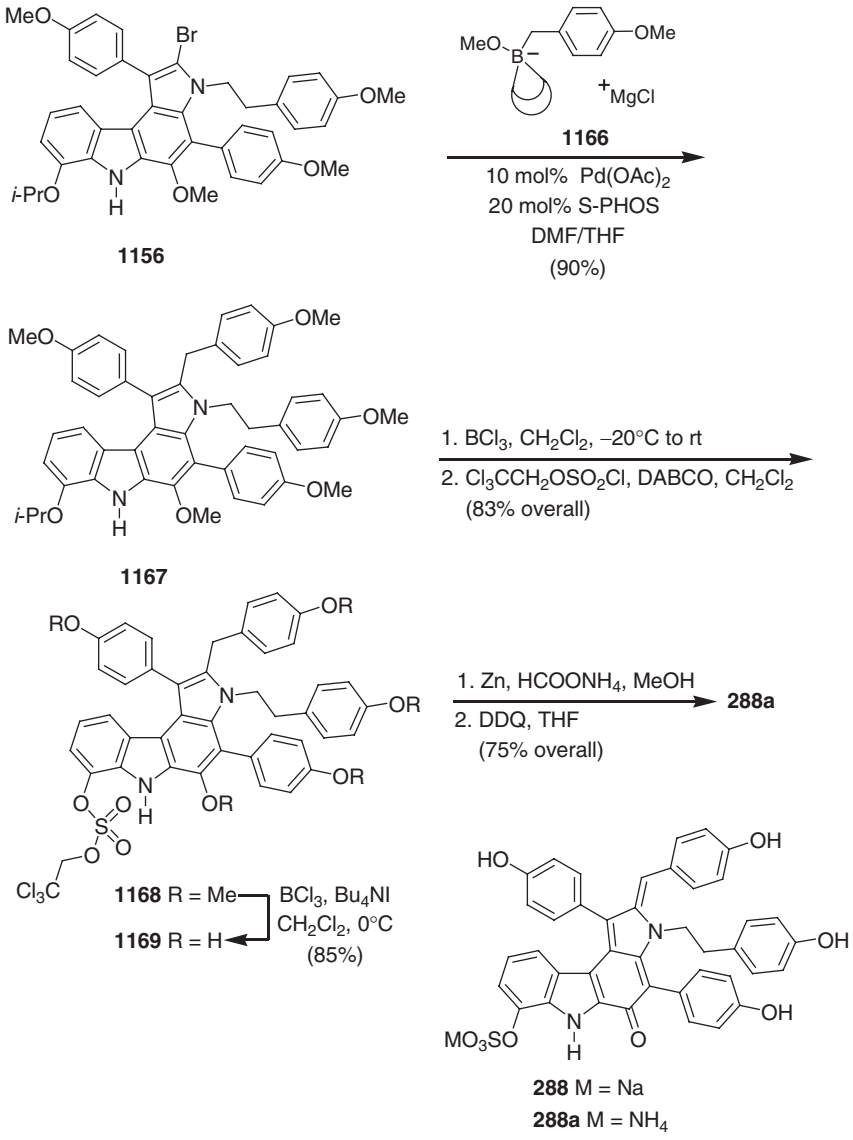

Scheme 5.192

been reviewed in this series by Gilbert (696), Cordell (697), Suffness and Cordell (408), and Gribble (192) in the Volumes 8, 17, 25, and 39, respectively. In addition to these comprehensive reviews, various reviews have appeared elsewhere, covering different aspects of the pyrido[4,3-*b*]carbazole alkaloids and their analogs (8,185–191,195,196,698,699). Further, in 1991 Gribble (193) and in 1994 Moody (525) wrote personal accounts on the synthesis of the antitumor pyridocarbazole alkaloids. Pindur *et al.* have published a series of articles on the intercalating properties of pyrido[4,3-*b*]carbazole alkaloids (190,194,405).

Herein, as an update of Volume 39 of this series (192), we summarize the total syntheses of natural pyrido[4,3-*b*]carbazole alkaloids developed since 1990.

Gribble *et al*. reported the total syntheses of ellipticine (**228**), olivacine (**238a**), 9-methoxyellipticine (**229**), and 9-hydroxyellipticine (**230**) starting from the keto lactam **1181** and its methoxy derivative **1182** (700,701) The ketolactam **1181** was available in four steps, and 71% overall yield, starting from indole **1170**. Thus, indole **1170** was converted to *N*-phenylsulfonylindole (**956**) by treatment with *n*-butyllithium followed by the addition of benzenesulfonyl chloride. Regiospecific 2-lithiation of **956** with LDA and quenching of the intermediate 2-lithioindole **1173** with pyridine 3,4-dicarboxylic anhydride (**1175**) led to the desired keto acid **1176** in 92% yield, along with 8% of the regioisomeric product **1178**. After cleavage of the *N*-phenylsulfonyl protecting group, the keto acid **1179** was smoothly cyclized to the keto lactam **1181** in quantitative yield. Low temperature addition of methyllithium to keto lactam **1181** led to the diol **1189** as two unstable diastereomers, which, without purification, were treated with sodium borohydride ($NaBH_4$) to afford ellipticine (**228**) in 82% yield (700,701) (Schemes 5.193 and 5.194).

An analogous sequence to that described for ellipticine was used to convert 5-methoxyindole (**1171**) to 9-methoxyellipticine (**229**). Noteworthy is the fact that none of the other regioisomeric keto acid could be detected by analysis of the crude product **1177**. Using this sequence, 9-methoxyellipticine (**229**) was obtained in 47% overall yield based on **1171**. *O*-Demethylation of 9-methoxyellipticine (**229**)

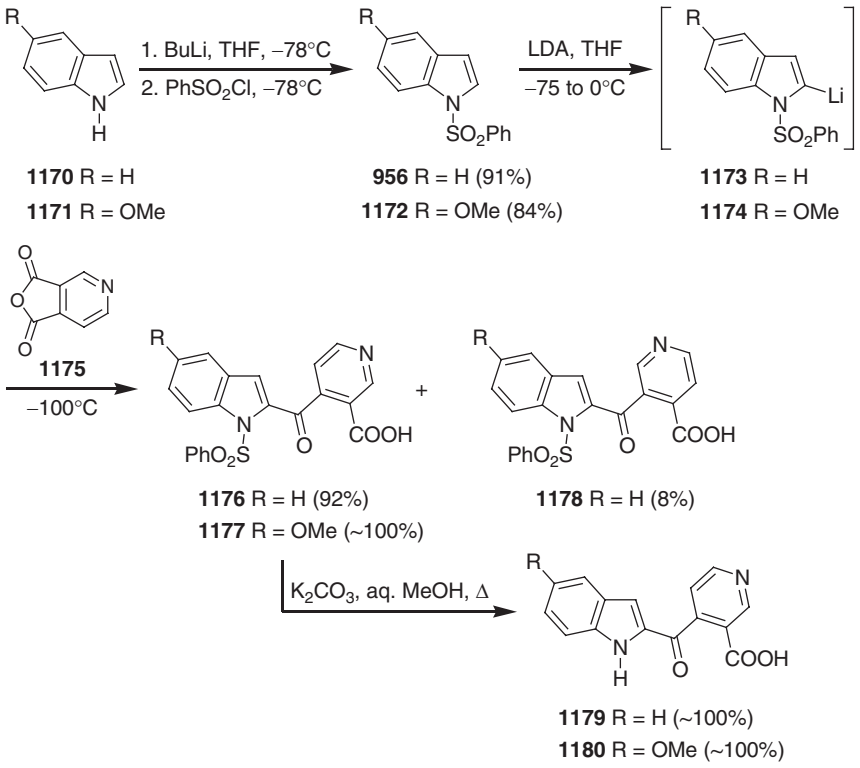

Scheme 5.193

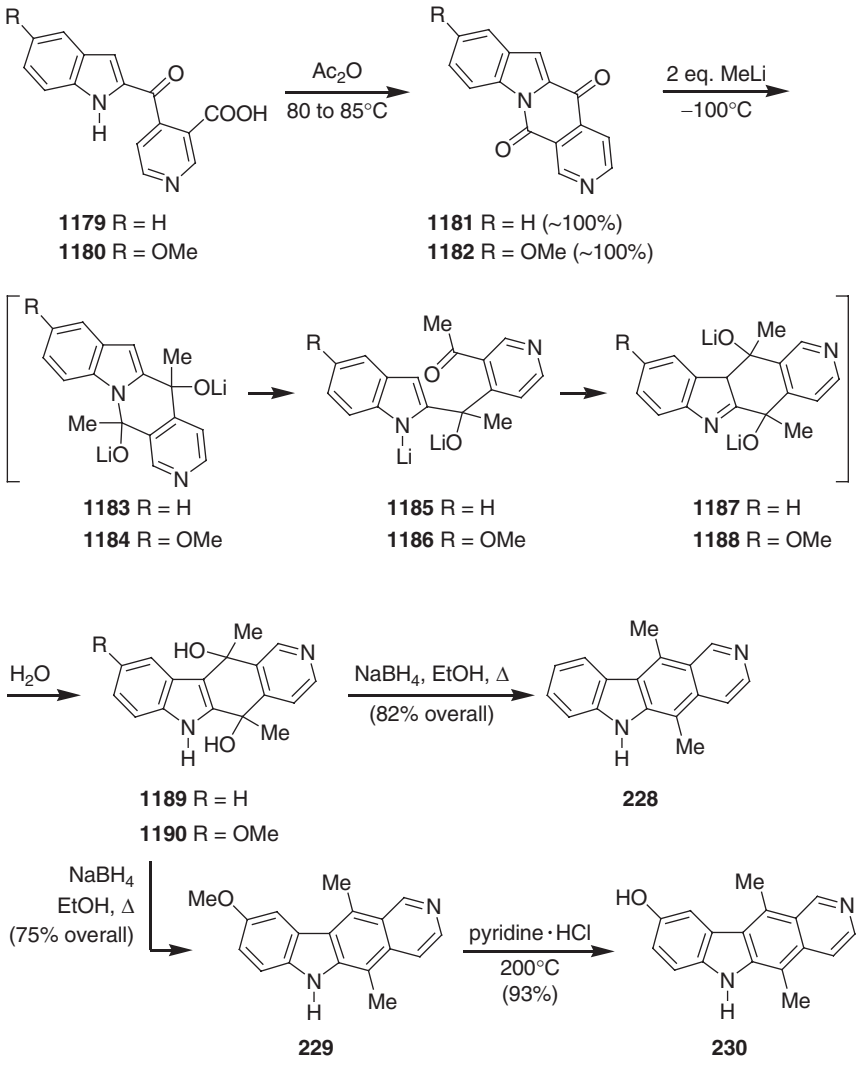

Scheme 5.194

with pyridine hydrochloride led to 9-hydroxyellipticine (**230**) (701) (Schemes 5.193 and 5.194).

As an extension of this methodology, Gribble *et al*. reported a formal total synthesis of olivacine (**238a**). This synthesis starts from the same keto lactam **1181**, used for the synthesis of ellipticine (**228**), and exploits the lower reactivity of the lactam carbonyl as compared to the carbonyl of the keto lactam. Reaction of the keto lactam **1181** sequentially with methyllithium and superhydride ($LiBHEt_3$) led to 11-demethylellipticine (**1191**) in 57% yield, along with 30% of ellipticine (**228**). Finally, using Kutney's procedure (220), 11-demethylellipticine (**1191**) could be transformed to olivacine (**238a**) (701) (Scheme 5.195).

Gribble *et al*. also reported a new annulation strategy for the total synthesis of ellipticine (**228**) (527). This methodology utilizes a Diels–Alder reaction between

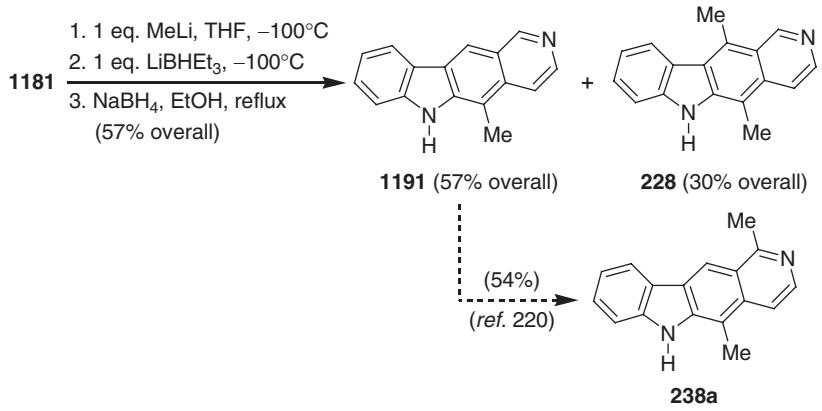

Scheme 5.195

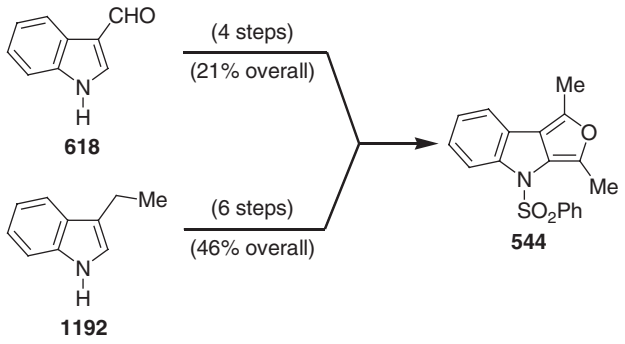

Scheme 5.196

1,3-dimethyl-4-(phenylsulfonyl)-4*H*-furo[3,4-*b*]indole (**544**) and 3,4-pyridyne (**1193**), followed by extrusion of the oxygen bridge. Furo[3,4-*b*]indole **544** was prepared from commercially available 3-formylindole (**618**) in 21% overall yield, using four simple functional group transformations. Alternatively, a longer, albeit higher yielding synthesis of **544** was also developed starting from 3-ethylindole (**1192**) (527) (Scheme 5.196).

Diels–Alder reaction of the furoindole **544** with 3,4-pyridyne (**1193**), generated *in situ via* two different ways, led to a mixture of the two possible cycloadducts **1194** and **1195** in approximately equal amounts. Without purification, the crude adducts **1194** and **1195** were treated with basic sodium borohydride ($NaBH_4$) to afford a separable mixture of ellipticine (**228**) and isoellipticine (**1196**) in 23% and 29% yield, respectively (527) (Scheme 5.197).

Six years later, the same authors reported an improved version of their earlier synthesis of ellipticine (**228**) (527) (Scheme 5.197) by using the 1-(*p*-methoxybenzyl)-5,6-dihydropyridone (**1197**) as 3,4-pyridyne surrogate (702,703). Thus, the dimethylfuroindole **544** was treated with the unsaturated lactam **1197** (prepared from δ-valerolactam in three steps) in the presence of trimethylsilyl triflate (TMSOTf) to afford the carbazole **1199** as a single product in 40% yield. The low yield is presumably a consequence of decomposition of the intermediate adduct **1198** during

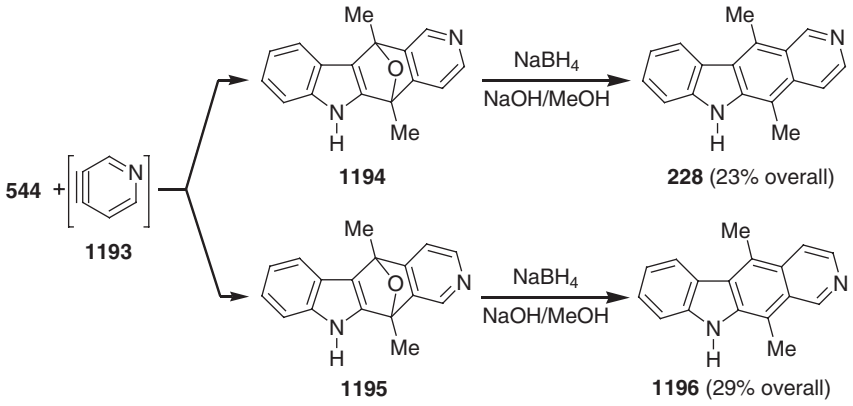

Scheme 5.197

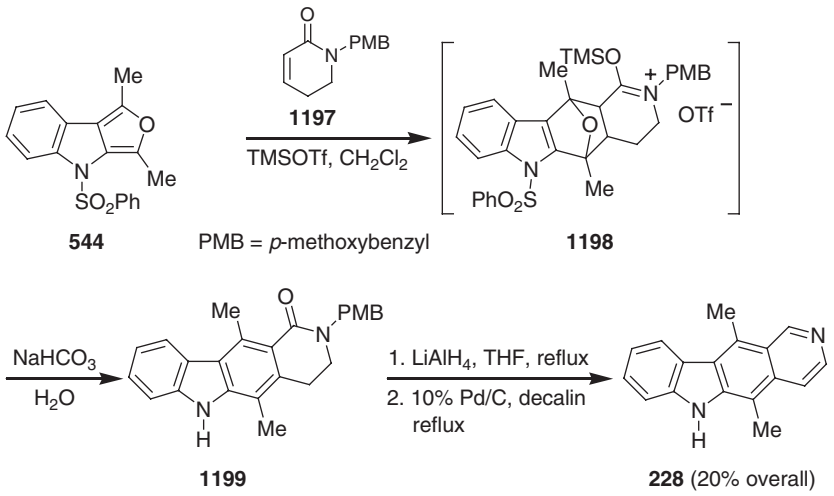

Scheme 5.198

the reaction. Reduction of the carbonyl group with lithium aluminum hydride, followed by aromatization with concomitant debenzylation, transformed the carbazole **1199** to ellipticine (**228**) (702,703) (Scheme 5.198).

Murakami *et al.* reported a total synthesis of ellipticine (**288**) starting from 9-benzyl-4-methyl-1,2,3,4-tetrahydro-9*H*-carbazole (**1200**) (704,705). Using an optimized Vilsmeier–Haack protocol, the tetrahydrocarbazole (**1200**) was transformed to the desired 3-formylcarbazole **1202** in 38% yield, along with the other minor carbazole derivatives **1201** and **1203** in 1% and 26% yield, respectively. The 3-formylcarbazole **1202** was converted to the imine **1204** and then to the tosyl amide **1205**. Finally, using modified Pomeranz–Fritsch cyclization conditions, the amide **1205** was transformed to ellipticine (**228**), involving a spontaneous sequence of detosylation, aromatization, and debenzylation. However, the Birch reduction, used for the removal of the benzyl group, also reduced the pyridine ring to dihydroellipticine, which subsequently had to be rearomatized with 10% Pd/C to

ellipticine (**228**). Therefore, an alternative route was developed involving removal of the benzyl group prior to formation of the pyridine ring. The Birch reduction of the imine **1204** removed the benzyl group with concomitant reduction of the C–N double bond. Tosylation of the resulting amine gave the acetal **1206**. Cyclization of the tosylate **1206** using Jackson and Shannon's conditions (706) with hydrochloric acid in dioxane provided ellipticine (**228**) along with 13% of 2-tosyl-1,2-dihydroellipticine (**1207**) (704,705) (Scheme 5.199). Following a similar synthetic sequence, starting from 9-benzyl-1,2,3,4-tetrahydro-9*H*-carbazole, the same authors also reported the synthesis of olivacine (**238a**) (704,705).

Bäckvall and Plobeck reported a formal synthesis of ellipticine (**228**) starting from indole (707). The [4+2] cycloaddition of 1-indolylmagnesium iodide (**1208**) with 3-(phenylsulfonyl)-2,4-hexadiene (**1209**) afforded the tetrahydrocarbazole

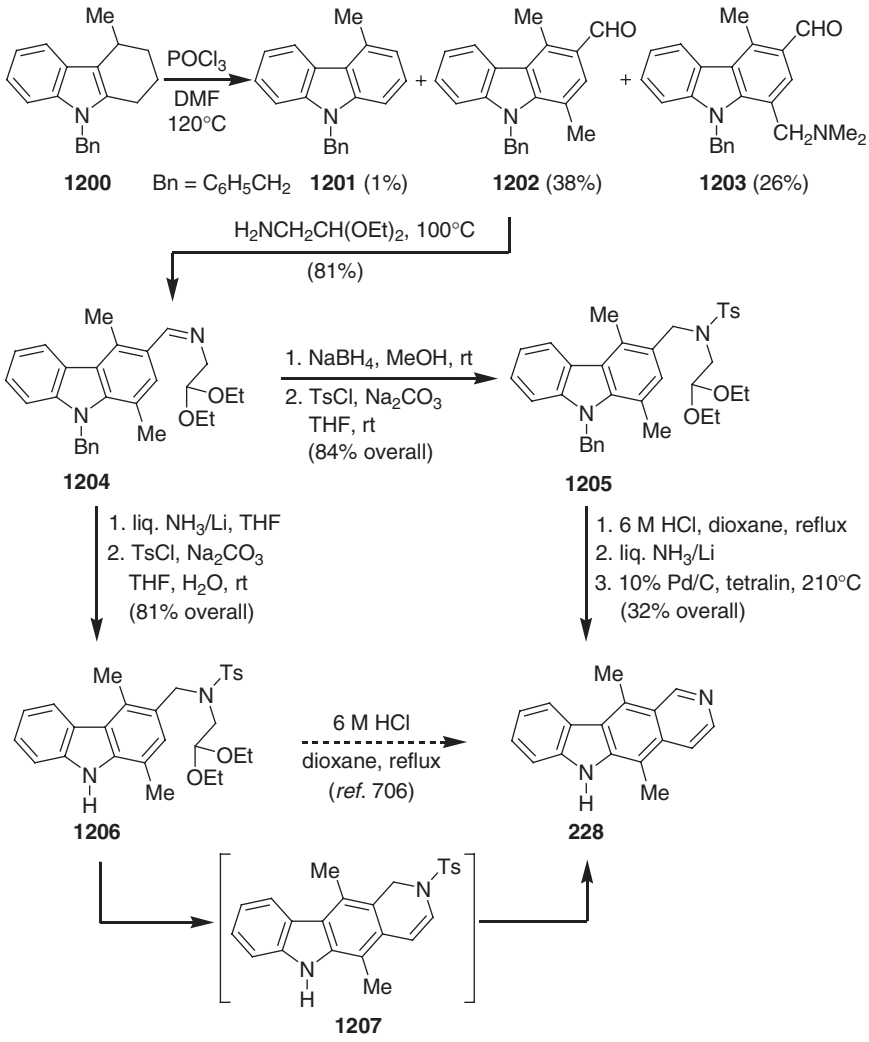

Scheme 5.199

1210 as the major diastereoisomer. Michael addition of lithio acetonitrile to the tetrahydrocarbazole **1210** gave the hexahydrocarbazole **1211**. Reductive desulfonation of **1211** with sodium amalgam in buffered methanol to **1212**, followed by aromatization with chloranil, provided the carbazole **1213**. Reduction of compound **1213** using $CoCl_2/NaBH_4$ to the amine, and subsequent formylation with ethyl formate, led to the formamide **1214**. The known formamide **1214** was previously reported (708) to provide ellipticine (**228**) in 77% overall yield, by Bischler–Napieralski cyclization to dihydroellipticine and subsequent aromatization (Scheme 5.200). Based on the cycloaddition of (*E*)-2-(phenylsulfonyl)-1,3-pentadiene with 1-indolylmagnesium iodide (**1208**) (84% yield), a similar reaction sequence was used for a formal synthesis of olivacine (**238a**) (707).

Hibino and Sugino reported a total synthesis of ellipticine (**228**) and olivacine (**238a**) starting from *N*-(phenylsulfonyl)indole (**956**) (709). This route involves a thermal electrocyclic reaction of a conjugated hexatriene system, which is generated by a [1,5]-sigmatropic reaction of the 2-alkenylindoles **1217** and **1218**. The 2-alkenylindoles **1217** and **1218** were obtained by condensation of 2-lithio-1-phenylsulfonylindole **1173** with the substituted 4-acetylpyridines **1215** and **1216**. Finally, thermal electrocyclic reaction of **1217** and **1218** at 460–500°C afforded ellipticine (**228**) and olivacine (**238a**) in 30% and 57% yield, respectively (709) (Scheme 5.201). This method was extended to the synthesis of the 11-demethylellipticine derivatives (709).

Archer *et al*. reported a total synthesis of 12-hydroxyellipticine (**232**) starting from Gribble's ketolactam intermediate **1181**, which was obtained in five simple steps

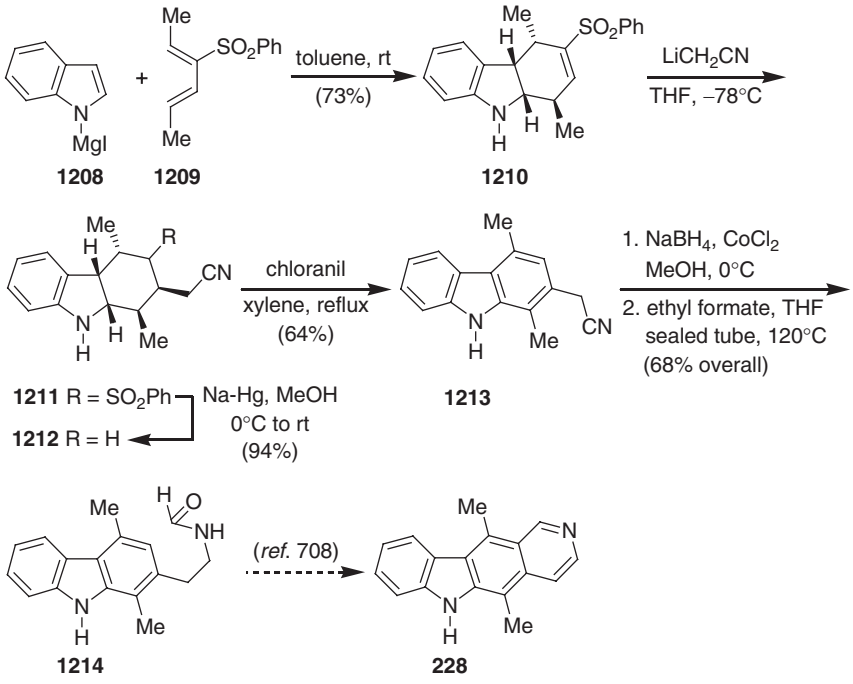

Scheme 5.200

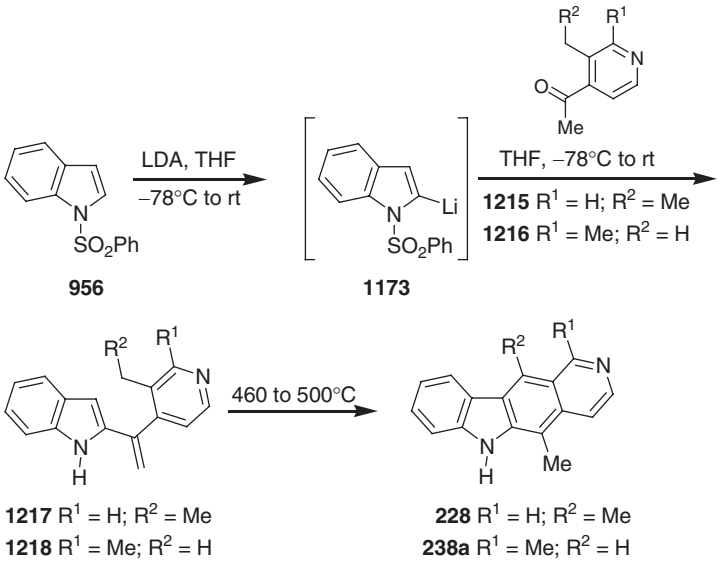

Scheme 5.201

starting from indole (**1170**) (710,711) (see Schemes 5.193 and 5.194). Treatment of the ketolactam **1181** with 1 equivalent of methyllithium, followed by quenching with solid ammonium chloride, gave the lactam carbinol **1220** as the major product. However, when the same reaction was quenched with water, the lactone **1219** was formed in 65% yield due to hydrolysis of the lactam carbinol **1220** by *in situ*-generated LiOH. The lactone **1219** was used as an intermediate for the introduction of different substituents at C-11.

Addition of methyllithium to the lactone **1219**, followed by reduction with sodium borohydride in refluxing ethanol, afforded, almost quantitatively, ellipticine (**228**). Reaction of the compound **1219** with the lithio derivative of formaldehyde diethylmercaptal, and reduction with sodium borohydride in refluxing ethanol, led to the mercaptal **1221**. Cleavage of the mercaptal **1221** with bis(trifluoroacetoxy) iodobenzene [$PhI(OCOCF_3)_2$] in aqueous acetonitrile gave the 11-formyl derivative, which was reduced with sodium cyanoborohydride ($NaBH_3CN$) to 12-hydroxyellipticine (**232**) (710,711) (Scheme 5.202). The same group also reported the synthesis of further pyrido[4,3-*b*]carbazole derivatives by condensation of 2-substituted indoles with 3-acetylpyridine (712).

Sha and Yang reported the total synthesis of ellipticine (**228**) using the 2,4-dihydropyrrolo[3,4-*b*]indole (**1225**) as a synthetic equivalent of indolo-2,3-quinodimethane in a Diels–Alder reaction with 3,4-pyridyne (**1193**) (713). The acetylation of 2-ethylindole (**1222**) with *N*,*N*-dimethylacetamide and phosphorus oxychloride, followed by protection of the indole as the corresponding phenylsulfonyl derivative, led to the *N*-protected indole **1223**. The compound **1223** was transformed to the bromide, and then to the azido compound **1224**. Staudinger reaction of the azido compound **1224** with triphenylphosphine gave the 2,4-dihydropyrrolo[3,4-*b*]indole, which, on protection of the pyrrolo nitrogen, led to the corresponding *N*-Boc derivative **1225**. The Diels–Alder cycloaddition of **1225** with 3,4-pyridyne (**1193**), generated by reaction of 1-aminotriazolo[4,5-*c*]pyridine

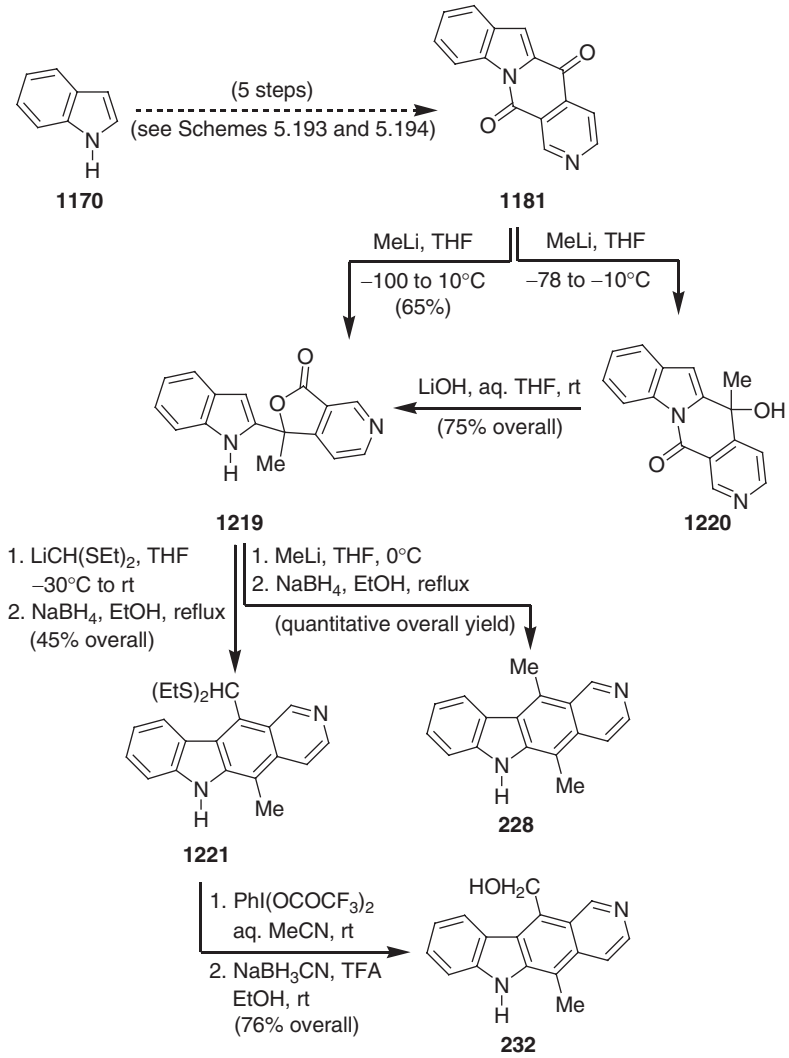

Scheme 5.202

with lead tetraacetate, provided the regioisomeric cycloadducts **1226** and **1227** in a ratio of 55:45 (62% yield). Hydrolysis of the cycloadducts **1226** and **1227** afforded the tetracyclic carbazoles **1228** and **1229** in 35% and 39% yield, respectively. Separate catalytic hydrogenation to the carbazole derivatives **1230** and **1231** (80% and 83% yield, respectively), followed by treatment with TFA provided ellipticine (**228**) (85% yield) and isoellipticine (**1196**) (78% yield) (713) (Scheme 5.203). This method was also applied to the synthesis of amino analogs of ellipticine (713).

Miki *et al.* reported the total synthesis of ellipticine (**228**) starting from *N*-benzylindole-2,3-dicarboxylic anhydride (**852**) (714,715). Reaction of (3-bromo-4-pyridyl)triisopropoxyltitanium (**1232**) with **852** gave 2-acylindole-3-carboxylic acid **1233** in 86% yield. Decarboxylation and debenzylation of **1233** led to the ketone **1234**. Wittig olefination of the ketone **1234**, followed by catalytic hydrogenation,

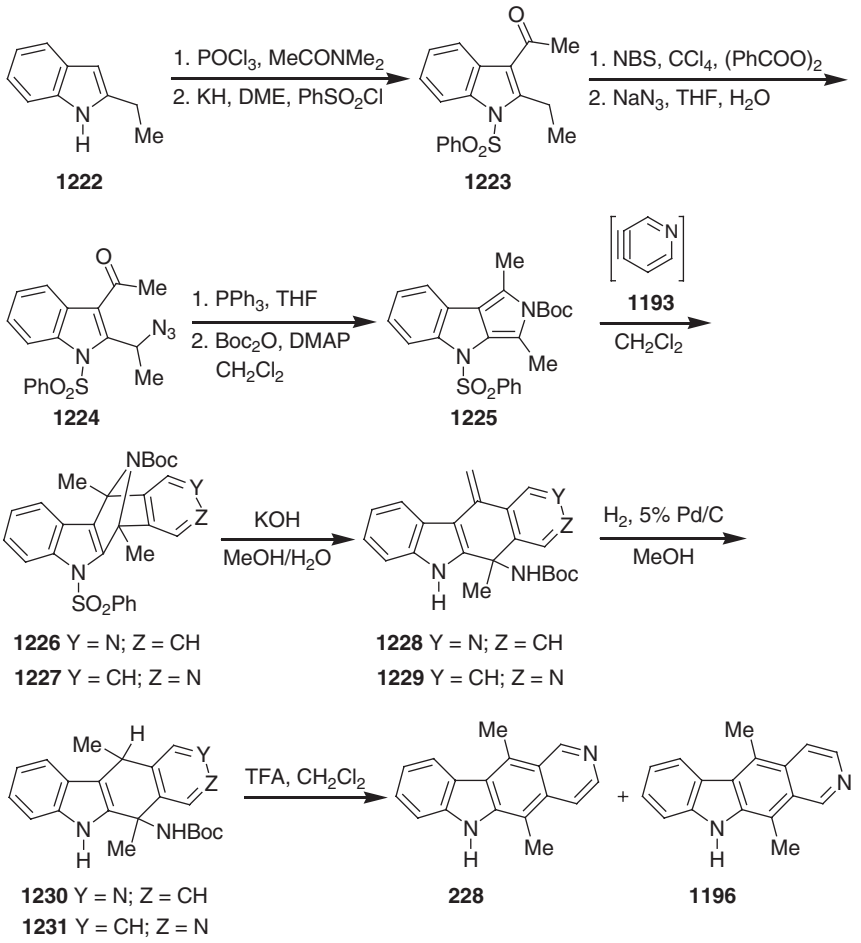

Scheme 5.203

provided 1-(3-bromo-4-pyridyl)-1-(2-indolyl)ethane (**1235**). Palladium(0)-catalyzed cross-coupling of **1235** with (1-ethoxyvinyl)tributyltin (**1236**) led to the corresponding ethoxyvinyl derivative **1237**. Finally, cyclization of **1237** with 10% hydrochloric acid led to ellipticine (**228**) in 87% yield (714,715) (Scheme 5.204).

Two years later, the same group reported a formal synthesis of ellipticine (**228**) using 6-benzyl-6*H*-pyrido[4,3-*b*]carbazole-5,11-quinone (6-benzylellipticine quinone) (**1241**) as intermediate (716). The optimized conditions, reaction of 1.2 equivalents of 3-bromo-4-lithiopyridine (**1238**) with *N*-benzylindole-2,3-dicarboxylic anhydride (**852**) at −96°C, led regioselectively to the 2-acylindole-3-carboxylic acid **1233** in 42% yield. Compound **1233** was converted to the corresponding amide **1239** by treatment with oxalyl chloride, followed by diethylamine. The ketone **1239** was reduced to the corresponding alcohol **1240** by reaction with sodium borohydride. Reaction of the alcohol **1240** with *t*-butyllithium led to the desired 6-benzylellipticine quinone (**1241**), along with a debrominated alcohol **1242,** in 40% and 19% yield, respectively. 6-Benzylellipticine quinone (**1241**) was transformed to 6-benzylellipticine (**1243**) in 38% yield by treatment with methyllithium, then hydroiodic acid, followed

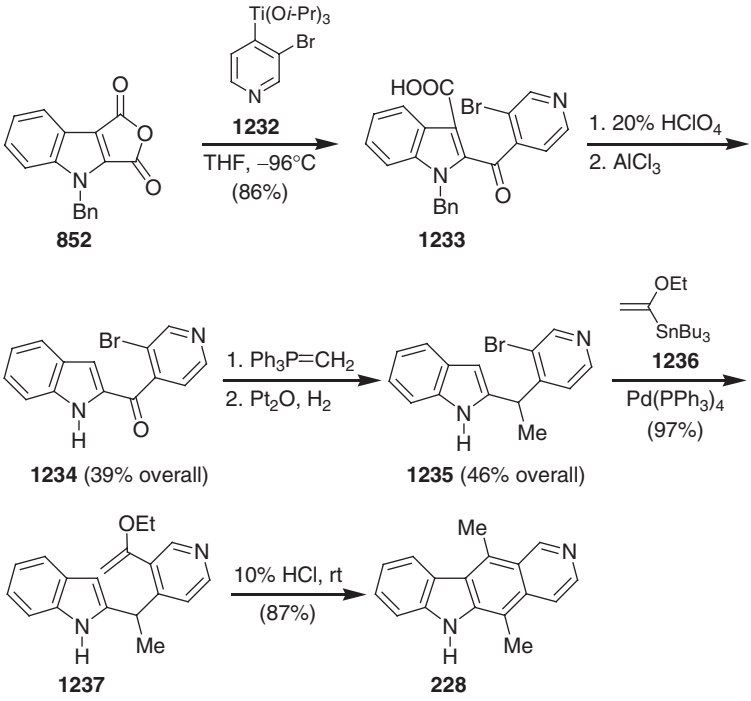

Scheme 5.204

by tin(II) chloride. 6-Benzylellipticine (**1243**) was previously transformed to ellipticine (**228**) (716) (Scheme 5.205).

Recently, the same authors reported a different route for the total synthesis of olivacine (**238a**) and ellipticine (**228**) starting from 2,4,6-trimethoxypyridine (**1244**) with *N*-benzylindole-2,3-dicarboxylic anhydride (**852**) (717,718). Interestingly, this method also uses the same common precursor, *N*-benzylindole-2,3-dicarboxylic anhydride (**852**) as shown in Schemes 5.204 and 5.205. Contrary to the earlier route, this sequence involves a Friedel–Crafts acylation of 2,4,6-trimethoxypyridine (**1244**) with *N*-benzylindole-2,3-dicarboxylic anhydride (**852**) (717,718).

For the synthesis of olivacine (**238a**), the required 6-methyl derivative **1247** was obtained in four steps and 64.5% overall yield starting from *N*-benzylindole-2,3-dicarboxylic anhydride (**852**). Thus, regioselective Friedel–Crafts reaction of **852** with 2,4,6-trimethoxypyridine (**1244**) in the presence of titanium(IV) chloride provided the corresponding 3-acylindole-2-carboxylic acid **1245**. Prior to *O*-demethylation, **1245** was subjected to decarboxylation by reacting with copper chromite in quinoline to afford the ketone **1246**. The compound **1246** was subjected to regioselective mono *O*-demethylation by treatment with 47% hydrobromic acid. Subsequent reaction with triflic anhydride (Tf_2O), followed by reaction of the corresponding triflate with MeMgBr in the presence of $NiCl_2(dppe)_2$, led to the methyl derivative **1247** in 70% overall yield.

Chemoselective demethylation of **1247** by treatment with boron tribromide led to a 4-hydroxy compound, which, after reduction with diborane, was reacted with triflic anhydride (Tf_2O) to afford the benzyl derivative **1248**. Palladium(0)-catalyzed

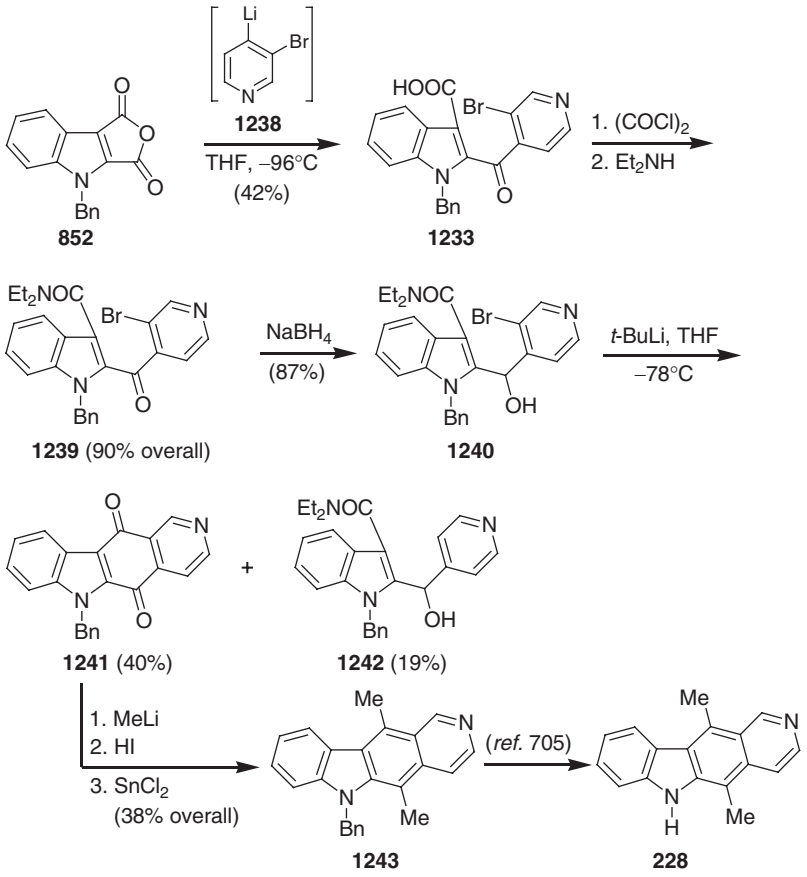

Scheme 5.205

cross-coupling of **1248** with (1-ethoxyvinyl)tributyltin (**1236**), followed by cyclization of the intermediate ethoxyvinyl derivative with 10% hydrochloric acid, afforded 6-benzyl-3-methoxyolivacine (**1249**) in 84% yield. Debenzylation of **1249** with 47% hydrobromic acid afforded 3-methoxyolivacine (**1250**). After *O*-demethylation of **1250**, the corresponding hydroxy derivative was transformed to the triflate, which on subsequent hydrogenation with ammonium formate in the presence of $Pd(PPh_3)_4$ in hot methanol afforded olivacine (**238a**) (717) (Scheme 5.206).

For the synthesis of ellipticine (**228**) (718), the required 2,4-dimethoxy derivative **1251** was prepared in three steps, and 76% overall yield, starting from the previously known ketone **1246** (717). Thus, regioselective demethylation of **1246** with 47% hydrobromic acid in hot acetic acid, followed by treatment with triflic anhydride (Tf_2O), gave the corresponding triflate, which, on reduction with ammonium formate in the presence of $Pd(PPh_3)_4$, was transformed to the 2,4-dimethoxy derivative **1251**. Selective *O*-demethylation of the 4-methoxy group of **1251** was performed by treatment with boron tribromide to provide the 4-hydroxy compound **1252**. After Wittig olefination of the keto derivative **1252**, the corresponding olefin was subjected to catalytic hydrogenation in the presence of Adam's catalyst (PtO_2) to afford the corresponding ethane derivative **1253**. The 4-hydroxy derivative was

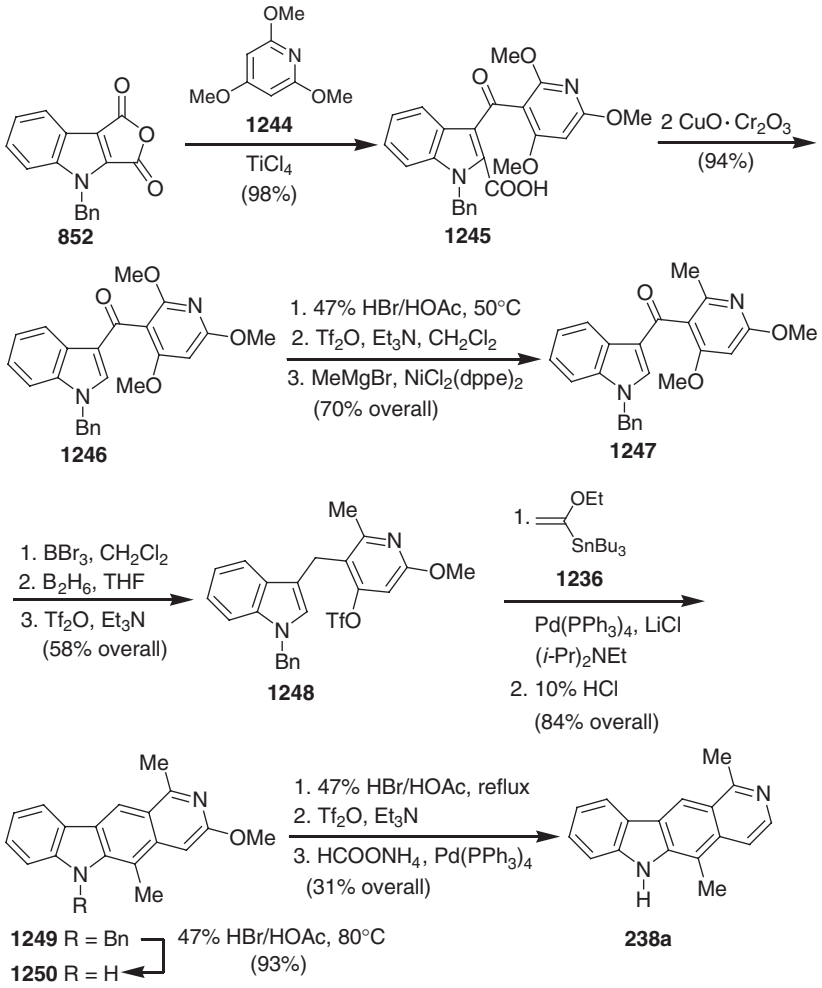

Scheme 5.206

transformed to the corresponding triflate, by reaction with triflic anhydride (Tf_2O) in the presence of triethylamine, which, on palladium(0)-catalyzed cross-coupling with (1-ethoxyvinyl)tributyltin (**1236**), followed by cyclization of the intermediate ethoxyvinyl derivative with 10% hydrochloric acid, afforded 6-benzyl-3-methoxyellipticine (**1254**) in 71% overall yield. Finally, 6-benzyl-3-methoxyellipticine (**1254**) was transformed to ellipticine (**228**) in 22.5% overall yield by executing the similar reaction sequence as shown for the conversion of 6-benzyl-3-methoxyolivacine (**1249**) to olivacine (**238a**) (717) (see Scheme 5.206) (718) (Scheme 5.207).

Ishikura *et al.* reported the total synthesis of ellipticine (**228**) starting from *N*-Boc indole (**1256**) and the vinyl bromide **1258** (719–721). This methodology involves a palladium-catalyzed, tandem cyclization-cross-coupling reaction of the indolyl borate **1257** with the vinyl bromide **1258** as the key step. Using a literature procedure, the vinyl bromide **1258** was prepared as an *E*/*Z* mixture starting from *cis*- and *trans*-crotyl alcohol. The indolyl borate **1257** was generated *in situ* from

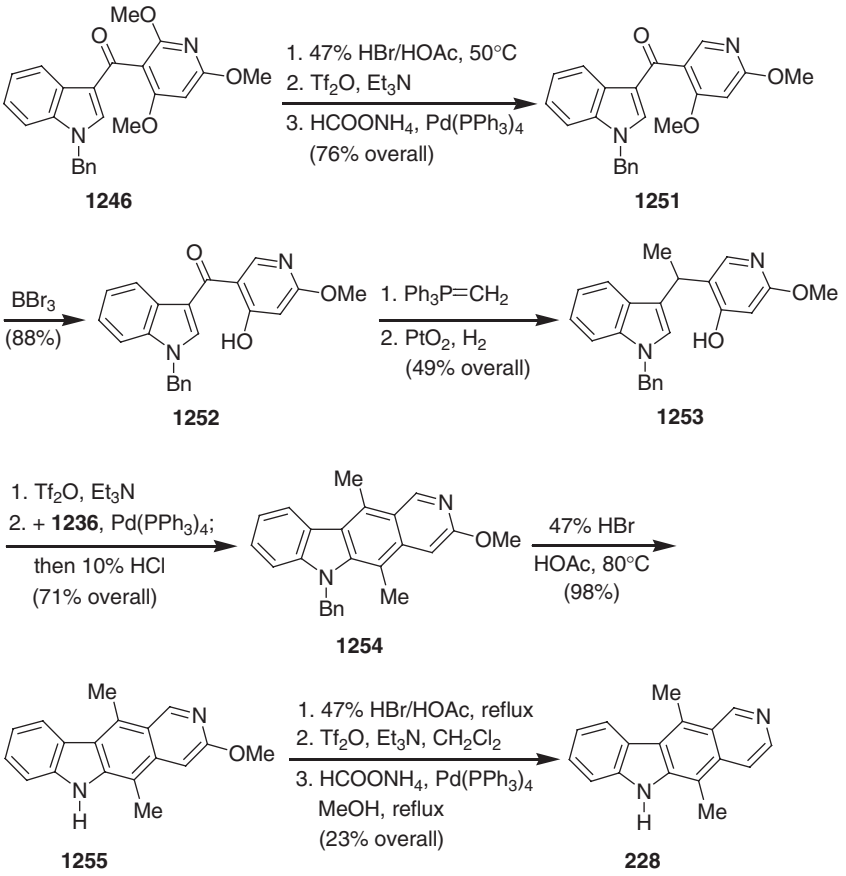

Scheme 5.207

N-Boc indole (**1256**) and *tert*-butyllithium, followed by treatment with triethylborane. A palladium-catalyzed, tandem cyclization-cross-coupling reaction by heating compound **1257** with the vinyl bromide **1258** in the presence of catalytic amounts of bis(triphenylphosphine)palladium(II) chloride provided the hexatriene **1259** in 64% yield. Photolytic electrocyclization of the hexatriene **1259** led to the tetrahydropyridocarbazole **1260**. Deprotection of **1260** by sequential removal of the Boc and benzyloxycarbonyl (Cbz) groups, and subsequent dehydrogenation, led to ellipticine (**228**) in low yield. The low yield of this step was ascribed to the presence of the free indole NH. Thus, reversal of the deprotection sequence starting from the same tetrahydropyridocarbazole **1260** led to ellipticine in an improved yield over three steps (719–721) (Scheme 5.208). This methodology was also applied to the synthesis of 6-methylellipticine derivatives starting from 1-methylindole (721).

Guitián *et al*. reported a total synthesis of ellipticine (**228**) using a modified Gribble methodology (722,723). This approach applied 2-chloro-3,4-pyridyne (**1267**) as a synthetic equivalent for 3,4-pyridyne and used the polar effect of the chlorine atom for improved yields and regiocontrol of the cycloaddition with the furoindole **544**. Silylation of 2-chloro-3-hydroxypyridine (**1263**), followed by treatment of **1264** with LDA, afforded the 4-trimethylsilylpyridine **1265**. This reaction probably involves

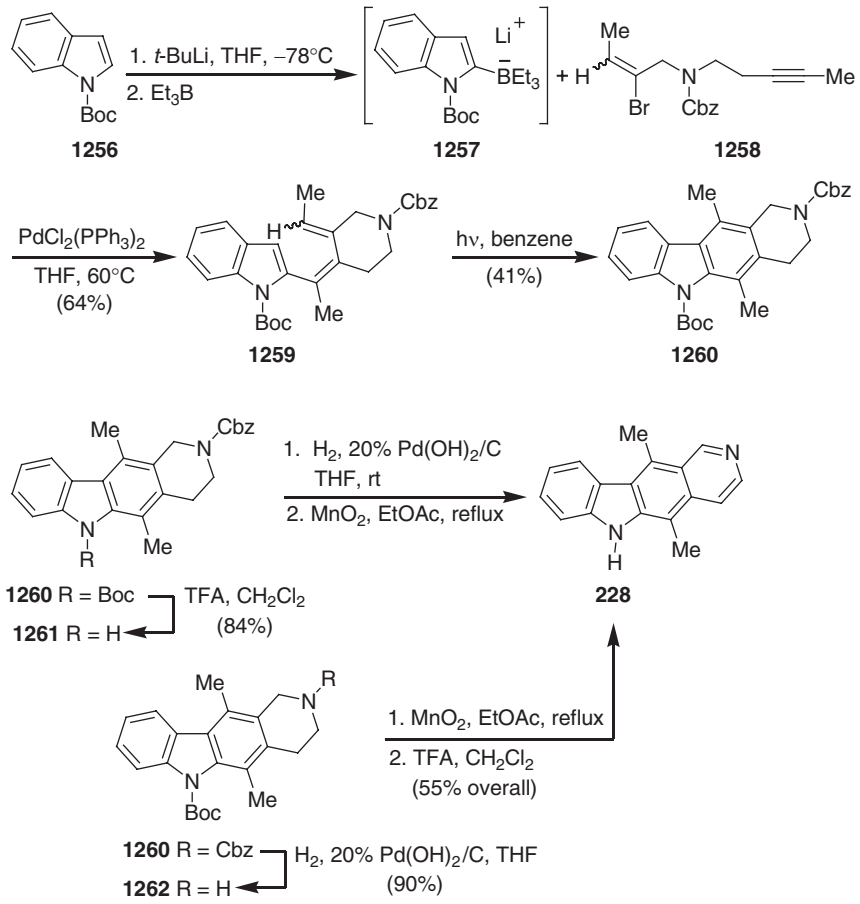

Scheme 5.208

proton abstraction at C-4 and subsequent migration of the TMS group. After transformation to the triflate **1266**, the 2-chloro-3,4-pyridyne (**1267**) is easily formed using Kobayashi's method by treatment with fluoride. The reaction of *in situ*-generated 2-chloro-3,4-pyridyne (**1267**) with the furoindole **544** provided the two regioisomers **1268** and **1269** in a ratio of 2.4:1 (89% yield). Reductive cleavage of the ether bridge of the major product **1268** with sodium borohydride and sodium hydroxide, followed by hydrogenolysis to remove the chlorine substituent, provided ellipticine (**228**) in 87% overall yield. The minor adduct **1269** was transformed to isoellipticine (**1196**) in 65% overall yield by the same sequence of steps (722,723) (Scheme 5.209).

Three years later, the same authors also reported a modified Moody approach for the total synthesis of ellipticine (**228**). In this route, an indolopyrone is used as a stable equivalent of indolo-2,3-quinodimethane in a Diels–Alder reaction with 2-chloro-3,4-pyridyne (**1267**) (723).

Mal *et al.* reported a formal total synthesis of ellipticine (**228**) starting from the furoindolone **649** (583,724). In this strategy, the key step is the anionic [4+2] cycloaddition of furoindolone **649** with 3,4-pyridyne (**1193**). Reaction of compound **1270** with 3,4-pyridyne (**1193**) in the presence of LDA gave ellipticine quinone (**1272**)

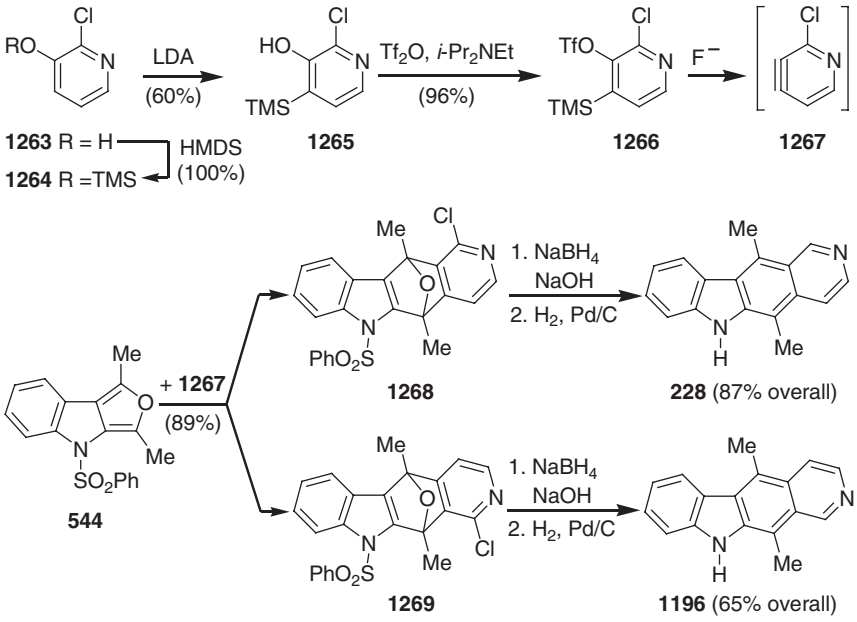

Scheme 5.209

and isoellipticine quinone (**1273**) in a ratio of 2:1 (45% combined yield). Previously (725–727), the quinones **1272** and **1273** were transformed to ellipticine (**228**) and isoellipticine (**1196**) (583,724) (Scheme 5.210).

Bennasar *et al*. reported a formal total synthesis of ellipticine (**228**) starting from the 3-formylindole **1274** (728). In this route, the key reaction is the regioselective, intramolecular cyclization of the 2-indolylacyl radical (*in situ* generated from *N*-benzyl selenoester **1278**) onto the 4-position of the pyridine ring. Reaction of **1274** with 3-pyridylmagnesium bromide (**1275**), followed by triethyl silane reduction of the resulting carbinol **1276**, led to the ester **1277** in 55% yield. Hydrolysis of **1277**, followed by phenylselenation of the corresponding carboxylic acid, gave the selenoester **1278**. The 2-indolylacyl radical generated from the corresponding *N*-benzyl selenoester **1278** under hexabutylditin–*hν* conditions underwent regioselective intramolecular reaction with pyridine to afford directly *N*-benzylellipticine quinone (**1241**). As previously described (705,716,729), the *N*-benzylellipticine quinone (**1241**) was transformed into ellipticine (**228**) (728) (Scheme 5.211).

One year later, the same authors extended the aforementioned methodology to the total synthesis of (±)-guatambuine (**233**) starting from the 3-formylindole **1279** (213). Executing a similar reaction sequence as shown for the formal total synthesis of ellipticine (**228**) (see Scheme 5.211), the 3-formylindole **1279** was transformed to the pyridylmethylindole **1281** in two steps in 50% overall yield. After quaternization of the pyridine nitrogen with methyl iodide, the *N*-methylpyridinium salt **1282** was reacted with methylmagnesium chloride, followed by reduction of the intermediate 2,3-disubstituted dihydropyridine, to afford the tetrahydropyridine **1283**. Hydrolysis of **1283** led to the corresponding carboxylic acid, which, on phenylselenation, afforded the selenoester **1284**. Radical cyclization of **1284** in dilute benzene solution led to the stereoisomeric mixture of pyridocarbazoles **1285**. Probably, this reaction

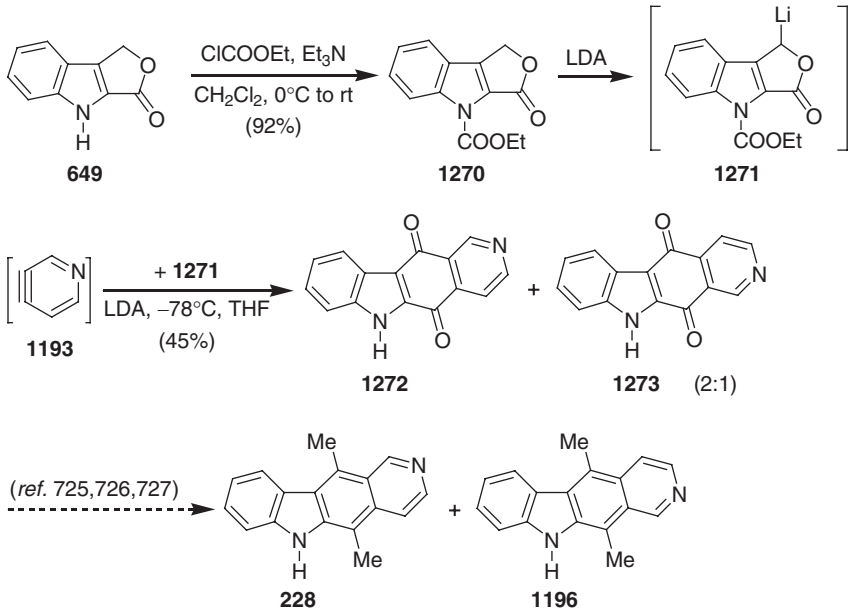

Scheme 5.210

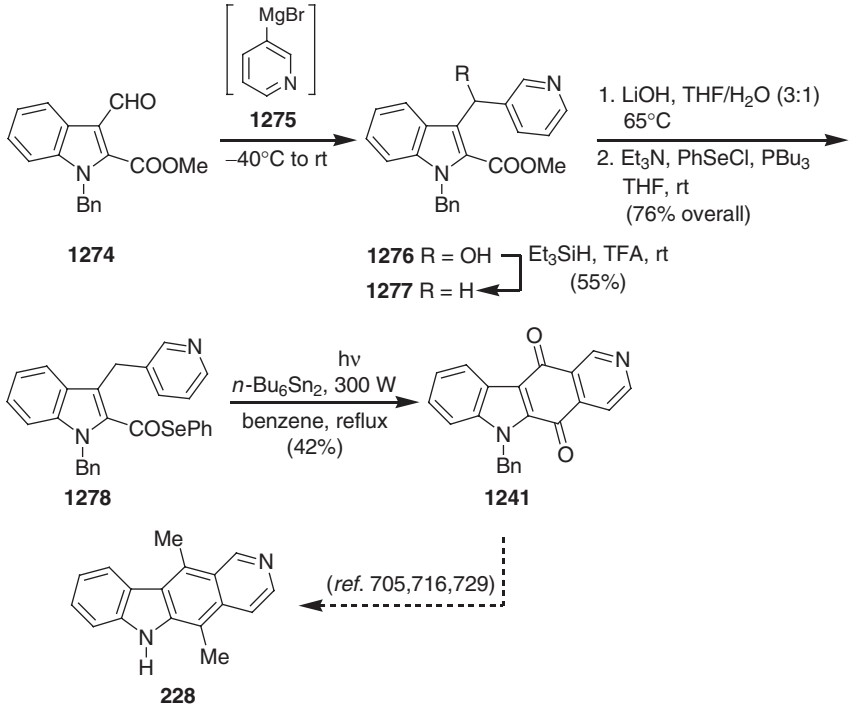

Scheme 5.211

proceeds through the formation of a 2-indolylacyl radical which could initiate the desired 6-endo cyclization without interference of the indole NH. Finally, the pyridocarbazole **1285** was transformed into (±)-guatambuine (**233**) by reaction with methyllithium, followed by TFA-Pd/C-promoted dehydration of the carbinol with concomitant dehydrogenation (213). Previously (211,376), (±)-guatambuine (**233**) was transformed to olivacine (**238a**) by dealkylative aromatization (213) (Scheme 5.212).

Bowman *et al*. reported the total synthesis of ellipticine (**228**) involving an imidoyl radical cascade reaction (730). For this key step, the required imidoyl radical was generated from the imidoyl selanide **1290**, which was obtained from ethyl 2-(4-pyridyl)acetate (**1286**). Reaction of **1286** with LDA, followed by addition of methyl iodide, led to the corresponding methyl derivative **1287**. Treatment of **1287** with 2-iodoaniline (**743**) in the presence of trimethylaluminum ($AlMe_3$) afforded the amide **1288**. Using Sonogashira conditions, propyne is coupled with the amide **1288** to afford the aryl acetylene **1289**. The aryl acetylene **1289** was transformed to the

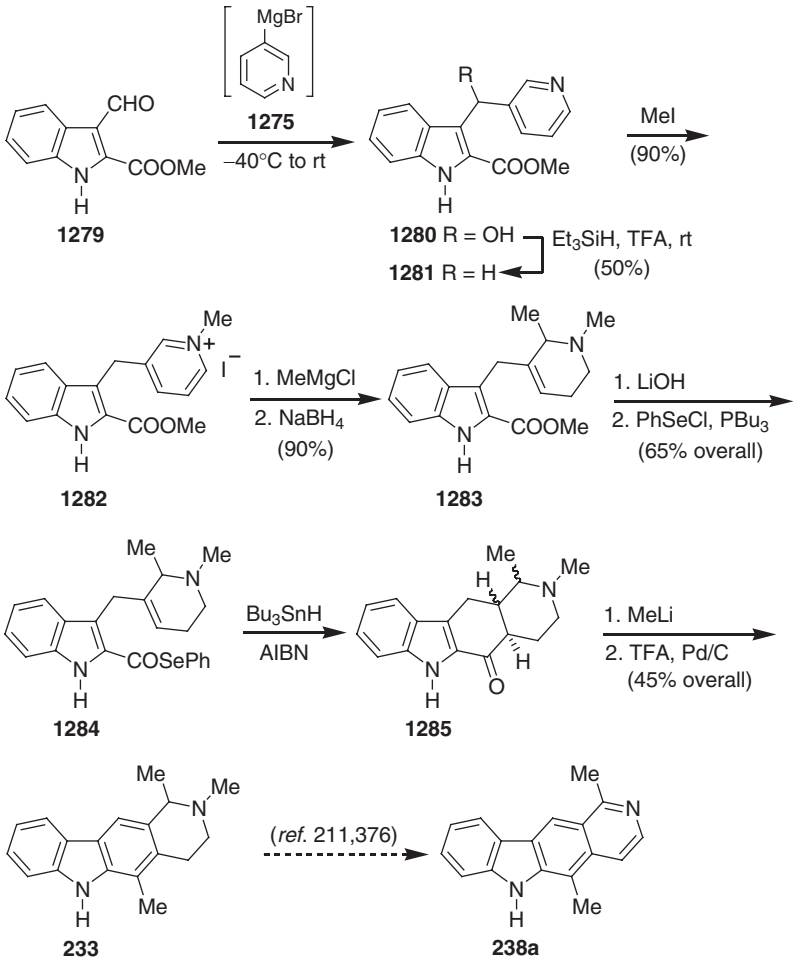

Scheme 5.212

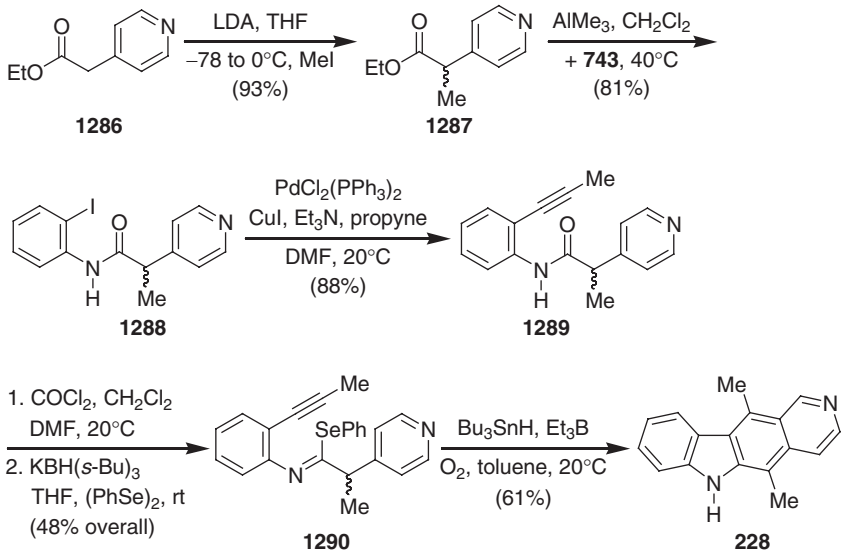

Scheme 5.213

imidoyl selanide **1290** by reaction with oxalyl chloride followed by K-Selectride treatment in the presence of diphenyl diselenide. Finally, in a one-pot operation, the imidoyl selanide **1290** was transformed to ellipticine (**228**) by reaction with tributyltin hydride in the presence of the radical initiator triethylborane (730) (Scheme 5.213).

Ho and Hsieh reported a total synthesis of ellipticine (**228**) starting from 4,7-dimethyl-1*H*-indene (731). In this route, the key step is the deoxygenative cyclization of the *o*-nitrobiaryl **1297** using Cadogan's method. 4,7-Dimethyl-indan-2-one (**1292**), which was obtained by oxidation of the corresponding indene, was reduced to the alcohol **1293** in the presence of sodium borohydride in almost quantitative yield. After iodination of **1293**, the corresponding iodo derivative **1294** was transformed to the acetate **1295**. Suzuki coupling of **1295** with 2-nitrobenzeneboronic acid (**1296**) afforded the nitrobiaryl **1297** in 79% yield. Reductive cyclization of **1297** by heating in the presence of triethylphosphite [$P(OEt)_3$] led to the carbazole **1298**. Oxidation of **1298** with DDQ, followed by *in situ* reduction of the keto acetate, led to the diols **1299**. Oxidation of **1299** with sodium periodate ($NaIO_4$), followed by reaction of the intermediate dicarbonyl derivative with ammonium acetate (NH_4OAc), resulted in ellipticine (**228**) (731) (Scheme 5.214).

In addition to the aforementioned total syntheses of naturally occurring pyrido[4,3-*b*]carbazole alkaloids, various groups have also developed synthetic strategies towards a range of pyrido[4,3-*b*]carbazole analogs (732–755).

H. Indolo[2,3-*a*]carbazole Alkaloids

Since the first isolation and the discovery of the potent inhibitory activity of the microbial alkaloid staurosporine (**295**) against protein kinase C (PKC), the indolo[2,3-*a*]carbazole alkaloids have emerged as a rapidly growing family. This was attested to by the isolation of about 70 natural products. In addition to this large

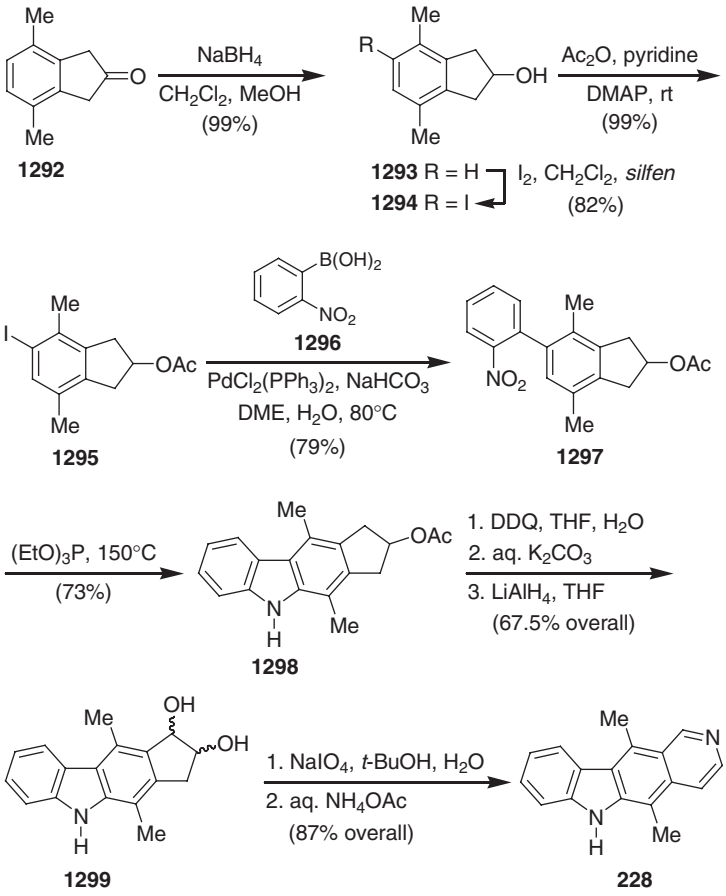

Scheme 5.214

number of natural products, a wide range of structural analogs was also reported due to their diverse and, in some cases, extraordinary biological activity. Because of this, a wide range of approaches has been developed for the synthesis of natural products as well as synthetic analogs of indolo[2,3-*a*]carbazole alkaloids. The explosive growth of this class of carbazole alkaloids was attested by the publication of various review articles covering different aspects (252–260,756–758). The present section describes a detailed discussion of the synthetic activity with regard to these natural products published since 1990.

Raphael *et al.* reported the total synthesis of arcyriaflavin B (**346**) (759) and staurosporinone (**293**) (760) starting from 2-nitrocinnamaldehyde (**1300**). This synthetic route involves a double nitrene insertion as the key step.

Wittig olefination of 2-nitro-Z-cinnamaldehyde (**1300**) with the phosphonium bromide **1301** led to the diene **1302**. The Diels–Alder cycloaddition of **1302** with maleimide (**1303**), followed by dehydrogenation with DDQ, afforded the phthalimide **1304**. Double deoxygenation of **1304** with triphenylphosphine (PPh_3) in collidine gave *O*-methylarcyriaflavin B (1**305**). Finally, heating of **1305** with molten pyridine hydrochloride led to arcyriaflavin B (**346**) (759) (Scheme 5.215).

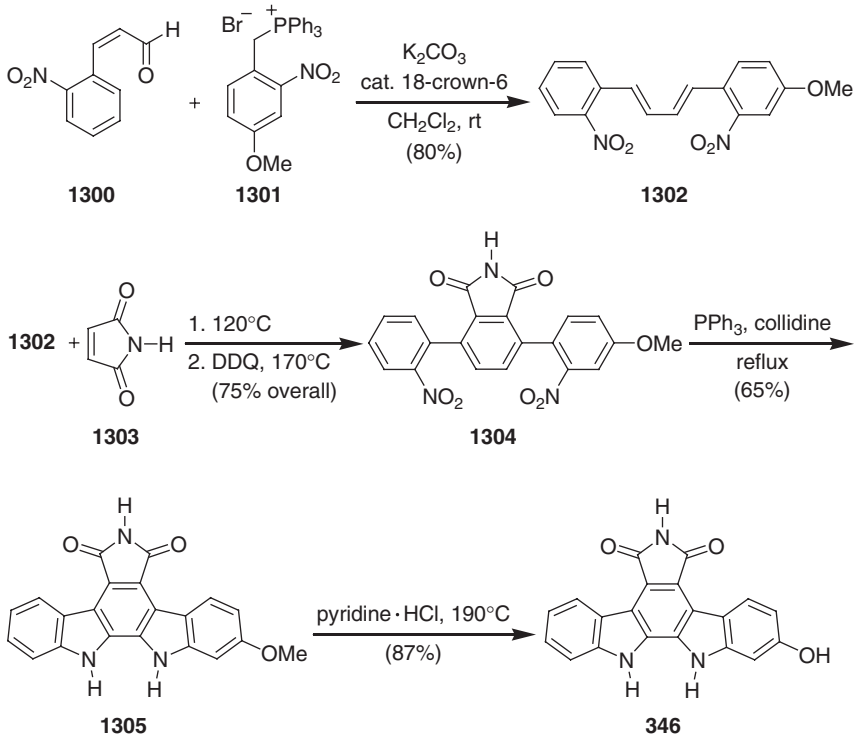

Scheme 5.215

Due to the difficulties associated with the removal of *N*-maleimide protecting groups and reduction of the imide to the lactam, Raphael *et al.* modified their method in 1990 for the synthesis of staurosporinone (**293**) (760). In this approach, the key steps are a Diels–Alder cycloaddition of dimethyl acetylenedicarboxylate (**535**) with 1,4-bis(*o*-nitrophenyl)butadiene (**1307**), conversion to the imide **1309** through the anhydride by reacting with ammonia, reduction to the lactam **1310**, and the final transformation to staurosporinone (**293**). Direct deoxygenation of the lactam **1310** to staurosporinone (**293**) proceeded well. However, the staurosporinone (**293**) produced formed a complex with the generated triphenylphosphine oxide. Due to this separation problem, prior to deoxygenation, the lactam **1310** nitrogen was protected as a tetrahydropyran-2-yl (THP) group. Thus, smooth deoxygenation of **1311** with triphenylphosphine (PPh_3) led to the THP-protected staurosporinone **1312**, which was readily transformed to staurosporinone (**293**) by aqueous sulfuric acid treatment (760) (Scheme 5.216).

Bergman *et al.* reported a synthesis of arcyriaflavin A (**345**) starting from indol-3-ylacetic acid (**680**) or the corresponding methyl ester (**1313**) (339). The key step of their methodology is an oxidative coupling of the indol-3-ylacetic acid trianion (**1314**) or the methyl indol-3-ylacetate dianion (**1315**). Sequential addition of 2 equivalents of butyllithium and 1 equivalent of *tert*-butyllithium to indol-3-ylacetic acid generated the trianion **1314**. Iodine-mediated oxidative coupling of **1314**, followed by acidic work-up, afforded the diacid **1316**. Treatment of **1316** with diazomethane led to bisindolylsuccinic acid methyl ester **1317** in 38% overall yield as a diastereomeric

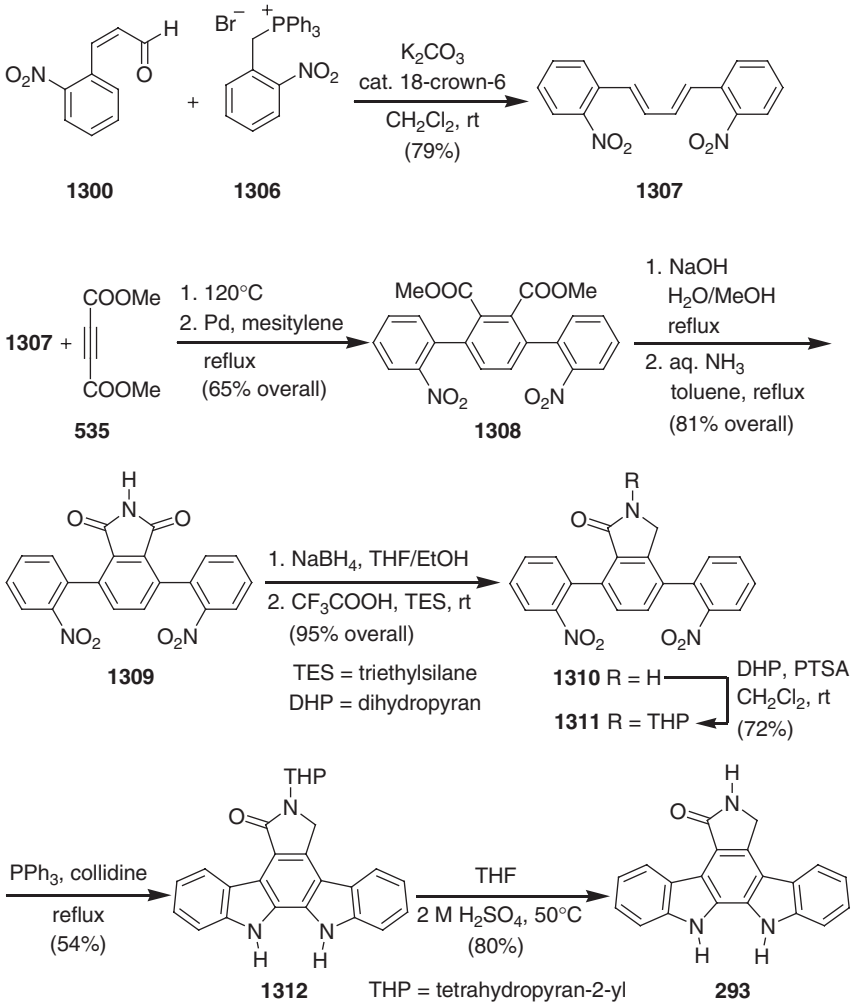

Scheme 5.216

mixture. However, the diester **1317** could be prepared directly in much better yield (85%) by the iodine-promoted, oxidative coupling of the dianion **1315**, obtained by the addition of 2 equivalents of LDA to methyl indol-3-ylacetate (**1313**). Heating of the diastereomeric mixture of diester **1317** with ammonium formate in refluxing triglyme led exclusively to the *trans*-imide **1318** indicating the cyclization of one of the two diastereoisomers to the imide. After dehydrogenation of **1318** with DDQ, the resulting arcyriarubin A (**349**) was hydrogenated to afford the required *cis*-succinimide **1319**. Finally, reaction of **1319** with refluxing TFA led to arcyriaflavin A (**345**) in 75% yield (339) (Schemes 5.217 and 5.218).

Moody and Rahimtoola reported a short synthesis of staurosporinone (**293**) without the use of protecting groups at the indole or the lactam nitrogen (761,762). This route involves an intramolecular Diels–Alder reaction of the pyrano[4,3-*b*]indol-3-one **1325** and a subsequent cyclization by nitrene insertion. The pyrano[4,3-*b*]indol-3-one **1325** was obtained in four steps from ethyl indol-2-yl

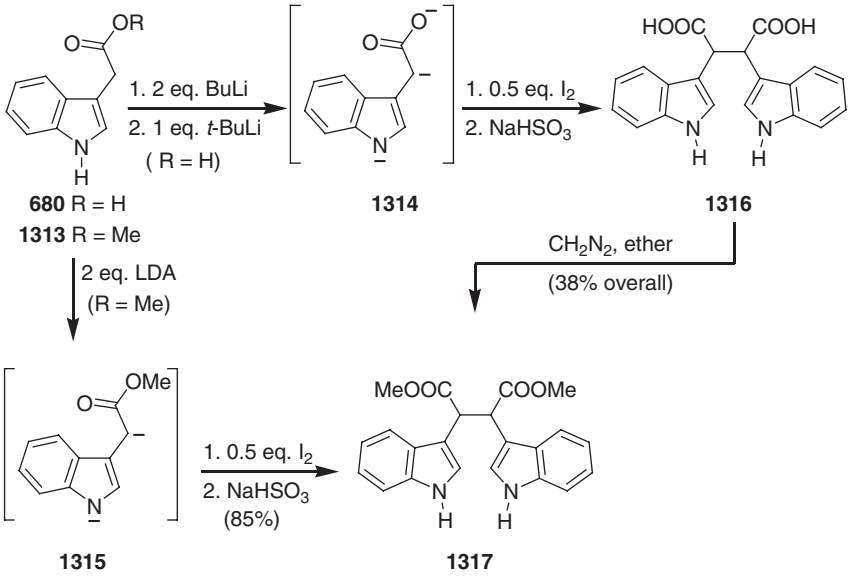

Scheme 5.217

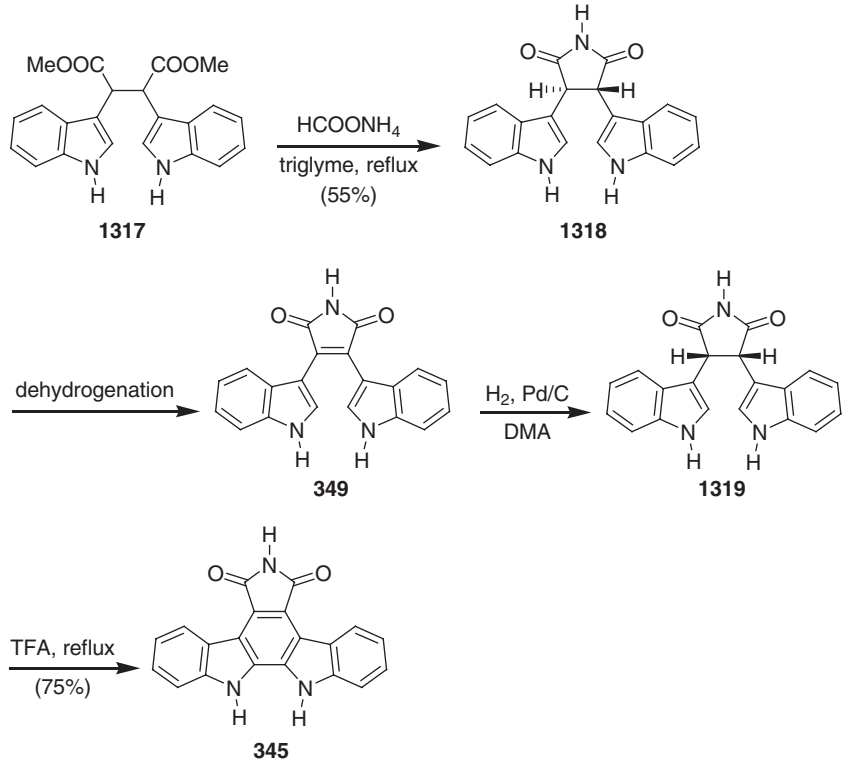

Scheme 5.218

acetate (**1322**). Reaction of **1322** with oxalyl chloride, followed by quenching with 2-nitrocinnamylamine (**1321**) [available in three steps from commercial 2-nitrocinnamaldehyde (**1320**)], afforded the 2,3-disubstituted indole **1323**. Hydrolysis of the ester **1323**, followed by cyclodehydration of the keto acid **1324** with acetic anhydride, led to the pyrano[4,3-*b*]indol-3-one **1325**. The intramolecular Diels–Alder reaction of the pyrano[4,3-*b*]indol-3-one **1325** with concomitant loss of carbon dioxide by heating in bromobenzene under reflux, and a subsequent aromatization by oxidation in air, gave the carbazole **1326**. Cyclization of **1326**, by Cadogan's method through heating in triethyl phosphite, provided staurosporinone (K-252c) (**293**) (761,762) (Scheme 5.219).

Bonjouklian and Moore *et al*. reported the total synthesis of the tjipanazoles D (**359**) and E (**370**) to support the assigned structures for these natural products. Condensation of 2 equivalents of 4-chlorophenylhydrazine hydrochloride (**1327**) with 1,2-cyclohexanedione (**1328**) in the presence of air and step-wise Fischer indolization provided tjipanazole D (**359**) in 54% yield. Coupling of **359** with

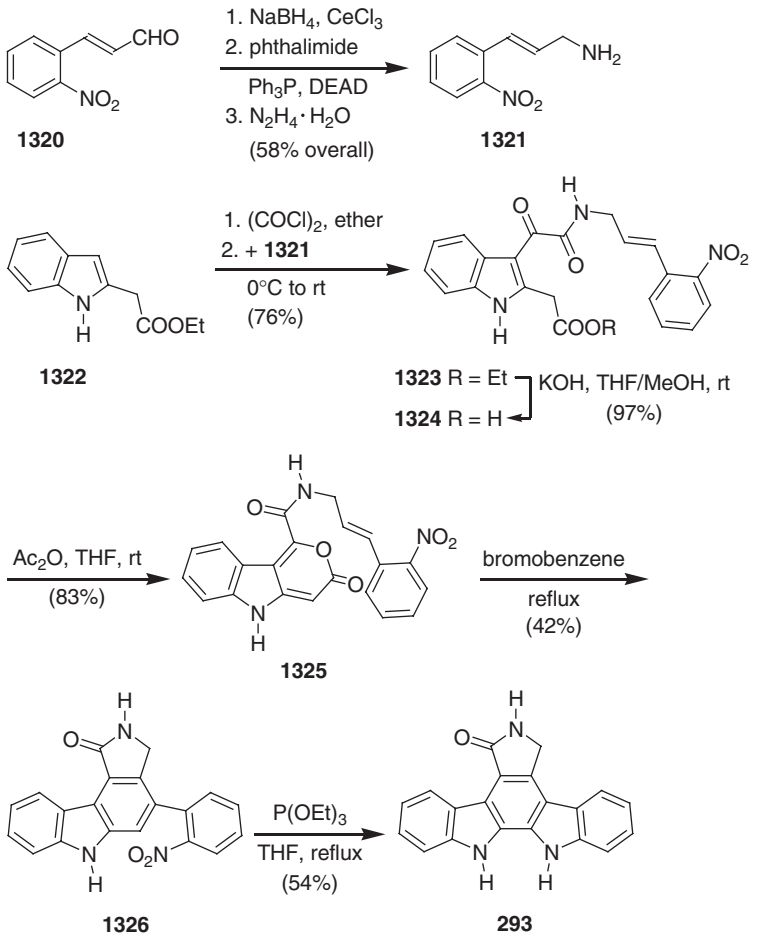

Scheme 5.219

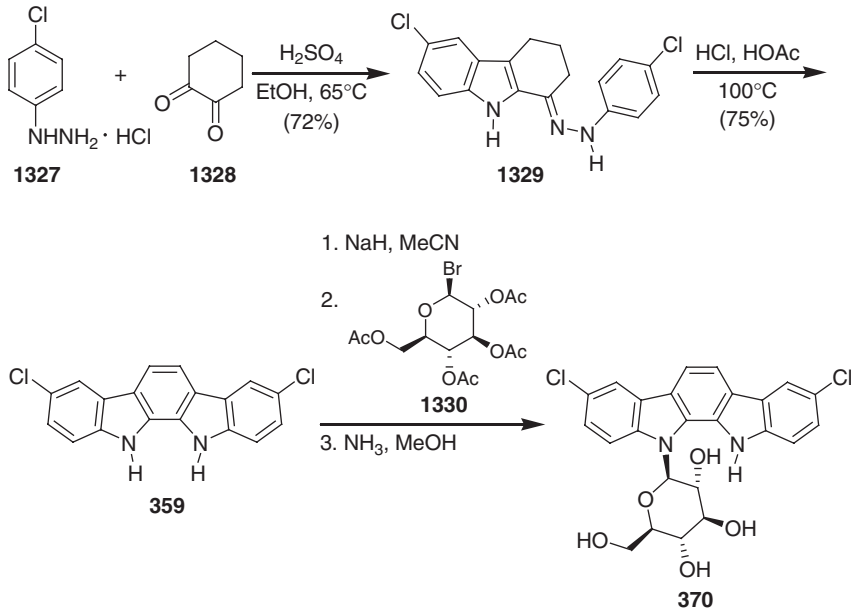

Scheme 5.220

1-bromo-α-D-glucopyranosyl-2,3,4,6-tetraacetate (**1330**), followed by removal of the acetyl protecting groups, led to tjipanazole E (**370**) (329) (Scheme 5.220).

Gribble and Berthel reported the synthesis of arcyriaflavin A (**345**) starting from the commercially available cyclohexene imide **1331** involving double Fischer indolization as key step (336). Although this approach is much shorter, the overall yield is lower. The cyclohexene derivative **1331** was converted to the labile dialdehyde **1332**, which, on further treatment with 2 equivalents of phenylhydrazine (**524**), led to the corresponding bis(phenylhydrazones) **1333**. Double Fischer indolization of **1333** with polyphosphoric acid trimethylsilyl ester (PPSE) in nitromethane under reflux provided arcyriaflavin A (**345**) (336) (Scheme 5.221). This methodology was also applied to the synthesis of 6-methylarcyriaflavin (AT2433-B aglycon) (336).

Danishefsky *et al.* described the total synthesis of rebeccamycin (**337**) using a stereoselective opening of the α-1,2-anhydrosugar **1339** with the sodium salt of the secoaglycon **1338** (763). Following Clardy's and Kaneko's procedure (325), starting from 7-chloroindole (**1334**), the secoaglycon **1338**, a precursor of rebeccamycin (**337**), was obtained in 59% overall yield in three steps. This method involves sequential indole Grignard additions to *N*-(benzyloxymethyl)dibromomaleimide (**1335**). Thus, deprotonation of 7-chloroindole (**1334**) with methylmagnesium iodide and addition of *N*-(benzyloxymethyl)dibromomaleimide **1335** afforded the monoindolyl derivative **1336**. After protection of the indole nitrogen with a SEM group to **1337**, 7-chloroindolemagnesium iodide was added to afford the secoaglycon **1338**.

The stereoselective glycosidation of the secoaglycon **1338** was achieved by reaction of the sodium salt of **1338** with the α-1,2-anhydrosugar **1339** to give the β-glucopyranoside **1340** in 48% yield. After the removal of the SEM protecting group with TBAF, the photocyclization of compound **1341** afforded the indolocarbazole

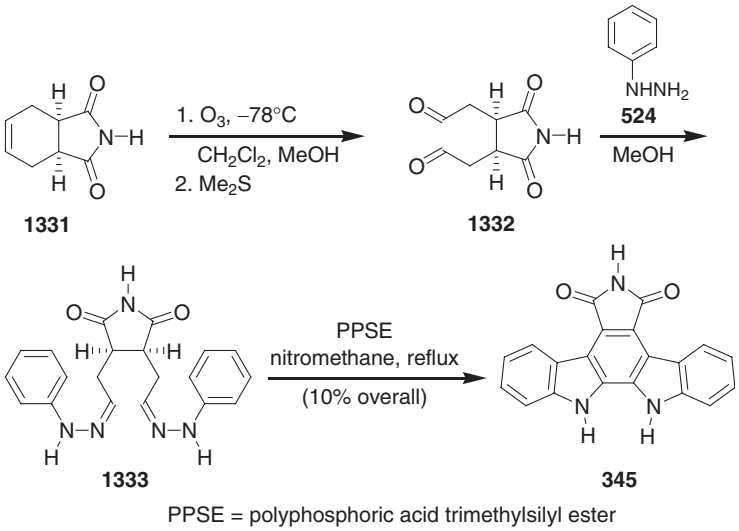

Scheme 5.221

glucopyranoside **1342**. Hydrogenation of **1342** over Pearlman's catalyst [$Pd(OH)_2$], followed by ammonolysis to complete the BOM deprotection, provided rebeccamycin (**337**) in 72% yield (763) (Scheme 5.222).

Danishefsky *et al*. also reported the first total synthesis of (+)-staurosporine (**295**) (764,765). This synthesis involves the preparation of the staurosporine secoaglycon **1343**, and sequential coupling of oxazolidinone glycol **1344** with the indolic nitrogens of the aglycon acceptor **1343**. Using sequential indole-Grignard additions to *N*-(benzyloxymethyl)dibromomaleimide, the unsymmetrical secoaglycon **1343** was obtained in three steps and 57% overall yield (see the synthesis of the secoaglycon **1338** in Scheme 5.222).

The glycosylation was achieved by reaction of the sodium salt of **1343** with the 1,2-anhydrosugar **1344**. The C2′-hydroxy function was removed from the indole glycoside **1345** by Barton deoxygenation to afford compound **1346**. Deprotection by removal of the C6′-PMB and the indole-SEM groups, followed by photocyclization of **1347**, provided the indolocarbazole glycoside **1348**. The alcohol was transformed into the iodo derivative **1349**, which, on subsequent elimination of hydrogen iodide with 1,8-diazabicyclo[5.4.0]undec-7-ene (DBU), afforded the exo-glycal **1350** (Scheme 5.223). The intramolecular glycosylation of **1350** with potassium *tert*-butoxide in the presence of iodine provided the glycoside **1351**. Deiodination of **1351** with tri-*n*-butyltin hydride, and removal of the BOM groups led to the compound **1352**. Selective installation of a Boc group on the oxazolidinone nitrogen of **1352**, and reprotection of the maleimide nitrogen with a BOM protecting group, furnished the indolo oxazolidinone **1353**. The Boc group at the oxazolidinone ring plays a crucial role in the smooth disconnection of the oxazolidinone. Thus, the oxazolidinone in **1353** was opened with cesium carbonate in methanol to provide the hydroxy amine **1354**. *O*-Methylation and mono-*N*-methylation, cleavage of the BOM group by hydrogenation over Pearlman's catalyst, and removal of the Boc group, led to 7-oxostaurosporine (**1355**) in 70% overall yield. Reduction of the imide with sodium borohydride to the hydroxy lactam, and further reduction with phenylselenol in the

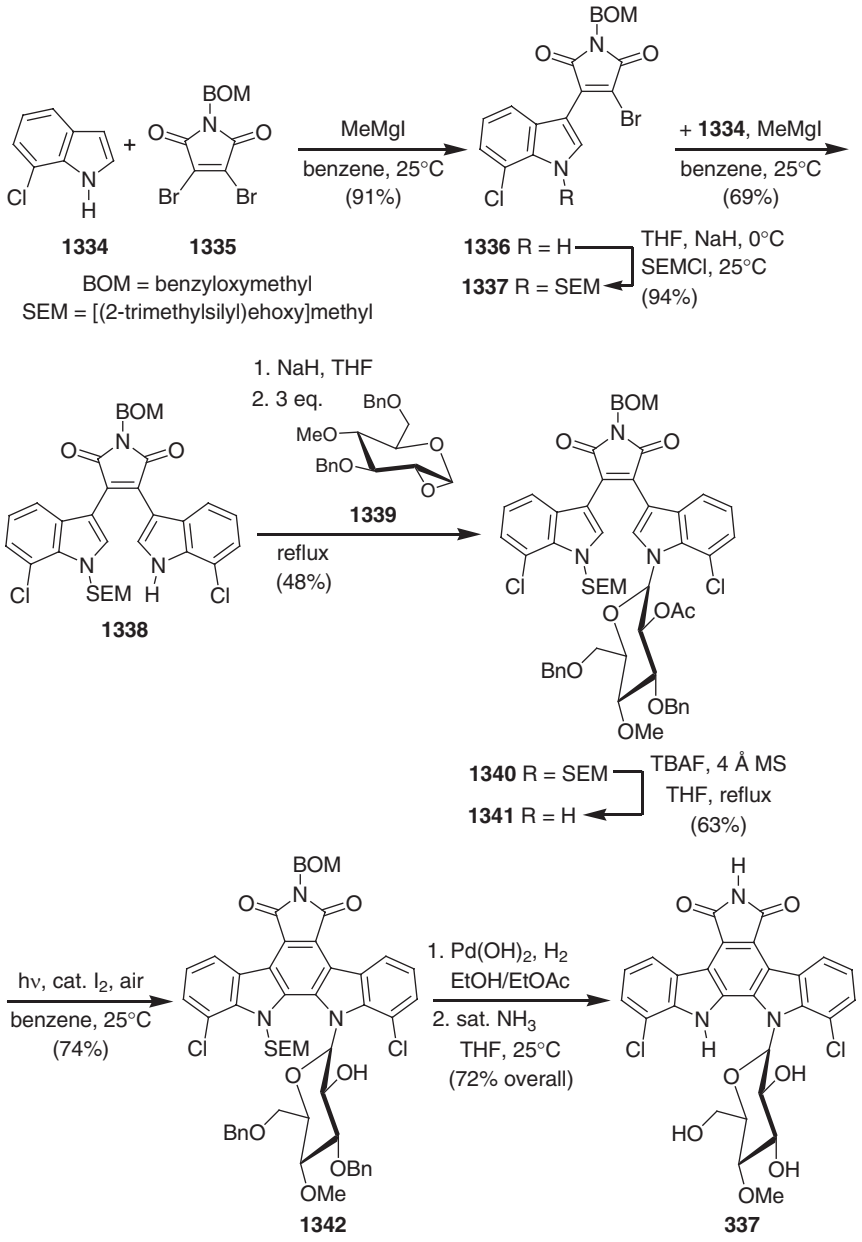

Scheme 5.222

presence of a catalytic amount of *p*-toluenesulfonic acid, provided a 1:1 mixture of (+)-staurosporine (**295**) and isostaurosporine (**1356**) (764,765) (Scheme 5.224).

Hill *et al.* reported an efficient short synthesis of staurosporinone (**293**) using a palladium-mediated oxidative cyclization of the bisindolylmaleimide arcyriarubin A (**349**) as the key step (766). The key intermediate, arcyriarubin A (**349**), was prepared

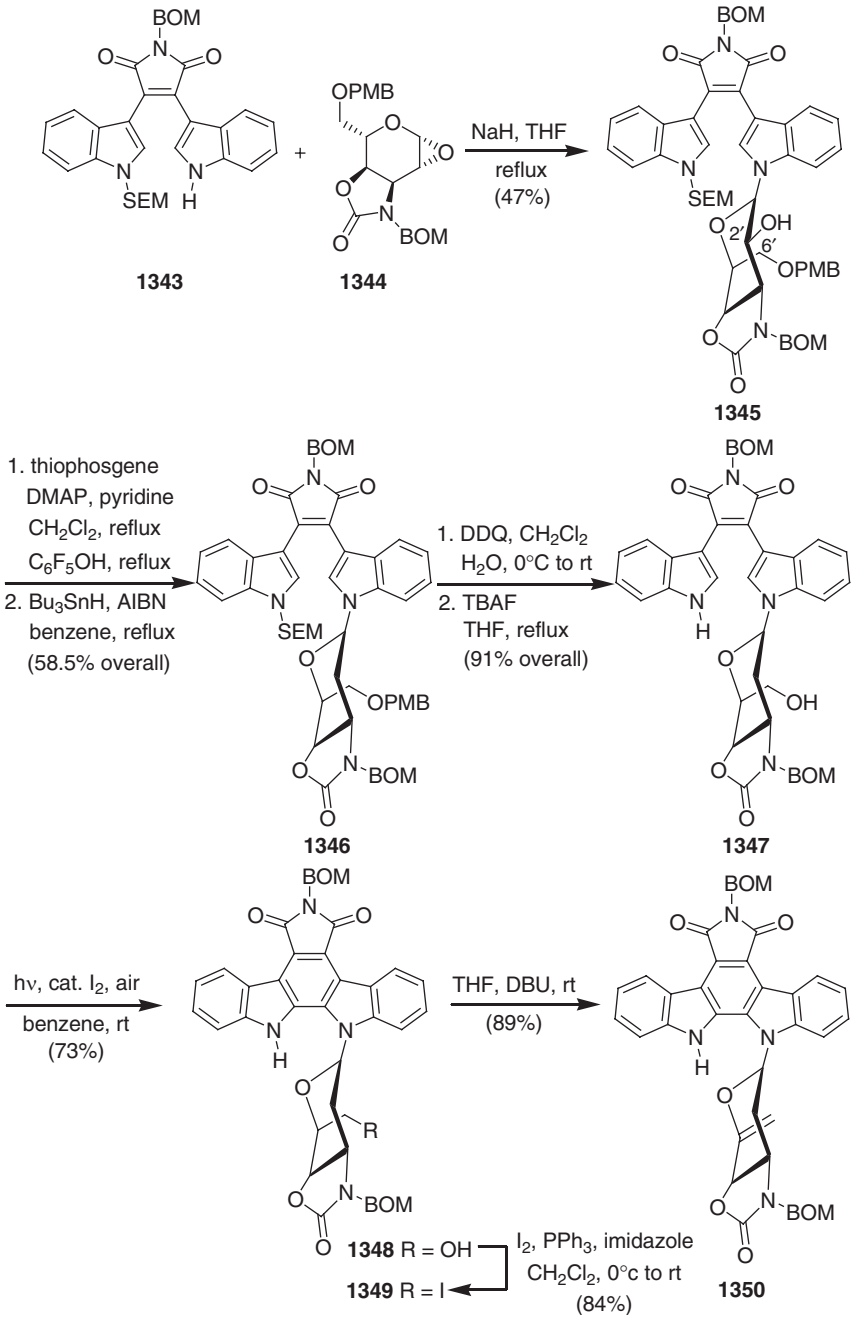

Scheme 5.223

in one step without protection of the imide nitrogen by reaction of dibromomaleimide (**1357**) with 4 equivalents of indolylmagnesium bromide (**1358**) in benzene under reflux. Oxidative cyclization of arcyriarubin A (**349**) with 1 equivalent of palladium(II) acetate in acetic acid led to arcyriaflavin A (**345**) in 75% yield.

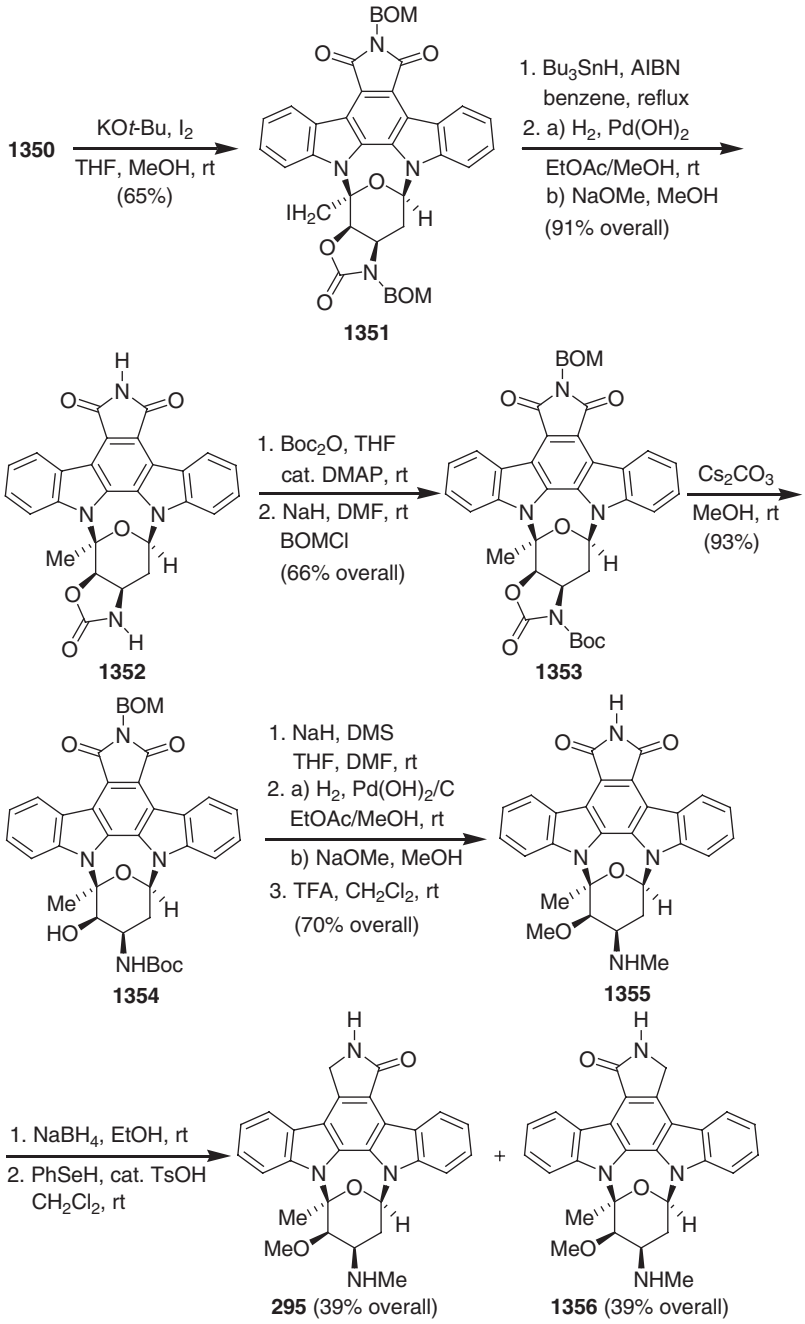

Scheme 5.224

Hydride reduction of **345**, followed by hydrogenolytic deoxygenation of the resulting hydroxylactam afforded staurosporinone (**293**) (766) (Scheme 5.225). The same sequence was applied to the synthesis of the 12-methyl analog of staurosporinone (766).

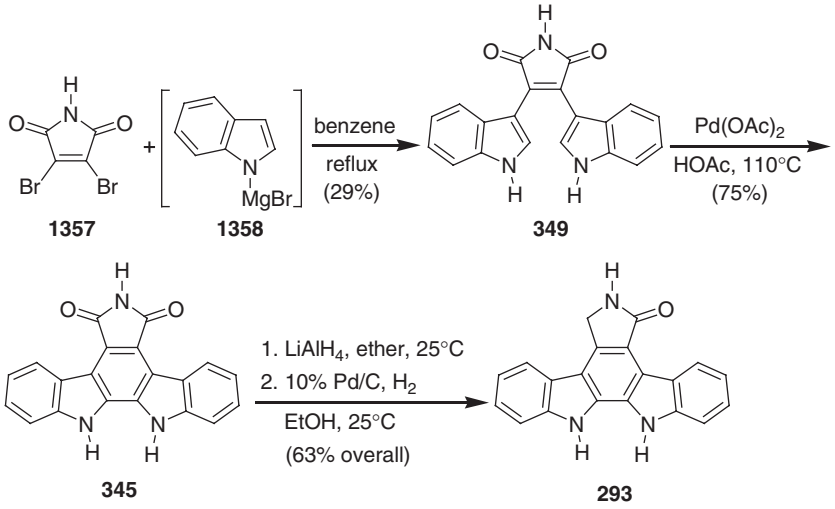

1357 **1358** **349** **345** **293**

Scheme 5.225

Xie and Lown reported a facile synthesis of staurosporinone (**293**) starting from the bisindolyl derivative **1361** (767). The key step of this synthesis is a photochemically induced oxidative cyclization of **1361**. A new coupling protocol was developed for an improved synthesis of *N*-benzyldibromomaleimide (**1359**). Thus, reaction of dibromomaleic acid with benzylamine in the presence of 1,3-dicyclohexylcarbodiimide (DCC) and a trace of DMAP afforded **1359** in 92% yield. Using the Grignard route, compound **1359** was transformed to the *N*-(benzyl)bis-indolylmaleimide (**1360**). Under alkaline conditions, compound **1360** was transformed to the bisindolyl maleic anhydride **1361**. The photolytically induced electrocyclization of **1361** in the presence of iodine as the oxidizing agent provided the indolocarbazole anhydride **1362** in 90% yield. Transformation of the anhydride **1362** to the corresponding imide by heating with ammonium acetate afforded arcyriaflavin A (**345**) in 92% yield. Finally, reduction of the symmetric imide **345** with zinc amalgam in a solvent mixture of hydrochloric acid, ethanol, and toluene at reflux led to staurosporinone (**293**) in a much improved yield (767) (Scheme 5.226).

Lobo and Prabhakar *et al.* described the synthesis of arcyriaflavin A (**345**) starting from 2,2′-bisindolyl-3,3′-dithiete (**1363**) (768,769). In a one-pot operation, heating of 2,2′-bisindolyl-3,3′-dithiete (**1363**) with maleimide (**1303**) in 1,2-dichlorobenzene at 188°C afforded arcyriaflavin A (**345**) in 36% yield. This reaction is believed to proceed *via* a Diels–Alder [4+2] adduct **1364**, followed by a retro-Diels–Alder reaction with extrusion of singlet-S_2 to 4c,7a-dihydroarcyriaflavin A (**1365**) and dehydrogenation by dissolved oxygen or extruded sulfur to arcyriaflavin A (**345**) (768,769) (Scheme 5.227). Five years later, starting from 2,2′-bisindolyl-3,3′-dithiete (**1363**), the same group developed an improved synthesis of arcyriaflavin A (**345**) by an intramolecular twofold sulfur extrusion reaction (770).

Faul *et al.* reported an improved synthesis of arcyriarubin A (**349**) by reaction of indolylmagnesium bromide (**1358**) with dichloromaleimide (**1366**). Following Hill's route, **349** was transformed to staurosporinone (**293**) in three steps and 47% overall yield (see Scheme 5.225). This approach provides, so far, the shortest access to staurosporinone (**293**) with the best overall yield (771) (Scheme 5.228).

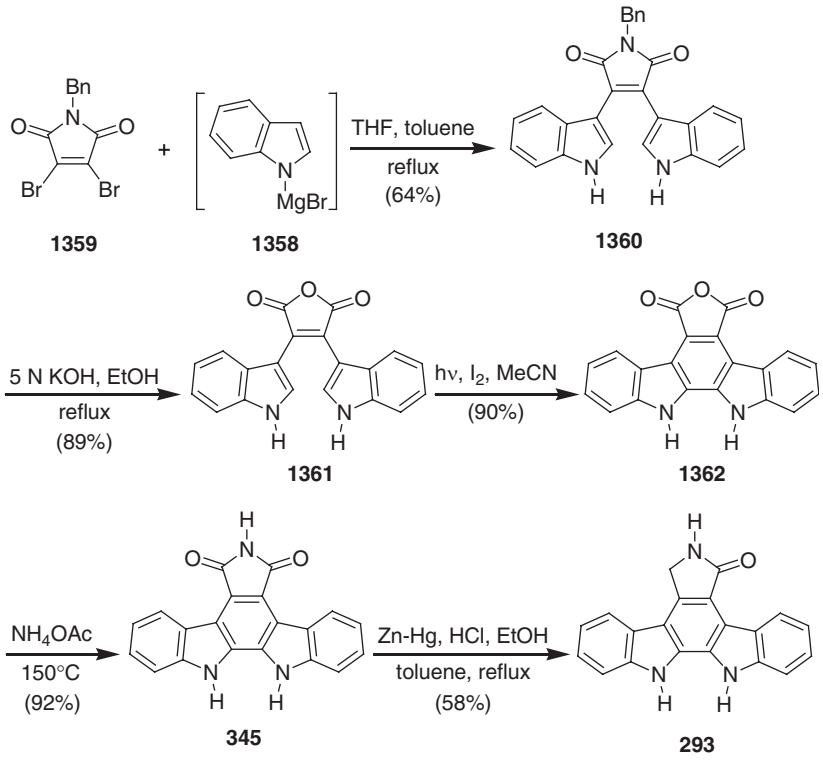

Scheme 5.226

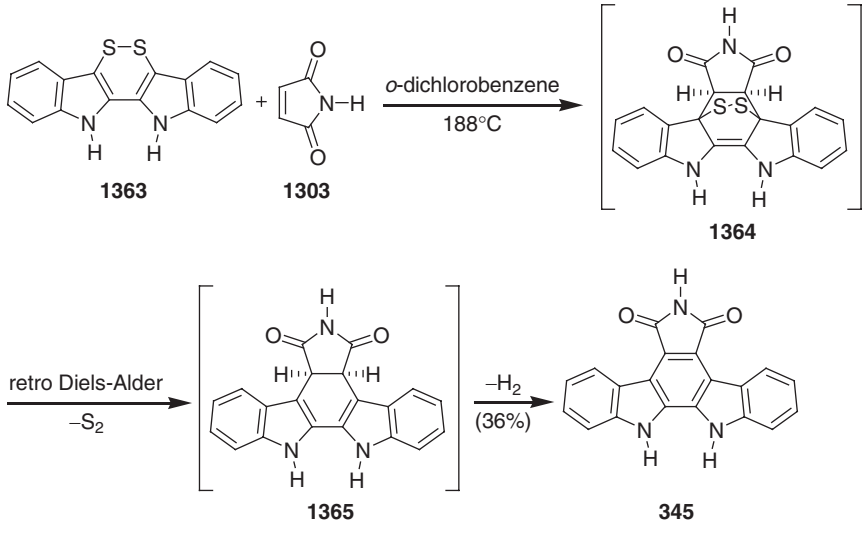

Scheme 5.227

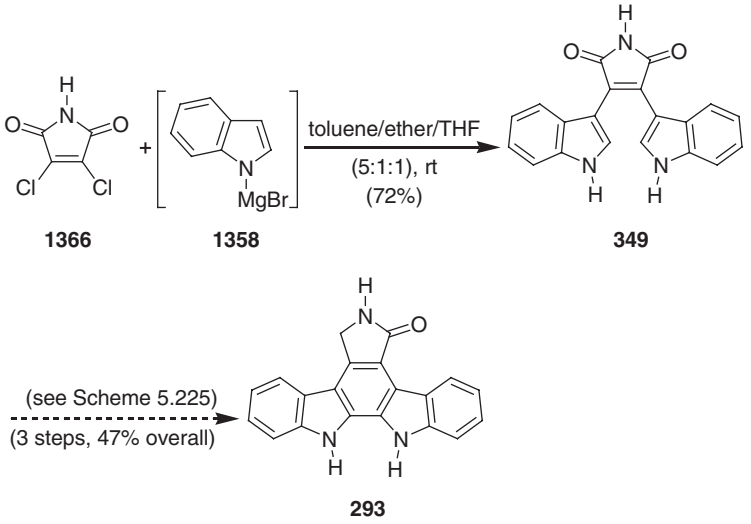

1366 **1358** **349** **293**

Scheme 5.228

Three years later, the same authors developed a new route to arcyriarubin A (**349**) starting from methyl indole-3-glyoxylate (**1368**) and indole-3-acetamide (**1369**) (772). Methyl indole-3-glyoxylate (**1368**) was prepared either by treatment of indole (**1170**) with oxalyl chloride followed by addition of sodium methoxide at low temperature, or by refluxing 3-indole glyoxylic acid (**1367**) in methanol with a Dowex 50X8–100 ion-exchange resin. An intramolecular Perkin-type condensation of methyl indole-3-glyoxylate (**1368**) and indole-3-acetamide (**1369**) in the presence of a 1 M solution of potassium *tert*-butoxide (KO*t*-Bu) in THF provided arcyriarubin A (**349**) quantitatively. Although this synthesis requires two steps, arcyriarubin A (**349**) was obtained in a high overall yield. Using Hill's three-step protocol (palladium-mediated oxidative cyclization, reduction, and deoxygenation), bisindolylmaleimide **349** was transformed to staurosporinone (**293**) (772) (see Scheme 5.225) (Scheme 5.229).

Faul *et al*. applied their condensation methodology, as shown in Scheme 5.229, for the total synthesis of rebeccamycin (**337**) and 11-dechlororebeccamycin (**338**) (323). For this methodology, the required symmetrical and unsymmetrical bisindolylmaleimides **1376** and **1377** were prepared by condensation of the glycosylated 7-chloroindole-3-acetamide (**1372**) with the methyl indole-3-glyoxylates **1373** and **1368**. Using Danishefsky's method, a selective formation of the β-*N*-glycoside of 7-chloroindole-3-acetamide **1372** was accomplished. The α-1,2-anhydro-sugar **1371** was prepared from commercially available tri-*O*-acetyl-D-glucal in four steps and 15:1 α/β-selectivity (80% overall yield). Deprotonation of 7-chloroindole-3-acetamide (**1370**) (obtained from 7-chloroindole in three steps and 65% overall yield) with sodium hydride in acetonitrile, followed by treatment with the α-1,2-anhydrosugar **1371**, afforded the β-*N*-glycoside **1372** in 40% yield. The β/α-selectivity of the reaction was 16:1, and the minor α-isomer was removed by chromatography to afford the β-isomer in $>98\%$ diastereomeric purity. The methyl indole-3-glyoxylates **1373** and **1368** were readily prepared from the indoles **1334** and **1170** by reaction with oxalyl chloride at room temperature followed by addition of sodium methoxide (323) (Scheme 5.230).

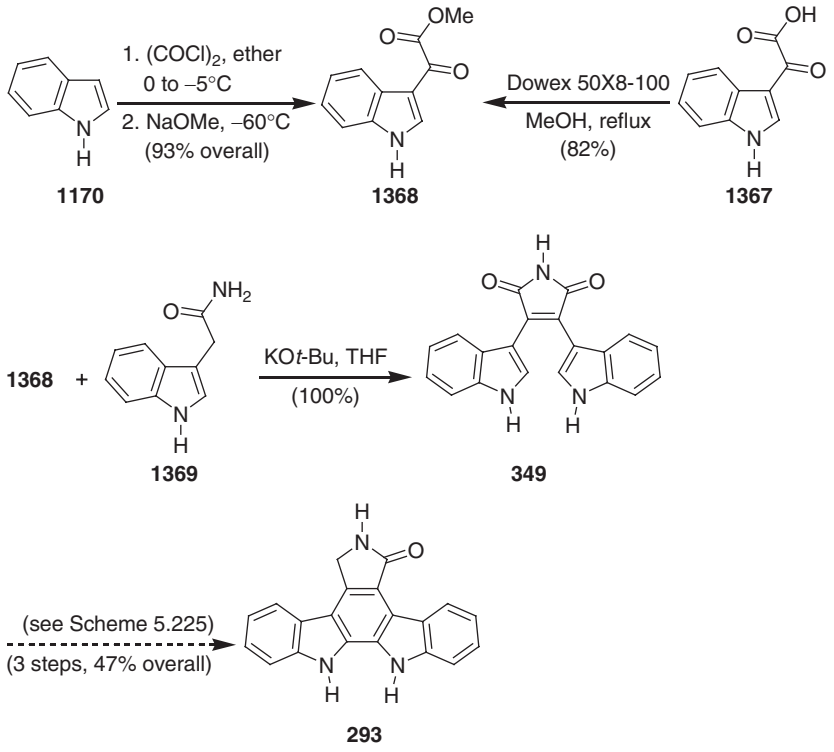

Scheme 5.229

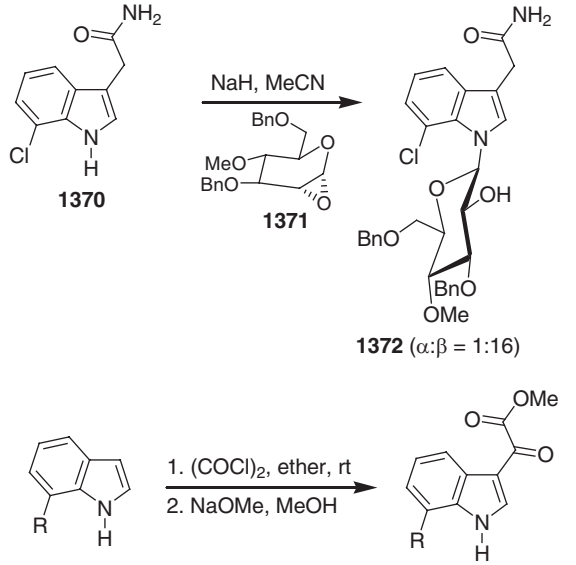

Scheme 5.230

The intramolecular Perkin-type condensation of the glycosylated 7-chloroindole-3-acetamide **1372** and the methyl indole-3-glyoxylate **1373**, initiated by a 1 M solution of potassium *tert*-butoxide in THF at room temperature, afforded the bisindolylmaleimide **1376** through an intermediate hydroxyimide **1374**. The oxidative cyclization of the bisindolylmaleimide **1376** using palladium(II) triflate in DMF at 90°C, followed by debenzylation with Pearlman's catalyst [$Pd(OH)_2/C$], provided rebeccamycin (**337**) in 55% yield. An analogous route, starting from methyl indole-3-glyoxylate (**1368**) and the methyl 7-chloroindole-3-glyoxylate **1372**, afforded 11-dechlororebeccamycin (**338**) in three steps and 52% overall yield (323) (Scheme 5.231).

Wood *et al.* envisaged an elegant synthetic strategy for the total syntheses of the series of indolocarbazole alkaloids, (+)-staurosporine (**295**), (−)-TAN-1030A (**313**), (+)-RK-286C (**318**), and (+)-MLR-52 (**320**) using a common intermediate, α-methoxy ketone **1378**, which was generated by Demjanov–Tiffeneau-like ring expansion of a furanosylated indolocarbazole **1380** (773–777). This common intermediate has all the required stereogenic centers of **295**, **313**, **318**, and **320** already in place, and additional stereocontrolled functionalizations at C-4′ and C-5′ are feasible. Starting from the

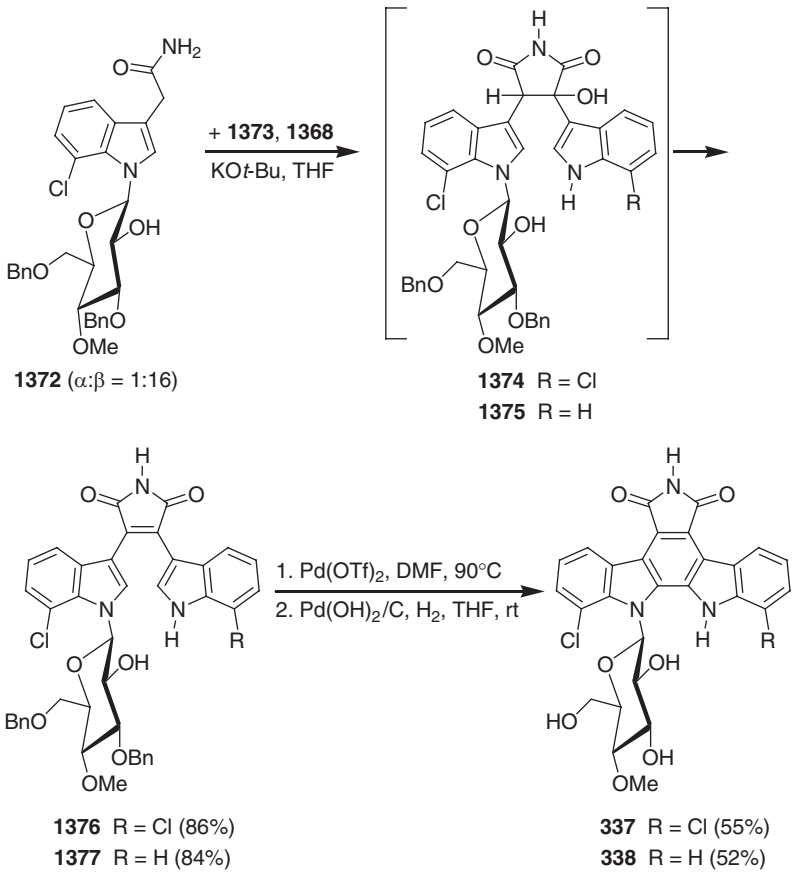

1372 (α:β = 1:16)

1374 R = Cl
1375 R = H

1376 R = Cl (86%)
1377 R = H (84%)

337 R = Cl (55%)
338 R = H (52%)

Scheme 5.231

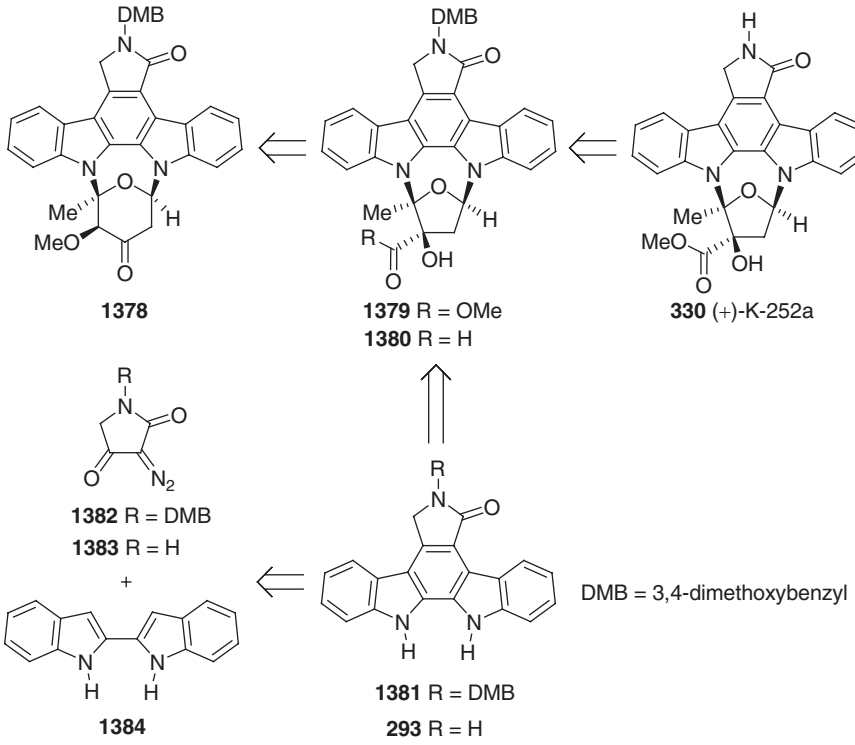

Scheme 5.232

ketone **1378**, a reductive amination would produce staurosporine (**295**), formation of the oxime would lead to (−)-TAN-1030A (**313**), reduction at C-4′ from the convex face would provide (+)-RK-286C (**318**), and β-elimination of either a C-4′-amine (*via* Cope elimination) or a C-4′-hydroxy (*via* Martin's sulfurane dehydration or Burgess dehydration), followed by dihydroxylation, would provide (+)-MLR-52 (**320**) (Schemes 5.232 and 5.233).

The required furanosylated indolocarbazole **1380** should be readily available by reduction of **1379**, a precursor of (+)-K-252a (**330**). For the synthesis of (+)-K-252a (**330**) a single-step cycloglycosidation of the selectively protected aglycon **1381** with an appropriate furanose was planned. The protected aglycon **1381** should be readily available by a rhodium-catalyzed coupling of 2,2′-bisindole **1384** with the α-diazo-β-keto-γ-lactam **1382** (Scheme 5.232).

The 2,2′-bisindole (**1384**), required for the synthesis of staurosporinone (**293**) and the protected aglycon **1381**, was prepared by a double Madelung cyclization as reported by Bergman. For the synthesis of the diazolactams **1382** and **1383**, the glycine esters **1385** and **1386** were transformed to the lactams **1389** and **1390** by DCC/DMAP-promoted coupling with monoethyl malonate, followed by Dieckmann cyclization. The lactams **1389** and **1390** were heated in wet acetonitrile, and then treated with mesyl azide (MsN_3) and triethylamine, to afford the diazolactams **1382** and **1383**. This one-pot process involves decarboethoxylation and a diazo transfer reaction (Scheme 5.234).

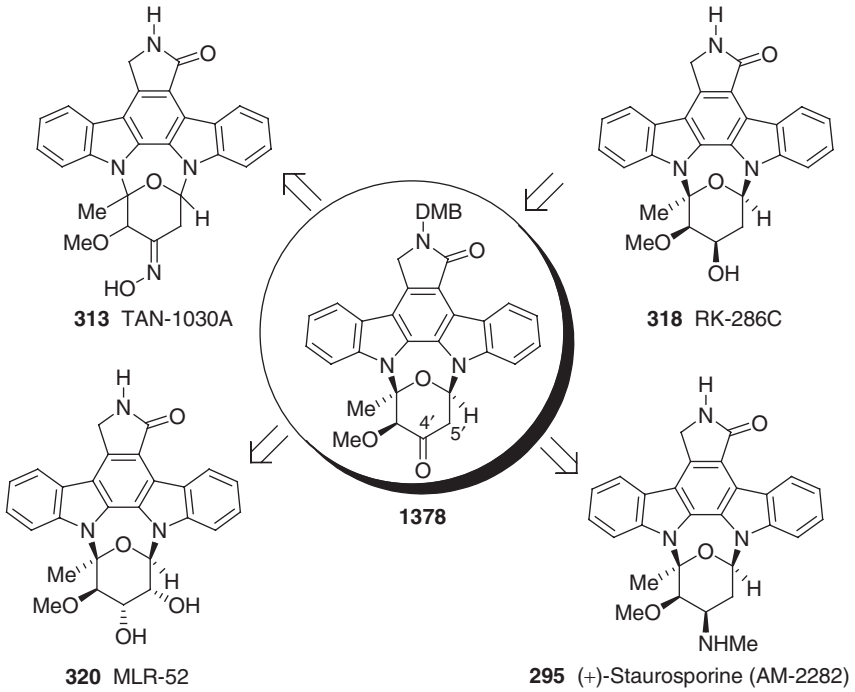

Scheme 5.233

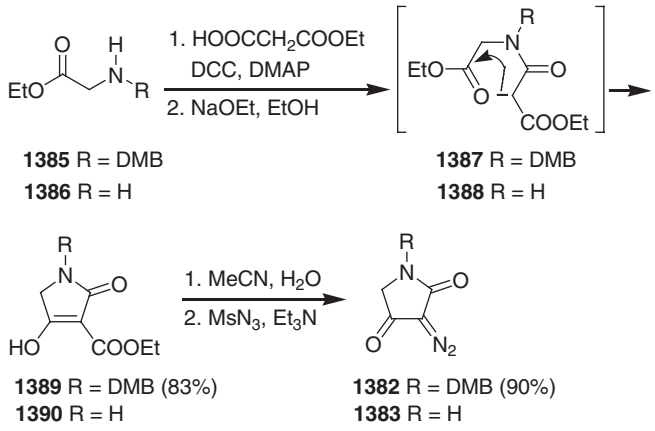

Scheme 5.234

Coupling of the diazolactams **1382** and **1383** with 2,2′-bisindole (**1384**) in the presence of catalytic amounts of $Rh_2(OAc)_4$ and degassed pinacolone provided staurosporinone (**293**) directly in 25% yield, and the protected aglycon **1381** in 62% yield. This annulation is believed to proceed *via* the intermediates **1391**, **1392** and **1393**, **1394**. The degassed pinacolone is both a good solvent for the 2,2′-bisindole substrate and compatible with the carbenoid chemistry (773,774) (Scheme 5.235).

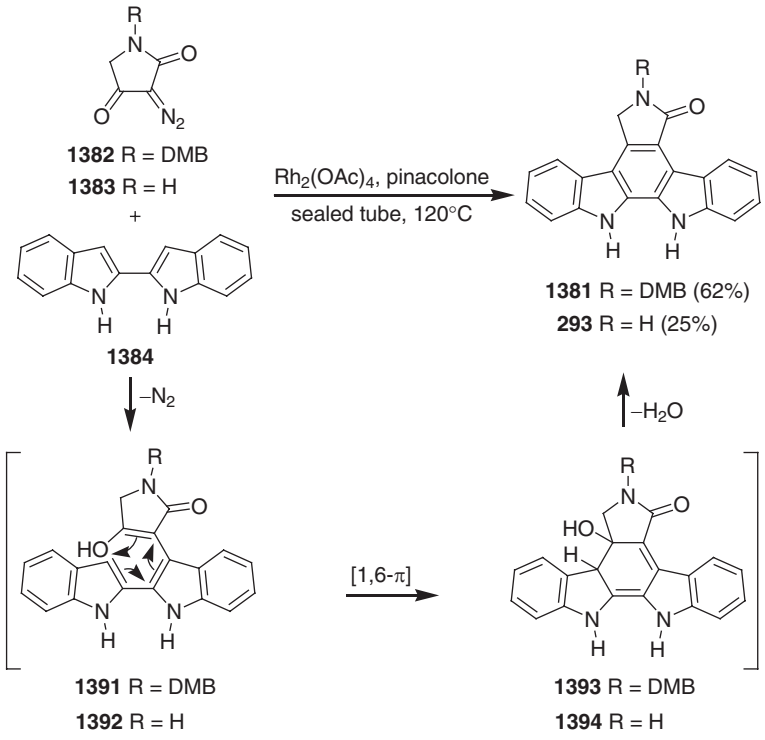

Scheme 5.235

For the asymmetric synthesis of the furanose (−)-**1398a,b**, a novel tandem [3,3]/[1,2] rearrangement protocol was developed to combine (*R*)-(−)-1-nonen-3-ol [(*R*)-(−)-**1395**] with methyl 2-diazo-3-oxobutyrate **1396**. The reaction of (*R*)-(−)-**1395** and **1396** in the presence of catalytic $Rh_2(OAc)_4$, followed by addition of boron trifluoride etherate, afforded (*R*)-(+)-**1397** in 77% yield. Ozonolysis of (*R*)-(+)-**1397**, and subsequent acid-mediated cyclization, provided a mixture of (−)-**1398a,b** and (+)-**1399** in 80% yield. A McCombie cycloglycosidation of the 3,4-dimethoxybenzyl (DMB)-protected aglycon **1381** with (−)-**1398a,b**/(+)-**1399** in 1,2-dichloroethane, using camphorsulfonic acid (CSA) as catalyst, afforded in 80% yield a 1:2 regioisomeric mixture of the furanosylated indolocarbazoles (+)-**1400** and (+)-**1379**. This reaction led selectively to a stereochemistry with the C-3′ hydroxy group oriented *syn* to the indolocarbazole moiety. Moreover, the major regioisomer corresponded to the *N*-protected K-252a (**330**). Removal of the DMB group, using TFA and thioanisole as cation scavenger, provided (+)-K-252a (**330**) in 83% yield (773,774) (Scheme 5.236). The same route was applied to the syntheses of racemic K-252a and non-natural (−)-K-252a from the DMB-protected aglycon **1381** and the carbohydrates (±)-**1398a,b**/(±)-**1399** and (+)-**1398a,b**/(−)-**1399** as precursors (773,774).

In order to achieve access to the entire family of glycosylated indolocarbazoles, (+)-staurosporine (**295**), (−)-TAN-1030A (**313**), (+)-RK-286C (**318**), and (+)-MLR-52 (**320**) from a common synthetic precursor, the *N*-protected K-252a **1379** was subjected

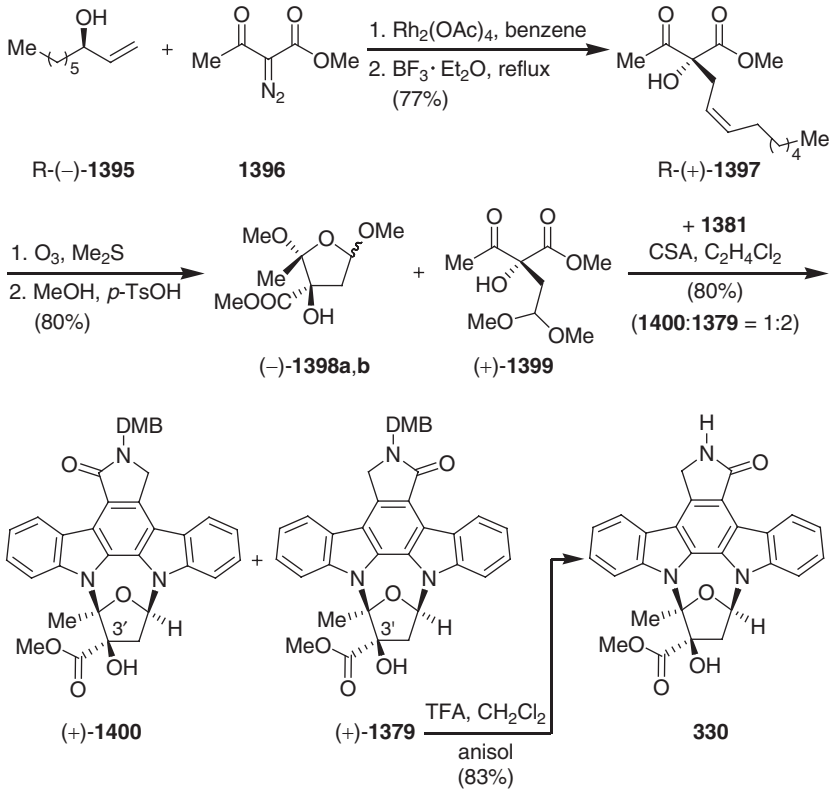

Scheme 5.236

to regio- and stereoselective ring expansion. Compound (+)-**1379** underwent lithium borohydride reduction to afford the alcohol (+)-**1401**, which, under Moffatt–Pfitzner oxidation conditions, led to the aldehyde (+)-**1380**. On treatment with boron trifluoride etherate, the aldehyde (+)-**1380** underwent a rearrangement with ring expansion to the α-hydroxyketone (+)-**1402** (775,776) (Scheme 5.237).

Reduction of the α-hydroxyketone (+)-**1402** with sodium borohydride, afforded the diol (+)-**1403**. The selective alkylation at the C-3′ hydroxy group with sodium hydride and iodomethane provided the alcohol (+)-**1404** in 80% yield. This selectivity was ascribed to the steric environment of the equatorial (C-3′) and the axial (C-4′) hydroxy groups. Removal of the DMB protecting group, by treatment of (+)-**1404** with TFA in anisole, afforded (+)-RK-286C (**318**) in 75% yield. Dehydration of the alcohol (+)-**1404** with Martin's sulfurane led to the olefin (+)-**1405**, which was stereoselectively dihydroxylated using osmium tetroxide in the presence of NMO to give the dihydroxy derivative (+)-**1406**. Finally, removal of the DMB group in (+)-**1406** led to (+)-MLR-52 (**320**) in 77% yield (775,776) (Scheme 5.238).

Reaction of the α-hydroxyketone (+)-**1402** with hydroxylamine hydrochloride gave the oxime (−)-**1407** in 95% yield. A bis-methylation of (−)-**1407** under phase transfer conditions afforded the corresponding dimethyl derivative (−)-**1408**. Stereoselective hydrogenation of (−)-**1408** using H_2/PtO_2 led to the amine

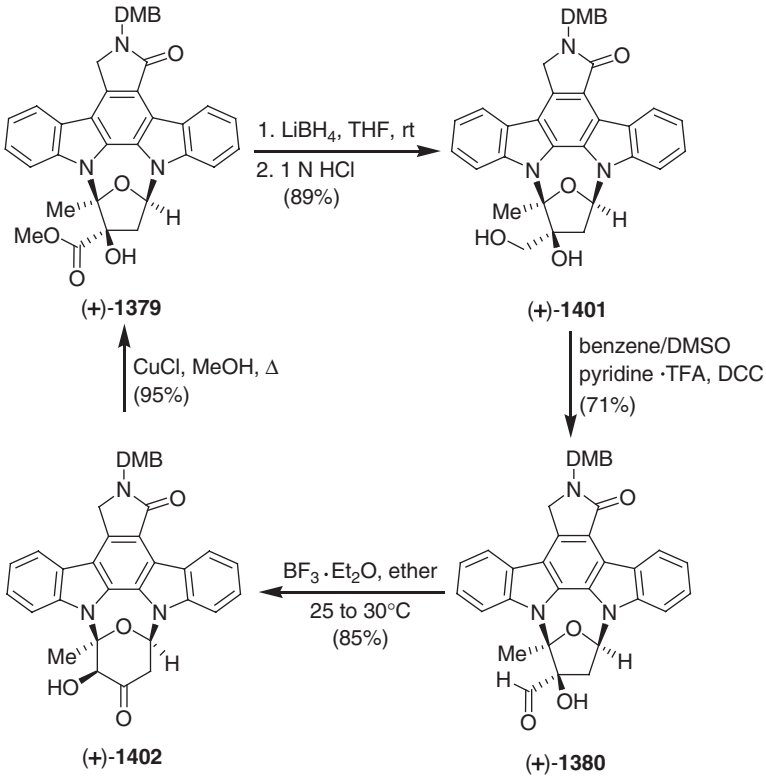

Scheme 5.237

(+)-**1409**. Monomethylation of the amine (+)-**1409** yielded compound (+)-**1410**, which, on deprotection, provided (+)-staurosporine (**295**) (775,776) (Scheme 5.239).

The reaction of the α-hydroxyketone (+)-**1402** with *O*-benzylhydroxylamine hydrochloride afforded the benzyl-protected oxime (−)-**1411**. *O*-Methylation under phase transfer conditions led to the corresponding methyl derivative (−)-**1412**. Removal of the DMB protecting group from (−)-**1412** followed by debenzylation of the lactam (−)-**1413** by treatment with iodotrimethylsilane afforded (−)-TAN-1030A (**313**) (776) (Scheme 5.240). In the following years, Wood *et al.* further explored the rhodium carbenoid approach for the synthesis C7−methyl derivatives of K-252a (777), C2′−alkyl derivatives of (±)-K-252a (778), and (−)-(7*S*)- and (+)-(7*R*)-K-252a dimers (779).

Lowinger *et al.* (780) applied Raphael's method (760) for the synthesis of (±)-K-252a [(±)-**330**]. This method uses the anhydride **1362** as a key-intermediate starting from 2-nitrocinnamaldehyde (**1300**). The condensation of 2-nitrocinnamaldehyde (**1300**) with the Wittig reagent prepared from the phosphonium bromide **1306** afforded 1,4-bis(*o*-nitrophenyl)butadiene **1307**. Diels–Alder cycloaddition of the butadiene **1307** with neat *N*-methylmaleimide **1414**, followed by dehydrogenation with DDQ, led to the terphenyl **1415**. Double nitrene insertion of **1415** by refluxing with triphenylphosphine in collidine provided, after basic hydrolysis, the anhydride **1362**. Aminolysis with *p*-methoxybenzylamine ($PMBNH_2$), followed by reduction,

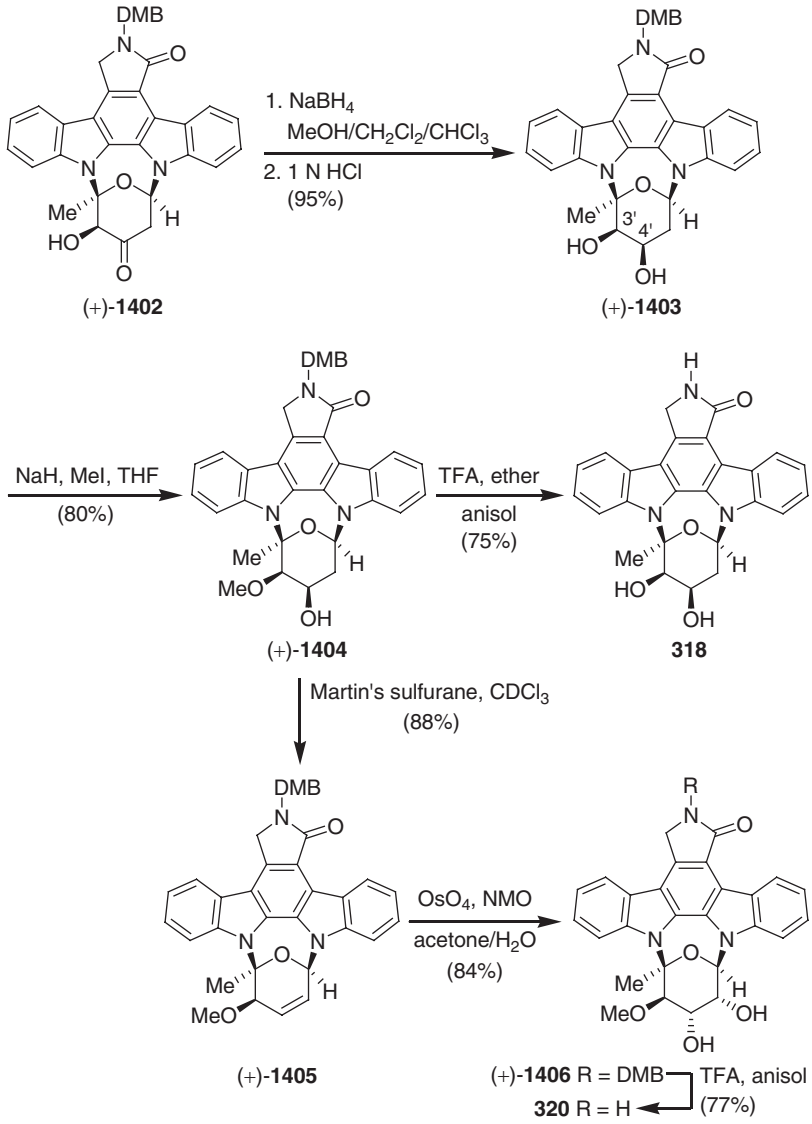

Scheme 5.238

afforded the PMB-protected aglycon **1416**. The CSA-catalyzed, double glycosidation of the aglycon **1416** with the furanose (±)-**1398** in refluxing dichloromethane gave a 2:1 mixture of the regioisomeric bis-glycosides (±)-**1417** and (±)-**1418** in 63% yield. Removal of the PMB group from compound (±)-**1417** using TFA in the presence of anisole provided (±)-K-252a [(±)-**330**] in 80% yield (780) (Scheme 5.241).

Ohkubo *et al*. reported the synthesis of the arcyriaflavins B (**346**), C (**347**), and D (**348**) involving a base-induced indolylation of dibromo-*N*-methylmaleimide **1420** and a palladium-mediated oxidative cyclization of the bisindolylmaleimides **1428**, **1429**, and **1430** as key steps (337). The reaction of 6-benzyloxyindole (**1419**) and

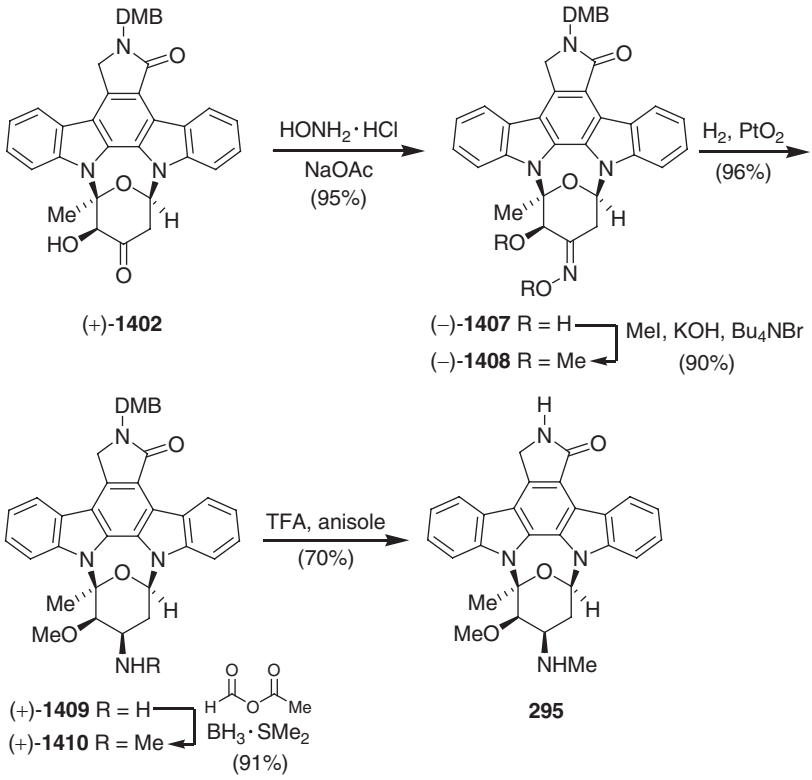

Scheme 5.239

dibromo-*N*-methylmaleimide **1420** with lithium hexamethyldisilazide (LiHMDS) as the base afforded the monoindolyl derivative **1421** in 93% yield. After protection of the indole nitrogen, the corresponding *N*-Boc derivative **1422** was coupled with the indoles **1423**, **1424**, and **1170** in the presence of base (LiHMDS) to afford the corresponding bisindolyl derivatives **1425**, **1426**, and **1427**. Removal of the Boc group with methylamine afforded, in good yields, the deprotected compounds **1428–1430**. Cyclization of **1428** and **1430** using DDQ, followed by debenzylation using catalytic amounts of palladium on charcoal, provided the corresponding products **1431** and **1433**. The cyclization of **1429** with DDQ gave only traces of the desired product. However, the oxidative cyclization of **1429** using palladium(II) chloride in DMF, followed by debenzylation, led to the desired compound **1432** in 86.5% yield over both steps. Treatment of **1431–1433** with aqueous potassium hydroxide afforded the corresponding anhydrides **1434–1436**. Finally, ammonolysis of the anhydrides **1434–1436** provided the arcyriaflavins C (**347**), D (**348**), and B (**346**) (337) (Scheme 5.242). In the following year, the same authors applied this method to the synthesis of the anticancer agent NB-506 (781), ED-110 (781), and some unsymmetrical indolocarbazole glycosides (782).

Gilbert and Van Vranken described the synthesis of tjipanazole F2 (**372**) by introduction of the halide and the glycosidic substituent at the heterocyclic skeleton without the use of protecting groups and with complete control of regioselectivity

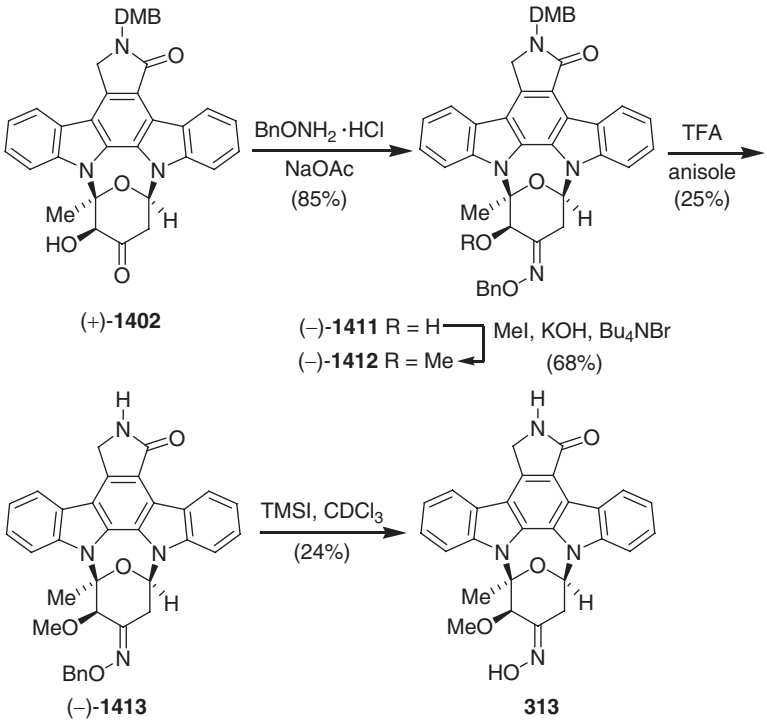

Scheme 5.240

(783). The indolo[2,3-*a*]carbazole framework required for this synthesis was obtained by a TFA-promoted, Mannich cyclization of the readily available 1,2-bis(indol-3-yl)ethane (**1437**). Subsequent bromination with NBS gave the racemic bromoindoline (±)-**1438**. Compound (±)-**1438** was regioselectively glycosylated at the indoline nitrogen with 3 equivalents of D-xylopyranose in methanol under reflux to afford a 1:1 diastereoisomeric mixture of **1439**. A convergent aromatization of the diastereoisomers **1439** with DDQ, followed by a halogen exchange using copper(I) chloride, provided tjipanazole F2 (**372**) in 61% yield over two steps (783) (Scheme 5.243).

In the following year, this method was also applied to the total synthesis of tjipanazole F1 (**371**) (784). For this synthesis, the required bisindole **1444** was obtained starting from 5-chloroindole (**1440**) in three steps and 47% overall yield. Acylation of **1440** with oxalyl chloride led to the glyoxylic acid chloride **1441**. Transmetalation of indolylmagnesium bromide with zinc chloride, followed by addition of the acid chloride, provided the α-diketone **1443**. Exhaustive reduction of **1443** with lithium aluminum hydride ($LiAlH_4$) afforded the corresponding bisindolylethane **1444**. Executing a similar reaction sequence as shown for the synthesis of tjipanazole F2 (**372**) (see Scheme 5.243), the chloroindoline (±)-**1445** was transformed to tjipanazole F1 (**371**) in two steps and 50% overall yield (784) (Scheme 5.244).

Three years later, Chisholm and Van Vranken reported the first total synthesis of AT2433-A1 (**339**) using their acid-promoted Mannich cyclization methodology (785).

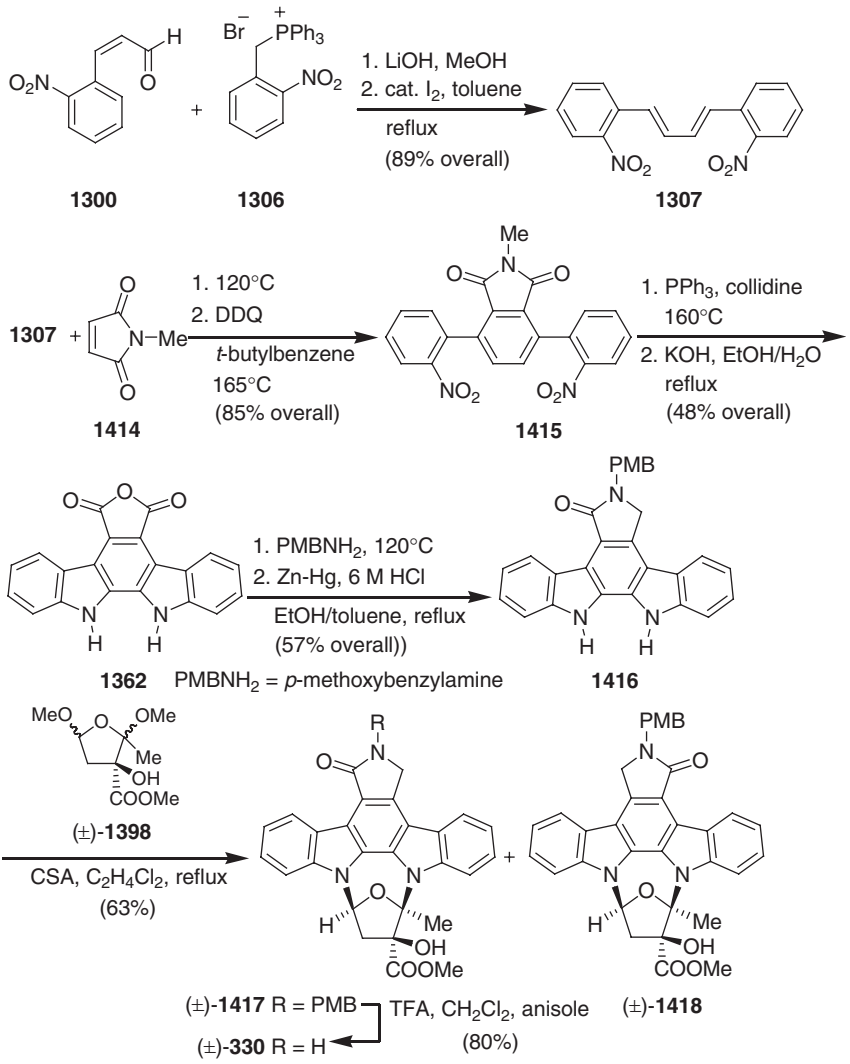

Scheme 5.241

For this methodology, the required chlorinated bisindolylsuccinimide (±)-**1450** was prepared following Clardy's and Kaneko's procedure. Reaction of the 7-chloroindole Grignard compound **1447** with 1 equivalent of (*N*-methyl)dibromomaleimide (**1420**) led to the monoaddition product **1448**, addition of indolylmagnesium bromide (**1358**) then afforded the unsymmetrical bisindolylmaleimide **1449** in 74% yield. Catalytic hydrogenation of **1449** to the bisindolylsuccinimide (±)-**1450**, followed by Mannich cyclization with methanesulfonic acid in chloroform, provided the hexacyclic compound (±)-**1451** with high regio- and stereoselectivity. Glycosylation of the racemic chlorinated indoline (±)-**1451** with the aminodisaccharide **1452** in the presence of CSA in DMF, and subsequent aromatization with DBU and iodine in dichloromethane, afforded the trimethylsilylethyl carbamate **1453**. Removal of the

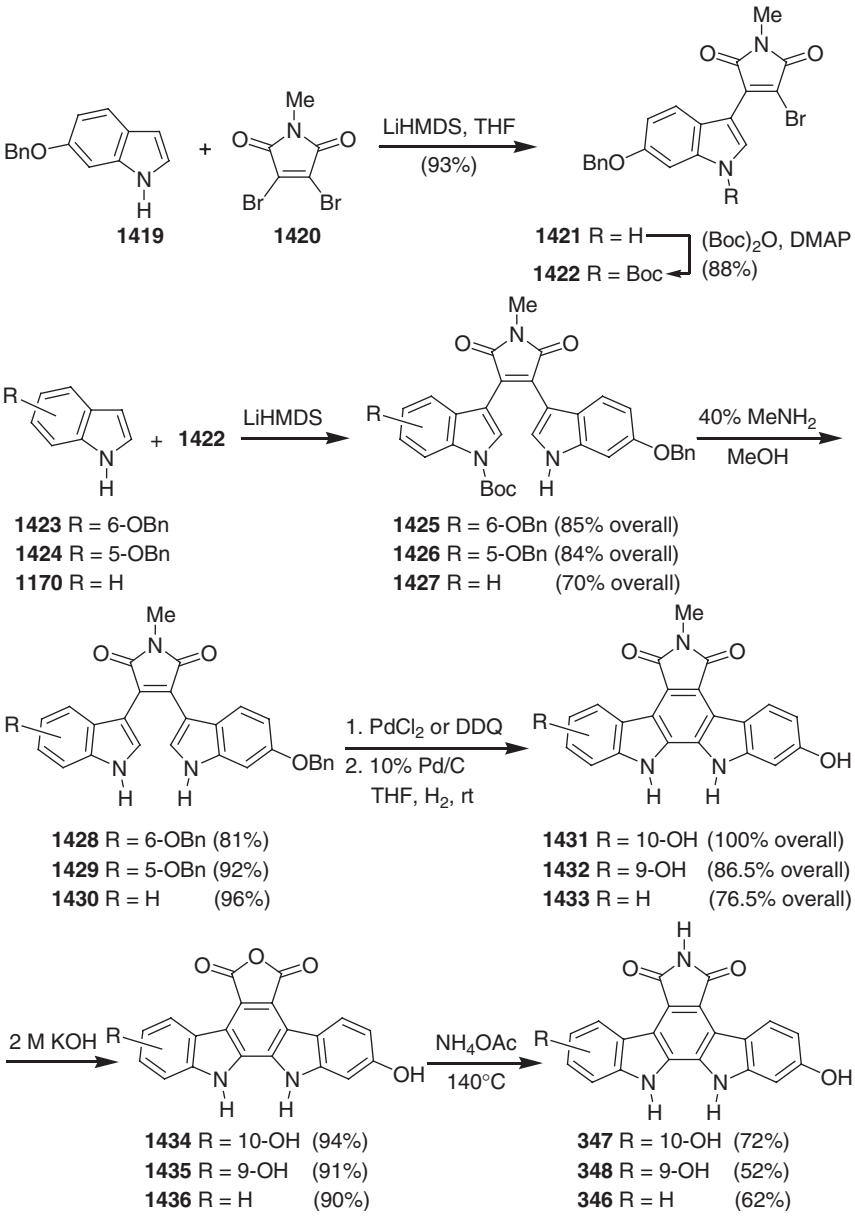

Scheme 5.242

2-trimethylsilylethoxycarbonyl (Teoc) group with TBAF provided AT2433-A1 (**339**) in 78% yield (785) (Scheme 5.245).

An extension of this methodology led to another indolo[2,3-*a*]carbazole, AT2433-B1 (**341**). For this synthesis, the required bisindolylsuccinimide (**1455**) was obtained through a catalytic hydrogenation of the readily available *N*-methylarcyriarubin A (**1454**). TFA-promoted Mannich cyclization of **1455** afforded the hexacyclic

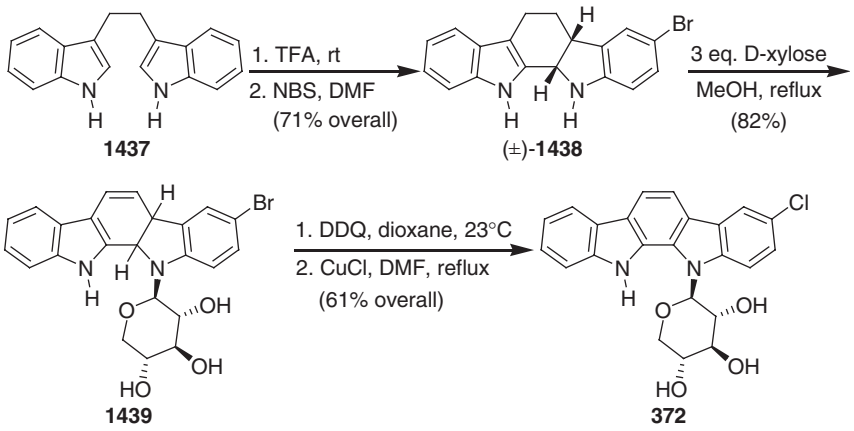

Scheme 5.243

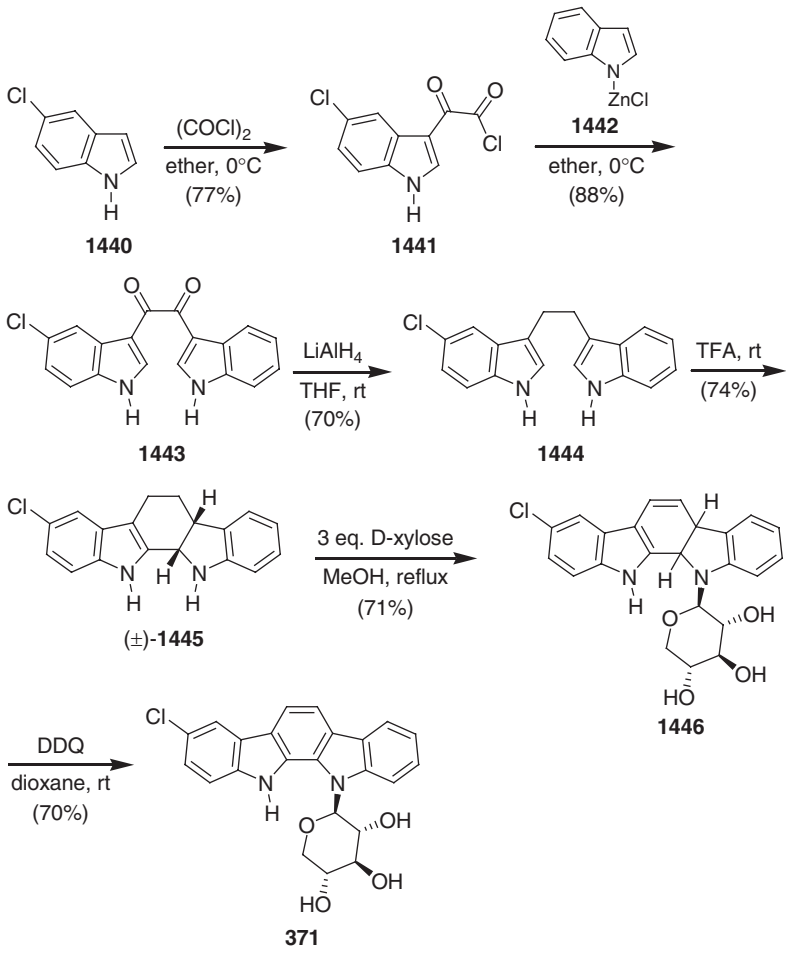

Scheme 5.244

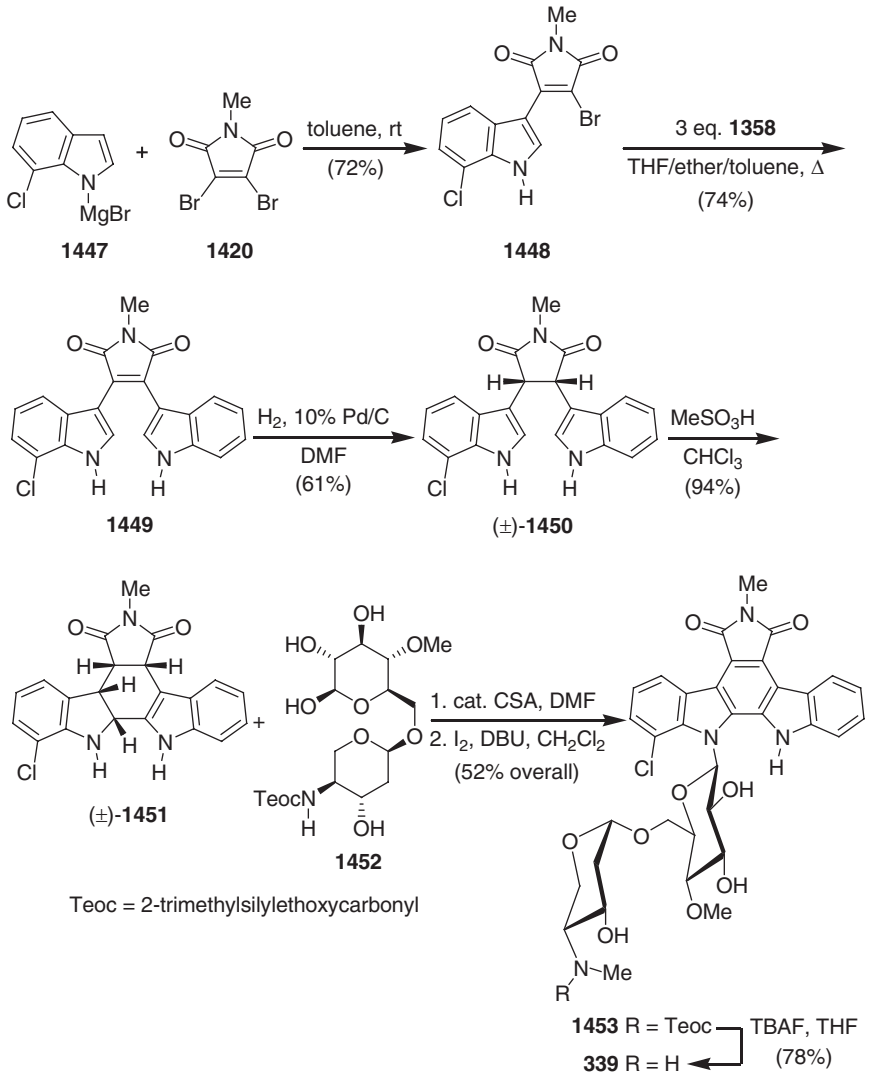

Scheme 5.245

compound (±)-**1456**. Glycosylation of (±)-**1456** with the aminodisaccharide **1452**, followed by oxidative aromatization with DDQ, led to the Teoc-protected AT2433-B1 (**1457**). Finally, deprotection of the Teoc carbamate with TBAF provided AT2433-B1 (**341**) in 78% yield (785) (Scheme 5.246).

Somei *et al.* reported the total synthesis of the cytotoxic and antiviral 5-cyano-6-methoxy-11-methylindolo[2,3-*a*]carbazole (**357**) starting from indigo (**1458**) (786,787). A reduction of indigo (**1458**) with tin in acetic acid/acetic anhydride afforded 3-acetoxy-2,2′-bisindolyl (**1459**) in 88% yield. Heating of **1459** with dichloroacetyl chloride in ethyl acetate under reflux provided 3-acetoxy-3′-dichloroacetyl-2,2′-bisindolyl (**1460**), which was treated with aqueous ammonia in methanol/DMF at room temperature to give the indolo[2,3-*a*]carbazole derivative **1461**. *N*-Methylation

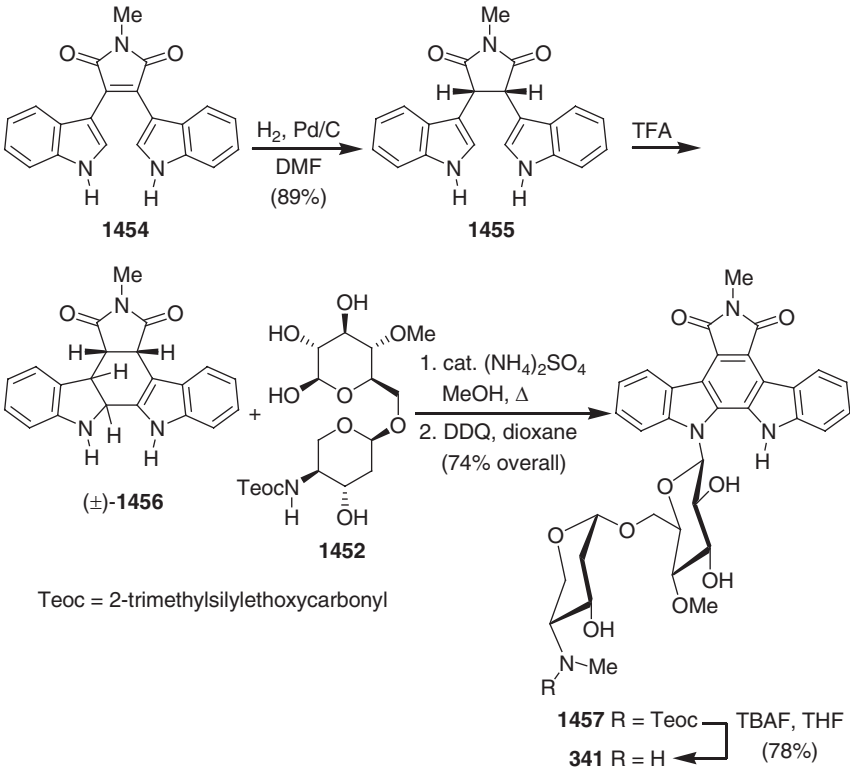

Scheme 5.246

to **1462** followed by reductive cyanation afforded 5-cyano-6-hydroxy-11-methylindolo[2,3-*a*]carbazole **1463**. Finally, *O*-methylation of **1463** with diazomethane afforded 5-cyano-6-methoxy-11-methylindolo[2,3-*a*]carbazole (**357**) in 86% yield (786,787) (Scheme 5.247).

The two previous total syntheses of 5-cyano-6-methoxy-11-methylindolo[2,3-*a*]carbazole (**357**) by Somei *et al*. started also from indigo, however, gave low overall yields (788). In the following year, the same group reported the syntheses of various indolo[2,3-*a*] carbazoles from indigo (789).

Beccalli *et al*. reported a new synthesis of staurosporinone (**293**) from 3-cyano-3-(1*H*-indol-3-yl)-2-oxo propionic acid ethyl ester (**1464**) (790). The reaction of **1464** with ethyl chlorocarbonate and triethylamine afforded the compound **1465**, which, on treatment with dimethylamine, led to the corresponding hydroxy derivative **1466**. The triflate **1467** was prepared from **1466** by reaction with trifluoromethanesulfonic anhydride (Tf_2O) in the presence of ethyldiisopropylamine. The palladium(0)-catalyzed cross-coupling of the triflate **1467** with the 3-(tributylstannyl)indole **1468** afforded the vinylindole **1469** in 89% yield. Deprotection of both nitrogen atoms with sodium ethoxide in ethanol to **1470**, followed by photocyclization in the presence of iodine as the oxidizing agent provided the indolocarbazole **1471**. Finally, reductive cyclization of **1471** with sodium borohydride-cobaltous chloride led to staurosporinone (**293**) in 40% yield (790) (Scheme 5.248).

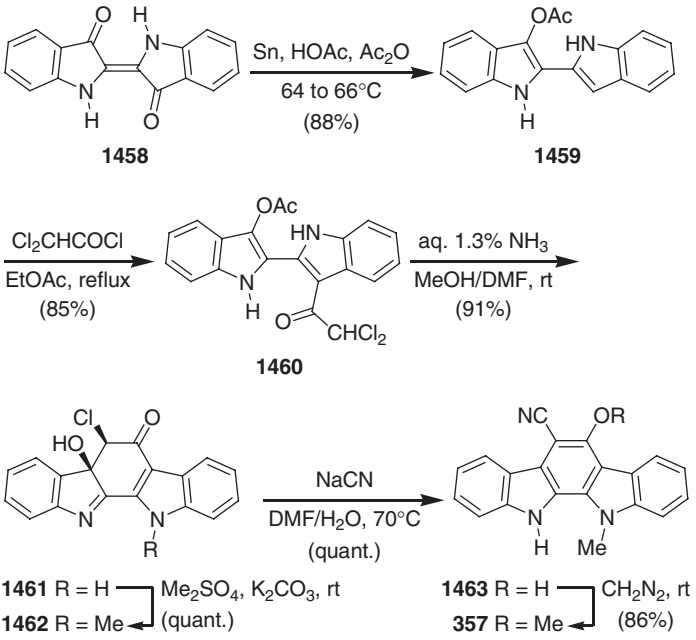

Scheme 5.247

Mahboobi *et al*. described a novel synthesis of staurosporinone (**293**) (791). The intermolecular Michael addition of 1-(indol-3-yl)-2-nitroethene (**1472**) to methyl indol-3-ylacetate (**1313**) provided with high diastereoselectivity methyl 2,3-bis(indol-3-yl)-4-nitrobutanoate (**1473**). Catalytic hydrogenation and lactamization afforded 2,3-bis(indol-3-yl)-γ-butyrolactam (**1474**) in 87% yield. Oxidative cyclization of the *cis*-lactam **1474** with DDQ in the presence of catalytic amounts of *p*-TsOH led to staurosporinone (**293**) (791) (Scheme 5.249).

Fukuyama *et al*. reported the total synthesis of (+)-K-252a (**330**) starting from indol-3-ylacetic acid (**680**) (792). Formation of the allyl ester, followed by regioselective bromination, led to the 2-bromoindole **1475**. The *N*-glycosidation of compound **1475** was carried out by deprotonation with sodium hydride and subsequent addition of the readily available 1-chloro-2-deoxy-3,5-di-*O*-*p*-toluoyl-α-D-*erythro*-pentofuranose (**1476**) and afforded the β-*N*-glycoside **1477** as the sole product. Compound **1477** was transformed to the diacetyl bisindole **1478** in four steps and 52% overall yield by cleavage of the allyl ester, reaction of the resulting acid with tryptamine to the amide, regioselective oxidation at the benzylic position to the ketone, and diacetylation of the indole and amide nitrogens. The base-catalyzed cyclization of the diacetyl bisindole **1478** with catalytic amounts of DBU and 4 Å MS afforded the lactam **1479**. A non-oxidative photocyclization of the lactam **1479** by sunlight, in the presence of *N*,*N*-diisopropylethylamine to promote the dehydrobromination, provided almost quantitatively the desired indolocarbazole **1480**. Hydrolysis of all acyl groups followed by treatment with iodine, triphenylphosphine, and imidazole led to selective conversion of the primary alcohol to the corresponding iodide **1481** (Scheme 5.250).

The conversion of the iodide **1481** to the olefin **1482** was achieved by a conventional four-step sequence. Treatment of **1482** with iodine, potassium iodide,

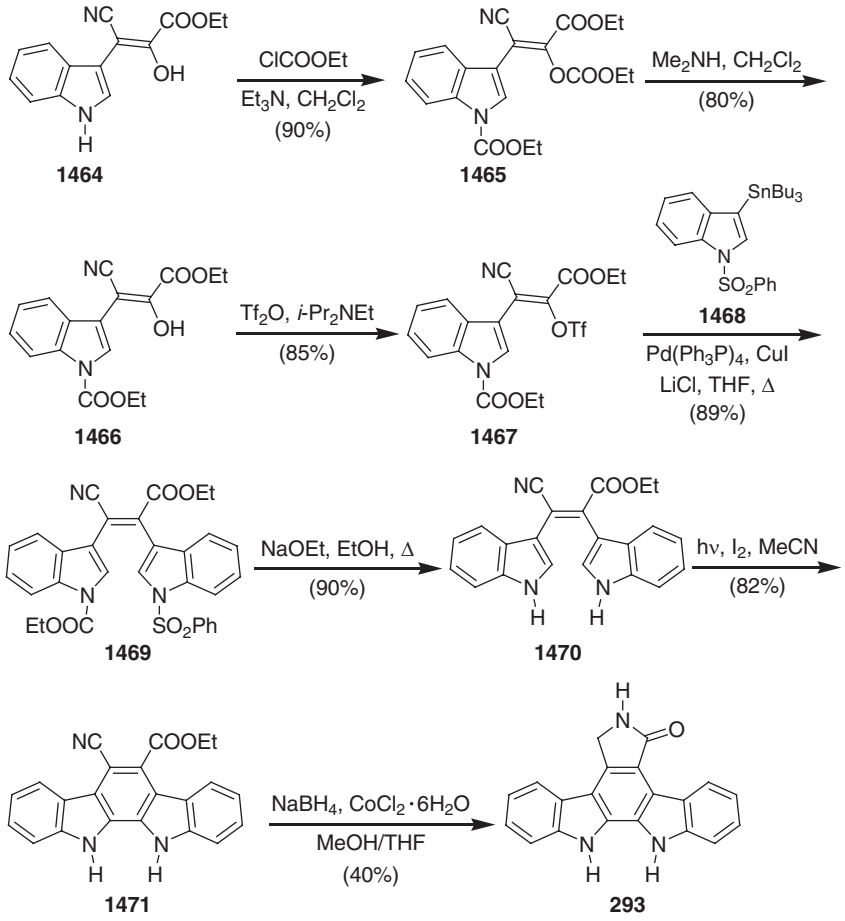

Scheme 5.248

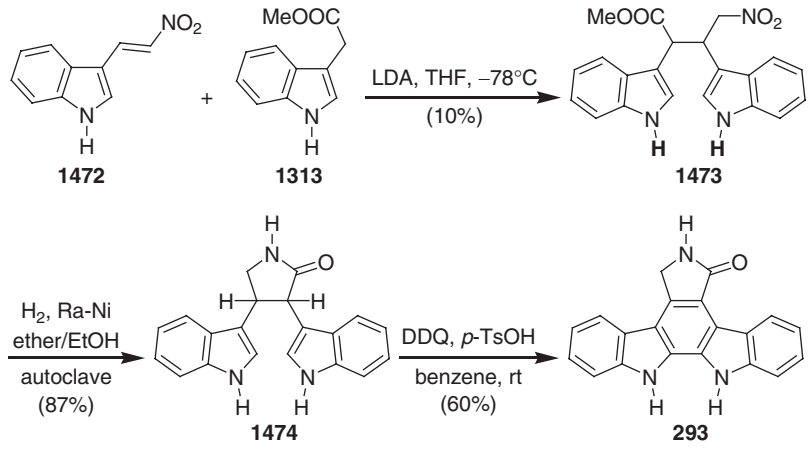

Scheme 5.249

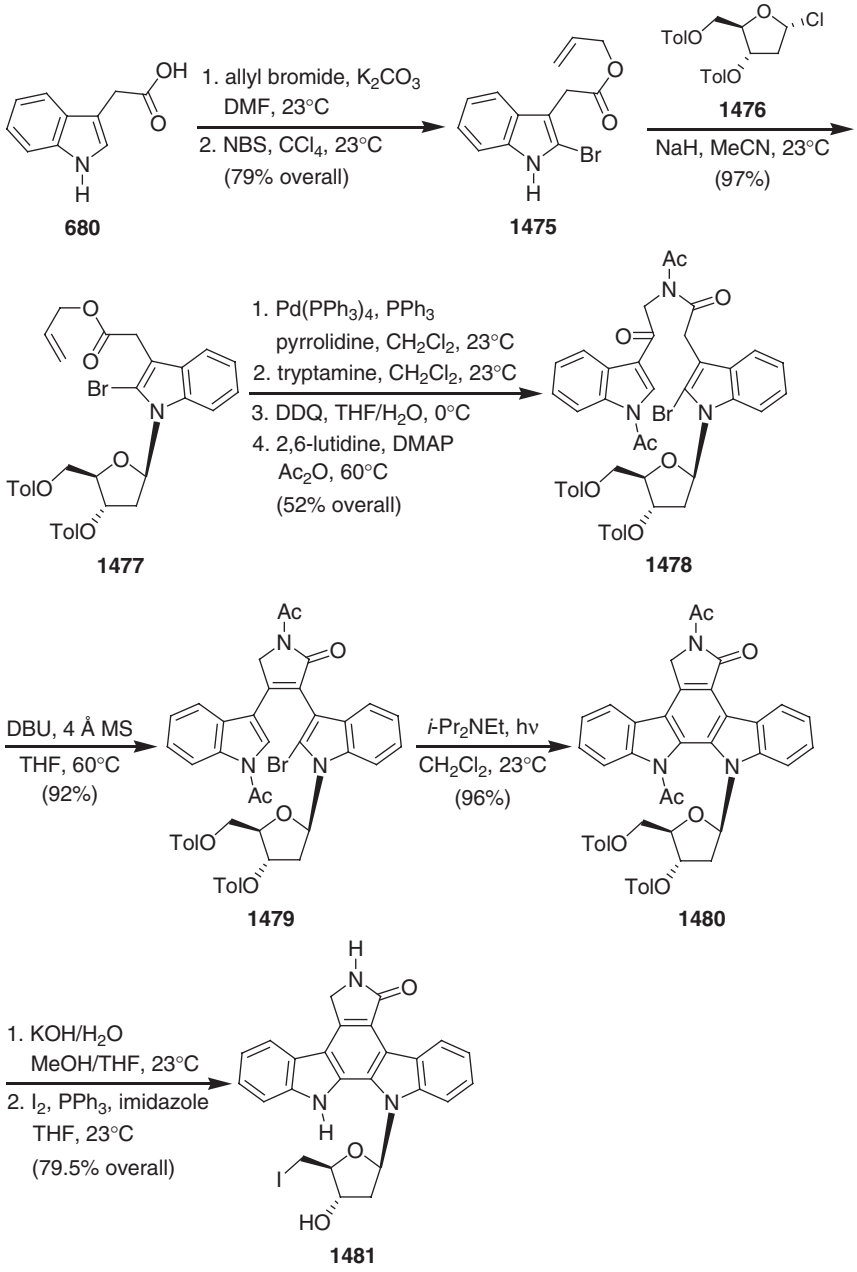

Scheme 5.250

and DBU provided the cycloglycoside **1483** in 93% yield. Radical deiodination of **1483**, followed by cleavage of the acetate, led to the hydroxy derivative **1484**. The compound **1484** was transformed to the acetylcyanohydrin **1485** over three steps in 98% overall yield by Moffatt–Pfitzner oxidation, followed by cyanation of the formed ketone with hydrogen cyanide, and acetylation. An attempted

acid-promoted methanolysis of **1485** afforded mainly the intermediate ketone (not shown in the scheme) along with only a trace of (+)-K-252a (**330**). Therefore, compound **1485** was transformed to the amide **1486**, followed by alkaline hydrolysis to the acid and treatment with diazomethane to provide (+)-K-252a (**330**) (792) (Scheme 5.251).

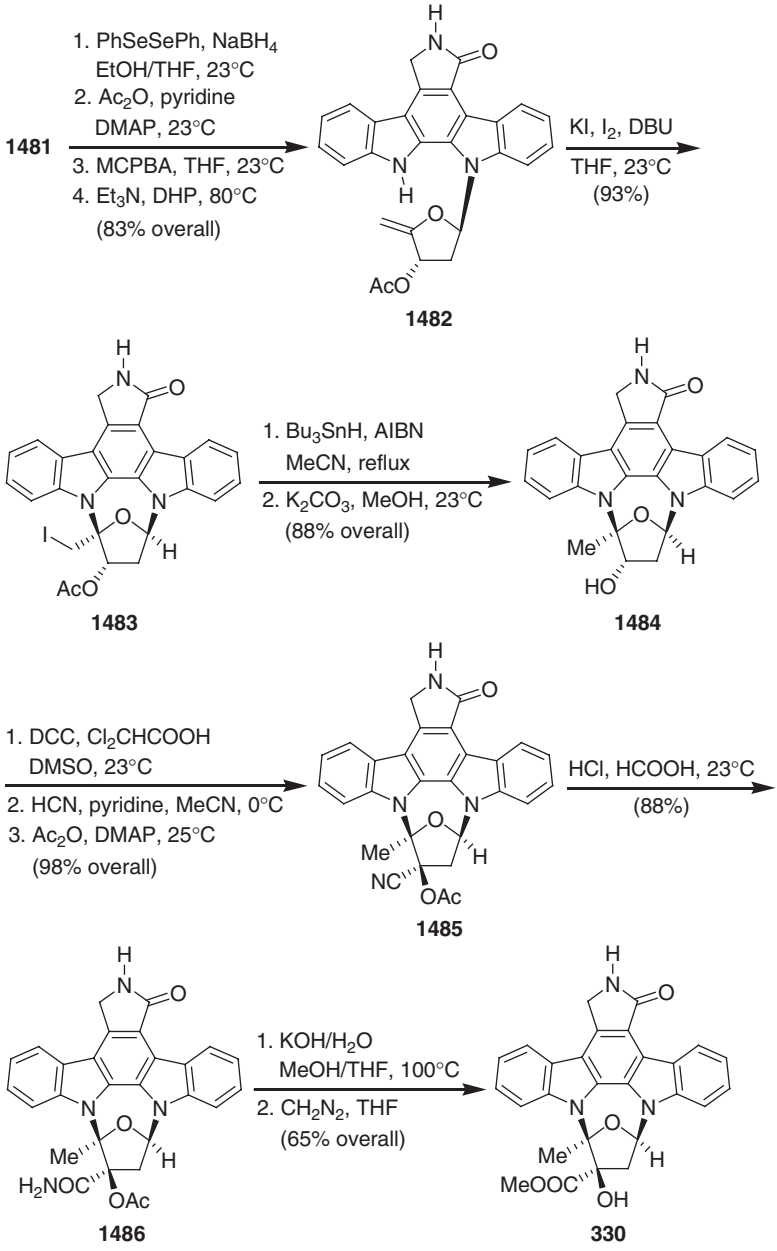

Scheme 5.251

Tomé *et al*. described a synthesis of arcyriaflavin A (**345**) from commercially available 2-nitrobenzaldehyde (**1487**) (793). The construction of the indolo[2,3-*a*] pyrrolo[3,4-*c*]carbazole framework was achieved by successive Diels–Alder cycloaddition, Fischer indolization, and nitrene insertion. A Wittig reaction of 2-nitrobenzaldehyde (**1487**) to the ketone **1488**, followed by reaction with *tert*-butyldimethylsilyl triflate (TBSOTf) in the presence of triethylamine, led to the diene **1489** in high yield. The Diels–Alder reaction of **1489** with maleimide (**1303**) afforded the *endo*-cycloadduct (±)-**1490**. Acidic hydrolysis of compound (±)-**1490** gave the perhydroisoindole-1,3,5-trione (±)-**1491**, which, on Fischer indolization with phenylhydrazine (**524**) provided the regioisomers (±)-**1492** and (±)-**1493** in a 2:1 ratio. Dehydrogenation of (±)-**1492** with DDQ to the carbazole **1494**, and nitrene insertion using Cadogan's procedure by heating in triethyl phosphite, afforded arcyriaflavin A (**345**) (793) (Scheme 5.252). This method was also applied to the synthesis of 3-methoxy-6-phenylarcyriaflavin A (793).

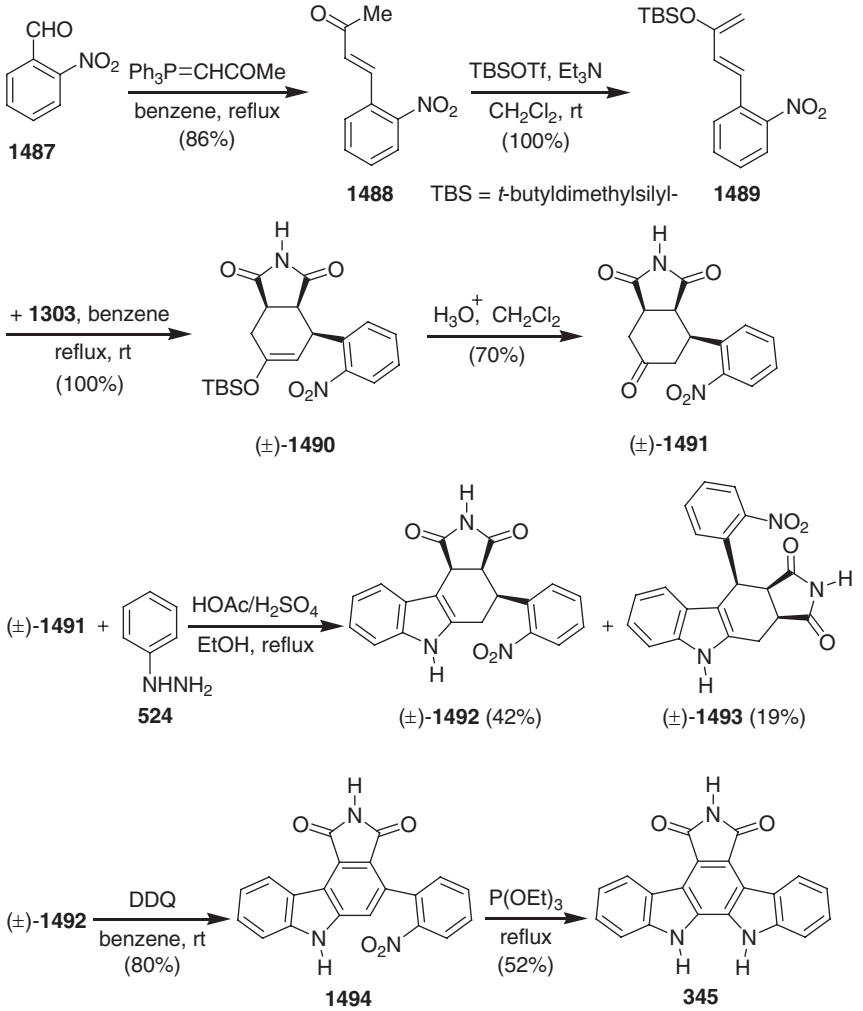

Scheme 5.252

Five years later, the same authors reported an improved total synthesis of arcyriaflavin A (**345**) starting from the TBS enol ether **1490** (for the synthesis see Scheme 5.252). This route involves two indolizations based on silyl enol ether nucleophilic attack and Fischer processes. Using Cadogan's procedure by heating in triethyl phosphite, the TBS enol ether **1490** was transformed into the ketone (±)-**1495**, involving silyl enol ether-mediated indolization. Finally, Fischer indolization of (±)-**1495** by reacting with phenylhydrazine (**524**) led directly to arcyriaflavin A (**345**) in 57% yield (794) (Scheme 5.253).

Uang *et al.* reported a synthesis of staurosporinone (**293**) starting from arcyriarubin A (**349**). Oxidative photocyclization of bisindolylmaleimide **349** in the presence of a catalytic amount of iodine in THF/acetonitrile led to arcyriaflavin A (**345**) in 85% yield. Finally, using modified Clemmensen reduction conditions, arcyriaflavin A (**345**) was transformed to staurosporinone (**293**) in 68% yield (795) (Scheme 5.254).

Kuethe *et al.* reported the synthesis of the tjipanazoles D (**359**), I (**360**), B (**369**), and E (**370**) starting from the nitro derivative **1496** (796). This route involves the synthesis of 2,2′-bisindoles, followed by a two-carbon insertion through condensation with (dimethylamino)acetaldehyde diethyl acetal to afford the indolocarbazole ring.

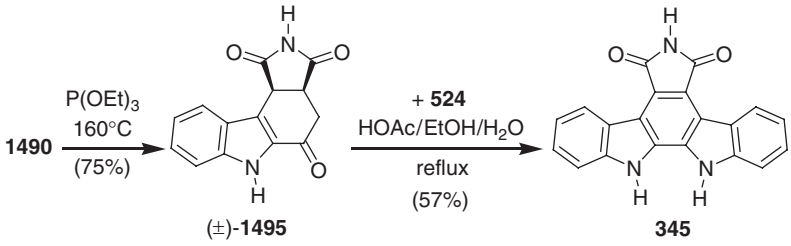

Scheme 5.253

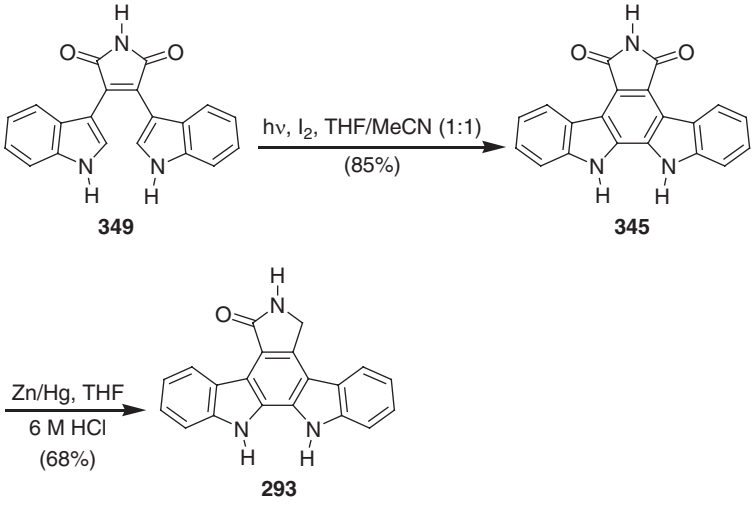

Scheme 5.254

Reaction of the TMS-nitro compound **1496** and the indole carboxaldehyde **1497** with a catalytic amount of TBAF led to the desired alcohol **1498**, which, on further treatment with TFAA, followed by elimination of the corresponding trifluoroacetate with DBU, afforded the *trans*-stilbene **1499**. Reductive cyclization of **1499** under Cadogan–Sundberg conditions afforded the bisindole **1500**. Finally, condensation of **1500** with (dimethylamino)acetaldehyde diethyl acetal led to tjipanazole D (**359**) in 71% yield (796) (Scheme 5.255).

Analogous to the aforementioned method, starting from the same nitro derivative **1496** and the indole carboxaldehyde **1501**, tjipanazole I (**360**) was obtained in five steps and 28% overall yield (796) (Scheme 5.256).

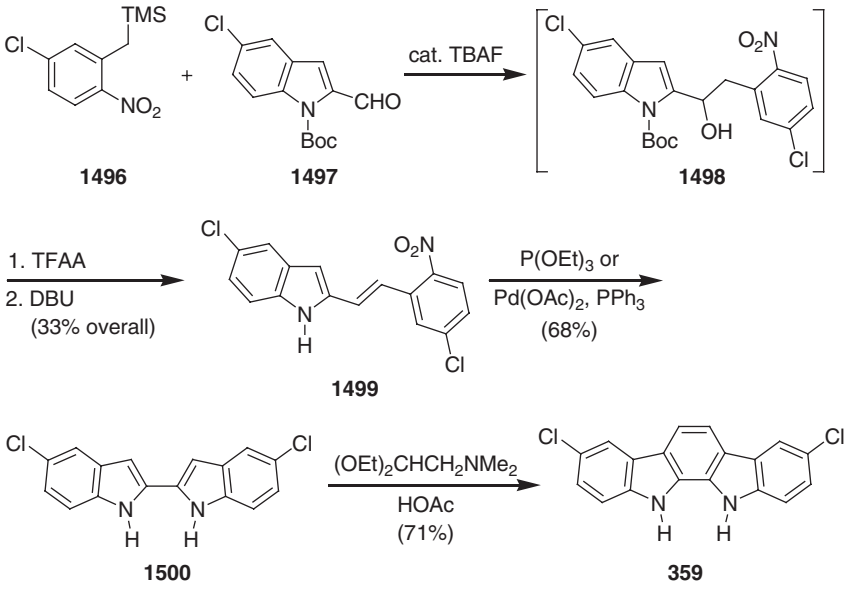

Scheme 5.255

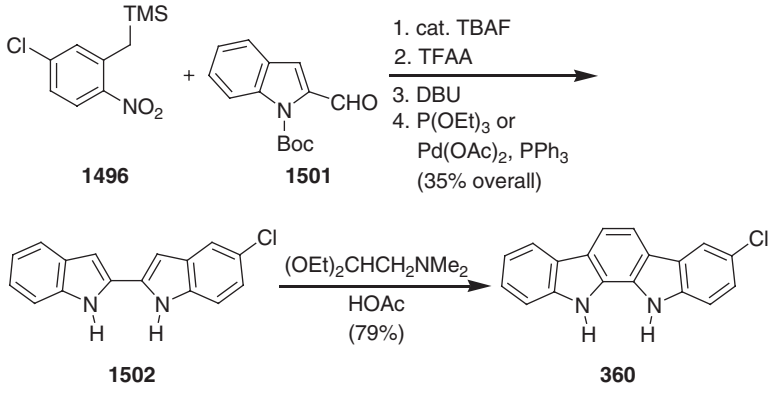

Scheme 5.256

The same authors also reported the total synthesis of tjipanazole B (**369**) in 66% overall yield, in two steps, by reacting tjipanazole D (**359**) with α-D-xylopyranosyl chloride (**1503**) in a biphasic mixture of MTBE and 45% aqueous KOH and Aliquat 336, followed by hydrogenation with $Pd(OH)_2$ (796). Similarly, reaction of tjipanazole D (**359**) with α-D-glycopyranosyl chloride (**1504**) led to tjipanazole E (**370**) in two steps and 77% overall yield (796) (Scheme 5.257).

Cai and Snieckus reported a total synthesis of 5-cyano-6-methoxy-11-methylindolo[2,3-*a*]carbazole (**357**) starting from the 2-bromoindolecarboxamide **1505** (797). This methodology uses a directed *ortho*- and remote metalation-cross-coupling strategy. Stille cross-coupling reaction of 2-bromoindolecarboxamide **1505** with the 2-stannylated *N*-carboxyindole **1506** afforded the bisindolyl derivative **1507** in 77% yield. On treatment with Eschenmoser's salt, **1507** gave the gramine derivative **1508**, which, upon sequential reaction with methyl iodide, followed by reaction with KCN/18-crown-6, afforded the acetonitrile **1509**. LDA-mediated cyclization of **1509**, followed by immediate methylation of the unstable phenol with diazomethane, led to 5-cyano-6-methoxy-11-methylindolo[2,3-*a*]carbazole (**357**) (797) (Scheme 5.258).

The powerful and varied biological activities of the indolocarbazole systems offer many potential therapeutic applications, particularly as anticancer agents, and several have reached the stage of clinical trials. Unsurprisingly, these fascinating structures have attracted substantial synthetic interest, both from the standpoint of total synthesis of the natural products themselves as discussed above, and the design of simpler analogs for probing structure activity relationships (435,437,439,440,798–852).

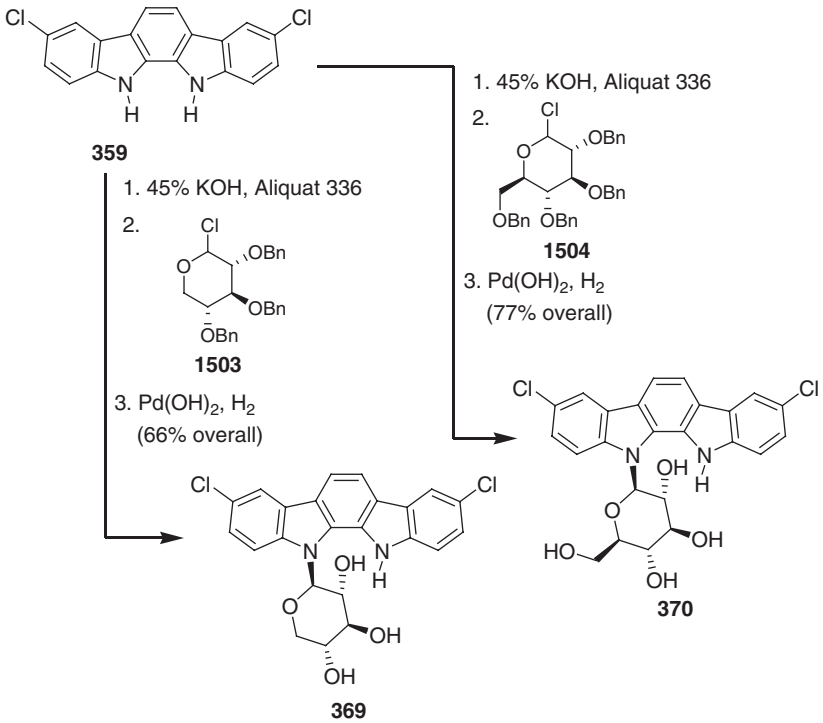

Scheme 5.257

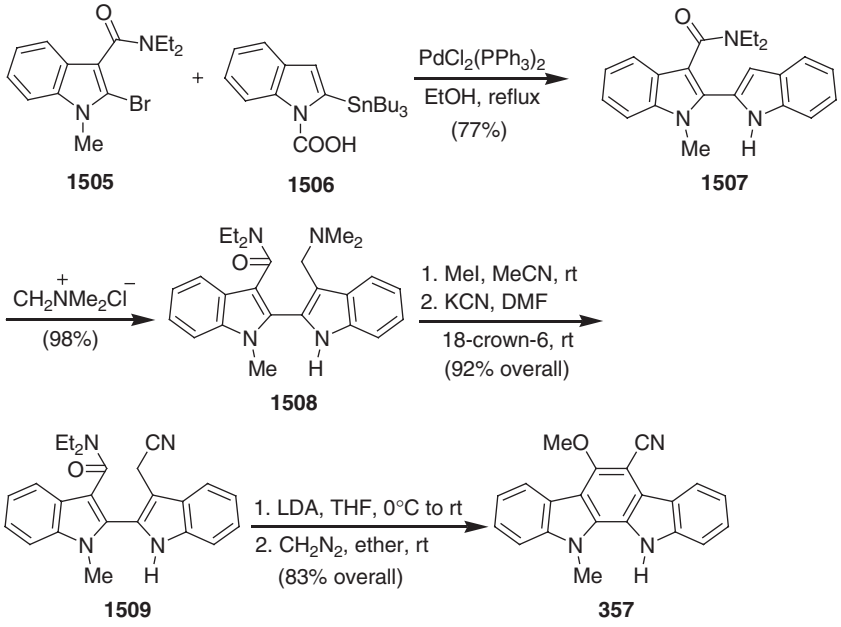

Scheme 5.258

I. Imidazo[4,5-*a*]pyrrolo[3,4-*c*]carbazole Alkaloids

Until now, this relatively new class of imidazo[4,5-*a*]pyrrolo[3,4-*c*]carbazole alkaloids includes only three natural products. These natural products showed G2 check point inhibitor activity, and thus represent a promising target for the development of new chemotherapeutic anticancer agents. Due to this fact, a wide range of analogs of imidazo[4,5-*a*]pyrrolo[3,4-*c*]carbazole alkaloids were reported for structure activity studies.

Berlinck, Piers, Anderson, and co-workers described the total synthesis of granulatimide (**374**) and isogranulatimide (**375**), along with its isolation (342). This short and efficient biomimetic synthesis was undertaken to establish the assigned structures, and uses a photolytic electrocyclization of didemnimide A (**373**) as the key step. Reaction of the substituted imidazole **1510** with butyllithium, followed by reaction of the intermediate 5-lithioimidazole with dimethyl oxalate, afforded the α-keto ester **1511** in 66% yield. Condensation of compound **1511** with indole-3-acetamide (**1369**) in the presence of potassium *tert*-butoxide (KO*t*-Bu) and 4 Å MS in DMF led to the maleimide **1512**. After desulfurization of **1512** with Raney nickel (Ra-Ni) to compound **1513**, the methoxymethyl group was cleaved with boron tribromide to give didemnimide A (**373**). Finally, the photolysis of a solution of didemnimide A (**373**) in acetonitrile containing a small amount of palladium on charcoal provided granulatimide (**374**) in 91% yield and isogranulatimide (**375**) in 8% yield (342) (Scheme 5.259).

Two years later, Piers *et al.* reported an improved synthesis of isogranulatimide (**375**) starting from didemnimide A (**373**). Heating of a solution of **373** in nitrobenzene containing palladium black as the hydrogen transfer reagent at

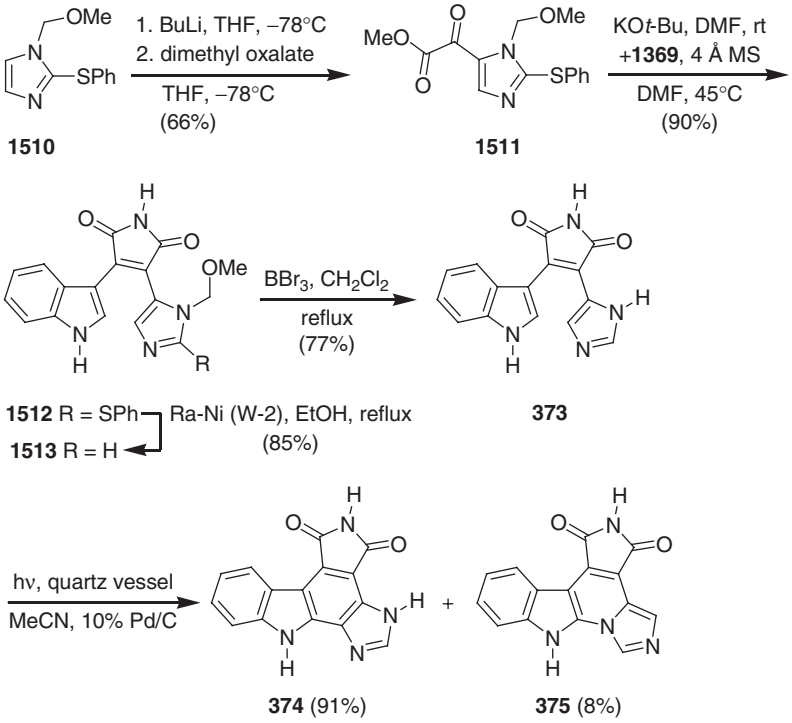

Scheme 5.259

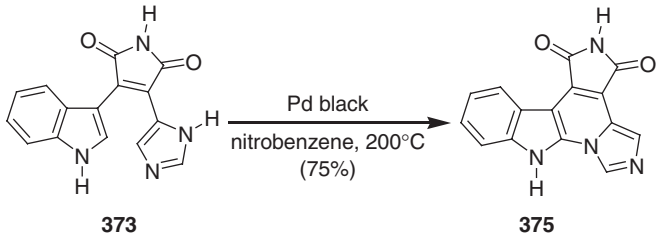

Scheme 5.260

200°C led to only isogranulatimide (**375**) in 75% yield (853) (Scheme 5.260). The same authors also reported a series of analogs of granulatimide and isogranulatimide (853).

Murase *et al.* reported a new synthesis of granulatimide (**374**) starting from 1-methoxyindole (**1514**) (854). This synthetic approach involves Stille coupling of stannylindole **1515** with the iodoimidazole **1516** to afford the indole–imidazole coupling product **1517** and photocyclization of the condensation product **1520** as key steps. Regioselective lithiation of 1-methoxyindole (**1514**) with butyllithium, followed by quenching of the intermediate 2-lithio derivative with chloro tributylstannane led to the stannylindole **1515**. The Stille coupling reaction of **1515** with 4-iodo-1-(methoxymethyl)imidazole (**1516**) in the presence of $PdCl_2(PPh_3)_2$

afforded the corresponding indole–imidazole coupling product **1517**. After removal of the methoxy group in **1517**, the deprotected compound **1518** was reacted with ethylmagnesium bromide to afford the corresponding Grignard reagent **1519**, which, on treatment with dibromomaleimide (**1357**), led to the corresponding coupling product **1520**. Following Pier's procedure, with some modifications, compound **1520** was transformed to MOM-protected granulatimide (**1521**). Finally, removal of the MOM group in **1521** led to granulatimide (**374**) in 72% yield (854) (Scheme 5.261). Further application of this synthetic approach led to the granulatimide structural analogs, 10-methylgranulatimide, 17-methylgranulatimide, and 10,17-dimethylgranulatimide (854). One year later, the same authors reported a further extension of the aforementioned methodology for the synthesis of various granulatimide positional analogs (855).

Prodhomme *et al.* reported the synthesis of a series of structurally related granulatimide and isogranulatimide isomers and analogs bearing modified heterocycles (856–860). These syntheses were undertaken to obtain an insight into the possible interactions of these analogs with the ATP binding site of the target kinase.

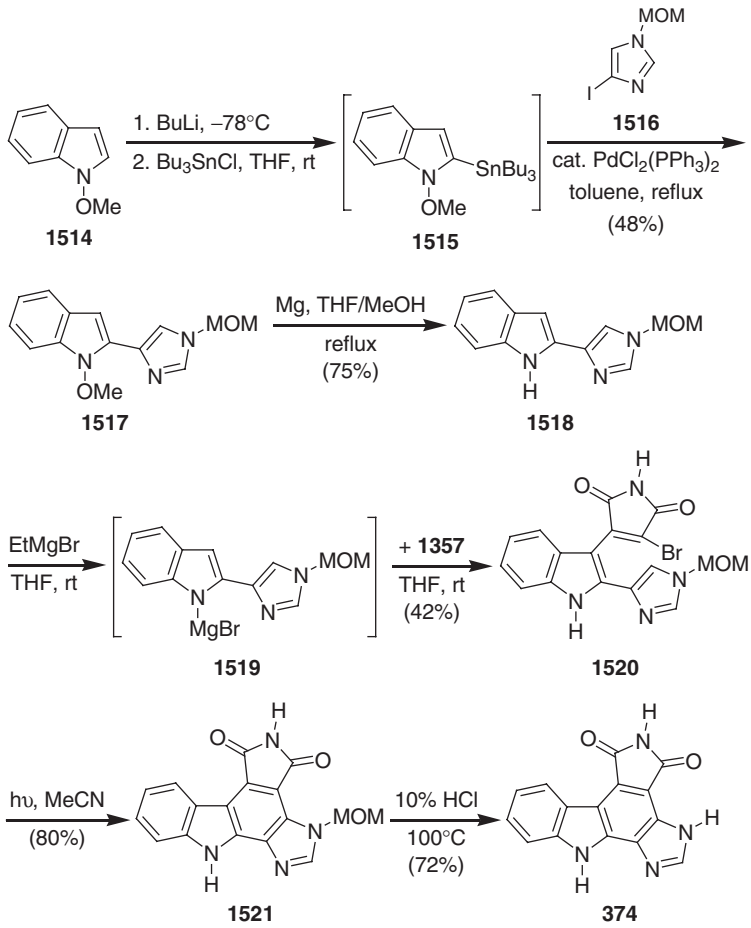

Scheme 5.261

J. Quinolino[4,3-*b*]carbazole-1,4-quinone Alkaloids

So far this class of carbazole alkaloids contains only two natural products, calothrixin A and its *N*-deoxy-derivative calothrixin B. These two pentacyclic metabolites with a quinolino[4,3-*b*]carbazole-1,4-quinone framework displayed potent inhibitory effects on the *in vitro* growth of both human malarial parasites and human cancer cells and inhibition of RNA polymerase activity. Owing to this pharmaceutical potential, these natural products have attracted the synthetic interest of various research groups (8).

Kelly *et al.* reported the first total synthesis of calothrixins A (**377**) and B (**378**) from 3-formyl indole (**618**) and quinoline-4-carboxylic acid (**1523**) involving an *ortho*-lithiation strategy for the construction of the pentacyclic ring system (861). The MOM-protected 3-formylindole (**1522**) and the quinoline-4-carboxamide (**1523**) were prepared in a one-pot operation from the commercially available compounds **618** and **1523**, respectively. Lithiation of **1524** using lithium tetramethylpiperidide (LiTMP), followed by coupling with **1522**, provided directly the MOM-protected calothrixin B (**1529**). None of the putative intermediates **1526**, **1527**, and **1528** shown in Scheme 5.262 was isolated. However, the use of LiTMP as base was crucial for this metalation. Finally, removal of the MOM protecting group of **1529** led to calothrixin B (**378**) in 74% yield. Selective oxidation of the pyridine nitrogen of calothrixin B (**378**) with MCPBA afforded calothrixin A (**377**) in 71% yield (861) (Scheme 5.262).

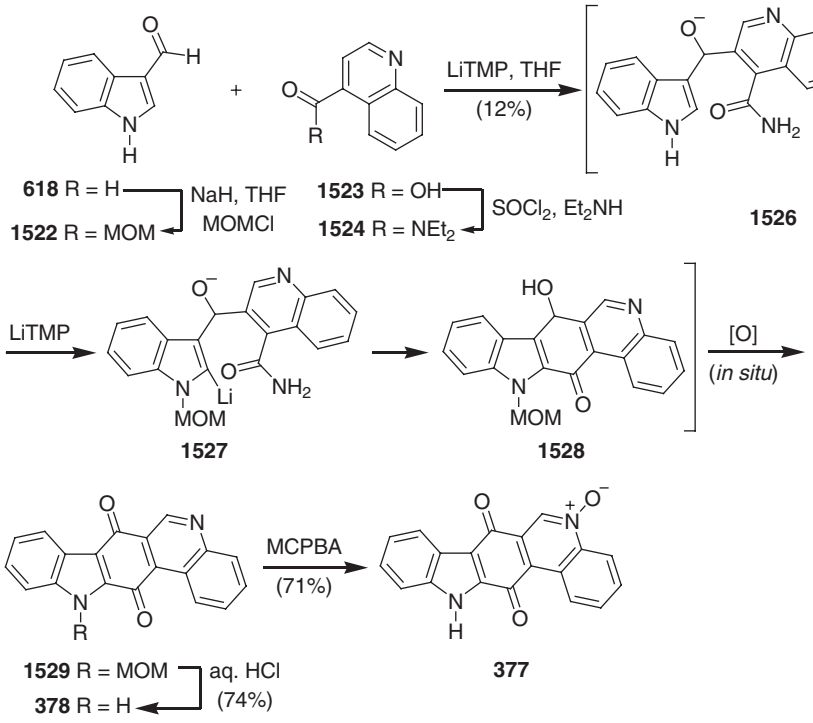

Scheme 5.262

Chai *et al*. reported an alternative synthesis to calothrixin A (**377**) and B (**378**) from readily available indole (**1170**) and the acid chloride **1532**. This methodology differs from Kelly's synthesis in that the pentacyclic ring system is constructed by using Friedel–Crafts acylation and metalation strategies. The acid chloride **1532** was obtained from the corresponding quinoline **1531**, which, in turn, is prepared from quinolin-3,4-anhydride (**1530**). The Friedel–Crafts acylation of indole (**1170**) with the acid chloride **1532** provided the diaryl ketone **1533** in 90% yield. Compound **1533** was protected as *N*-MOM derivative **1534**. Reaction of **1534** with LiHMDS in the presence of tetramethylethylenediamine (TMEDA), followed by intramolecular nucleophilic substitution of the ester, led to *N*-MOM-calothrixin B (**1529**) in 92% yield. Finally, cleavage of the *N*-MOM group provided calothrixin B (**378**) (862–864). Conversion of **378** to calothrixin A (**377**) was then readily achieved by using MCPBA as the oxidant (see Scheme 5.262) (861) (Scheme 5.263).

Collet, Guingant, and co-workers reported a convergent synthesis of calothrixin B (**378**) starting from the commercially available tetrahydro-4*H*-carbazole-4-one (**859**) (865,866). This methodology is based on the regioselective hetero-Diels–Alder reaction between 9-bromocarbazole-1,4-dione **1534** and '*push pull*' 2-aza-1,3-diene **1535** to construct the pentacyclic core structure of calothrixin B (**378**). Dehydrogenation of tetrahydro-4*H*-carbazole-4-one (**859**) on Pd/C afforded carbazol-4-ol **1530**, which, on bis-protection with the Cbz group using benzylchloroformate, led to the bis-Cbz carbazole **1531**. Chemoselective monodeprotection of **1531** by treatment with aqueous sodium hydroxide led to the *N*-Cbz-carbazole **1532**, which on bromination with NBS in acetonitrile, furnished the corresponding 3-bromocarbazole **1533**.

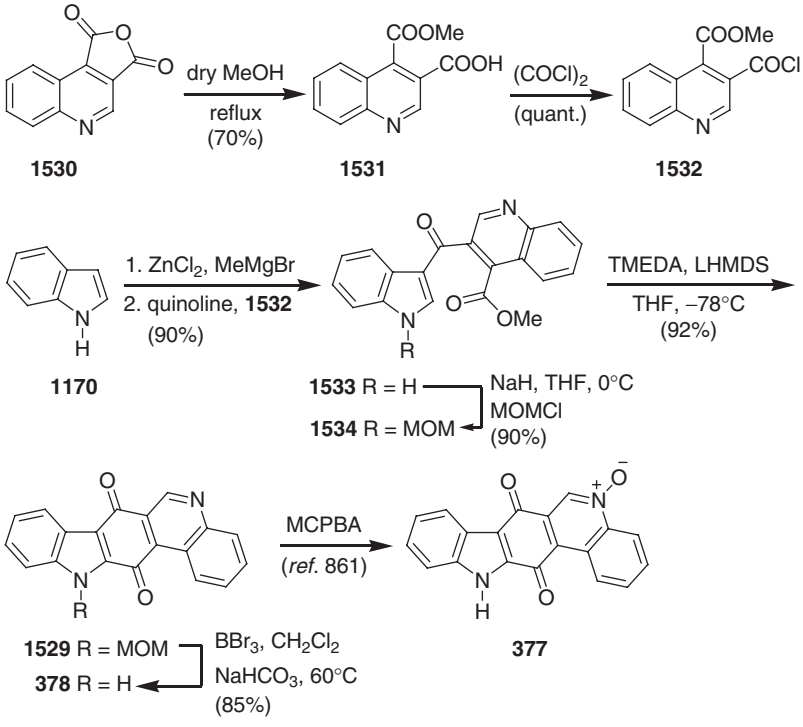

Scheme 5.263

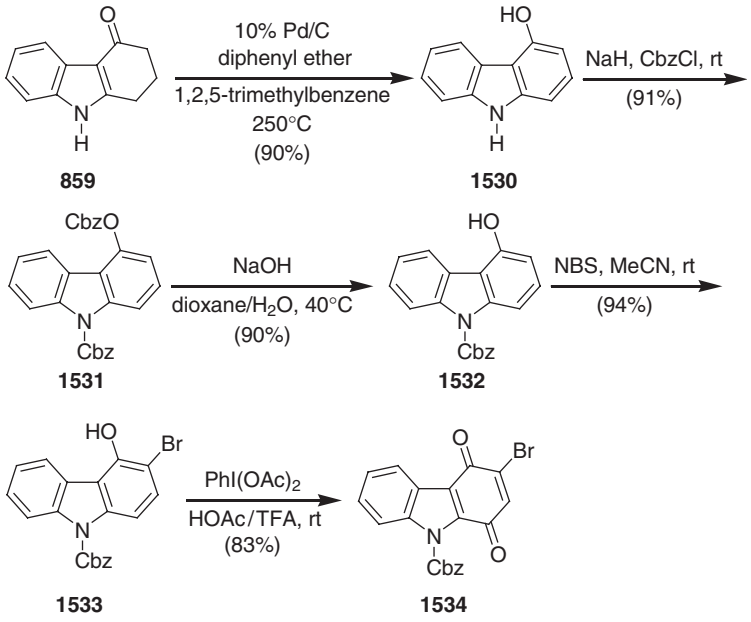

Scheme 5.264

Oxidation of **1533** with diacetoxyiodobenzene [$PhI(OAc)_2$] led to the desired bromo-activated dienophile **1534** (Scheme 5.264).

The key [4+2] cycloaddition reaction of **1534** with an excess of 2-aza-1,3-diene **1535** in acetonitrile at 40°C afforded the Cbz-deprotected adduct **1536** in 80% yield, along with 5% of the Cbz cycloadduct **1537**. The high yield of this cycloadduct is attributed to the electron-acceptor nature of the Cbz protecting group, as well as the removal of the Cbz group with the liberated dimethylamine hydrobromide. Deprotonation of **1536**, followed by triflation, afforded a mixture of the enol triflate **1538** and the aryl triflate **1539**, which, without separation, were subsequently heated in dioxane in the presence of DDQ to afford the triflate **1539**. Finally, exposure of **1539** to palladium(0)-catalyzed reductive elimination conditions completed the synthesis of calothrixin B (**378**) (865,866) (Scheme 5.265). Execution of this sequence with the benzyl protecting group turned out to be less efficient due to the poor yield in the key cycloaddition step, as well as difficult removal of the *N*-benzyl protecting group at a later stage of the synthesis (865,866).

Hibino *et al*. reported a new total synthesis of calothrixin B (**378**) starting from 2-formyl-*N*-phenylsulfonylindole (**1540**) (867). The key step in this synthesis is an allene-mediated, electrocyclic reaction of a 6π-electron system involving the indole-2,3-bond for the construction of the 4-oxygenated carbazole ring system **1546**. The Wittig reaction of **1540** with 2-nitrobenzyltriphenylphosphorane (**1541**) gave the *trans*-styrylindole **1542**. Treatment of **1541** with 1,1-dichloromethyl methyl ether in the presence of $AlCl_3$ afforded the 3-formylindole **1543**. Grignard reaction of **1543** with ethynyl magnesium bromide led to the corresponding propargyl alcohol **1544**, which was protected as the methoxymethyl ether **1545**. The propargyl ether **1545** was subjected to an allene-mediated electrocyclic reaction by treatment with potassium *tert*-butoxide (KO*t*-Bu) in *tert*-butanol (*t*-BuOH) and THF at 90°C to

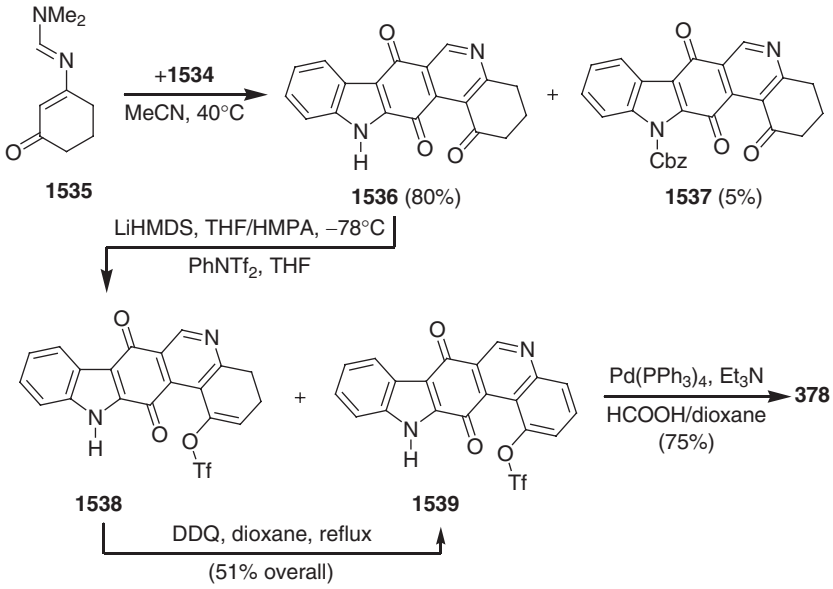

Scheme 5.265

afford the required 4-oxygenated carbazole **1546**. Oxidation of **1546** with DDQ in the presence of lithium perchlorate gave the 3-formyl-4-hydroxy-carbazole **1547** with elimination of the MOM group. Reduction of the nitro group of **1547** with 10% Pd/C, followed by the intramolecular cyclization and subsequent oxidation to the quinone with CAN, afforded calothrixin B (**378**) in 67% yield (867) (Scheme 5.266).

One year later, the same authors reported a biomimetic synthesis to calothrixin B (**378**) *via* a hypothetical metabolite, 6-formylindole[2,3-*a*]carbazole (868). This synthesis is based on an allene-mediated, electrocyclic reaction involving two[*b*]-bonds of indoles and starts from 2-bromoindole-3-carbaldehyde (**1548**). Suzuki–Miyaura coupling of **1548** with indole-2-boronic acid **1549** gave the bisindole **1550**. Cleavage of the *N*-Boc group in **1550** with TFA, followed by protection of both nitrogen atoms with chloromethyl methyl ether (MOMCl) and NaH, afforded the bis-MOM-bisindole **1551**. The Grignard reaction of **1551** with ethynyl magnesium bromide yielded the propargyl alcohol **1552**, which was protected with MOMCl to afford the MOM ether **1553**. An allene-mediated electrocyclic reaction of **1553** led to the desired indolocarbazole **1554**. Oxidation of the 6-methylindolocarbazole **1554** to 6-formylindolocarbazole **1555** was achieved by reaction with DDQ. Further oxidation with CAN led to *N*-MOM-calothrixin B (**1529**) involving the quinone imine **1556** and the quinone **1557** as intermediates. Finally, cleavage of the MOM group using Kelly's method afforded calothrixin B (**378**) in 65% yield (868) (Scheme 5.267).

Bennasar *et al*. reported a new radical-based route for the synthesis of calothrixin B (**378**) (869). This synthesis starts from the 2,3-disubstituted *N*-Boc indole **1558** and uses a regioselective intramolecular acylation of a quinoline ring as the key step for the construction of the calothrixin pentacyclic framework. Chemoselective reaction of *in situ*-generated 3-lithio-2-bromoquinoline [from 2-bromoquinoline **1559** with LDA] with the 3-formylindole **1558** followed by triethylsilane reduction of the

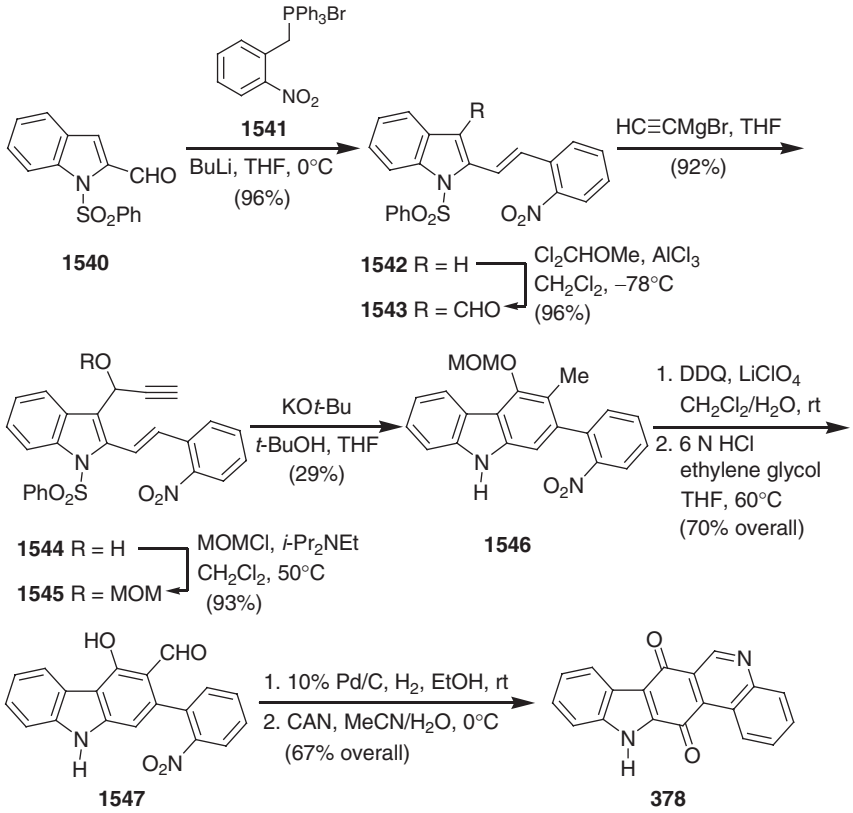

Scheme 5.266

resulting carbinol afforded the 2-bromoquinoline **1560** in 65% yield. Reaction of **1560** with tributyltin hydride followed by protection of the indole nitrogen with MOMCl led to the *N*-MOM methyl ester **1561** in 81% yield. Hydrolysis of **1561**, followed by phenylselenation of the intermediate carboxylic acid gave the required selenoester **1562**. Treatment of the selenoester **1562** with tri(trimethylsilyl)silane (TTMSS) in the presence of the radical initiator AIBN at 80°C led to the pentacyclic phenol **1563**. Mild oxidation of the phenol **1563** with molecular oxygen in basic medium furnished a nearly quantitative yield of *N*-MOM-calothrixin B (**1529**), a known immediate precursor of calothrixin B (**378**) (869) (Scheme 5.268).

Recently, Moody *et al.* reported a biomimetic synthesis of calothrixin B (**378**) by oxidation of Hibino's 6-formylindole[2,3-*a*]carbazole **1555** (870). The key intermediate 6-formyl-indole[2,3-*a*]carbazole was readily obtained in six steps from indigo (**1458**). Using Somei's procedure, indigo (**1458**) was transformed to the *cis*-chlorohydrin **1461** in three steps and 50% overall yield (see Scheme 5.247). The reduction of the chlorohydrin **1461** gave 5-hydroxy-indolo[2,3-*a*]carbazole **1564**, and subsequent Vilsmeier formylation delivered the desired 6-formyl-indole[2,3-*a*]carbazole **1565** in 45% yield. Reaction of hydroxy-indolocarbazole **1565** with an excess of chloromethyl methyl ether (MOMCl) afforded the tris-MOM-protected compound **1555**. Following Hibino's approach, the tris-MOM-protected indolocarbazole **1555**

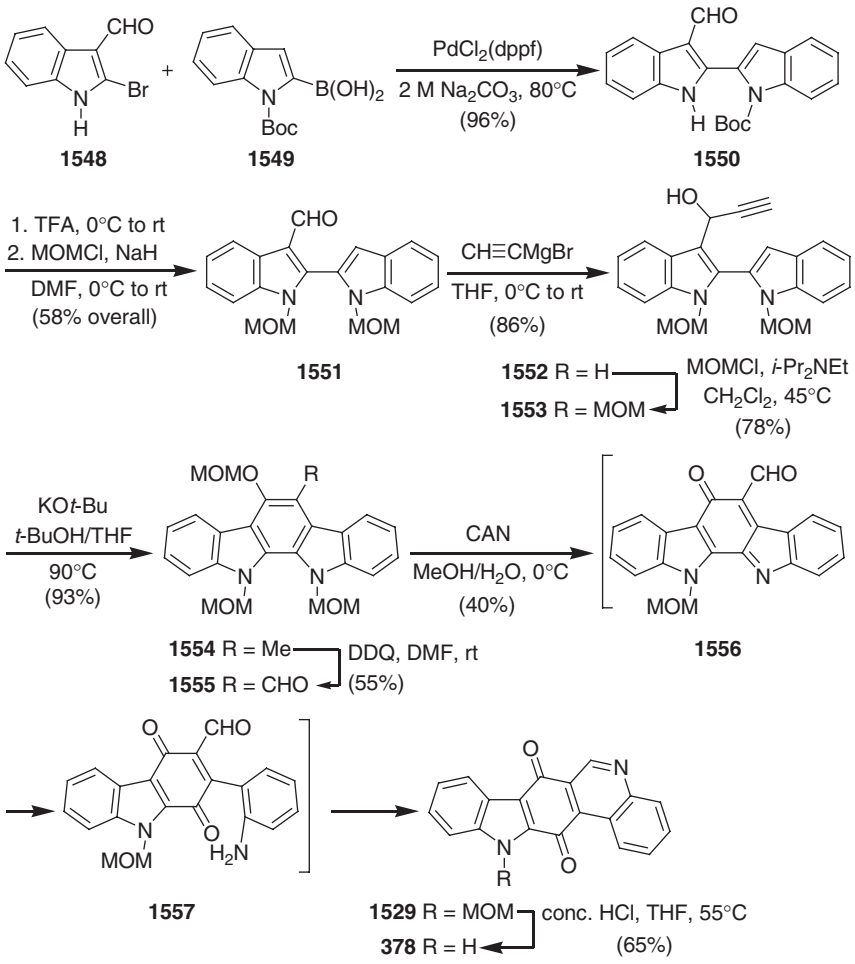

Scheme 5.267

was transformed to calothrixin B (**378**) in two steps and 26% overall yield (870) (Scheme 5.269).

K. Miscellaneous Carbazole Alkaloids

In this section, we cover the total synthesis of carbazole alkaloids that are not discussed in the previous sections because of their unique substitution pattern.

Filimonov *et al.* reported a synthesis of 3,6-diiodocarbazole (**387**) by iodination of carbazole (**1**). For the iodination, the required electrophilic iodine was generated by reacting iodine monochloride (ICl) with silver trifluoroacetate (CF_3COOAg) in acetonitrile. Following this procedure, 3,6-diiodocarbazole (**387**) was obtained in almost quantitative yield (871) (Scheme 5.270).

Müllen *et al.* reported an efficient, two-step synthesis of 2,7-dibromocarbazole (**388**) starting from 4,4′-dibromobiphenyl (**1566**). This method uses Cadogan's

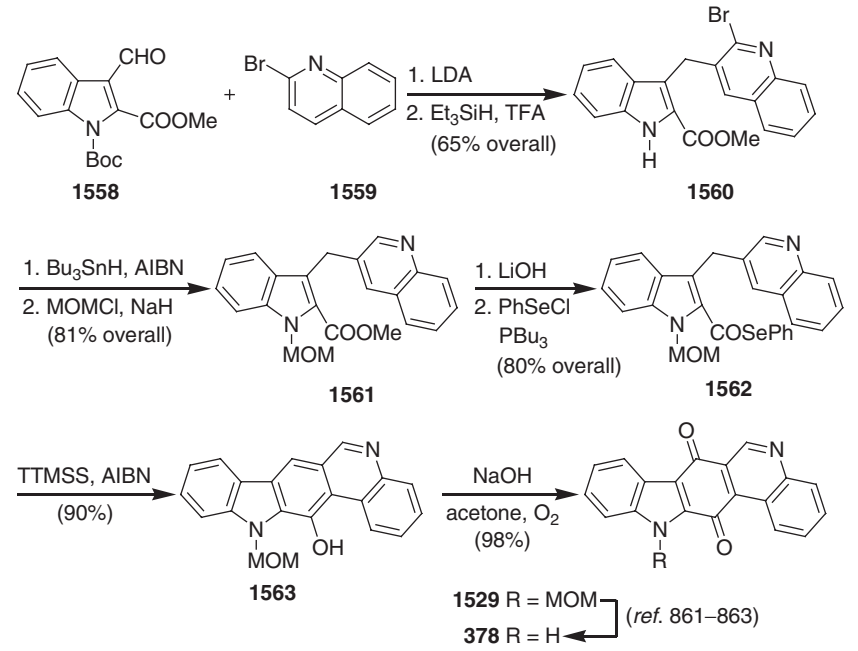

Scheme 5.268

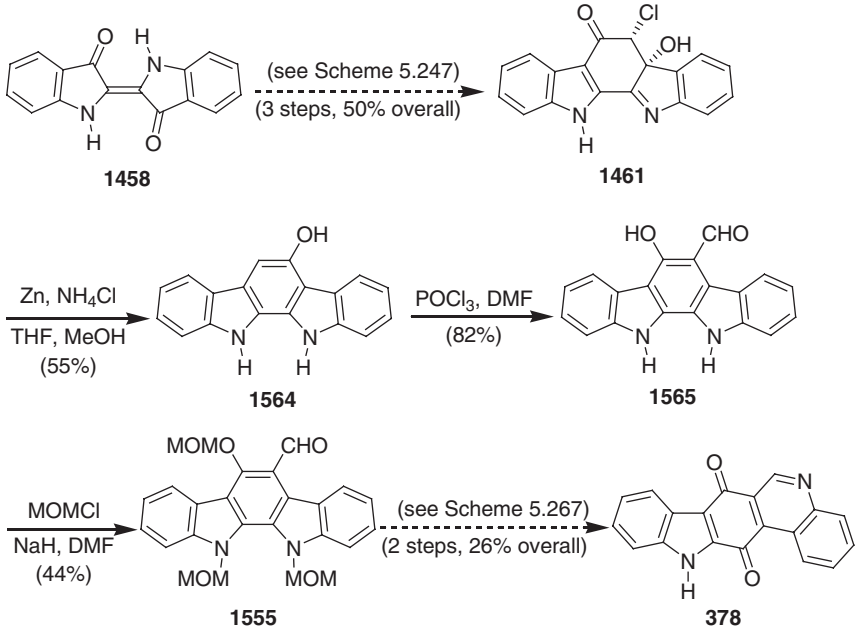

Scheme 5.269

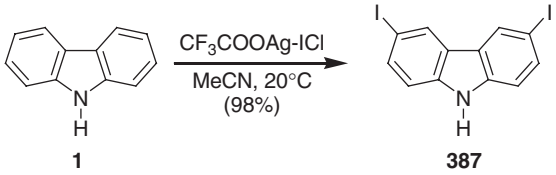

1 **387**

Scheme 5.270

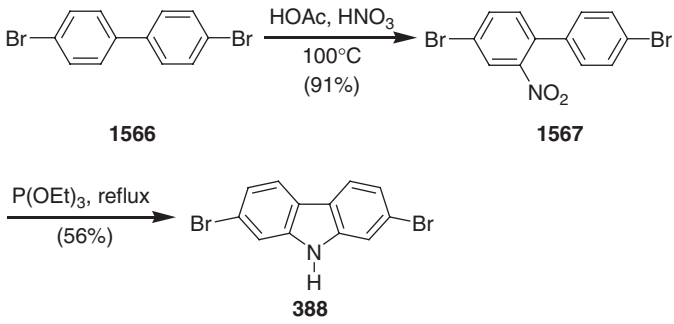

1566 **1567**

388

Scheme 5.271

deoxygenative cyclization as the key step for the formation of the carbazole framework. Nitration of the dibromobiphenyl **1566** with concentrated nitric acid gave the corresponding 2-nitro derivative **1567** in 91% yield. Finally, a reductive Cadogan's ring closure of **1567** by refluxing in triethylphosphite led to 2,7-dibromocarbazole (**388**) in 56% yield (872) (Scheme 5.271).

Over the past few years, the heteroaryl-condensed non-natural carbazoles emerged as a rapidly growing class of compounds because of their broad spectrum of useful biological activities (8,249,873). This relatively new class of non-natural carbazoles with a great variety of heterocyclic systems has been extensively investigated in order to understand the structure activity relationships for the various biological activities (843,874–895).

CHAPTER 6

Addendum

Pindur *et al*. reported the synthesis of carazostatin (**247**) starting from the 2-vinylindole **958**, which previously served as the key building block in the total synthesis of carbazoquinocin C (**274**) (see Scheme 5.130). The 2-vinylindole (**958**), readily available in four steps starting from *N*-(phenylsulfonyl)indole (**956**), was transformed to the indolylacetic acid (**1568**) by treatment with KCN and paraformaldehyde followed by alkaline hydrolysis. Subsequent acid-catalyzed polar cyclization of **1568** led to carazostatin (**247**) (648) (Scheme 6.1).

Recently, Tripathi *et al*. reported a new pyrano[3,2-*a*]carbazole alkaloid, 7-isovaleryl-oxy-8-methoxygirinimbine (**1569**) from the leaves of *Murraya koenigii* (896) (Scheme 6.2).

Liu and Larock reported a new total synthesis of mukonine (**11**) starting from commercially available 4-amino-3-methoxybenzoic acid (**1570**) (897). This method

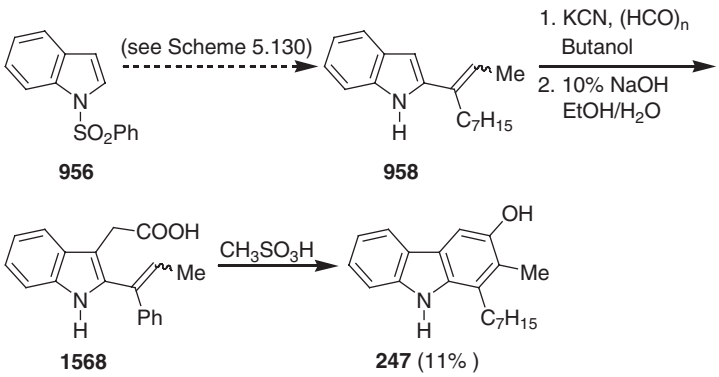

Scheme 6.1

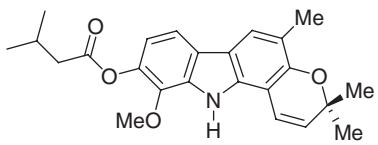

1569 7-Isovaleryloxy-8-methoxygirinimbine

Scheme 6.2

involves a cross-coupling of a 2-iodoaniline with silylaryl triflate and subsequent Pd(0)-catalyzed cyclization as the key step. Reaction of the aminobenzoic acid **1570** with methanol led to the corresponding methyl benzoate **600**. Iodination of **600** with iodine monochloride (ICl) in dichloromethane afforded methyl 4-amino-3-iodo-5-methoxybenzoate (**1571**) in 82% yield. Finally, cross-coupling of **1571** with silylaryl triflate in the presence of CsF, followed by Pd(0)-catalyzed intramolecular cyclization, led to mukonine (**11**) in 95% yield (897) (Scheme 6.3).

Ackermann and Althammer reported an efficient synthesis of murrayafoline A (**7**) starting from the easily accessible 2-methoxy-4-methylaniline (**598**) (see Scheme 5.33) (898). This methodology involves a Pd(0)-catalyzed domino N–H/C–H bond activation to afford the carbazole framework directly. Thus, in a one-pot operation, 2-chloro-bromobenzene (**1573**) and the aniline **598** were directly transformed into murrayafoline A (**7**) in 74% yield by reacting with a catalytic amount of Pd(II) acetate in the presence of K_3PO_4, PCy_3, and *N*-methylpyrrolidone (NMP). This reaction also proceeds with 1,2-dichlorobenzene, albeit in 72% yield (898) (Scheme 6.4).

Lebold and Kerr reported the total synthesis of the eustifolines-A (**172**), -B (**173**), -C (**93**), -D (**227**), and glycomaurrol (**92**) starting from the readily available quinine imine **1574** and diene **1575** (899). This methodology uses the Diels–Alder reaction of a quinone monoimine **1574** and subsequent Plieninger indolization of the adduct **1576** for the synthesis of the key tetrahydrocarbazole framework.

Reaction of the quinine imine **1574** and diene **1575** in refluxing dichloromethane, followed by treatment of the resulting adduct with a catalytic amount of DBU, afforded the desired aromatic compound **1576** as a 1:1 diastereoisomeric mixture in

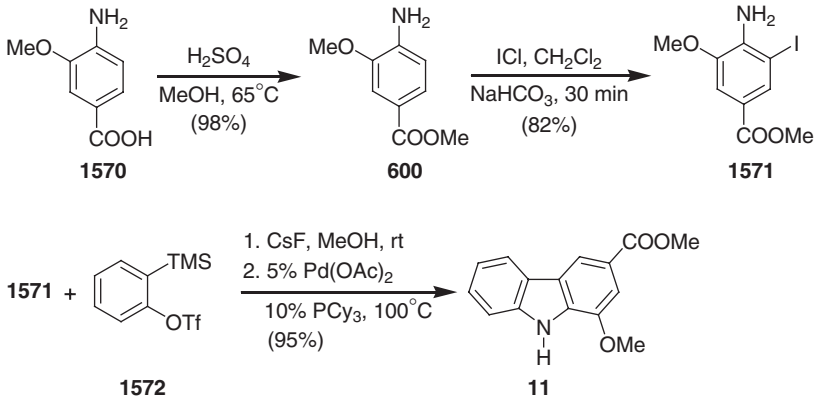

Scheme 6.3

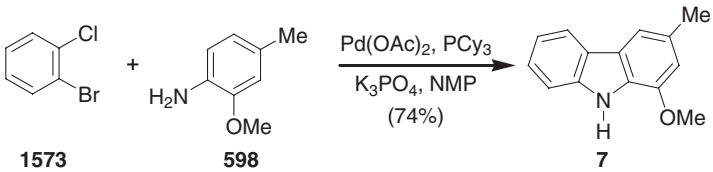

Scheme 6.4

91% yield. Without separation, both diastereoisomers of the dihydronaphthalene **1576** were transformed to the tetrahydrocarbazole **1577** *via* an oxidative cleavage of the double bond of the protected phenol (*via* the diol) followed by treatment of the resulting dicarbonyl with acid. Using this four-step sequence, tetrahydrocarbazole **1577** was obtained in 61% yield. Compound **1577** was transformed to methylcarbazole **1578** in 89% overall yield involving aldehyde reduction, tosyl removal, and dehydrogenation (899) (Scheme 6.5).

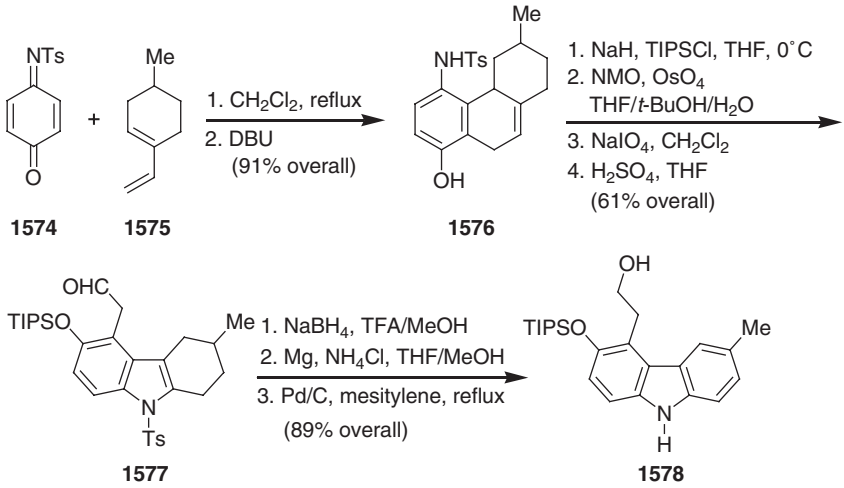

Scheme 6.5

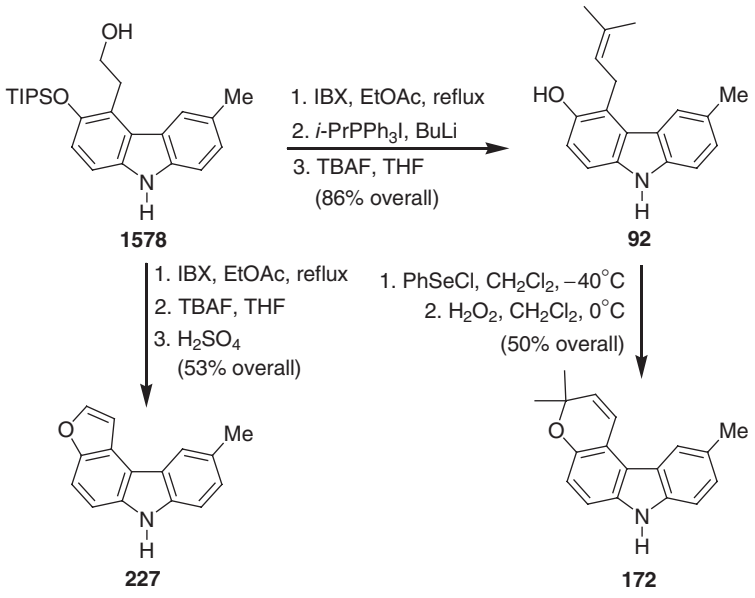

Scheme 6.6

Oxidation of the methylcarbazole **1578** to the corresponding aldehyde, followed by olefination of the crude aldehyde with triphenylphosphonium isopropyl ylide and desilylation, afforded glycomaurrol (**92**) in 86% yield over three steps. Cyclization of glycomaurrol (**92**) with PhSeCl, followed by oxidation with hydrogen peroxide (H_2O_2), afforded eustifoline-A (**172**) in 50% overall yield over two steps. Eustifoline-D (**227**) was prepared by oxidizing the 3-methylcarbazole **1578**, and subjecting the resulting aldehyde to desilylation, followed by treatment with acid to effect benzofuran formation. This three-step sequence led to eustifoline-D (**227**) in 53% overall yield (Scheme 6.6).

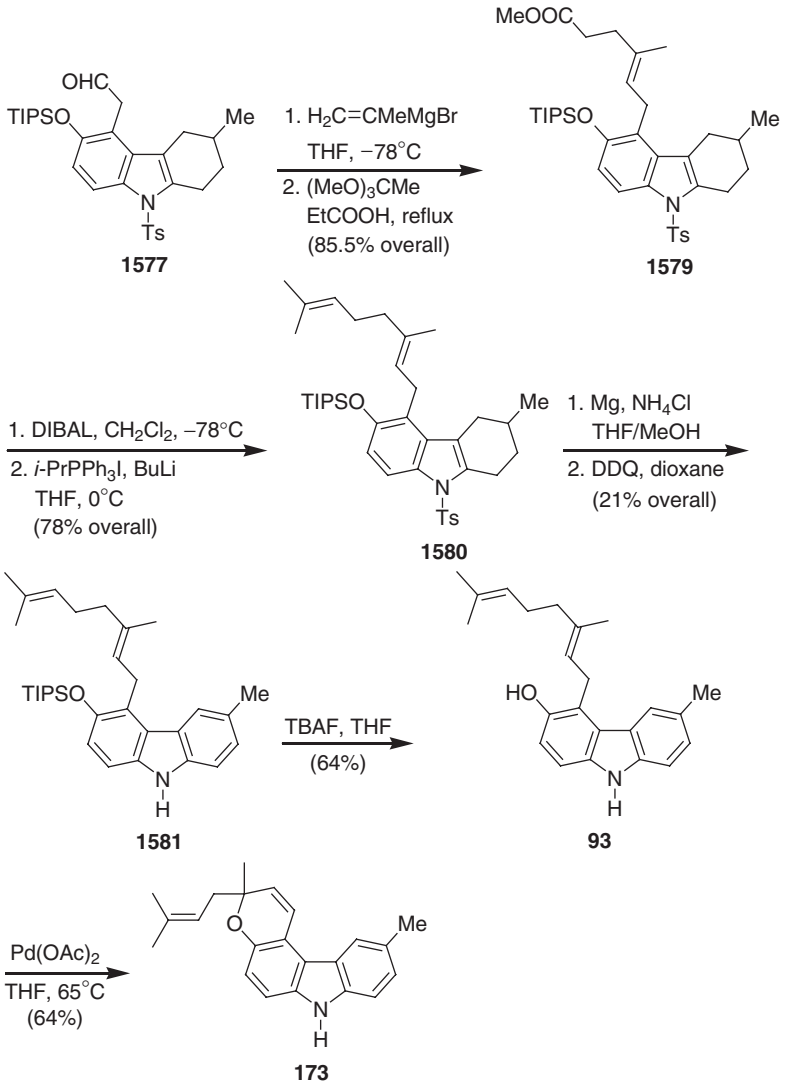

Scheme 6.7

Treatment of tetrahydrocarbazole **1577** with isopropenyl magnesium bromide followed by *in situ* generation of a ketene acetal *en route* to a Johnson–Claisen rearrangement, led to the formation of ester **1579** with the required *E*-double bond. Reduction to the aldehyde using DIBAL, and olefination with triphenylphosphonium isopropyl ylide, gave the corresponding tetrahydrocarbazole **1580** with the requisite isopropylidine moiety in 78% overall yield. After *N*-tosyl removal with magnesium metal in methanolic aqueous ammonium chloride, the corresponding tetrahydrocarbazole was subjected to DDQ-mediated aromatization to afford *O*-TIPS-eustifoline-C (**1581**). Desilylation with TBAF furnished eustifoline-C (**93**) in 64% yield. Oxidative cyclization of eustifoline-C (**93**) with Pd(II) acetate then generated eustifoline-B (**173**) in 64% yield (899) (Scheme 6.7).

REFERENCES

[1] R. S. Kapil, *in* "The Alkaloids" (R. H. F. Manske, ed.), vol. 13, p. 273. Academic Press, New York, 1971.
[2] H.-P. Husson, *in* "The Alkaloids" (A. Brossi, ed.), vol. 26, p. 1. Academic Press, New York, 1985.
[3] D. P. Chakraborty, *in* "The Alkaloids" (G. A. Cordell, ed.), vol. 44, p. 257. Academic Press, New York, 1993.
[4] D. P. Chakraborty, *in* "Progress in the Chemistry of Organic Natural Products" (W. Herz, H. Grisebach and G. W. Kirby, eds.), vol. 34, p. 299. Springer-Verlag, Wien, 1977.
[5] P. Bhattacharyya and D. P. Chakraborty, *in* "Progress in the Chemistry of Organic Natural Products" (W. Herz, H. Grisebach, G. W. Kirby and C. Tamm, eds.), vol. 52, p. 159. Springer-Verlag, Wien, 1987.
[6] D. P. Chakraborty and S. Roy, *in* "Progress in the Chemistry of Organic Natural Products" (W. Herz, H. Grisebach, G. W. Kirby, W. Steglich and C. Tamm, eds.), vol. 57, p. 71. Springer-Verlag, Wien, 1991.
[7] D. P. Chakraborty and S. Roy, *in* "Progress in the Chemistry of Organic Natural Products" (W. Herz, H. Grisebach, G. W. Kirby, W. Steglich and C. Tamm, eds.), vol. 85, p. 125. Springer-Verlag, Wien, 2003.
[8] H.-J. Knölker and K. R. Reddy, *Chem. Rev.* **102**, 4303 (2002).
[9] H.-J. Knölker, *Curr. Org. Synth.* **1**, 309 (2004).
[10] H.-J. Knölker, *Top. Curr. Chem.* **244**, 115 (2005).
[11] B. S. Joshi, *Heterocycles* **3**, 837 (1975).
[12] C. Graebe and C. Glaser, *Ber. Dtsch. Chem. Ges.* **5**, 12 (1872).
[13] B. K. Chowdhury, A. Mustapha, M. Garba, and P. Bhattacharyya, *Phytochemistry* **26**, 2138 (1987).
[14] A. Roy, P. Bhattacharyya, and D. P. Chakraborty, *Phytochemistry* **13**, 1017 (1974).
[15] B. S. Joshi and D. H. Gawad, *Indian J. Chem.* **12**, 437 (1974).
[16] B. T. Ngadjui, J. F. Ayafor, B. L. Sondengam, and J. D. Connolly, *Phytochemistry* **28**, 1517 (1989).
[17] M. Chakrabarty, A. C. Nath, S. Khasnobis, M. Chakrabarty, Y. Konda, Y. Harigaya, and K. Komiyama, *Phytochemistry* **46**, 751 (1997).
[18] T.-S. Wu, Y.-Y. Chan, M.-J. Liou, F.-W. Lin, L.-S. Shi, and K.-T. Chen, *Phytother. Res.* **12**, S80 (1998).
[19] R. E. Richards, *J. Chem. Soc.* 978 (1947).
[20] D. P. Chakraborty, J. Datta, and A. Ghosh, *Sci. Cult. (India)* **31**, 529 (1965).
[21] D. P. Chakraborty, K. C. Das, and S. P. Basak, *J. Indian Chem. Soc.* **45**, 84 (1968).
[22] C. Ito, T.-S. Wu, and H. Furukawa, *Chem. Pharm. Bull.* **36**, 2377 (1988).
[23] W.-S. Li, J. D. McChesney, and F. S. El-Feraly, *Phytochemistry* **30**, 343 (1991).
[24] S. S. Jash, G. K. Biswas, S. K. Bhattacharyya, P. Bhattacharyya, A. Chakraborty, and B. K. Chowdhury, *Phytochemistry* **31**, 2503 (1992).
[25] P. H. Carter, S. G. P. Plant, and M. Tomlinson, *J. Chem. Soc.* 2210 (1957).
[26] B. S. Joshi, V. N. Kamat, A. K. Saksena, and T. R. Govindachari, *Tetrahedron Lett.* 4019 (1967).
[27] F. Anwar, A. S. Masaldan, R. S. Kapil, and S. P. Popli, *Indian J. Chem.* **11**, 1314 (1973).
[28] T.-S. Wu, T. Ohta, H. Furukawa, and C.-S. Kuoh, *Heterocycles* **20**, 1267 (1983).
[29] H. Furukawa, T.-S. Wu, T. Ohta, and C.-S. Kuoh, *Chem. Pharm. Bull.* **33**, 4132 (1985).
[30] N. M. Cuong, T. Q. Hung, T. V. Sung, and W. C. Taylor, *Chem. Pharm. Bull.* **52**, 1175 (2004).
[31] D. P. Chakraborty and B. K. Chowdhury, *J. Org. Chem.* **33**, 1265 (1968).
[32] M. Fiebig, J. M. Pezzuto, D. D. Soejarto, and A. D. Kinghorn, *Phytochemistry* **24**, 3041 (1985).
[33] D. P. Chakraborty, B. K. Barman, and P. K. Bose, *Tetrahedron* **21**, 681 (1965).
[34] P. Bhattacharyya and D. P. Chakraborty, *Phytochemistry* **12**, 1831 (1973).
[35] K. C. Das, D. P. Chakraborty, and P. K. Bose, *Experientia* **21**, 340 (1965).
[36] B. K. Chowdhury and D. P. Chakraborty, *Chem. Ind. (London)* 549 (1969).
[37] B. K. Choudhury and D. P. Chakraborty, *Phytochemistry* **10**, 1967 (1971).
[38] H. Furukawa, C. Ito, M. Yogo, and T.-S. Wu, *Chem. Pharm. Bull.* **34**, 2672 (1986).
[39] P. Bhattacharyya and B. K. Chowdhury, *Chem. Ind. (London)* 301 (1984).

[40] A. Chakraborty, B. K. Chowdhury, and P. Bhattacharyya, *Phytochemistry* **40**, 295 (1995).
[41] D. Lontsi, J. F. Ayafor, B. L. Sondengam, J. D. Connolly, and D. S. Rycroft, *Tetrahedron Lett.* **26**, 4249 (1985).
[42] A. Chakraborty, C. Saha, G. Podder, B. K. Chowdhury, and P. Bhattacharyya, *Phytochemistry* **38**, 787 (1995).
[43] T.-S. Wu, S.-C. Huang, P.-L. Wu, and C.-S. Kuoh, *Phytochemistry* **52**, 523 (1999).
[44] C. Ito, S. Katsuno, M. Itoigawa, N. Ruangrungsi, T. Mukainaka, M. Okuda, Y. Kitagawa, H. Tokuda, H. Nishino, and H. Furukawa, *J. Nat. Prod.* **63**, 125 (2000).
[45] P. Bhattacharyya, A. K. Maiti, K. Basu, and B. K. Chowdhury, *Phytochemistry* **35**, 1085 (1994).
[46] T.-S. Wu, S.-C. Huang, P.-L. Wu, and C.-M. Teng, *Phytochemistry* **43**, 133 (1996).
[47] C. Ito, S. Katsuno, H. Ohta, M. Omura, I. Kajiura, and H. Furukawa, *Chem. Pharm. Bull.* **45**, 48 (1997).
[48] B. K. Chowdhury, S. Jha, P. Bhattacharyya, and J. Mukherjee, *Indian J. Chem.* **40B**, 490 (2001).
[49] C. Saha and B. K. Chowdhury, *Phytochemistry* **48**, 363 (1998).
[50] T.-S. Wu and S.-C. Huang, *Chem. Pharm. Bull.* **40**, 1069 (1992).
[51] T.-S. Wu, S.-C. Huang, and P.-L. Wu, *Phytochemistry* **43**, 1427 (1996).
[52] O. Potterat, C. Puder, W. Bolek, K. Wagner, C. Ke, Y. Ye, and F. Gillardon, *Pharmazie* **60**, 637 (2005).
[53] T.-S. Wu, S.-C. Huang, and P.-L. Wu, *Tetrahedron Lett.* **37**, 7819 (1996).
[54] T.-S. Wu and H. Furukawa, *Chem. Pharm. Bull.* **31**, 901 (1983).
[55] P. Bhattacharyya and B. K. Chowdhury, *Indian J. Chem.* **24B**, 452 (1985).
[56] D. P. Chakraborty, D. Chatterji, and S. N. Ganguly, *Chem. Ind. (London)* 1662 (1969).
[57] N. Ruangrungsi, J. Ariyaprayoon, G. L. Lange, and M. G. Organ, *J. Nat. Prod.* **53**, 946 (1990).
[58] B. Kongkathip, N. Kongkathip, A. Sunthitikawinsakul, C. Napaswat, and C. Yoosook, *Phytother. Res.* **19**, 728 (2005).
[59] T.-S. Wu, S.-C. Huang, J.-S. Lai, C.-M. Teng, F.-N. Ko, and C.-S. Kuoh, *Phytochemistry* **32**, 449 (1993).
[60] D. P. Chakraborty and B. P. Das, *Sci. Cult. (India)* **32**, 182 (1966).
[61] D. P. Chakraborty, B. P. Das, and S. P. Basak, *Plant Biochem. J. (India)* **1**, 73 (1974).
[62] A. K. Chakravarty, T. Sarkar, K. Masuda, and K. Shiojima, *Phytochemistry* **50**, 1263 (1999).
[63] S. P. Kureel, R. S. Kapil, and S. P. Popli, *Chem. Ind. (London)* 1262 (1970).
[64] A. Islam, P. Bhattacharyya, and D. P. Chakraborty, *J. Chem. Soc., Chem. Commun.* 537 (1972).
[65] P. Bhattacharyya, P. K. Chakrabarty, and B. K. Chowdhury, *Phytochemistry* **24**, 882 (1985).
[66] S. Mukherjee, M. Mukherjee, and S. N. Ganguly, *Phytochemistry* **22**, 1064 (1983).
[67] P. Bhattacharyya, T. Sarkar, A. Chakraborty, and B. K. Chowdhury, *Indian J. Chem.* **23B**, 49 (1984).
[68] C. Ito, M. Itoigawa, A. Sato, C. M. Hasan, M. A. Rashid, H. Tokuda, T. Mukainaka, H. Nishino, and H. Furukawa, *J. Nat. Prod.* **67**, 1488 (2004).
[69] C. Ito, T.-S. Wu, and H. Furukawa, *Chem. Pharm. Bull.* **35**, 450 (1987).
[70] C. Ito, M. Nakagawa, T.-S. Wu, and H. Furukawa, *Chem. Pharm. Bull.* **39**, 2525 (1991).
[71] J. Reisch, O. Goj, A. Wickramasinghe, H. M. T. B. Herath, and G. Henkel, *Phytochemistry* **31**, 2877 (1992).
[72] P. Bhattacharyya and B. K. Chowdhury, *J. Nat. Prod.* **48**, 465 (1985).
[73] D. A. Okorie, *Phytochemistry* **14**, 2720 (1975).
[74] C. Ito, H. Ohta, H. T.-W. Tan, and H. Furukawa, *Chem. Pharm. Bull.* **44**, 2231 (1996).
[75] P. Bhattacharyya, S. S. Jash, and B. K. Chowdhury, *Chem. Ind. (London)* 246 (1986).
[76] P. Bhattacharyya and A. Chakraborty, *Phytochemistry* **23**, 471 (1984).
[77] D. P. Chakraborty, P. Bhattacharyya, A. Islam, and S. Roy, *Chem. Ind. (London)* 165 (1974).
[78] D. P. Chakraborty, S. Roy, and R. Guha, *J. Indian Chem. Soc.* **55**, 1114 (1978).
[79] M. R. R. Bhagwanth, A. V. Rama Rao, and K. Venkataraman, *Indian J. Chem.* **7**, 1065 (1969).
[80] H.-J. Knölker and M. Wolpert, *Tetrahedron Lett.* **38**, 533 (1997).
[81] H.-J. Knölker and M. Wolpert, *Tetrahedron* **59**, 5317 (2003).
[82] C. Ito, Y. Thoyama, M. Omura, I. Kajiura, and H. Furukawa, *Chem. Pharm. Bull.* **41**, 2096 (1993).
[83] J. Reisch, A. C. Adebajo, V. Kumar, and A. J. Aladesanmi, *Phytochemistry* **36**, 1073 (1994).
[84] A. V. Rama Rao, K. S. Bhide, and R. B. Mujumdar, *Chem. Ind. (London)* 697 (1980).
[85] K. M. Meragelman, T. C. McKee, and M. R. Boyd, *J. Nat. Prod.* **63**, 427 (2000).
[86] T. Pacher, M. Bacher, O. Hofer, and H. Greger, *Phytochemistry* **58**, 129 (2001).
[87] C. Ito, M. Nakagawa, T.-S. Wu, and H. Furukawa, *Chem. Pharm. Bull.* **39**, 1668 (1991).
[88] Y. Tachibana, H. Kikuzaki, N. H. Lajis, and N. Nakatani, *J. Agric. Food Chem.* **49**, 5589 (2001).
[89] C. Chaichantipyuth, S. Pummangura, K. Naowsaran, and D. Thanyavuthi, *J. Nat. Prod.* **51**, 1285 (1988).

[90] D. Prakash, K. Raj, R. S. Kapil, and S. P. Popli, *Indian J. Chem.* **19B**, 1075 (1980).
[91] B. S. Joshi, V. N. Kamat, D. H. Gawad, and T. R. Govindachari, *Phytochemistry* **11**, 2065 (1972).
[92] D. P. Chakraborty, K. C. Das, and A. Islam, *J. Indian Chem. Soc.* **47**, 1197 (1970).
[93] B. S. Joshi, D. H. Gawad, and V. N. Kamat, *Indian J. Chem.* **10**, 1123 (1972).
[94] C. Chaichantipyuth, S. Pummangura, K. Naowsaran, and D. Thanyavuthi, *J. Nat. Prod.* **52**, 375 (1989).
[95] D. P. Chakraborty, *Tetrahedron Lett.* 661 (1966).
[96] D. P. Chakraborty, *Phytochemistry* **8**, 769 (1969).
[97] D. P. Chakraborty, K. C. Das, and B. K. Chowdhury, *Chem. Ind. (London)* 1684 (1966).
[98] A. K. Chakravarty, T. Sarkar, K. Masuda, T. Takey, H. Doi, E. Kotani, and K. Shiojima, *Indian J. Chem.* **40B**, 484 (2001).
[99] P. Bhattacharyya, G. K. Biswas, A. K. Barua, C. Saha, I. B. Roy, and B. K. Chowdhury, *Phytochemistry* **33**, 248 (1993).
[100] V. Kumar, J. Reisch, and A. Wickramasinghe, *Aust. J. Chem.* **42**, 1375 (1989).
[101] C. Ito and H. Furukawa, *Chem. Pharm. Bull.* **38**, 1548 (1990).
[102] S. Roy, L. Bhattacharyya, and D. P. Chakraborty, *J. Indian Chem. Soc.* **59**, 1369 (1982).
[103] C. Ma, R. J. Case, Y. Wang, H.-J. Zhang, G. T. Tan, N. V. Hung, N. M. Cuong, S. G. Franzblau, D. D. Soejarto, H. H. S. Fong, and G. F. Pauli, *Planta Med.* **71**, 261 (2005).
[104] C. Ito, N. Okahana, T.-S. Wu, M.-L. Wang, J.-S. Lai, C.-S. Kuoh, and H. Furukawa, *Chem. Pharm. Bull.* **40**, 230 (1992).
[105] H. Furukawa, *J. Indian Chem. Soc.* **71**, 303 (1994).
[106] Z. Bouaziz, P. Nebois, A. Poumaroux, and H. Fillion, *Heterocycles* **52**, 977 (2000).
[107] T.-S. Wu, S.-C. Huang, P.-L. Wu, and K.-H. Lee, *Bioorg. Med. Chem. Lett.* **4**, 2395 (1994).
[108] D. P. Chakraborty, B. K. Barman, and P. K. Bose, *Sci. Cult. (India)* **30**, 445 (1964).
[109] N. L. Dutta and C. Quasim, *Indian J. Chem.* **7**, 307 (1969).
[110] B. S. Joshi, V. N. Kamat, and D. H. Gawad, *Tetrahedron* **26**, 1475 (1970).
[111] N. S. Narasimhan, M. V. Paradkar, and V. P. Chitguppi, *Tetrahedron Lett.* 5501 (1968).
[112] S. P. Kureel, R. S. Kapil, and S. P. Popli, *Experientia* **25**, 790 (1969).
[113] N. S. Narasimhan, M. V. Paradkar, and S. L. Kelkar, *Indian J. Chem.* **8**, 473 (1970).
[114] I. H. Bowen and K. P. W. C. Perera, *Phytochemistry* **21**, 433 (1982).
[115] T.-S. Wu, *Phytochemistry* **30**, 1048 (1991).
[116] T. Tachibana, H. Kikuzaki, N. H. Lajis, and N. Nakatani, *J. Agric. Food Chem.* **51**, 6461 (2003).
[117] I. Mester and J. Reisch, *Justus Liebigs Ann. Chem.* 1725 (1977).
[118] M. Mukherjee, S. Mukherjee, A. K. Shaw, and S. N. Ganguly, *Phytochemistry* **22**, 2328 (1983).
[119] Y.-S. Wang, H.-P. He, Y.-M. Shen, X. Hong, and X.-J. Hao, *J. Nat. Prod.* **66**, 416 (2003).
[120] D. P. Chakraborty and K. C. Das, *Chem. Commun.* 967 (1968).
[121] D. P. Chakraborty, K. C. Das, and B. K. Chowdhury, *J. Org. Chem.* **36**, 725 (1971).
[122] S. Ray and D. P. Chakraborty, *Phytochemistry* **15**, 356 (1976).
[123] D. P. Chakraborty, P. Bhattacharyya, A. Islam, and S. Roy, *Chem. Ind. (London)* 303 (1974).
[124] D. P. Chakraborty, P. Bhattacharyya, A. Islam, and S. Roy, *J. Indian Chem. Soc.* **62**, 670 (1985).
[125] T.-S. Wu, M.-L. Wang, and P.-L. Wu, *Phytochemistry* **43**, 785 (1996).
[126] D. P. Chakraborty and A. Islam, *J. Indian Chem. Soc.* **48**, 91 (1971).
[127] P. Bhattacharyya, A. Chakraborty, and B. K. Chowdhury, *Phytochemistry* **23**, 2409 (1984).
[128] T.-S. Wu, S.-C. Huang, and P.-L. Wu, *Heterocycles* **45**, 969 (1997).
[129] H. Furukawa, T.-S. Wu, and C.-S. Kuoh, *Heterocycles* **23**, 1391 (1985).
[130] T.-S. Wu, M.-L. Wang, P.-L. Wu, C. Ito, and H. Furukawa, *Phytochemistry* **41**, 1433 (1996).
[131] C. Ito, M. Itoigawa, K. Nakao, T. Murata, M. Tsuboi, N. Kaneda, and H. Furukawa, *Phytomedicine* **13**, 359 (2006).
[132] D. P. Chakraborty, K. C. Das, and P. K. Bose, *Sci. Cult. (India)* **32**, 83 (1966).
[133] N. S. Narasimhan, M. V. Paradkar, V. P. Chitguppi, and S. L. Kelkar, *Indian J. Chem.* **13**, 993 (1975).
[134] C. Ito, H. Kanbara, T.-S. Wu, and H. Furukawa, *Phytochemistry* **31**, 1083 (1992).
[135] S. Roy, S. Gosh, and D. P. Chakraborty, *Chem. Ind. (London)* 669 (1979).
[136] S. P. Kureel, R. S. Kapil, and S. P. Popli, *Chem. Ind. (London)* 958 (1970).
[137] R. S. Ramsewak, M. G. Nair, G. M. Strasburg, D. L. DeWitt, and J. L. Nitiss, *J. Agric. Food Chem.* **47**, 444 (1999).
[138] K. Nakahara, G. Trakoontivakorn, N. S. Alizoreky, H. Ono, M. Onishi-Kameyama, and M. Yoshida, *J. Agric. Food Chem.* **50**, 4796 (2002).
[139] F. Anwer, R. S. Kapil, and S. P. Popli, *Experientia* **28**, 769 (1972).

[140] N. L. Dutta, C. Quasim, and M. S. Wadia, *Indian J. Chem.* **7**, 1168 (1969).
[141] N. S. Narasimhan and S. L. Kelkar, *Indian J. Chem.* **14B**, 430 (1976).
[142] D. P. Chakraborty, A. Islam, S. P. Basak, and R. Das, *Chem. Ind. (London)* 593 (1970).
[143] S. P. Kureel, R. S. Kapil, and S. P. Popli, *Tetrahedron Lett.* 3857 (1969).
[144] W. M. Bandaranayake, M. J. Begley, B. O. Brown, D. G. Clarke, L. Crombie, and D. A. Whiting, *J. Chem. Soc., Perkin Trans. 1* 998 (1974).
[145] A. T. McPhail, T.-S. Wu, T. Ohta, and H. Furukawa, *Tetrahedron Lett.* **24**, 5377 (1983).
[146] H. Furukawa, C. Ito, T.-S. Wu, and A. T. McPhail, *Chem. Pharm. Bull.* **41**, 1249 (1993).
[147] D. P. Chakraborty, P. Bhattacharyya, and A. R. Mitra, *Chem. Ind. (London)* 260 (1974).
[148] D. P. Chakraborty, S. N. Ganguly, P. N. Maji, A. R. Mitra, K. C. Das, and B. Weinstein, *Chem. Ind. (London)* 322 (1973).
[149] S. N. Ganguly and A. Sarkar, *Phytochemistry* **17**, 1816 (1978).
[150] T.-S. Wu, M.-L. Wang, and P.-L. Wu, *Tetrahedron Lett.* **36**, 5835 (1995).
[151] T.-S. Wu, M.-L. Wang, P.-L. Wu, and T.-T. Jong, *Phytochemistry* **40**, 1817 (1995).
[152] N. L. Dutta, C. Quasim, and M. S. Wadia, *Indian J. Chem.* **7**, 1061 (1969).
[153] J. Bordner, D. P. Chakraborty, B. K. Chowdhury, S. N. Ganguli, K. C. Das, and B. Weinstein, *Experientia* **28**, 1406 (1972).
[154] L. Bhattacharya, S. K. Roy, and D. P. Chakraborty, *Phytochemistry* **21**, 2432 (1982).
[155] L. Bhattacharyya, S. K. Chatterjee, S. Roy, and D. P. Chakraborty, *J. Indian Chem. Soc.* **66**, 140 (1989).
[156] Z. A. Ahmad, *Indian Drugs* **31**, 32 (1994).
[157] H. Furukawa, M. Yogo, C. Ito, T.-S. Wu, and C.-S. Kuoh, *Chem. Pharm. Bull.* **33**, 1320 (1985).
[158] H. Furukawa, *Trends Heterocycl. Chem.* **3**, 185 (1993).
[159] S. Tasler and G. Bringmann, *Chem. Record* **2**, 114 (2002).
[160] H. Furukawa, T.-S. Wu, and C.-S. Kuoh, *Chem. Pharm. Bull.* **33**, 2611 (1985).
[161] C. Ito, T.-S. Wu, and H. Furukawa, *Chem. Pharm. Bull.* **38**, 1143 (1990).
[162] G. Bringmann, S. Tasler, H. Endress, J. Kraus, K. Messer, M. Wohlfarth, and W. Lobin, *J. Am. Chem. Soc.* **123**, 2703 (2001).
[163] M. M. Rahman and A. I. Gray, *Phytochemistry* **66**, 1601 (2005).
[164] H. Furukawa, T.-S. Wu, and T. Ohta, *Chem. Pharm. Bull.* **31**, 4202 (1983).
[165] A. Zhang and G. Lin, *Bioorg. Med. Chem. Lett.* **10**, 1021 (2000).
[166] G. Bringmann, A. Ledermann, and G. François, *Heterocycles* **40**, 293 (1995).
[167] G. Bringmann, A. Ledermann, M. Stahl, and K.-P. Gulden, *Tetrahedron* **51**, 9353 (1995).
[168] G. Bringmann, A. Ledermann, J. Holenz, M.-T. Kao, U. Busse, H. G. Wu, and G. François, *Planta Med.* **64**, 54 (1998).
[169] Y. S. Wang, H. P. He, X. Hong, Q. Zhao, and X. J. Hao, *Chin. Chem. Lett.* **13**, 849 (2002).
[170] T.-S. Wu, M.-L. Wang, J.-S. Lai, C. Ito, and H. Furukawa, *Phytochemistry* **30**, 1052 (1991).
[171] C. Ito and H. Furukawa, *Chem. Pharm. Bull.* **39**, 1355 (1991).
[172] M. T. H. Nutan, C. M. Hasan, and M. A. Rashid, *Fitoterapia* **70**, 130 (1999).
[173] C. Ito, S. Katsuno, N. Ruangrungsi, and H. Furukawa, *Chem. Pharm. Bull.* **46**, 344 (1998).
[174] T.-S. Wu, S.-C. Huang, and P.-L. Wu, *Chem. Pharm. Bull.* **46**, 1459 (1998).
[175] W. Fröhner, M. P. Krahl, K. R. Reddy, and H.-J. Knölker, *Heterocycles* **63**, 2393 (2004).
[176] H.-J. Knölker and K. R. Reddy, *in* "Selected Methods for Synthesis and Modification of Heterocycles: The Chemistry and Biological Activity of Natural Indole Systems, Part 1" (V. G. Kartsev, ed.), vol. 4, p. 166. ICSPF Press, Moscow, 2005.
[177] S. Goodwin, A. F. Smith, and E. C. Horning, *J. Am. Chem. Soc.* **81**, 1903 (1959).
[178] R. B. Woodward, G. A. Iacobucci, and F. A. Hochstein, *J. Am. Chem. Soc.* **81**, 4434 (1959).
[179] G. H. Svoboda, G. A. Poore, and M. L. Montfort, *J. Pharm. Sci.* **57**, 1720 (1968).
[180] K. N. Kilminster, M. Sainsbury, and B. Webb, *Phytochemistry* **11**, 389 (1972).
[181] A. Ahond, H. Fernandez, M. Julia-Moore, C. Poupat, V. Sánchez, P. Potier, S. K. Kan, and T. Sévenet, *J. Nat. Prod.* **44**, 193 (1981).
[182] Y.-M. Lin, M. Juichi, R.-Y. Wu, and K.-H. Lee, *Planta Med.* 545 (1985).
[183] S. Michel, F. Tillequin, and M. Koch, *J. Nat. Prod.* **43**, 294 (1980).
[184] S. Michel, F. Tillequin, and M. Koch, *J. Nat. Prod.* **45**, 489 (1982).
[185] M. Sainsbury, *Synthesis* 437 (1977).
[186] R. Barone and M. Chanon, *Heterocycles* **16**, 1357 (1981).
[187] M. J. E. Hewlins, A.-M. Oliveira-Campos, and P. V. R. Shannon, *Synthesis* 289 (1984).
[188] G. W. Gribble and M. G. Saulnier, *Heterocycles* **23**, 1277 (1985).

[189] V. K. Kansal and P. Potier, *Tetrahedron* **42**, 2389 (1986).
[190] U. Pindur, *Pharm. Unserer Zeit* 47 (1987).
[191] G. W. Gribble, *in* "Advances in Heterocyclic Natural Product Synthesis" (W. H. Pearson, ed.), vol. 1, p. 43. JAI Press, Greenwich, 1990.
[192] G. W. Gribble, *in* "The Alkaloids" (A. Brossi, ed.), vol. 39, p. 239. Academic Press, New York, 1990.
[193] G. W. Gribble, *Synlett* 289 (1991).
[194] U. Pindur, M. Haber, and K. Sattler, *Pharm. Unserer Zeit* 21 (1992).
[195] P. Potier, *Chem. Soc. Rev.* **21**, 113 (1992).
[196] M. Álvarez and J. A. Joule, *in* "The Alkaloids" (G. A. Cordell, ed.), vol. 57, p. 235. Academic Press, New York, 2001.
[197] P. Juret, A. Tanguy, A. Girard, J. Y. Le Talaer, J. S. Abbatucci, N. Dat-Xuong, J. B. Le Pecq, and C. Paoletti, *Eur. J. Cancer* **14**, 205 (1978).
[198] C. Paoletti, J.-B. Le Pecq, N. Dat-Xuong, P. Juret, H. Garnier, J.-L. Amiel, and J. Rouesse, *Recent Results Cancer Res.* **74**, 107 (1980).
[199] P. Juret, J. F. Heron, J. E. Couette, T. Delozier, and J. Y. Le Talaer, *Cancer Treat. Rep.* **66**, 1909 (1982).
[200] P. Dodion, M. Rozencweig, C. Nicaise, M. Piccart, E. Cumps, N. Crespeigne, D. Kisner, and Y. Kenis, *Eur. J. Cancer Clin. Oncol.* **18**, 519 (1982).
[201] A. Clarysse, A. Brugarolas, P. Siegenthaler, R. Abele, F. Cavalli, R. D. Jager, G. Renard, M. Rozencweig, and H. H. Hansen, *Eur. J. Cancer Clin. Oncol.* **20**, 243 (1984).
[202] T. S. Mansour, T. C. Wong, and E. M. Kaiser, *Org. Magn. Res.* **21**, 71 (1983).
[203] J. W. Loder, *Aust. J. Chem.* **19**, 1947 (1966).
[204] N. Dat-Xuong, M.-T. Adeline, P. Lecointe, and M.-M. Janot, *C. R. Acad. Sci. Paris* **281C**, 623 (1975).
[205] S. Michel, F. Tillequin, and M. Koch, *Tetrahedron Lett.* **21**, 4027 (1980).
[206] J. Schmutz, F. Hunziker, and R. Hirt, *Helv. Chim. Acta* **40**, 1189 (1957).
[207] J. Schmutz and F. Hunziker, *Helv. Chim. Acta* **41**, 288 (1958).
[208] P. Carvalho-Ferreira, G. B. M. Bettolo, and J. Schmutz, *Experientia* **15**, 179 (1959).
[209] G. B. M. Bettolo and P. Carvalho-Ferreira, *Ann. Chim.* **49**, 869 (1959).
[210] M. A. Ondetti and V. Deulofeu, *Tetrahedron Lett.* 18 (1960).
[211] M. A. Ondetti and V. Deulofeu, *Tetrahedron* **15**, 160 (1961).
[212] R. H. Burnell and D. D. Casa, *Can. J. Chem.* **45**, 89 (1967).
[213] M.-L. Bennasar, T. Roca, and F. Ferrando, *J. Org. Chem.* **71**, 1746 (2006).
[214] M. Azoug, A. Loukaci, B. Richard, J.-M. Nuzillard, C. Moreti, M. Zèches-Hanrot, and L. L. Men-Olivier, *Phytochemistry* **39**, 1223 (1995).
[215] H. Lehner and J. Schmutz, *Helv. Chim. Acta* **44**, 444 (1961).
[216] G. Büchi, D. W. Mayo, and F. A. Hochstein, *Tetrahedron* **15**, 167 (1961).
[217] J. Schmutz and F. Hunziker, *Pharm. Acta Helv.* **33**, 341 (1958).
[218] M. A. Ondetti and V. Deulofeu, *Tetrahedron Lett.* 1 (1959).
[219] M. Gorman, N. Neuss, N. J. Cone, and J. A. Deyrup, *J. Am. Chem. Soc.* **82**, 1142 (1960).
[220] J. P. Kutney, M. Noda, N. G. Lewis, B. Monteiro, D. Mostowicz, and B. R. Worth, *Can. J. Chem.* **60**, 2426 (1982).
[221] S. Michel, F. Tillequin, and M. Koch, *J. Chem. Soc., Chem. Commun.* 229 (1987).
[222] J. Bruneton, T. Sévenet, and A. Cavé, *Phytochemistry* **11**, 3073 (1972).
[223] J. R. Garlich, E. M. Kaiser, and E. O. Schlemper, *Acta Cryst.* **C40**, 1871 (1984).
[224] G. Kusano, M. Shibano, M. Idoji, and K. Minoura, *Heterocycles* **36**, 2367 (1993).
[225] J. H. Cardellina II, M. P. Kirkup, R. E. Moore, J. S. Mynderse, K. Seff, and C. J. Simmons, *Tetrahedron Lett.* **51**, 4915 (1979).
[226] S. Kato, H. Kawai, T. Kawasaki, Y. Toda, T. Urata, and Y. Hayakawa, *J. Antibiot.* **42**, 1879 (1989).
[227] M. Iwatsuki, E. Niki, S. Kato, and K. Nishikori, *Chem. Lett.* **21**, 1735 (1992).
[228] C.-J. Mo, K. Shin-ya, K. Furihata, K. Furihata, A. Shimazu, Y. Hayakawa, and H. Seto, *J. Antibiot.* **43**, 1337 (1990).
[229] N. Kotoda, K. Shin-ya, K. Furihata, Y. Hayakawa, and H. Seto, *J. Antibiot.* **50**, 770 (1997).
[230] Y. Nihei, H. Yamamoto, M. Hasegawa, M. Hanada, Y. Fukagawa, and T. Oki, *J. Antibiot.* **46**, 25 (1993).
[231] K. Sakano, K. Ishimaru, and S. Nakamura, *J. Antibiot.* **33**, 683 (1980).
[232] K. Sakano and S. Nakamura, *J. Antibiot.* **33**, 961 (1980).
[233] M. Kaneda, K. Sakano, S. Nakamura, Y. Kushi, and Y. Iitaka, *Heterocycles* **15**, 993 (1981).
[234] K. Yamasaki, M. Kaneda, K. Watanabe, Y. Ueki, K. Ishimaru, S. Nakamura, R. Nomi, N. Yoshida, and T. Nakajima, *J. Antibiot.* **36**, 552 (1983).

[235] S. Kondo, M. Katayama, and S. Marumo, *J. Antibiot.* **39**, 727 (1986).
[236] T. Naid, T. Kitahara, M. Kaneda, and S. Nakamura, *J. Antibiot.* **40**, 157 (1987).
[237] D. J. Hook, J. Y. Yacobucci, S. O'Connor, M. Lee, E. Kerns, B. Krishnan, J. Matson, and G. Hesler, *J. Antibiot.* **43**, 1347 (1990).
[238] M. Kaneda, T. Naid, T. Kitahara, S. Nakamura, T. Hirata, and T. Suga, *J. Antibiot.* **41**, 602 (1988).
[239] S. Kato, K. Shindo, Y. Kataoka, Y. Yamagishi, and J. Mochizuki, *J. Antibiot.* **44**, 903 (1991).
[240] S. Urban, J. W. Blunt, and M. H. G. Munro, *J. Nat. Prod.* **65**, 1371 (2002).
[241] K. Shin-ya, M. Tanaka, K. Furihata, Y. Hayakawa, and H. Seto, *Tetrahedron Lett.* **34**, 4943 (1993).
[242] H. Seto and Y. Hayakawa, Japanese Patent JP 06032778 A (1994).
[243] K. Shin-ya, T. Kunigami, J.-S. Kim, K. Furihata, Y. Hayakawa, and H. Seto, *Biosci. Biotech. Biochem.* **61**, 1768 (1997).
[244] H. Grammel, H. Wolf, E.-D. Gilles, F. Huth, and H. Laatsch, *Z. Naturforsch.* **53c**, 325 (1998).
[245] K. Shin-ya, S. Shimizu, T. Kunigami, K. Furihata, K. Furihata, and H. Seto, *J. Antibiot.* **48**, 574 (1995).
[246] M. Tanaka, K. Shin-ya, K. Furihata, and H. Seto, *J. Antibiot.* **48**, 326 (1995).
[247] G. W. Chan, T. Francis, D. R. Thureen, P. H. Offen, N. J. Pierce, J. W. Westley, and R. K. Johnson, *J. Org. Chem.* **58**, 2544 (1993).
[248] H. Kang and W. Fenical, *J. Org. Chem.* **62**, 3254 (1997).
[249] M. Chakrabarty and S. Khasnobis, *J. Indian Chem. Soc.* **74**, 917 (1997).
[250] A. Sato, T. Morishita, T. Shiraki, S. Yoshioka, H. Horikoshi, H. Kuwano, H. Hanzawa, and T. Hata, *J. Org. Chem.* **58**, 7632 (1993).
[251] K. Warabi, S. Matsunaga, R. W. M. van Soest, and N. Fusetani, *J. Org. Chem.* **68**, 2765 (2003).
[252] M. Gill and W. Steglich, *in* "Progress in the Chemistry of Organic Natural Products" (W. Herz, H. Grisebach, G. W. Kirby and C. Tamm, eds.), vol. 51, p. 216. Springer-Verlag, Wien, 1987.
[253] J. Bergman, *in* "Studies in Natural Product Chemistry: Stereoselective Synthesis (Part A)" (Atta-ur-Rahman, ed.), vol. 1, p. 3. Elsevier, Amsterdam, 1988.
[254] W. Steglich, *Pure Appl. Chem.* **61**, 281 (1989).
[255] G. W. Gribble and S. J. Berthel, *in* "Studies in Natural Product Chemistry: Stereoselective Synthesis (Part H)" (Atta-ur-Rahman, ed.), vol. 12, p. 365. Elsevier, Amsterdam, 1988.
[256] M. Prudhomme, *Curr. Pharm. Des.* **3**, 265 (1997).
[257] U. Pindur and T. Lemster, *Recent Res. Dev. Org. Bioorg. Chem.* **1**, 33 (1997).
[258] U. Pindur, Y.-S. Kim, and F. Mehrabani, *Curr. Med. Chem.* **6**, 29 (1999).
[259] M. Prudhomme, *Curr. Med. Chem.* **7**, 1189 (2000).
[260] M. Prudhomme, *Eur. J. Med. Chem.* **38**, 123 (2003).
[261] M. L. Trudell, A. S. Basile, H. E. Shannon, P. Skolnick, and J. M. Cook, *J. Med. Chem.* **30**, 456 (1987).
[262] M. L. Trudell, S. L. Lifer, Y.-C. Tan, M. J. Martin, L. Deng, P. Skolnick, and J. M. Cook, *J. Med. Chem.* **33**, 2412 (1990).
[263] A. B. Okey, D. S. Riddick, and P. A. Harper, *Trends Pharmacol. Sci.* **15**, 226 (1994).
[264] O. Hankinson, *Annu. Rev. Pharmacol. Toxicol.* **35**, 307 (1995).
[265] J. V. Schmidt and C. A. Brandfield, *Annu. Rev. Cell. Dev. Biol.* **12**, 55 (1996).
[266] N. Wahlström, I. Romero, and J. Bergman, *Eur. J. Org. Chem.* 2593 (2004).
[267] H. Morioka, M. Ishihara, H. Shibai, and T. Suzuki, *Agric. Biol. Chem.* **49**, 1959 (1985).
[268] S. Oka, M. Kodama, H. Takeda, N. Tomizuka, and H. Suzuki, *Agric. Biol. Chem.* **50**, 2723 (1986).
[269] J. A. Bush, B. H. Long, J. J. Catino, W. T. Bradner, and K. Tomita, *J. Antibiot.* **40**, 668 (1987).
[270] B. H. Long and B. N. Balasubramanian, *Exp. Opin. Ther. Patents* **10**, 635 (2000).
[271] T. Tamaoki, H. Nomoto, I. Takahashi, Y. Kato, M. Morimoto, and F. Tomita, *Biochem. Biophys. Res. Commun.* **135**, 397 (1986).
[272] H. Kase, K. Iwahashi, and Y. Matsuda, *J. Antibiot.* **39**, 1059 (1986).
[273] S. Nakanishi, Y. Matsuda, K. Iwahashi, and H. Kase, *J. Antibiot.* **39**, 1066 (1986).
[274] T. Yasuzawa, T. Iida, M. Yoshida, N. Hirayama, M. Takahashi, K. Shirahata, and H. Sano, *J. Antibiot.* **39**, 1072 (1986).
[275] P. A. Horton, R. E. Longley, O. J. McConnell, and L. M. Ballas, *Experientia* **50**, 843 (1994).
[276] H. Nakano, E. Kobayashi, I. Takahashi, T. Tamaoki, Y. Kuzuu, and H. Iba, *J. Antibiot.* **40**, 706 (1987).
[277] P. D. Davis, C. H. Hill, E. Keech, G. Lawton, J. S. Nixon, A. D. Sedgwick, J. Wadsworth, D. Westmacott, and S. E. Wilkinson, *FEBS Lett.* **259**, 61 (1989).
[278] U. T. Ruegg and G. M. Burgess, *Trends Pharmacol. Sci.* **10**, 218 (1989).
[279] I. Takahashi, Y. Saitoh, M. Yoshida, H. Sano, H. Nakano, M. Morimoto, and T. Tamaoki, *J. Antibiot.* **42**, 571 (1989).

[280] S. Ōmura, Y. Sasaki, Y. Iwai, and H. Takeshima, *J. Antibiot.* **48**, 535 (1995).
[281] S. Ōmura, Y. Iwai, A. Hirano, A. Nakagawa, J. Awaya, H. Tsuchiya, Y. Takahashi, and R. Masuma, *J. Antibiot.* **30**, 276 (1977).
[282] A. Furusaki, N. Hashiba, T. Matsumoto, A. Hirano, Y. Iwai, and S. Ōmura, *J. Chem. Soc., Chem. Commun.* 800 (1978).
[283] A. Furusaki, N. Hashiba, T. Matsumoto, A. Hirano, Y. Iwai, and S. Ōmura, *Bull. Chem. Soc. Jpn.* **55**, 3681 (1982).
[284] H. Takahashi, H. Osada, M. Uramoto, and K. Isono, *J. Antibiot.* **43**, 168 (1990).
[285] N. Funato, H. Takayanagi, Y. Konda, Y. Toda, Y. Harigaya, Y. Iwai, and S. Ōmura, *Tetrahedron Lett.* **35**, 1251 (1994).
[286] S. Ōmura, Y. Iwai, and A. Hirano, *Japan Kokai* 53,073,501; *Chem. Abstr.* **89**, 178086b (1978).
[287] S. Ōmura, Y. Iwai, and A. Hirano, *Ger. Offen.* 2,754,326; *Chem. Abstr.* **89**, 58348y (1978).
[288] T. Oikawa, M. Shimamura, H. Ashino, O. Nakamura, T. Nanayasu, I. Morita, and S.-I. Murota, *J. Antibiot.* **45**, 1155 (1992).
[289] Y. Cai, A. Fredenhagen, P. Hug, T. Meyer, and H. H. Peter, *J. Antibiot.* **49**, 519 (1996).
[290] D. Meksuriyen and G. A. Cordell, *J. Nat. Prod.* **51**, 884 (1988).
[291] S. Tanida, M. Takizawa, T. Takahashi, S. Tsubotani, and S. Harada, *J. Antibiot.* **42**, 1619 (1989).
[292] S. Tanida, T. Takahashi, S. Tsuboya, and S. Harada, *Japan Kokai* 01,149,791; *Chem. Abstr.* **112**, 75314v (1990).
[293] S. Tsubotani, S. Tanida, and S. Harada, *Tetrahedron* **47**, 3565 (1991).
[294] P. Hoehn, O. Ghisalba, T. Moerker, and H. H. Peter, *J. Antibiot.* **48**, 300 (1995).
[295] R. B. Kinnel and P. J. Scheuer, *J. Org. Chem.* **57**, 6327 (1992).
[296] C. L. Cantrell, A. Groweiss, K. R. Gustafson, and M. R. Boyd, *Nat. Prod. Lett.* **14**, 39 (1999).
[297] P. Schupp, C. Eder, P. Proksch, V. Wray, B. Schneider, M. Herderich, and V. Paul, *J. Nat. Prod.* **62**, 959 (1999).
[298] L. M. C. Hernández, J. A. F. Blanco, L. P. Baz, J. L. F. Puentes, F. R. Millán, F. E. Vázquez, and R. I. Fernández-Chimeno, *J. Antibiot.* **53**, 895 (2000).
[299] P. Schupp, P. Proksch, and V. Wray, *J. Nat. Prod.* **65**, 295 (2002).
[300] Y. Cai, A. Fredenhagen, P. Hug, and H. H. Peter, *J. Antibiot.* **49**, 1060 (1996).
[301] Y. Cai, A. Fredenhagen, P. Hug, and H. H. Peter, *J. Antibiot.* **48**, 143 (1995).
[302] C. Murakata, A. Sato, M. Kasai, M. Morimoto, and S. Akinaga, *W08907105* (1989); European Patent Application EP 383919 (1989); *Chem. Abstr.* **112**, 77240 (1990).
[303] H. Osada, H. Takahashi, K. Tsunoda, H. Kusakabe, and K. Isono, *J. Antibiot.* **43**, 163 (1990).
[304] H. Koshino, H. Osada, S. Amano, R. Onose, and K. Isono, *J. Antibiot.* **45**, 1428 (1992).
[305] J. B. McAlpine, J. P. Karwowski, M. Jackson, M. M. Mullally, J. E. Hochlowski, U. Premachandran, and N. S. Burres, *J. Antibiot.* **47**, 281 (1994).
[306] X.-X. Han, C.-B. Cui, Q.-Q. Gu, W.-M. Zhu, H.-B. Liu, J.-Y. Gu, and H. Osada, *Tetrahedron Lett.* **46**, 6137 (2005).
[307] D. Schroeder, K. S. Lam, J. Mattei, and G. A. Hesler, European Patent Application EP 388,962 (1990); *Chem. Abstr.* **114**, 162431r (1991).
[308] H. Osada, H. Koshino, T. Kudo, R. Onose, and K. Isono, *J. Antibiot.* **45**, 189 (1992).
[309] H. Koshino, H. Osada, and K. Isono, *J. Antibiot.* **45**, 195 (1992).
[310] H. Nomoto, H. Nakano, I. Takahashi, T. Tamaoki, F. Tomita, I. Kawamoto, K. Asano, and M. Morimoto, European Patent Application EP 238,011 (1987); *Chem. Abstr.* **108**, 93097y (1988).
[311] I. Takahashi, E. Kobayashi, K. Asano, M. Yoshida, and H. Nakano, *J. Antibiot.* **40**, 1782 (1987).
[312] I. Takahashi, K. Asano, I. Kawamoto, T. Tamaoki, and H. Nakano, *J. Antibiot.* **42**, 564 (1989).
[313] D. E. Williams, V. S. Bernan, F. V. Ritacco, W. M. Maiese, M. Greenstein, and R. J. Andersen, *Tetrahedron Lett.* **40**, 7171 (1999).
[314] M. Sezaki, T. Sasaki, T. Nakazawa, U. Takeda, M. Iwata, and T. Watanabe, *J. Antibiot.* **38**, 1437 (1985).
[315] H. Osada, M. Satake, H. Koshino, R. Onose, and K. Isono, *J. Antibiot.* **45**, 278 (1992).
[316] N. Matsuura, N. Tamehiro, T. Andoh, A. Kawashima, and M. Ubukata, *J. Antibiot.* **55**, 355 (2002).
[317] N. Tamehiro, N. Matsuura, Y. Feng, N. Nakajima, and M. Ubukata, *J. Antibiot.* **55**, 363 (2002).
[318] Y. Feng, N. Matsuura, and M. Ubukata, *J. Antibiot.* **57**, 627 (2004).
[319] D. E. Nettleton, T. W. Doyle, B. Krishnan, G. K. Matsumoto, and J. Clardy, *Tetrahedron Lett.* **26**, 4011 (1985).
[320] K. S. Lam, J. Mattei, and S. Forenza, *J. Ind. Microbiol.* **4**, 105 (1989).
[321] J. A. Matson, *US* 4524145; *Chem. Abstr.* **103**, 159104d (1985).

[322] D. P. Labeda, K. Hatano, R. M. Kroppenstedt, and T. Tamura, *Int. J. Syst. Evol. Microbiol.* **51**, 1045 (2001).
[323] M. M. Faul, L. L. Winneroski, and C. A. Krumrich, *J. Org. Chem.* **64**, 2465 (1999).
[324] Y. Yamashita, N. Fujii, C. Murakata, T. Ashizawa, M. Okabe, and H. Nakano, *Biochemistry* **31**, 12069 (1992).
[325] T. Kaneko, H. Wong, K. T. Okamoto, and J. Clardy, *Tetrahedron Lett.* **26**, 4015 (1985).
[326] A. C. Horan, J. Golik, J. A. Matson, and M. G. Patel, European Patent Application EP 175,284 (1986); *Chem. Abstr.* **105**, 5184j (1986).
[327] J. A. Matson, C. Claridge, J. A. Bush, J. Titus, W. T. Bradner, T. W. Doyle, A. C. Horan, and M. Patel, *J. Antibiot.* **42**, 1547 (1989).
[328] J. Golik, T. W. Doyle, B. Krishnan, G. Dubay, and J. Matson, *J. Antibiot.* **42**, 1784 (1989).
[329] R. Bonjouklian, T. A. Smitka, L. E. Doolin, R. M. Molloy, M. Debono, S. A. Shaffer, R. E. Moore, J. B. Stewart, and G. M. L. Patterson, *Tetrahedron* **47**, 7739 (1991).
[330] K. Kojiri, H. Kondo, T. Yoshinari, H. Arakawa, S. Nakajima, F. Satoh, K. Kawamura, A. Okura, H. Suda, and M. Okanishi, *J. Antibiot.* **44**, 723 (1991).
[331] W. Steglich, B. Steffan, L. Kopanski, and G. Eckhardt, *Angew. Chem. Int. Ed.* **19**, 459 (1980); *Angew. Chem.* **92**, 463 (1980).
[332] W. Steglich, *Pure Appl. Chem.* **53**, 1233 (1981).
[333] L. Kopanski, G.-R. Li, H. Besl, and W. Steglich, *Liebigs Ann. Chem.* 1722 (1982).
[334] S. Nakatani, A. Naoe, Y. Yamamoto, T. Yamauchi, N. Yamaguchi, and M. Ishibashi, *Bioorg. Med. Chem. Lett.* **13**, 2879 (2003).
[335] J. Bergman and B. Pelcman, *J. Org. Chem.* **54**, 824 (1989).
[336] G. W. Gribble and S. J. Berthel, *Tetrahedron* **48**, 8869 (1992).
[337] M. Ohkubo, T. Nishimura, H. Jona, T. Honma, and H. Morishima, *Tetrahedron* **52**, 8099 (1996).
[338] M. Brenner, H. Rexhausen, B. Steffan, and W. Steglich, *Tetrahedron* **44**, 2887 (1988).
[339] J. Bergman, E. Koch, and B. Pelcman, *J. Chem. Soc., Perkin Trans. 1* 2609 (2000).
[340] G. Knübel, L. K. Larsen, R. E. Moore, I. A. Levine, and G. M. L. Patterson, *J. Antibiot.* **43**, 1236 (1990).
[341] K. Ramasamy, N. Imamura, R. K. Robins, and G. R. Revankar, *J. Heterocycl. Chem.* **25**, 1893 (1988).
[342] R. G. S. Berlinck, R. Britton, E. Piers, L. Lim, M. Roberge, R. M. da Rocha, and R. J. Andersen, *J. Org. Chem.* **63**, 9850 (1998).
[343] H. C. Vervoort, S. E. Richards-Gross, and W. Fenical, *J. Org. Chem.* **62**, 1486 (1997).
[344] R. Britton, J. H. H. L. de Oliveira, R. J. Andersen, and R. G. S. Berlinck, *J. Nat. Prod.* **64**, 254 (2001).
[345] R. W. Rickards, J. M. Rothschild, A. C. Willis, N. M. de Chazal, J. Kirk, K. Kirk, K. J. Saliba, and G. D. Smith, *Tetrahedron* **55**, 13513 (1999).
[346] M. R. TePaske, J. B. Gloer, D. T. Wicklow, and P. F. Dowd, *J. Org. Chem.* **54**, 4743 (1989).
[347] M. R. TePaske, J. B. Gloer, D. T. Wicklow, and P. F. Dowd, *Tetrahedron Lett.* **30**, 5965 (1989).
[348] M. R. TePaske, J. B. Gloer, D. T. Wicklow, and P. F. Dowd, *J. Org. Chem.* **55**, 5299 (1990).
[349] H. L. Sings, G. H. Harris, and A. W. Dombrowski, *J. Nat. Prod.* **64**, 836 (2001).
[350] R. L. Dillman and J. H. Cardellina II, *J. Nat. Prod.* **54**, 1056 (1991).
[351] D. Hoffmann, G. Rathkamp, and H. Woziwodzki, *Beitr. Tabakforsch.* **4**, 253 (1968); *Chem. Abstr.* **71**, 19643z (1969).
[352] D. N. Chowdhury, S. K. Basak, and B. P. Das, *Curr. Sci.* **47**, 490 (1978).
[353] E. J. LaVoie, G. Briggs, V. Bedenko, and D. Hoffmann, *Mutat. Res.* **101**, 141 (1982).
[354] K.-C. Luk, L. Stern, and M. Weigele, *J. Nat. Prod.* **46**, 852 (1983).
[355] B. Åkermark, L. Eberson, E. Jonsson, and E. Pettersson, *J. Org. Chem.* **40**, 1365 (1975).
[356] S.-C. Lee, G. A. Williams, and G. D. Brown, *Phytochemistry* **52**, 537 (1999).
[357] L. Zhu and R. A. Hites, *Environ. Sci. Technol.* **39**, 9446 (2005).
[358] B. Irlinger, A. Bartsch, H.-J. Krämer, P. Mayser, and W. Steglich, *Helv. Chim. Acta* **88**, 1472 (2005).
[359] K. M. Meragelman, L. M. West, P. T. Northcote, L. K. Pannell, T. C. McKee, and M. R. Boyd, *J. Org. Chem.* **67**, 6671 (2002).
[360] B. K. Chowdhury, S. K. Hirani, A. Mustapha, and P. Bhattacharyya, *Chem. Ind. (London)* 298 (1987).
[361] D. P. Chakraborty, *Planta Med.* **39**, 97 (1980).
[362] A. R. Battersby, R. T. Brown, R. S. Kapil, A. O. Plunkett, and J. B. Taylor, *Chem. Commun.* 46 (1966).
[363] E. Leistner and M. H. Zenk, *Tetrahedron Lett.* 1395 (1968).
[364] H. Erdtman, *in* "Perspectives in Phytochemistry" (J. B. Harborne and T. Swain, eds.), p. 107. Academic Press, New York, 1969.

[365] Y.-C. Kong, K.-F. Cheng, K.-H. Ng, P. P.-H. But, Q. Li, S.-X. Yu, H.-T. Chang, R. C. Cambie, T. Kinoshita, W.-S. Kan, and P. G. Waterman, *Biochem. Syst. Ecol.* **14**, 491 (1986).
[366] P. M. Dewick, "Medicinal Natural Products: A Biosynthetic Approach", 2nd Edition, Wiley, England, 2002.
[367] D. P. Chakraborty, *J. Indian Chem. Soc.* **46**, 177 (1969).
[368] I. Mester, *in* "Chemistry and Chemical Taxonomy of the Rutales" (P. G. Waterman and M. F. Grundon, eds.), p. 31. Academic Press, London, 1983.
[369] S. Roy, R. Guha, S. Ghosh, and D. P. Chakraborty, *Indian J. Chem.* **21B**, 617 (1982).
[370] S. P. Kureel, R. S. Kapil, and S. P. Popli, *Chem. Commun.* 1120 (1969).
[371] D. P. Chakraborty, *J. Indian Chem. Soc.* **66**, 843 (1989).
[372] J. P. Kutney, *Heterocycles* **4**, 429 (1976).
[373] G. Kunesch, C. Poupat, N. von Bac, G. Henry, T. Sévenet, and P. Potier, *C. R. Acad. Sci. Paris* **285C**, 89 (1977).
[374] E. Wenkert, *J. Am. Chem. Soc.* **84**, 98 (1962).
[375] P. Potier and M.-M. Janot, *C. R. Acad. Sci. Paris* **276C**, 1727 (1973).
[376] R. Besselièvre and H.-P. Husson, *Tetrahedron* **37**, 241 (1981).
[377] A. Ahond, A. Cavé, C. Kan-Fan, Y. Langlois, and P. Potier, *Chem. Commun.* 517 (1970).
[378] M. Kaneda, T. Kitahara, K. Yamasaki, and S. Nakamura, *J. Antibiot.* **43**, 1623 (1990).
[379] D. Meksuriyen and G. A. Cordell, *J. Nat. Prod.* **51**, 893 (1988).
[380] S.-W. Yang and G. A. Cordell, *J. Nat. Prod.* **60**, 44 (1997).
[381] C. J. Pearce, T. W. Doyle, S. Forenza, K. S. Lam, and D. R. Schroeder, *J. Nat. Prod.* **51**, 937 (1988).
[382] S.-W. Yang, L.-J. Lin, G. A. Cordell, P. Wang, and D. G. Corley, *J. Nat. Prod.* **62**, 1551 (1999).
[383] K. Goeke, P. Hoehn, and O. Ghisalba, *J. Antibiot.* **48**, 428 (1995).
[384] A. Fredenhagen and H. H. Peter, *Tetrahedron* **52**, 1235 (1996).
[385] R. Fröde, C. Hinze, I. Josten, B. Schmidt, B. Steffan, and W. Steglich, *Tetrahedron Lett.* **35**, 1689 (1994).
[386] T. Hoshino, Y. Kojima, T. Hayashi, T. Uchiyama, and K. Kaneko, *Biosci. Biotech. Biochem.* **57**, 775 (1993).
[387] A. R. Howard-Jones and C. T. Walsh, *J. Am. Chem. Soc.* **128**, 12289 (2006).
[388] H. Onaka, S.-I. Taniguchi, Y. Igarashi, and T. Furumai, *J. Antibiot.* **55**, 1063 (2002).
[389] A. P. Salas, L. Zhu, C. Sánchez, A. F. Brana, J. Rohr, C. Méndez, and J. A. Salas, *Mol. Microbiol.* **58**, 17 (2005).
[390] S. Asamizu, Y. Kato, Y. Igarashi, T. Furumai, and H. Onaka, *Tetrahedron Lett.* **47**, 473 (2006).
[391] C. Sánchez, I. A. Butovich, A. F. Brana, J. Rohr, C. Méndez, and J. A. Salas, *Chem. Biol.* **8**, 519 (2002).
[392] H. Onaka, S.-I. Taniguchi, Y. Igarashi, and T. Furumai, *Biosci. Biotech. Biochem.* **67**, 127 (2003).
[393] T. Nishizawa, S. Grüschow, D. H.-E. Jayamaha, C. Nishizawa-Harada, and D. H. Shermann, *J. Am. Chem. Soc.* **128**, 724 (2006).
[394] E. E. Shults and G. A. Tolstikov, *in* "Selected Methods for Synthesis and Modification of Heterocycles: The Chemistry and Biological Activity of Natural Indole Systems, Part 1" (V. G. Kartsev, ed.), vol. 4, p. 241. ICSPF Press, Moscow, 2005.
[395] Y.-Z. Shu, *J. Nat. Prod.* **61**, 1053 (1998).
[396] M. Prudhomme, *Curr. Med. Chem.* **4**, 509 (2004).
[397] C. Ito, *Nat. Med.* **54**, 117 (2000).
[398] M. T. H. Nutan, A. Hasnat, and M. A. Rashid, *Fitoterapia* **69**, 173 (1998).
[399] M. Itoigawa, Y. Kashiwada, C. Ito, H. Furukawa, Y. Tachibana, K. F. Bastow, and K.-H. Lee, *J. Nat. Prod.* **63**, 893 (2000).
[400] L. M. Rice and K. R. Scott, *J. Med. Chem.* **13**, 308 (1970).
[401] N. P. Buu-Hoï, N. Hoán, and N. H. Khôi, *J. Org. Chem.* **14**, 492 (1949).
[402] E. von Angerer and J. Prekajac, *J. Med. Chem.* **29**, 380 (1986).
[403] A. Segall, H. Pappa, R. Casaubon, G. Martin, R. Bergoc, and M. T. Pizzorno, *Eur. J. Med. Chem.* **30**, 165 (1995).
[404] M. Dräger, M. Haber, H. Erfanian-Abdoust, U. Pindur, and K. Sattler, *Monatsh. Chem.* **124**, 559 (1993).
[405] U. Pindur, M. Haber, and K. Sattler, *J. Chem. Ed.* **70**, 263 (1993).
[406] G. W. Gribble and M. G. Saulnier, *J. Chem. Soc., Chem. Commun.* 168 (1984).
[407] U. Kuckländer, H. Pitzler, and K. Kuna, *Arch. Pharm.* **327**, 137 (1994).
[408] M. Suffness and G. A. Cordell, *in* "The Alkaloids" (A. Brossi, ed.), vol. 25, p. 1. Academic Press, New York, 1985.
[409] Ditercalinium chloride, *Drugs of the Future* **10**, 116 (1985).

[410] C. Auclair, A. Pierre, E. Voisin, O. Pepin, S. Cros, C. Colas, J.-M. Saucier, B. Verschuere, P. Gros, and C. Paoletti, *Cancer Res.* **47**, 6254 (1987).
[411] G. Atassi, P. Dumont, O. Pepin, O. Gros, and P. Gros, *Proc. Annu. Meet. Am. Assoc. Cancer Res.* **30**, A2458 (1989).
[412] V. Pierson, A. Pierre, Y. Pommier, and P. Gros, *Cancer Res.* **48**, 1404 (1988).
[413] B. H. Long, W. C. Rose, D. M. Vyas, J. A. Matson, and S. Forenza, *Curr. Med. Chem.* **2**, 255 (2002).
[414] S. Goel, S. Wadler, A. Hoffman, F. Volterra, C. Baker, E. Nazario, P. Ivy, A. Silverman, and S. Mani, *Investigational New Drugs* **21**, 103 (2003).
[415] M. Hussain, U. Vaishampayan, L. K. Heilbrun, V. Jain, P. M. LoRusso, P. Ivy, and L. Flaherty, *Investigational New Drugs* **21**, 465 (2003).
[416] G. W. Rewcastle, *IDrugs* **8**, 838 (2005).
[417] W. A. Denny, *IDrugs* **7**, 173 (2004).
[418] H. Arakawa, M. Morita, T. Kodera, A. Okura, M. Ohkubo, H. Morishima, and S. Nishimura, *Jpn. J. Cancer Res.* **90**, 1163 (1999).
[419] T. Yoshinari, M. Matsumoto, H. Arakawa, H. Okada, K. Noguchi, H. Suda, A. Okura, and S. Nishimura, *Cancer Res.* **55**, 1310 (1995).
[420] H. Arakawa, T. Iguchi, M. Morita, T. Yoshinari, K. Kojiri, H. Suda, A. Okura, and S. Nishimura, *Cancer Res.* **55**, 1316 (1995).
[421] H. Komatani, M. Morita, N. Sakaizumi, K. Fukasawa, E. Yoshida, A. Okura, T. Yoshinari, and S. Nishimura, *Cancer Res.* **59**, 2701 (1999).
[422] M. G. Saulnier, B. N. Balasubramanian, B. H. Long, D. B. Frennesson, E. Ruediger, K. Zimmermann, J. T. Eummer, D. R. St. Laurent, K. M. Stoffan, B. N. Naidu, M. Mahler, F. Beaulieu, C. Bachand, F. Y. Lee, C. R. Fairchild, L. K. Stadnick, W. C. Rose, C. Solomon, H. Wong, A. Martel, J. J. Wright, R. Kramer, D. R. Langley, and D. M. Vyas, *J. Med. Chem.* **48**, 2258 (2005).
[423] R.-G. Shao, C.-X. Cao, T. Shimizu, P. M. O'Connor, K. W. Kohn, and Y. Pommier, *Cancer Res.* **57**, 4029 (1997).
[424] S. Akinaga, K. Sugiyama, and T. Akiyama, *Anti-Cancer Drug Des.* **15**, 43 (2000).
[425] M. Bayés, X. Rabasseda, and J. R. Prous, *Methods Find Exp. Clin. Pharmacol.* **25**, 747 (2003).
[426] A. M. Senderowicz, *Cancer Biol. Ther.* **2**, S84 (2003).
[427] D. J. Propper, A. C. McDonald, A. Man, P. Thavasu, F. Balkwill, J. P. Braybrooke, F. Caponigro, P. Graf, C. Dutreix, R. Blackie, S. B. Kaye, T. S. Ganesan, D. C. Talbot, A. L. Harris, and C. Twelves, *J. Clin. Oncol.* **19**, 1485 (2001).
[428] J. P. Eder Jr., R. Garcia-Carbonero, J. W. Clark, J. G. Supko, T. A. Puchalski, D. P. Ryan, P. Deluca, A. Wozniak, A. Campbell, J. Rothermel, and P. LoRusso, *Investigational New Drugs* **22**, 139 (2004).
[429] B. D. Smith, M. Levis, M. Beran, F. Giles, H. Kantarjian, K. Berg, K. M. Murphy, T. Dauses, J. Allebach, and D. Small, *Blood* **103**, 3669 (2004).
[430] H. A. M. Mucke, *IDrugs* **6**, 377 (2003).
[431] L. H. Wang, C. G. Besirli, and E. M. Johnson Jr., *Annu. Rev. Pharmacol. Toxicol.* **44**, 451 (2004).
[432] P. B. Jacobson, S. L. Kuchera, A. Metz, C. Schächtele, K. Imre, and D. J. Schrier, *J. Pharmacol. Exp. Therap.* **275**, 995 (1995).
[433] M. R. Jirousek, J. R. Gillig, C. M. Gonzalez, W. F. Heath, J. H. McDonald III, D. A. Neel, C. J. Rito, U. Singh, L. E. Stramm, A. Melikian-Badalian, M. Baevsky, L. M. Ballas, S. E. Hall, L. L. Winneroski, and M. M. Faul, *J. Med. Chem.* **39**, 2664 (1996).
[434] H. Ishii, M. R. Jirousek, D. Koya, C. Takagi, P. Xia, A. Clermont, S.-E. Bursell, T. S. Kern, L. M. Ballas, W. F. Heath, L. E. Stramm, E. P. Feener, and G. L. King, *Science* **272**, 728 (1996).
[435] J. Kleinschroth, J. Hartenstein, C. Rudolph, and C. Schächtele, *Bioorg. Med. Chem. Lett.* **3**, 1959 (1993).
[436] J. Kleinschroth, J. Hartenstein, C. Rudolph, and C. Schächtele, *Bioorg. Med. Chem. Lett.* **5**, 55 (1995).
[437] E. R. Pereira, L. Belin, M. Sancelme, M. Prudhomme, M. Ollier, M. Rapp, D. Sevère, J.-F. Riou, D. Fabbro, and T. Meyer, *J. Med. Chem.* **39**, 4471 (1996).
[438] M. J. Slater, R. Baxter, R. W. Bonser, S. Cockerill, K. Gohil, N. Parry, E. Robinson, R. Randall, C. Yeates, W. Snowden, and A. Walters, *Bioorg. Med. Chem. Lett.* **11**, 1993 (2001).
[439] C. Sanchez-Martinez, C. Shih, G. Zhu, T. Li, H. B. Brooks, B. K. R. Patel, R. M. Schultz, T. B. DeHahn, C. D. Spencer, S. A. Watkins, C. A. Ogg, E. Considine, J. A. Dempsey, and F. Zhang, *Bioorg. Med. Chem. Lett.* **13**, 3841 (2003).
[440] C. Sanchez-Martinez, C. Shih, M. M. Faul, G. Zhu, M. Paal, C. Somoza, T. Li, C. A. Kumrich, L. L. Winneroski, Z. Xun, H. B. Brooks, B. K. R. Patel, R. M. Schultz, T. B. DeHahn, C. D. Spencer, S. A.

Watkins, E. Considine, J. A. Dempsey, C. A. Ogg, R. M. Campbell, B. A. Anderson, and J. Wagner, *Bioorg. Med. Chem. Lett.* **13**, 3835 (2003).
[441] C. Saha, A. Chakraborty, and B. K. Chowdhury, *Indian J. Chem.* **35B**, 677 (1996).
[442] A. Sunthitikawinsakul, N. Kongkathip, B. Kongkathip, S. Phonnakhu, J. W. Daly, T. F. Spande, Y. Nimit, and S. Rochanaruangrai, *Planta Med.* **69**, 155 (2003).
[443] T. A. Choi, R. Czerwonka, W. Fröhner, M. P. Krahl, K. R. Reddy, S. G. Franzblau, and H.-J. Knölker, *Chem. Med. Chem.* **1**, 812 (2006).
[444] T. A. Choi, R. Czerwonka, J. Knöll, M. P. Krahl, K. R. Reddy, S. G. Franzblau, and H.-J. Knölker, *Med. Chem. Res.* **15**, 28 (2006).
[445] T. A. Choi, R. Czerwonka, R. Forke, A. Jäger, J. Knöll, M. P. Krahl, T. Krause, K. R. Reddy, S. G. Franzblau, and H.-J. Knölker, *Med. Chem. Res.* **16**, in press (2008).
[446] B. E. Randelia and B. P. J. Patel, *Experientia* **38**, 529 (1982).
[447] A. M. El-Naggar, F. S. M. Ahmed, A. M. Abd El-Salam, and M. A. El-Gazzar, *Arab. Gulf J. Sci. Res.* **1**, 131 (1983).
[448] A. Domański and J. B. Kyziol, *Pol. J. Chem.* **59**, 613 (1985).
[449] K. Asres, A. Seyoum, C. Veeresham, F. Bucar, and S. Gibbons, *Phytother. Res.* **19**, 557 (2005).
[450] J. Wang, Y. Zheng, T. Efferth, R. Wang, Y. Shen, and X. Hao, *Phytochemistry* **66**, 697 (2005).
[451] A. A. Asselin, L. G. Humber, T. A. Dobson, and J. Komlossy, *J. Med. Chem.* **19**, 787 (1976).
[452] A. H. Conney, C. Coutinho, B. Koechlin, R. Swarm, J. A. Cheripko, C. Impellizzeri, and H. Baruth, *Clin. Pharmacol. Ther.* **16**, 176 (1974).
[453] E. Storch, H. Kirchner, K. Huller, M. G. Martinotti, and D. Gemsa, *J. Gen. Virol.* **67**, 1211 (1986).
[454] A. Tursi, M. P. Loria, G. Specchia, and D. Casamassima, *Eur. J. Rheumatol. Inflamm.* **5**, 488 (1882).
[455] M. Masaki, T. Yushiro, S. Tsutomu, and N. Keji, *Nippon Yakurigaku Zasshi* **73**, 757 (1977); *Chem. Abstr.* **88**, 69038c (1978).
[456] C. Yenjai, S. Sripontan, P. Sriprajun, P. Kittakoop, A. Jintasirikul, M. Tanticharoen, and Y. Thebtaranonth, *Planta Med.* **66**, 277 (2000).
[457] V. H. Brown, M. Keyanpour-Rad, and J. I. DeGraw, *J. Med. Chem.* **14**, 549 (1971).
[458] A. Shoeb, F. Anwer, R. S. Kapil, and S. P. Popli, *J. Med. Chem.* **16**, 425 (1973).
[459] R. M. Ferris, H. L. White, F. L. M. Tang, A. Russell, and M. Harfenist, *Drug Dev. Res.* **9**, 171 (1986).
[460] B. Levant, G. Bissette, E. Widerlöv, and C. B. Nemeroff, *Regul. Pept.* **32**, 193 (1991).
[461] D. L. Gilmore, Y. Liu, and R. R. Matsumoto, *CNS Drug Rev.* **10**, 1 (2004).
[462] J. A. Pointek and R. Y. Wang, *Life Sci.* **39**, 651 (1986).
[463] D. Lednicer and L. A. Mitscher, ''The Organic Chemistry of Drug Synthesis'', vol. 3, p. 168. Wiley, New York, 1984.
[464] P. L. Wood and P. S. McQuade, *Prog. Neuropsychopharmacol. Biol. Psychiatry* **8**, 773 (1984).
[465] G. Z. Feuerstein, N. H. Schusterman, and R. R. Ruffolo Jr., *Drugs Today* **33**, 453 (1997).
[466] Y.-C. Lee, *Maryland Med. J.* **47**, 67 (1998).
[467] C. C. Gerhardt, J. Gros, A. D. Strosberg, and T. Issad, *Mol. Pharmacol.* **55**, 255 (1999).
[468] L. A. Nikolaidis, I. Poornima, P. Parikh, M. Magovern, Y.-T. Shen, and R. P. Shannon, *J. Am. Coll. Cardiol.* **47**, 1871 (2006).
[469] T.-L. Yue, R. R. Bufflolo Jr., and G. Feuerstein, *Heart Fail. Rev.* **4**, 39 (1999).
[470] B. B. Innis, F. M. A. Correa, and S. H. Snyder, *Life Sci.* **24**, 2255 (1979).
[471] P. St. Janiak, *Drugs Today* **17**, 53 (1981).
[472] N. Chaiyabutr, C. Buranakarl, T. Tesaprateep, and P. Loypetjra, *Br. Vet. J.* **143**, 448 (1987).
[473] K. Takeya, M. Itoigawa, and H. Furukawa, *Eur. J. Pharmacol.* **169**, 137 (1989).
[474] H. Nagai, H. Takeda, S. Yamaguchi, H. Tanaka, A. Matsuo, and N. Inagaki, *Prostaglandins* **50**, 75 (1995).
[475] T. Ishizuka, T. Matsui, Y. Okamoto, A. Ohta, and M. Shichiji, *Cardiovasc. Drug Rev.* **22**, 71 (2004).
[476] S. Kato, T. Kawasaki, T. Urata, and J. Mochizuki, *J. Antibiot.* **46**, 1859 (1993).
[477] M. Iwatsuki, E. Niki, and S. Kato, *BioFactors* **4**, 123 (1993).
[478] R. Narlawar, B. I. Pérez Revuelta, K. Baumann, R. Schubenel, C. Haass, H. Steiner, and B. Schmidt, *Bioorg. Med. Chem. Lett.* **17**, 176 (2007).
[479] J. G. Pecca and S. M. Albonico, *J. Med. Chem.* **13**, 327 (1970).
[480] J. A. Joule, *Adv. Heterocycl. Chem.* **35**, 83 (1984).
[481] P. T. Gallagher, *in* ''Science of Synthesis (Houben–Weyl)'' (E. J. Thomas, ed.), Vol. 10, p. 693. Thieme, Stuttgart, 2001.
[482] H. C. Waterman and D. L. Vivian, US Patent 2,292,808 (1942).

[483] H. C. Waterman and D. L. Vivian, *J. Org. Chem.* **14**, 289 (1949).
[484] J. I. G. Cadogan, M. Cameron-Wood, R. K. Mackie, and R. J. G. Searle, *J. Chem. Soc.* 4831 (1965).
[485] B. Iddon, O. Meth-Cohn, E. F. V. Scriven, H. Suschitzky, and P. T. Gallagher, *Angew. Chem. Int. Ed. Engl.* **18**, 900 (1979).
[486] B. C. G. Söderberg, *Curr. Org. Chem.* **4**, 727 (2000).
[487] J. H. Smitrovich and I. W. Davies, *Org. Lett.* **6**, 533 (2004).
[488] P. A. S. Smith and B. B. Brown, *J. Am. Chem. Soc.* **73**, 2435 (1951).
[489] P. A. S. Smith, J. M. Clegg, and J. H. Hall, *J. Org. Chem.* **23**, 524 (1958).
[490] R. J. Sundberg, D. W. Gillespie, and B. A. DeGraff, *J. Am. Chem. Soc.* **97**, 6193 (1975).
[491] T. Täuber, *Ber. Dtsch. Chem. Ges.* **24**, 200 (1891).
[492] T. Täuber, *Ber. Dtsch. Chem. Ges.* **25**, 128 (1892).
[493] H. Leditschke, *Chem. Ber.* **86**, 522 (1953).
[494] S. F. Gait, M. E. Peek, C. W. Rees, and R. C. Storr, *J. Chem. Soc., Perkin Trans. 1* 1248 (1974).
[495] R. Robinson, *Chem. Rev.* **63**, 373 (1963).
[496] R. Robinson, *Chem. Rev.* **69**, 227 (1969).
[497] E. Fischer and F. Jourdan, *Ber. Dtsch. Chem. Ges.* **16**, 2241 (1883).
[498] W. Borsche, A. Witte, and W. Bothe, *Justus Liebigs Ann. Chem.* **359**, 49 (1908).
[499] F. R. Japp and F. Klingemann, *Ber. Dtsch. Chem. Ges.* **20**, 2942, 3284, 3398 (1887).
[500] F. R. Japp and F. Klingemann, *Justus Liebigs Ann. Chem.* **247**, 190 (1888).
[501] R. R. Phillips, *Org. React.* **10**, 143 (1959).
[502] C. Graebe and F. Ullmann, *Justus Liebigs Ann. Chem.* **291**, 16 (1896).
[503] R. W. G. Preston, S. H. Tucker, and J. M. L. Cameron, *J. Chem. Soc.* 500 (1942).
[504] F. Ullmann, *Justus Liebigs Ann. Chem.* **332**, 82 (1904).
[505] J. J. Lie, *in* "Name Reactions in Heterocyclic Chemistry" Wiley, New Jersey, 2005.
[506] J.-L. Bernier, J.-P. Hénichart, C. Vaccher, and R. Houssin, *J. Org. Chem.* **45**, 1493 (1980).
[507] R. Littell, G. O. Morton, and G. R. Allen Jr., *J. Am. Chem. Soc.* **92**, 3740 (1970).
[508] H. T. Bucherer and F. Seyde, *J. Prakt. Chem.* **77**, 403 (1908).
[509] F. R. Japp and W. Maitland, *J. Chem. Soc.* **83**, 267 (1903).
[510] H. Seeboth, *Angew. Chem. Int. Ed. Engl.* **6**, 307 (1967).
[511] Y. Oikawa and O. Yonemitsu, *J. Org. Chem.* **41**, 1118 (1976).
[512] S. Takano, K. Yuta, S. Hatakeyama, and K. Ogasawara, *Tetrahedron Lett.* 369 (1979).
[513] S. Takano, Y. Suzuki, and K. Ogasawara, *Heterocycles* **16**, 1479 (1981).
[514] U. Pindur and H. Erfanian-Abdoust, *Chem. Rev.* **89**, 1681 (1989).
[515] T. Gallagher and P. Magnus, *Tetrahedron* **37**, 3889 (1981).
[516] E. R. Marinelli, *Tetrahedron Lett.* **23**, 2745 (1982).
[517] B. Saroja and P. C. Srinivasan, *Tetrahedron Lett.* **25**, 5429 (1984).
[518] T. Kurihara, M. Hanakawa, T. Wakita, and S. Harusawa, *Heterocycles* **23**, 2221 (1985).
[519] T. Kurihara, M. Hanakawa, S. Harusawa, and R. Yoneda, *Chem. Pharm. Bull.* **34**, 4545 (1986).
[520] M. V. B. Rao, J. Satyanarayana, H. Ila, and H. Junjappa, *Tetrahedron Lett.* **36**, 3385 (1995).
[521] H. Plieninger, W. Müller, and K. Weinerth, *Chem. Ber.* **97**, 667 (1964).
[522] C. J. Moody, *J. Chem. Soc., Chem. Commun.* 925 (1984).
[523] C. J. Moody, *J. Chem. Soc., Perkin Trans. 1* 2505 (1985).
[524] C. J. Moody and P. Shah, *J. Chem. Soc., Perkin Trans. 1* 1407 (1988).
[525] C. J. Moody, *Synlett* 681 (1994).
[526] M. G. Saulnier and G. W. Gribble, *Tetrahedron Lett.* **24**, 5435 (1983).
[527] G. W. Gribble, M. G. Saulnier, M. P. Sibi, and J. A. Obaza-Nutaitis, *J. Org. Chem.* **49**, 4518 (1984).
[528] G. W. Gribble, M. G. Saulnier, E. T. Pelkey, T. L. S. Kishbaugh, Y. Liu, J. Jiang, H. A. Trujillo, D. J. Keavy, D. A. Davis, S. C. Conway, F. L. Switzer, S. Roy, R. J. Silva, J. A. Obaza-Nutaitis, M. P. Sibi, N. V. Moskalev, T. C. Barden, L. Chang, W. M. Habeski, B. Pelcman, W. R. Sponholtz III, R. W. Chau, B. D. Allison, S. D. Guraas, M. S. Sinha, M. A. McGowan, M. R. Reese, and K. S. Harpp, *Curr. Org. Chem.* **9**, 1493 (2005).
[529] J. T. Vessels, S. Z. Janicki, and P. A Petillo, *Org. Lett.* **2**, 73 (2000).
[530] W. E. Noland, W. C. Kuryla, and R. F. Lange, *J. Am. Chem. Soc.* **81**, 6010 (1959).
[531] W. E. Noland and S. R. Wann, *J. Org. Chem.* **44**, 4402 (1979).
[532] M. Eitel and U. Pindur, *Synthesis* 364 (1989).
[533] U. Pindur and M. Eitel, *J. Heterocycl. Chem.* **28**, 951 (1991).
[534] S. Kano, E. Sugino, S. Shibuya, and S. Hibino, *J. Org. Chem.* **46**, 3856 (1981).

[535] S. Hibino, A. Tonari, T. Choshi, and E. Sugino, *Heterocycles* **35**, 441 (1993).
[536] T. Choshi, T. Sada, H. Fujimoto, C. Nagayama, E. Sugino, and S. Hibino, *Tetrahedron Lett.* **37**, 2593 (1996).
[537] T. Choshi, T. Sada, H. Fujimoto, C. Nagayama, E. Sugino, and S. Hibino, *J. Org. Chem.* **62**, 2535 (1997).
[538] T. Kawasaki, Y. Nonaka, and M. Sakamoto, *J. Chem. Soc., Chem. Commun.* 43 (1989).
[539] T. Kawasaki, Y. Nonaka, M. Akahane, N. Maeda, and M. Sakamoto, *J. Chem. Soc., Perkin Trans. 1* 1777 (1993).
[540] E. M. Beccalli, A. Marchesini, and T. Pilati, *J. Chem. Soc., Perkin Trans. 1* 579 (1994).
[541] S. V. Ley and A. W. Thomas, *Angew. Chem. Int. Ed.* **42**, 5400 (2003).
[542] J. F. Hartwig, *Angew. Chem. Int. Ed.* **37**, 2046 (1998).
[543] A. R. Muci and S. L. Buchwald, *Top. Curr. Chem.* **219**, 131 (2002).
[544] H.-J. Knölker and N. O'Sullivan, *Tetrahedron* **50**, 10893 (1994).
[545] H.-J. Knölker, W. Fröhner, and K. R. Reddy, *Synthesis* 557 (2002).
[546] M. P. Krahl, A. Jäger, T. Krause, and H.-J. Knölker, *Org. Biomol. Chem.* **4**, 3215 (2006).
[547] R. Forke, M. P. Krahl, T. Krause, G. Schlechtingen, and H.-J. Knölker, *Synlett* 268 (2007).
[548] B. Åkermark, J. D. Oslob, and U. Heuschert, *Tetrahedron Lett.* **36**, 1325 (1995).
[549] H. Hagelin, J. D. Oslob, and B. Åkermark, *Chem. Eur. J.* **5**, 2413 (1999).
[550] T. Iwaki, A. Yasuhara, and T. Sakamoto, *J. Chem. Soc., Perkin Trans. 1* 1505 (1999).
[551] D. E. Ames and A. Opalko, *Tetrahedron* **40**, 1919 (1984).
[552] R. B. Bedford and C. S. J. Cazin, *Chem. Commun.* 2310 (2002).
[553] M. A. Campo, Q. Huang, T. Yao, Q. Tian, and R. C. Larock, *J. Am. Chem. Soc.* **125**, 11506 (2003).
[554] Z. Liu and R. C. Larock, *Org. Lett.* **6**, 3739 (2004).
[555] J. Zhao and R. C. Larock, *Org. Lett.* **7**, 701 (2005).
[556] J. Zhao and R. C. Larock, *J. Org. Chem.* **71**, 5340 (2006).
[557] H.-J. Knölker, *in* "Transition Metals for Organic Synthesis: Building Blocks and Fine Chemicals" (M. Beller and C. Bolm, eds.), vol. 1, p. 534. Wiley-VCH, Weinheim, 1998; H.-J. Knölker, *Chem. Soc. Rev.* **28**, 151 (1999).
[558] H.-J. Knölker, *in* "Transition Metals for Organic Synthesis: Building Blocks and Fine Chemicals" (2nd Edition) (M. Beller and C. Bolm, eds.), vol. 1, p. 585. Wiley-VCH, Weinheim, 2004.
[559] H.-J. Knölker and M. Bauermeister, *J. Indian Chem. Soc.* **71**, 345 (1994).
[560] H.-J. Knölker, H. Goesmann, and C. Hofmann, *Synlett* 737 (1996).
[561] B. Witulski and C. Alayrac, *Angew. Chem.* **114**, 3415 (2002).
[562] W. E. Bauta, W. D. Wulff, S. F. Pavkovic, and E. J. Zaluzec, *J. Org. Chem.* **54**, 3249 (1989).
[563] M. Rawat and W. D. Wulff, *Org. Lett.* **6**, 329 (2004).
[564] K. H. Dötz and T. Leese, *Bull. Soc. Chim. Fr.* **134**, 503 (1997).
[565] K. H. Dötz and P. Tomuschat, *Chem. Soc. Rev.* **28**, 187 (1999).
[566] Q. Huang and R. C. Larock, *J. Org. Chem.* **68**, 7342 (2003).
[567] K. Nozaki, K. Takahashi, K. Nakano, T. Hiyama, H.-Z. Tang, M. Fujiki, S. Yamaguchi, and K. Tamao, *Angew. Chem.* **115**, 2097 (2003).
[568] A. Kuwahara, K. Nakano, and K. Nozaki, *J. Org. Chem.* **70**, 413 (2005).
[569] C.-Y. Liu and P. Knochel, *Org. Lett.* **7**, 2543 (2005).
[570] H.-J. Knölker, *in* "Organic Synthesis via Organometallics" (K. H. Dötz and R. W. Hoffmann, eds.), p. 119. Vieweg, Braunschweig, 1991.
[571] H.-J. Knölker, *Synlett* 371 (1992).
[572] H.-J. Knölker, *in* "Advances in Nitrogen Heterocycles" (C. J. Moody, ed.), vol. 1, p. 173. JAI Press, Greenwich, 1995.
[573] H.-J. Knölker and M. Bauermeister, *J. Chem. Soc., Chem. Commun.* 664 (1990).
[574] H.-J. Knölker and M. Bauermeister, *Tetrahedron* **49**, 11221 (1993).
[575] Y. Murakami, H. Yokoo, and T. Watanabe, *Heterocycles* **49**, 127 (1998).
[576] E. Brenna, C. Fuganti, and S. Serra, *Tetrahedron* **54**, 1585 (1998).
[577] G. Bringmann, S. Tasler, H. Endress, K. Peters, and E.-M. Peters, *Synthesis* 1501 (1998).
[578] G. Lin and A. Zhang, *Tetrahedron Lett.* **40**, 341 (1999).
[579] Y. Kikugawa, Y. Aoki, and T. Sakamoto, *J. Org. Chem.* **66**, 8612 (2001).
[580] A. Zempoalteca and J. Tamariz, *Heterocycles* **57**, 259 (2002).
[581] A. Benavides, J. Peralta, F. Delgado, and J. Tamariz, *Synthesis* 2499 (2004).
[582] L.-C. Campeau, M. Parisien, A. Jean, and K. Fagnou, *J. Am. Chem. Soc.* **128**, 581 (2006).
[583] D. Mal, B. K. Senapati, and P. Pahari, *Synlett* 994 (2006).

[584] D. Mal, B. K. Senapati, and P. Pahari, *Tetrahedron Lett.* **47**, 1071 (2006); see also ref. 724.
[585] V. Sridharan, M. A. Martin, and J. C. Menéndez, *Synlett* 2375 (2006).
[586] J. W. Faller, H. H. Murray, D. L. White, and K. H. Chao, *Organometallics* **2**, 400 (1983).
[587] J. S. McCallum, J. T. Sterbenz, and L. S. Liebeskind, *Organometallics* **12**, 927 (1993).
[588] O. Kataeva, M. P. Krahl, and H.-J. Knölker, *Org. Biomol. Chem.* **3**, 3099 (2005).
[589] R. B. Bedford and M. Betham, *J. Org. Chem.* **71**, 9403 (2006).
[590] R. L. Danheiser, R. G. Brisbois, J. J. Kowalczyk, and R. F. Miller, *J. Am. Chem. Soc.* **112**, 3093 (1990).
[591] C. J. Moody and P. Shah, *J. Chem. Soc., Perkin Trans. 1* 376 (1989).
[592] C. J. Moody and P. Shah, *J. Chem. Soc., Perkin Trans. 1* 2463 (1989).
[593] P. M. Jackson and C. J. Moody, *Synlett* 521 (1990).
[594] P. M. Jackson, C. J. Moody, and R. J. Mortimer, *J. Chem. Soc., Perkin Trans. 1* 2941 (1991).
[595] Y. Nonaka, T. Kawasaki, and M. Sakamoto, *Heterocycles* **53**, 1681 (2000).
[596] K. Shin and K. Ogasawara, *Chem. Lett.* **24**, 289 (1995).
[597] H.-J. Knölker and T. Hopfmann, *Synlett* 981 (1995).
[598] H.-J. Knölker and T. Hopfmann, *Tetrahedron* **58**, 8937 (2002).
[599] H.-J. Knölker, E. Baum, and T. Hopfmann, *Tetrahedron Lett.* **36**, 5339 (1995).
[600] H.-J. Knölker, E. Baum, and T. Hopfmann, *Tetrahedron* **55**, 10391 (1999).
[601] U. Azzena, G. Meloni, and L. Pisano, *Tetrahedron Lett.* **34**, 5635 (1993).
[602] H.-J. Knölker, W. Fröhner, and R. Heinrich, *Synlett* 2705 (2004).
[603] H.-J. Knölker and J. Knöll, *Chem. Commun.* 1170 (2003).
[604] H.-J. Knölker and J. Knöll, *Synlett* 651 (2006).
[605] H.-J. Knölker and J. Knöll, *Tetrahedron Lett.* **47**, 6079 (2006).
[606] E. Duval and G. D. Cuny, *Tetrahedron Lett.* **45**, 5411 (2004).
[607] H.-J. Knölker, M. Bauermeister, D. Bläser, R. Boese, and J.-B. Pannek, *Angew. Chem. Int. Ed.* **28**, 223 (1989); *Angew. Chem.* **101**, 225 (1989).
[608] H.-J. Knölker and M. Bauermeister, *J. Chem. Soc., Chem. Commun.* 1468 (1989).
[609] H.-J. Knölker and M. Bauermeister, *Helv. Chim. Acta* **76**, 2500 (1993).
[610] H.-J. Knölker and W. Fröhner, *Tetrahedron Lett.* **40**, 6915 (1999).
[611] H.-J. Knölker and G. Schlechtingen, *J. Chem. Soc., Perkin Trans. 1* 349 (1997).
[612] H.-J. Knölker and M. Bauermeister, *Heterocycles* **32**, 2443 (1991).
[613] R. Czerwonka, K. R. Reddy, E. Baum, and H.-J. Knölker, *Chem. Commun.* 711 (2006).
[614] H.-J. Knölker, W. Fröhner, and A. Wagner, *Tetrahedron Lett.* **39**, 2947 (1998).
[615] M. Tokunaga, J. F. Larrow, F. Kakiuchi, and E. J. Jacobsen, *Science* **277**, 936 (1997).
[616] S. E. Schaus, J. Brånalt, and E. N. Jacobsen, *J. Org. Chem.* **63**, 4876 (1998).
[617] S. E. Schaus, B. D. Brandes, J. F. Larrow, M. Tokunaga, K. B. Hansen, A. E. Gould, M. E. Furrow, and E. N. Jacobsen, *J. Am. Chem. Soc.* **124**, 1307 (2002).
[618] D. L. J. Clive, N. Etkin, T. Joseph, and J. W. Lown, *J. Org. Chem.* **58**, 2442 (1993).
[619] U. Pindur and L. Pfeuffer, *Heterocycles* **26**, 325 (1987).
[620] E. M. Beccalli and A. Marchesini, *Synth. Commun.* **23**, 2945 (1993).
[621] E. M. Beccalli and A. Marchesini, *Tetrahedron* **52**, 3029 (1996).
[622] D. Crich and S. Rumthao, *Tetrahedron* **60**, 1513 (2004).
[623] M. Yogo, C. Ito, and H. Furukawa, *Chem. Pharm. Bull.* **39**, 328 (1991).
[624] Y. Miki and H. Hachiken, *Synlett* 333 (1993).
[625] G. R. Clemo and D. G. I. Felton, *J. Chem. Soc.* 700 (1951).
[626] A. Osuka, Y. Mori, and H. Suzuki, *Chem. Lett.* **11**, 2031 (1982).
[627] H. Iida, Y. Yuasa, and C. Kibayashi, *J. Org. Chem.* **44**, 1236 (1979).
[628] H. Iida, Y. Yuasa, and C. Kibayashi, *J. Org. Chem.* **45**, 2938 (1980).
[629] K. Matsuo and S. Ishida, *Chem. Express* **8**, 321 (1993).
[630] K. Matsuo and S. Ishida, *Chem. Pharm. Bull.* **42**, 1325 (1994).
[631] A. Wada, S. Hirai, and M. Hanaoka, *Chem. Pharm. Bull.* **42**, 416 (1994).
[632] T. Martin and C. J. Moody, *J. Chem. Soc., Perkin Trans. 1* 235 (1988).
[633] W. S. Murphy and M. Bertrand, *J. Chem. Soc., Perkin Trans. 1* 4115 (1998).
[634] B. K. Chowdhury, S. Jha, B. R. Kar, and C. Saha, *Indian J. Chem.* **38B**, 1106 (1999).
[635] H.-J. Knölker and K. R. Reddy, *Heterocycles* **60**, 1049 (2003).
[636] H. Hagiwara, T. Choshi, H. Fujimoto, E. Sugino, and S. Hibino, *Chem. Pharm. Bull.* **46**, 1948 (1998).
[637] H. Hagiwara, T. Choshi, J. Nobuhiro, H. Fujimoto, and S. Hibino, *Chem. Pharm. Bull.* **49**, 881 (2001).
[638] T. L. Scott and B. C. G. Söderberg, *Tetrahedron* **59**, 6323 (2003).

[639] K. Shin and K. Ogasawara, *Synlett* 922 (1996).
[640] H.-J. Knölker and W. Fröhner, *Tetrahedron Lett.* **38**, 1535 (1997).
[641] H.-J. Knölker and W. Fröhner, *Synlett* 1108 (1997).
[642] H.-J. Knölker and W. Fröhner, *Tetrahedron Lett.* **39**, 2537 (1998).
[643] H.-J. Knölker, E. Baum, and K. R. Reddy, *Tetrahedron Lett.* **41**, 1171 (2000).
[644] H.-J. Knölker, E. Baum, and K. R. Reddy, *Chirality* **12**, 526 (2000).
[645] H.-J. Knölker, K. R. Reddy, and A. Wagner, *Tetrahedron Lett.* **39**, 8267 (1998).
[646] H.-J. Knölker and K. R. Reddy, *Synlett* 596 (1999).
[647] A. Aygün and U. Pindur, *Synlett* 1757 (2000).
[648] U. Pindur and T. Lemster, *Recent Res. Dev. Org. Bioorg. Chem.* **5**, 99 (2002).
[649] A. Aygün and U. Pindur, *J. Heterocycl. Chem.* **40**, 411 (2003).
[650] H.-J. Knölker and W. Fröhner, *Tetrahedron Lett.* **38**, 4051 (1997).
[651] H.-J. Knölker, W. Fröhner, and K. R. Reddy, *Eur. J. Org. Chem.* 740 (2003).
[652] H.-J. Knölker and W. Fröhner, *J. Chem. Soc., Perkin Trans. 1* 173 (1998).
[653] H. Hagiwara, T. Choshi, H. Fujimoto, E. Sugino, and S. Hibino, *Tetrahedron* **56**, 5807 (2000).
[654] T. Kawasaki and M. Somei, *Heterocycles* **31**, 1605 (1990).
[655] M. Somei and T. Kawasaki, *Heterocycles* **29**, 1251 (1989).
[656] B. K. Chowdhury and C. Saha, *Indian J. Chem.* **33B**, 892 (1994).
[657] N. Selvakumar, M. K. Khera, B. Y. Reddy, D. Srinivas, A. M. Azhagan, and J. Iqbal, *Tetrahedron Lett.* **44**, 7071 (2003).
[658] N. Selvakumar, B. Y. Reddy, A. M. Azhagan, M. K. Khera, J. M. Babu, and J. Iqbal, *Tetrahedron Lett.* **44**, 7065 (2003).
[659] T. L. Scott, X. Yu, S. P. Gorugantula, G. Carrero-Martínez, and B. C. G. Söderberg, *Tetrahedron* **62**, 10835 (2006).
[660] H.-J. Knölker and C. Hofmann, *Tetrahedron Lett.* **37**, 7947 (1996).
[661] G. Bringmann and S. Tasler, *Tetrahedron* **57**, 331 (2001).
[662] G. Bringmann and S. Tasler, *Tetrahedron* **57**, 2337 (2001).
[663] G. Bringmann, S. Tasler, H. Endress, and J. Mühlbacher, *Chem. Commun.* 761 (2001).
[664] S. Tasler, H. Endress, and G. Bringmann, *Synthesis* 1993 (2001).
[665] G. Lin and A. Zhang, *Tetrahedron* **56**, 7163 (2000).
[666] T. Kitawaki, Y. Hayashi, and N. Chida, *Heterocycles* **65**, 1561 (2005).
[667] T. Kitawaki, Y. Hayashi, A. Ueno, and N. Chida, *Tetrahedron* **62**, 6792 (2006).
[668] P. Dharmasena, A. M. F. Oliveira-Campos, M. J. R. P. Queiroz, M. M. M. Raposo, P. V. R. Shannon, and C. M. Wedd, *J. Chem. Res.* (S) 398 (1997); (M) 2501.
[669] M. W. Davies, C. N. Johnson, and J. P. A. Harrity, *J. Org. Chem.* **66**, 3525 (2001).
[670] A. Yasuhara, Y. Takeda, N. Suzuki, and T. Sakamoto, *Chem. Pharm. Bull.* **50**, 235 (2002).
[671] Y. Miki, Y. Tsuzaki, and H. Matsukida, *Heterocycles* **57**, 1645 (2002).
[672] J. C. Barcia, J. Cruces, J. C. Estévez, R. J. Estévez, and L. Castedo, *Tetrahedron Lett.* **43**, 5141 (2002).
[673] C. B. de Koning, J. P. Michael, J. M. Nhlapo, R. Pathak, and W. A. L. van Otterlo, *Synlett* 705 (2003).
[674] S. R. Flanagan, D. C. Harrowven, and M. Bradley, *Tetrahedron Lett.* **44**, 1795 (2003).
[675] A. K. Singh and P. K. Hota, *Indian J. Chem.* **42B**, 2048 (2003).
[676] J. Barluenga, M. Trincado, E. Rubio, and J. M. González, *Angew. Chem.* **115**, 2508 (2003).
[677] M. Fernandez, C. Barcia, J. C. Estévez, R. J. Estévez, and L. Castedo, *Synlett* 267 (2004).
[678] V. Mamane, P. Hannen, and A. Fürstner, *Chem. Eur. J.* **10**, 4556 (2004).
[679] M.-L. Bennasar, T. Roca, and F. Ferrando, *Tetrahedron Lett.* **45**, 5605 (2004).
[680] M. M. Oliveira, M. A. Salvador, P. J. Coelho, and L. M. Carvalho, *Tetrahedron* **61**, 1681 (2005).
[681] S. Routier, J.-Y. Mérour, N. Dias, A. Lansiaux, C. Bailly, O. Lozach, and L. Meijer, *J. Med. Chem.* **49**, 789 (2006).
[682] F. Dufour and G. Kirsch, *Synlett* 1021 (2006).
[683] H.-Y. Hu, Y. Liu, M. Ye, and J.-H. Xu, *Synlett* 1913 (2006).
[684] R. Pathak, J. M. Nhlapo, S. Govender, J. P. Michael, W. A. L. van Otterlo, and C. B. de Koning, *Tetrahedron* **62**, 2820 (2006).
[685] H. Çavdar and N. Saracoğlu, *J. Org. Chem.* **71**, 7793 (2006).
[686] C. Peschko and W. Steglich, *Tetrahedron Lett.* **41**, 9477 (2000).
[687] A. Hamasaki, J. M. Zimpleman, I. Hwang, and D. L. Boger, *J. Am. Chem. Soc.* **127**, 10767 (2005).
[688] H.-J. Knölker and W. Fröhner, *Tetrahedron Lett.* **37**, 9183 (1996).
[689] H.-J. Knölker and W. Fröhner, *Synthesis* 2131 (2000).

[690] H.-J. Knölker and M. P. Krahl, *Synlett* 528 (2004).
[691] E. M. Beccalli, F. Clerici, and A. Marchesini, *Tetrahedron* **54**, 11675 (1998).
[692] T. Soós, G. Timári, and G. Hajós, *Tetrahedron Lett.* **40**, 8607 (1999).
[693] A. Yasuhara, N. Suzuki, and T. Sakamoto, *Chem. Pharm. Bull.* **50**, 143 (2002).
[694] A. Fürstner, M. M. Domostoj, and B. Scheiper, *J. Am. Chem. Soc.* **127**, 11620 (2005).
[695] A. Fürstner, M. M. Domostoj, and B. Scheiper, *J. Am. Chem. Soc.* **128**, 8087 (2006).
[696] B. Gilbert, *in* "The Alkaloids" (A. Brossi, ed.), vol. 8, p. 205. Academic Press, New York, 1968.
[697] G. A. Cordell, *in* "The Alkaloids" (A. Brossi, ed.), vol. 17, p. 199. Academic Press, New York, 1979.
[698] M. Lounasmaa and H. Merikallio, *Kem. Kemi.* **8**, 51 (1981).
[699] M. Lounasmaa and H. Merikallio, *Kem. Kemi.* **8**, 137 (1981).
[700] M. G. Saulnier and G. W. Gribble, *J. Org. Chem.* **47**, 2810 (1982).
[701] G. W. Gribble, M. G. Saulnier, J. A. Obaza-Nutaitis, and D. M. Ketcha, *J. Org. Chem.* **57**, 5891 (1992).
[702] D. A. Davis and G. W. Gribble, *Tetrahedron Lett.* **31**, 1081 (1990).
[703] G. W. Gribble, D. J. Keavy, D. A. Davis, M. G. Saulnier, B. Pelcman, T. C. Barden, M. P. Sibi, E. R. Olson, and J. J. BelBruno, *J. Org. Chem.* **57**, 5878 (1992).
[704] Y. Murakami, Y. Yokoyama, and N. Okuyama, *Tetrahedron Lett.* **24**, 2189 (1983).
[705] Y. Yokoyama, N. Okuyama, S. Iwadata, T. Momoi, and Y. Murakami, *J. Chem. Soc., Perkin Trans. 1* 1319 (1990).
[706] A. H. Jackson, P. R. Jenkins, and P. V. R. Shannon, *J. Chem. Soc., Perkin Trans. 1* 1698 (1977).
[707] J.-E. Bäckvall and N. A. Plobeck, *J. Org. Chem.* **55**, 4528 (1990).
[708] Y. Oikawa, O. Yonemitsu, and J. Chem. Soc., *J. Chem. Soc., Perkin Trans. 1* 1479 (1976).
[709] S. Hibino and E. Sugino, *J. Heterocycl. Chem.* **27**, 1751 (1990).
[710] S. P. Modi, J. J. Carey, and S. Archer, *Tetrahedron Lett.* **31**, 5845 (1990).
[711] S. P. Modi, M. A. Michael, and S. Archer, *Tetrahedron* **47**, 6539 (1991).
[712] S. P. Modi, T. McComb, A.-H. Zayed, R. C. Oglesby, and S. Archer, *Tetrahedron* **46**, 5555 (1990).
[713] C.-K. Sha and J.-F. Yang, *Tetrahedron* **48**, 10645 (1992).
[714] Y. Miki, Y. Tada, N. Yanase, H. Hachiken, and K. Matsushita, *Tetrahedron Lett.* **37**, 7753 (1996).
[715] Y. Miki, H. Hachiken, and N. Yanase, *J. Chem. Soc., Perkin Trans. 1* 2213 (2001).
[716] Y. Miki, Y. Tada, and K. Matsushita, *Heterocycles* **48**, 1593 (1998).
[717] Y. Miki, Y. Tsuzaki, H. Hibino, and Y. Aoki, *Synlett* 2206 (2004).
[718] Y. Miki, Y. Aoki, Y. Tsuzaki, M. Umemoto, and H. Hibino, *Heterocycles* **65**, 2693 (2005).
[719] M. Ishikura, T. Yaginuma, I. Agata, Y. Miwa, R. Yanada, and T. Taga, *Synlett* 214 (1997).
[720] M. Ishikura, A. Hino, and N. Katagiri, *Heterocycles* **53**, 11 (2000).
[721] M. Ishikura, A. Hino, T. Yaginuma, I. Agata, and N. Katagiri, *Tetrahedron* **56**, 193 (2000).
[722] M. T. Díaz, A. Cobas, E. Guitián, and L. Castedo, *Synlett* 157 (1998).
[723] M. Díaz, A. Cobas, E. Guitián, and L. Castedo, *Eur. J. Org. Chem.* 4543 (2001).
[724] D. Mal, B. K. Senapati, and P. Pahari, *Tetrahedron* **63**, 3768 (2007).
[725] D. A. Taylor, M. M. Baradarani, S. J. Martinez, and J. A. Joule, *J. Chem. Res.* (S) 387 (1979); (M) 4801.
[726] D. A. Taylor, M. M. Baradarani, S. J. Martinez, and J. A. Joule, *J. Chem. Res.* (S) 4801 (1979).
[727] M. G. Saulnier and G. W. Gribble, *J. Org. Chem.* **48**, 2690 (1983).
[728] M.-L. Bennasar, T. Roca, and F. Ferrando, *J. Org. Chem.* **70**, 9077 (2005).
[729] M. Watanabe and V. Snieckus, *J. Am. Chem. Soc.* **102**, 1457 (1980).
[730] J. M. Pedersen, W. R. Bowman, M. R. J. Elsegood, A. J. Fletcher, and P. J. Lovell, *J. Org. Chem.* **70**, 10615 (2005).
[731] T.-L. Ho and S.-Y. Hsieh, *Helv. Chim. Acta* **89**, 111 (2006).
[732] I. Hogan, P. Jenkins, and M. Sainsbury, *Tetrahedron Lett.* **29**, 6505 (1988).
[733] I. Hogan, P. D. Jenkins, and M. Sainsbury, *Tetrahedron* **46**, 2943 (1990).
[734] R. J. Hall, A. H. Jackson, A. M. F. Oliveira-Campos, M.-J. R. P. Queiroz, and P. V. R. Shannon, *Heterocycles* **31**, 401 (1990).
[735] R. J. Hall, A. H. Jackson, A. M. F. Oliveira-Campos, and P. V. R. Shannon, *J. Chem. Res.* (S) 314 (1990); (M) 2501.
[736] A. M. F. Oliveira-Campos, M.-J. R. P. Queiroz, and P. V. R. Shannon, *Chem. Ind. (London)* 352 (1991).
[737] R. J. Hall, P. V. R. Shannon, A. M. F. Oliveira-Campos, and M. J. R. P. Queiroz, *Chem. Res.* (S) 2 (1992); (M) 0114.
[738] R. J. Hall, J. Marchant, A. M. F. Oliveira-Campos, M. J. R. P. Queiroz, and P. V. R. Shannon, *J. Chem. Soc., Perkin Trans. 1* 3439 (1992).
[739] P. M. Dharmasena and P. V. R. Shannon, *Tetrahedron Lett.* **35**, 7119 (1994).

[740] A. M. F. Oliveira-Campos, M.-J. R. P. Queiroz, M. M. M. Raposo, and P. V. R. Shannon, *Tetrahedron Lett.* **36**, 133 (1995).
[741] L. Chunchatprasert, P. Dharmasena, A. M. F. Oliveira-Campos, M. J. R. P. Queiroz, M. M. M. Raposo, and P. V. R. Shannon, *Chem. Res.* (S) 84 (1996); (M) 0630.
[742] I. Praly-Deprez, C. Rivalle, C. Huel, J. Belehradek, C. Paoletti, and E. Bisagni, *J. Chem. Soc., Perkin Trans. 1* 3165 (1991).
[743] I. Praly-Deprez, C. Rivalle, J. Belehradek, C. Huel, and E. Bisagni, *J. Chem. Soc., Perkin Trans. 1* 3173 (1991).
[744] F. Marsais, Ph. Pineau, F. Nivolliers, M. Mallet, A. Turck, A. Godard, and G. Queguiner, *J. Org. Chem.* **57**, 565 (1992).
[745] P. Molina, P. M. Fresneda, and P. Almendros, *Tetrahedron* **49**, 1223 (1993).
[746] J.-R. Dormoy and A. Heymes, *Tetrahedron* **49**, 2885 (1993).
[747] J.-R. Dormoy and A. Heymes, *Tetrahedron* **49**, 2915 (1993).
[748] P. W. Groundwater and R. Lewis, *Chem. Res.* (S) 215 (1995); (M) 1477.
[749] S. Blechert, R. Knier, H. Schroers, and T. Wirth, *Synthesis* 592 (1995).
[750] N. Haider, K. Mereiter, and R. Wanko, *Heterocycles* **41**, 1445 (1995).
[751] E. Desarbre, S. Coudret, C. Meheust, and J.-Y. Mérour, *Tetrahedron* **53**, 3637 (1997).
[752] Y. Ergün, S. Patir, and G. Okay, *J. Heterocycl. Chem.* **35**, 1445 (1998).
[753] Y. Ergün, S. Patir, and G. Okay, *J. Heterocycl. Chem.* **40**, 1005 (2003).
[754] Y. Ergün, S. Patir, and G. Okay, *Synth. Commun.* **34**, 435 (2004).
[755] A. R. Grummitt, M. M. Harding, P. I. Anderberg, and A. Rodger, *Eur. J. Org. Chem.* 63 (2003).
[756] J. Bergman, *Chem. Scr.* **27**, 539 (1987).
[757] J. Bergman, T. Janosik, and N. Wahlström, *Adv. Heterocycl. Chem.* **80**, 1 (2001).
[758] C. Sánchez, C. Méndez, and J. A. Salas, *Nat. Prod. Rep.* **23**, 1007 (2006).
[759] I. Hughes and R. A. Raphael, *Tetrahedron Lett.* **24**, 1441 (1983).
[760] I. Hughes, W. P. Nolan, and R. A. Raphael, *J. Chem. Soc., Perkin Trans. 1* 2475 (1990).
[761] C. J. Moody and K. F. Rahimtoola, *J. Chem. Soc., Chem. Commun.* 1667 (1990).
[762] C. J. Moody, K. F. Rahimtoola, B. Porter, and B. C. Ross, *J. Org. Chem.* **57**, 2105 (1992).
[763] M. Gallant, J. T. Link, and S. J. Danishefsky, *J. Org. Chem.* **58**, 343 (1993).
[764] J. T. Link, S. Raghavan, and S. J. Danishefsky, *J. Am. Chem. Soc.* **117**, 552 (1995).
[765] J. T. Link, S. Raghavan, M. Gallant, S. J. Danishefsky, T. C. Chou, and L. M. Ballas, *J. Am. Chem. Soc.* **118**, 2825 (1996).
[766] W. Harris, C. H. Hill, E. Keech, and P. Malsher, *Tetrahedron Lett.* **34**, 8361 (1993).
[767] G. Xie and J. W. Lown, *Tetrahedron Lett.* **35**, 5555 (1994).
[768] A. P. Fonseca, A. M. Lobo, and S. Prabhakar, *Tetrahedron Lett.* **36**, 2689 (1995).
[769] M. M. B. Marques, A. M. Lobo, S. Prabhakar, and P. S. Branco, *Tetrahedron Lett.* **40**, 3795 (1999).
[770] M. M. B. Marques, M. M. M. Santos, A. M. Lobo, and S. Prabhakar, *Tetrahedron Lett.* **41**, 9835 (2000).
[771] M. M. Faul, K. A. Sullivan, and L. L. Winneroski, *Synthesis* 1511 (1995).
[772] M. M. Faul, L. L. Winneroski, and C. A. Krumrich, *J. Org. Chem.* **63**, 6053 (1998).
[773] J. L. Wood, B. M. Stolz, and H.-J. Dietrich, *J. Am. Chem. Soc.* **117**, 10413 (1995).
[774] J. L. Wood, B. M. Stolz, H.-J. Dietrich, D. A. Pflum, and D. T. Petsch, *J. Am. Chem. Soc.* **119**, 9641 (1997).
[775] J. L. Wood, B. M. Stolz, and S. N. Goodman, *J. Am. Chem. Soc.* **118**, 10656 (1996).
[776] J. L. Wood, B. M. Stolz, S. N. Goodman, and K. Onwueme, *J. Am. Chem. Soc.* **119**, 9652 (1997).
[777] J. L. Wood, D. T. Petsch, B. M. Stolz, E. M. Hawkins, D. Elbaum, and D. R. Stover, *Synthesis* 1529 (1999).
[778] K. Tamaki, J. B. Shotwell, R. D. White, I. Drutu, D. T. Petsch, T. V. Nheu, H. He, Y. Hirokawa, H. Maruta, and J. L. Wood, *Org. Lett.* **3**, 1689 (2001).
[779] Y. Tamaki, E. W. D. Huntsman, D. T. Petsch, and J. L. Wood, *Tetrahedron Lett.* **43**, 379 (2002).
[780] T. B. Lowinger, J. Chu, and P. L. Spence, *Tetrahedron Lett.* **36**, 8383 (1995).
[781] M. Ohkubo, H. Kawamoto, T. Ohno, M. Nakano, and H. Morishima, *Tetrahedron* **53**, 585 (1997).
[782] M. Ohkubo, T. Nishimura, H. Jona, T. Honma, S. Ito, and H. Morishima, *Tetrahedron* **53**, 5937 (1997).
[783] E. J. Gilbert and D. L. Van Vranken, *J. Am. Chem. Soc.* **118**, 5500 (1996).
[784] E. J. Gilbert, J. W. Ziller, and D. L. Van Vranken, *Tetrahedron* **53**, 16553 (1997).
[785] J. D. Chisholm and D. L. Van Vranken, *J. Org. Chem.* **65**, 7541 (2000).
[786] H. Hayashi, Y. Suzuki, and M. Somei, *Heterocycles* **51**, 1233 (1999).
[787] M. Somei, F. Yamada, Y. Suzuki, S. Ohmoto, and H. Hayashi, *Heterocycles* **64**, 483 (2004).
[788] H. Hayashi, S. Ohmoto, and M. Somei, *Heterocycles* **45**, 1647 (1997).

[789] M. Somei, F. Yamada, J. Kato, Y. Suzuki, and Y. Ueda, *Heterocycles* **56**, 81 (2002).
[790] E. M. Beccalli, M. L. Gelmi, and A. Marchesini, *Tetrahedron* **54**, 6909 (1998).
[791] S. Mahboobi, E. Eibler, M. Koller, S. Kumar KC, A. Popp, and D. Schollmeyer, *J. Org. Chem.* **64**, 4697 (1999).
[792] Y. Kobayashi, T. Fujimoto, and T. Fukuyama, *J. Am. Chem. Soc.* **121**, 6501 (1999).
[793] M. Adeva, F. Buono, E. Caballero, M. Medarde, and F. Tomé, *Synlett* 832 (2000).
[794] D. Alonso, E. Caballero, M. Medarde, and F. Tomé, *Tetrahedron Lett.* **46**, 4839 (2005).
[795] G. M. Reddy, S.-Y. Chen, and B.-J. Uang, *Synthesis* 497 (2003).
[796] J. T. Kuethe, A. Wong, and I. W. Davies, *Org. Lett.* **5**, 3721 (2003).
[797] X. Cai and V. Snieckus, *Org. Lett.* **6**, 2293 (2004).
[798] T. Kaneko, H. Wong, J. Utzig, J. Schurig, and T. W. Doyle, *J. Antibiot.* **43**, 125 (1990).
[799] M. Somei and A. Kodama, *Heterocycles* **34**, 1285 (1992).
[800] S. Tanaka, M. Ohkubo, K. Kojiri, H. Suda, A. Yamada, and D. Uemura, *J. Antibiot.* **45**, 1797 (1992).
[801] J. Brüning, T. Hache, and E. Winterfeldt, *Synthesis* 25 (1994).
[802] U. Pindur, Y.-S. Kim, and D. Schollmeyer, *J. Heterocycl. Chem.* **31**, 377 (1994).
[803] U. Pindur, Y. S. Kim, and D. Schollmeyer, *J. Heterocycl. Chem.* **32**, 1335 (1995).
[804] M. G. Saulnier, D. B. Frennesson, M. S. Deshpande, and D. M. Vyas, *Tetrahedron Lett.* **36**, 7841 (1995).
[805] J. F. Barry, T. W. Wallace, and N. D. A. Walshe, *Tetrahedron* **51**, 12797 (1995).
[806] B. M. Stoltz and J. L. Wood, *Tetrahedron Lett.* **36**, 8543 (1995).
[807] U. Pindur and Y.-S. Kim, *J. Heterocycl. Chem.* **33**, 623 (1996).
[808] B. M. Stoltz and J. L. Wood, *Tetrahedron Lett.* **37**, 3929 (1996).
[809] J. L. Wood, B. M. Stolz, K. Onwueme, and S. N. Goodman, *Tetrahedron Lett.* **37**, 7335 (1996).
[810] R. L. Hudkins and J. L. Diebold, *Tetrahedron Lett.* **38**, 915 (1997).
[811] U. Pindur and Y.-S. Kim, *J. Heterocycl. Chem.* **35**, 97 (1998).
[812] S. Eils and E. Winterfeldt, *Synthesis* 275 (1999).
[813] D. E. Zembower, H. Zhang, J. P. Lineswala, M. J. Kuffel, S. A. Aytes, and M. M. Ames, *Bioorg. Med. Chem. Lett.* **9**, 145 (1999).
[814] M. Ohkubo, K. Kojiri, H. Kondo, S. Tanaka, H. Kawamoto, T. Nishimura, I. Nishimura, T. Yoshinari, H. Arakawa, H. Suda, H. Morishima, and S. Nishimura, *Bioorg. Med. Chem. Lett.* **9**, 1219 (1999).
[815] M. Ohkubo, T. Nishimura, H. Kawamoto, M. Nakano, T. Honma, T. Yoshinari, H. Arakawa, H. Suda, H. Morishima, and S. Nishimura, *Bioorg. Med. Chem. Lett.* **10**, 419 (2000).
[816] G. E. Burtin, D. J. Madge, and D. L. Selwood, *Heterocycles* **53**, 2119 (2000).
[817] M. F. Faul and K. A. Sullivan, *Tetrahedron Lett.* **42**, 3271 (2001).
[818] R. Nomak and J. K. Snyder, *Tetrahedron Lett.* **42**, 7929 (2001).
[819] A. Akao, S. Hiraga, T. Iida, A. Kamatani, M. Kawasaki, T. Mase, T. Nemoto, N. Satake, S. A. Weissman, D. M. Tschaen, K. Rossen, D. Petrillo, R. A. Reamer, and R. P. Volante, *Tetrahedron* **57**, 8917 (2001).
[820] J. Wang, M. Rosingana, D. J. Watson, E. D. Dowdy, R. P. Discordia, N. Soundarajan, and W.-S. Li, *Tetrahedron Lett.* **42**, 8935 (2001).
[821] A. Marotto, Y.-S. Kim, E. Schulze, and U. Pindur, *Pharmazie* **57**, 194 (2002).
[822] A. M. Lobo and P. Prabhakar, *J. Heterocycl. Chem.* **39**, 429 (2002).
[823] S. Routier, G. Coudert, J.-Y. Mérour, and D. H. Caignard, *Tetrahedron Lett.* **43**, 2561 (2002).
[824] B. M. Trost, M. J. Krische, V. Berl, and E. M. Grenzer, *Org. Lett.* **4**, 2005 (2002).
[825] S. A. Lakatosh, J. Balzarini, G. Andrei, R. Snoeck, E. De Clercq, and M. N. Preobrazhenskaya, *J. Antibiot.* **55**, 768 (2002).
[826] D. E. Gingrich and R. L. Hudkins, *Bioorg. Med. Chem. Lett.* **12**, 2829 (2002).
[827] T. A. Engler, K. Furness, S. Malhotra, C. Sanchez-Martinez, C. Shih, W. Xie, Z. Zhu, X. Zhou, S. Conner, M. F. Faul, K. A. Sullivan, S. P. Kolis, H. B. Brooks, B. Patel, R. M. Schultz, T. B. DeHahn, K. Kirmani, C. D. Spencer, S. A. Watkins, E. L. Considine, J. A. Dempsey, C. A. Ogg, N. B. Stamm, B. D. Anderson, R. M. Campbell, V. Vasudevan, and M. L. Lytle, *Bioorg. Med. Chem. Lett.* **13**, 2261 (2003).
[828] C. Sanchez-Martinez, M. M. Faul, C. Shih, K. A. Sullivan, J. L. Grutsch, J. T. Cooper, and S. P. Kolis, *J. Org. Chem.* **68**, 8008 (2003).
[829] E. Caballero, M. Adeva, S. Calderón, H. Sahagún, F. Tomé, M. Medarde, J. L. Fernández, M. López-Lázaro, and M. J. Ayuso, *Bioorg. Med. Chem. Lett.* **11**, 3413 (2003).
[830] B. N. Balasubramanian, D. R. St. Laurent, M. G. Saulnier, B. H. Long, C. Bachand, F. Beaulieu, W. Clarke, M. Deshpande, J. Eummer, C. R. Fairchild, D. B. Frennesson, R. Kramer, F. Y. Lee,

M. Mahler, A. Martel, B. N. Naidu, W. C. Rose, J. Russell, E. Ruediger, C. Solomon, K. M. Stoffan, H. Wong, K. Zimmermann, and D. M. Vyas, *J. Med. Chem.* **47**, 1609 (2004).
[831] M. M. Faul, K. A. Sullivan, J. L. Grutsch, L. L. Winneroski, C. Shih, C. Sanchez-Martinez, and J. T. Cooper, *Tetrahedron Lett.* **45**, 1095 (2004).
[832] M. M. Faul, T. A. Engler, K. A. Sullivan, J. L. Grutsch, M. T. Clayton, M. J. Martinelli, J. M. Pawlak, M. LeTourneau, D. S. Coffey, S. W. Pedersen, S. P. Kolis, K. Furness, S. Malhotra, R. S. Al-awar, and J. E. Ray, *J. Org. Chem.* **69**, 2967 (2004).
[833] M. M. M. Santos, A. M. Lobo, S. Prabhakar, and M. M. B. Marques, *Tetrahedron Lett.* **45**, 2347 (2004).
[834] R. S. Al-awar, J. E. Ray, K. A. Hecker, J. Huang, P. P. Waid, C. Shih, H. B. Brooks, C. D. Spencer, S. A. Watkins, B. R. Patel, N. B. Stamm, C. A. Ogg, R. M. Schultz, E. L. Considine, M. M. Faul, K. A. Sullivan, S. P. Kolis, J. L. Grutsch, and S. Joseph, *Bioorg. Med. Chem. Lett.* **14**, 3217 (2004).
[835] G. Zhu, S. E. Conner, X. Zhou, H.-K. Chan, C. Shih, T. A. Engler, R. S. Al-awar, H. B. Brooks, S. A. Watkins, C. D. Spencer, R. M. Schultz, J. A. Dempsey, E. L. Considine, B. R. Patel, C. A. Ogg, V. Vasudevan, and M. L. Lytle, *Bioorg. Med. Chem. Lett.* **14**, 3057 (2004).
[836] J. T. Kuethe and I. W. Davies, *Tetrahedron Lett.* **45**, 4009 (2004).
[837] R. S. Al-awar, J. E. Ray, K. A. Hecker, S. Joseph, J. Huang, C. Shih, H. B. Brooks, C. D. Spencer, S. A. Watkins, R. M. Schultz, E. L. Considine, M. M. Faul, K. A. Sullivan, S. P. Kolis, M. A. Carr, and F. Zhang, *Bioorg. Med. Chem. Lett.* **14**, 3925 (2004).
[838] S. Bartlett and A. Nelson, *Org. Biomol. Chem.* **2**, 2874 (2004).
[839] S. Massaoudi, F. Anizon, B. Pfeiffer, R. Golsteyn, and M. Prudhomme, *Tetrahedron Lett.* **45**, 4643 (2004).
[840] N. Wahlström and J. Bergman, *Tetrahedron Lett.* **45**, 7273 (2004).
[841] C. J. Nichols and N. S. Simpkins, *Tetrahedron Lett.* **45**, 7469 (2004).
[842] C. Sánchez, L. Zhu, A. F. Brana, A. P. Salas, J. Rohr, C. Méndez, and J. A. Salas, *Proc. Natl. Acad. Sci. USA* **102**, 461 (2005).
[843] J. Wang, N. Soundarajan, N. Liu, K. Zimmermann, and B. N. Naidu, *Tetrahedron Lett.* **46**, 907 (2005).
[844] M. G. Saulnier, D. R. Langley, D. B. Frennesson, B. H. Long, S. Huang, Q. Gao, D. Wu, C. R. Fairchild, E. Ruediger, K. Zimmermann, D. R. St. Laurent, B. N. Balasubramanian, and D. M. Vyas, *Org. Lett.* **7**, 1271 (2005).
[845] B. Witulski and T. Schweikert, *Synthesis* 1959 (2005).
[846] S. Messaoudi, F. Anizon, B. Pfeiffer, and M. Prudhomme, *Tetrahedron* **61**, 7304 (2005).
[847] D. Moffat, C. J. Nichols, D. A. Riley, and N. S. Simpkins, *Org. Biomol. Chem.* **3**, 2953 (2005).
[848] S. Barrett, S. Bartlett, A. Bolt, A. Ironmonger, C. Joce, A. Nelson, and T. Woodhall, *Chem. Eur. J.* **11**, 6277 (2005).
[849] A. Bourderioux, S. Routier, V. Bénéteau, and J.-Y. Mérour, *Tetrahedron Lett.* **46**, 6071 (2005).
[850] W. Fröhner, B. Monse, T. M. Braxmeier, L. Casiraghi, H. Sahagún, and P. Seneci, *Org. Lett.* **7**, 4573 (2005).
[851] S. Roy, A. Eastman, and G. W. Gribble, *Tetrahedron* **62**, 7838 (2006).
[852] S. Roy, A. Eastman, and G. W. Gribble, *Org. Biomol. Chem.* **4**, 3228 (2006).
[853] E. Piers, R. Britton, and R. J. Andersen, *J. Org. Chem.* **65**, 530 (2000).
[854] T. Yoshida, M. Nishiyachi, N. Nakashima, M. Murase, and E. Kotani, *Chem. Pharm. Bull.* **50**, 872 (2002).
[855] T. Yoshida, M. Nishiyachi, N. Nakashima, M. Murase, and E. Kotani, *Chem. Pharm. Bull.* **51**, 209 (2003).
[856] B. Hugon, B. Pfeiffer, P. Renard, and M. Prudhomme, *Tetrahedron Lett.* **44**, 3927 (2003).
[857] B. Hugon, B. Pfeiffer, P. Renard, and M. Prudhomme, *Tetrahedron Lett.* **44**, 3935 (2003).
[858] B. Hugon, B. Pfeiffer, P. Renard, and M. Prudhomme, *Tetrahedron Lett.* **44**, 4607 (2003).
[859] H. Hénon, S. Messaoudi, B. Hugon, F. Anizon, B. Pfeiffer, and M. Prudhomme, *Tetrahedron* **61**, 5599 (2005).
[860] H. Hénon, F. Anizon, N. Kucharczyk, A. Loynel, P. Casara, B. Pfeiffer, and M. Prudhomme, *Synthesis* 711 (2006).
[861] T. R. Kelly, Y. Zhao, M. Cavero, and M. Torneirao, *Org. Lett.* **2**, 3735 (2000).
[862] P. H. Bernardo, C. L. L. Chai, and J. A. Elix, *Tetrahedron Lett.* **43**, 2939 (2002).
[863] P. H. Bernardo and C. L. L. Chai, *J. Org. Chem.* **68**, 8906 (2003).
[864] P. H. Bernardo, C. L. L. Chai, G. A. Heath, P. J. Mahon, G. D. Smith, P. Waring, and B. A. Wilkes, *J. Med. Chem.* **47**, 4958 (2004).
[865] D. Sissouma, S. C. Collet, and A. Y. Guingant, *Synlett* 2612 (2004).

[866] D. Sissouma, L. Maingot, S. Collet, and A. Guingant, *J. Org. Chem.* **71**, 8384 (2006).
[867] S. Tohyama, T. Choshi, K. Matsumoto, A. Yamabuki, K. Ikegata, J. Nobuhiro, and S. Hibino, *Tetrahedron Lett.* **46**, 5263 (2005).
[868] A. Yamabuki, H. Fujinawa, T. Choshi, S. Tohyama, K. Matsumoto, K. Ohmura, J. Nobuhiro, and S. Hibino, *Tetrahedron Lett.* **47**, 5859 (2006).
[869] M.-L. Bennasar, T. Roca, and F. Ferrando, *Org. Lett.* **4**, 561 (2006).
[870] J. Sperry, C. S. P. McErlean, A. M. Z. Slawin, and C. J. Moody, *Tetrahedron Lett.* **48**, 231 (2007).
[871] V. D. Filimonov, E. A. Krasnokutskaya, and Y. A. Lesina, *Russ. J. Org. Chem.* **39**, 875 (2003).
[872] F. Dierschke, A. C. Grimsdale, and K. Müllen, *Synthesis* 2470 (2003).
[873] G. H. Kirsch, *Curr. Org. Chem.* **5**, 507 (2001).
[874] D. Joseph, L. Martarello, and G. Kirsch, *J. Chem. Res.* (S) 448 (1995); (M) 2557.
[875] N. Haider, *J. Heterocycl. Chem.* **39**, 511 (2002).
[876] N. Haider and E. Sotelo, *Chem. Pharm. Bull.* **50**, 1479 (2002).
[877] S. Routier, N. Ayerbe, J.-Y. Mérour, G. Coudert, C. Bailly, A. Pierré, B. Pfeiffer, D.-H. Caignard, and P. Renard, *Tetrahedron* **58**, 6621 (2002).
[878] I. C. F. R. Ferreira, M.-J. R. P. Queiroz, and G. Kirsch, *Tetrahedron* **58**, 7943 (2002).
[879] I. C. F. R. Ferreira, M.-J. R. P. Queiroz, and G. Kirsch, *Tetrahedron* **59**, 3737 (2003).
[880] I. C. F. R. Ferreira, M.-J. R. P. Queiroz, and G. Kirsch, *Tetrahedron Lett.* **44**, 4327 (2003).
[881] M. A. Fousteris, A. I. Koutsourea, E. S. Arsenou, L. Leondiadis, S. S. Nikolaropoulos, and I. K. Stamos, *J. Heterocycl. Chem.* **41**, 349 (2004).
[882] M. Chakrabarty, N. Ghosh, and Y. Harigaya, *Heterocycles* **62**, 779 (2004).
[883] R. Nagarajan and P. T. Perumal, *Synthesis* 1269 (2004).
[884] G. Desforges, C. Bossert, C. Montagne, and B. Joseph, *Synlett* 1306 (2004).
[885] M. Chakrabarty, N. Ghosh, and Y. Harigaya, *Tetrahedron Lett.* **45**, 4955 (2004).
[886] N. Haider and J. Käferböck, *Tetrahedron* **60**, 6495 (2004).
[887] T. Tsuchimoto, H. Matsubayashi, M. Kaneko, E. Shirakawa, and Y. Kawakami, *Angew. Chem.* **117**, 1360 (2005).
[888] H. Bregman, D. S. Williams, and E. Meggers, *Synthesis* 1521 (2005).
[889] D. S. Williams, G. K. Atilla, H. Bregman, A. Arzoumanian, P. S. Klein, and E. Meggers, *Angew. Chem.* **117**, 2020 (2005).
[890] S. C. Pelly, C. J. Parkinson, W. A. L. van Otterlo, and C. B. de Koning, *J. Org. Chem.* **70**, 10474 (2005).
[891] P. A. Kumar, R. Chakrabarty, and A. K. Saxene, *Med. Chem. Res.* **15**, 112 (2006).
[892] H. Bregman, P. J. Carroll, and E. Meggers, *J. Am. Chem. Soc.* **128**, 877 (2006).
[893] E. Meggers, G. E. Atilla-Gokcumen, H. Bregman, J. Maksimoska, S. P. Mulcahy, N. Pagano, and D. S. Williams, *Synlett* 1177 (2007).
[894] H. Hénon, F. Anizon, B. Pfeiffer, and M. Prudhomme, *Tetrahedron* **62**, 1116 (2006).
[895] E. Conchon, F. Anizon, R. M. Golsteyn, S. Léonce, B. Pfeiffer, and M. Prudhomme, *Tetrahedron* **32**, 11136 (2006).
[896] B. B. Mishra, V. K. Tiwari, D. D. Singh, A. Singh, and V. J. Tripathi, *Med. Chem. Res.* **15**, 119 (2006).
[897] Z. Liu and R. C. Larock, *Tetrahedron* **63**, 347 (2007).
[898] L. Ackermann and A. Althammer, *Angew. Chem.* **119**, 1652 (2007).
[899] T. P. Lebold and M. A. Kerr, *Org. Lett.* **9**, 1883 (2007).

CUMULATIVE INDEX OF TITLES

SUBJECT INDEX